UC Irvine
UC Irvine Electronic Theses and Dissertations

Title

Radical-Polar Crossover Cyclizations in the Total Synthesis of Paxilline Indole Diterpenes

Permalink

https://escholarship.org/uc/item/581373c7

Author

Schatz, Devon

Publication Date

2020

Copyright Information

Peer reviewed|Thesis/dissertation

UNIVERSITY OF CALIFORNIA,
IRVINE

Radical-Polar Crossover Cyclizations in the Total Synthesis of Paxilline Indole Diterpenes

DISSERTATION

submitted in partial satisfaction of the requirements
for the degree of

DOCTOR OF PHILOSOPHY

in Chemistry

by

Devon James Schatz

Dissertation Committee:
Assistant Professor Sergey V. Pronin, Chair
Distinguished Professor Larry E. Overman
Professor Christopher D. Vanderwal

2020

DEDICATION

To my Mom and Dad,

in recognition of their unrelenting support.

TABLE OF CONTENTS

LIST OF FIGURES

LIST OF SCHEMES

LIST OF TABLES

ACKNOWLEDGMENTS

VITAE

DEVON SCHATZ

EDUCATION
- PhD in Chemistry, University of California, Irvine; 2015 – 2020 (3.9 GPA)
- B.Sc. with Specialization in Chemistry, University of Alberta, 2010 – 2014 (3.3 GPA)

RESEARCH EXPERIENCE
- Graduate Research Assistant, University of California – Irvine; supervised by Professor Sergey V. Pronin (December 2015 – Present)
- Undergraduate Research Assistant, University of Alberta; supervised by Professor Frederick G. West, (January 2014 – August 2015)
- Undergraduate Research Assistant, University of Alberta; supervised by Professor Eric Rivard (May – August 2013)

PUBLICATIONS
- Thomas, W.P.; **Schatz, D. J.;** George, D. T.; Pronin, S. V. A Radical-Polar Crossover Annulation to Access Terpenoid Motifs*, J. Am. Chem. Soc.* **2019,** *141,* 12246-12250.
- **Schatz, D. J.;** Lin., W.; Pronin, S. V. Catalytic Enantioselective Conjugate Addition en route to Paxilline Indoloterpenoids, *Tetrahedron,* **2019,** *75,* 3361-3365.
- Godfrey, N. A.*; **Schatz, D. J.*;** Pronin, S. V. Twelve-Step Asymmetric Synthesis of (–)-Nodulisporic Acid C, *J. Am. Chem. Soc.* **2018,** *140,* 12770-12774. (*equally contributing authors)
- **Schatz, D. J.;** Kwon, Y.; Scully, T. W.; West, F. G. Interrupting the Nazarov Cyclization with Bromine, *J. Org. Chem.* **2016,** *81,* 12494-12498.
- Kwon, Y.; **Schatz, D. J.;** West, F. G. 1,4-Diketones from Cross-Conjugated Dienones: Potassium Permanganate-Interrupted Nazarov Reaction, *Angew. Chem. Int. Ed.* **2015,** *54,* 9940-9943.
- He, G.; Gelgado, W. T.; **Schatz, D. J.;** Merten, C.; Mohammadpour, A.; Mayr, L.; Ferguson, M. J.; McDonald, R.; Brown, A.; Shankar, K.; Rivard, E. Coaxing Solid State Phosphorescence from Tellurophenes, *Angew. Chem. Int. Ed.* **2014,** *53,* 4587-4591.

PRESENTATIONS
- **Schatz, D. J.;** Godfrey, N. A.; Pronin, S. V. Total Synthesis of (–)-Nodulisporic Acid C. Presented at the 2019 ACS DOC Graduate Research Symposium, July 2019 (Presentation).
- **Schatz, D. J.;** Godfrey, N. A.; Pronin, S. V. A Concise Approach to the Nodulisporic Acids. Presented at the 101st Canadian Chemistry Conference and Exhibition, May 2018 (Presentation).
- **Schatz, D. J.;** Kwon, Y.; West, F. G. Interrupting the Nazarov Cyclization with Bromine. Presented at the 98th Canadian Chemistry Conference and Exhibition, June 2015 (Poster).

AWARDS
- NSERC Postgraduate Scholarship – Doctorate (2015)
- Dr. Robert Schutte Award in Science (2014)

- Chemistry 401 Undergraduate Research Award (2014)
- Association of the Chemical Profession of Alberta Undergraduate Scholarship in Chemistry (2014)
- Jason Lang Scholarship (2013 and 2014)
- Gilead Sciences Prize in Carbohydrate Chemistry (2013)

ABSTRACT OF THE DISSERTATION

Radical-Polar Crossover Cyclizations in the Total Synthesis of Paxilline Indole Diterpenes

by

Devon James Schatz

Doctor of Philosophy in Chemistry

University of California, Irvine, 2020

Assistant Professor Sergey V. Pronin

In Chapter 1, a thorough overview of the paxilline indoloterpenoids will be covered with an emphasis on the diterpene congeners. Their notable biological activities will be discussed, as well as their challenging structural features from a synthetic organic chemistry standpoint. A brief discussion on the biosynthetic origin of the natural product family is also provided. Prior synthetic art will then be discussed at length, with an emphasis on the terpene core, as knowledge of synthetic challenges intrinsic to this system has intimately guided the work discussed in Chapters 2 and 3.

Chapter 2 describes our lab's efforts towards a total synthesis of (–)-nodulisporic acid C. Development of a key radical-polar crossover cascade and an enantioselective conjugate addition permitted expedient access the terpene core. Completion of the highly convergent synthesis was facilitated by an efficient, intermolecular ketone α-arylation between two complex fragments that required extensive optimization. Taken together, a 12-step, asymmetric synthesis of (–)-nodulisporic acid C was completed.

Chapter 3 describes recent efforts to elaborate on the utility of the key radical-polar crossover cyclization to access additional paxilline indole diterpene congeners, particularly

flagship congener paxilline itself. Various strategies were assessed for transforming the original polycyclization product into the desired oxidation pattern. The lack of success in this endeavour forced a revision of the polycyclization substrate altogether. Proof of concept with this strategy has been demonstrated towards the core of paxilline.

In Chapter 4, a brief review of carbon-carbon bond forming processes enabled by hydrogen atom transfer is described. Our labs methodology expanding the radical-polar crossover cascade to a well-functioning annulation is then discussed. Highly decorated cyclohexanols, complementary to Diels-Alder adducts, were efficiently accessed. The methodology permitted a facile synthesis of labdane diterpene forskolin.

Chapter 1: A Review of the Paxilline Indoloterpenoids

1.1 The Paxilline Indoloterpenoids

1.1.1 Introduction and Bioactivity of Notable Isolates

The paxilline indoloterpenoids are a diverse class of secondary metabolites produced by various species of fungi, found frequently in agricultural crops, that induce neurotoxic effects on grazing insects and animals.[1] One of the early isolates, and representative member, paxilline (**1.1**)[2] was found to reversibly block high conductance calcium-activated potassium (maxi-K) channels in vascular smooth muscle tissue (Figure 1.1).[3] Following this study was the identification of the structurally more complex and potent lolitrem B (**1.2**).[4] Known as the causative agent for ryegrass staggers in grazing livestock, the lolitrems also target maxi-K channels[5], though demonstrate prolonged tremors and resistance to washout indicating higher binding affinity.[6] Molecules that target potassium channels have been pursued as treatments for cardiac arrhythmia, hypertension, chronic pain, and neurological diseases such as epilepsy and memory disorders.[7] Additionally, lolitrem B has been found to inhibit cytokines IL-6 and TNFa while showing no toxicity towards the host cells.[8] The lolitrems have therefore garnered attention as potential therapies for sepsis. Penitrem A (**1.3**)[9] was another early isolate shown to interfere with amino acid release

Figure 1.1 Paxilline Indole Diterpenes Notable for their Bioactivity

paxilline (**1.1**)

lolitrem B (**1.2**)

penitrem A (**1.3**)

nodulisporic acid A (**1.4**)

terpendole E (**1.5**)
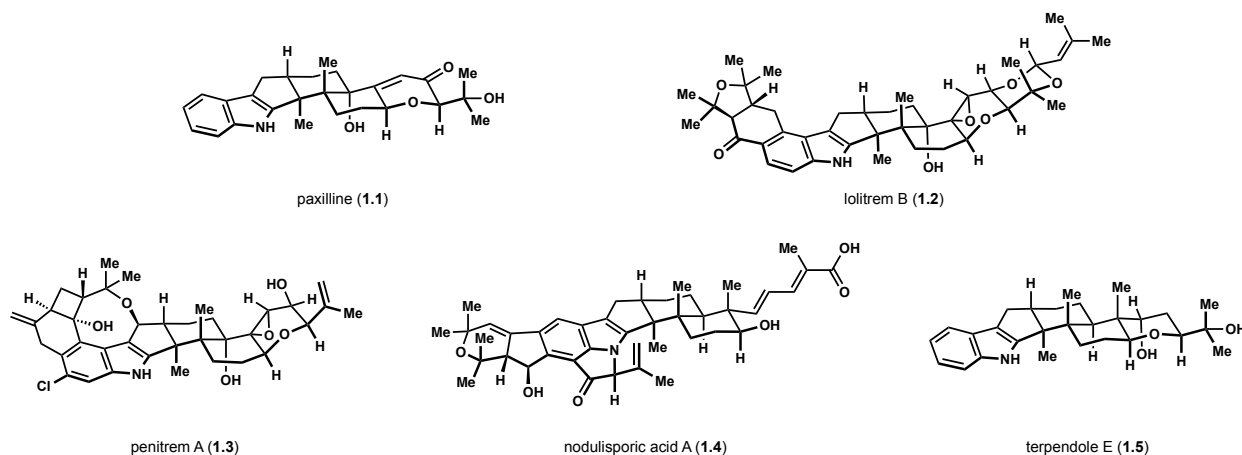
mechanisms, increasing the amount of glutamate, aspartate and γ-aminobutyric acid (GABA)[10], leading to similar muscular contractions produced by lolitrem B.[3a] These secondary metabolites, while detrimental to livestock well-being, cause analogous effects on invertebrates, inspiring pursuit of non-toxic congeners to control insect infestations on crops.[11] Nodulisporic acid A (**1.4**)[12] possesses this profile, modulating a subset of ligand-gated chloride ion channels exclusively found in arthropods, rendering them harmless to mammalian cells.[13] As more studies are conducted, additional unrelated activities continue to be discovered. Terpendole E[14] for example has garnered attention for inhibition of kinesin Eg5, arresting cell division and proliferation, a promising trait for developing cancer therapies.[15]

1.1.2 Distinguishing Features of the Paxilline Indole Diterpenes

Since the initial discovery of aflatrem (**1.6**)[16], >150 diterpene and sesquiterpene congeners have been disclosed (Figure 1.2), constituting a vast resource for therapies and tools for studying biological systems perhaps not yet recognized. Illustrated on paspaline (**1.7**)[17] in Figure 1.2, the paxilline indole diterpenes (PIDs) share a characteristic pentacyclic core possessing an indole fused to a tricarbocyclic framework containing two *trans*-fused ring junctures at C3–C16 and C4–C13. Another hallmark feature is the vicinal quaternary carbon pair at C3 and C4. In many congeners, the presence of an axial methyl group at C12 adds further steric demand due to the transannular interaction with the C4 methyl group. These features are highlighted as synthetic efforts have demonstrated on multiple occasions that they are challenging to construct (*vide infra*).

2

Figure 1.2 Known Paxilline Indoloterpenoids

paspaline (**1.7**)[17]

emindole SB (**1.8**)[18]

paspaline B (**1.9**)[19]

4a-demethylpaspaline-4a-carboxyllic acid (**1.10**)[20]

4a-demethylpaspaline-3,4,4a-triol (**1.11**)[20]

3-deoxo-4b-deoxypaxilline (**1.12**)[20]

PC-M6 (**1.13**)[21]

3-deoxopaxilline (**1.14**)[20]

13-dehydroxypaxilline (**1.15**)[18]

α-paxitriol (**1.16**)[22]

β-paxitriol (**1.17**)[22]

paxilline (**1.1**)[2]

1'-O-acetylpaxilline (**1.18**)[23]

4b-deoxy-1'-O-acetylpaxilline (**1.19**)[23]

2'-hydroxypaxilline (**1.20**)[20]

PC-M5' (**1.21**)[21]

21-isopentenylpaxilline (**1.22**)[24]

penijanthine A (**1.23**)[25]

4b-deoxypenijanthine A (**1.24**)[23]

penijanthine B (**1.25**)[26]

rhizovarin F (**1.26**)[27]

Sulpinine A (**1.27**)[28]

Sulpinine B (**1.28**)[28]

Sulpinine C (**1.29**)[28]

3

terpendole A (**1.30**): C33 undefined[15a]
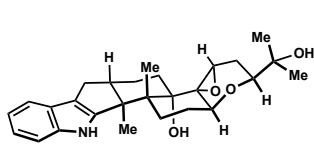
terpendole B (**1.31**)[15a]
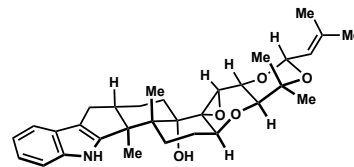
terpendole C (**1.33**)[15a]
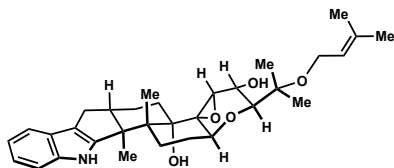
terpendole D (**1.33**)[15a]
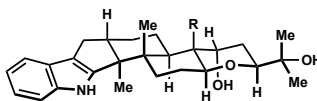
terpendole E (**1.5**)[14a]: R = Me
terpendole F (**1.34**)[14a]: R = CH$_2$OH
terpendole G (**1.35**)[14a]: R = CHO
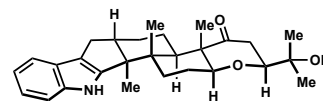
11-ketopaspalline (**1.36**)[15c]
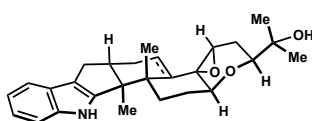
terpendole H (**1.37**): C13–C14 epoxide[14a]
stereochemistry unconfirmed
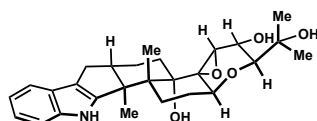
terpendole I (**1.38**)[14a]
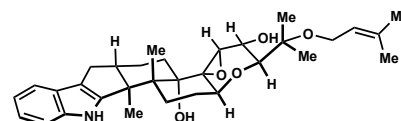
terpendole J (**1.39**)[14a]
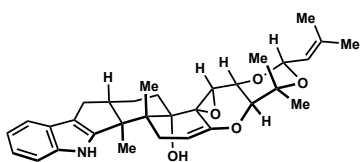
terpendole K (**1.40**)[14a]
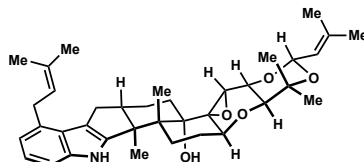
terpendole L (**1.41**)[14a]
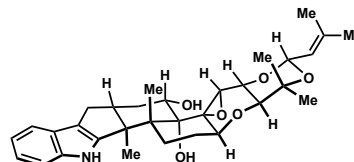
terpendole M (**1.42**)[14c]
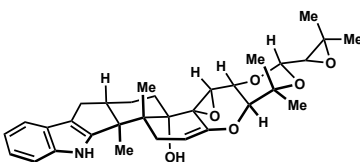
6,7-dehydroterpendole A (**1.43**)[29]
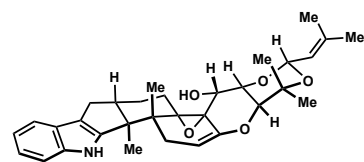
11-hydroxy-12,13-epoxyterpendole K (**1.44**)[29]
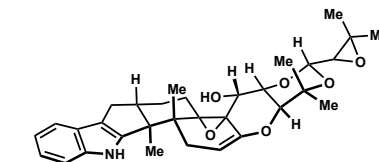
6,7-dehydro-11-hydroxy-12,13-epoxyterpendole A (**1.45**)[29]
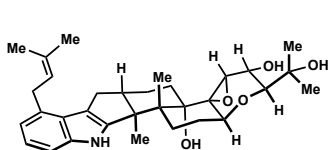
tolypocladin A (**1.46**)[30]
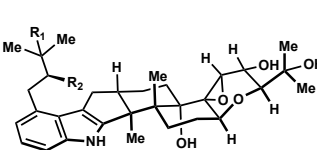
tolypocladin B (**1.47**)[30]: R$_1$ = Cl; R$_2$ = OH
tolypocladin C (**1.48**)[30]: R$_1$ = OMe; R$_2$ = OH
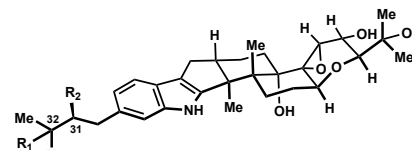
tolypocladin D (**1.49**)[30]: R$_1$ = Cl; R$_2$ = OH
tolypocladin K (**1.50**)[30]: Δ^{31,32}
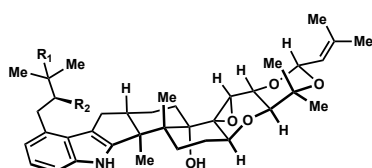
tolypocladin E (**1.51**)[30]: R$_1$ = Cl; R$_2$ = OH
tolypocladin F (**1.52**)[30]: R$_1$ = R$_2$ = OH
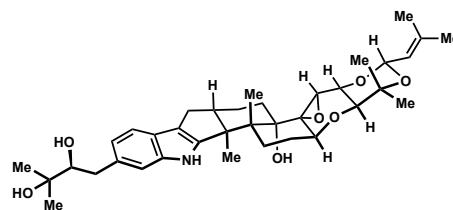
tolypocladin G (**1.53**)[30]

4
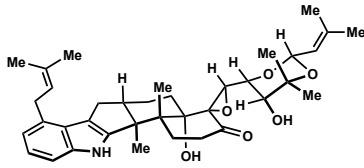
tolypocladin H (**1.54**)[30]
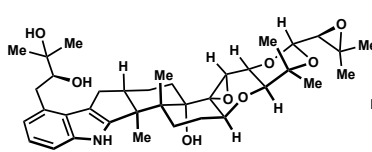
tolypocladin I (**1.55**)[30]
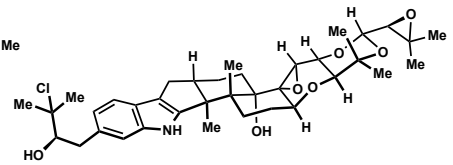
tolypocladin J (**1.56**)[30]
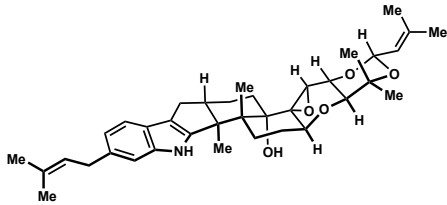
tolypocladin L (**1.57**)[30]
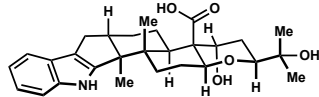
drechmerin B (**1.58**)[31]
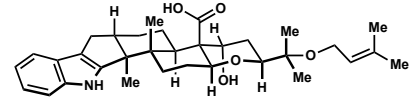
drechmerin C (**1.59**)[31]
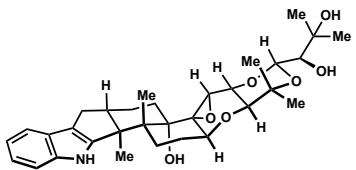
drechmerin D (**1.60**)[31]
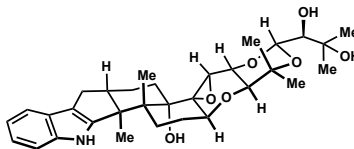
drechmerin E (**1.61**)[31]
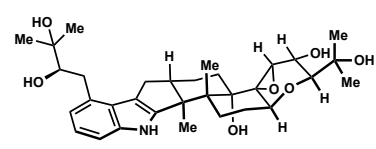
drechmerin F (**1.62**)[31]
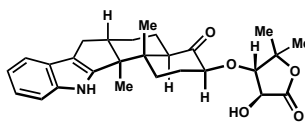
drechmerin G (**1.63**)[31]
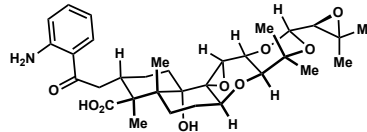
drechmerin H (**1.64**)[32]
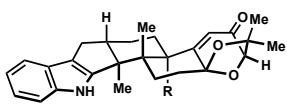
paspalicine (**1.65**)[17]: R = H
paspalinine (**1.66**)[33]: R = OH
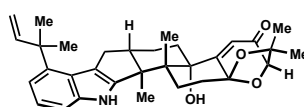
aflatrem (**1.6**)[16]
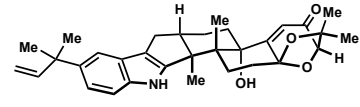
β-aflatrem (**1.67**)[34]
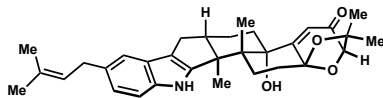
paspalitrem A (**1.68**)[35]
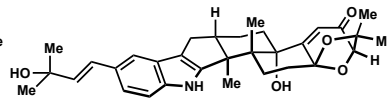
paspalitrem B (**1.69**)[35]
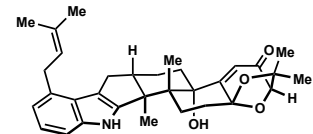
paspalitrem C (**1.70**)[34]
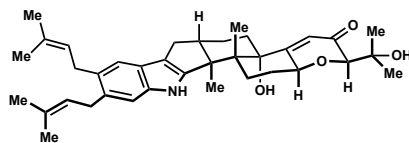
9,10-diisopentenylpaxilline (**1.71**)[20]

pyrapaxilline (**1.72**)[36]

shearinine A (**1.73**)[24]: R = H
shearinine D (**1.74**)[37]: R = OH
shearinine E (**1.75**)[37]: R = OMe

shearinine B (**1.76**)[24]

shearinine C (**1.77**)[24]

shearinine F (**1.78**)[37]

shearinine G (**1.79**)[37]

shearinine H (**1.80**)[37]

shearinine I (**1.81**)[37]

shearinine J (**1.82**)[37]

shearinine K (**1.83**)[37]

janthitrem A (**1.84**)[38]: R = OH
janthitrem D (**1.85**)[38]: R = H

janthitrem B (**1.86**)[39]: R = OH
janthitrem C (**1.87**)[40]: R = H

janthitrem E (**1.88**)[39]: R$_1$ = OH; R$_2$ = H
janthitrem F (**1.89**)[39]: R$_1$ = OH; R$_2$ = Ac
janthitrem G* (**1.90**)[39]: R$_1$ = R$_2$ = H
*C23 stereochemistry not confirmed

lolicine A (**1.91**)[41]: R = Me
lolicine B (**1.92**)[41]: R = CHO

lolitriol (**1.93**)[41]

lolitrem A (**1.94**)[42]

lolitrem B (**1.2**)[4a]

31-*epi*-lolitrem B (**1.95**)[43]

6

lolitrem E (**1.96**)[44]

lolitrem F (**1.97**)[43]
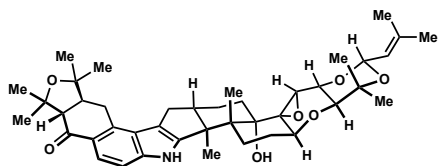
31-*epi*-lolitrem F (**1.98**)[43]
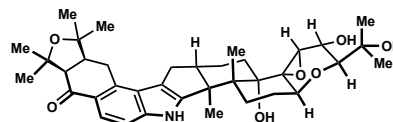
lolitrem N (**1.99**)[41]
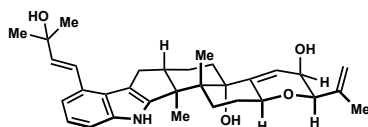
PC-M5 (**1.100**)[45]
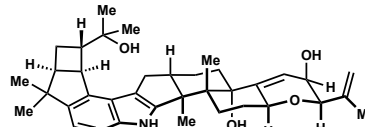
PC-M4 (**1.101**)[45]
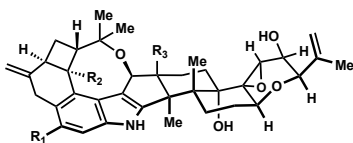
penitrem A (**1.3**)[9b,c]: R₁ = Cl; R₂ = OH; R₃ = H
penitrem B (**1.102**)[9b]: R₁ = H; R₂ = H; R₃ = H
penitrem E (**1.103**)[9b]: R₁ = H; R₂ = OH; R₃ = H
penitrem F (**1.104**)[9b]: R₁ = Cl; R₂ = H; R₃ = H
penitrem H (**1.105**)[26]: R₁ = Cl; R₂ = OH; R₃ = OMe
19-hydroxypenitrem A (**1.106**)[46]: R₁ = Cl; R₂ = OH; R₃ = OH
19-hydroxypenitrem E (**1.107**)[46]: R₁ = H; R₂ = OH; R₃ = OH
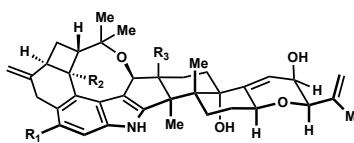
penitrem C (**1.108**)[9b]: R₁ = Cl; R₂ = H; R₃ = H
penitrem D (**1.109**)[9b]: R₁ = H; R₂ = H; R₃ = H
penitrem G (**1.110**)[11]: R₁ = H; R₂ = H; R₃ = OH
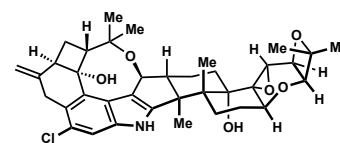
pennigritrem (**1.111**)[47]
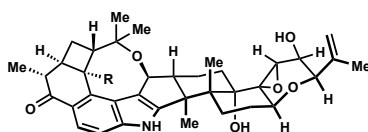
penitrenome A (**1.112**)[48]: R = H
penitrenome B (**1.113**)[48]: R = OH
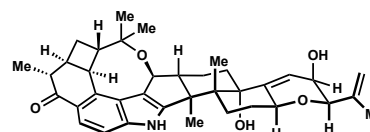
penitrenome C (**1.114**)[48]
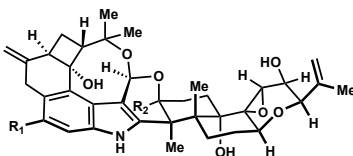
rhizovarin A (**1.115**)[27]: R₁ = Cl; R₂ = OH
rhizovarin B (**1.116**)[27]: R₁ = Cl; R₂ = OMe
rhizovarin C (**1.117**)[27]: R₁ = H; R₂ = OMe
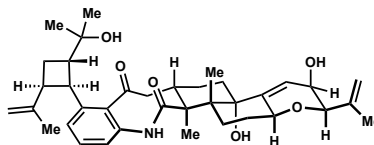
rhizovarin D (**1.118**)[27]
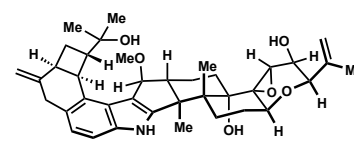
rhizovarin E (**1.119**)[27]

7
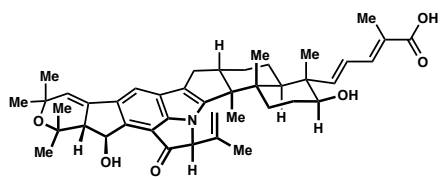
nodulisporic acid A (**1.4**)[12a]
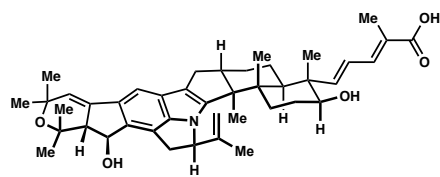
nodulisporic acid B (**1.120**)[12c]
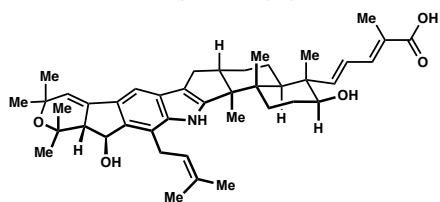
nodulisporic acid C (**1.121**)[12d]
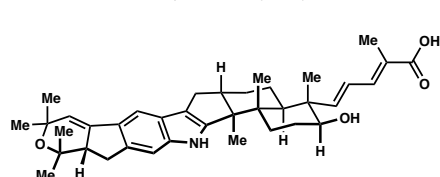
nodulisporic acid D (**1.122**)[12e]
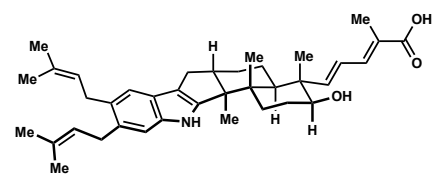
nodulisporic acid E (**1.123**)[12e]
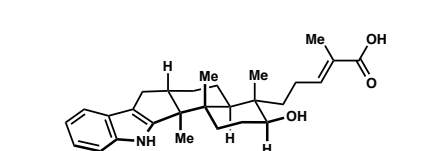
nodulisporic acid F (**1.124**)[12e]
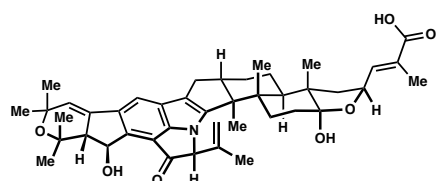
nodulisporic acid A$_1$ (**1.125**)[12b]
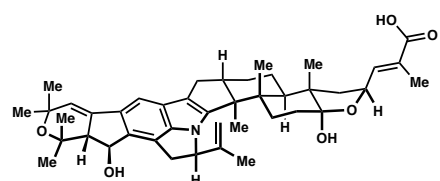
nodulisporic acid B$_1$ (**1.126**)[12c]
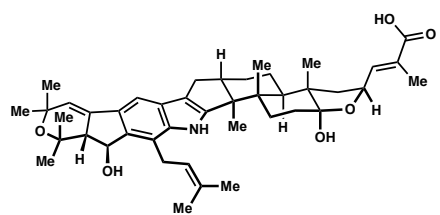
nodulisporic acid C$_1$ (**1.127**)[12d]
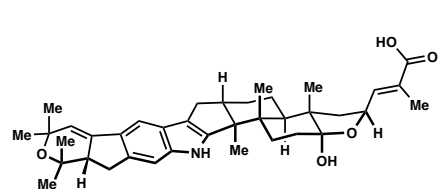
nodulisporic acid D$_1$ (**1.128**)[12e]
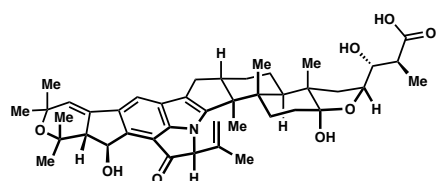
nodulisporic acid A$_2$ (**1.129**)[12b]
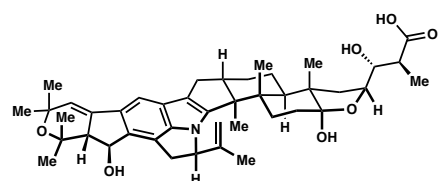
nodulisporic acid B$_2$ (**1.130**)[12c]
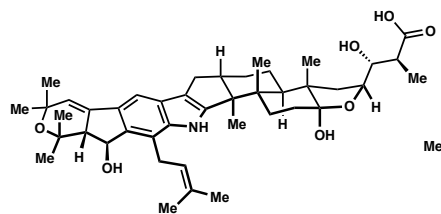
nodulisporic acid C$_2$ (**1.131**)[12d]
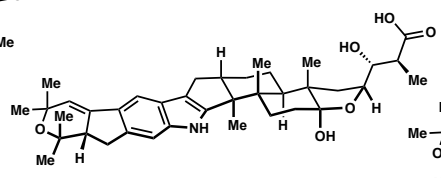
nodulisporic acid D$_2$ (**1.132**)[12e]
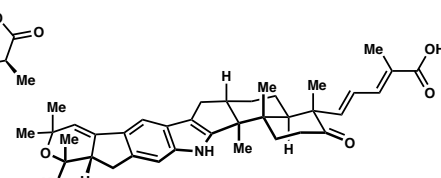
nodulisporic acid D$_3$ (**1.133**)[12e]
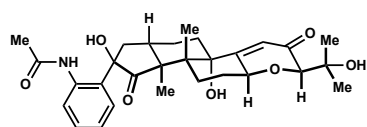
secopaxilline (**1.134**)[49]
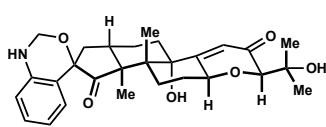
penerpene A (**1.135**)[50]
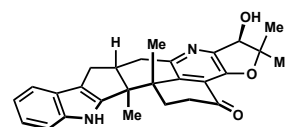
penerpene B (**1.136**)[50]
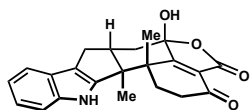
penerpene C (**1.137**)[50]
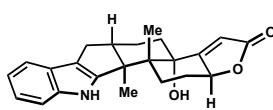
penerpene D (**1.138**)[50]
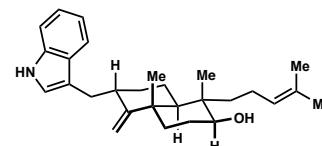
emeniveol (**1.139**)[51]
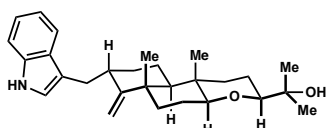
anthcolorin (**1.140**)[52]
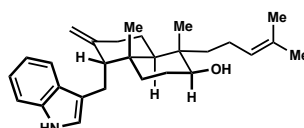
emindole DA (**1.141**)[53]
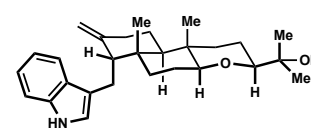
emindole DB (**1.142**)[53]
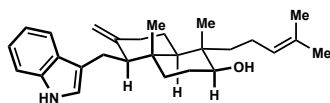
emindole SA (**1.143**)[54]
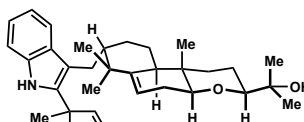
emindole PA (**1.144**)[55]
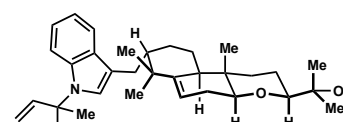
emindole PB (**1.145**)[55]
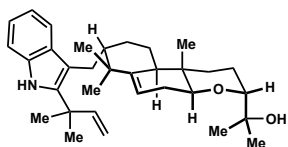
emindole PC (**1.146**)[55]
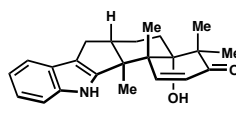
lecanindole A (**1.147**)[56]
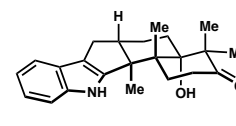
lecanindole B (**1.148**)[56]
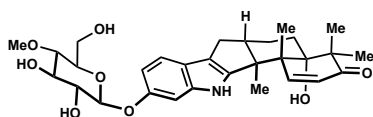
lecanindole C (**1.149**)[56]
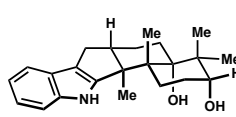
lecanindole D (**1.150**)[56]
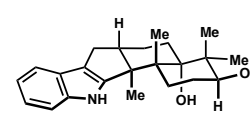
7-epi-lecanindole D (**1.151**)[56]
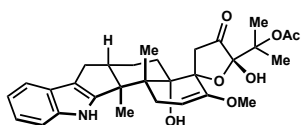
thiersinine A (**1.152**)[57]
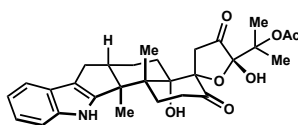
thiersinine B (**1.153**)[57]
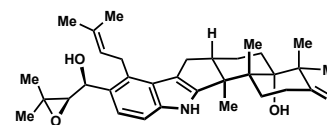
sespendole (**1.154**)[58]

1.1.3 Biosynthetic Production of the Paxilline Indole Diterpenes

The fascinating framework that these molecules consist of arises from a unique polyene cyclization pathway. Studies by Arigoni confirmed the polyene origin through incorporation of

C13 into geranylgeranyl pyrophosphate (GGPP) from labelled acetate (Scheme 1.1).[59] Oikawa and co-workers[60] later elaborated that 3-geranylgeranyl indole, derived from either tryptophan[61] or indole glycerol pyrophosphate[62], was the next precursor to polyene cyclization through deuterium incorporation.

Scheme 1.1. Arigoni's ^{13}C Labelling of Paspaline

• ^{13}C labelled acetate   mevalonate   isopentenyl pyrophosphate   paspaline (**1.7**)
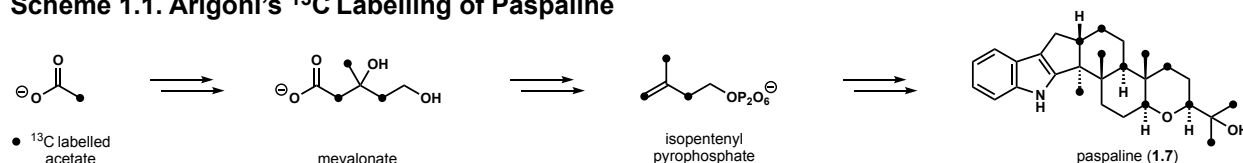
From these early studies and the aid of gene cluster elucidation experiments[63], biosynthetic pathways to most of the PID congeners have been proposed (Scheme 1.2).[64] Extension of farnesyl pyrophosphate to GGPP and indole alkylation produces polyene **1.157**. Regioselective epoxidation produces the polycyclization precursor **1.158** that undergoes the unique initial cyclization where C3' attacks C7' in anti-Markovnikov fashion to result in bicyclic secondary carbocation **1.159**. Wagner-Meerwein shift leaves a tertiary carbocation at C3' that is attacked by the C2 of the indole to produce emindole SB (**1.8**). This intermediate is the branching point for production of the nodulisporic acids, whose gene clusters (Nod)[65] have only been partially resolved. Otherwise, **1.8** is carried on to paspaline (**1.7**) and then paxilline (**1.1**). It is worth highlighting that paspaline and paxilline each represent one of the two core oxidation patterns found throughout the PIDs. As such, more complex congeners may be referred to as paspaline or paxilline-type. In the past two decades, a significant amount of effort from Scott and Oikawa has elucidated several genes responsible for these transformations.[66] Scott and co-workers identified PaxG for GGPP synthesis, PaxC the prenyltransferase, a monooxygenase PaxM and membrane protein PaxB as the minimum constituents necessary for paspaline production.[63b] Additional gene deletion experiments clarified two P450 monooxygenases (PaxP and PaxQ) are responsible for the conversion of paspaline (**1.7**)

to paxilline (**1.1**).[67] Several additional studies have helped at least partially elucidate machinery responsible for several other congeners such as the terpendoles (Ter)[68], aflatrems (Atm)[69], lolitrems (Ltm)[70], shearinines and janthitrems (Jan)[71] and the penitrems (Ptm).[72]

Scheme 1.2. Biosynthetic Production of PIDs with Identified Gene Clusters
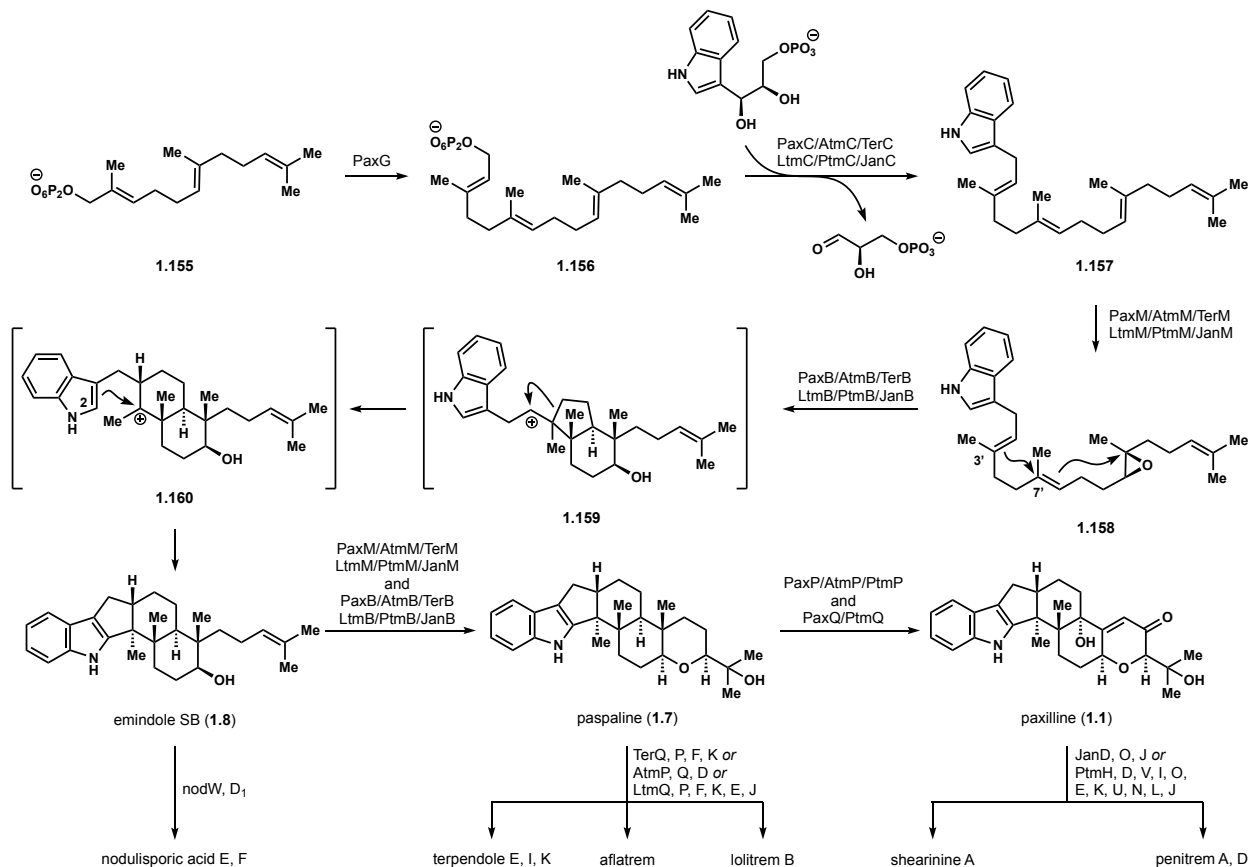
1.2 Prior Syntheses of Paxilline Indoloterpenoids and the Terpene Core

1.2.1 Conspectus

This section of Chapter 1 will serve to highlight the synthetic work related to the paxilline indoloterpenoids, focusing on completed syntheses along with studies related to the terpene core. The work presented is intended to follow an organizational approach based loosely on chronological evolution strategies. Attention is given to both complete and incomplete strategies, which often provide valuable insight surrounding stereocontrolled transformations necessary to

access the natural products efficiently. Methods that have been developed and indirectly associated with the paxilline indoloterpenoids are not discussed. Beginning with Amos B. Smith (III)'s foundational synthesis of (–)-paspaline in 1984, his body of work over the following two decades will be discussed. Contributions from other groups over this time-period and after will follow. The discussion will return to Smith and his most recent accomplishment, the syntheses of (–)-nodulisporic acids B and C, that have been subject to Smith's study for the past two decades. Finally, our lab's synthesis of (±)-emindole SB is introduced, leading into our synthesis of (–)-nodulisporic acid C described in Chapter 2.

1.2.2 Amos B. Smith (III)'s First Generation Total Synthesis of (–)-Paspaline

The seminal completion of a paxilline indole diterpene total synthesis came from the lab of Amos B. Smith (III) with the completion of (–)-paspaline (**1.7**).[73] Smith's approach featured appendage of the indole motif late stage on a cyclopentanone **1.161** (Scheme 1.3). Generation of the *trans*-hydrindane at C3–C16 was first accomplished with a reductive methylation of enonone **1.162**. These stereocenters were a major driving force in the evolution of Smith's strategies to the terpene core, resulting in multiple generations of approaches that will be discussed in detail.[74] In contrast, Smith's initial generation of the relative C12–C13 orientation through a reductive allylation transform has not been substantially modified in over three decades. The enone **1.162** leads Smith back to (+)-Wieland–Miescher ketone (**1.163**)[75], providing the key C4 stereocenter in one step and in enantioenriched form. This point of initiation is ubiquitous to Smith's syntheses.

Scheme 1.3. Key Stereodefining Transformations Employed by Smith

(–)-paspaline (**1.7**) — late stage indole formation → **1.161** — reductive methylation → **1.162** — reductive allylation → (+)-Wieland-Miescher ketone (**1.163**)
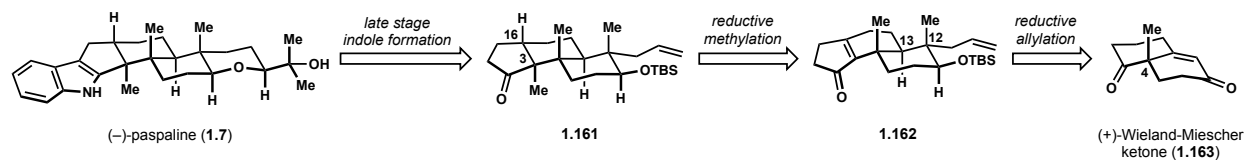
In the forward sense, Baudin's protocol[76] for selective ketalization of the C3 ketone of Wieland–Miesher ketone (**1.163**) permitted alkylation of enone **1.164** at C12 to thioether **1.165** as reported by Kirk and Petrow (Scheme 1.4).[77] Smith extensively screened reductive alkylation of enone **1.165**, ultimately employing dissolving metal conditions and allyl bromide as the alkylating reagent to set stereocenters at C12 and C13 with the axial methyl group at C4 directing the electrophile to the opposite face.[78] In contrast, sodium borohydride reduction of ketone **1.166** at the C7 carbonyl modestly favoured production of equatorial alcohol **1.167**. Following removal of the ketal, a protected propargyl alcohol equivalent was added to ketone **1.168** to produce an inconsequential mixture of tertiary alcohols. Treatment of this mixture with concentrated sulfuric acid in methanol induced a Meyer–Schuster rearrangement/Nazarov cyclization cascade to produce cyclopentenone **1.171** in modest yield.[79] Following silylation, Smith faced the onerous challenge of stereoselectively generating the C16, C3 and C4 stereotriad. Reduction of enone **1.162** set the C16 stereocenter as desired, but methylation of the resulting enolate provided a modest yield of diastereomers that favoured the undesired cyclopentanone **1.172** bearing the *cis*-fused 5,6 ring-juncture. Smith advanced the minor alkene diastereomer **1.161** through a hydroboration, oxidation and olefination sequence to provide disubstituted alkene **1.175** as a mixture of geometric isomers. Notably, this was carried out with the ethyl and not isopropyl derived Wittig reagent. This rendered the stereochemical outcome of the following epoxidation inconsequential, as concomitant tetrahydropyran formation was followed by oxidation of the resulting alcohol **1.176**, which in turn could be epimerized to equatorial ketone **1.177**. Following methylmagnesium chloride addition to the equatorial ketone **1.177**, the indole moiety was installed in four steps via the Gassman indole synthesis[80] to complete the first total synthesis of a paxilline indole diterpene in (−)-paspaline (**1.7**).

Scheme 1.4. Smith's First Generation Total Synthesis of (–)-Paspaline
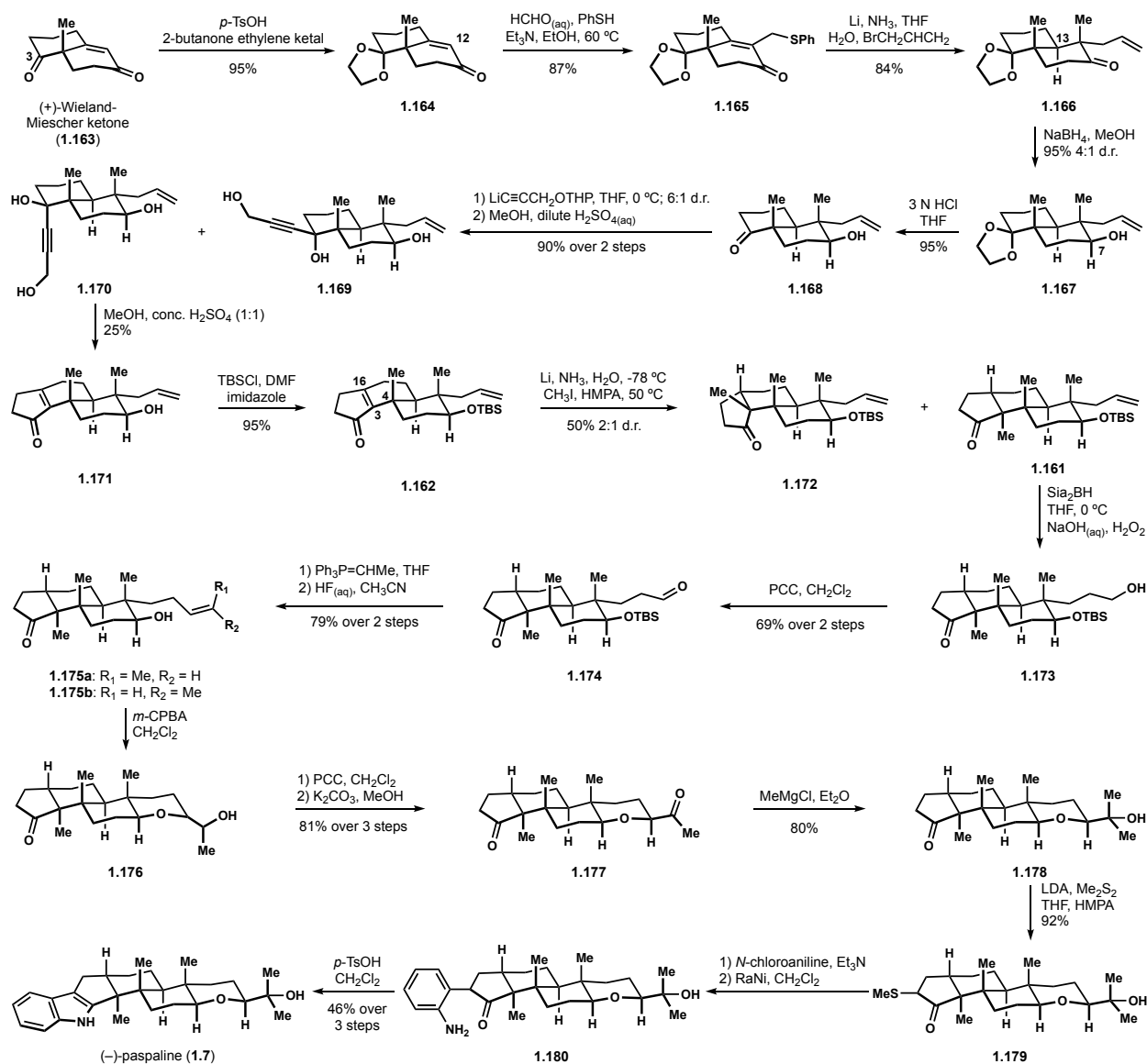
1.2.3 Amos B. Smith (III)'s Revised Approach to (–)-Paspaline

To improve upon the stereoselectivity at C3 provided by the reductive methylation strategy, Smith developed a second-generation approach towards the terpene core (Scheme 1.5).[81] A modified transketalization procedure[82] installed a ketal at C7 of (+)-Wieland–Miescher ketone to provide β,γ-unsaturated ketone **3.181**. Benzylamine condensation on the remaining C3 ketone

Scheme 1.5. Smith's Second Generation Total Synthesis of (–)-Paspaline
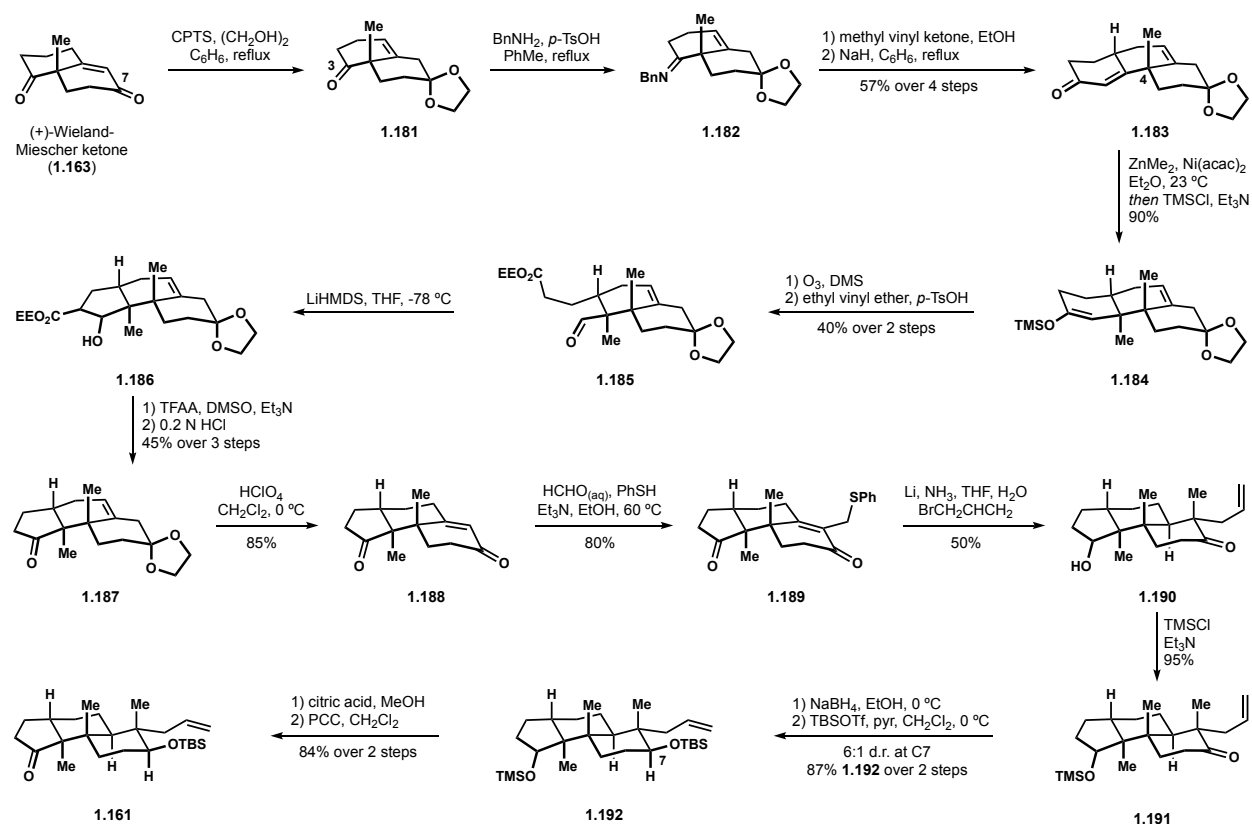
generated imine **3.182,** which was next subjected to a Robinson annulation[83], providing enone **1.183**. A nickel catalyzed conjugate addition of dimethyl zinc[84] was directed by the C4 axial methyl group to the opposite face, setting the C3 stereochemistry with complete control. The zinc enolate was subsequently trapped as the silyenol ether **1.184**. Ozonolysis of the enol and conversion of the resulting carboxylic acid to ester **1.185** provided a system to complete construction of the cyclopentanone. Aldol reaction between the ester and aldehyde of **3.185** generated the requisite cyclopentane as the *β*-hydroxy ester **1.186**. Swern oxidation of the alcohol and decarboxylation completed formation of the cyclopentanone **1.187**. Removal of the ketal generated ketoenone **1.188**, which once again successfully underwent the thioetherification, reductive allylation sequence to furnish the fully substituted, tricyclic intermediate **1.190**. Redox

and protecting group manipulations yielded key intermediate **1.161** in 18 (previously 10) steps in nearly the same overall yield owing to the improved stereocontrol.

1.2.4 Amos B. Smith (III)'s Total Syntheses of (–)-Paspalicine and (–)-Paspalinine

Following the seminal publications on paspaline, Smith directed efforts to other PID congeners containing the paxilline-type oxidation patterns. In 1990, Smith published the first total syntheses of (–)-paspalicine (**1.65**) and (–)-paspalinine (**1.66**).[85] Notably, the axial methyl substituent at C12 has been excised and the tetrahydropyran ring oxidized, which necessitated an alternative strategy in which Smith envisioned uniting enone **1.193** with epoxide **1.194** through Stork metalloenamine alkylation (Scheme 1.6).[86] Each of these fragments were readily prepared in enantioenriched form from (+)-Wieland-Miescher (**1.163**) and prenylalcohol[87] respectively. Paspalinine (**1.66**) also carries a tertiary alcohol at C13, which has proven necessary for pronounced biological activity.

Scheme 1.6 Smith's Strategy to access the Paxilline-type Core of (–)-Paspalicine and (–)-Paspalinine

	1.193	**1.194**

(+)-Wieland-Miescher ketone (**1.163**)
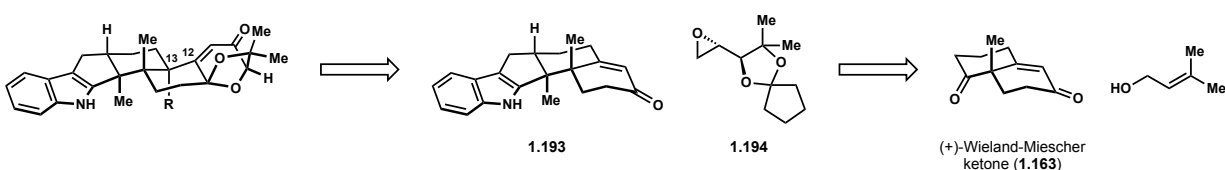
Utilizing intermediate **1.187** from the second-generation approach to paspaline (Scheme 1.4), Smith elected to carry out the four-step Gassman protocol early on to prepare indole **1.195**, thereby removing the need to protect the C2 ketone (Scheme 1.7). The diversion of routes with respect to the terpene core began with removal of the ketal on **1.195** and condensation of *N,N*-dimethylhydrazine to access hydrazone **1.195**. Alkylation with functionalized epoxide **1.194** provided secondary alcohol **1.197** that was subsequently protected as the acetate. Hydrolysis of the hydrazone restored the enone as the elaborated derivative **1.198**. Treatment with acid induced

16

Scheme 1.7 Smith's Total Synthesis of (–)-Paspalicine and (–)-Paspalinine
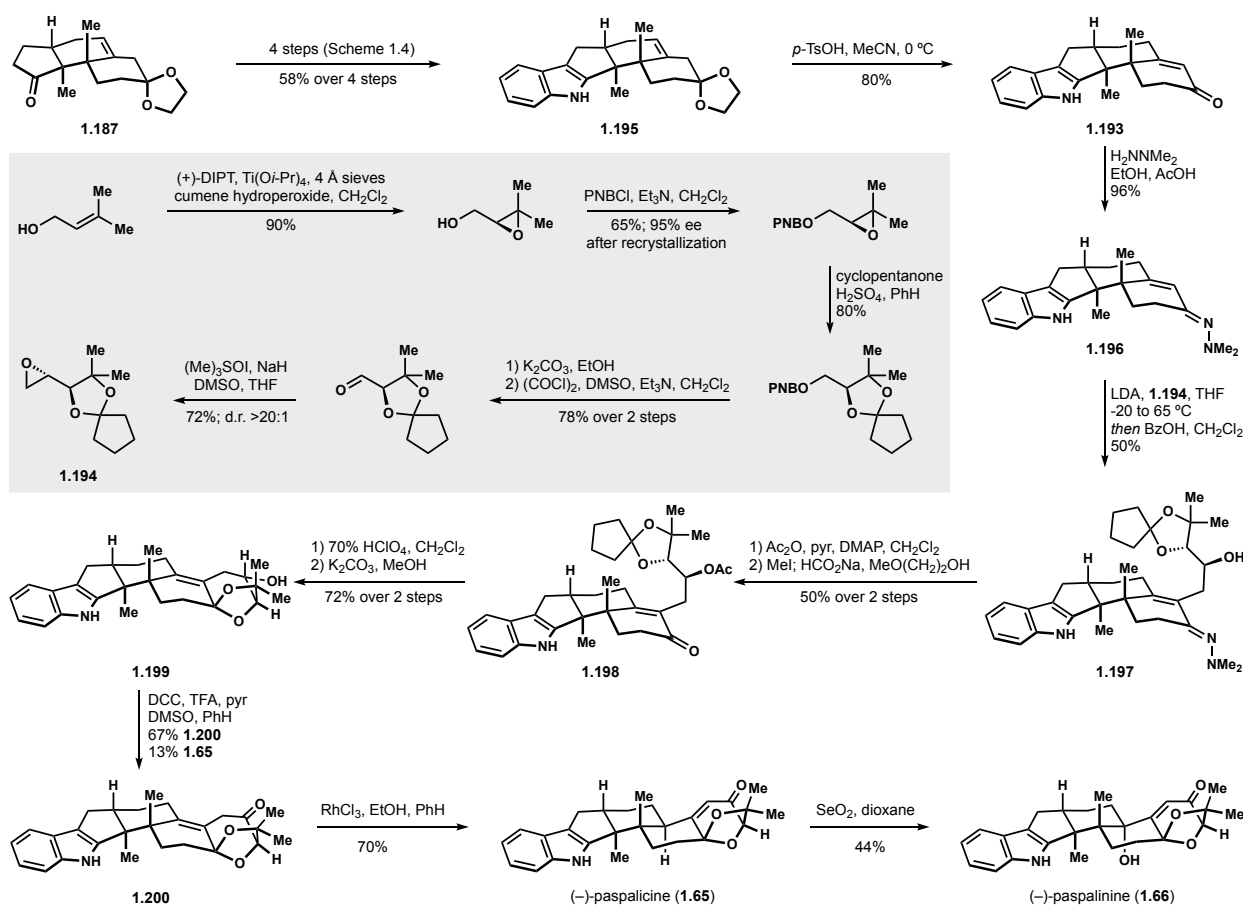
trans-ketalization to produce the requisite bridged ketal, which following removal of the acetate protecting group yielded alcohol **1.199**. Oxidation of the remaining alcohol afforded β,γ-unsaturated ketone **1.200**, along with partial formation of (–)-paspalicine (**1.65**). Grieco's rhodium(III) chloride[88] protocol to isomerize the alkene into conjugation converted the material fully into (–)-paspalicine (**1.65**). Selenium(IV) oxide accomplished the final γ-oxidation of the enone to complete (–)-paspalinine (**1.66**).

1.2.5 Amos B. Smith (III)'s Total Synthesis of (–)-Penitrem D

Smith's work on paspalinine laid the foundation for a more daunting target, (–)-penitrem D.[89] The route to the terpenoid core was substantially reworked to employ a novel method for

constructing the indole late stage. Seeking to unite *ortho*-toluidine **1.201** with lactone **1.202** utilizing a modified Madelung indole synthesis[90], these fragments became Smith's new sub targets (Scheme 1.8). The lactone **1.202** would be accessed through a Stork metalloenamine alkylation, analogous to paspalinine, between epoxide **1.203** and lactone containing enone **1.204**.

Scheme 1.8 Smith's Retrosynthetic Plan for (−)-Penitrem D

penitrem D (**1.109**)   **1.201**   **1.202**   **1.203**   **1.204**
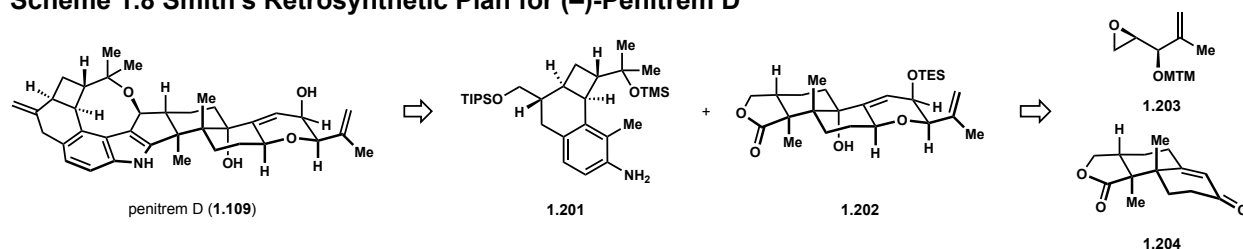
Synthesis of (−)-penitrem D began with (−)-Wieland–Miescher ketone **1.205** (Scheme 1.9).[91] *Trans*-ketalization protected the C22 ketone (penitrem D numbering) and the enone was subsequently deprotonated at the γ-position and trapped as silylenol ether **1.207**. Functionalization at the γ-position with dithiane **1.208** was followed by 1,2-reduction of enone **1.209** from the convex face to yield allylic alcohol **1.210**, which was subsequently protected as the acetate **1.211**. The dithiane was removed and the resulting aldehyde **1.212** reduced and protected as silyl ether **1.214**. Removal of the acetate from **1.214** provided allylic alcohol **1.215**, to which Smith applied a tactic from Saxton's approach to paspalicine (*vide infra*)[92], utilizing the alcohol to direct cyclopropanation[93] of the alkene on the concave face and provide cyclopropane **1.216**. Oxidation of the alcohol reintroduced the carbonyl as **1.217**, which under dissolving metal conditions induced fragmentation of the cyclopropane to install the C32 methyl group.[94] Quenching the reductive fragmentation reaction with Comins' reagent[95] to trap the enolate in situ delivered vinyl triflate **1.218**. Coupling with a Gilman reagent produced methyl substituted cyclohexene **1.219** that was oxidatively cleaved to ketoacid **1.220**. Refluxing the highly-functionalized cyclohexane **1.220** in acidic media induced desilylation of the primary alcohol and subsequent lactonization with the

18

Scheme 1.9 Synthesis of an Enone Subtarget for the Penitrems
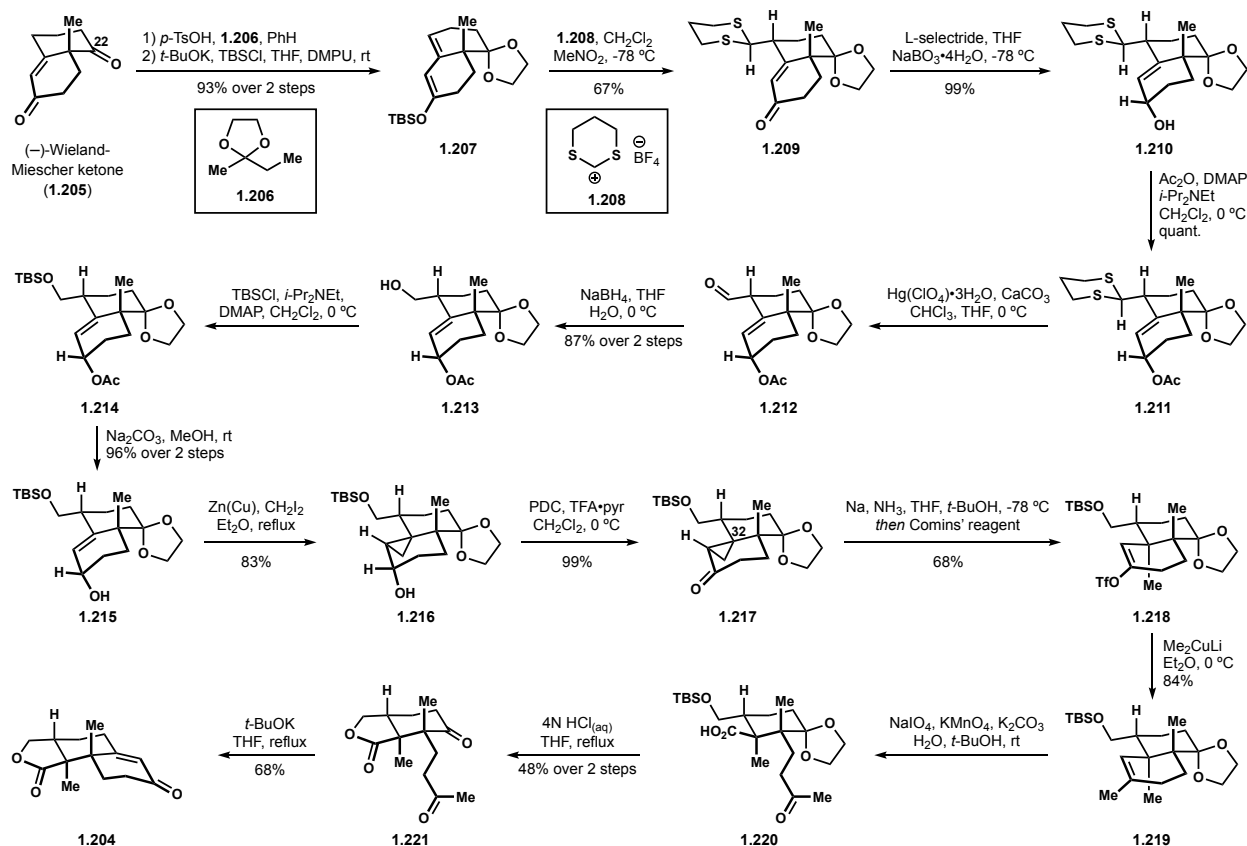
acid, as well as hydrolysis of the ketal to afford diketolactone **1.221**. Treatment with potassium

tert-butoxide instigated an aldol condensation between the two ketones, constructing the tricyclic

enone **1.204** for metalloenamine alkylation.

Before further elaborating enone **1.204**, the ketone was protected as ketal **1.222**, allowing

selective reduction of the lactone to provide an inconsequential mixture of lactol **1.223**

diastereomers (Scheme 1.10). Treatment of the lactol with methanolic acid converted the substrate

to a mixed acetal and coincided with removal of the ketal to deliver enone **1.224**. The purpose of

converting the lactone to the acetal was to avoid compatability issues between a lactone and

metalloenamine conditions. The acetals α-**1.223** and β-**1.223** were separated and each

diastereomer was converted to hydrazone **1.225** before being carried through the alkylation

protocol with epoxide **1.203** to deliver alcohols α-**1.227** and β-**1.227**. The alcohols were protected

19

Scheme 1.10 Elaboration of Enone 1.204 to the Coupling Fragment
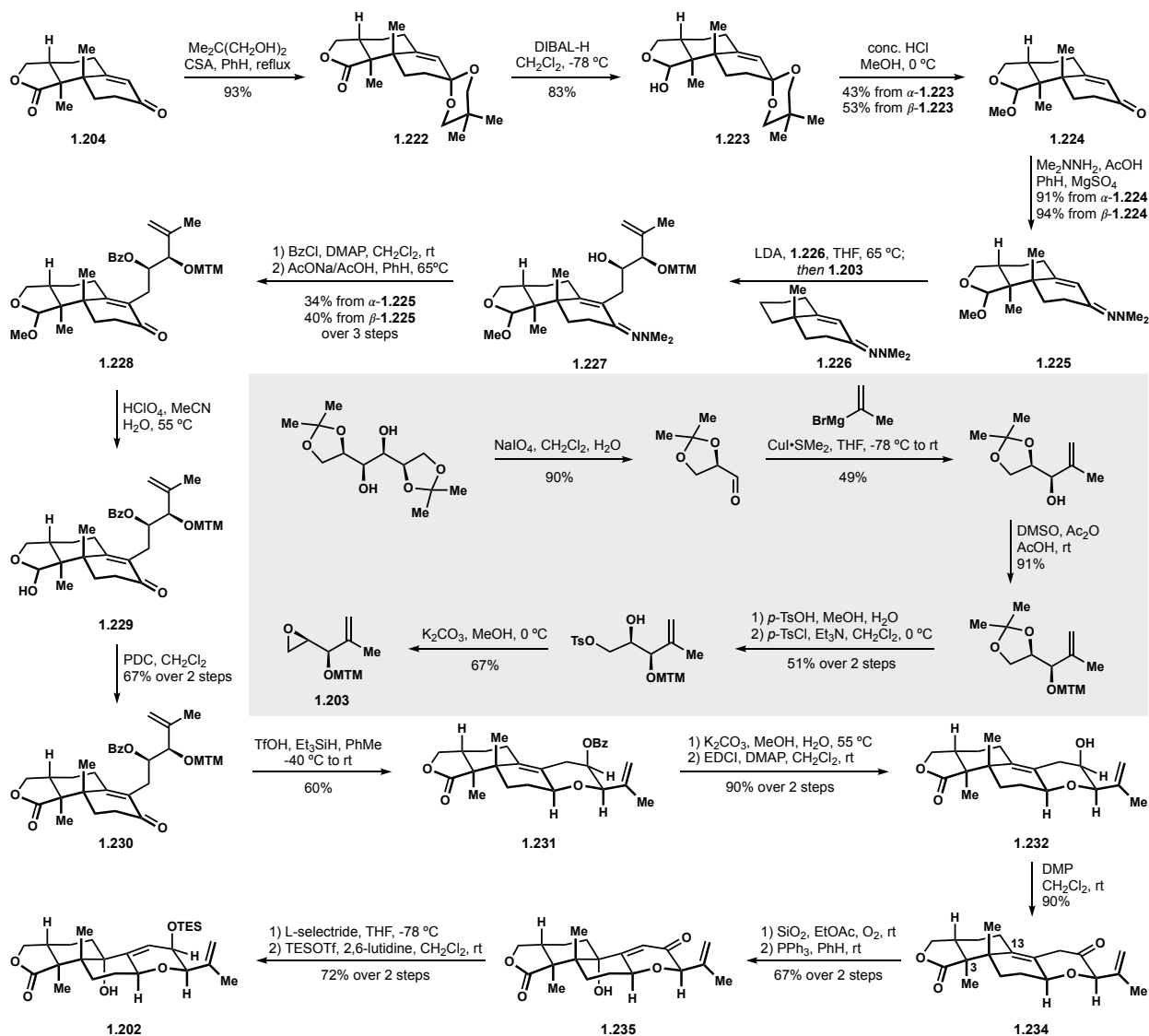
as the benzoates and the hydrazone next removed to provide enones α-**1.228** and β-**1.228**, at which

point the diastereomers were recombined. The acetals of α-**1.228** and β-**1.228** were converted back

to the lactone oxidation state over two steps to deliver the proper coupling handle in lactone **2.230**.

Treatment of **2.30** with triflic acid and triethylsilane, a modification to Nicolaou's protocol[96],

induced a cascade beginning with removal of the methylthioether, permitting reductive

condensation of the resulting alcohol onto the enone carbonyl to form the *cis*-pyran **1.231**,

proceeding with high levels of stereocontrol. Removal of the benzoate protecting group resulted

20

in partial hydrolysis of the lactone, necessitating treatment with EDCI to recover tetracycle **1.232**. Smith extensively studied photooxidations of alkene **1.232** to no avail. Based on comparisons with model studies, it was evident the C3 methyl group dissuaded approach by singlet oxygen. Nonetheless, upon oxidation to ketone **2.134**, Smith ultimately found that mild enolizing conditions in an oxygen atmosphere led to oxidation of the desired face at C13 as desired. Further optimization meant the Grieco alkene isomerization-selenium oxidation sequence could be replaced, providing efficient access to hydroxy enone **1.235** after reduction of the peroxide intermediate. A brief screen of reductants identified L-selectride as a competent hydride source to deliver complete diastereoselectivity for 1,2-reduction of enone **1.235**, which was subsequently protected as the silyl ether, completing the eastern fragment **1.202** for coupling.

With respect to the western hemisphere of (–)-penitrem D,[97] dihydroresorcinol methyl ether **1.236** was alkylated with BOMCl and the ketoenol ether **1.237** dehydrated by reduction and elimination (Scheme 1.11). Hydrogenation of the resulting enone provided meso ketone **1.238**. Smith procured enantioenriched material from this substrate via deprotonation of ketone **1.238** with lithiated chiral amine **1.239**.[98] The resulting enolate was trapped as the silyl enol ether **1.240** and then oxidized to enone **1.241** under Schenk-ene conditions.[99] With enantioenriched material at hand, a key [2+2] photocycloaddition between the enone **1.241** and methyl acrylate was directed anti to the benzyl ether group and with high regioselectivity to produce cyclobutane **1.242**.[100] Smith noted that material was primarily lost as the C14 epimer and that attempts to epimerize crude material led to diminished overall yields. Moving forward, the ketone of **1.242** was interconverted to the dimethylacetal **1.243**, allowing for two equivalents of methylmagnesium bromide to be added to the ester and deliver tertiary alcohol **1.244**. Following protection of this

Scheme 1.11 Synthesis of Aniline Coupling Fragment 1.201 for (–)-Penitrem D
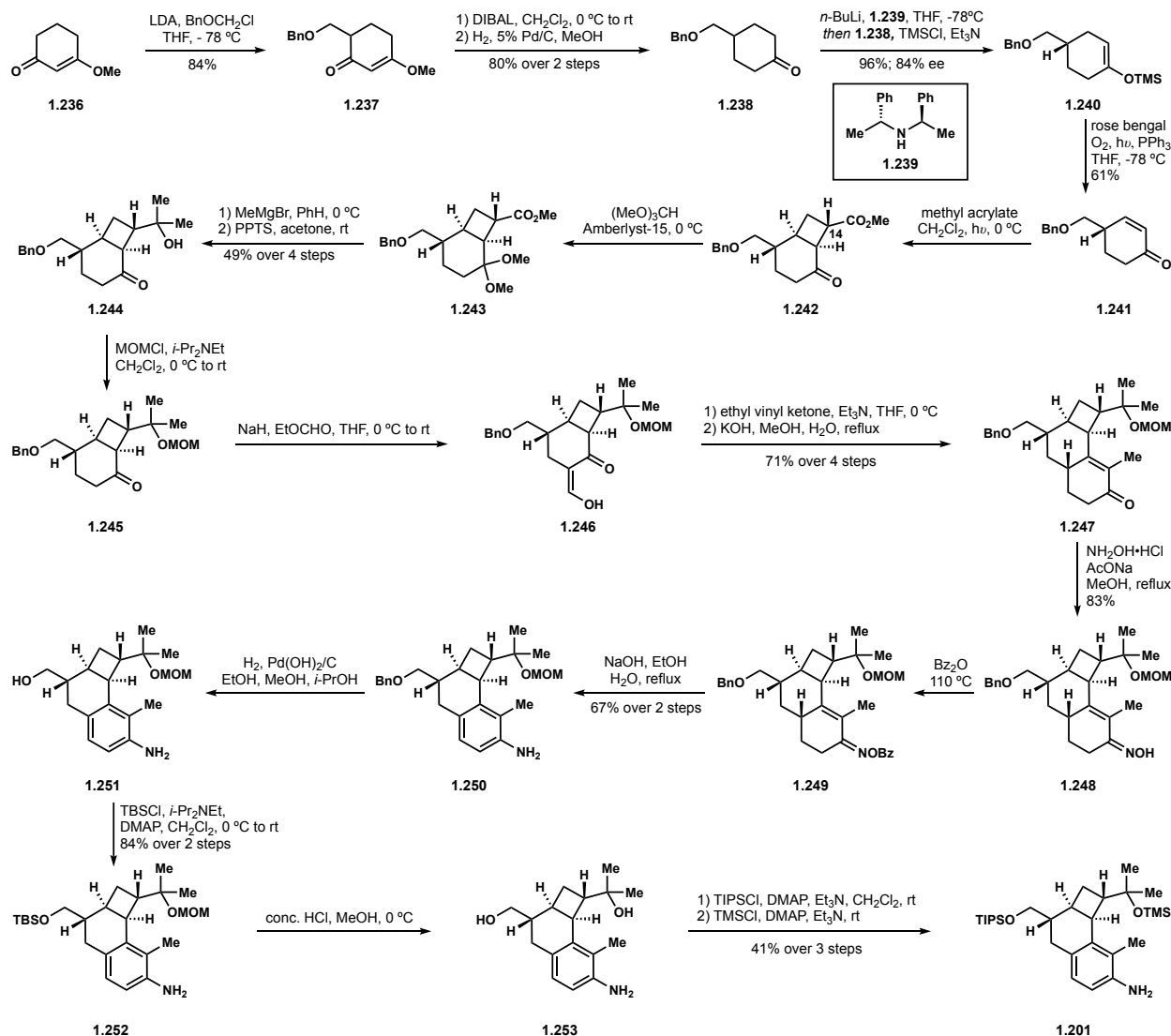
alcohol, construction of the D ring commenced. A three-step modified Robinson annulation installed the carbon framework in the form of enone **1.247**.[101] Following condensation of hydroxylamine to form oxime **1.248**, a modified Semmler–Wolff reaction[102] sequence aromatized the system to provide *ortho*-toluidine **1.250**. The benzyl protecting group was converted to silyl ether **1.252**, as the envisioned late stage intermediates contained alkenes susceptible to hydrogenation. Additionally, Smith predicted the MOM group would be a liability as it would require harsher conditions to remove. Deprotection of MOM ether **1.252** did coincide with loss of

the TBS group of the primary alcohol. TIPS and TMS protection of the primary and secondary alcohols respectively completed assembly of the western coupling fragment **1.201** of (–)-penitrem D.

With coupling partners **1.201** and **1.202** in hand, Smith employed the dianion addition between the two fragments (Scheme 1.12). The order of operations for this sequence was critical. The *ortho*-toluidine **1.201** was deprotonated once with *n*-butyllithium and then silylated. A second equivalent of *n*-butyllithium was added to deprotonate the aniline again, followed by *sec*-butyllithium to deprotonate the *ortho*-methyl group and generate the dianion. Finally, adding lactone **1.202** to the reaction mixture saw addition of the carbanion to the lactone, leading to ketoaniline **1.254**. While this transformation is remarkable with respect to complexity of fragments united, the procedure did require 12 equivalents of *ortho*-toluidine relative to lactone **1.202**. Nonetheless, treatment with silica gel induced condensation to form the indole nucleus and Parikh–Doering conditions[103] oxidized the primary alcohol to deliver indole aldehyde **1.255**. Acidic deprotection of the more labile silyl ethers allowed for treatment with scandium(III) triflate to induce a cascade of condensations to form the F ring as well as the oxocane A ring. The secondary allylic alcohol of the eastern hemisphere was next esterified and the TIPS group on the other end of the molecule removed to provide primary alcohol **1.257**. These protecting group manipulations allowed for selenation of the primary alcohol[104], which was eliminated to provide exocyclic alkene **1.259**. Deacetylation of the remaining alcohol completed the monumental synthesis of (–)-penitrem D (**1.209**), a feat that has not yet been matched.

Scheme 1.12 Fragment Union and Synthesis of (–)-Penitrem D
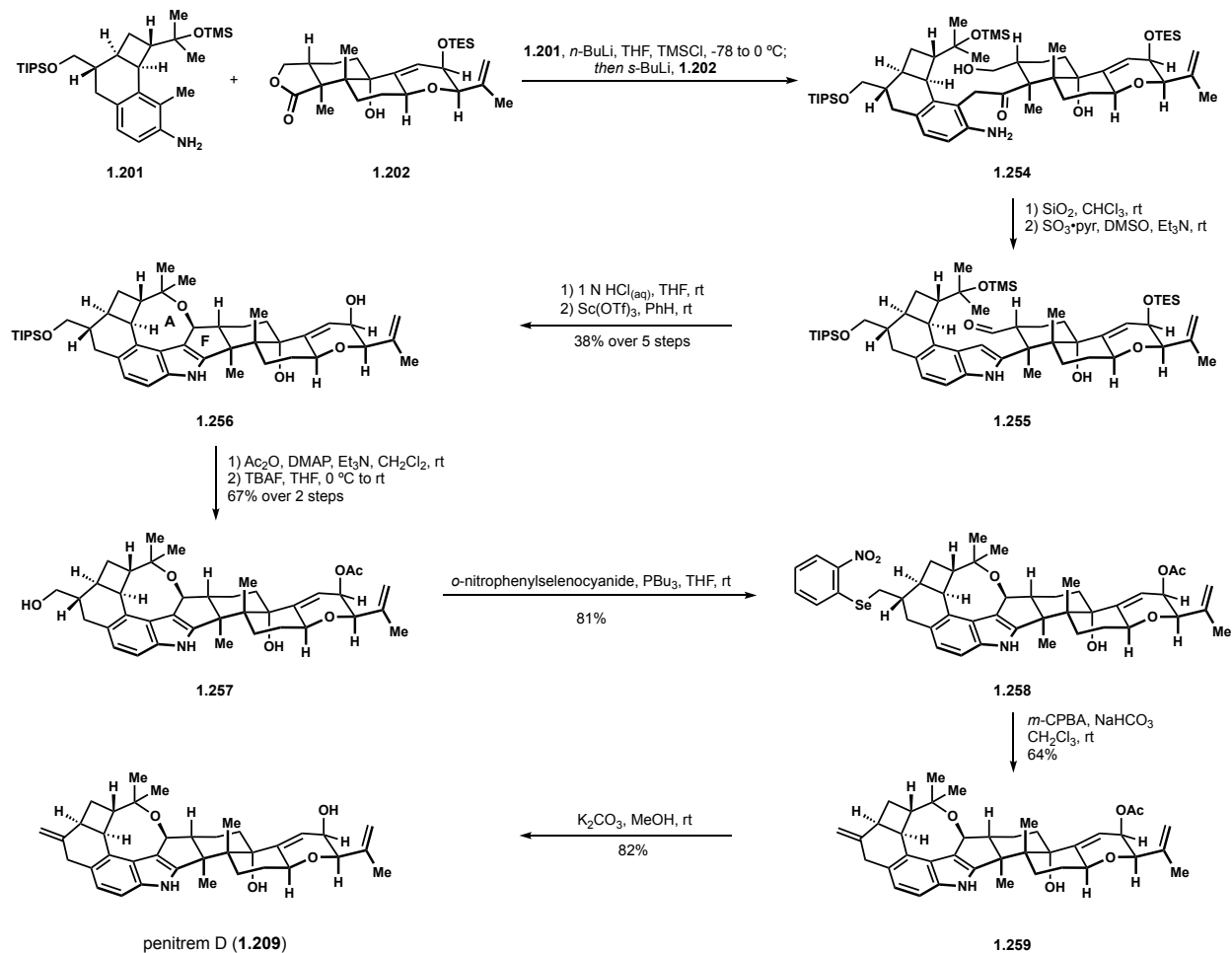
1.2.6 Amos B. Smith (III)'s Total Syntheses of (–)-21-Isopentenylpaxilline

Smith utilized a similar strategy used for (–)-penitrem D (**1.109**) to access (–)-21-isopentenylpaxilline (**1.22**).[105] Smith used this target to explore installation of alternative oxidation patterns found throughout the PIDs and improved the efficiency of the route, illustrated in Scheme 2.13. Hydrazone **1.224** was alkylated with a modified epoxide **1.260** to provide the oxidized chain as alcohol **1.261**. Protection of the alcohol as the benzoate was followed with removal of the hydrazone to restore the enone and provide protected triol **1.262**. The methyl acetal was reverted to the lactol **1.264** and oxidized back to lactone **1.265** before inducing methylthioether deprotection and reductive condensation to *cis*-pyran **1.266**. The tetrasubstituted alkene was oxidized with *m*-

Scheme 1.13 Smith's Total Synthesis of (–)-21-Isopentenylpaxilline
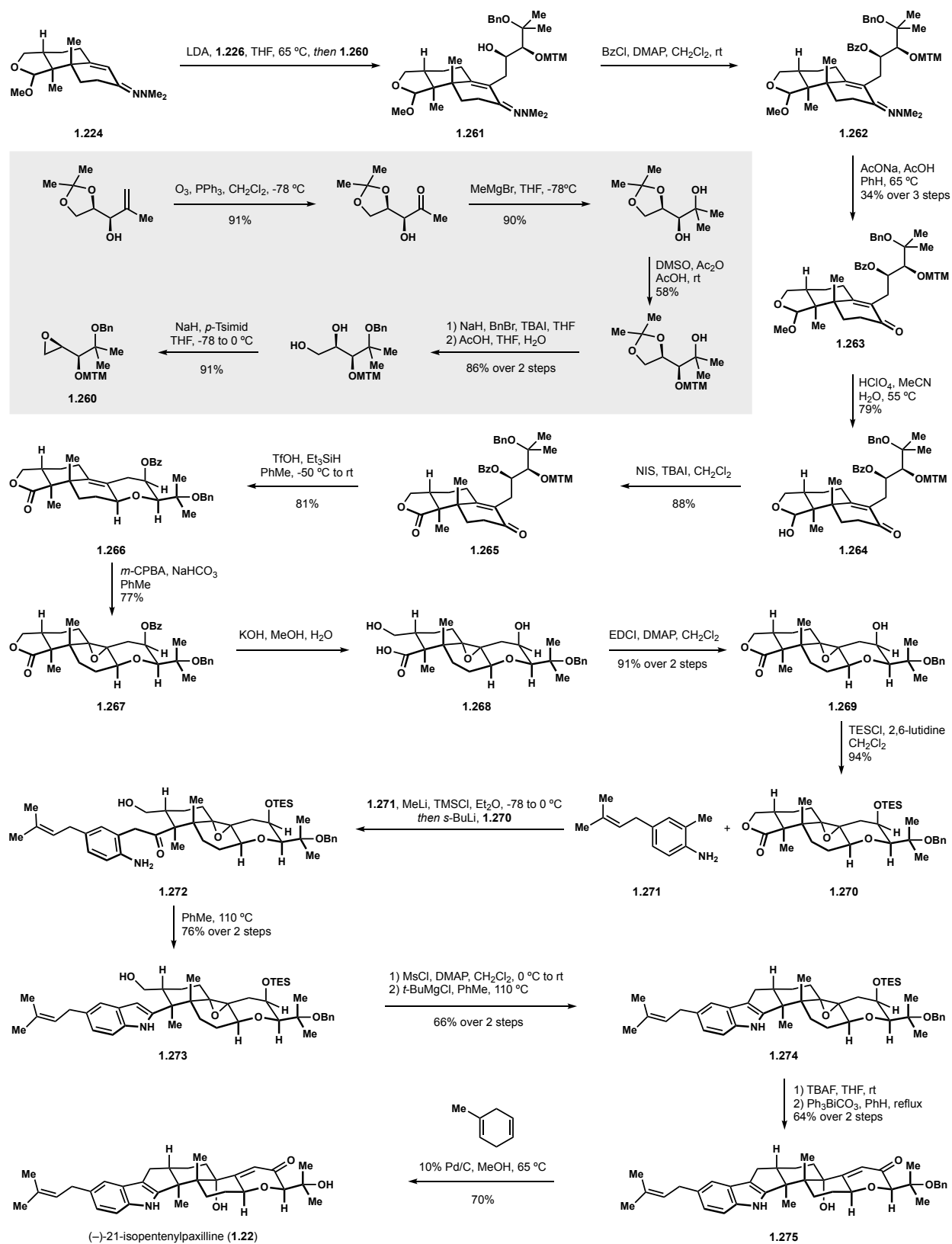
CPBA, *anti* to the C3 axial methyl group, to provide α-epoxide **1.267**. Removal of the benzoate coincided with partial hydrolysis of the lactone. As such, treating hydroxy acid **1.268** with EDCI regenerated lactone **1.269** and the alcohol was reprotected with a more labile TES group, completing the synthesis of coupling fragment **1.270**. Utilizing the modified Madelung indole synthesis previously developed for penitrem D (*vide supra*), *ortho*-toluidine **1.271** and lactone **1.270** were united to construct indole **1.274** in four steps. Following removal of the TES group, Smith utilized a very mild oxidation developed by Barton[106], notably tolerant of indoles, to carry out tandem oxidation-epoxide fragmentation to afford γ-hydroxyenone **1.275**. Lastly, removal of the benzyl group required optimization to avoid hydrogenation of the prenyl substituent. Transfer hydrogenation proved to be the most successful, yielding only minor amounts of the over reduced material and completing the synthesis of (−)-21-isopentenylpaxilline (**1.22**).

1.2.7 Amos B. Smith (III)'s Biomimetic Synthesis of (+)-Emindole SA

Following completion of penitrem D, Smith released the first study towards a PID that did not rely on Wieland–Miesher ketone as an initiation point. Smith instead explored the viability of a biomimetic polyene cyclization as an alternative way to construct the terpene core, demonstrating the utility in a synthesis of (+)-emindole SA (**1.143**, Scheme 1.14).[107] *trans,trans*-Farnesyl acetate was converted to sulfone **1.276** according to Kato's protocol in five steps.[108] The allylic alcohol was then converted to the bromide and used to alkylate indole[109] to provide indole triene **1.277**. The sulfone was then alkylated with epoxyiodide **1.279**[110] and the sulfones subsequently reduced off, necessitating protection of the indole once more to provide polyene **1.281**. Treatment of the epoxide with a Lewis acid induced the polyene cyclization to provide a modest yield of exocyclic alkene and a substantial (~50%) quantity of presumed alkene isomers. Nonetheless, reduction of

Scheme 1.14 Smith's Biomimmetic Synthesis of (+)-Emindole SA

the desired isomer completed a concise synthesis of emindole SA (**1.143**). In contrast to the biosynthetic pathway to emindole SB, the polyene cyclization did not proceed with *anti*-Markovnikov selectivity of the terminal alkene (Scheme 1.2), underscoring the need for novel approaches to access the more elaborate terpene ring systems efficiently.

1.2.8 Masato Oikawa's Approach to (–)-Terpendole E

Masato Oikawa also published an approach utilizing a polyene cascade to access (–)-terpendole E.[111] While the strategy remains incomplete, Oikawa developed a facile approach to the tetrahydropyran ring and disclosed valuable insight for stereoselective installation of the C11 hydroxyl group (terpendole E numbering, Scheme 1.15). To access the polycyclization precursor, Sharpless allylic oxidation[87,112] of *trans,trans*-farnesyl acetate was followed by asymmetric epoxidation of the resultant alcohol to afford epoxyalcohol **1.283**. After TBS protection of the alcohol, treatment of epoxy diene **1.284** with titanocene dichloride and Zinc initiated a reasonably efficient cyclization, terminated by elimination to yield *trans*-decalin **1.285** in merely four steps. PMB protection of the secondary alcohol followed by desilylation and oxidation of the primary

Scheme 1.15 Oikawa's Approach to the Terpenoid Core of (–)-Terpendole E
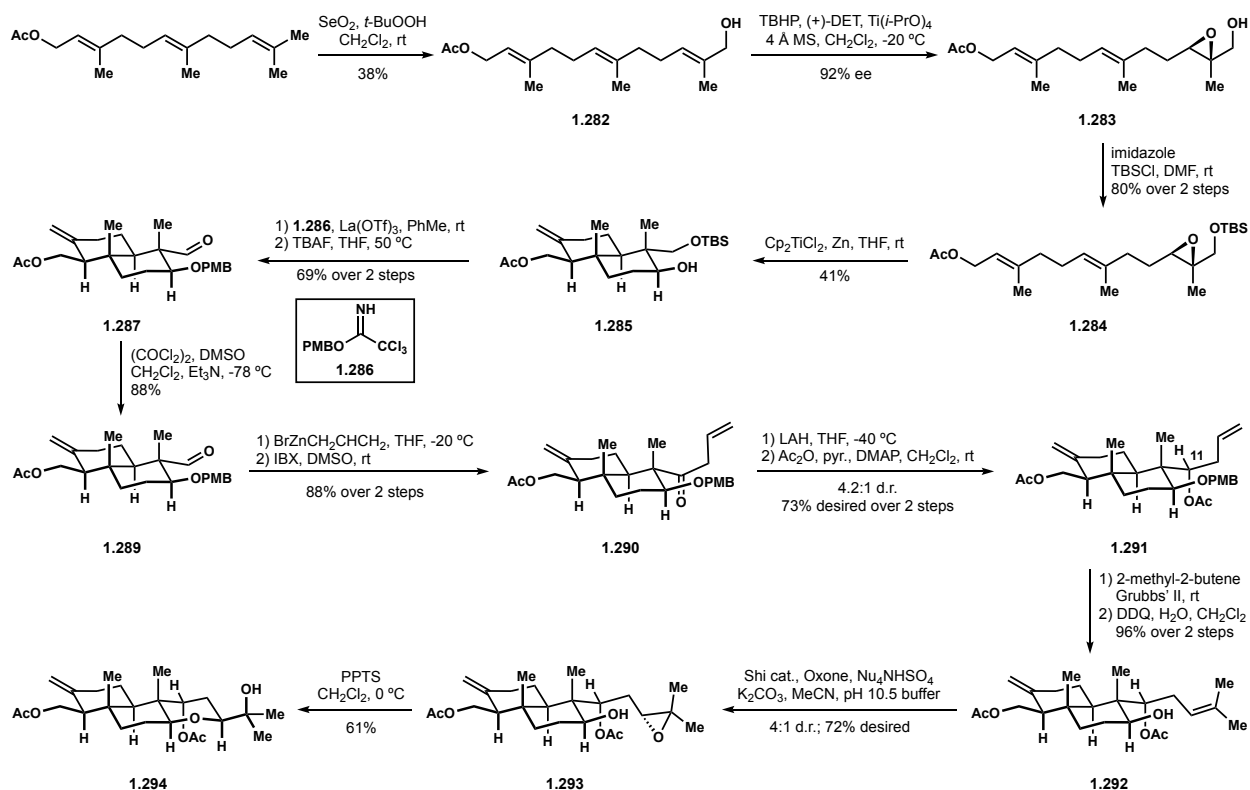
alcohol provided protected hydroxy aldehyde **1.287**, a notable moiety seen in several future studies (*vide infra*). Oikawa extensively studied prenylations and allylations of aldehyde **1.287**[113], which failed to proceed with any appreciable level of stereocontrol in the desired sense. Oikawa conceded and made use of the high yield obtained with allyl zinc bromide to access a diasteromeric mixture of homoallylic alcohols. Following oxidation of the alcohol[114], the resulting ketone **1.290** could be reduced in an appreciable 4.2:1 ratio favouring the desired α-alcohol at C11, that was subsequently protected as acetate **1.291**. Cross metathesis[115] with 2-methyl-2-butene and PMB removal provided trisubstituted alkenyl alcohol **1.292**. Shi epoxidation[116] of the alkene provided modest levels of diastereoselectivity, but high yields of **1.293** were nonetheless obtained. Treatment with PPTS then catalyzed epoxide opening to yield the *cis*-tetrahydropyran and eastern hemisphere derivative of terpendole E **1.294**.

1.2.9 J. Edwin Saxton's Approach to Paspalicine

Around the time Smith published his work on paspalicine and paspalinine, Saxton reported incomplete strategies to both the ketal containing ring and installation of the vicinal quaternary carbons at C2 and C3 (Scheme 1.16).[117] Following Smith's lead, Saxton began with Wieland–Miesher ketone and protected the C2 carbonyl as ketal **1.164**. Reductive allylation of the enone provided alkene **1.295**, which was converted to furan **1.296** via ozonolysis of the alkene and treatment with an acetic acid-acetic anhydride mixture. Vilsmeier–Haack formylation provided furaldehyde **1.297**, which was subjected to a Wittig reaction to provide trisubstituted alkene **1.298**. Dihydroxylation of the alkene produced a 1:1 mixture of diastereomeric diols **1.29**. These intermediates set the stage for Saxton's key transformation, an Achmatowicz reaction[118] that transformed the furan into the dihydropyanone, isolated as the hemiacetals **1.300** and **1.301**. Dehydration induced by tosic acid converted both hemiacetals to their respective ketal diastereomers **1.302** and **1.303**. Inherently, the absence of selectivity in the dihydroxylation is a drawback, however, if a similar substrate was procured in a diastereoselective manner, Saxton's strategy could be rendered very efficient.

Scheme 1.16 Saxton's Approach to the Dihydropyranone

29
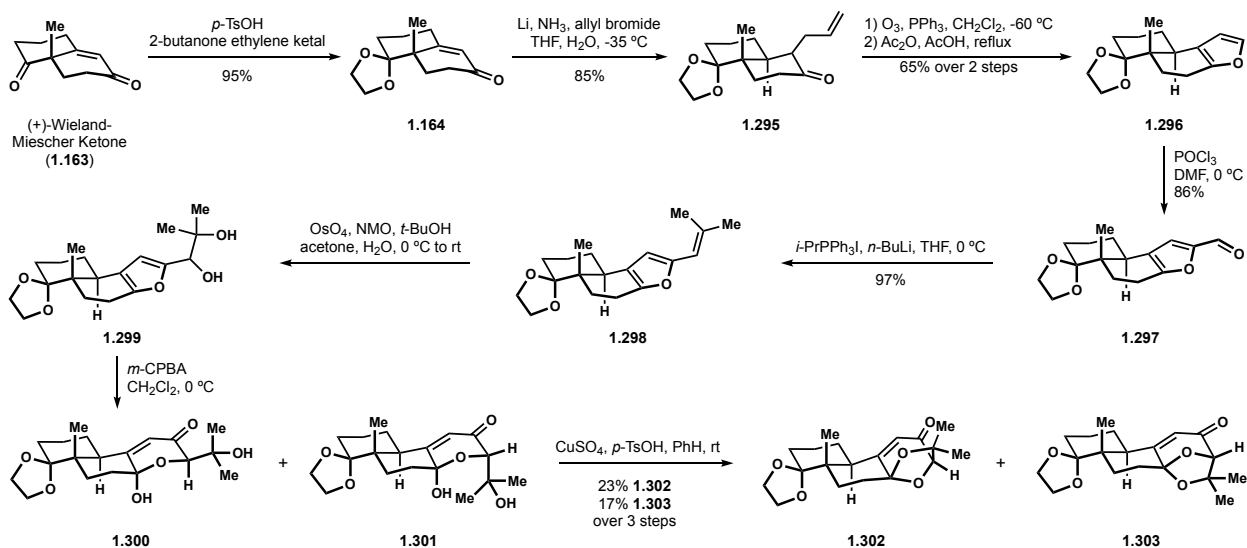
In a separate report[92], Saxton also disclosed a straightforward approach to an adequately

functionalized tricycle with respect to the hydrindane ring system. Beginning with Wieland–

Miesher ketone derivative **1.181** (Scheme 1.5), alkylation with propynyl phosphonate[119] was

followed with hydration of the alkyne in the presence of mercury(II) chloride to provide β-

ketophosphonate **1.305** (Scheme 1.17). Intramolecular Horner–Wadsworth–Emmons reaction

delivered cyclopentenone **1.306**, that underwent diastereoselective 1,2-reduction to allylic alcohol

1.307. This alcohol then successfully directed a Simmons–Smith cyclopropanation to the concave

face of the cyclopentene, as first demonstrated by Corey[120], to provide cyclopropane **1.308**.

Finally, re-oxidation of the alcohol and reduction of the ketone fragmented the cyclopropane to

the axial methyl group at C3 and afforded cyclopentanone **1.309**. While Saxton did not complete

a total synthesis of paspalicine of any other PID, it should be recognized that his contributions

were utilized by others to do so, demonstrating the impact of his work.

Scheme 1.17 Saxton's Approach to the *trans*-Hydrindane Ring System
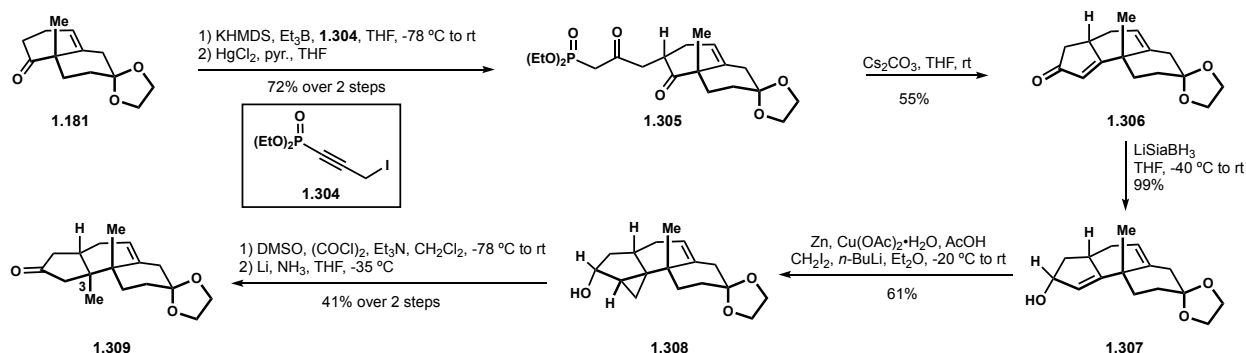
1.2.10 Shigefumi Kuwahara's Total Synthesis of (–)-Paspalinine

Saxton never unified his strategies to complete a total synthesis of (–)-paspalinine or (–)-

paspalicine. Shigefumi Kuwahara ultimately utilized Saxton's approach to finally lend it credence

with a successful synthesis of paspalinine.[121] Kuwahara prepared the cyclopropane intermediate

Scheme 1.18 Kuwahara's Total Synthesis of (–)-Paspalinine
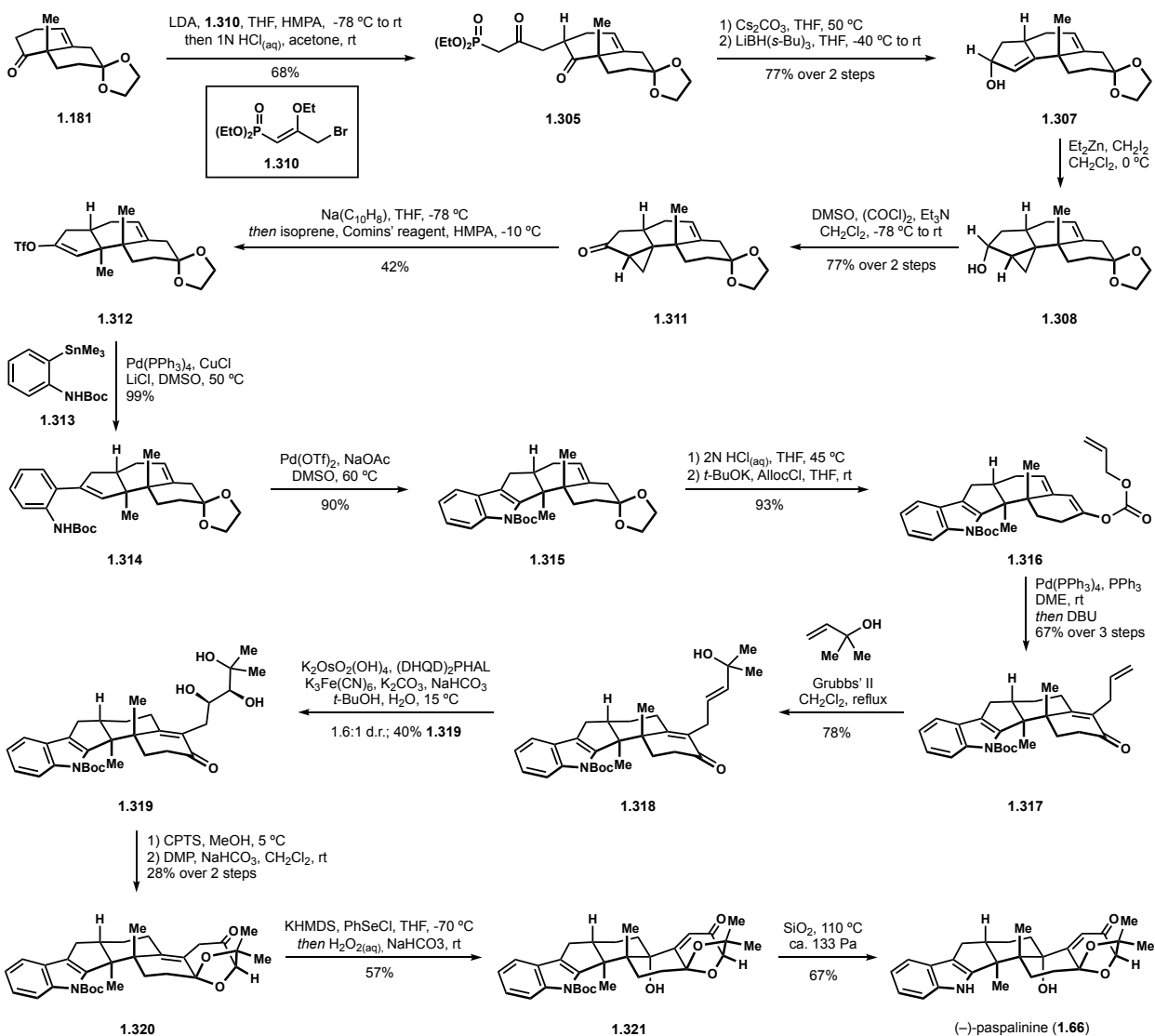
1.311 in near identical fashion to Saxton, only slightly modifying procedures (Scheme 1.18).

Kuwahara also utilized Smith's protocol for cyclopropane fragmentation and *in situ* trapping of

the enolate as the vinyl triflate **1.312**, thus the fragment was immediately available for elaboration.

Stille coupling with stannylated *N*-Boc aniline (**1.313**) afforded the styrenyl aniline **1.314**, which

then underwent intramolecular Heck type cyclization[122] to produce the Boc protected indole **1.315**.

With Saxton's strategy successfully employed to provide the pentacyclic intermediate, Kuwahara

moved to the dihydropyranone ring, where he developed a novel approach. Removal of the ketal

from **1.315** was followed with conversion of the enone to allyl carbonate **1.316**. Tsuji–Trost allylation[123] and alkene isomerisation provided substituted enone **1.317**. Cross metathesis with 2-methyl-3-buten-2-ol provided allylic alcohol **1.318**.[124] Sharpless' asymmetric dihydroxylation conditions yielded a poor diastereomeric ratio of diol **1.319** products from alkene **1.318**.[125] Pushing forward the appropriate diastereomer, condensation of the diol onto the ketone generated the ketal and oxidation of the remaining free alcohol afforded the β,γ-unsaturated ketone **1/320**. Kuwahara then developed an alternative oxidation protocol to Smith's by generating the α-selenyl ether and treating the intermediate with hydroperoxide to induce a 2,3-rearrangement[126] to efficiently access γ-hydroxy enone **1.321**. Removal of the Boc protecting group with silica gel at elevated temperatures completed the synthesis of (–)-paspalinine (**1.66**).

1.2.11 Shigefumi Kuwahara's Total Synthesis of (±)-Lecanindole D

Kuwahara utilized the directed cyclopropanation strategy to access additional congers such as indole sesquiterpenoid (±)-lecanindole D (Scheme 1.19).[127] With the advanced cyclopropane intermediate **1.308**, Kuwahara benzyl protected the alcohol and removed the ketal protecting group. Double α-methylation of the enone **1.322** left β,γ-unsaturated ketone **1.323**. Reduction with L-selectride slightly favoured the pseudo-axial alcohol **1.324**. Presence of this alcohol likely aided in directing the following epoxidation to the concave face, which was opened with lithium aluminium hydride to install the C9 hydroxyl group (lecanindole D numbering) and provide diol **1.325**. Notably, this provides an alternative oxidation sequence that could be applied to other PID congeners. Orthogonal protection of the C6 alcohol allowed for deprotection and oxidation of the cyclopentanol **1.326**. This intermediate allowed Kuwahara to employ the rest of the endgame

Scheme 1.19 Kuwahara's Total Synthesis of (±)-Lecanindole D
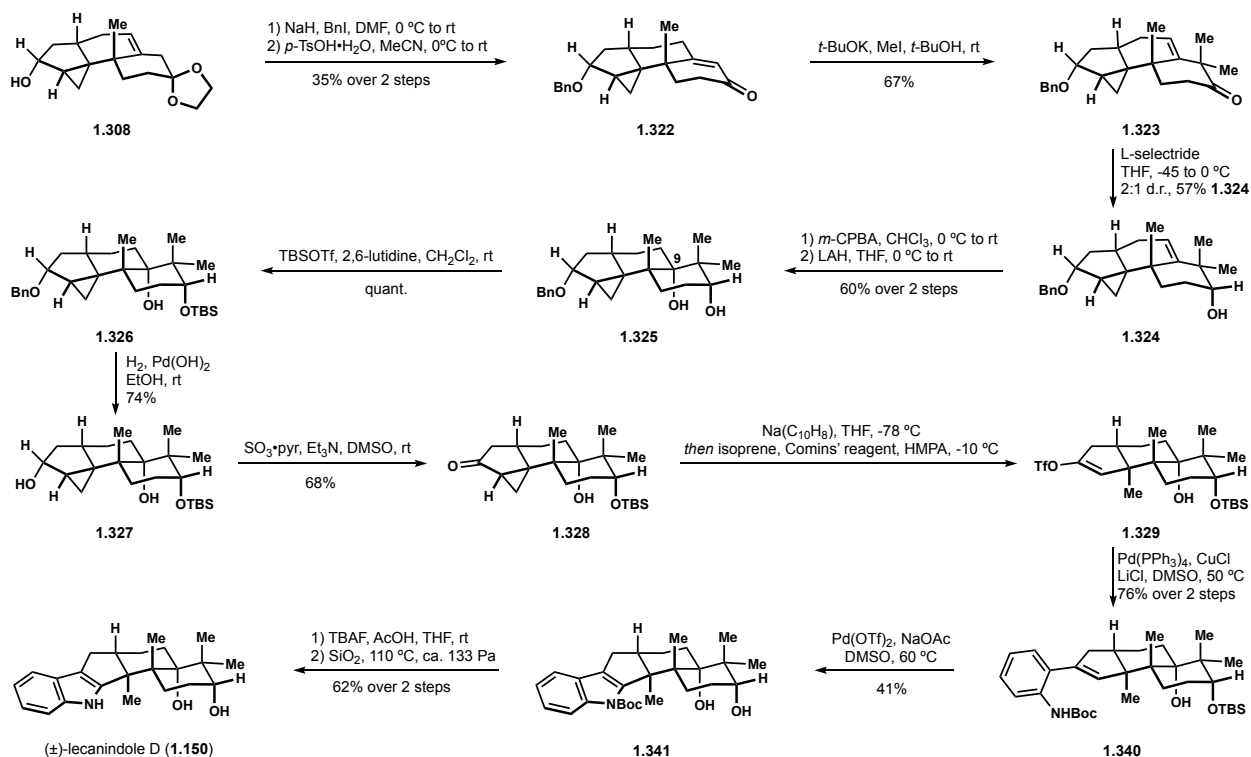
developed for paspalinine to incorporate the indole and effect global deprotection to access (±)-lecanindole (**1.150**) in five additional steps.

1.2.12 Shigefumi Kuwahara's Total Synthesis of (±)-Terpendole E

Kuwahara ultimately capitalized on the allylation studied by Oikawa (*vide supra*) and combined the findings with his own work to complete a synthesis of (±)-terpendole E (Scheme 1.20).[128] Reductive carboxylation of Wieland–Miesher type enone **1.342**[129] efficiently provided ketoester **1.343**. Reduction of the ketone and PMB protection of the resulting secondary alcohol was followed with conversion of the ester to the requisite aldehyde **3.146**. Following a slightly modified allylation procedure of Oikawa's[111], Kuwahara produced the mixture of homoallylic alcohols **3.147** and **3.148** in high yield. Material could be recycled by converting **3.147** to the desired stereoisomer **3.148** as reported by Oikawa. Protection of alcohol **3.148** as MOM ether

Scheme 1.20 Kuwahara's Total Synthesis of (±)-Terpendole E
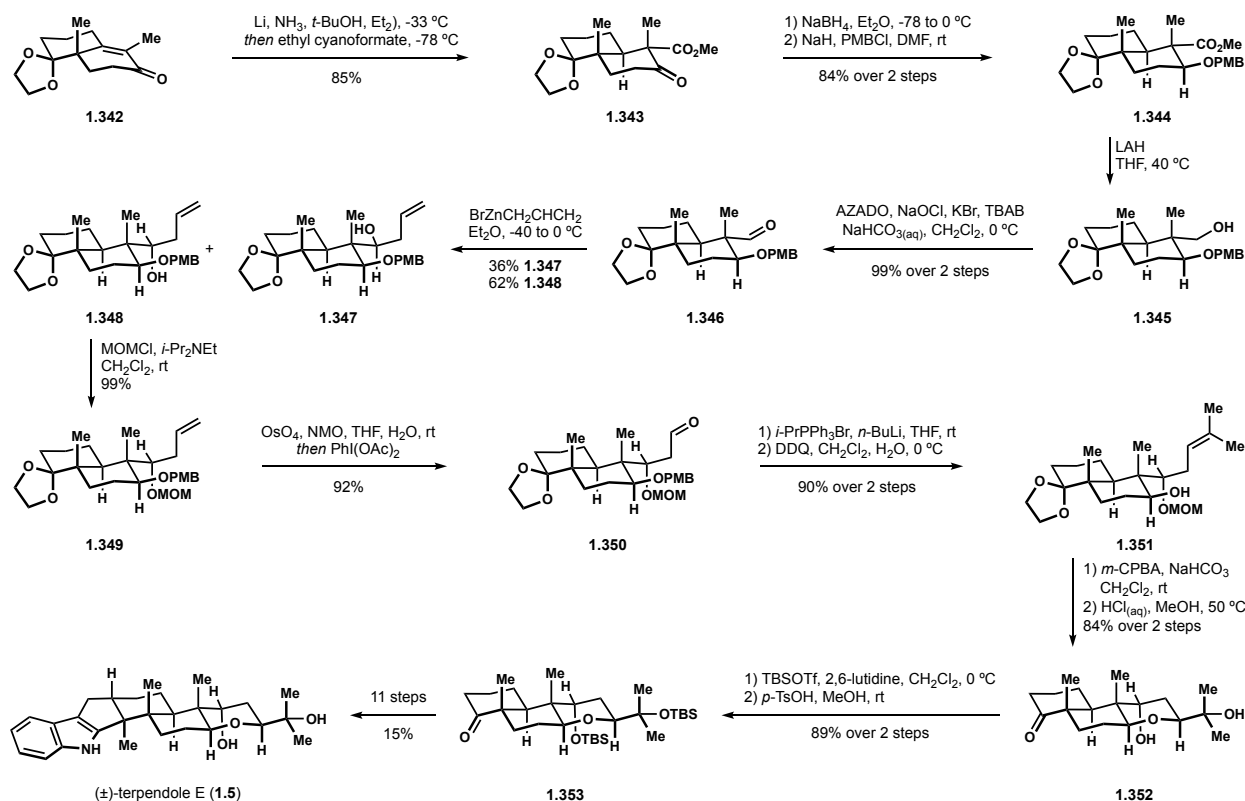
3.149 was followed by ozonolysis of the alkene and Wittig reaction of aldehyde **3.150** to homoprenylalcohol derivative **3.151**. Epoxidation of the alkene with *m*-CPBA not only proceeded with high diastereoselectivity, but was immediately followed by epoxide opening to *cis*-pyran with high efficiency. The observed selectivity in the epoxidation, presumably directed by the alcohol, could be of great use to future synthetic endeavours. This result rendered use of chiral catalysts as Oikawa had used (Scheme 1.15), or the four-step sequence utilized by Smith in his synthesis of paspaline (Scheme 1.4) unnecessary for this transformation. Removal of the ketal and MOM ether afforded ketodiol **1.352** and global silylation was followed by selective hydrolysis of the silylenol ether to afford ketone **3.153**. At this stage, Kuwahara employed the 11-step sequence optimized for (−)-paspalinine (**1.66**) and (±)-lecanindole D (**1.150**) to complete the first synthesis of (±)-terpendole E (**1.5**).

34

1.2.13 Athanassios Giannis' Synthesis of (+)-16-*epi*-Terpendole E

In 2010, Athanessios Giannis published a thwarted attempt towards (−)-terpendole E (**1.5**).[130] His approach to the challenging *trans*-5,6 ring juncture was a Nazarov cyclization[131] of vinyligous amide **1.354** (Scheme 1.21). Giannis utilized Smith's first generation approach to paspaline (Scheme 1.4) to initiate his sequence with functionalized *trans*-decalin **1.166**.

Scheme 1.21 Giannis' Proposed Nazarov Cyclization *en route* to (−)-Terpendole E
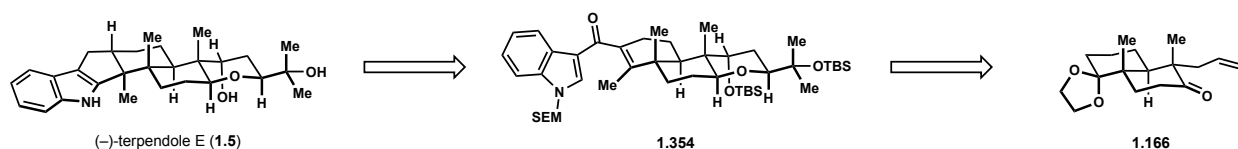
Reduction of the ketone **1.166** and hydroboration-oxidation of the alkene provided diol **1.355**, which was further oxidized to lactone **3.156** and then dihydropyranone **1.358** via a modified Cope elimination (Scheme 1.22).[132] Substrate controlled epoxidation of enone **1.358** with hydrogen peroxide was followed with reductive fragmentation of the epoxide[133] to install the key C11 alcohol in **3.159**, which was subsequently protected as the MOM ether **3.160**. The lactone was reduced to the lactol **3.161** and subjected to a Wittig reaction to provide a mixture of alkene isomers, that were then epoxidized and cyclized to tetrahydropyran **3.162** as a mixture of diastereomers, analogous to Smith's synthesis of paspaline (Scheme 1.4).[134] Oxidation and epimerization merged the mixture into equatorial ketone **3.164**, at which point methyl group addition and protecting group manipulation prepared ketone **1.353** for indole installation. Aldol condensation onto indoloaldehyde **3.165** provided an enone intermediate that was hydrogenated to diastereoselectively provide ketoindole **3.166**. Methyllithium addition to the ketone provided allylic alcohols **1.367a** and **1.367b** in an undisclosed and inconsequential ratio. Allylic C-H oxidation of the indole provided β-hydroxyketones **1.368a** and **1.368b**, that were treated with Burgess' reagent to facilitate elimination to the requisite enone **1.354** for electrocyclization. Where

Scheme 1.22 Giannis' Synthesis of (+)-16-*epi*-Terpendole E
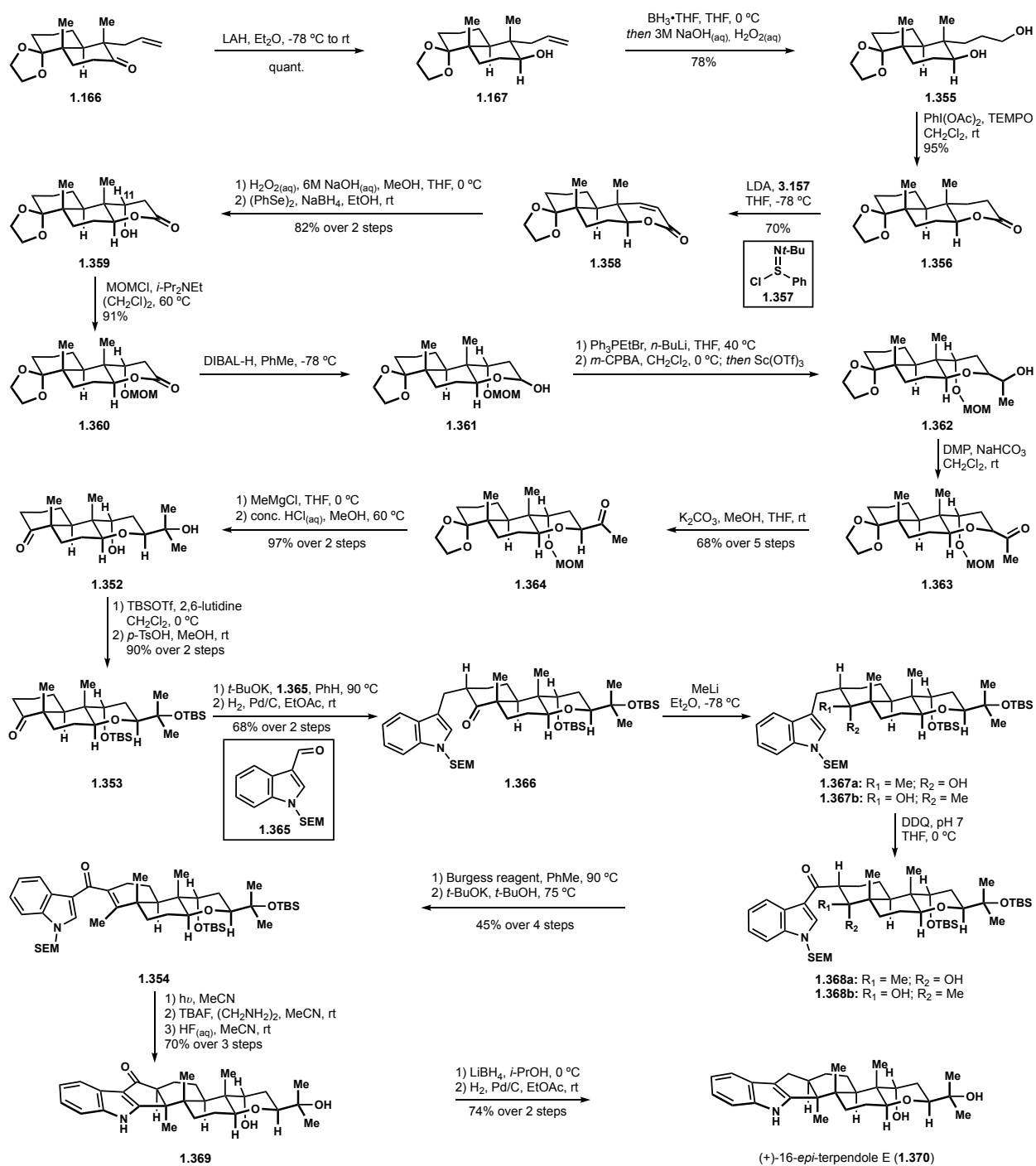
Lewis and protic acids failed to induce the desired Nazarov cyclization, irradiation with light produced cyclized product **3.169** in good yield with C3 set as desired, but epimeric at C16. Attempts to epimerize C16 returned **3.169**, indicating a thermodynamic preference for the *cis* ring

juncture. Giannis completed the synthesis of 16-*epi*-terpendole E (**1.370**) in a four-step sequence consisting of global deprotection and ketone reduction. Notably, Giannis analyzed the analogue for kinesin spindle protein inhibition known to terpendoles[15], finding the activity had been completely lost.

1.2.14 Jeffery S. Johnson's Total Synthesis of (–)-Paspaline

In the first deviation from a synthetic strategy that relied on Wieland-Miesher ketone or a polyene cyclization, Jeffery S. Johnson published a synthesis of (–)-paspaline (**1.7**), whereby multiple desymmetrizing tactics were used to build the terpene core in a highly stereoselective manner.[135] Beginning with 1,3-diketone **1.371**, Johnson developed a protocol to bias *C*, rather than *O*-alkylation through use of hydrazone **3.372** and permit access to substituted diketone **1.373** (Scheme 1.23).[136] In order to access enantioenriched material, Johnson employed enzyme YSC-2 to effect a mono reduction and provide *β*-hydroxyketone **1.374** in high yield, enantioselectivity and diastereoselectivity.[137] Effecting an epoxidation of alkene **1.374** resulted in poor levels of diastereocontrol. Furthermore, the desired ring closure of the alcohol onto the epoxide was out competed by attack of the enol tautomer of the carbonyl, resulting a higher ratio of diol **1.375** relative to ketone **1.376**. Remarkably, by converting the remaining ketone of **3.174** to a hydrazone, epoxidation of the alkene became highly diastereoselective. Additionally, the hydrazone enforced opening of the epoxide with the alcohol to afford *cis*-tetrahydropyran **1.377**. Presence of the hydrazone produces a notably curios case of substrate control, the origins of which are not well understood. There is possibly a geometric argument for the hydrazone directing the alkene into proximity to the alcohol.[135b] Alternatively, if not additionally, a favourable interplay of hydrogen-bonding between the peroxide and the hydrazone may promote stereoselective epoxidation.

Scheme 1.23 Johnson's Total Synthesis of (–)-Paspaline
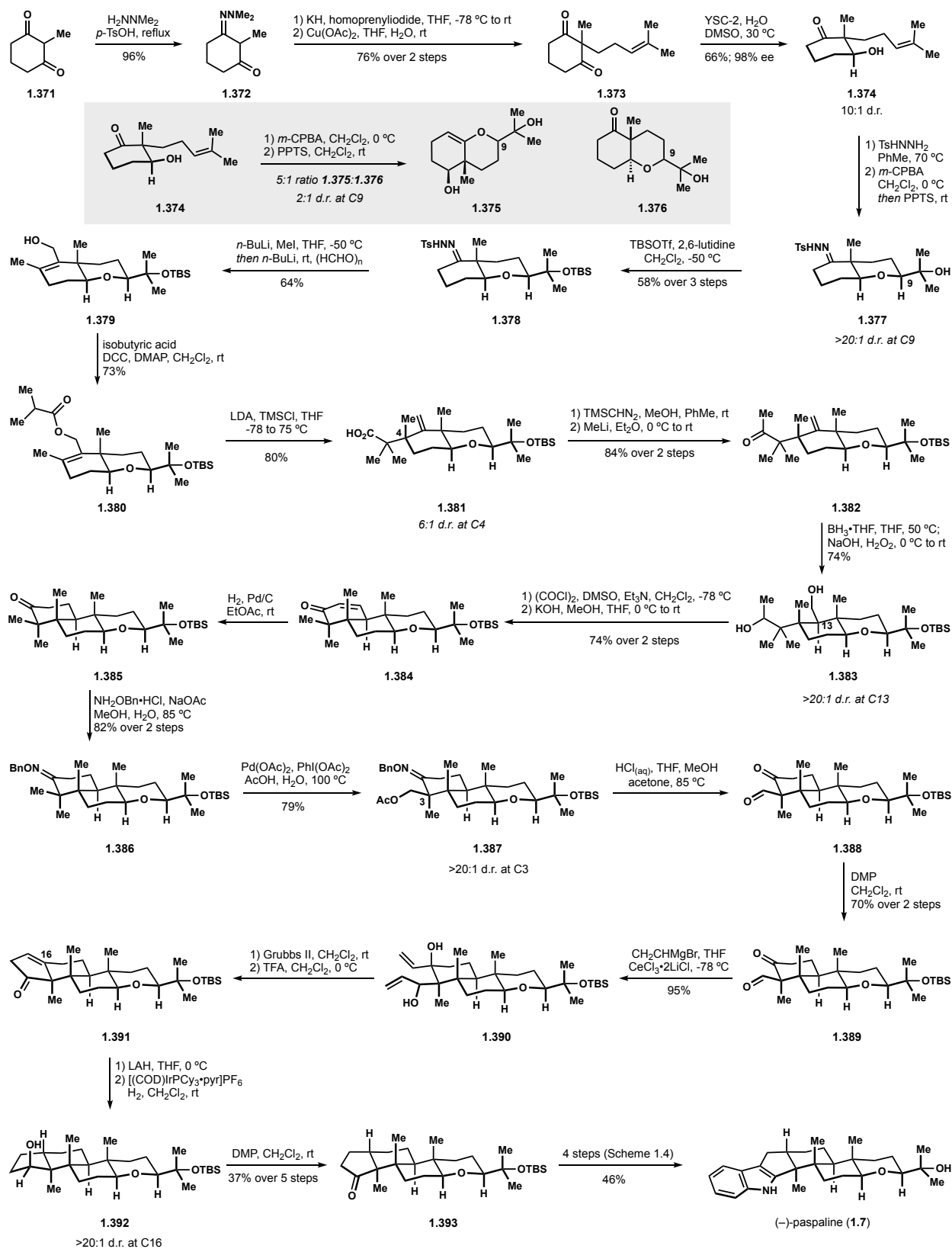
Protection of tertiary alcohol **1.377** was followed by a one pot α-methylation of hydrazone **1.378** and Shapiro reaction trapped with formaldehyde to provide allylic alcohol **1.379**.[138] Conversion of the alcohol to the isobutyrate **1.380** set the stage for an Ireland–Claisen rearrangement[139] to introduce the stereocenter at C4 with appreciable levels of control, leaving carboxylic acid and alkene functional handles on decalin **1.381** for constructing the next ring. Esterification of the acid **1.381** and methyllithium addition provided ketone **1.382**. Hydroboration-oxidation of the alkene **1.382** proceeded with high selectivity at C13 to produce diol **1.383**, which underwent double oxidation and aldol condensation to afford enone **1.384**. Hydrogenation and conversion to oxime **1.386** set the stage for Johnson's key C-H oxidation. With the application of Sanford's conditions[140], oxime **1.386** competently directed the oxidation to the equatorial methyl group in plane with the nitrogen atom, setting the C3 stereochemistry as desired and providing acetate **1.387**. Removal of the oxime and acetate protecting group was followed by DMP oxidation to yield dicarbonyl **1.389**. An equivalent of vinyl Grignard was added to each carbonyl, which was followed by ring closing metathesis to furnish the cyclopentyl ring. Treatment of the cyclopentenol with trifluoroacetic anhydride induced elimination of the tertiary alcohol and formal oxidation of the secondary alcohol to provide γ,δ-unsaturated cyclopentanone **1.391**. Hydrogenation of **1.391** yielded the epimeric product at C16. Johnson therefore reduced the ketone with LAH to yield secondary alcohol, which directed an iridium catalyzed hydrogenation with excellent selectivity to provide cyclopentanol **1.392**, overriding the bias to hydrogenate the convex face.[141] Following oxidation of **1.392**, Johnson applied the Gasman indole synthesis and complete the target (−)-paspaline (**1.7**).

1.2.15 Timothy R. Newhouse's Total Syntheses of (–)-Paspaline and (–)-Emindole PB

Representing the most recent synthesis of a paxilline indole diterpene, the Newhouse lab looked combine more modern methods with a biomimetic cyclization to construct the C ring in a synthesis of (–)-paspaline (**1.7,** Scheme 1.24).[142] Newhouse used computational analysis to predict the kinetic barrier for indole cyclization onto carbocation **1.394** along with two other potential derivatives in the gas phase. Calculations for an undesired 1,2-methyl shift pathway were also carried out. These calculations directed Newhouse to what was expected to be the optimal substrate for the indole cyclization and application towards a synthesis of (–)-paspaline from Wieland–Miesher ketone derivative **1.395**.

Scheme 1.24 Newhouse's Proposed Biomimmetic Cyclization

(–)-paspaline (**1.7**)   **1.394**   **1.395**
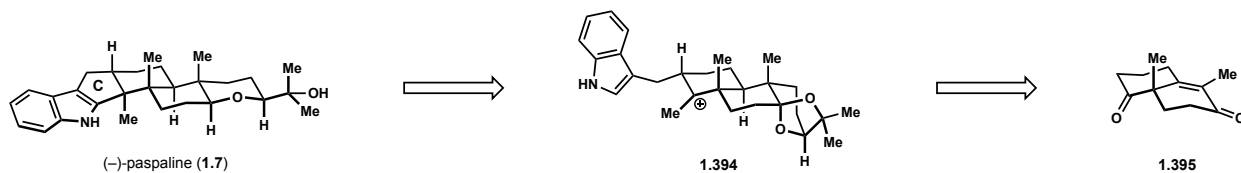
Newhouse procured the optimal substrate very rapidly, beginning with diketone **1.371** and employing the enantioselective Robinson annulation utilized to make Wieland–Miesher ketone derivative **1.395** (Scheme 1.25).[129] Deprotonation at the γ-position of enone **1.395** and α-alkylation with homoprenyl iodide yielded alkene **1.397** with modest diastereoselctivity. Sharpless' asymmetric dihydroxylation[125] of the homoprenyl alkene proceeded with poor diastereoselectivity. Nevertheless, treatment with TFA promoted ketal formation and iron mediated hydrogen atom transfer reduced the bridging alkene to provide the *trans*-decalin intermediate **1.399**.[143] Alkylation of the ketone with indole **1.400** and epimerization to the equatorial diastereomer coincided with deprotection of the indole to provide ketoindole **1.401**. Methyllithium addition into the ketone generated the key tertiary alcohol **1.402**. Ionization of the tertiary alcohol did not proceed as

Scheme 1.25 Newhouse's Total Syntheses of (–)-Paspaline and (–)-Emindole PB
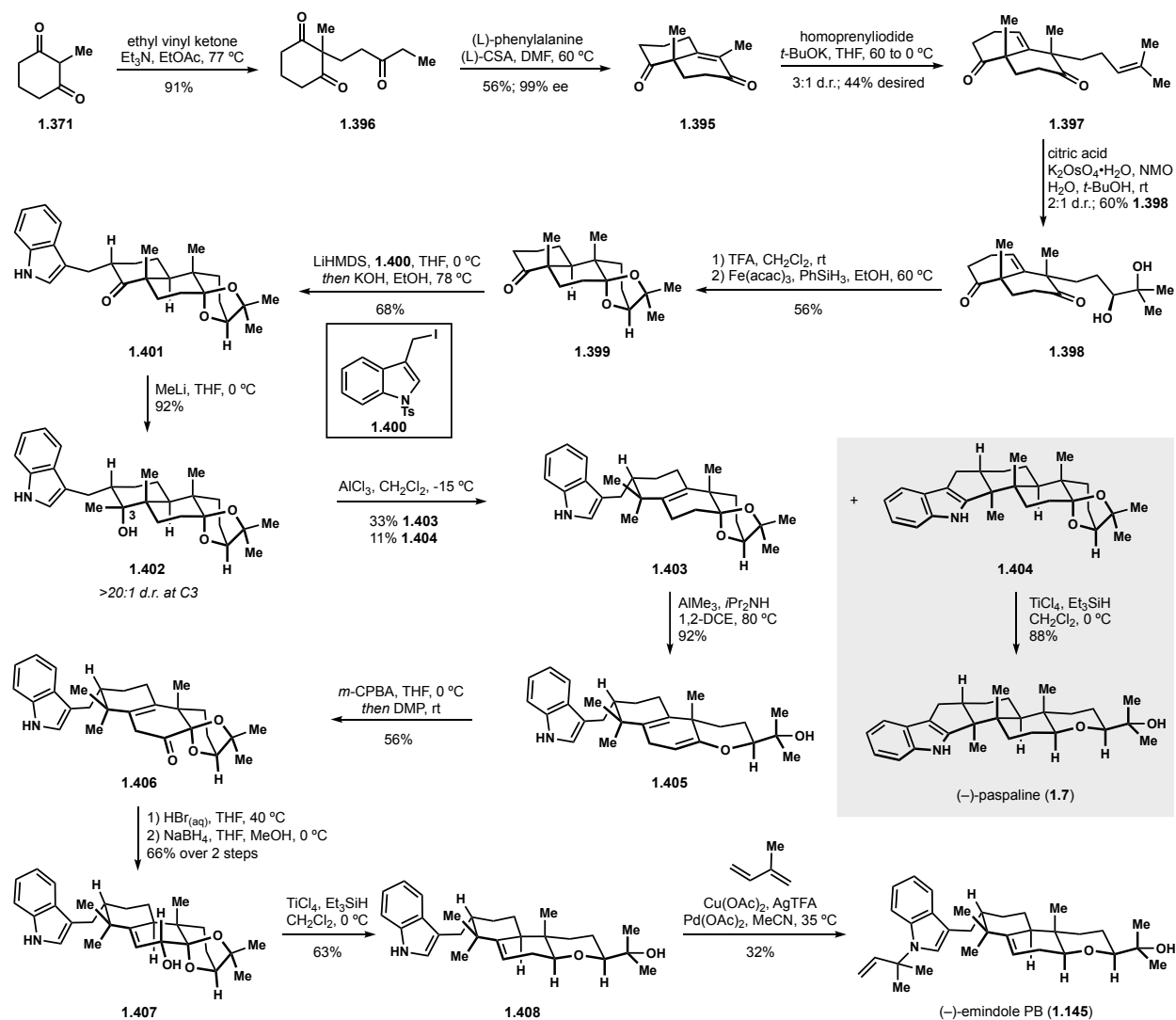
predicted by the calculations, with the 1,2-methyl shift, leading to tetrasubstituted alkene **1.403,** outcompeting indole attack by a ratio of 3:1. Closer analysis reveals that the C3 axial methyl is *anti*-periplanar to C-O σ* of the ionizing alcohol, allowing for facile migration of the methyl group and elimination to produce **1.403**. With the desired indole **1.404** that they could procure, reduction with triethylsilane in the presence of titanium(IV) chloride completed the synthesis of (–)-paspaline (**1.7**) in merely 9 steps, with a modest improvement to Johnson and Smith's overall yields. The oversight to investigate a concerted pathway highlights there are still significant challenges when it comes to computational modeling, as programs rely on the intuition of the

chemist to select pathways for analysis. Nonetheless, Newhouse made use of the product arising from the methyl shift by converting the material to (−)-emindole PB (**1.145**), likely arising biosynthetically from the same methyl shift. Treatment of ketal **1.403** with base opened the ketal to enol ether **1.405**, which was then converted to ketone **1.406** via epoxidation of the enol, fragmentation of the intermediate oxirane and oxidation of the resulting alcohol. Oxirane fragmentation also facilitated regeneration of the ketal from the intermediate oxocarbenium. Isomerization of alkene **1.406** into conjugation was followed by reduction of both the enone carbonyl and ketal to provide the tricyclic terpene core **1.408** of emindole PB. Reverse *N*-prenylation[144] of the indole **1.408** completed the first synthesis of (−)-emindole PB (**1.145**).

1.2.16 Toshio Nishikawa's Approach to (−)-Sespendole

A more unique strategy for indole construction is being developed by Toshio Nishikawa. Focusing on the first known paxilline sesquiterpenoid (−)-sespendole (**1.154**), Nishikawa planned to construct the indole from hydration of alkyne **1.409**, which in turn would be constructed from Sonogashira cross-coupling between aryl triflate **1.410** and alkyne **1.411** (Scheme 1.26).[145] Stereoselective approaches to each fragment have been completed, but are yet to be implemented in Nishikawa's endgame.

Scheme 1.26 Nishikawa's Approach to (−)-Sespendole
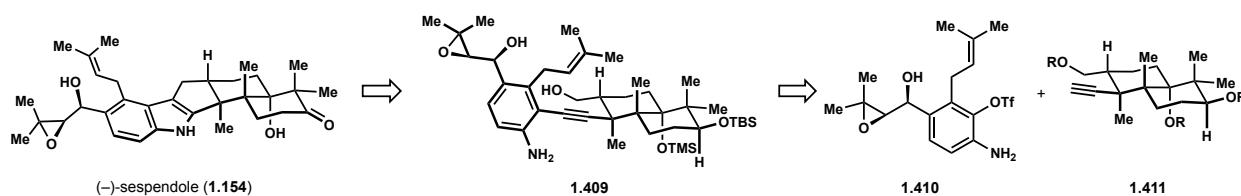
With respect to the terpene core, Nishikawa began with (+)-Wieland–Miesher ketone (**1.163,** Scheme 1.27). Double *α*-methylation of the enone and reduction of the residual ketone produced homoallylic alcohol **1.412**. Epoxidation of the bridging alkene was followed by reductive

Scheme 1.27 Nishikawa's Synthesis of an Alkyne Coupling Fragment
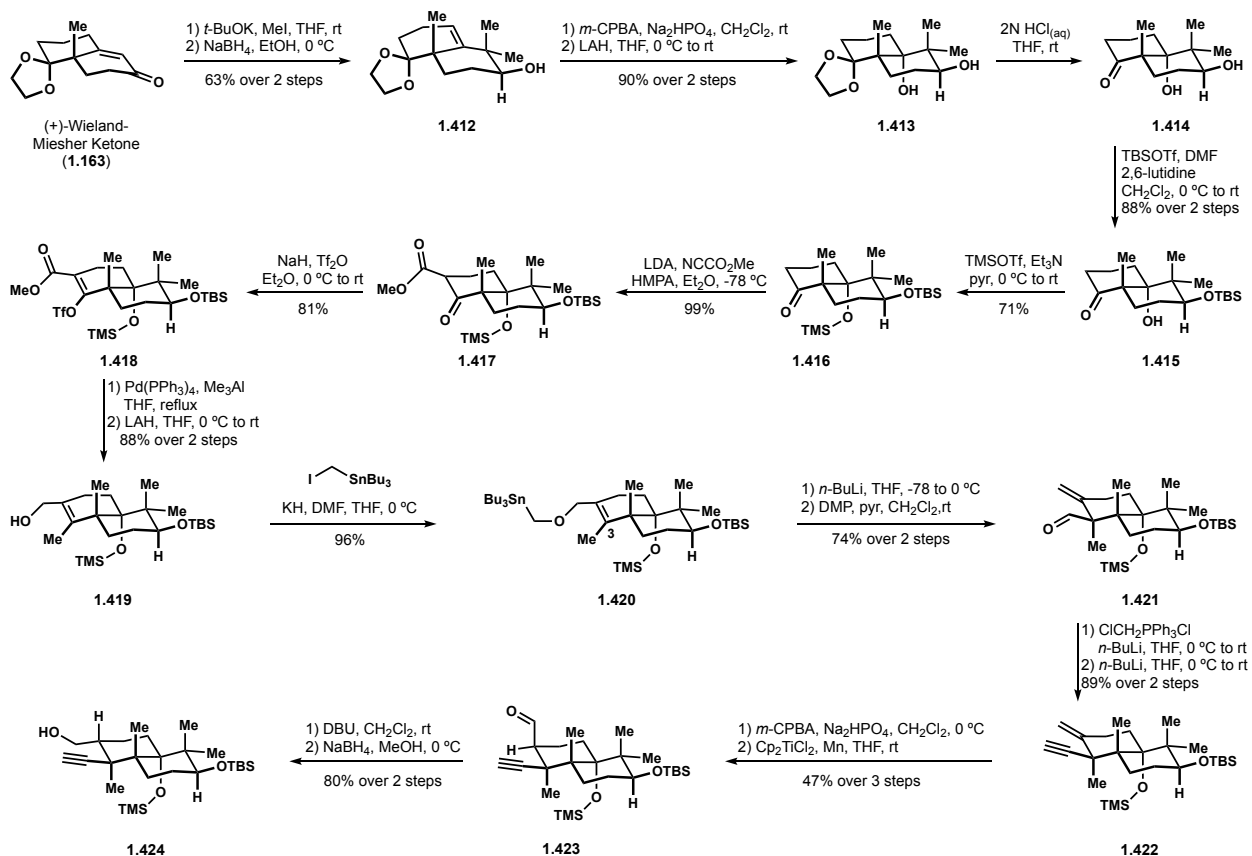
opening of the oxirane to generate tertiary alcohol **1.413**. Removal of the ketal on **1.413** and

protection of each alcohol provided ketone **1.416**, which was functionalized to with Mander's

reagent to provide β-ketoester **1.417**. The ketone was subsequently converted to vinyl triflate **1.418**

and functionalized with a methyl group. Reduction of the ester left allylic alcohol **1.419** that was

alkylated with an iodostannane to prepare stannane **1.420** for a key, stereodefining 2,3-Wittig

rearrangement to set the C3 quaternary center.[146] Treatment of **1.420** with *n*-butyllithium induced

the desired rearrangement, setting C3 with high control. Notably, conjugate addition strategies

were applied to carbonyl derivatives of alcohol **1.419** to no avail, thus, the 2,3-Wittig

rearrangement is an excellent method for generating the C3 stereocenter in this setting. Oxidation

of the alcohol provided alkenyl aldehyde **1.421**, which was converted to the requisite alkyne **1.422**

via a modified Corey–Fuchs protocol.[147] The exocyclic alkene was next converted to the epoxide

and reductive opening led to axial aldehyde **1.423**, requiring epimerization prior to carbonyl

reduction to provide coupling fragment **1.424**.

Synthesis of the aryl triflate began with S_NAr of dihalonitrobenzene **1.425** with 2-methyl-

3-buten-2-ol to provide aryl ether **1.426** (Scheme 1.28). Claisen rearrangement installed the prenyl

substituent on the arene and the resulting phenol **1.427** was TBS protected. Nitro arene **1.428** was

reduced to the aniline, which was then tosylated to provide protected arene **1.429**. The

epoxyalcohol fragment was next installed using enantioenriched epoxyaldehyde **1.430**.[87,148]

Lithium-bromide exchange of **1.429** and addition of aldehyde **1.430** provided a diastereomeric

alcohols favouring the desired *syn* epoxyalcohol **1.431** by a ratio of 3.3:1. Recrystallization

permitted isolation of diastereomerically pure material. The protected phenol was subsequently

converted to the triflate **1.410** required for Sonogoshira coupling that has yet to be disclosed.

Scheme 1.28 Nishikawa's Synthesis of an Aryl Triflate Coupling Fragment
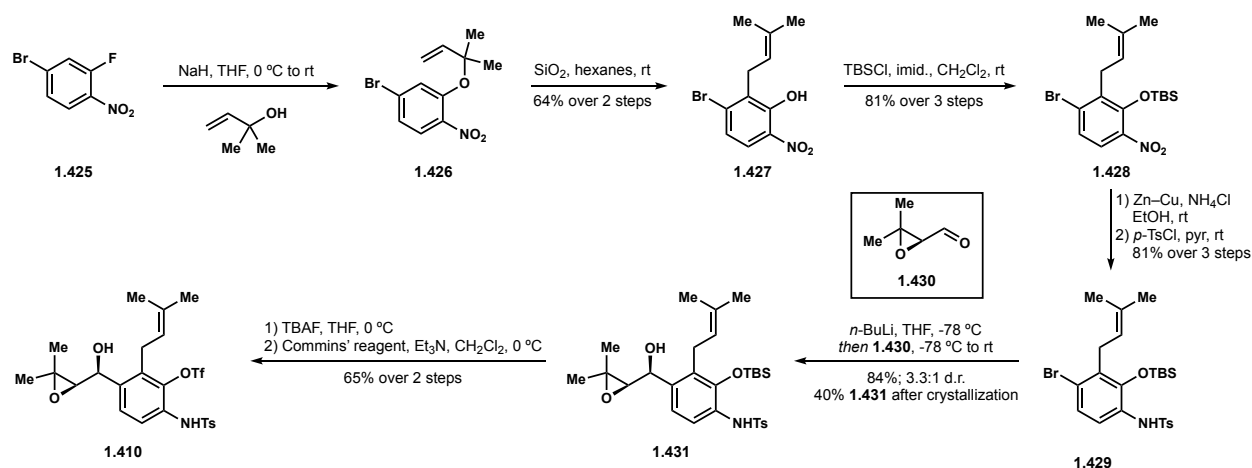
1.2.17 Amos B. Smith (III)'s Total Synthesis of (+)-Nodulisporic Acid F

The nodulisporic acids[12] represent one of the more recently discovered subclasses of the

PIDs. Notable features of flagship congener nodulisporic acid A (**1.4**) include a western

hemisphere indenopyran similar, though inverted to that found in the shearinines[24,37] and

janthitrems[38-40], bearing stereogenic carbons at C23 and C24 (Figure 1.3). An additional ring system fuses the indole nitrogen to C26, and a dienoic acid chain in place of the typical dihydropyran ring found in congeners discussed thus far. Smith's synthetic foray into the nodulisporic acids began with the simpler analogue, nodulisporic acid F (**1.124**)[149], which lacks the indenopyran and 3-pyrrolidinone motifs. Doing so provided Smith with another opportunity to revisit his strategy to the paspaline-type terpene core.[150]

Figure 1.3 New Structural Challenges Introduced by the Nodulisporic Acids

nodulisporic acid A (**1.4**)   nodulisporic acid F (**1.124**)
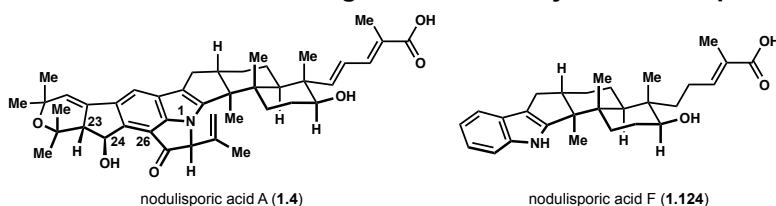
Still commencing his sequence with a Wieland–Miesher ketone derivative **1.165**, the enone was reduced under dissolving metal conditions and intercepted as silylenol ether **1.432** (Scheme 1.29). This allowed for production of β-hydroxy ketone **1.433** via Mukaiyama aldol reaction with formaldehyde. Stereoselective reduction of the ketone and removal of the ketal was followed with silylation of both alcohols to provide ketone **1.436**. Conversion of the ketone to enal[151] **1.438** began Smith's revised sequence to set the C12 and C3 (nodulisporic acid numbering) stereochemistry through a conjugate addition and methylation respectively. To this end, Smith employed an auxiliary in the form of chiral amine **1.439**,[152] condensing it onto aldehyde **1.438** to yield imine **1.440**. To their chagrin, vinylmagnesium bromide addition proceeded with the complete opposite stereoselectivity at C12. In contrast, alkylation with methyliodide performed as desired at C3 to provide functionalized decalin **1.441**. Following hydrolysis of the imine, Smith was left with alkenyl aldehyde **1.442**, which was oxidized to the carboxylic acid **1.443** and methylated to form the ester. Ozonolysis of the alkene permitted epimerization of the aldehyde at C12, which was then reduced to afford hydroxy ester **1.445**. Treatment of **1.445** with acid induced lactone formation

45

Scheme 1.29 Smith's Total Synthesis of Nodulisporic Acid F
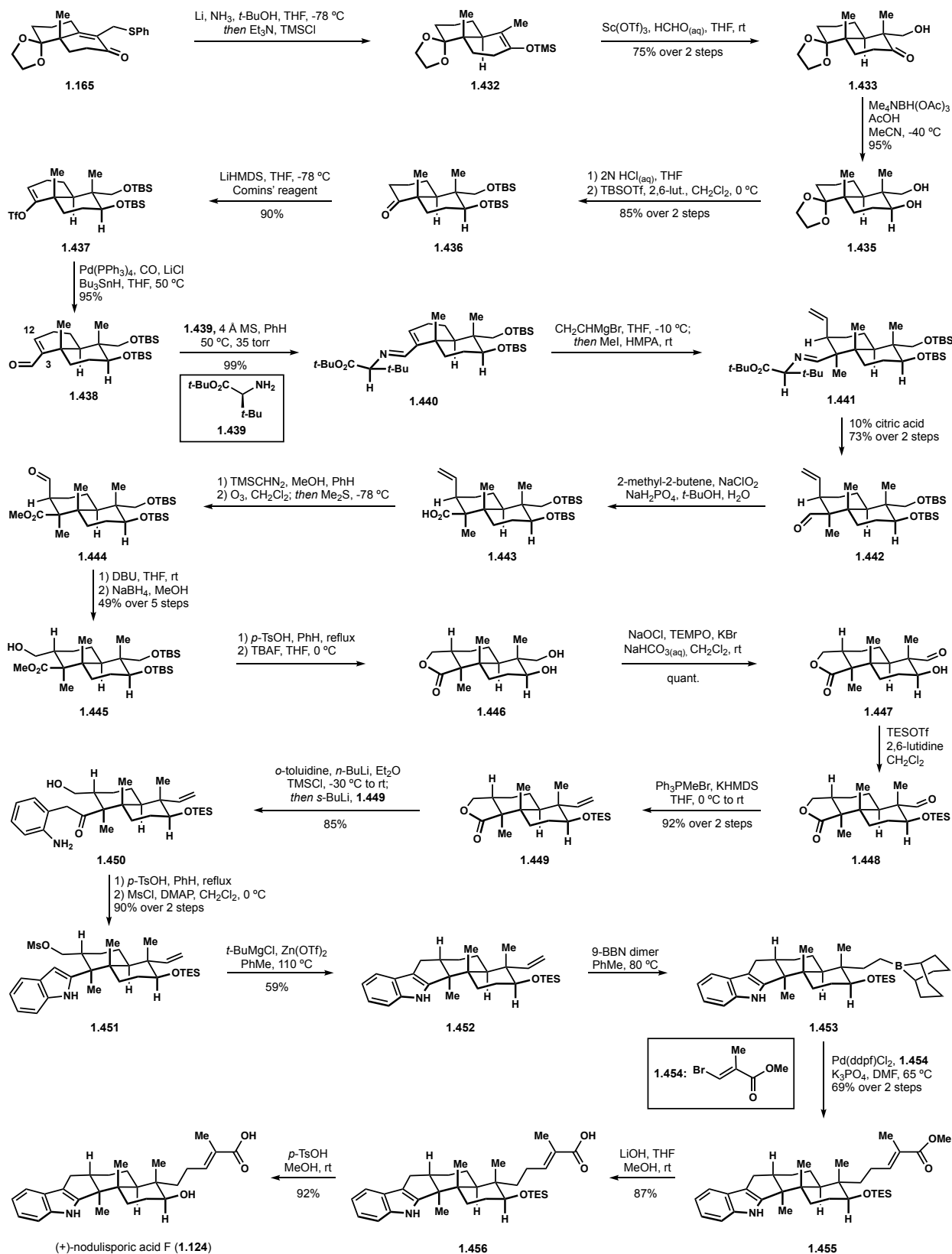
and TBAF removed the TBS groups to produce diol **1.446**.[153] The primary alcohol was subsequently oxidized[154] to afford hydroxyaldehyde **1.447** and the secondary alcohol was silylated again to give protected hydroxy aldehyde **1.448**. A Witting reaction of the aldehyde prepared the lactone **1.449**, suitable for indolization. The four-step modified Madelung coupling protocol with *o*-toluidine proceeded smoothly, yielding indole **1.452**.[155] Hydroboration[156] and Suzuki–Miyaura cross-coupling of the alkene with 3-bromo-methylmethacrylate installed the acid side-chain as α,β-unsaturated ester **1.445**. Saponification of the ester side chain and desilylation of the secondary alcohol completed the synthesis of (+)-nodulisporic acid F (**1.124**).

1.2.18 Revision of Smith's Indole Coupling Strategy

During his pursuit of the more complex nodulisporic acids A–D, Smith realized that use of the modified Madelung indole synthesis in his lab's syntheses of (–)-penitrem D and (–)-nodulisporic acid F would have to be reconsidered. The benzylic alcohol found in these targets introduced a liability, as the silylether **1.457** was prone to elimination once the benzyl anion was generated (Scheme 1.30a).[150b] The free alcohol was also prone to elimination under acidic conditions, a problem identified during the isolation of these compounds. Smith overcame these issues for initial fragment coupling by treating hydroxyaniline **1.460** with 3 equivalents of *tert*-butyllithium to produce the lithium alkoxide trianion **1.462** and before adding lactone **1.462** to provide ketoaniline **1.463** (Scheme 1.30b). However, attempts to condense ketoaniline and forge the indole **1.464** were futile, as the benzyllic alcohol became increasingly prone to elimination once the aniline was deprotected. Furthermore, the modified Madelung protocol necessitated use of stoichiometric quantities of *o*-toluidine ten-fold higher relative to the lactone partner. Thus, Smith sought a milder and more efficient approach to the indole nucleus, choosing a Buchwald–

Scheme 1.30 Evolution of Smith's Indole Construction Strategies

a)

1.457 → (n-BuLi, TMSCl, Et₂O then s-BuLi) → 1.458 → 1.459

b)

1.460 → (t-BuLi, Et₂O, -78 to 25 °C) → 1.461 + 1.462 → (HMPA, Et₂O, -25 °C, 67%) → 1.463

1.464 ← (conditions) ← 1.463

c)

nodulisporic acid D (**1.122**) ⟹ 1.465 + 1.466
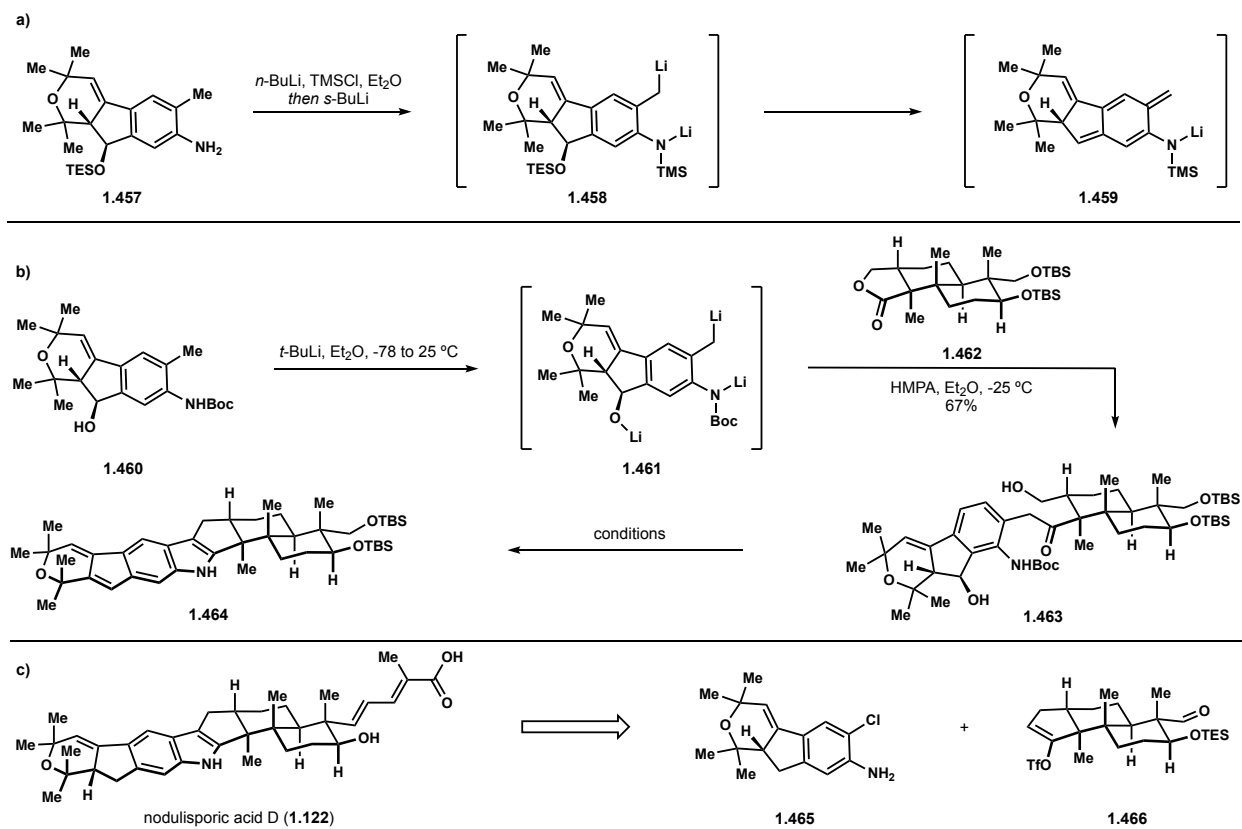
Hartwig amination and Heck reaction cascade developed by Barluenga for coupling *ortho-*haloanilines with vinyl halides or psuedohalides.[157] (–)-Nodulisporic acid D (**1.122**) was chosen to demonstrate a proof of concept coupling between chloroaniline **1.465** and vinyltriflate **1.466**. (Scheme 1.31c).[158]

1.2.19 Amos B. Smith (III)'s Total Synthesis of (–)-Nodulisporic Acid D

Smith diverted from previous strategy at enal **1.438**. In this iteration, it was discovered that the use of an auxiliary to direct vinyl cuprate addition was superfluous, and Normant cuprate addition to enal **1.438** provided the desired C12 stereoisomer exclusively (Scheme 1.31).[159] Silyl enol ether **1.467** was generated *in situ* during the conjugate addition and was methylated at C3 to provide the alkenyl aldehyde **1.468** with high levels of stereocontrol at C3. Vinyl group addition

Scheme 1.31 Synthesis of a Revised Eastern Hemisphere Fragment
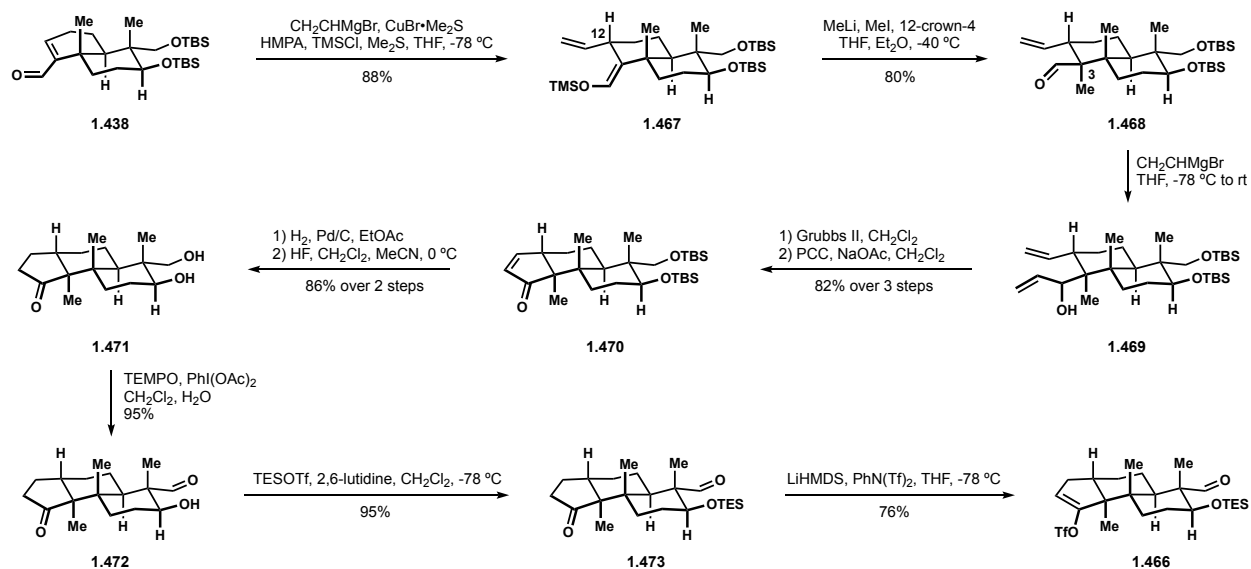
into the aldehyde, ring-closing metathesis[115] and oxidation[160] efficiently provided cyclopentenone **1.470**. Hydrogenation of the enone completed construction of the *trans*-5,6 ring system. Deprotection of the diol and selective oxidation of the primary alcohol provided hydroxyaldehyde **1.472**.[161] The secondary alcohol of **1.472** required reprotection and cyclopentanone **1.473** was converted into the vinyl triflate coupling partner **1.466**.

To access chloroaniline **1.465**, Smith began with 4-chloro-3-nitrobenzoic acid (Scheme 1.32). Reduction of the acid to the alcohol and Appel reaction[162] delivered benzyl iodide **1.474**.

Scheme 1.32 Synthesis of a Western Coupling Fragment for (–)-Nodulisporic Acid D
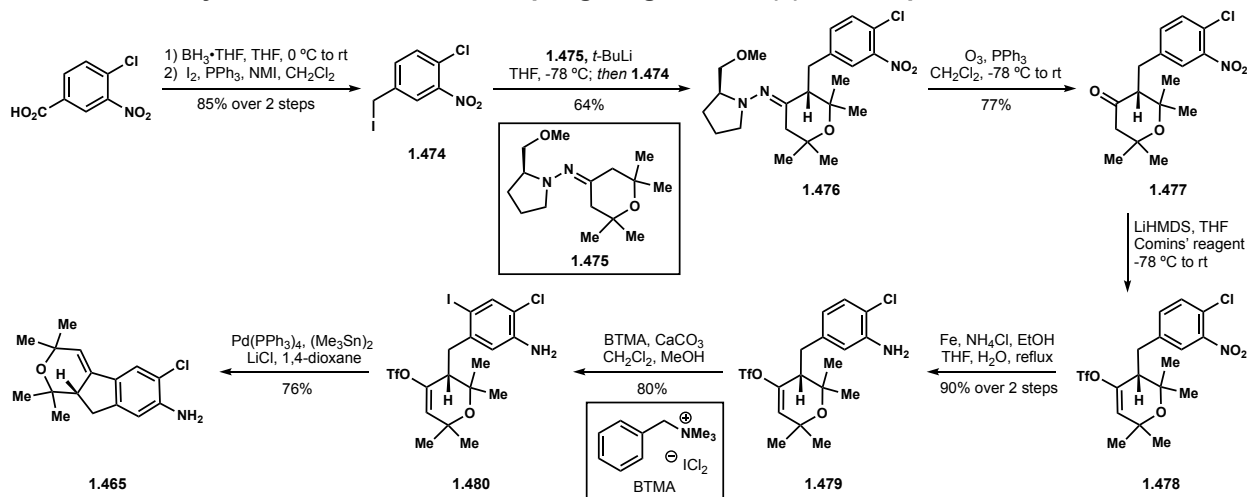
Ender's alkylation[163] of hydrazone **1.475** with iodide **1.474** delivered enantioenriched hydrazone **1.476**. Following ozonolysis of the hydrazone to ketone **1.477** the kinetic enolate was generated and trapped as the vinyl triflate **1.478**. Nitro group reduction and iodination[164] *para* to the amine preceded a Stille–Kelly reaction[165] that completed synthesis of the western coupling fragment **1.465**.

With both tricyclic fragments now in hand, utilization of a palladium precatalyst containing the phosphine ligand RuPhos,[166] developed by Buchwald, successfully united the two fragments to forge indole **1.481** (Scheme 1.33). Installation of the dienoic acid side chain was to be carried out through a Horner–Wadsworth–Emmons reaction[167] with phosphonate **1.483,** though the silylether **1.481** was evidently too sterically encumbered. Desilylation of **1.481** and reprotection as the acetate permitted the HWE reaction of aldehyde **1.482**. Saponification of the diester completed the synthesis of (–)-nodulisporic acid D (**1.122**).

Scheme 1.33 Completion of Smith's Total Synthesis of (–)-Nodulisporic Acid D
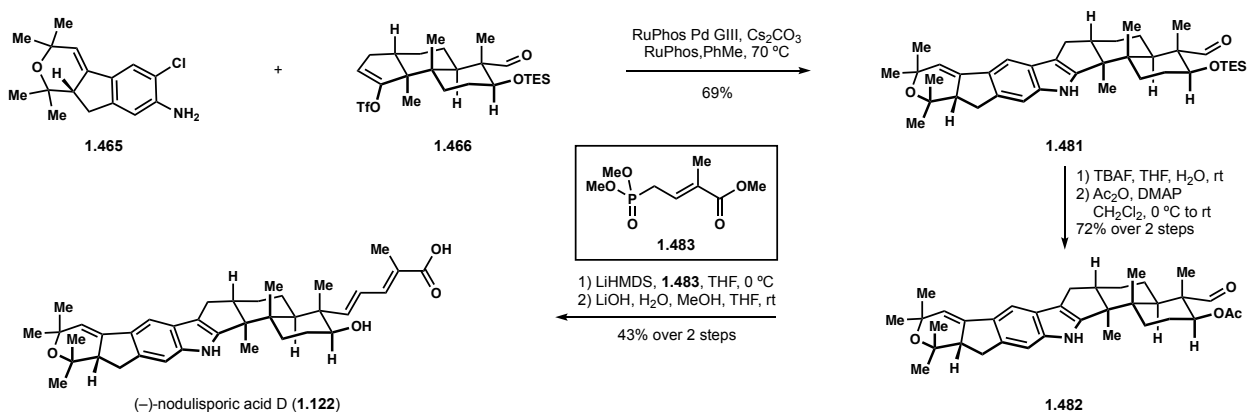
1.2.20 Amos B. Smith (III)'s Total Synthesis of (–)-Nodulisporic Acid C

Taking another step forward, Smith looked to nodulisporic acid C, containing the troublesome benzylic alcohol as well as a prenyl substituent *ortho* to the indole nitrogen.[168] The presence of these additional functionalities forced minor modifications to Smith's route that were

Scheme 1.34 Synthesis of a Western Coupling Fragment for (–)-Nodulisporic Acid C
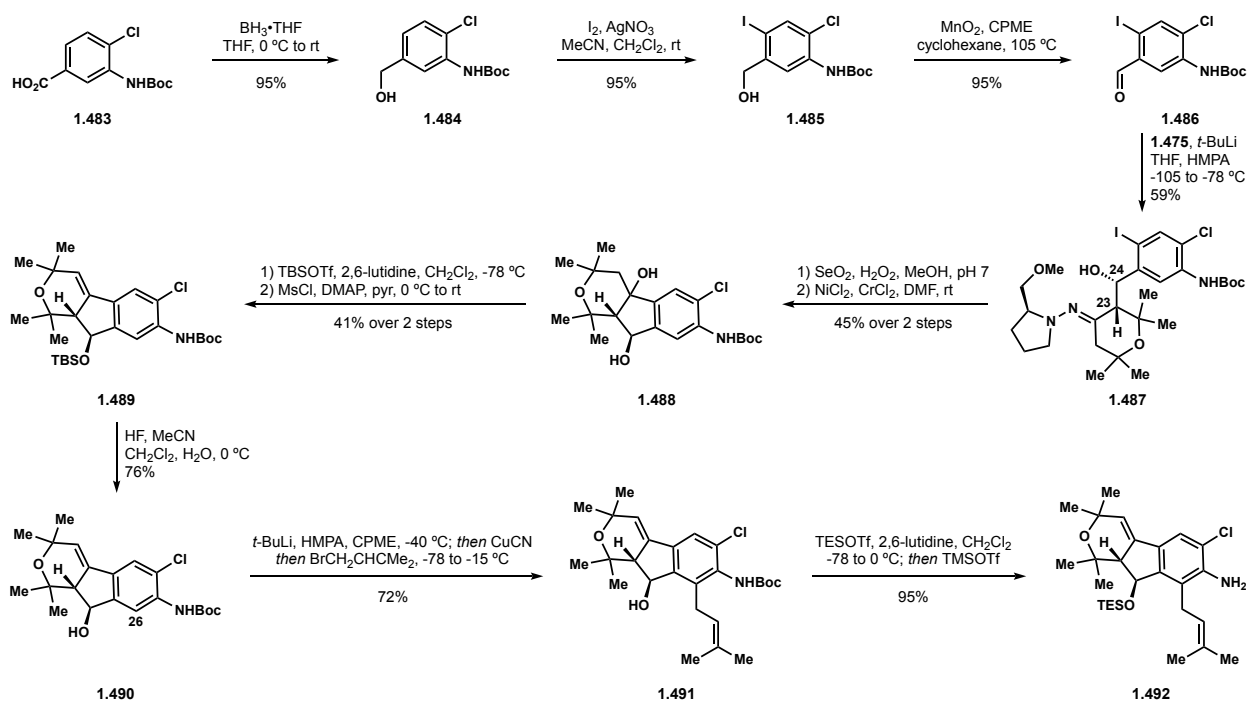
mainly implemented to improve synthetic efficiency. The new sequence began with *N*-Boc aniline

1.483, bypassing the need to carry out nitro reduction in the presence of the problematic benzylic

alcohol (Scheme 1.34).[3a] The carboxylic acid of **1.483** was reduced to the alcohol **1.484** and

iodinated to afford tetrasubstituted arene **1.485**. Treating the alcohol with manganese(II) oxide

provided benzaldehyde **1.486**, which was reacted with the hydrazone **1.475** to provide benzylic

alcohol **1.487**, setting the C23 stereochemistry, as done previously, along with the C24 benzylic

alcohol orientation.[169] Following removal of the hydrazone, Smith elected to employ the Nozaki–

Hiyama–Kishi reaction[170] to cyclize to the tricyclic core as tertiary alcohol **1.488**, citing toxicity

concerns in handling hexamethylditin on scale as the reason for sequence modification. Protection

of the secondary alcohol on **1.488** allowed for elimination of the tertiary alcohol and provided the

indenopyran **1.489**. To complete the western hemisphere subtarget, **1.489** was deprotected and the

resulting alcohol **1.490** treated with three equivalents of *tert*-butyllithium for directed

deprotonation at C26. Transmetallation and alkylation with prenyl bromide afforded prenylated

benzyl alcohol **1.491**.[171] Silyl protection of the alcohol and removal of the Boc group completed

preparation of coupling fragment **1.492**.

Silyl ether **1.446** was converted to acetate **1.493** to permit the HWE reaction following

fragment coupling (Scheme 1.35). Smith then attempted coupling with vinyl triflate **1.493** and

chloroaniline **1.492**; however, initial coupling reactions failed to provide the indole. Evidently, the

prenyl substituent introduced an additional steric restraint for the amination step. Additional

screening identified APhos[172] as a competent ligand for the transformation, likely owing to the

smaller size relative to RuPhos. Further optimization led to appreciable yields of indole **1.494**. The

HWE reaction with phosphonate **1.483** once again installed the dienoic acid side chain to afford

protected nodulisporic acid C **1.495**. Global deprotection and treatment with sodium carbonate

made it possible to isolate pure (−)-nodulisporic acid C (**1.121**) as the sodium salt.

Scheme 1.35 Completion of Smith's Total Synthesis of (−)-Nodulisporic Acid C
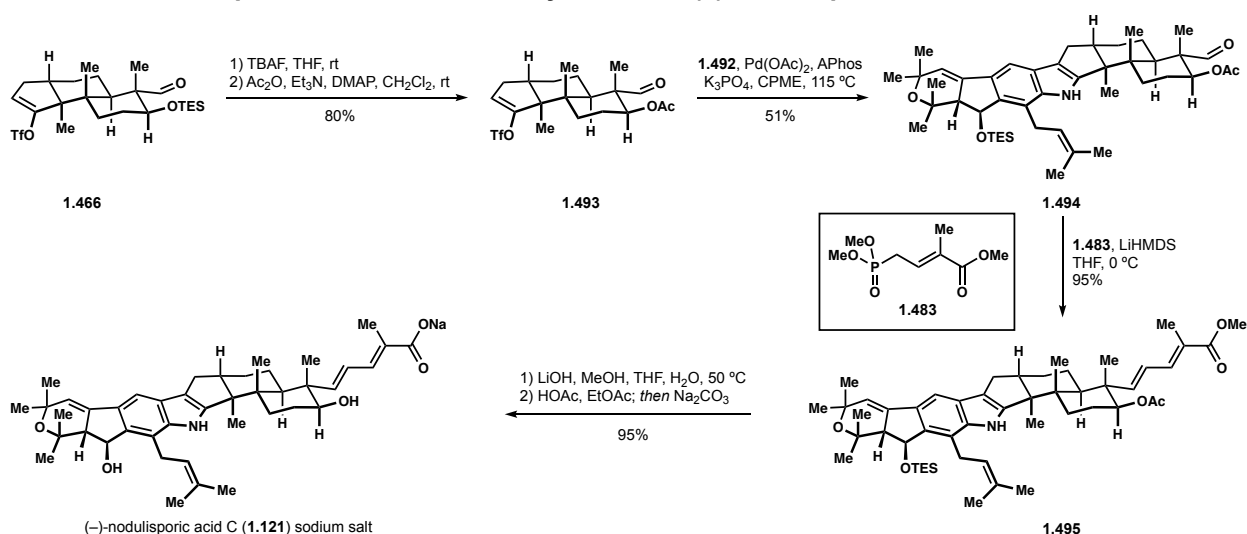
1.2.21 Amos B. Smith (III)'s Total Synthesis of (−)-Nodulisporic Acid B

Having overcome the challenges associated with the western hemisphere in the context of

(−)-nodulisporic acid C (**1.121**), Smith looked to address the outstanding challenge of the

Figure 1.4 Outstanding Structural Challenges in the Nodulisporic Acids

nodulisporic acid A (**1.4**)　　　　　nodulisporic acid B (**1.120**)

additional ring found in nodulisporic acids A (**1.4**) and B (**1.21**) shown in Figure 1.4. Given the

sensitivity of other functionalities in the molecule and substantial amount of strain imparted by

this ring, constructing this moeity with stereocontrol at C2' represents a substantial challenge.

Notably, Smith's attempts to carry out Buchwald-Hartwig aminations with an indane model

system have been well documented, but lack the isopropenyl substituent, which becomes

epimerizable should the C1' ketone be present.[150,173] Smith ultimately decided to construct this

ring after indole formation, targeting nodulisporic acid B via nitrogen allylation.[174]

Accessing the appropriate substrate only required functionalizing the arene with an

oxidized prenyl halide derivative. Nonetheless, the order of operations to the indenopyran were

further optimized during the studies toward nodulisporic acid B. Following Ender's aldol addition,

the resulting benzyl alcohol **1.487** was protected with a TES group prior to hydrolysis to ketone

1.497 (Scheme 1.36). With the alcohol protected, the NHK reaction and elimination evidently

worked more efficiently, as desilylation afforded des-prenyl indenopyran **1.490** in 34% yield over

5 steps compared to 14% in the previous route. Alcohol **1.490** was alkylated with allyl iodide **1.500**

in reasonable yield. Silylation of the benzylic alcohol and removal of the Boc group prepared the

chloroaniline **1.502** for fragment coupling. Uniting chloroaniline **1.502** and vinyl triflate **1.466**

proceeded with the same efficiency as it had for (−)-nodulisporic acid C (**1.121**) to forge indole

1.503. The allylic, primary alcohol was carefully and selectively desilylated with ammonium

fluoride, permitting conversion of silyl ether **1.503** to carbonate **1.504**. This substrate was now

Scheme 1.36 Smith's Total Synthesis of (–)-Nodulisporic Acid B
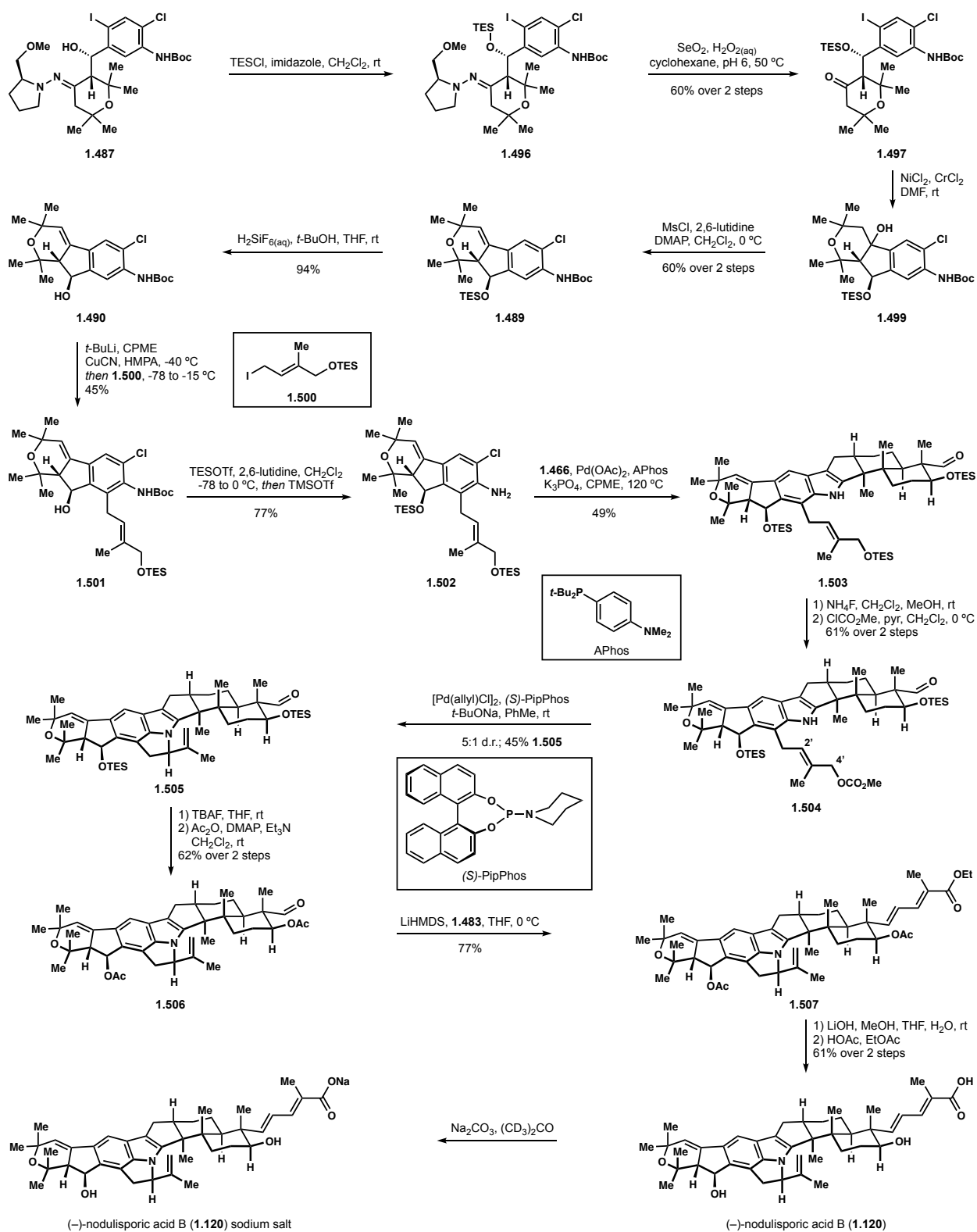
suitable for indole allylation assessment. Extensive experimentation provided several interesting

pieces of insight. Initial experiments produced three distinct results. Either the desired C2'

allylation product **1.505** was obtained as a mixture of diastereomers at C2', the carbonate was

eliminated prior to cyclization, or allylation occurred at C4' (products not shown). The system

possesses no evident source of substrate control for this transformation. Furthermore, Smith

demonstrated a rare example of reversible reductive elimination to form the C–N bond[175], thus a

thermodynamic mixture or diastereomers are likely to be produced. This issue was surmounted by

employing Feringa's chiral phosphoramidite ligand PipPhos[176] to place reductive elimination

under kinetic control and favour production of epimer **1.505** by a ratio of 5:1. Having successfully

overcome the challenge of the final ring system, protecting group manipulations, HWE reaction

of the aldehyde and global deprotection yielded nodulisporic acid B (**1.120**) as the sodium salt.

1.2.22 Sergey V. Pronin's Total Synthesis of (±)-Emindole SB

Our lab's entry into the synthetic field of PIDs began with emindole SB (**1.8**), the

biosynthetic precursor for all diterpene congeners.[177] Central to the strategy was a polycyclization

to construct the decalin core, a rarity in the context of the PIDs. Beginning with 2-methylcyclopent-

2-en-1-one, conjugate addition with homoprenyl Grignard reagent **1.508** was terminated by

trapping the metal enolate as silyl enol ether **1.509** (Scheme 1.37). An indium-promoted

alkenylation was developed for facile preparation of 1,1-disubstituted alkene **1.511** with control of

the C3 stereocenter.[178] Sharpless allylic hydroxylation[179] and Fischer indolization[180] provided

indole diol **1.512**, which was oxidized to the dialdehyde and funneled to hemiaminal **1.513**. The

alkene was then reduced using hydrogen atom transfer conditions to generate a teriary alkyl

radical, which underwent intramolecular conjugate addition with the pendant enal to generate

hydrindane **1.514**.[181,182] By inducing hemiaminal formation, the tertiary alkyl radical that results

Scheme 1.37 Pronin's Total Synthesis of (±)-Emindole SB
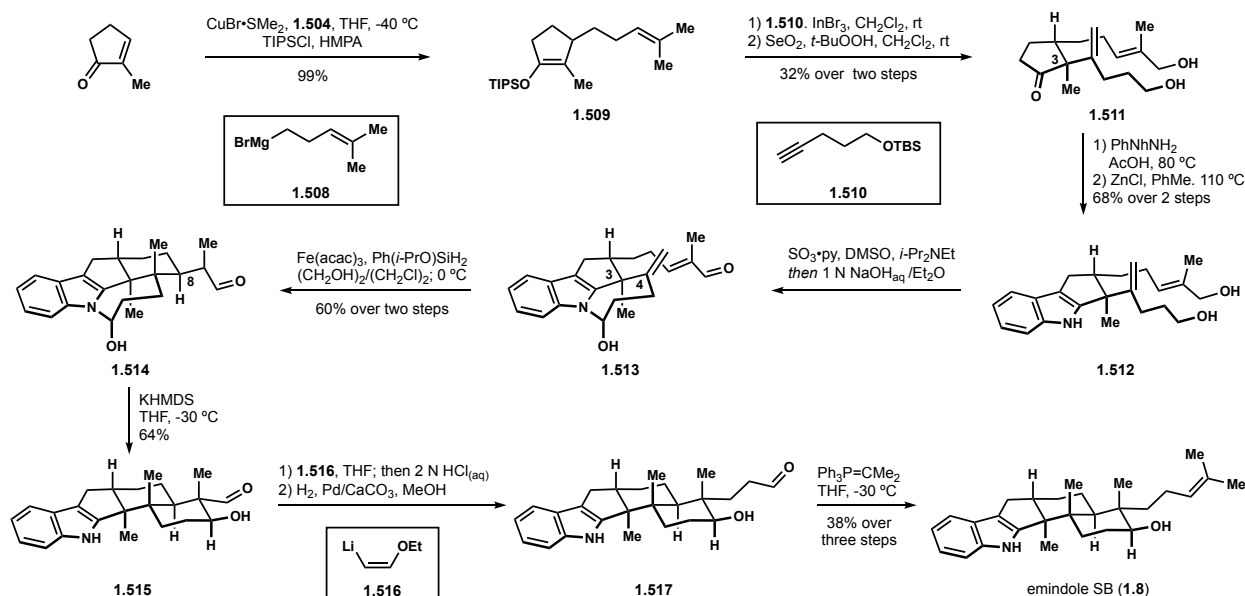
from subsequent hydrogen atom transfer is unable to undergo bond rotation at C3–C4. This led to a very efficient intramolecular Giesse addition, forging the C4–C8 bond with complete stereocontrol. Treatment of **1.514** with KHMDS released the aldehyde from the indole and promoted aldol addition to complete construction of the *trans*-decalin core as hydroxyaldehyde **1.515**. Lithioenol ether addition[183] to the aldehyde **1.515** and hydrogenation of the resulting enal afforded the extended aldehyde **1.517**. A Wittig reaction completed the synthesis of (±)- emindole SB (**1.8**).

1.3 Additional Approaches to Western Hemispheres of Various PIDs

1.3.1 Hidetoshi Tokuyama's Approach to the Western Hemisphere of Penitrem E

A more recent approach to the western hemisphere of the penitrems has been published by Tokuyama.[184] Focusing on penitrem E, reactivity was explored on model indole **1.518** (Scheme 1.38). A key [2+2] cycloaddition analogous to Smith's work[89], but under thermal conditions was explored to produce the cyclobutane. In contrast to Smith, Tokuyama constructed tricyclic

precursor **1.519** in a dramatically different fashion via a Catellini reaction[185] between alkyl and aryl iodides **1.520** and **1.521**. Additionally, alkyl iodide **1.520** was prepared in enantioenriched for through use of a lipase acetylation.[186]

Scheme 1.38 Tokuyama's Approach to the Western Hemisphere of Penitrem E
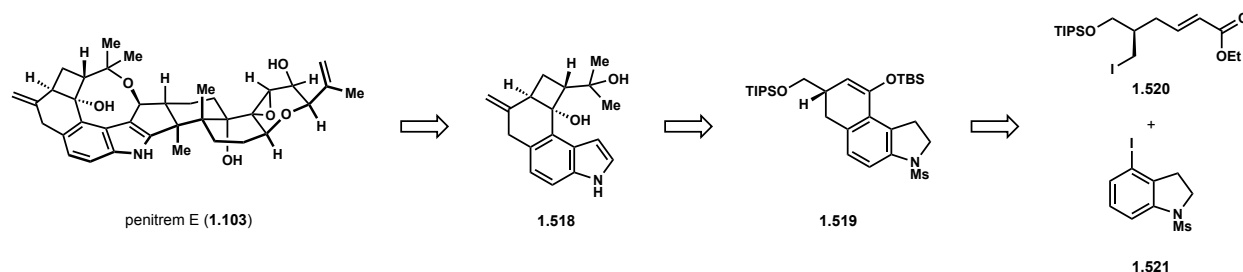
Standard Catellini reaction conditions successfully annulated the indoline to construct the indenotetralin **1.522** (Scheme 1.39). The unsaturated ester was then oxidatively cleaved to afford ketone **1.523**. Converting this ketone to silylenol ether **1.524** prepared the fragment for the [2+2] cycloaddition. As was observed in Smith's synthesis of penitrem, the acrylate was directed *anti* to the pendant TIPS ether, providing a modest yield of desired diastereomer **1.525** along with substantial amounts of the C14 epimer. As Smith had already detailed, epimerization of this

Scheme 1.39 Tokuyama's Synthesis of a Penitrem E Western Fragment
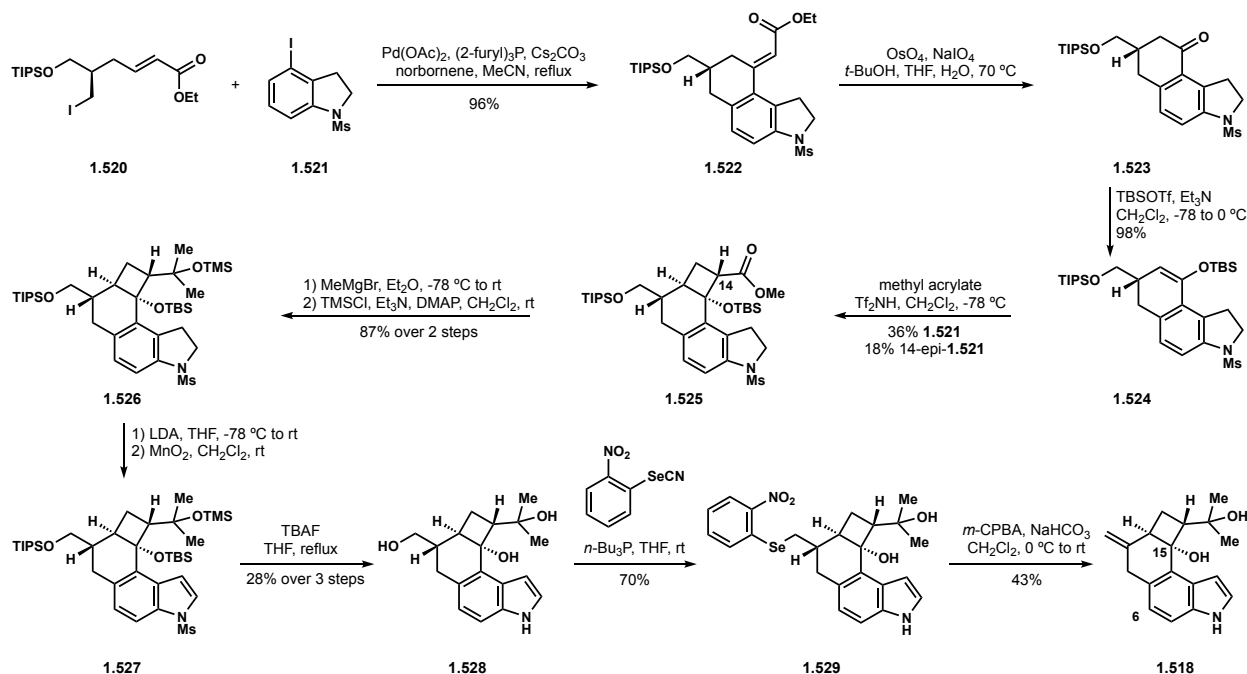
intermediate was futile. Addition of two equivalents of methyl magnesium bromide converted ester **1.525** into the tertiary alcohol, which was subsequently protected as TMS ether **1.526**. Treatment with LDA removed the indoline mesyl group that was then oxidized back to the indole **1.527**. Global deprotection to afford triol **1.528** was followed with Grieco–Nishizawa elimination[88] of the primary alcohol to complete Tokuyama's synthesis of the western hemisphere subtarget **1.518** of penitrem E. Notably, this fragment possesses the C15 hydroxyl group, but not the C6 chloride, both of which are found in penitrem A.

1.3.2 Michael A. Kerr's Approach to the Western Hemisphere of Lolitrem B

In contrast to the indenopyran motif shared by the nodulisporic acids[12], shearinines[24,37] and janthitrems[38-40], the lolicines[41] and lolitrems[4] contain a unique tetralone with a fused tetrahydrofuran on the western hemisphere, illustrate with lolitrem B (**1.2**) in Scheme 1.40. Despite the enticing bioactivity displayed by lolitrem B, Kerr is the only researcher to publish an approach to the lolitrems in the form of indolotetralone **1.530**.[187] Central to Kerr's strategy were a conjugate addition – aldol cascade[188] to access tetralone and Plieninger indole synthesis of indole **1.531**.

Scheme 1.40 Kerr's Conjugate Addition-Aldol Strategy Towards Lolitrem B

lolitrem B (**1.2**)   **1.530**   **1.531**   **1.532**
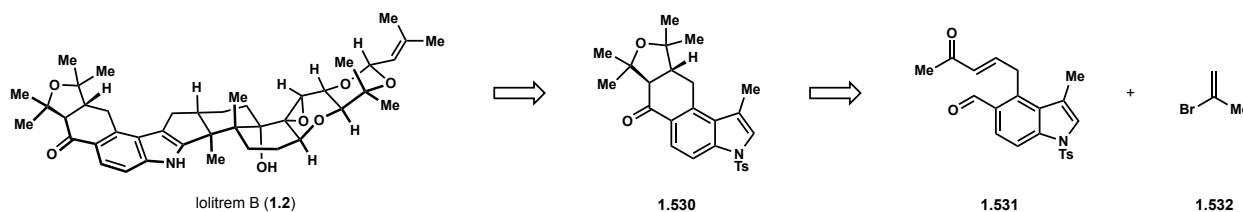
In the forward sense, the Diels–Alder reaction between the iminoquinone **1.533** and *trans*-1,3-pentadiene was followed with aromatization to provide phenol **1.534**, which was converted to the aryl triflate **1.535** (Scheme 1.41).[189] Oxidative cleavage of the alkene to the dialdehyde **1.536** and condensation yielded indole **1.537**. The remaining aldehyde of **1.537** required reduction and

Scheme 1.41 Kerr's Synthesis of a Lolitrem B Western Fragment
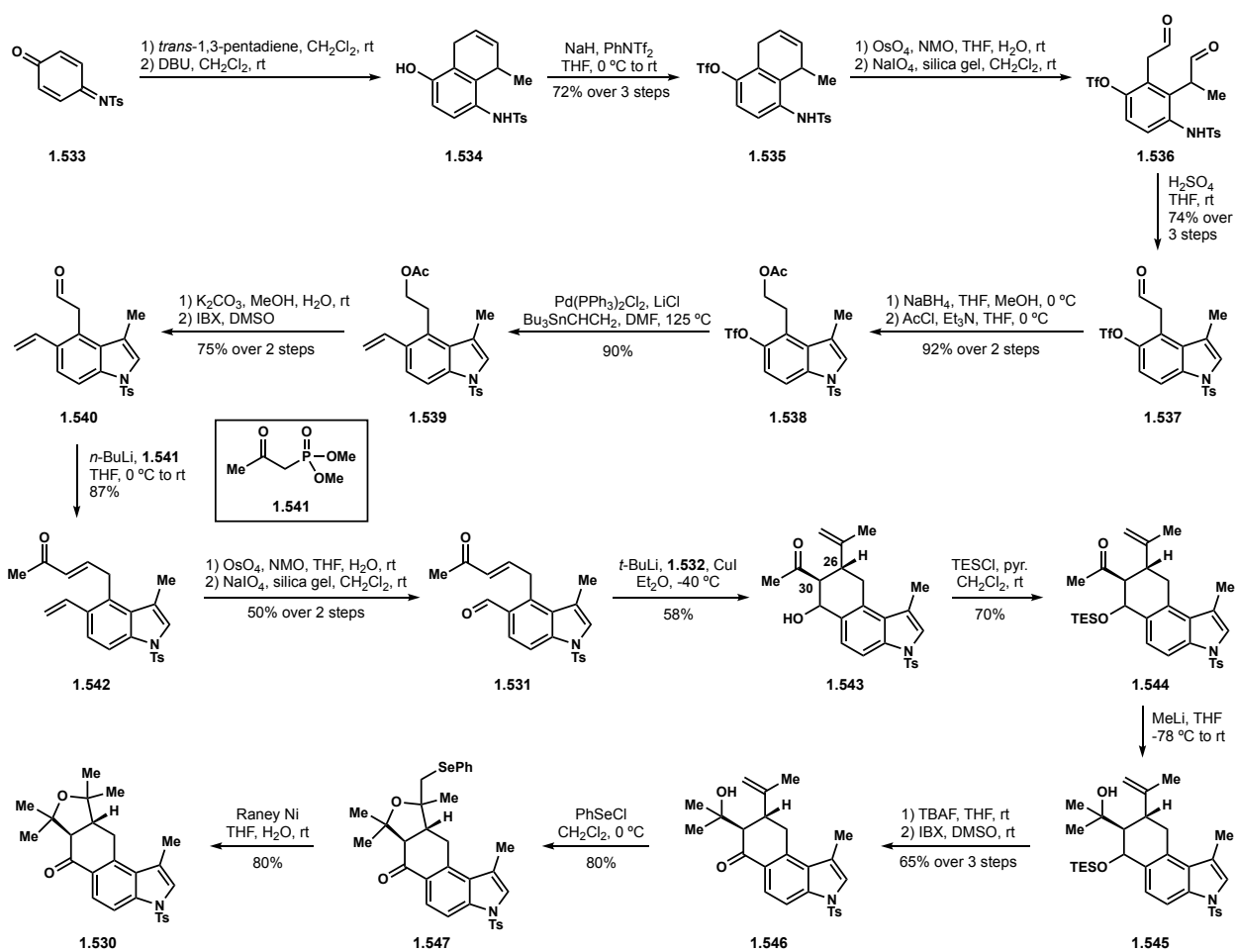
conversion to the acetate **1.538** to permit Stille cross-coupling of the aryl triflate, which provided

styrene **1.539**. The aldehyde was reinstalled to give **1.540** which was converted to enone **1.542**

through an HWE reaction with phosphonate **1.541**. Oxidative cleavage of the styrene prepared the

conjugate addition cascade precursor **1.531**. Treatment of **1.531** with isopropenyl cuprate effected

the desired reaction, forming β-hydroxyketone **1.543** diastereoselectively with respect to C26 and

C30 (lolitrem B numbering). Following protection of alcohol as the silyl ether **1.544**,

methyllithium addition produced tertiary alcohol **1.545**. Deprotection and oxidation of the benzylic

alcohol converged the epimeric mixture to ketone **1.546**. The tetrahydrofuran was next generated

via oxyselenation[190] of the isopropene moiety and reduction to complete the tetracyclic subunit **1.530** of the lolitrems.

1.3.3 Philip Magnus's Approach to the Indenopyran of the Nodulisporic Acids

The first to study the nodulisporic acids from a synthetic standpoint was Phillip Magnus.[191] His approach centered on constructing the C23–C24 bond through a diastereoselective ene reaction (Scheme 1.42).[192] Utilizing dienone **1.548**, ketopyran **1.549** was prepared. Lithium halogen exchange of arene **1.550,** addition into ketone **1.549** and elimination afforded styrene **1.551.** Deprotection of the aldehyde afforded model substrate **1.552** for exploring Magnus' key ene reaction. Treatment of the aldehyde **1.548** with various Lewis acids led to a mixture of products with minor quantities of alcohol **1.553**. Magnus instead optimized for diene **1.555** and attempted to make use of the undesired outcome. Oxidation with DMDO and oxirane opening provided indanone **1.555**, allowing Magnus to explore stereoselective reductions. Unfortunately, treatment with sodium borohydride favoured formation of undesired diastereomer **1.557** by a ratio of 3.6:1. Reduction with K-selectride provided exclusively the undesired diastereomer, illustrating that introduction of the benzyl alcohol would undoubtedly require an alternative approach.

Scheme 1.42 Magnus' Approach to the Indenopyran of the Nodulisporic Acids
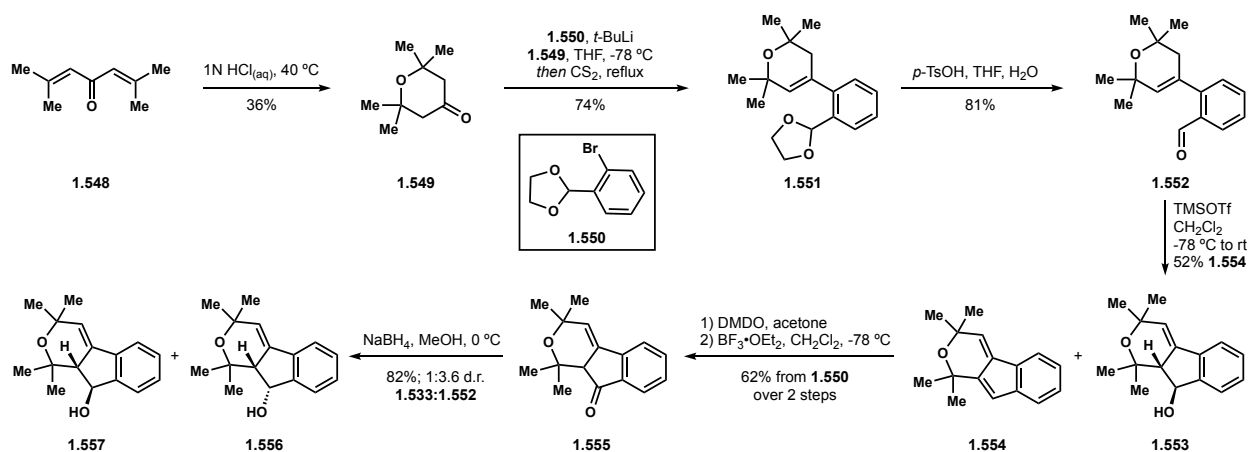
1.4 References and Notes

1. (a) Imlach, W. L.; Finch, S. C.; Dunlop, J.; Meredith, A. L.; Aldrich, R. W.; Dalziel, J. E. *J. Pharmacol. Exp. Ther*. **2008**, *327*, 657. (b) Evans, T. J.; Gupta, R. C. (Ed) Tremorgenic Mycotoxins. In *Veterinary Toxicology, Basic and Clinical Principles, Third Edition,* Academic Press: **2018**, 1033. (c) Kozák, K.; Szilágyi, Z.; Tóth, L.; Pócsi, I.; Molnár, I. Appl. Microbiol. Biotechnol. **2019**, *103*, 1599. (d) Reddy, P.; Guthridge, K.; Vassiliadis, S.; Hemsworth, J.; Hettiarachchige, I.; Spangenberg, G.; Rochfort, S. *Toxins*, **2019**, *11,* 302.

2. Springer, J. P.; Clardy, J.; Wells, J. M.; Cole, R. J.; Kirksey, J. W. *Tetrahedron Lett*. **1975**, *16*, 2531.

3. (a) Knaus, H.-G.; McManus, O. B.; Lee, S. H.; Schmalhofer, W. A.; Garcia-Calvo, M.; Helms, L. M. H.; Sanchez, M.; Giangiacomo, K.; Reuben, J. P.; Smith, A. B., III.; Kaczorowski, G. J.; Garcia, M. L. *Biochemistry*, **1994**, *33*, 5819. (b) Sanchez, M.; McManus, O. B. *Neuropharmacology*, **1996**, *35*, 963.

4. Gallagher, R. T.; Hawkes, A. D.; Steyn, P. S.; Vleggaar, R. *J. Chem. Soc., Chem. Commun.* **1984**, 614.

5. (a) Rowan, D. D. *Agric., Ecosyst. Environ.* **1993**, *44*, 103. (b) McCleay, L. M.; Munday-Finch, S. C. *Res. Vet. Sci*. **1999**, *66*, 119. (c) Imlach, W. L.; Finch, S. C.; Dunlop, J.; Dalziel, J. E. *Eur. J. Pharmacol*. **2009**, *605*, 36. (d) Philippe, G. *Toxins*, **2016**, *8*, 47.

6. (a) Dalziel, J. E.; Finch, S. C.; Dunlop, J. *Toxicol. Lett.* **2005**, *155*, 421. (b) Zhou, Y.; Xia, X.-M.; Lingle, C. L. *J. Proc. Natl. Acad. Sci. U.S.A.* **2020,** *117,* 1021.

7. Wulff, H.; Zhorov, B. S. *Chem. Rev*. **2008**, *108*, 1744.

8. Dalziel, J. E.; Dunlop, J.; Finch, S. C.; Wong, S. S. Immune Response Inhibition Using Indole Diterpene Compound. International Publication Number WO 2006/115423 A1, November 2, 2006.

9. For isolation and structure determination of the penitrems, see: (a) Wilson, B. J.; Wilson, C. H.; Hayes, A. W. *Nature*, **1968**, *220*, 77. (b) De Jesus, A. E.; Steyn, P. S.; Van Heerden, F R.; Vleggaar, R.; Wessels, P. L. *J. Chem. Soc., Chem. Commun*. **1981**, 289. (c) De Jesus, A. E.; Steyn, P. S.; Van Heerden, F R.; Vleggaar, R.; Wessels, P. L. *J. Chem. Soc. Perkin Trans. 1,* **1983**, 1847. (d) De Jesus, A. E.; Steyn, P. S.; Van Heerden, F R.; Vleggaar, R.; Wessels, P. L. *J. Chem. Soc. Perkin Trans. 1,* **1983**, 1857.

10. (a) Norris, P.J.; Smith, C.C.T.; de Belleroche, J.; Bradford, H.F.; Mantle, P.G.; Thomas, A.J.; Penny, R.H. *J. Neurochem*. **1980**, *34*, 33. (b) Moldes-Anaya, A. S.; Fonnum, F.; Eriksen, G. S.; Rundberget, T.; Walaas, S. I.; Wigestrand, M. B. *Neurochem. Int*. **2011**, *59*, 1074.

11. González, M. C.; Lull, C.; Moya, P.; Ayala, I.; Primo, J.; Yúfera, E. P. *J. Agric. Food. Chem*. **2003**, *51*, 2156.

12. For isolation and structure determination of the nodulisporic acids, see: (a) Ondeyka, J. G.; Helms, G. L.; Hensens, O. D.; Goetz, M. A.; Zink, D. L.; Tsipouras, A.; Shoop, W. L.; Slayton, L.; Dombrowski, A. W.; Polishook, J. D.; Ostlind, D. A.; Tsou, N. N.; Ball, R. G.; Singh, S. B. *J. Am. Chem. Soc.* **1997**, *119*, 8809−8816. (b) Hensens, O. D.; Ondeyka, J. D.; Dombrowski, A. W.; Ostlind, D. A.; Zink, D. L. *Tetrahedron Lett*. **1999**, *40*, 5455. (c) Ondeyka, J. G.; Dahl-Roshak, A. M.; Tkacz, J. S.; Zink, D. L.; Zakson-Aiken, M.; Shoop, W. L.; Goetz, M. A.; Singh, S. B. *Bioorg. Med. Chem. Lett.* **2002,** *12,* 2941. (d) Ondeyka, J. G.; Byrne, K.; Vesey, D.; Zink, D. L.; Shoop, W. L.; Goetz, M. A.; Singh, S. B. *J. Nat.*

Prod. **2003**, *66,* 121. (e) Singh, S. B.; Ondeyka, J. G.; Jayasuriya, H.; Zink, D. L.; Ha, S. N.; Dahl-Roshak, A.; Greene, J.; Kim, J, A.; Smith, M. M.; Shoop, W.; Tkacz, J. S. *J. Nat. Prod.* **2004, 67,** 1496.

13. (a) Smith, M. M.; Warren, V. A.; Thomas, B. S.; Brochu, R. M.; Ertel, E. A.; Rohrer, S.; Schaeffer, J.; Schmatz, D.; Petuch, B. R.; Tang, Y.-S.; Meinke, P. T.; Kaczorowski, G. J.; Cohen, C. J. *Biochemistry* **2000, 39,** 5543. (b) Shoop, W. L.; Gregory, L. M.; Zakson-Aiken, M.; Michael, B. F.; Haines, H. W.; Ondeyka, J. G.; Meinke, P. T.; Schmatz, D. M. *J. Parasitol.* **2001**, *87*, 419. (c) Ludmerer, S. W.; Warren, V. A.; Williams, B. S.; Zheng, Y.; Hunt, D. C.; Ayer, M. B.; Wallace, M. A.; Chaudhary, A. G.; Egan, M. A.; Meinke, P. T.; Dean, D. C.; Garcia, M. L.; Cully, D. F.; Smith, M. M. *Biochemistry* **2002**, *41*, 6548−6560.

14. (a) Huang, X.-H.; Nishida, H.; Tomoda, H.; Tabata, N.; Shiomi, K.; Yang, D.-Y.; Takayanagi, H.; Ōmura, S. *J. Antibiot.* **1995**, *48*, 5. (b) Tomoda, H.; Tabata, N.; Yang, D.-J.; Takayanagi, H.; Ōmura, S. *J. Antibiot.* **1995**, *48*, 793. (c) Gatenby, W. A.; Munday-Finch, S. C.; Wilkins, A. L.; Miles, C. O. *J. Agric. Food Chem.* **1999**, *47*, 1092.

15. (a) Huang, X.-H.; Tomoda, H.; Nishida, H.; Masuma, R.; Ōmura, S. *J. Antibiot.* **1995**, *48*, 1. (b) Nakazawa, J.; Yajima, J.; Usui, T.; Ueki, M.; Takatsuki, A.; Imoto, M.; Toyoshima, Y. Y.; Osada, H. *Chem. Biol.* **2003**, *10*, 131. (c) Tarui, Y.; Chinen, T.; Nagumo, Y.; Motoyama, T.; Hayashi, T.; Hirota, H.; Muroi, M.; Ishii, Y.; Kondo, H.; Osada, H.; Usui, T. *ChemBioChem.* **2014**, *14*, 934.

16. (a) Wilson, B. J.; Wilson, C. H. *Science*, **1964**, *144*, 177. (b) Gallagher, R. T.; Clardy, J.; Wilson, B. J. *Tetrahedron Lett.* **1980**, *21*, 239.

17. (a) von Fehr, T.; Acklin, W. *Helv. Chim. Acta* **1966**, *49*, 1907. (b) Springer, J. P.; Clardy, J. *Tetrahedron Lett.* **1980**, *21*, 231.

18. Nozawa, K.; Nakajima, S.; Kawai, K. *J. Chem. Soc. Perkin Trans. 1,* **1988**, 2607.

19. Munday-Finch, S. C.; Wilkins, A. L.; Miles, C. O. *Phytochemistry*, **1996**, *41*, 327.

20. Fan, Y.; Wang, Y.; Liu, P.; Fu, P.; Zhu, T.; Wang, W.; Zhu, W. *J. Nat. Prod.* **2013**, *76*, 1328.

21. Hosoe, T.; Nozawa, K.; Udagawa, S.; Nakajima, S.; Kawai, K. *Chem. Pharm. Bull.* **1990**, *12*, 3473.

22. Miles, C. O.; Wilkins, A. L.; Gallagher, R. T.; Hawkes, A. D.; Munday, S. C.; *J. Agric. Food Chem.* **1992**, *40*, 234.

23. Zhang, Y.-H.; Huang, S.-D.; Pan, H.-Q.; Bian, X.-Q.; Wang, Z.-Y.; Han, A.-H.; Bai, J. *Magn. Reson. Chem.* **2014**, *52*, 306.

24. Belofsky, G. N.; Gloer, J. B.; Wicklow, D. T.; Dowd, P. F. *Tetrahedron*, **1995**, *51*, 3959.

25. Itabashi, T.; Hosoe, T.; Wakana, D.; Fukushima, K.; Takizawa, K.; Yaguchi, T.; Okada, K.; de Campos Takaki, G. M.; Kawai, K. *J. Nat. Med.* **2009**, *63*, 96.

26. Su, S.-S.; Song, A.-H.; Chen, G.; Wang, H.-F.; Li, Z.-Q.; Pei, Y.-Hu. *J. Asian Nat. Prod. Res.* **2014**, *16*, 285.

27. Gao, S.-S.; Li, X.-M.; Williams, K.; Proksch, P.; Ji, N.-Y.; Wang, B.-G. *J. Nat. Prod.* **2016**, *79*, 2066.

28. (a) Laakso, J. A.; TePaske, M. R.; Dowd, P. F.; Gloer, J. B.; Wicklow, D. T. Sulpinine, Secopenitrem B, and Aflatrem B Antiinsectan Metabolites. U.S. Patent Number 5,130,326, July 14, 1992. (b) Laakso, J. A.; Gloer, J. B.; Wicklow, D. T.; Dowd, P. F. *J. Org. Chem.* **1992**, *57*, 2066.

29. Gardner, D. R.; Welch, K. D.; Lee, S. T.; Cook, D.; Riet-Correa, F. *J. Nat. Prod*. **2018**, *81*, 1682.
30. Xu, L.-L.; Hai, P.; Zhang, S.-B.; Xiao, J.-F.; Gao, Y.; Ma, B.-J.; Fu, H.-Y.; Chen, Y.-M.; Yang, X.-L. *J. Nat. Prod*. **2019**, *82*, 221.
31. Zhao, J.-C.; Wang, Y.-L.; Zhang, T.-Y.; Chen, Z.-J.; Yang, T.-M.; Wu, Y.-Y.; Sun, C.-P.; Ma, X.-C.; Zhang, Y.-X. *Phytochemistry*, **2018**, *148*, 21.
32. Zhao, J.-C.; Luan, Z.-L.; Liang, J.-H.; Cheng, Z.-B.; Sun, C.-P.; Wang, Y.-L.; Zhang, M.-Y.; Zhang, T.-Y.; Wang, Y.; Yang, T.-M.; Wu, Y.-Y.; Zhang, X.-Y.; Ma, X.-C. *Biorg. Chem.* **2018**, *79*, 250.
33. Gallagher, R. T.; Finer, J.; Clardy, J. *Tetrahedron Lett*. **1980**, *21*, 235.
34. TePaske, M. R.; Gloer, J. B. *J. Nat. Prod*. **1992**, *55*, 1080.
35. Cole, R. J.; Dorner, J. W.; Lansden, J. A.; Cox, R. H.; Pape, C.; Cunfer, B.; Nicholson, S. S.; Bedell, D. M. *J. Agric. Food Chem*. **1977**, *25*, 1197.
36. Matsui, C.; Ikeda, Y.; Iinuma, H.; Kushida, N.; Kunisada, T.; Simizu, S.; Umezawa, K. *J. Antibiot.* **2014**, *67*, 787.
37. Xu, M.; Gessner, G.; Groth, I.; Lange, C.; Christner, A.; Bruhn, T.; Deng, Z.; Li, X.; Heinemann, S. H.; Grabley, S.; Bringmann, G.; Sattler, I.; Lin, W. **Tetrahedron**, *2007*, *63*, 435.
38. Babu, J. V.; Popay, A. J.; Miles, C. O.; Wilkins, A. L.; di Menna, M. E.; Finch, S. C. *J. Agric. Food Chem.* **2018**, *66*, 13116.
39. Wilkins, A. L.; Miles, C. O.; Ede, R. M.; Gallagher, R. T.; Munday, S. C. *J. Agric. Food. Chem.* **1992**, *40*, 1307.
40. Penn, J.; Swift, R.; Wigley, L. J.; Mantle, P. G.; Bilton, J. N.; Sheppard, R. N. *Phytochemistry*, **1993**, *32*, 1431.
41. Munday-Finch, S. C.; Wilkins, A. L.; Miles, C. O. *J. Agric. Food Chem*. **1998**, *46*, 590.
42. Munday-Finch, S. C.; Miles, C. O.; Wilkins, A. L.; Hawkes, A. D. *J. Agric. Food Chem*. **1995**, *43*, 1283.
43. Munday-Finch, S. C.; Wilkins, A. L.; Miles, C. O.; Ede, R. M.; Thomson, R. A. *J. Agric. Food Chem.* **1996**, *44*, 2782.
44. Miles, C. O.; Finch, S. C.; Wilkins, A. L.; Ede, R. M.; Towers, N. R. *J. Agric. Food Chem.* **1994**, *42*, 1488.
45. Yamaguchi, T.; Nozakawa, K.; Hosoe, T.; Nakajima, S.; Kawai, K. *Phytochemistry*, **1993**, *32*, 1177.
46. Zhang, P.; Li, X.-M.; Li, X.; Wang, B.-G. *Phytochem. Lett*. **2015**, *12*, 182.
47. Penn, J.; Biddle, J. R.; Mantle, P. G.; Bilton, J. N.; Sheppard, R. N. *J. Chem. Soc. Perkin Tran. 1*, **1992**, 23.
48. Naik, J. T.; Mantle, P. G.; Sheppard, R. N.; Waight, E. S. *J. Chem. Soc. Perkin Trans. 1*, **1995**, 1121.
49. Fan, Y.; Wang, Y.; Fu, P.; Chairoungdua, A.; Piyachaturawat, P.; Zhu, W. *Org. Chem. Front*. **2018**, *5*, 2835.
50. Kong, F.-D.; Fan, P.; Zhou, L.-M.; Ma, Q.-Y.; Xie, Q.-Y.; Zheng, H.-Z.; Zheng, Z.-H.; Zhang, R.-S.; Yuan, J.-Z.; Dai, H.-F.; Luo, D.-Q.; Zhao, Y.-X. *Org. Lett*. **2019**, *21*, 4864.
51. Kimura, Y.; Nishibe, M.; Nakajima, H.; Hamasaki, T.; Shigemitsu, N.; Sugawara, F.; Stout, T. J.; Clardy, J. *Tetrahedron Lett*. **1992**, *33*, 6987.
52. Elsbaey, M.; Tanaka, C.; Miyamoto, T. *Phytochem. Lett*. **2019**, *32*, 70.
53. Nozawa, K.; Nakajima, S.; Kawai, K. *J. Chem. Soc. Perkin Trans. 1,* **1988**, 1689.

54. Nozawa, K.; Yuyama, M.; Nakajima, S.; Kawai, K. *J. Chem. Soc. Perkin Trans. 1,* **1988**, 2155.

55. Hosoe, T.; Itabashi, T.; Kobayashi, N.; Udagawa, S.; Kawai, K. *Chem. Pharm. Bull*. **2006**, *54*, 185.

56. Roll, D. M.; Barbieri, L. R.; Bigelis, R.; McDonald, L. A.; Arias, D. A.; Chang, L.-P.; Singh, M. P.; Luckman, S. W.; Berrodin, T. J.; Yudt, M. R. *J. Nat. Prod*. **2009**, *72*, 1944.

57. Li, C.; Gloer, J. B.; Wicklow, D. T.; Dowd, P. F. *Org. Lett*. **2002**, *4*, 3095.

58. (a) Uchida, R.; Kim, Y.-P.; Namatame, I.; Tomoda, H.; Ōmura, S. *J. Antibiot*. **2006**, *59*, 93. (b) Uchida, R.; Kim, Y.-P.; Nagamitsu, T.; Tomoda, H.; Ōmura, S. *J. Antibiot.* **2006**, *59*, 338.

59. (a) Acklin, W.; Weibel, F.; Arigoni, D. *Chimia*, **1977**, *31*, 63. (b) de Jesus, A. E.; Gorst-Allman, C. P.; Steyn, P. S.; van Heerden, F. R.; Vieggaar, R.; Wessels, P. L.; Hull, W. E. *J. Chem. Soc., Perkin Trans*. **1983**, 1863.

60. Fueki, S.; Tokiwano, T.; Toshima, H.; Oikawa, H. *Org. Lett.* **2004**, *6*, 2697.

61. Laws, I., Mantle, P.G. *J. Gen. Microbiol* **1989**, *135*, 2679.

62. Byrne, K. M.; Smith, S. K.; Ondeyka, J. G. *J. Am. Chem. Soc.* **2002**, *124*, 7055.

63. (a) Young, C.; McMillan, L.; Telfer, E.; Scott, B. *Mol. Microbio*. **2001**, *39*, 754. (b) Saika, S.; Parker, E. J.; Koulman, A.; Scott, B. *FEBS Lett*. **2006**, *580*, 1625.

64. For summaries of the biosynthesis of PIDs and the roles of gene clusters, see: (a) Nicholson, M. J.; Eaton, C. A.; Stärkel, C.; Tapper, B. A.; Cox, M. P.; Scott, B. *Toxins*, **2015**, *7*, 2701. (b) Matsuda, Y.; Abe, I. *Nat. Prod. Rep*. **2016**, *33*, 26. and references therein.

65. (a) Van de Bittner, K. C.; Nicholson, M. J.; Bustamante, L. Y.; Kessans, S. A.; Ram, A.; van Dolleweerd, C. J.; Scott, B.; Parker, E. J. *J. Am. Chem. Soc*. **2018**, *140*, 582. (b) Van de Bittner, K. C.; Cameron, R. C.; Bustamante, L. Y.; Bundela, R.; Kessans, S. A.; Vorster, J.; Nicholson, M. J.; Parker, E. J. *Med. Chem. Commun.* **2019,** *10,* 1160.

66. Tagami, K.; Liu, C.; Minami, A.; Noike, M.; Isaka, T.; Fueki, S.; Shichijo, Y.; Toshima, H.; Gomi, K.; Dairi, T.; Oikawa, H. *J. Am. Chem. Soc.* **2013**, *135*, 1260.

67. (a) L. McMillan, R. Carr, C. Young, J. Astin, R. Lowe, E. Parker, G. Jameson, S. Finch, C. Miles, O. McManus, W. A. Schmalhofer, M. L. Garcia, G. J. Kaczorowski, M. Goetz, J. S. Tkacz and B. Scott, *Mol. Genet. Genomics*, **2003**, *270*, 9. (b) Saikia, S.; Parker, E. J.; Koulman, A.; Scott, B. *J. Biol. Chem*. **2007**, *282*, 16829.

68. Motoyama, T.; Hayashi, T.; Hirota, H.; Ueki, M. Osada, H. *Chem. Biol*. **2012**, *19*, 1611.

69. Nicholson, M. J.; Koulman, A.; Monahan, B. J.; Pritchard, B. L.; Payne, G. A.; Scott, B. *Applied Environ. Sci*. **2009**, *75*, 7469.

70. (a) Young, C. A.; Bryant, M. K.; Christensen, M. J.; Tapper, B. A.; Bryan, G. T.; Scott, B. *Mol. Genet. Genomics* **2005**, *274*, 13. (b) Young, C. A.; Felitti, S.; Shields, K.; Spangenberg, G.; Johnson, R. D.; Bryan, G. T.; Saika, S.; Scott, B. *Fungal. Genet. Biol*. **2006**, *43*, 679. (c) Saikia, S.; Takemoto, D.; Tapper, B. A.; Lane, G. A.; Fraser, K.; Scott, B. *FEBS Lett*. **2012**, *586*, 2563.

71. Liu, C.; Minami, A.; Dairi, T.; Gomi, K.; Scott, B.; Oikawa, H. *Org. Lett*. **2016**, *18*, 5026.

72. Liu, C.; Tagami, K.; Minami, A.; Matsumoto, T.; Frisvad, J. C.; Suzuki, H.; Ishikawa, J.; Gomi, K.; Oikawa, H. *Angew. Chem., Int. Ed*. **2015**, 54, 5748.

73. Mewshaw, R. Smith, A. B., III. *J. Am. Chem. Soc*. **1985**, *107*, 1769.

74. Zou, Y.; Smith, A. B., III. *J. Antibiot*. **2018**, *71*, 185.

75. (a) Hajos, Z. G.; Parrish, D. R. *J. Org. Chem*. **1974**, *39*, 1615. (b) Eder, U.; Sauer, G.; Wiechert, R. *Angew. Chem., Int. Ed. Engl*. **1971**, *10*, 496.

76. Baudin, G.; Pietrasanta, Y. *Tetrahedron* **1973**, *29*, 4225.

77. Kirk, D. N.; Petrow, V. *J. Chem. Soc*. **1962**, 1091.

78. Smith, A. B., III.; Mewshaw, R. *J. Org. Chem*. **1984**, *49*, 3685.

79. Islam, A.M.; Raphael, R. A. *J. Chem. Soc*. **1953**, 2247

80. Gassman, P. G.; van Bergen, T. J.; Gilbert, D. P.; Cue, B. W., Jr. *J. Am. Chem. Soc*. **1974**, *96*, 5495.

81. (a) Smith, A.B., III.; Leenay, T.L. *Tetrahedron Lett*. **1988**, *29*, 2787. (b) Smith, A.B., III.; Leenay, T.L. *Tetrahedron Lett*. **1988**, *29*, 2791.

82. Buchschacher, P.; Furst, A. *Org. Synth*. **1984**, *63*, 37.

83. Jung, M. *Tetrahedron* **1976**, *32*, 3.

84. Luche, J. L.; Petrier, C.; Lansard, J. P.; Greene, A. E. *J. Org. Chem*. **1983**, *48*, 3837.

85. (a) Smith, A. B., III.; Sunazuka, T.; Leenay, T.L.; Kingery-Wood, J. *J. Am. Chem. Soc*. **1990**, *112*, 8197. (b) Smith, A. B., III.; Kingery-Wood, J.; Leenay, T. L.; Nolen, E. G.; Sunazuka, T. *J. Am. Chem. Soc*. **1992**, *114*, 1438.

86. Stork, G.; Benaim, J. *J. Am. Chem. Soc*. **1971,** *93,* 5938.

87. Gao, Y.; Hanson, R. M.; Klunder, J. M.; Ko, S. Y.; Masamune, H.; Sharpless, K. B. *J. Am. Chem. Soc*. **1987**, *109*, 5765.

88. (a) Clive, D. L. J.; Joussef, A. C. *J. Org. Chem*. **1990**, *55,* 1096. (b) Grieco. P.A.; Nishizawa. M.; Marinovic. N.; Ehmann, W. J. *J. Am. Chem. Soc*. **1976**, *98.* 7102.

89. (a) Smith, A. B., III.; Kanoh, N.; Haruaki, I.; Hartz, R. A. *J. Am. Chem. Soc*. **2000**, *122*, 11254. (b) Smith, A. B., III.; Kanoh, N.; Haruaki, I.; Minakawa, N.; Rainier, J. D.; Hartz, R. A.; Cho, Y. S.; Cui, H.; Moser, W. H. *J. Am. Chem. Soc*. **2003**, *135*, 8228.

90. (a) Smith, A. B., III; Visnick, M. *Tetrahedron Lett*. **1985**, *26*, 3757. (b) Smith, A. B., III; Visnick, M.; Haseltine, J. N.; Sprengeler, P. A. *Tetrahedron* **1986**, *42*, 2957.

91. For preparation of lactone **1.204**, see: Smith, A. B., III.; Hartz, R. A.; Spoors, P. G.; Rainier, J. D. *Israel J. Chem*. **1997**, *37*, 69.

92. Guile, S. D.; Saxton, J. E.; Thornton-Pett, M *J. Chem. Soc. Perkin Trans. 1,* **1992**, 1763.

93. For a review of the cyclopropanation of allylic alcohols with iodomethyl- zinc reagents, see: Charette, A.B.; Marcoux J.-F. *Synlett* **1995**, 1197

94. (a) Dauben, W. G.; Deviny, E. J. *J. Org. Chem*. **1966**, *31*, 3794. (b) Stork, G.; Uyeo, S.; Wakamatsu, T.; Grieco, P.; Labovitz, J. *J. Am. Chem. Soc*. **1971**, *93*, 4945.

95. Comins, D.L.; Dehghani, A *Tetrahedron Lett*. **1992***, 33*, 6299.

96. Nicolaou, K. C.; Hwang, C.-K.; Nugiel, D. A. *J. Am. Chem. Soc*. **1989**, *111*, 4136.

97. For preparation of enone **1.241**, see: Smith, A. B., III; Nolen, E. G., Jr.; Shirai, R.; Blase, F. R.; Ohta, M.; Chida, N.; Hartz, R. A.; Fitch, D. M.; Clark, W. M.; Sprengeler, P. A. *J. Org. Chem*. **1995**, *60*, 7837.

98. (a) Shirai, R.; Tanaka, M.; Koga, K. *J. Am. Chem. Soc*. **1986**, *108*, 543. (b) Whitesell, J. K.; Felmen, S. W. *J. Org. Chem*. **1980**, *45*, 755,

99. (a) Ito, Y.; Hirato, T.; Saegusa, T. *J. J. Org. Chem*. **1978**, *43*, 1011. (b) Fridrich, E.; Lutz, W. *Angew. Chem., Int. Ed*. **1977**, *16*, 413.

100. Smith, A. B., III; Haseltine, J. H.; Visnick, M. *Tetrahedron,* **1989**, *45*, 2431.

101. (a) Shunk, H.; Wilds, A. L. *J. Am. Chem. Soc*. **1949**, *71*, 3946. (b) Woodward, R. B.; Sondheimer, F.; Taub, D.; Heusler, K.; McLamore, W. M. *J. Am. Chem. Soc*. **1952**, *74*, 4223.

102. (a) Semmler, W. *Chem. Ber*. **1892**, *25*, 3352-3354. (b) Wolff, L. *Annalen* **1902**, *322*, 351.

103. Parikh, J. R.; Doering, W. E.; *J. Am. Chem. Soc*. **1967**, *89*, 5505.

104. (a) Grieco, P. A.; Gilman, S.; Nishizawa, M. *J. Org. Chem*. **1976**, *41*, 1485. (b) Sharpless, K. B.; Young, M. W. J. *Org. Chem*. **1975**, *40*, 947.

105. (a) Smith, A. B., III; Cui, H. Helv. Chim. Acta 2003, 86, 3908. (b) Smith, A. B., III; Cui, H. *Org. Lett*. **2003**, 5, 587.

106. Barton, D. H. R.; Kitchin, J. P.; Lester, D. J.; Motherwell, W. B.; Papoula, M. T. B. *Tetrahedron*, **1981**, 37, 73.

107. Rainier, J. D.; Smith, A. B., III. *Tetrahedron Lett*. **2000**, *41*, 9419.

108. Kato, T.; Takayanagi, H.; Uyehara, T.; Kitihara, Y. *Chem. Lett*. **1977**, 1009.

109. Jackson A. H.; Smith, P. *Tetrahedron* **1968**, *24*, 2227.

110. Nicolaou, K. C.; Duggan, M. E.; Ladduwahetty, T. *Tetrahedron Lett*. **1984**, 25, 2069.

111. Oikawa, M.; Hashimoto, R.; Sasaki, M. *Eur. J. Org. Chem*. **2011**, 538.

112. Lan, J.; Liu, Z.; Yuan, H.; Peng, L.; Li, W.-D. Z.; Li, Y.; Li, Y.; Chan, A. C. S. *Tetrahedron Lett.* **2000**, *41*, 2181.

113. (a) Yanagisawa, A.; Habaue, S.; Yasue, K.; Yamamoto, H.; *J. Am. Chem. Soc*. **1994**, *116*, 6130. (b) Wilson, S. R.; Haque, M. S.; Misra, R. N. *J. Org. Chem*. **1982**, *47*, 747.

114. Frigerio, M.; Santagostino, M. *Tetrahedron Lett*. **1994**, *35*, 8019.

115. Scholl, M.; Ding, S. Lee, C. W.; Grubbs, R. H. *Org. Lett*. **1999**, *1,* 953.

116. Wang, Z.-X.; Tu, Y.; Frohn, M.; Zhang, J.-R.; Shi, Y. *J. Am. Chem. Soc*. **1997**, *119*, 11224.

117. (a) Ali, A.; Saxton, J. E. *Tetrahedron Lett*. **1989**, *30*, 3197. (b) Ali, A.; Guile, S. D.; Saxton, J. E.; Thornton-Pett, M. *Tetrahedron*, **1991**, *47*, 6407.

118. Achmatowicz, O.; Bukowski, P.; Szechner, B.; Zwierzchoska, Z.; Zamojski, A. *Tetrahedron*, **1973**, *27*, 1973.

119. Poss, A. J.; Belter, R. K. *J. Org. Chem*. **1987**, *52*, 4810.

120. Corey, E. J.; Virgil, S. C. *J. Am. Chem. Soc*. **1990**, *112*, 6429.

121. Enomoto, M.; Morita, A.; Kuwahara, S. *Angew. Chem., Int. Ed*. **2012**, *51*, 12833.

122. Harrington, P. J.; Hegedus, L. S.; McDaniel, K. F. *J. Am. Chem. Soc*. **1987**, *109*, 4335.

123. Tsuji, T.; Minami, I.; Shimizu, I. *Tetrahedron Lett*. **1983**, *24*, 1793.

124. Kuwaraha also used intermediate **1.318** in a synthesis of JBIR-03: Murokawa, T.; Enomoto, M.; Teranishi, T.; Ogura, Y.; Kuwahara, S. *Tetrahedron Lett*. **2018**, *59*, 4107.

125. (a) Sharpless, K. B.; Amberg, W.; Bennani, Y. L.; Crispino, G. A.; Hartung, J.; Jeong, K.-S.; Kwong, H.-L.; Morikawa, K.; Wang, Z.-M.; Xu, D.; Zhang, X.-L. *J. Org. Chem*. **1992**, *57*, 2768. (b) Vanhessche, K. P. M.; Wang, Z.-M.; Sharpless, K. B. *Tetrahedron Lett*. **1994**, *35*, 3469

126. Sharpless, K. B.; Lauer, R. F. *J. Am. Chem. Soc*. **1973**, *95*, 2697.

127. Asanuma, A.; Enomoto, M; Nagasawa, T.; Kuwahara, S. *Tetrahedron Lett*. **2013**, *54*, 4561.

128. (a) Teranishi, T.; Kuwahara, S. Tetrahedron Lett. 2014, 55, 1486. (b) Teranishi, T.; Murokawa, T.; Enomoto, M.; Kuwahara, S. *Biosci., Biotechnol., Biochem*. **2015**, *79*, 11.

129. (a) Uma, M. R.; Swaminathan, S.; Rajagopalan, K. *Tetrahedron Lett*. **1984**, *25*, 5825. (b) Hagiwara, H.; Uda, H. *J. Org. Chem*. **1988**, *53*, 2308.

130. Curruca, F.; Fousteris, M.; Ishikawa, Y.; Rekowski, M. W.; Hounsou, C.; Surrey, T.; Giannis, A. *Org. Lett*. **2010**, *12*, 2096.

131. (a) Habermas, K. L.; Denmark, S. E.; Jones, T. K. *Org. React*. **1994**, *45*, 1. (b) Pellissier, H. *Tetrahedron* **2005**, *61*, 6479. (c) Frontier, A. J.; Collison, C. *Tetrahedron* **2005**, *61*, 7577.

132. Matsuo, J.; Aizawa, Y. *Tetrahedron Lett*. **2005**, *46*, 407.

133. Miyashita, M.; Suzuki, T.; Hoshino, M.; Yoshikoshi, A. *Tetrahedron* **1997**, *53*, 12469.

134. Giannis' report predates Kuwahara's synthesis of terpendole E (reference 121), thus the more efficient Wittig reaction-epoxidation sequence was presumably unknown to Giannis.

135. (a) Sharpe, R. J.; Johnson, J. S. *J. Am. Chem. Soc*. **2015**, *137*, 4968. (b) Sharpe, R. J.; Johnson, J. S. *J. Org. Chem*. **2015**, *137*, 15410.

136. Sharpe, R. J.; Portillo, M.; Vélez, R. A.; Johnson, J. S. *Synlett*. **2015**, *26*, 2293.

137. (a) Watanabe, H.; Iwamoto, M.; Nakada, M. *J. Org. Chem*. **2005**, *70*, 4652. (b) Katoh, T.; Mizumoto, S.; Fudesaka, M.; Nakashima, Y.; Kajimoto, T.; Node, M. *Synlett* **2006**, 2176. (c) Katoh, T.; Mizumoto, S.; Fudesaka, M.; Takeo, M.; Kajimoto, T.; Node, M. *Tetrahedron: Asymmetry* **2006**, *17*, 1655.

138. Shapiro, R. H.; Heath, M. J. *J. Am. Chem. Soc*. **1967**, *89*, 5734.

139. (a) Ireland, R. E.; Mueller, R. H. *J. Am. Chem. Soc*. **1972**, *94*, 5897. (b) Ireland, R. E.; Mueller, R. H.; Willard, A. K. *J. Am. Chem. Soc*. **1976**, *98*, 2868.

140. (a) Desai, L. V.; Hull, K. L.; Sanford, M. S. *J. Am. Chem. Soc*. **2004**, *126*, 9542. (b) Neufeldt, S. R.; Sanford, M. S. *Org. Lett*. **2010**, *12*, 532.

141. (a) Evans, D. A.; Morrissey, M. *J. Am. Chem. Soc*. **1984**, *106*, 3866. (b) Evans, D. A.; Morrissey, M. *Tetrahedron Lett*. **1984**, *25*, 4637.

142. Kim, D. E.; Zweig, J. E.; Newhouse, T. R. *J. Am. Chem. Soc*. **2019**, *141*, 1479.

143. (a) Iwasaki, K.; Wan, K. K.; Oppedisano, A.; Crossley, S. W. M.; Shenvi, R. A. *J. Am. Chem. Soc*. **2014**, *136*, 1300. (b) King, S. M.; Ma, X.; Herzon, S. B. *J. Am. Chem. Soc*. **2014**, *136*, 6884.

144. Luzung, M. R.; Lewis, C. A.; Baran, P. S. *Angew. Chem., Int. Ed*. **2009**, *48*, 7025.

145. (a) Sugino, K.; Nakazaki, A.; Isobe, M.; Nishikawa, T. *Synlett*. **2011**, 647. (b) Adachi, M; Higuchi, K.; Thasana, N.; Yamada, Y.; Nishikawa, T. *Org. Lett*. **2012**, *14*, 114. (c) Ono, Y.; Nakazaki, A.; Ueki, K.; Higuchi, K.; Sriphana, U.; Adachi, M.; Nishikawa, T. *J. Org. Chem*. **2019**, *84*, 9750.

146. Mori, K.; Amaike, M.; Itou, M. *Tetrahedron* **1993**, *49*, 1871.

147. (a) Corey, E. J.; Fuchs, P. L. *Tetrahedron Lett*. **1972**, *13,* 3769. (b) Armstrong, A.; Bhonoah, Y.; Shanahan, S. E. *J. Org. Chem*. **2007**, *72*, 8019. (c) Frye, L. L.; Robinson, C. H. *J. Org. Chem*. **1990**, *55*, 1579.

148. Zou, Y.; Lobera, M.; Snider, B. B. *J. Org. Chem*. **2005**, *70*, 1761.

149. Smith, A. B., III; Davulcu, A. H.; Kürti, L. *Org. Lett*. **2006**, *8*, 1665.

150. (a) Smith, A. B., III; Cho, Y. S.; Ishiyama, H.; *Org. Lett*. **2001**, *3*, 3971. (b) Smith, A. B., III; Davulcu, A. H.; Cho, Y. S.; Ohmoto, K.; Kürti, L.; Ishiyama, H. *J. Org. Chem*. **2007**, *72*, 4596.

151. (a) Scott, W. J.; Crisp, G. T.; Stille, J. K. *J. Am. Chem. Soc*. **1984,** *106*, 4630. (b) Cacchi, S.; Morera, E.; Ortar, G. *Tetrahedron Lett*. **1985**, *26*, 1109.

152. Kogen, H.; Tomioka, K.; Hashimoto, S.; Koga, K. *Tetrahedron* **1981**, *37*, 3951.

153. For complete preparation of lactone **1.446**, see reference 150(a).

154. de Nooy, A. E. J.; Basemer, A. C.; van Bekkum, H. *Synthesis* **1996**, 1153.

155. For an updated procedure to indole **1.452**, see reference 150(b).

156. Sabat, M.; Johnson, C. *Org. Lett*. **2000**, *2*, 1089.

157. (a) Barluenga, J.; Fernandez, M. A.; Aznar, F.; Valdes, C. *Chem. Eur. J*. **2005**, *11*, 2276. (b) Barluenga, J.; Valdes, C. *Chem. Commun*. **2005**, 4891.

158. Zou, Y.; Melvin, J. E.; Gonzales, S. S.; Spafford, M. J.; Smith, A. B., III. *J. Am. Chem. Soc*. **2015**, *137*, 7095.

159. (a) Corey, E. J.; Boaz, N. W. *Tetrahedron Lett*. **1984**, *25*, 3063. (b) Corey, E. J.; Boaz, N.

W. *Tetrahedron Lett*. **1985**, *26*, 6015. (c) Normant, J. F.; Bourgain, M. *Tetrahedron Lett.* **1971**, *12*, 2583.

160. Corey, E. J.; Suggs, J. W. *Tetrahedron Lett*. **1975**, *16*, 2647.

161. De Mico, A.; Margarita, R.; Parlanti, L.; Vescovi, A.; Piancatelli, G. *J. Org. Chem.* **1997**, *62*, 6974.

162. Garegg, P. J.; Samuelsson, B. *J. Chem. Soc., Chem. Commun*. **1979**, 978.

163. Enders, D.; Zamponi, A.; Raabe, G.; Runsink, J. *Synthesis* **1993**, *1993*, 725.

164. Kajigaeshi, S.; Kakinami, T.; Yamasaki, H.; Fujisaki, S.; Kondo, M.; Okamoto, T. *Chem. Lett*. **1987**, *16*, 2109.

165. (a) Ross Kelly, T.; Li, Q.; Bhushan, V. *Tetrahedron Lett*. **1990**, *31*, 161. (b) Sheffy, F. K.; Godschalx, J. P.; Stille, J. K. *J. Am. Chem. Soc*. **1984**, *106*, 4833. (c) Azarian, D.; Dua, S. S.; Eaborn, C.; Walton, D. R. M. *J. Organomet. Chem*. **1976**, *117*, C55.

166. (a) Bruno, N. C.; Tudge, M. T.; Buchwald, S. L. *Chem. Sci*. **2013**, *4*, 916. (b) Kinzel, T.; Zhang, Y.; Buchwald, S. L. *J. Am. Chem. Soc*. **2010**, *132*, 14073. (c) Biscoe, M. R.; Fors, B. P.; Buchwald, S. L. *J. Am. Chem. Soc*. **2008**, *130*, 6686.

167. (a) Horner, L.; Hoffmann, H.; Wippel, H. G. Chem. Ber. 1958, 91, 61. (b) Wadsworth, W. S.; Emmons, W. D. *J. Am. Chem. Soc*. **1961**, *83*, 1733.

168. Zou, Y.; Li, X.; Yang, Y.; Berritt, S.; Melvin, J.; Gonzales, S.; Spafford, M.; Smith, A. B., III. *J. Am. Chem. Soc*. **2018**, *140*, 9502.

169. Enders, D.; Kipphardt, H.; Fey, P.; Guzmań, B.; Hall, S. S.; Saucy, G. *Org. Synth*. **2003**, 183.

170. (a) Okude, Y.; Hirano, S.; Hiyama, T.; Nozaki, H. *J. Am. Chem. Soc*. **1977**, *99*, 3179. (b) Takai, K.; Kimura, K.; Kuroda, T.; Hiyama, T.; Nozaki, H. *Tetrahedron Lett*. **1983**, *24*, 5281. (c) Jin, H.; Uenishi, J.; Christ, W. J.; Kishi, Y. J. Am. Chem. Soc. 1986, 108, 5644.

171. Normant, J. F. *Synthesis* **1972**, *1972*, 63.

172. (a) Guram, A. S.; King, A. O.; Allen, J. G.; Wang, X.; Schenkel, L. B.; Chan, J.; Bunel, E. E.; Faul, M. M.; Larsen, R. D.; Martinelli, M. J.; Reider, P. J. *Org. Lett*. **2006**, *8*, 1787. (b) Guram, A. S.; Wang, X.; Bunel, E. E.; Faul, M. M.; Larsen, R. D.; Martinelli, M. J. *J. Org. Chem*. **2007**, *72*, 5104.

173. (a) Smith, A. B., III; Kürti, L.; Davulcu, A. H. Org. Lett. 2006, 8, 2167. (b) Smith, A. B., III; Kürti, L.; Davulcu, A. H.; Cho, Y. S.; Ohmoto, K. *J. Org. Chem*. **2007**, *72*, 4611.

174. (a) Tsuji, J.; Takahashi, H.; Morikawa, M. *Tetrahedron Lett*. **1965**, *6*, 4387. (b) Trost, B. M.; Fullerton, T. J. *J. Am. Chem. Soc*. **1973**, *95*, 292. (c) Trost, B. M. *Tetrahedron* **2015**, *71*, 5708.

175. (a) Amatore, C.; Geńin, E.; Jutand, A.; Mensah, L. *Organometallics* **2007**, *26*, 1875. (b) Caminiti, N. S.; Goodstein, M. B.; Leibler, I. N. M.; Holtzman, B. S.; Jia, Z. B.; Martini, M. L.; Nelson, N. C.; Bunt, R. C. *Tetrahedron Lett*. **2015**, *56*, 5445.

176. Teichert, J. F.; Feringa, B. L. *Angew. Chem., Int. Ed*. **2010**, *49*, 2486.

177. George, D. T.; Kuenstner, E. J., Pronin, S. V. *J. Am. Chem. Soc*. **2015,** *137,* 15410.

178. Holmbo, S. D.; Godfrey, N. A.; Hirner, J. J.; Pronin, S. V. *J. Am. Chem. Soc*. **2016**, *138*, 12316.

179. Umbreit, M. A.; Sharpless, K. B. *J. Am. Chem. Soc*. **1977**, *99*, 5526.

180. Vaswani, R. G.; Day, J. J.; Wood, J. L. *Org. Lett*. **2009**, *11*, 4532.

181. (a) Lo, J. C.; Yabe, Y.; Baran, P. S. *J. Am. Chem. Soc*. **2014**, *136*, 1304. (b) Lo, J. C.; Gui, J.; Yabe, Y.; Pan, C.–M.; Baran, P. S. *Nature*, **2014**, *516*, 343. (c) Lo, J. C.; Kim, D.; Pan, C.–M.; Edward, J. T.; Yabe, Y.; Gui, J. Qin, T.; Gutiérrez, S.; Giacoboni, J.; Smith, M. W.;

Holland, P. L.; Baran, P. S. *J. Am. Chem. Soc.* **2017**, *139*, 2484.

182. Obradors, C.; Martinez, R. M.; Shenvi, R. A. *J. Am. Chem. Soc.* **2016**, *138*, 4962.

183. Lau, K. S. Y.; Schlosser, M. *J. Org. Chem*. **1978**, *43*, 1595.

184. Yoshi, Y.; Otsu, T.; Hosokawa, N.; Takasu, K.; Okano, K.; Tokuyama, H. *Chem. Commun*. **2015**, *51*, 1070.

185. M. Catellani and M. C. Fagnola, *Angew. Chem., Int. Ed*. **1994**, *33*, 2421; (b) M. Lautens and S. Piguel, *Angew. Chem., Int. Ed*. **2000**, *39*, 1045.

186. E. García-Urdiales, I. Alfonso and V. Gotor, *Chem. Rev*., **2005**, *105*, 313.

187. England, D. B.; Magolan, J.; Kerr. M. A. *Org. Lett*. **2006**, *8*, 2209.

188. Little, R. D.; Dawson, J. R. *Tetrahedron Lett.* **1980**, 2609.

189. England, D. B.; Kerr, M. A. *J. Org. Chem*. **2005**, *70*, 6519.

190. Nicolaou, K. C.; Lysenko, Z. *Tetrahedron Lett.* **1977**, 1257

191. Magnus, P.; Mansley, T. E. *Tetrahedron Lett.* **1999**, *40*, 6909.

192. (a) Oppolzer, W.; Snieckus, V. *Angew. Chem., Int. Ed*. **1978**, *17*, 476. (b) Andersen, N. H.; Hadley, S. W.; Kelly, J. D.; Bacon, E. R. *J. Org. Chem*. **1985**, *50*, 4144.

Chapter 2: Total Synthesis of (–)-Nodulisporic Acid C

2.1 The Nodulisporic Acids: Target Introduction and Synthetic Planning

2.1.1 Isolation and Biological Activity

In 1997, Ondeyka and co-workers at Merck disclosed the structure and bioactivity of nodulisporic acid A, (**2.1**, Figure 2.1).[1] What garnered this molecule immediate attention was the high binding affinity towards chloride ion channels found in arthropods.[2] Using ivermectin as a benchmark (LC_{50} of 0.02 and 0.045 ppb respectively), nodulisporic acid A performed admirably at 0.5 and 0.3 ppm in each assay.[3] Of further note was the inactivity of paxilline (25 and 250 ppm respectively). Meinke and co-workers determined nodulisporic acid A binds a subset of ligand gated ion channels modulated by ivermectin.[2] Opening of these channels leads to cell hyperpolarization, which in turn causes paralysis, starvation and death of the organism. While fatal to invertebrates, these ion channels do not exist within mammalian cells and no toxicity has been observed for orally treated dogs and cats at concentrations 10 times higher than needed to treat infestation.[4] These results corroborate that the differences in bioactivity with paxilline, which does have strong tremorgenic activity in mammals[5], stem from separate binding sites.

Figure 2.1 Nodulisporic Acid A and Development Candidate *N-tert*-butyl Nodulisporamide

nodulisporic acid A (**2.1**)   *N-tert*-butyl nodulisporamide (**2.2**)
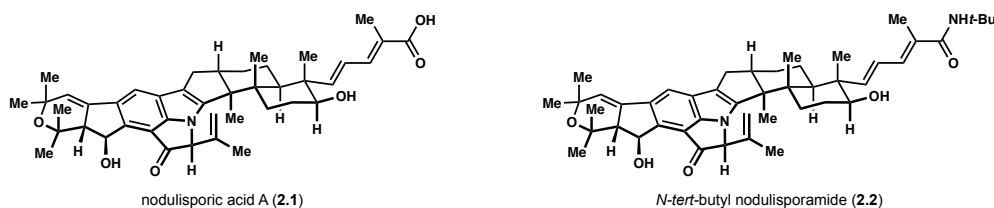
Further isolation efforts revealed several other congeners, none of which outperformed the flagship congener **2.1**.[6] Nonetheless, the appealing profile of **2.1** instigated further structure-activity relationship studies with the purpose of developing an orally available flea and tick treatment for companion animals.[7] Merck quickly found that modifications to the oxidation state

at any position on the polycyclic core led to substantial decreases in the observed activity.[6] In contrast, converting the carboxylic acid moiety into other functional groups, particularly amides, could enhance efficacy against fleas. From a library of over 300 nodulisporamides, *N-tert*-butyl nodulisporamide (**2.2**) was identified as the most promising candidate for development, increasing potency by an order of magnitude compared to **2.1**.[7] Since that report in 2009, no further studies have been disclosed pertaining to commercialization of a nodulisporic acid derived molecule.

2.1.2 Prior Studies and Retrosynthetic Analysis

Shortly after Merck disclosed nodulisporic acid A, Smith initiated a research program focusing on these targets that has spanned the course of two decades thus far. The work performed in his lab has culminated in the syntheses of nodulisporic acids F,[9] D,[10] C,[11] and B.[11] Along with his studies on the broader family of paxilline indole diterpenes (PIDs), these reports informed the community on key challenges associated with synthetic construction of these molecules.[12] As highlighted by Smith's synthesis of nodulisporic acid B (**2.3**) in Chapter 1, the tetrahydropyrole ring system introduces significant strain to the system[13], which Smith overcame utilizing a palladium catalyzed indole allylation (Scheme 2.1). Additionally, Smith employed an efficient coupling of chloroaniline **2.4** and vinyltriflate **2.5** to construct the indole late stage. The lability of the benzylic alcohol and the challenging stereotriad of C12, C3 and C4 forming the *trans-*

Scheme 2.1 Smith's Key Disconnections and Stereoselective Bond Formations

nodulisporic acid B (**2.3**)

• N1–C2': indole allylation

2.4

• C23 and C24: Enders alkylation
• C16–C17: NHK reaction

2.5

• C9 and C8: conjugate reduction–alkylation
• C12 and C3: conjugate addition–methylation

(+)-Wieland–Miescher ketone (**2.6**)
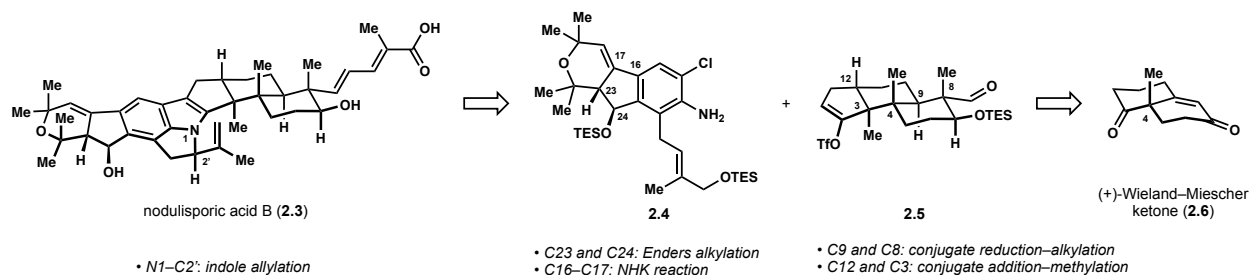
hydrindane are also noted in many of Smith's studies.[12] Despite three decades of evolution, Smith's strategy to tricyclic intermediate **2.5** alone requires twenty steps to access.[9,10,14]

Our synthetic program surrounding the paxilline indole diterpenes arose through the possibility of an efficient polycyclization strategy to access the terpenoid core of these molecules. The advent of an iron mediated hydrogen atom transfer (HAT) process has allowed for chemoselective reduction of electron rich alkenes at a faster rate than electron deficient ones.[15] We initially hypothesized that this reactivity would allow generation of tertiary alkyl radical **2.8** from 1,1-disubstituted alkene **2.7** (Scheme 2.2). An intramolecular conjugate addition would then form the C4-C9 bond, whereby radical reactivity would ease formation of this congested system.[16] Reduction of the resulting enol radical to leave enolate **2.9** and aldol addition would complete formation of a tricyclic core **2.10** found throughout the paspaline-type PIDs.[17]

Scheme 2.2 Hypothesized Construction of a Common Terpenoid Core
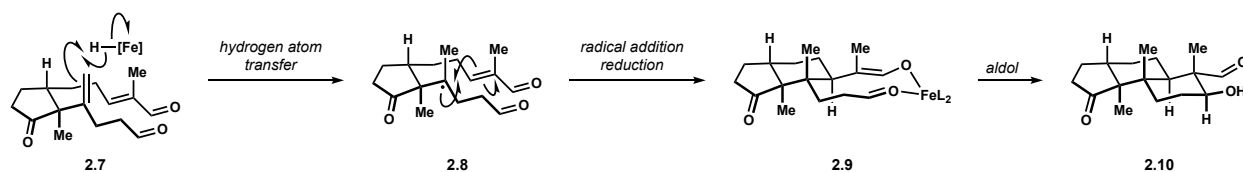
This strategy was first employed in the synthesis of (±)-emindole SB.[18] The studies of former group members Dr. David T. George and Dr. Eric J. Kuenstner on ketodialdehyde **2.7** revealed that rotation about the C3–C4 bond led to no difference in kinetic barrier of the conjugate addition (Scheme 2.3a). As a result, a nearly stoichiometric mixture of the desired *trans* and undesired *cis*-decalins **2.10** and **2.11** were produced. Further investigation on cyclopentanol **2.12** indicated that an equilibrium exists between the cyclopentanol and lactol **2.13** in solution, slightly favouring the lactol in a 2:1 ratio (Scheme 2.3b). Stereochemical models suggested that the lactol predisposes the 1,1-disubstituted alkene in a conformation that translates to proper orientation of the vicinal quaternary stereocenters. Indeed, subjecting this substrate mixture to the optimized

Scheme 2.3 Developing a Diastereocontrolled Approach to Emindole SB

a) Absent Selectivity

b) Lactol Promoted Selectivity

c) Hemiaminal Enforced selectivity
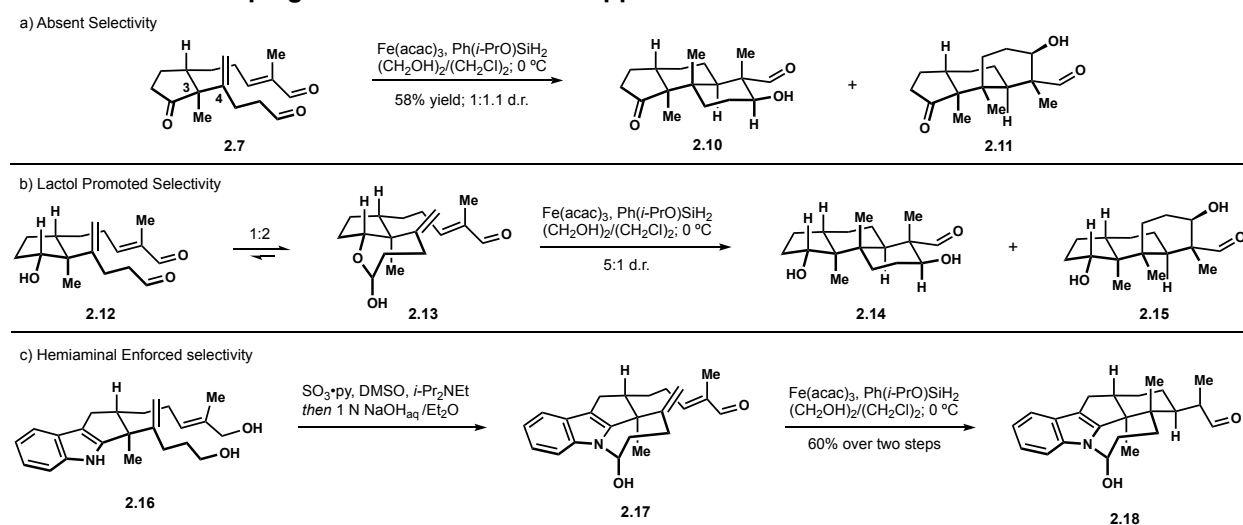
HAT conditions provided an amplified diastereomeric ratio of 5:1, favouring *trans*-decalin **2.14**. It remains unclear why there is a higher ratio of products relative to the equilibrium ratio observed. One possibility is that the ratio of dialdehyde to lactol in chloroform is not representative of what is in the reaction mixture containing a protic solvent. Alternatively, there may be a higher rate of HAT to the alkene rigidified in the lactol. Regardless, synthesis of **2.12** proved rather circuitous and differentiation of the two secondary alcohols in product **2.14** was anticipated to bring forth additional complications. The solution to these challenges for emindole SB was solved utilizing the indole moiety of the PIDs. Oxidation of the indole diol **2.16,** followed by treatment with base, induced the analogous tethering of the indole and aldehyde to produce hemiaminal **2.17**, though in this instance there was no observable equilibrium (Scheme 2.3c). This allowed for complete stereocontrol over the conjugate addition in the formation of hydrindane **2.18**. Due to the lack of equilibrium, the aldol addition required subsequent treatment with base to complete construction of the pentacyclic core.

The drawback to this strategy is that in utilizing the indole to effect substrate control, any strategy that relies on a late stage indole construction to maximize convergent assembly of more elaborate congeners is undermined. For this purpose, we looked to preserve the ketone

Scheme 2.4 Retrosynthetic Analysis of Nodulisporic Acid C
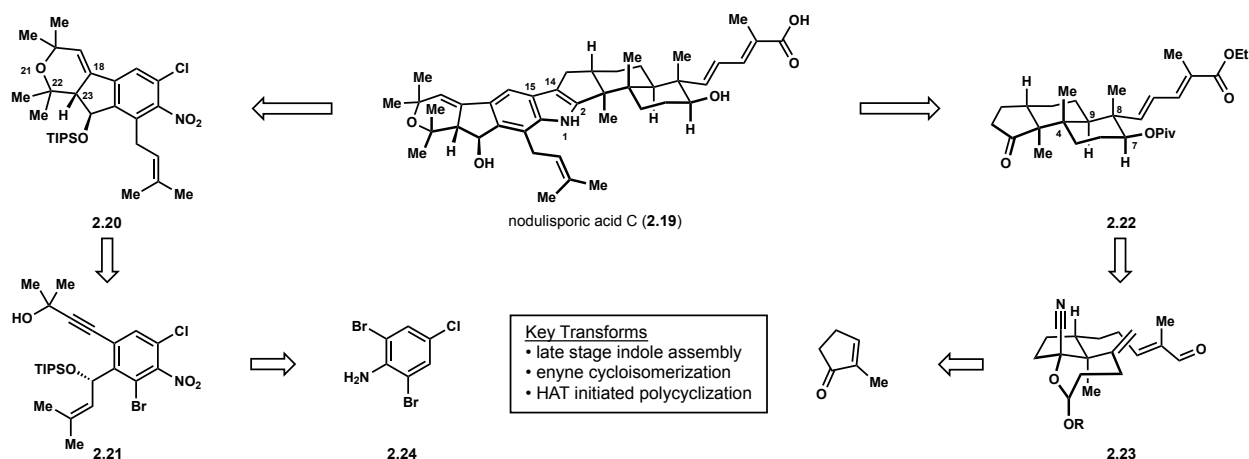
functionality in the polycyclization substrate. To this end, nodulisporic acid C (**2.19**) was chosen

as complex target which could be disconnected about the indole into two tricyclic fragments. The

highly-functionalized western hemisphere, in the form indenopyran **2.20**, could arise through a

cycloisomerization[19] of enyne **2.21** to forge the C18–C23 and O21–C22 bonds, and was former

group member Dr. Nicole A. Godfrey's subject of study. To access terpene fragment **2.22**, we

elected to pursue a cyanohydrin derivative **2.23** as our new polycyclization precursor. We

postulated that lactol formation analogous to secondary alcohol **2.13** would control reactivity as

desired, while also differentiating the functional groups present in the product. If the equilibrium

distribution did not sufficiently translate to high diastereomeric ratios, silylation of the lactol to

force this conformation was expected to promote the desired outcome. Each polycyclization

precursor can be traced back to commercial material in aniline **2.24** and 2-methylcyclopent-2-en-

1-one with reasonable brevity.

2.2 Total Synthesis of Nodulisporic Acid C

2.2.1 Development of a Diastereoselective Polycyclization

The first task undertaken for the synthesis of nodulisporic acid C was developing the key, diastereoselective polycyclization to access the tricyclic terpene core. Ketodiol **2.25** was prepared according to the procedures developed for emindole SB,[18] allowing for immediate optimization of cyanohydrin formation. Treatement of ketone **2.25** with trimethylsilyl cyanide (TMSCN) in the presence of zinc(II) iodide provided a modest amount of the desired cyanohydrin **2.26** (Table 1, entry 1).[20] Other zinc salts failed to produce any of the desired product, returning only starting material (entries 2 and 3). Ytterbium(III) trifluoromethanesulfonate also returned starting material (entry 4), whereas the corresponding scandium(III) salt restored the desired reactivity (entry 5), although a substantial amount of silyl-protected primary alcohols were also produced. Carrying out the reaction in ethereal solvents mitigated this issue and cyanohydrin diol **2.27** could be obtained as the sole product (entry 6). To avoid interference by the free alcohols, we attempted the reaction prior to installation of the allylic alcohol. Gratifyingly, use of desoxyketone **2.27** provided quantitative yields of protected cyanohydrin **2.28** and allowed reduction of TMSCN equivalents used by half (entry 7). It should also be noted that cyanohydrin formation provided a single detectable isomer as illustrated. The relative configuration was confirmed through reduction of nitrile **2.29** and analyzing NOE correlations between the amino and allylic methylene protons of aminoalcohol **2.30**. The stereoselectivity is analogous to hydride reduction of the ketone used to

Table 2.1 Optimization of Cyanohydrin Formation

R = OH (**2.25**) → R = OH (**2.26**)
R = H (**2.27**) → R = H (**2.28**)

TMSCN (10 equiv), Lewis acid, solvent, rt

entry	R	Lewis acid (10 mol%)	solvent (0.5 M)	% yield
1	OH	ZnI$_2$	Et$_2$O	37
2	OH	ZnBr$_2$	CH$_2$Cl$_2$	n.r.
3	OH	Zn(OTf)$_2$	CH$_2$Cl$_2$	n.r.
4	OH	Yb(OTf)$_2$	CH$_2$Cl$_2$	n.r.
5	OH	Sc(OTf)$_3$	CH$_2$Cl$_2$	67
6	OH	Sc(OTf)$_3$	Et$_2$O	77
7[a]	H	Sc(OTf)$_3$	Et$_2$O	quant.

[a]Reaction ran with 5 equiv. of TMSCN and at 0.6 M.

75

Scheme 2.5 Confirmation of Cyanohydrin Relative Stereochemistry
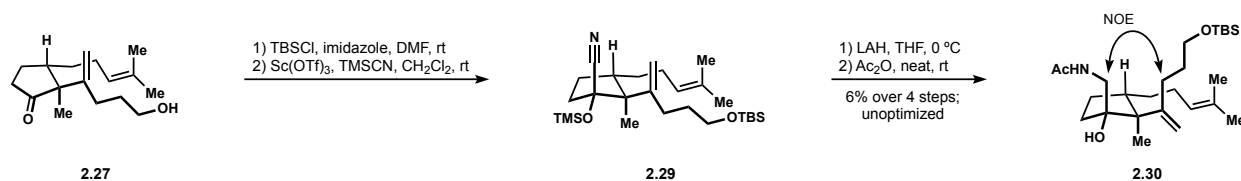
access alcohol **2.12,** where the face of attack appears to be dictated by β-substitution of the cyclopentanone blocking the required Bürgi–Dunitz trajectory.

With the cyanohydrin formation optimized, material suitable for polycyclization studies was quickly prepared (Scheme 2.6). Previously optimized Sharpless allylic hydroxylation conditions[21] were applied to cyanohydrin **2.28**, producing a mixture of the desired diol **2.26** and hydroxyaldehyde **2.31**. With this mixture, oxidation conditions were explored to access dialdehyde **2.32**. Swern[22] and Parikh–Doering[23] conditions proved to be too basic, resulting in reversion of the cyanohydrin back to the ketone **2.25**. Anelli conditions[24] and 2-iodoxybenzoic acid[25] were competent oxidants, but were outperformed by Dess–Martin periodinane.[26] With dialdehyde **2.32** in hand, we began exploring the possibility of lactol formation.

Scheme 2.6 Synthesis of Dialdehyde 2.33 and Initial Polycyclization Results
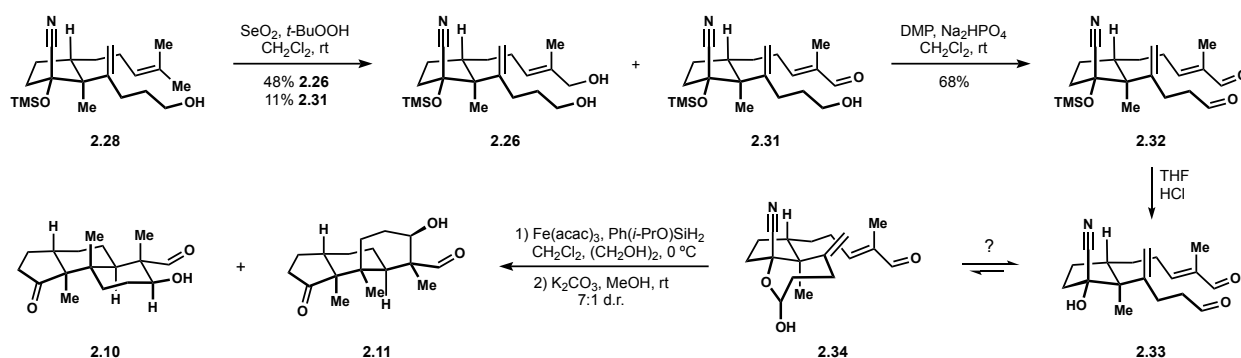
Following desilylation of produce the free cyanohydrin **2.33**, NMR analysis showed no evidence for the presence of lactol **2.34**. This is potentially due to the delocalization of oxygen lone pairs into σ* of the nitrile and lowering of the nucleophilicity of the alcohol. This effect also made handling the deprotected cyanohydrin **2.33** quite challenging, as attempts to funnel the

dialdehyde to the lactol by trapping as a silylether were thwarted by reversion of the cyanohydrin to the ketone. In consideration of secondary alcohol **2.12** and lactol **2.13** leading to a 5:1 ratio of products from a 1:2 ratio of starting materials and our ambiguous understanding of this result, we were curious to see if even the slightest amount of diastereoselectivity could be produced from cyanohydrin **2.33**. To our surprise, subjecting dialdehyde **2.33** to our standard HAT conditions and produced a 7:1 ratio of diastereomers. By treating the crude mixture with potassium carbonate and comparing the unpurified spectra to those previously reported,[18] we confirmed that the desired trans-decalin **2.10** was favoured. This was an unexpected result as we predicted that formation of the lactol would be the sole stereochemical determinant. As there was no evidence we were forming this species, we assumed the ratio of products would be lower than 5:1, if not 1:1. We speculated that substrate control must instead be related to the axial nitrile substituent.

We next chose to subject the silyl protected cyanohydrin **2.32** to the same conditions to confirm selectivity could be obtained without any possible formation of lactol. Indeed, following subjection to the same HAT conditions and subsequent potassium carbonate treatment, an even greater diastereomeric ratio favouring the *trans*-decalin **2.10** was obtained (Scheme 2.7). While satisfied with the outcome of the silyl cyanohydrin substrate, we felt understanding this interesting

Scheme 2.7 Substituent Effects on Controlling Polycyclization Diastereoselectivity

77
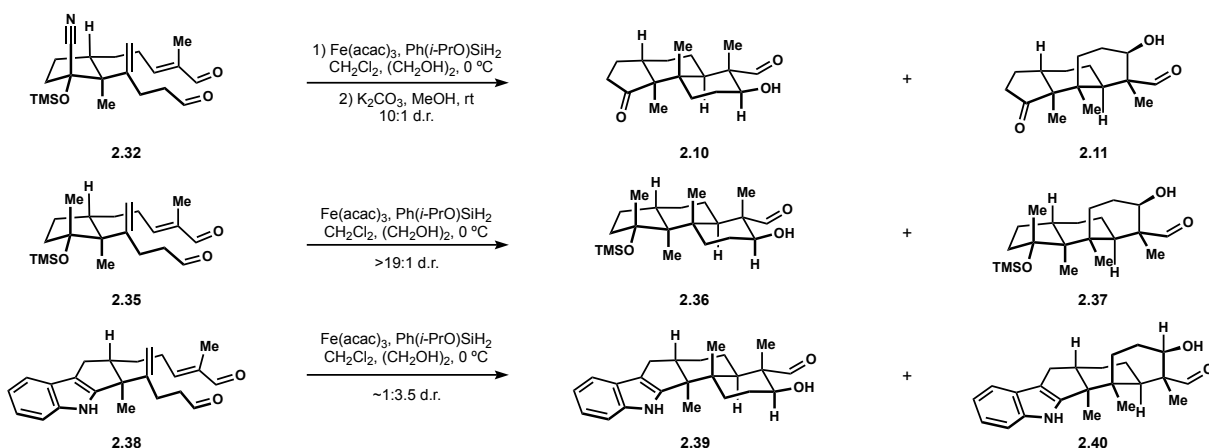
display of substrate control could be of great value to our lab. For this purpose, methyl derivative **2.35** was prepared, replacing the nitrile with a bulkier substituent allowed us to assess if this was in fact a steric effect or a more obscure influence of the nitrile. Subjecting **2.35** to the standard conditions resulted in *trans*-decalin **2.36** as the exclusive product isolated. In contrast to these examples, cyclization of indole dialdehyde **2.38**,[27] without formation of the hemiaminal as utilized for emindole SB, had the inverse selectivity with *cis*-decalin **2.40** now favoured slightly, but to noticeably greater extent than ketodialdehyde **2.7**.

It appears to us that rotation about the C3–C4 bond produces two conformers leading to two separate transition states for the conjugate addition. The conformation leading to the minor product **2.39** from cyanohydrin **2.34** is depicted in Scheme 2.8. Following HAT, the 1,3-diaxial interaction of radical **2.43** is likely minimized by rotating the aldehyde bearing, alkyl chain away from the nitrile. This in turn forces the alkyl chain to rotate towards the enal. As the bond begins to form, these two portions of the molecule would come into proximity with each other, producing a higher kinetic barrier for the pathway leading to *cis*-decalin **2.39**. In the case of indole dialdehyde **2.44**, the *N–H* presumably causes an analogous effect and disfavours the *trans*-decalin **2.41** pathway.

Scheme 2.8 Substituent Effects Leading to Biases in Transition States
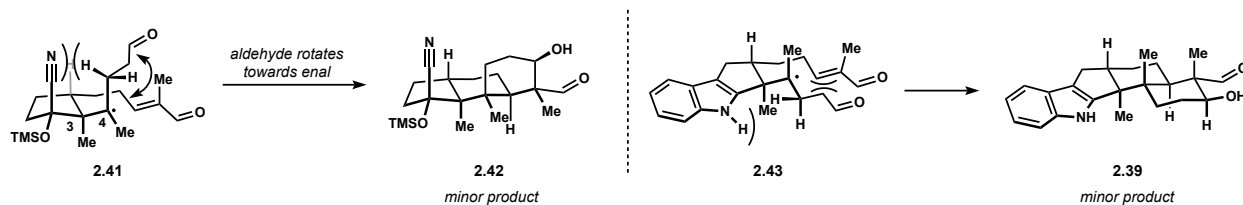
2.2.2 Development of an Enantioselective Conjugate Addition

To apply a convergent synthesis of nodulisporic acid C, production of enantioenriched material was paramount to maximizing throughput during fragment union. Furthermore, as we had already optimized for a highly diastereoselective approach to dialdehyde **2.32**, we wished to

preserve as much of the route as possible. The efficiency in accessing **2.32** is facilitated by our

lab's alkenylation method[28] to generate the requisite 1,1-disubstituted alkene from alkyne **2.44** and

silylenol ether **2.45** (Scheme 2.9a). This transformation also dramatically increases the brevity of

our approach. We therefore focused on methods to procure enantioenriched silylenol ether **2.45.**

Prior to my own efforts, alternative strategies had been explored by group members Dr. Eric

Kuenstner and Christopher A. Discolo (Scheme 2.9b). One promising strategy was the Stork–

Danheiser reaction[29] of a ketoenol such as **2.46** and subsequent conjugate reduction of the resulting

enone **2.47**. An alternative was the anionic oxy-Cope rearrangement of 1,2-allyl addition product

2.48.[30] Both methods proved to be rather circuitous and unsuccessful, further urging us to assess

direct conjugate addition reactions between an organometallic nucleophile and 2-methylcyclopent-

2-en-1-one as is done in the racemic route.

Scheme 2.9 Enantioselective Approaches Considered

a) General Retrosynthetic Plan to Access Dialdehyde **2.32**

b) Stork–Danheiser-conjugate Reduction Approach

c) Anionic oxy-Cope Approach
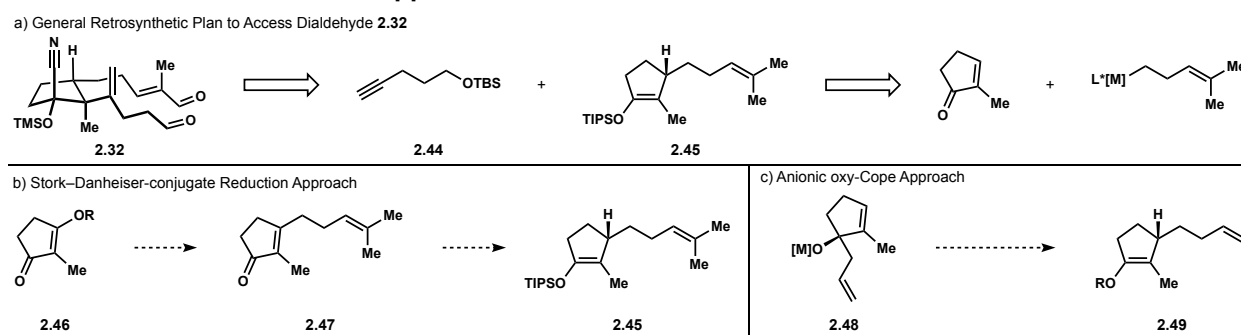
Evaluation of existing methods for this transformation revealed that amongst the plethora

of reports on enantioselective conjugate additions, very few methods exist that are applicable to

cyclopentenones, especially α-substituted derivatives.[31] The pioneering efforts by Pfaltz[32],

Hoveyda[33] and Leighton[34] groups identified three competent ligand classes that include oxazoline-

phosphites (**2.50**), peptide-based phosphines (**2.51**) and phosphine sulfonamides (**2.52**, Figure

2.2a). Each of these reports enabled highly enantioselective copper-catalyzed conjugate additions

of dialkylzinc nucleophiles to cyclopent-2-en-1-one. Extension of these systems to α-substituted

Figure 2.2 Enantioselective 1,4-Additions of Organometallic Alkyl Nucleophiles to Cyclopentenones

a) Additions to Cyclopent-2-en-1-one

2.50
R = Et, 94% ee

2.51
R = Et; 97% ee

2.52
R = i-Pr, 86% ee

b) Additions to 2-methylcyclopent-2-en-1-one

2.53
R = Et, 60% ee
R = i-Pr, 84% ee
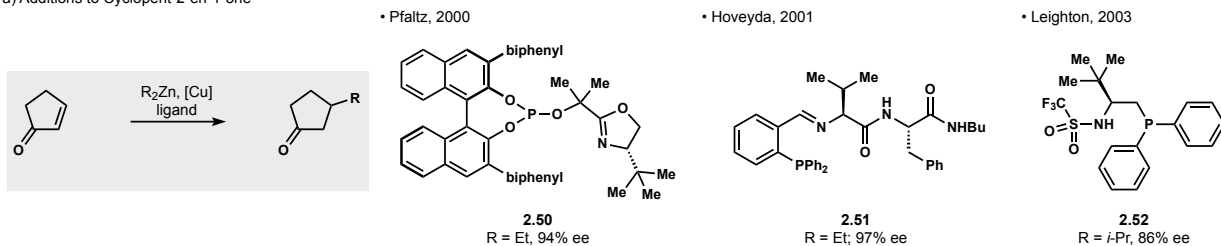
2.54
R = ... 70% ee
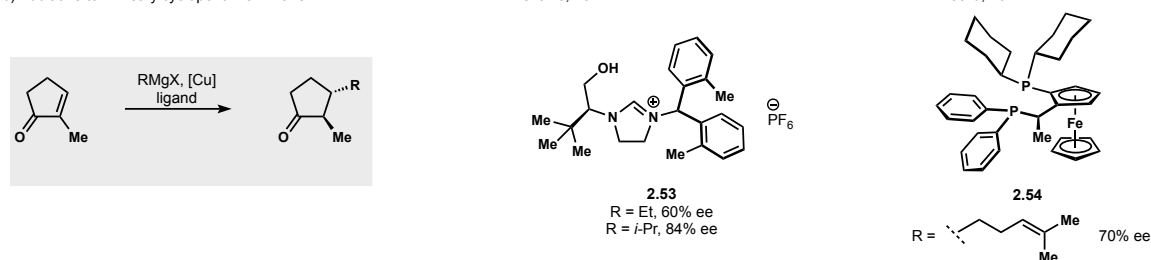
cycloalkenones have not been reported. The Alexakis group first demonstrated a solution to that substrate class utilizing *N*-heterocyclic carbene ligands such as **2.53**, obtaining high levels of enantioenrichment for copper catalyzed conjugate additions of bulky alkyl Grignard nucleophiles to 2-methylcyclopent-2-en-1-one.[35] In contrast, only moderate levels of enrichment were obtained for primary alkyl nucleophiles that were needed for our system. The Minnaard group recently discovered that the JosiPhos ligand family introduced by Feringa provided a modest improvement to Alexakis for this primary alkyl nucleophiles.[36] Most notably was the successful addition of the desired homoprenyl substituent to 2-methylcyclopent-2-en-1-one, with a synthetically useful 70% enantiomeric excess from the aid of JosiPhos **2.54**.[37] We chose this report as a starting point for further investigation as it lacked thorough investigation of the many available JosiPhos ligands as well as reaction parameters. We hoped within these conditions might lie further improvement of selectivity.

The optimal ligand, JosiPhos SL-J004-1 (**2.54**), and reaction conditions identified by Minnaard facilitated enantioselective addition of homoprenylmagnesium bromide to 2-methylcyclopent-2-en-1-one at a comparable level in our hands at 65% ee (Table 2.2, entry 1).

There was also a significant amount (>15 mol%) of 1,2-addition product. These two products and levels of selectivity provided us a reference point for further investigation. Evaluation of a series of JosiPhos ligands revealed both reactivity and selectivity depend dramatically on the ligand used. Replacement of the diphenyl phosphine of **2.54** with a dialkylphophine found in **2.57** and **2.58** resulted in complete loss of enantioenduction (entries and 3). Increasing the bulk of cyclohexylphosphine **2.54** to *tert*-butylphosphine **2.59** afforded no 1,4-addition product (entry 4). The same result was obtained when the placement of alkyl and aryl phosphines were switched as in SL-J002-1 (**2.60**) and the corresponding bis(trifluoromethyl) derivative **2.61** (entries 5 and 6). We speculate that racemic 1,4-addition product is the result of poor to no chelation to copper by the ligand, allowing free copper salt to catalyze uncontrolled addition. In contrast, 1,2 addition may be caused by ligand sequestration of copper, preventing transmetalation necessary for 1,4– addition to be favoured. The desired 1,4-reactivity was restored with *o*-tolyl derivative **2.62**, though the product obtained was racemic (entry 7). JosiPhos ligands SL-J007-1 (**2.63**) and SL-J005-1 (**2.64**) produced low, but measurable levels of enantioenrichment (entries 8 and 9). Gratifyingly, replacing the phenyl substituents of SL-J005-1 with 2-furyl in ligand **2.65** represented the first result comparable to Minnaard's original report (entry 10). While the improvement in enantioselectivity was modest, no 1,2-addition product was observed. Further changes to the aryl substituents once again eroded all enantioselectivity or desired reactivity (entries 11 – 15). Changes to other parameters such as concentration and solvents proved detrimental to the desired outcome as well (entries 16 – 20). Additional screening of representative diphosphines including JosPOPhos (**2.71**), WalPhos derivatives **2.72–2.74**, BINAP (**2.75**), BIPHEP (**2.76**), PhanePhos (**2.77**), DuPhos (**2.78**), ChiraPhos (**2.79**) and DIOP (**2.80**) all resulted in formation of racemic product (entries 21 – 30).

Table 2.2 Optimization of a Catalytic System to Access Enantioenriched Cyclopentanones

5 mol% CuBr•SMe$_2$
6 mol% ligand
MTBE (0.075 M), −78 °C

2.55

2.56
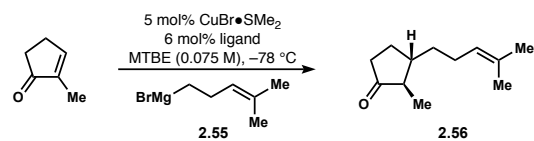
entry	ligand	%ee	entry	ligand	%ee	entry	ligand	%ee
1	SL-J004-1 (**2.54**)	65	11	**2.66**	0	21	SL-J618-1 (**2.71**)	0
2	SL-J003-1 (**2.57**)	0	12	SL-J452-1 (**2.67**)	0	22	SL-W001-1 (**2.72**)	0
3	SL-J009-1 (**2.58**)	0	13	SL-J425-1 (**2.68**)	0	23	SL-W002-1 (**2.73**)	0
4	SL-J502-1 (**2.59**)	–^{a}	14	SL-J008-1 (**2.69**)	0	24	SL-W008-1 (**2.74**)	0
5	SL-J002-1 (**2.60**)	–^{a}	15	SL-J418-1 (**2.70**)	–^{a}	25	(R)-BINAP (**2.75**)	0
6	SL-J011-1 (**2.61**)	–^{a}	16	SL-J015-1 (**2.65**)	50^b	26	(S)-MeOBIPHEP (**2.76**)	0
7	SL-J505-1 (**2.62**)	0	17	SL-J015-1 (**2.65**)	15^c	27	(S)-Phanephos (**2.77**)	0
8	SL-J007-1 (**2.63**)	37	18	SL-J015-1 (**2.65**)	10^d	28	(R,R)-Me-Duphos (**2.78**)	0
9	SL-J005-1 (**2.64**)	30	19	SL-J015-1 (**2.65**)	50^e	29	(S,S)-Chiraphos (**2.79**)	0
10	SL-J015-1 (**2.65**)	73	20	SL-J015-1 (**2.65**)	63^f	30	(S,S)-DIOP (**2.80**)	0

^{a}No 1,4 addition product observed. ^{b}Reaction ran at 0.2 M. ^{c}Reaction ran in Et$_2$O. ^{d}Reaction ran in i-Pr$_2$O. ^{e}Reaction ran in CH$_2$Cl$_2$. ^{f}Reaction ran in toluene.

SL-J004-1 (**2.54**)   SL-J003-1 (**2.57**)   SL-J009-1 (**2.58**)   SL-J502-1 (**2.59**)   SL-J002-1 (**2.60**)

SL-J011-1 (**2.61**)   SL-J505-1 (**2.62**)   SL-J007-1 (**2.63**)   SL-J005-1 (**2.64**)   SL-J015-1 (**2.65**)

2.66   SL-J452-1 (**2.67**)   SL-J425-1 (**2.68**)   SL-J008-1 (**2.69**)   SL-J418-1 (**2.70**)

SL-J618-1 (**2.71**)   SL-W001-1 (**2.72**)   SL-W002-1 (**2.73**)   SL-W008-1 (**2.74**)   (R)-BINAP (**2.75**)

(S)-MeOBIPHEP (**2.76**)   (S)-Phanephos (**2.77**)   (R,R)-Me-Duphos (**2.78**)   (S,S)-Chiraphos (**2.79**)   (S,S)-DIOP (**2.80**)
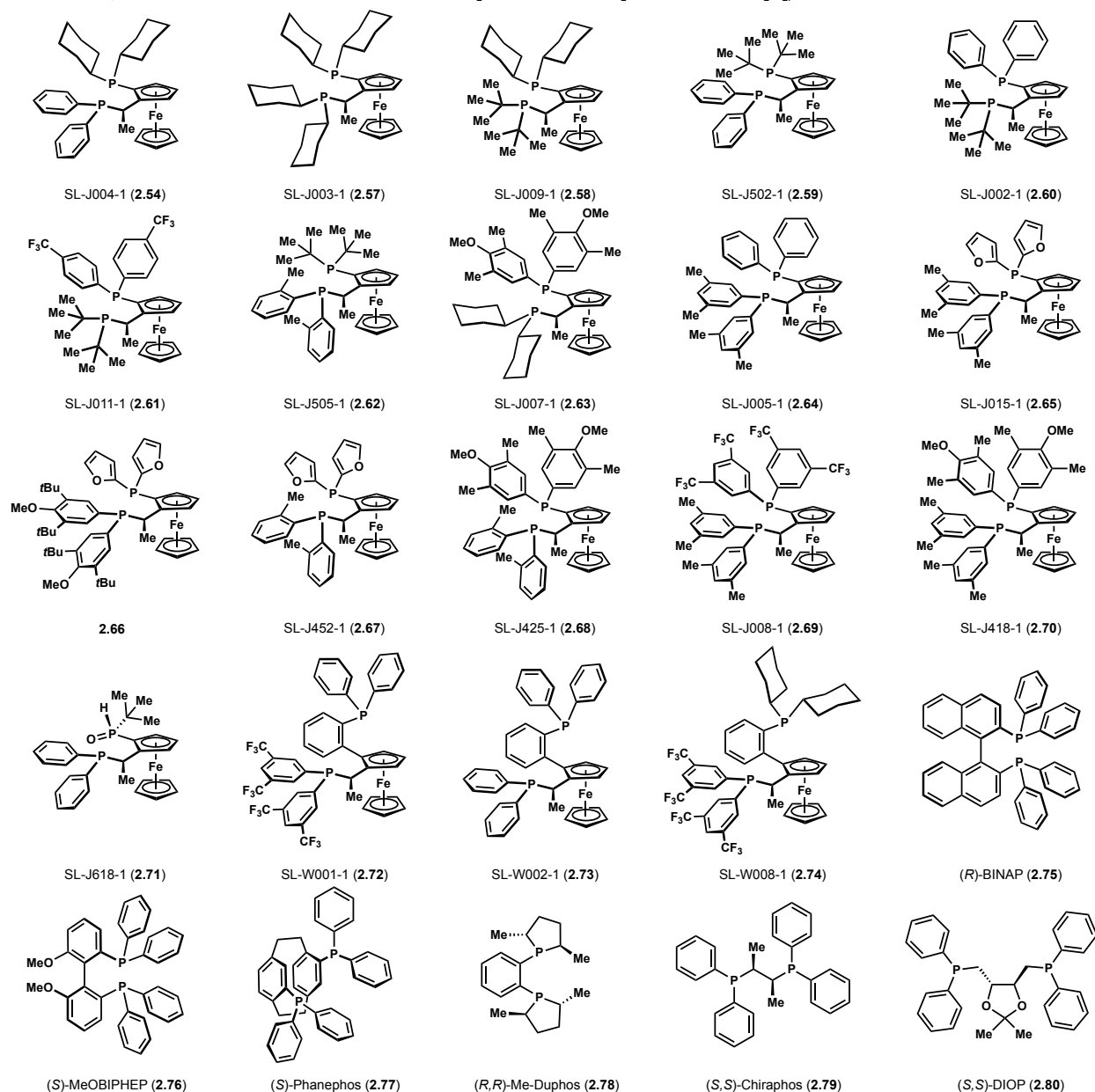
Considering the lack of information available regarding enantioselective conjugate additions to 2-methylcyclopent-2-ene-1-one, we felt it would be instructive to evaluate other nucleophiles with our optimal JosiPhos ligand **2.69**. With the aid of undergraduate researcher Wenqin Li, a variety of alkylmagnesium bromide Grignard reagents were assessed. We discovered that 2-phenethyl-, but-1-en-4-yl-, and 1-pentyl were all subject to reasonable levels of enantioinduction (Table 2.3, entries 1 – 3). These reactions were treated with triisopropylchloride, triethylamine, hexamethylphosphor-

Table 2.3 Evaluation of Nucleophiles with Josiphos Ligand 2.65
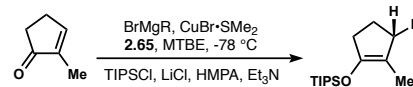
entry	Grignard reagent	yield	% ee[a]
1		80	59
2		80	52
3		84	64
4		75	0
5		80	0
6		1,2 addition	-
7		1,2 addition	-

[a]Values correspond to analysis of the major diastereomer resulting from acid hydrolysis of the isolated silyl enol ether.

amide and lithium chloride to trap the metal enolates as the silyl enol ethers, allowing for ease of separation from the ligand and evaluation of enantioenrichment. Larger nucleophiles such as isobutyl and isopropyl Grignard reagents delivered racemic products whereas allyl and phenyl Grignard reagents underwent preferential 1,2-addition. While the performance of this system was deemed acceptable for our purposes, it is clear asymmetric conjugate additions to α-substituted cyclic alkenones persists as an unresolved challenge.

2.2.3 Synthesis of the Nodulisporic Acid Eastern Hemisphere Sub-target

With both issues of diastereoselectivity and enantioselectivity resolved, synthesis of the complete fragment **2.22** commenced as illustrated in Scheme 2.10. Further reaction engineering of the conjugate addition permitted efficient formation of silylenol ether **2.45** on decagram scale. Isolation of this material was immediately followed by alkenylation[28], performing best with sub-

Scheme 2.10 Full Synthetic Sequence to Eastern Coupling Fragment 2.22
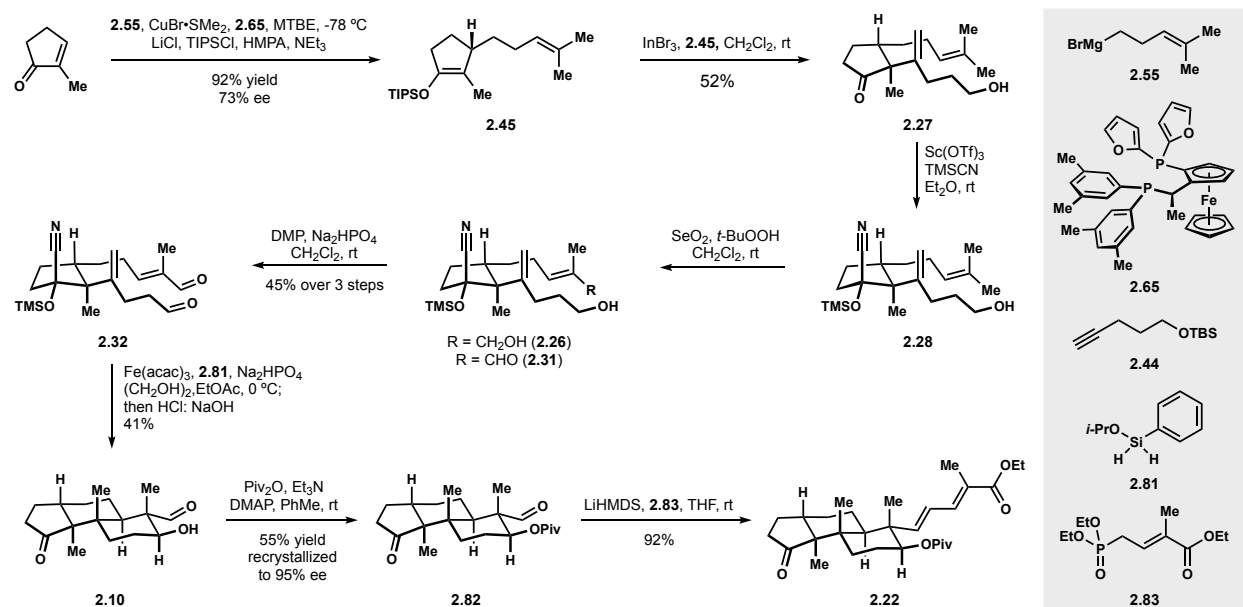
stoichiometric amounts of indium, to produce ketone **2.27**. Conversion of the ketone to the

cyanohydrin, allylic oxidation and double DMP oxidation prepares the polycyclization precursor

2.32. While several modifications to the polycyclization conditions were explored, a tangible

improvement from conditions previously reported was not observed. We did find that quenching

the polycyclization with HCl in THF and heating the mixture overnight adequately desilylated the

tricyclic cyanohydrin. A simple wash with aqueous NaOH during extraction was sufficiently basic

to reform the ketone moiety. Ultimately, 41% of the desired *trans*-decalin **2.10** could be separated

and isolated cleanly from the undesired *cis*-decalin. Protection of the secondary alcohol of **2.10**

with a pivalate group provided an opportunity for further enantioenrichment through

recrystallization of ester **2.82**. Dissolving in boiling hexanes and slow cooling afforded

enantiopure material. Lastly, a Horner–Wadsworth–Emmons reaction[38] of the aldehyde **2.82**

completed synthesis of our sub-target **2.22**.

2.2.4 Synthesis of the Nodulisporic Acid C Western Hemisphere Sub-target

Preparation of an indenopyran coupling fragment was carried out by Dr. Nicole Godfrey. Beginning with commercial aniline **2.24**, Sandmeyer iodination delivered tetrahaloarene **2.84** (Scheme 2.11). Chemoselective metal–iodide exchange permitted formylation of **2.84** with *N,N*-dimethylformamide and nitration of the resulting aldehyde **2.85** provided nitroarene **2.86**. At this stage, enantioenriched material was obtained through an asymmetric addition of an isobutenyl zinc reagent **2.87** in the presence of chiral aminoalcohol **2.88**. These conditions delivered benzylic alcohol **2.89** in quantitative yield and high levels of enantioenrichment.[39] Optimization of a chemoselective Sonogoshira coupling[40] with propargyl alcohol **2.90** secured access to the desired enyne framework in **2.91**. Protection of the benzylic alcohol as the TIPS ether readied the substrate for the key transformation. Treatment of alkyne **2.92** with a gold(I) NHC catalyst induced the desired cycloisomerization. Incredibly, the reaction proceeds with complete diastereocontrol and indenopyran **2.94** was procured in excellent yield. Stille coupling[41] installed the prenylsubstituent

Scheme 2.11 Synthetic Sequence to Western Coupling Fragments 2.20 and 2.96
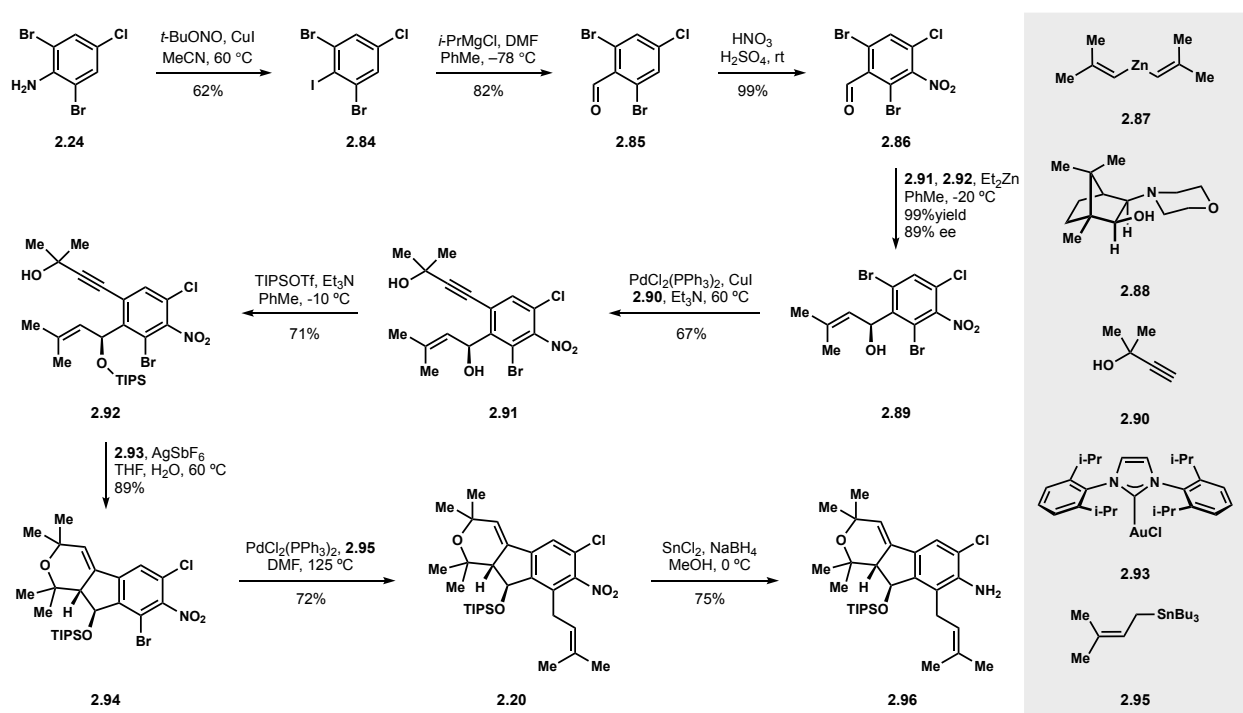
of nodulisporic acid C, providing nitroarene **2.20**, which can be easily reduced to the aniline **2.96**. Both indenopyran derivatives **2.20** and **2.96** were utilized for fragment coupling studies.

2.2.5 Fragment Union Studies

We initially looked to capitalize on Barluenga's conditions[42] utilized by Smith in his synthesis of nodulisporic acid D.[10] At the outset of this work, Smith had not reported his synthesis of (−)-nodulisporic acids B and C[11], thus the coupling of chloroaniline **2.4** and vinyl triflate **2.5** (Scheme 2.1) was unknown to us. After converting ketone **2.22** into vinyl triflate **2.97**, we attempted a model reaction with Smith's conditions to couple **2.97** with 2-chloroaniline (Scheme 2.12a). Proceeding via Buchwald–Hartwig amination, followed by a formal Heck cascade, the reaction worked well on the model system to provide indole **2.98**. Unfortunately, this result did not translate to the complex system involving chloroaniline **2.96** and formation of indole **2.99** was not observed under these conditions (Scheme 2.12b). We reasoned that the presence of an additional *ortho* substituent to the amine for the nodulisporic acid C system was at fault, creating a higher kinetic barrier for C–N bond formation.

Scheme 2.12 Unsuccessful Application of Smith's Indole Formation Strategy

a) Simplified Coupling Attempt

b) Application to Complex Fragments
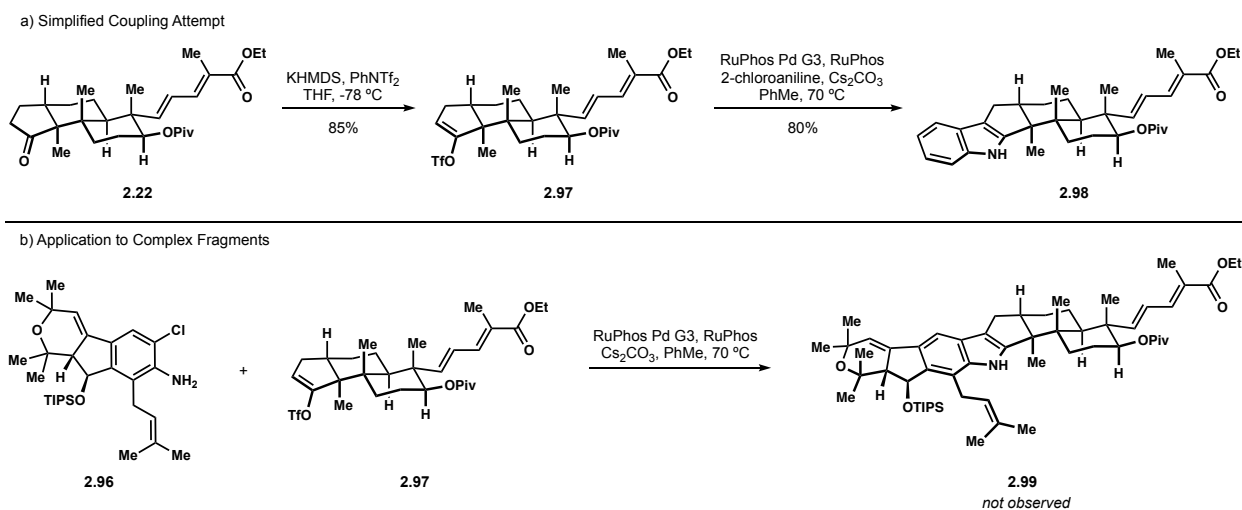
To further probe this reaction and determine if the challenge was surmountable, we explored the coupling of vinyl triflate **2.97** and 2-chloro-6-methylaniline (Scheme 2.13). A survey of available Buchwald-type ligands[43] including RuPhos (**2.102**), DavePhos (**2.103**) and BrettPhos (**2.104**) afforded none of the desired indole **2.100**. Bidentate phosphine **2.105**, tri-*tert*-butylphosphine (**2.106**) and NHC ligands **2.107–2.109** were explored as alternatives unsuccessfully. The only observable product in these reactions was protodemetallated tricycle **2.101**. To our disappointment, Smith revealed a solution with the use of a less bulky ligand, successfully coupling di-*ortho*-substituted anilines with a vinyl triflate for the syntheses of nodulisporic acids B and C.

Scheme 2.13 Alternative Ligands Explored for Coupling of Vinyl Triflate 2.97
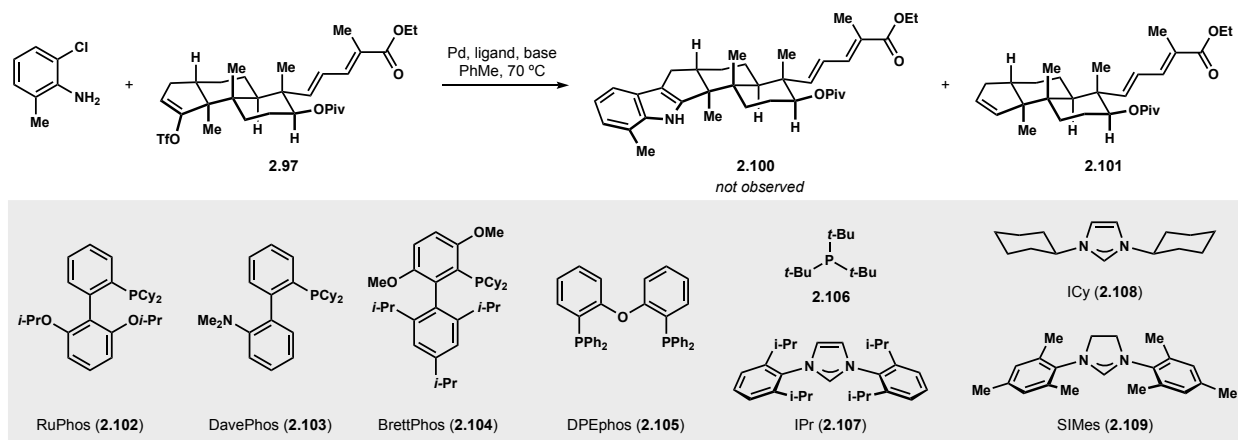
By the time Smith's synthesis of nodulisporic acid C was reported, we had begun to find our own success, but not before exhaustively exploring alternatives. The lack of reactivity forced us to consider more circuitous strategies to unite our fragments. To this end, Dr. Godfrey and I exhaustively explored alternatives. The first approach was the Fisher indolization (Scheme 2.14a). While this proved to be effective in the synthesis of emindole SB[18], the tricyclic ketone **2.22** was far more reluctant to undergo any condensation with tosylhydrazine in comparison to a pre-polycyclization derivative. An axial methyl substituent flanking each face of the cyclopentanone

2.22 likely dissuades approach by the nucleophile and hydrazone **2.110** was not detected. We then considered the lengthier Gasman sequence employed successfully by Smith[44] and Johnson[45] in various syntheses of PIDs (Scheme 2.14b). This strategy was quickly dismissed as formation of the *N*-chloroaniline was outcompeted by chlorination at the styrenyl position to give chloroindenopyran **2.113**. Though it proved to be inconsequential, we were reluctant to pursue these two strategies as they both require forcing acidic conditions to facilitate condensation reactions, which we expected to introduce additional issues due to the lability of the benzylic alcohol.[5b,10] We eventually decided that since the C–N bond formation was so sterically demanding, we should move away from this reaction center and instead focus on C–C bond formation instead and effect some form of ketone α-arylation. For this reason, we briefly explored S_NAr reactions[46] between nitroarene **2.94** and silyenol ether **2.114**, but only found desilylation products in the reaction mixtures (Scheme 2.14c). We decided to next explore transition metal catalyzed ketone arylation, which provided us a wealth of options to assess.[47]

Scheme 2.14 Unsuccessful Indole Construction Attempts

a) Fisher Indolization

2.22 **2.110**
not observed

b) Gasman Indolization

2.111 **2.112** **2.113**

c) S_NAr

2.94 **2.114** **2.115**
not observed

88
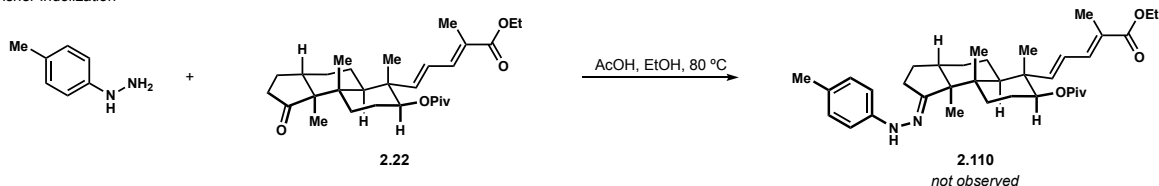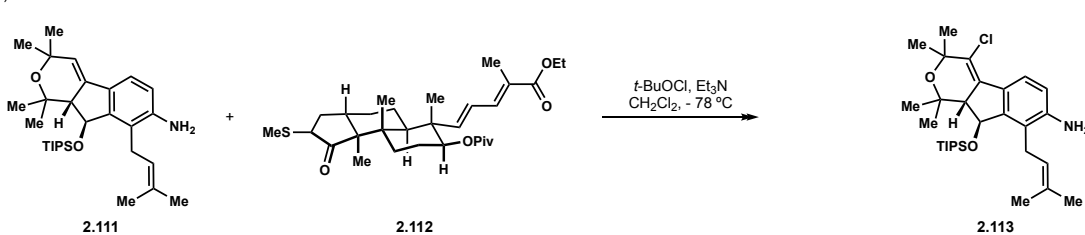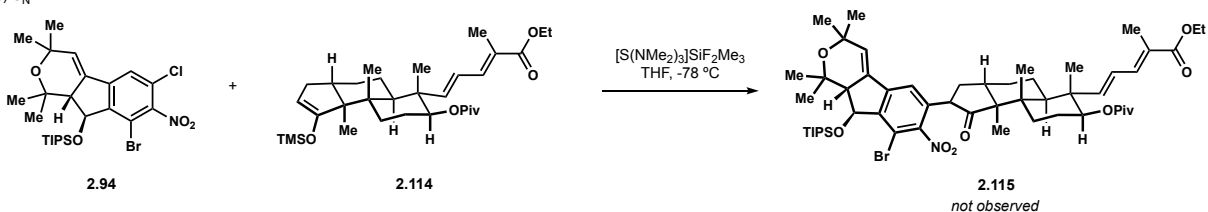
We were initially drawn to Buchwald's protocols for direct coupling of ketones with aryl halides (Scheme 2.15a).[48] In considering chloronitroarene **2.20** for this reactivity, we were concerned about the benzylic methylene, as deprotonation would produce an anion in conjugation with the vinylnitro moiety. We decided to shift to the milder methods developed by Hartwig[49] and Rawal[50], whereby *in situ* generated tin enolates from the silylenol ether precursors underwent intermolecular coupling with aryl halides (Scheme 2.15b and 2.15c). These conditions lack the presence of a strong base and showed promise in sterically demanding systems. The exact conditions reported by Hartwig or Rawal did not result in detectable product from chloronitro arene **2.20** and silyl enol ether **2.114**. Gratifyingly, by replacing tri-*tert*-butyl phosphine with Buchwald's DavePhos ligand[43], we detected the desired arylketone **2.116** through ESI-MS (Scheme 2.15d). Thus, we were reinvigorated and this reactivity was extensively explored.

Scheme 2.15 Select Ketone Arylation Strategies
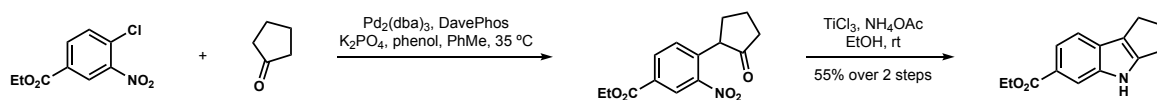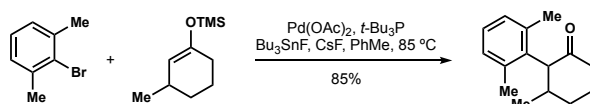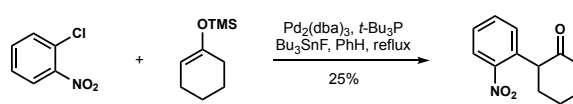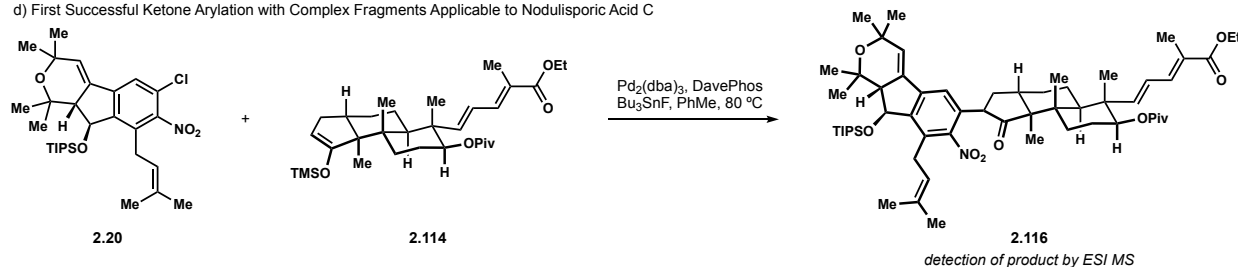
A substantial amount of time was dedicated to optimizing the arylation of silyl enol ether **1.114**. Arylketone **2.116** was confirmed as a mixture of diastereomers through NMR analysis. The material brought forth allowed us to explore the final stages of the synthesis, which was carried

out by Dr. Godfrey while the arylation was still being evaluated. The arylation diastereomers were taken forward as a mixture by reducing the nitro group. Gratifyingly, cyclocondensation to the desired indole **2.104** was observed under these conditions (Scheme 2.16). However, in addition to the indole product, a single diastereomer of reduced, but uncyclized aniline was observed. We subsequently isolated each nitroarene diastereomer and assigned their relative configurations utilizing two-dimensional NMR analyses.[51] We then subjected each diastereomer to the reduction conditions and determined that diastereomer **2.116b** was not undergoing the condensation and stalling at aniline **2.117** (Scheme 2.15). We hypothesized that the C3 methyl group adjacent to the ketone prohibits addition of the aniline into the carbonyl from that face. Efforts to epimerize nitroarene diastereomer **2.116b** with amine bases resulted in decomposition of the substrate. This outcome is worth comparing to past syntheses, particularly Smith[44] and Johnson's[45] indole constructions. The Gasman protocol they employ proceeds through a ketoaniline analogous to **2.117**. To effect cyclocondensation to the indole, their substrates were treated with tosic acid in refluxing benzene. Subjecting aniline **2.117** to similar conditions did induce cyclocondensation,

Scheme 2.16 Nitro Group Reduction and Amine Condensation Results

90
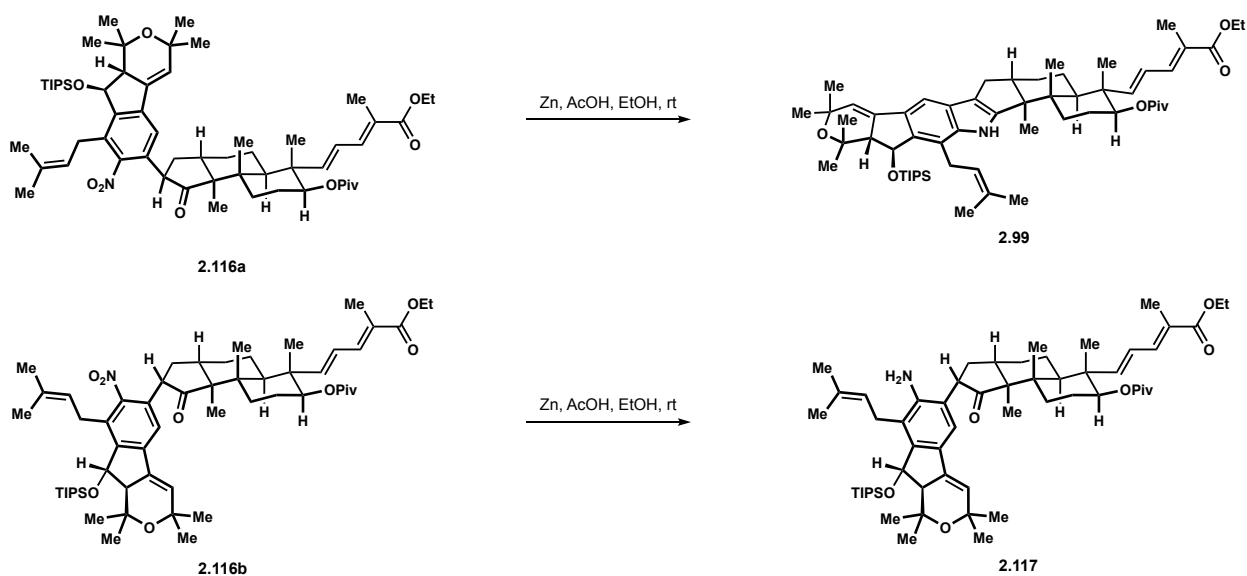
but not without concomitant elimination of the benzylic ether. These results highlight the need for

mild indole-forming tactics in the context of these complex natural products.

Given the newfound success in the coupling reaction, we decided to revisit direct arylation

of ketone **2.22** as opposed to the silyenol ether derivative. Indeed, by generating the tin enolate

with NaHMDS and tributyltin chloride before adding the chloronitroarene **2.20**, the coupling could

be accomplished in comparable yield with the same catalyst and ligand DavePhos (**2.103,** Table

2.4, entry 1). As control over which diastereomer we produced was now of paramount importance,

we thoroughly explored reaction parameters for this transformation. Other alkali metal bases

yielded no product (entries 2 and 3). By changing the ligand, a marked change in

diastereoselectivity was observed. However, in the case of *tert*-butylphosphine and XPhos (**2.118**)

ligands, the undesired diastereomer became favoured (entries 4 and 5). BrettPhos (**2.104**) restored

the desired selectivity at a lower overall yield (entry 6) and SPhos (**2.119**) performed comparably

to DavePhos (**2.103**) G3 (entry 7). RuPhos (**2.102**) G3 provided both a favourable yield and ratio

of products (entry 8). Of greater note was the fact that in all prior cases, most the arylchloride was

consumed unproductively. When using RuPhos, 60% of the arylchloride could be recovered along

with the 34% combined yield of products. When we applied DavePhos (**2.103**) G4, we noticed

improved product ratio (entry 9). This is possibly due to the carbazole by-product of G3 catalyst

activation epimerizing the highly acidic, α-proton in the product, though the appropriate

experiment has not been performed to confirm this. Nonetheless, we suspected fourth generation

precatalysts, releasing *N*-methylcarbazole as a by-product of activation, were likely optimal

regardless of the ligand. Despite the promising performances with respect to product ratio of

DavePhos (**2.103**), CPhos (**2.120**), CyJohnPhos (**2.121**) and (*t*-Bu)PhCPhos (**2.122**) fourth

generation precatalysts (entries 9 – 12), we felt RuPhos still contained the most potential for further

Table 2.4 Optimization of Ketone 2.22 Arylation with Chloronitroarene 2.20

2.20 + 2.22 → (precatalyst, ligand, base, Bu$_3$SnCl, PhMe, −20 to 60 °C) → **2.116a** + **2.116b**
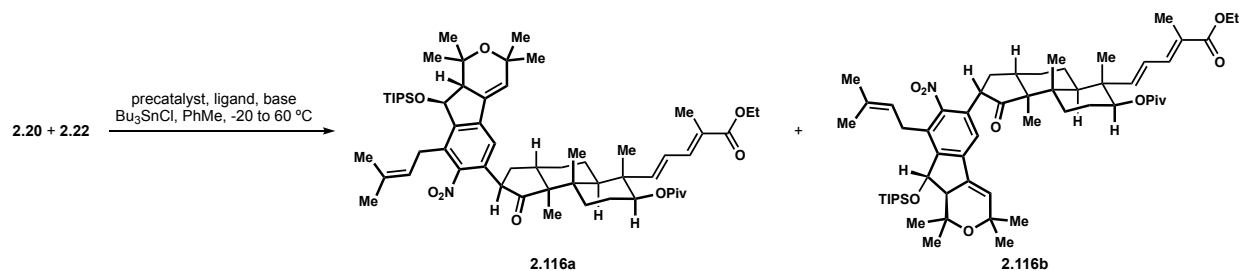
precatalyst version			entry	precatalyst	base	% yield 2.116a[a]	% yield 2.116b[a]
G2	G3	G4	1	DavePhosPd G3	NaHMDS	14	14
			2	DavePhosPd G3	KHMDS	0	0
			3	DavePhosPd G3	LiHMDS	0	0
			4	*t*-Bu$_3$PPd G3	NaHMDS	2	9
			5	XPhosPd G3	NaHMDS	9	27
ligand structure			6	BrettPhosPd G2	NaHMDS	14	2
			7	SPhosPd G2	NaHMDS	16	14
DavePhos (**2.103**)	XPhos: R = H (**2.118**); BrettPhos: R = OMe (**2.104**)	SPhos: R = OMe (**2.119**); RuPhos: R = O*i*-Pr (**2.102**); CPhos: R = NMe$_2$ (**2.120**); CyJohnPhos: R = H (**2.121**)	8	RuPhosPd G3	NaHMDS	26	8
			9	DavePhosPd G4	NaHMDS	15	9
			10	CPhosPd G4	NaHMDS	21	2
			11	CyJohnPhosPd G4	NaHMDS	25	5
			12	(*t*-Bu)PhCPhosPd G4	NaHMDS	27	0
(*t*-Bu)PhCPhos (**2.122**)	MorDalPhos (**2.123**)	**2.106**, **2.124**	13	MorDalPhosPd G4	NaHMDS	0	0
			14	*t*-Bu$_2$PMePd G4	NaHMDS	0	0
			15	RuPhosPd G4	NaHMDS	44[b]	10[b]

[a]Yields determined by inclusion of mesitylene as an internal NMR standard. [b]Isolated yield,

optimization due to a higher return of mass balance. In contrast, MorDalPhos (**2.123**) and di-*tert*-butyl-methylphosphine (**2.124**) produced no product (entries 13 and 14). Ultimately, further engineering of the reaction with RuPhos permitted production of the desired diastereomer **2.116a** in 44% isolated yield on nearly 100 mg scale (entry 15).

2.2.6 Total Synthesis of (–)-Nodulisporic Acid C

With acceptable yields of the desired arylketone diastereomer, we completed the synthesis of (–)-nodulisporic acid C in three additional steps. Zinc metal and acetic acid proved mild and effective for reducing the nitro group of **2.116a** bearing the sensitive benzylic alcohol (Scheme

2.17). Removal of the TIPS protecting group and saponification of the two esters yielded (–)-nodulisporic acid C in twelve steps (longest linear sequence).

Scheme 2.17 Synthesis of (–)-Nodulisporic Acid C

2.116a

1) Zn, AcOH, EtOH, rt
2) TASF, DMF, 60 °C
3) LiOH$_{(aq)}$, dioxane, MeOH, 100 °C

73% over 3 steps

(–)-nodulisporic acid C (**2.19**)
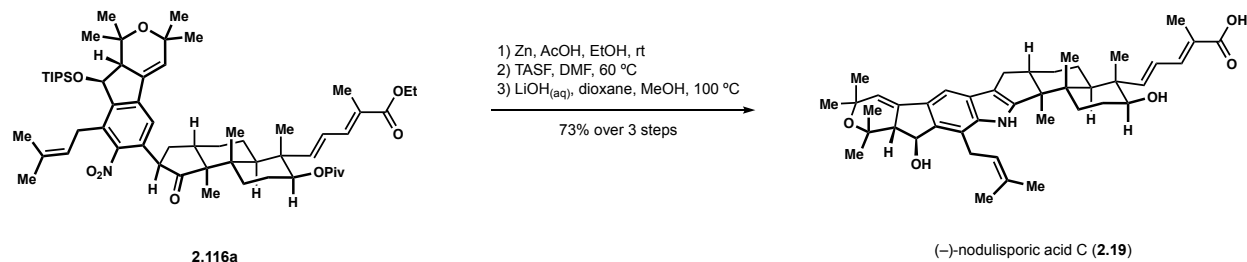
Through this work, we developed several transformations and pushed the limitations of known chemistry in the forms of enantioselective conjugate additions and ketone arylations. Furthermore, two key cyclization cascades were successfully developed and applied, of which the enyne cycloisomerization may lend itself to additional members of the paxilline indoloterpenoids such as the shearinines and janthitrems. The HAT initiated polycyclization is also well suited for accessing the greater family of targets and is reported in the following chapter.

2.3 Experimental Section

2.3.1 General Experimental Details

All reactions were carried out in flame-dried glassware under positive pressure of dry nitrogen unless otherwise noted. Reaction solvents (Fisher, HPLC grade) including tetrahydrofuran (THF), diethyl ether (Et$_2$O), dichloromethane (CH$_2$Cl$_2$), and toluene (PhMe) were dried by percolation through a column packed with neutral alumina and a column packed with a supported copper catalyst for scavenging oxygen (Q5) under positive pressure of argon. Methyl *tert*-butyl ether (MTBE, Millipore Sigma, ACS grade) was distilled from sodium diphenylketyl under positive pressure of nitrogen. Anhydrous 1,2-dichloroethane (DCE, Fisher, ACS Grade) and anhydrous triethylamine (Et$_3$N, Oakwood Chemical) were distilled from calcium hydride (10% w/v) under positive pressure of nitrogen. Anhydrous hexamethylphosphoramide (HMPA, Oakwood Chemical) was distilled from calcium hydride (10% w/v) under vacuum (*ca*. 0.1 torr). Solvents for extraction, thin layer chromatography (TLC), and flash column chromatography were purchased from Fischer (ACS Grade) and VWR (ACS Grade) and used without further purification. Chloroform-d, benzene-d$_6$, acetone-d$_6$ and methanol-d$_4$ for ^{1}H and ^{13}C NMR analysis were purchased from Cambridge Isotope Laboratories and used without further purification. Commercially available reagents were used without further purification unless otherwise noted. Reactions were monitored by thin layer chromatography (TLC) using precoated silica gel plates (EMD Chemicals, Silica gel 60 F$_{254}$). Flash column chromatography was performed over silica gel (Acros Organics, 60 Å, particle size 0.04-0.063 mm). GC/FID analysis was performed on Agilent 7820A system with helium as carrier gas. HPLC analysis was performed on an Agilent 1100 series. Optical rotation readings were obtained using JASCO P-1010 polarimeter. ^{1}H NMR and ^{13}C NMR spectra were recorded on Bruker DRX-500 (BBO probe), Bruker DRX-500 (TCI cryoprobe),

94

Bruker AVANCE600 (TBI probe), and Bruker AVANCE600 (BBFO cryoprobe) spectrometers using residual solvent peaks as internal standards (CHCl$_3$ @ 7.26 ppm ^{1}H NMR, 77.16 ppm ^{13}C NMR; C$_6$H$_6$ @ 7.16 ppm ^{1}H NMR, 128.00 ppm ^{13}C NMR; MeOH @ 3.31 ppm ^{1}H NMR, 49.00 ppm ^{13}C NMR; (CH$_3$)$_2$CO @ 2.05 ppm ^{1}H NMR, 29.84 ppm ^{13}C NMR). High-resolution mass spectra (HRMS) were recorded on Waters LCT Premier TOF spectrometer with ESI and CI sources.

2.3.2 Experimental Procedures
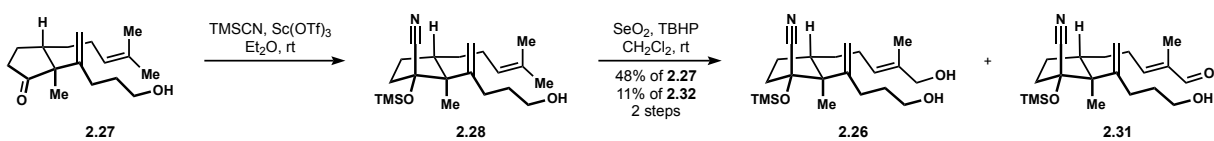
Diol 2.26 and Hydroxyaldehyde 2.31. Scandium(III) trifluoromethanesulfonate (0.71 g, 1.45 mmol) was prepared by drying under vacuum and a heat gun until the solid became a free-flowing powder. After cooling, the powder was dissolved in trimethylsilyl cyanide (9.1 mL, 72.6 mmol) and transferred to a solution of cyclopentanone **2.26** (3.48 g, 11.9 mmol) in diethyl ether (0.6 M) at room temperature. The reaction was stirred for 1 h, then quenched with 10% (w/v) aqueous solution of Na$_2$CO$_3$. The layers were separated and the aqueous layer was extracted twice with diethyl ether (100 mL combined). The organic layers were combined, washed with water (50 mL), brine (50 mL), dried over anhydrous magnesium sulfate, filtered and concentrated under reduced pressure. Crude cyanohydrin **2.28** (11.9 mmol) was subjected to previously reported conditions[18] to afford diol **2.26** (2.17 g, 48% yield) and hydroxyaldehyde **2.31** (0.48 g, 11% yield) as colorless oils.

Diol **2.26**

<superscript>1</superscript>H NMR (500 MHz, CDCl$_3$)

δ 5.43 – 5.40 (m, 1 H)	2.30 – 2.17 (m, 2 H)	1.49 – 1.41 (m, 1 H)
5.07 (s, 1H)	2.12 – 2.06 (m, 2 H)	1.22 – 1.14 (m, 1 H)
4.99 (s, 1 H)	2.02 – 1.89 (m, 2 H)	0.97 (s, 3 H)
4.00 (s, 2 H)	1.80 – 1.74 (m, 2H)	0.22 (s, 9 H)
3.71 – 3.66 (m, 2 H)	1.66 (s, 3 H)	
2.40 – 2.32 (m, 2 H)	1.60 – 1.54 (m, 3 H)	

<superscript>13</superscript>C NMR (125 MHz, CDCl$_3$)

δ 149.7	63.0	26.0
135.5	56.1	25.5
125.5	40.3	13.8
122.3	37.1	13.2
111.2	31.7	1.3
82.6	31.3	
68.9	27.8	

HRMS ES calculated for C$_{21}$H$_{37}$NO$_3$SiNa [M+Na]$^+$: 402.2440, found: 402.2433

TLC: R$_f$ = 0.38 (50% v/v ethyl acetate in hexanes)

$[\alpha]_D^{23}$ 25.0 (c = 1.0, CHCl$_3$); 73% ee

Hydroxyaldehyde **2.31**

^{1}H NMR (500 MHz, CDCl$_3$)

δ 9.39 (s, 1 H)	2.32 – 2.26 (m, 2 H)	1.73 – 1.70 (m, 1H)
6.49 – 6.46 (m, 1 H)	2.23 – 2.16 (m, 1 H)	1.53 – 1.45 (m, 1 H)
5.10 (t, J = 1.5 Hz, 1 H)	2.14 – 2.07 (m, 1 H)	1.33 – 1.27 (m, 2 H)
4.97 (s, 1 H)	1.98 – 1.91 (m, 1 H)	1.00 (s, 3 H)
3.73 – 3.65 (m, 2 H)	1.81 – 1.77 (m, 2 H)	0.23 (s, 9 H)
2.43 – 2.36 (m, 3 H)	1.75 (d, J = 1.2 Hz, 3 H)	

^{13}C NMR (125 MHz, CDCl$_3$)

δ 195.3	111.0	36.9	25.4
153.8	82.7	31.7	12.9
149.5	63.0	30.2	9.3
139.8	56.3	27.7	1.3
122.0	40.8	27.7	

HRMS ES calculated for C$_{21}$H$_{35}$NO$_3$SiNa [M+Na]$^+$: 400.2284, found 400.2290

TLC: R$_f$ = 0.64 (50% v/v ethyl acetate in hexanes)

$[\alpha]_D^{24}$ 22.9 (c = 1.0, CHCl$_3$); 73% ee
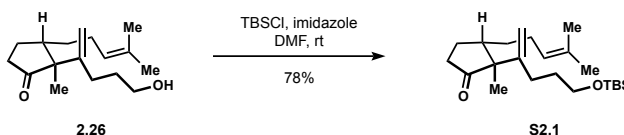
TBS Ether S2.1. To a room temperature solution of alcohol **2.26** (0.19 g, 0.72 mmol) in DMF (0.5 M) was added *tert*-butyldimethylsilyl chloride (0.14 g, 0.90 mmol) followed by imidazole (0.12 g, 1.80 mmol). The reaction was stirred for 2 h, then diluted with hexanes and quenched with water. The layers were separated and the aqueous layer was extracted twice with hexanes (30 mL combined). The organic layers were combined, washed twice with water (20 mL combined), brine (10 mL), dried over anhydrous magnesium sulfate, filtered and concentrated under reduced

pressure. Purification by flash chromatography (gradient elution: 100 % hexanes to 10% v/v ethyl acetate in hexanes) afforded TBS ether **S2.1** (0.21 g, 78% yield) of as a colorless oil.

TBS ether **S2.1**

^{1}H NMR (500 MHz, CDCl$_3$)

δ 5.10 – 5.07 (m, 1 H)	2.22 – 2.17 (m, 2 H)	1.55 –1.50 (m, 1 H)
5.06 (s, 1 H)	2.09 – 2.03 (m, 1 H)	1.26 – 1.20 (m, 1 H)
4.98 (s, 1 H)	1.99 – 1.90 (m, 3 H)	0.99 (s, 3 H)
3.64 – 3.55 (m, 2 H)	1.68 (s, 3 H)	0.88 (s, 9 H)
2.46 – 2.39 (m, 1 H)	1.66 – 1.63 (m, 2 H)	0.04 (s, 6H)
2.28 – 2.26 (m, 1 H)	1.60 (s, 3 H)	

^{13}C NMR (125 MHz, CDCl$_3$)

δ 221.9	63.0	29.8	25.4
149.4	58.8	29.2	18.4
132.0	43.3	26.2	17.8
124.4	38.0	26.1	15.1
112.1	32.2	25.8	5.1

HRMS ES calculated for C$_{23}$H$_{42}$O$_2$SiNa [M+Na]$^+$: 401.2852, found: 401.2867

TLC: R$_f$= 0.86 (50% v/v ethyl acetate in hexanes)
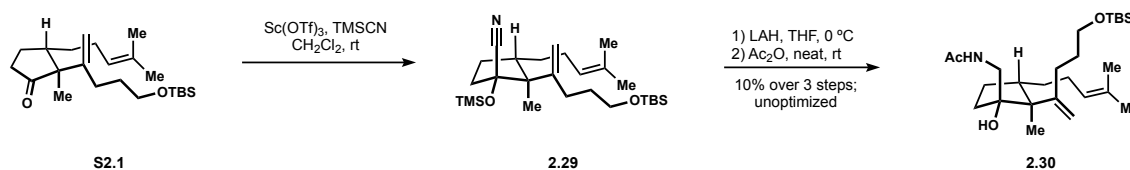
Amide 2.30. Scandium(III) trifluoromethanesulfonate (9.0 mg, 0.02 mmol) was prepared by drying under vacuum and a heat gun until the solid became a free-flowing powder. After cooling, the powder was dissolved in trimethylsilyl cyanide (0.36 mL, 2.83 mmol) and transferred to a

solution of ketone **S2.1** (0.10 g, 0.26 mmol) in CH_2Cl_2 (1.0 M). The reaction was stirred for 1 h, then quenched with 10% (w/v) aqueous solution of Na_2CO_3. The layers were separated and the aqueous layer was extracted twice with CH_2Cl_2 (20 mL combined). The organic layers were combined, washed with water (10 mL), brine (10 mL), dried over anhydrous magnesium sulfate, filtered and concentrated under reduced pressure. Crude cyanohydrin **2.30** was analytically pure and taken forward without further purification.

To a solution of lithium aluminium hydride (11 mg, 0.28 mmol) in THF (1 M) at 0 ℃ was added crude cyanohydrin **2.29** (47 mg, 0.10 mmol) dropwise as a solution in THF (0.5 M). The reaction was stirred for 1 h, then quenched with 1 N aqueous HCl. The layers were separated and the aqueous layer was extracted twice with diethyl ether (20 mL combined). The organic layers were combined, washed with water (10 mL), brine (10 mL), dried over anhydrous magnesium sulfate, filtered and concentrated under reduced pressure.

The crude mixture was dissolved in acetic anhydride (0.1 M) and stirred at 50 ℃ until starting material had been consumed by TLC analysis. The Reaction was diluted with diethyl ether and quenched with saturated aqueous $NaHCO_3$. The layers were separated and the aqueous layer was extracted twice with diethyl ether (20 mL combined). The organic layers were combined, washed with water (10 mL), brine (10 mL), dried over anhydrous magnesium sulfate, filtered and concentrated under reduced pressure. Purification by flash chromatography (gradient elution: 100 % hexanes to 40% v/v ethyl acetate in hexanes) afforded amide **2.30** (4.7 mg, 10 % yield over three steps) as a colorless oil.

Amide **2.30**

¹H NMR (500 MHz, CDCl₃)

δ 5.84 (d, J = 5.5 Hz, 1 H) 2.21 – 2.14 (m, 3 H) 1.60 (s, 3 H)

5.11 (d, J = 7.2 Hz, 1 H) 2.05 – 2.01 (m, 1 H) 1.54 – 1.48 (m, 2 H)

4.93 (s, 1 H) 2.00 (s, 3 H) 1.37 – 1.31 (m, 1 H)

4.80 (s, 1 H) 1.89 – 1.83 (m, 3 H) 1.14 – 1.06 (m, 1 H)

3.64 (t, J = 6.5 Hz, 2 H) 1.74 – 1.71 (m, 1 H) 1.00 (s, 3 H)

3.41 (dd, J = 14.2, 8.4 Hz, 1 H) 1.68 (s, 3 H) 0.89 (s, 9 H)

2.90 – 2.87 (m, 1 H) 1.65 – 1.63 (m, 1 H) 0.05 (s, 6 H)

¹³C NMR (125 MHz, CDCl₃)

δ 171.6	63.2	32.0	23.4
151.25	53.9	28.3	18.5
131.9	46.0	26.7	17.8
124.6	41.5	26.1	14.5
109.6	33.9	25.9	5.1
84.6	32.1	25.2	5.1

HRMS ES calculated for $C_{26}H_{49}NO_3SiNa$ [M+Na]$^+$: 474.3380, found: 474.3383

TLC: R_f = 0.26 (50% v/v ethyl acetate in hexanes)
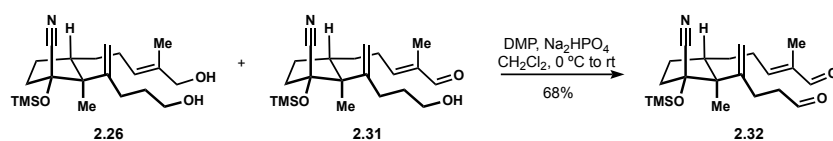
Dialdehyde 2.32. A 250 mL round bottom flask was charged with Dess-Martin periodinane (11.8 g, 27.9 mmol), sodium phosphate dibasic (3.96 g, 27.9 mmol) and CH_2Cl_2 (50 mL). The heterogeneous solution was cooled to 0 °C before adding diol **2.26** (2.17 g, 5.72 mmol) and hydroxyaldehyde **2.31** (0.47 g, 1.25 mmol) in CH_2Cl_2 (20 mL split into three portions) then warmed to room temperature. The solution was stirred 3 h, cooled back down to 0 °C, quenched with saturated aqueous $NaHCO_3$, and the aqueous layer was extracted with CH_2Cl_2 three times

(150 mL combined). The combined organic layers were washed with water (100 mL), brine (100mL), dried over anhydrous magnesium sulfate, filtered and concentrated under reduced pressure. Purification by flash chromatography (gradient elution: 100 % hexanes to 10% v/v ethyl acetate in hexanes) afforded dialdehyde **2.32** (1.79 g, 68% yield) of as a colorless oil.

Dialdehyde **2.32**

^{1}H NMR (500 MHz, CDCl$_3$)

δ 9.81 (t, J = 1.4 Hz, 1 H)	2.47 – 2.36 (m, 4 H)	1.53 – 1.47 (m, 1 H)
9.40 (s, 1 H)	2.33 – 2.26 (m, 1 H)	1.34 – 1.25 (m, 1 H)
6.49 – 6.45 (m, 1 H)	2.15 – 2.08 (m, 1 H)	1.02 (s, 3 H)
5.01 (s, 1 H)	1.99 – 1.92 (m, 1 H)	0.23 (s, 9 H)
4.99 (s, 1 H)	1.75 (d, J = 0.8 Hz, 3 H)	
2.68 – 2.57 (m, 3 H)	1.73 – 1.70 (m, 1 H)	

^{13}C NMR (125 MHz, CDCl$_3$)

δ 202.1	121.8	40.8	23.8
195.3	111.5	36.7	12.8
153.6	82.7	30.1	9.4
148.5	56.2	27.6	1.3
139.9	42.8	25.4	

HRMS ES calculated for C$_{21}$H$_{33}$NO$_3$SiNa [M+Na]$^+$: 398.2127, found: 398.2145

TLC: R$_f$ = 0.83 (50% v/v ethyl acetate in hexanes)

$[\alpha]_D^{22}$ 29.4 (c = 1.0, CHCl$_3$); 73% ee

Fe(acac)$_3$, Na$_2$HPO$_4$
PhSiH$_2$(Oi-Pr), (CH$_2$OH)$_2$, AcOEt
then HCl, THF
41%, d. r. 10:1

2.32 → **2.10**
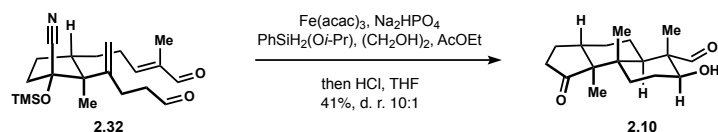
***trans*-decalin 2.10.** A Schlenk flask charged with iron(III) acetylacetonate (1.03 g, 2.92 mmol), dialdehyde **2.32** (0.910 g, 2.42 mmol), sodium phosphate dibasic (0.343 g, 2.42 mmol) ethyl acetate (48 mL) and anhydrous ethylene glycol (0.96 mL). The solution was degassed by freeze-pump-thaw technique (4 cycles), and the flask charged with nitrogen before cooling the solution to 0 °C and adding (isopropoxy)phenylsilane (0.60 mL, 3.63 mmol). The reaction was stirred 1 h at 0 °C, then quenched with 50% (v/v) 1 N aqueous HCl in THF (40 mL) and heated to 60 °C until the product had been fully desilylated by TLC analysis. The aqueous layer was extracted twice with ethyl acetate (200 mL combined) the combined organic layers washed twice with 1 N aqueous HCl (50 mL) or until the aqueous layer appeared colorless. The organic layer was then washed with 2 N aqueous NaOH three times (150 mL combined), brine (100 mL), dried over anhydrous magnesium sulfate, filtered and concentrated under reduced pressure. Purification by flash chromatography (gradient elution 100% hexanes to 20% v/v ethyl acetate in hexanes) afforded *trans*-decalin **2.10** (0.239 g, 35% yield) as a white solid. A set of impure fractions was purified a second time by flash chromatography to afford additional **2.10** (0.040 g, 6% yield). The diastereomeric ratio of products was determined by comparison of the crude ^{1}H NMR with isolated **11** and previously reported *cis* decalin.[18] ^{1}H and ^{13}C NMR data for *trans*-decalin **2.10** match that provided in the literature.[18]

$[\alpha]_D^{22}$ -33.7 (c = 1.0, CHCl$_3$); 73% ee

2.26 → **S2.2** (MeLi, CeCl₃, THF, -78 °C, 59%)
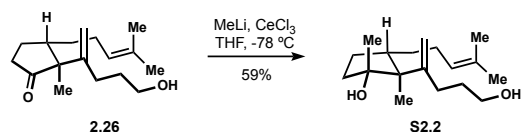
Tertiary alcohol S2.2. Anhydrous CeCl₃ (606 mg, 2.5 mmol) was suspended in THF (2.5 mL) and sonicated under argon atmosphere for 1 h. The resulting slurry was then cooled to -78 °C before adding MeLi (1.7 mL of 1.39 M solution in THF, 2.5 mmol) dropwise. The resulting suspension was stirred 30 min before adding cyclopentanone **2.26** (130 mg, 0.49 mmol) in THF (0.5 mL). The reaction mixture was stirred for 30 min, quenched with saturated aqueous ammonium chloride solution (5 mL) and the aqueous layer was extracted with diethyl ether three times (30 mL combined). The combined organic layers were washed with water (10 mL), brine (10 mL), dried over anhydrous magnesium sulfate, filtered and concentrated under reduced pressure. Purification by flash chromatography (gradient elution: 100% hexanes to 20% v/v ethyl acetate in hexanes) afforded tertiary alcohol **S2.2** (81.2 mg, 59% yield) as a colorless oil.

Tertiary alcohol **S2.2**
^{1}H NMR (500 MHz, CDCl₃)

δ 5.12 (app t, J = 7.2 Hz, 1 H)	2.05 – 1.98 (m, 2 H)	1.35 – 1.28 (m, 1 H)
4.90 (s, 1 H)	1.91 – 1.82 (m, 3 H)	1.14 – 1.09 (m, 1 H)
4.76 (s, 1 H)	1.80 – 1.71 (4 H)	1.07 (s, 3 H)
3.71 – 3.63 (m, 2 H)	1.68 (s, 3 H)	0.98 (s, 3 H)
2.25 (ddd, J = 16.5, 9.4, 6.9 Hz, 1 H)	1.60, (s, 3 H)	
2.16 – 2.09 (m, 1 H)	1.53 – 1.47 (m, 1 H)	

¹³C NMR (125 MHz, CDCl₃)

^{13}C NMR (125 MHz, CDCl$_3$)

δ 151.6	54.4	26.8
131.6	41.6	26.6
124.8	38.6	25.8
108.9	32,2	25.4
82.1	31.7	17.7
62.7	27.9	14.4

HRMS ES calculated for C$_{18}$H$_{32}$O$_2$Na [M+Na]$^+$: 303.2300, found: 303.2296

TLC: R$_f$ = 0.33 (50% v/v ethyl acetate in hexanes)
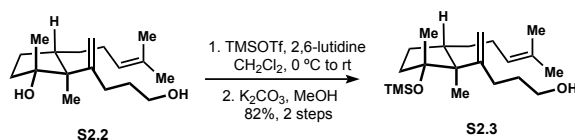
Silyl ether S2.3. To a solution of diol **S2.2** (95.0 mg, 0.34 mmol) and 2,6-lutidine (0.20 mL, 1.7 mmol) in CH$_2$Cl$_2$ (3.4 mL) at 0 °C, was added TMSOTf (0.24 mL, 1.4 mmol) dropwise. The solution was warmed to room temperature and stirred for 30 min, quenched with saturated aqueous ammonium chloride solution (5 mL) and the aqueous layer was extracted with CH$_2$Cl$_2$ three times (30 mL combined). The combined organic layers were washed with water (10 mL), brine (10 mL), dried over anhydrous magnesium sulfate, filtered and concentrated under reduced pressure. The crude material was then dissolved in methanol (3.4 mL) and treated with K$_2$CO$_3$ (5.0 mg, 0.03 mmol). The solution was stirred until the primary alcohol was deprotected as determined by TLC analysis. Once complete, methanol was removed under reduced pressure evaporation. Purification by flash chromatography (gradient elution: 100% hexanes to 10% v/v ethyl acetate in hexanes) yielded 98.8 mg (82% yield) of silyl ether **S2.3** as a colorless oil.

Silyl ether **S2.3**

^{1}H NMR (500 MHz, CDCl$_3$)

δ 5.13 (t, J = 7.1 Hz, 1 H)	2.07 – 1.98 (m, 2H)	1.54 – 1.48 (m, 2H)
4.87 (s, 1 H)	1.92 – 1.81 (m, 3H)	1.36 – 1.27 (m, 1 H)
4.70 (s, 1 H)	1.78 – 1.70 (m, 2 H)	1.12 – 1.06 (m, 1 H)
3.66 (t, J = 6.7 Hz, 2 H)	1.68 (s, 3 H)	1.04 (s, 3 H)
2.29 (ddd, J = 16.4, 10.3, 6.1 Hz, 1 H)	1.67 – 1.62 (m, 1 H)	0.93(s, 3 H)
2.13 (ddd, J = 16.1, 10.3, 5.7 Hz, 1 H)	1.60 (s, 3 H)	0.09 (s, 9H)

^{13}C NMR (125 MHz, CDCl$_3$)

δ 152.3	40.4	25.9
131.5	37.9	25.8
125.0	32.3	17.8
108.3	32.0	14.9
84.3	27.4	2.4
63.4	27.2	
55.3	26.9	

HRMS ES calculated for C$_{21}$H$_{40}$O$_2$SiNa [M+Na]$^+$: 375.2695, found: 375.2684

TLC: R$_f$ = 0.34 (20% v/v ethyl acetate in hexanes)

S2.3 → S2.4
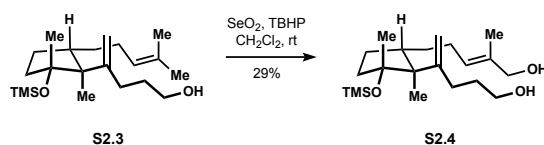
Diol S2.4. Silyl ether **S2.3** (97.0 mg, 0.28 mmol) was subjected to previously reported

conditions[18] to yield diol **S2.4** (30.4 mg, 29% yield) as a colorless oil.
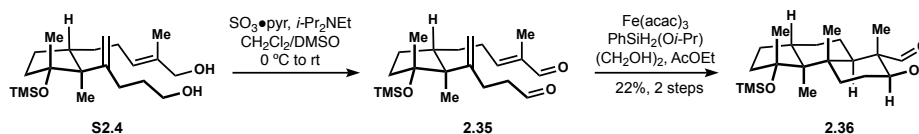
Diol **S2.4**

***Trans*-Decalin 2.36.** To a solution of diol **S2.4** (30.4 mg, 0.08 mmol) in CH_2Cl_2 (0.4 mL) at 0 °C

was added *i*-Pr₂Net (0.11 mL, 0.65mmol) followed by a solution of SO₃•pyr (78.0 mg, 0.49 mmol)

in DMSO (0.25 mL). The solution was stirred at 0 °C for 30 min, then warmed to room temperature

and stirred for 1 h before being diluted with CH_2Cl_2 (5 mL) and quenched with water (5 mL). The

aqueous layer was extracted with CH_2Cl_2 twice (20 mL combined) and the combined organic layers

washed with water (10 mL), brine (10 mL), dried over anhydrous magnesium sulfate, filtered and

concentrated under reduced pressure. Crude dialdehyde **2.35** was then subjected to polycyclization

conditions described for dialdehyde **2.32** above to yield *trans*-decalin **2.36** (6.4 mg, 22% yield) as

a thin film.

Trans-decalin **2.36**

^{1}H NMR (500 MHz, CDCl$_3$)

δ 9.34 (s, 1H)	1.73 – 1.65 (m, 3 H)	1.32 – 1.20 (m, 3 H)
3.71 (dd, J = 10.7, 4.6 Hz, 1 H)	1.63 – 1.54 (m, 3 H)	1.16 (s, 3 H)
2.06 – 2.00 (m, 2 H)	1.52 – 1.47 (m, 1 H)	1.11 (s, 3 H)
1.91 (td, J = 12.7, 3.7 Hz, 1 H)	1.43 – 1.40 (m, 1 H)	1.02 (s, 3 H)
1.79 (dd, J = 14.3, 4.2 Hz, 1 H)	1.38 (s, 3 H)	0.08 (s, 9 H)

^{13}C NMR (125 MHz, CDCl$_3$)

δ 206.9	39.9	24.2
87.0	37.3	19.3
72.3	32.0	13.1
55.1	31.7	9.6
54.0	27.4	2.5
41.6	26.6	
41.3	25.6	

HRMS ES calculated for C$_{21}$H$_{38}$O$_3$SiNa [M+Na]$^+$: 389.2488, found 389.2494

TLC: R$_f$ = 0.38 (20% v/v ethyl acetate in hexanes)
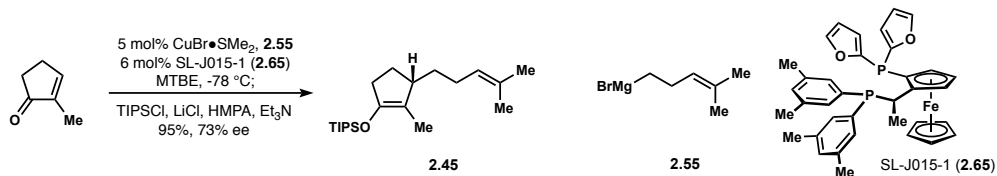
Silyl enol ether 2.45. In a glovebox under nitrogen atmosphere, a 1 L Schlenk flask was charged with JosiPhos **2.65** (SL-J015-1, 1.11g, 1.8 mmol). The flask was sealed with a plastic cap, removed from the glovebox and connected to a vacuum manifold. Under continuous flow of nitrogen, the plastic cap was removed to add CuBr•SMe$_2$ (0.30 g, 1.5 mmol) and replaced with a rubber septum. Methyl *tert*-butyl ether (400 mL) was added to the flask and the suspension sonicated 1 hour. Once CuBr•SMe$_2$ was no longer visible in solution, 2-methylcyclopent-2-en-1-one (2.88 g, 30 mmol) was added to the flask and the solution cooled to -78 °C. A solution of (4-methylpent-3-en-1-yl)magnesium bromide **2.55** (41 mL of 1.1 M solution in diethyl ether, 45 mmol; prepared from 5-bromo-2-methylpent-2-ene) was added dropwise with a syringe pump (0.67 mL/min). The reaction mixture was stirred 24 h at -78 °C and then added in succession, LiCl (60 mL, 0.5 M in THF), TIPSCl (19.2 mL, 90 mmol), HMPA (41.8 mL, 240 mmol) and Et$_3$N (14.6 mL, 105 mmol). The heterogeneous mixture was brought to room temperature and then heated to 50 °C until conversion of the magnesium enolate to the enoxysilane was complete as determined by TLC analysis. The reaction mixture was cooled back down to 0 °C and quenched with a 3:1 (v/v) mixture of saturated aqueous NH$_4$Cl and 28% (v/v) aqueous NH$_3$ (200 mL). The resulting emulsion was warmed to room temperature and diluted with hexanes (300 mL). The layers were separated and the organic layer washed twice with the NH$_4$Cl/NH$_3$ solution (200 mL combined). The aqueous layers were combined and extracted with hexanes twice (400 mL combined). The organic layers were then combined, washed with water (500 mL), brine (500 mL), dried over anhydrous magnesium sulfate, filtered and concentrated under reduced pressure. Purification by flash

chromatography on Et$_3$N-treated silica gel (elution with hexanes) afforded silyl enol ether **2.45** (9.61 g, 95% yield, 73% ee) as a colorless oil.

^{1}H and ^{13}C NMR data match that provided in the literature.[18] Enantiopurity was assessed by hydrolyzing (1N HCl in MeOH) a sample of silyl enol ether **2.45** to the corresponding ketone **S2.5** and analyzing the major diastereomer on a GC/FID (HP – Chiral – 20B; 6.88 psi; 0.5 mL/min; column temperature 105 °C for 180 min, then 10 °C/min to 200 °C, hold for 0 min): t_R = 179.79, 181.97 min.

$[\alpha]_D^{21}$ -1.34 (c = 1.0, CHCl$_3$); 73% ee
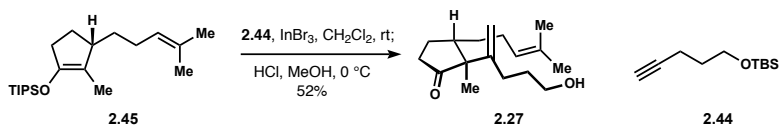
Cyclopentanone 2.27. Prepared from enoxysilane **2.45** according to previously reported procedures.[18]

Cyclopentanone **2.27**

$[\alpha]_D^{24}$ -13.1 (c = 1.0, CHCl$_3$); 73% ee
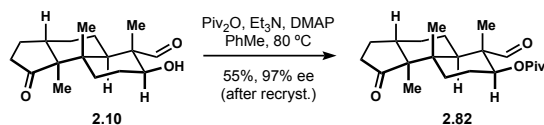
Pivalate 2.82. A 25 mL round bottom flask was charged with alcohol **2.10** (0.280 g, 1.01 mmol) suspended in toluene (2.0 mL). To the solution was added pivalic anhydride (0.82 mL, 4.04 mmol), Et$_3$N (0.70 mL, 5.05 mmol) and then DMAP (0.012 g, 0.10 mmol). The reaction mixture was heated at 80 °C for 8 h, then cooled back down to room temperature and quenched with saturated aqueous ammonium chloride solution (15 mL). The aqueous layer was extracted with diethyl ether

three times (45 mL combined) and the combined organic layers washed with water (20 mL), brine (20 mL), dried over anhydrous magnesium sulfate, filtered and concentrated under reduced pressure. Purification by flash chromatography (gradient elution: 100% hexanes to 10% v/v ethyl acetate in hexanes) afforded pivalate **2.82** (0.317 g, 87% yield) as a white solid. Pivalate **2.82** (0.291 g) was recrystallized by dissolving in boiling hexanes (distilled) and slow cooling to 4 °C. The supernatant was decanted to afford 0.183 g (63% recovery) of needle-like crystals. Recrystallization batches varied between 97 to 99% enantiomeric excess, which was determined on the following compound **2.22**.

Pivalate **2.82**

^{1}H NMR (500 MHz, CDCl$_3$)

δ 9.25 (s, 1 H)	2.03 (dt, J = 19.3, 9.5 Hz, 1 H)	1.12 (s, 9 H)
4.90 (dd, J = 10.3, 5.7 Hz, 1 H)	1.93 – 1.89 (m, 1H)	1.10 (s, 3 H)
2.35 (ddd, J = 19.5, 8.3, 0.8 Hz, 1 H)	1.86 – 1.68 (m, 5 H)	1.06 (s, 3 H)
2.26 – 2.23 (m, 1 H)	1.60 – 1.53 (m, 2 H)	1.00 (s, 3H)
2.22 – 2.16 (m, 1 H)	1.46 – 1.39 (m, 2 H)	

^{13}C NMR (125 MHz, CDCl$_3$)

δ 220.3	54.5	37.4	23.8
203.8	40.4	30.3	22.7
177.7	39.8	27.2	17.6
72.9	39.0	25.5	10.5
55.8	38.5	24.5	9.2

HRMS ES calculated for C$_{22}$H$_{34}$O$_4$Na [M+Na]$^+$: 385.2355, found: 385.2362

TLC: R$_f$ = 0.82 (50% v/v ethyl acetate in hexanes)

$[\alpha]_D^{24}$ -50.8 (c = 1.0, CHCl$_3$); 99% ee
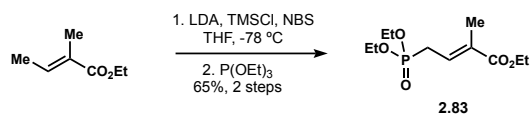
Phosphonate 2.83. Ethyl tiglate (8.3 mL, 60 mmol) was added dropwise to a solution of LDA

(120 mL of 0.52 M solution in THF, 63 mmol) at -78 °C over the course of 1 h. The solution was

stirred for an additional 20 min before adding TMSCl (11.4 mL, 90 mmol) as a solution in THF

(12 mL). The solution was stirred 1 h at -78 °C before being cannula transferred over to a

suspension of NBS (16.02 g, 90 mmol) in THF (30 mL) at -78 °C and stirred for an additional 2

h. The reaction was quenched with brine (200 mL) and the aqueous layer was extracted with

hexanes (three times, 300 mL combined). The combined organic layers were washed with brine

(200 mL), dried over anhydrous magnesium sulfate, filtered through a plug of silica and

concentrated to provide crude ethyl (E)-4-bromo-2-methylbut-2-enoate, which was used without

further purification. The crude bromide was subjected to previously reported conditions[2] to afford

phosphonate **2.83** (10.41 g, 65% yield) as a pale-yellow oil. ^{1}H and ^{13}C NMR data match that

provided in the literature.[52]
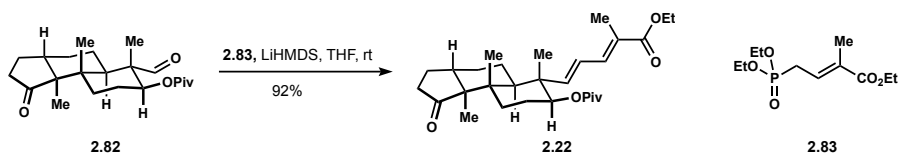
Dieneoate 2.22. To a solution of phosphonate **2.83** (1.12 g, 4.56 mmol) in THF (4.6 mL) at 0 °C

was added LiHMDS (3.2 mL, 1.0 M solution in THF, 3.2 mmol). The resulting solution was stirred

at 0 °C for 30 min, then added aldehyde **2.82** (0.165 g, 0.46 mmol) in THF (4.6 mL split into three

portions). The reaction mixture was then warmed to room temperature and stirred overnight (16

h). The reaction was quenched with 1 N aqueous HCl (10 mL) and the aqueous layer was extracted

with diethyl ether three times (45 mL combined). The combined organic layers were washed with

water (20 mL), brine (20 mL), dried over anhydrous magnesium sulfate, filtered and concentrated under reduced pressure. Purification by flash chromatography (gradient elution: 100% hexanes to 10% v/v ethyl acetate in hexanes) afforded dienoate **2.22** (0.198 g, 92% yield) as a white solid. Enantiopurity was assessed by HPLC (Chiralcel AS-H (w/o guard); 1 mL/min; 1% v/v i-PrOH in hexanes): t_R = 7.64, 19.15 min.

Dienoate **2.22**

^{1}H NMR (500 MHz, CDCl$_3$)

δ 7.13 (d, J = 11.1 Hz, 1 H)	2.22 – 2.15 (m, 2 H)	1.42 – 1.34 (m, 3 H)
6.23 (dd, J = 15.4, 11.2 Hz, 1 H)	2.01 (dt, J = 19.4, 9.4 Hz, 1 H)	1.30 (t, J = 7.1 Hz, 3 H)
5.76 (d, J = 15.3 Hz, 1 H)	1.90 (d, J = 1.3 Hz, 3 H)	1.12 (s, 3 H)
4.62 (dd, J = 10.7, 6.1 Hz, 1 H)	1.83 – 1.78 (m, 1 H)	1.09 (s, 9 H)
4.19 (q, J = 7.2 Hz, 2 H)	1.72 – 1.65 (m, 4 H)	1.07 (s, 3 H)
2.33 (dd, J = 19.3, 8.2 Hz, 1 H)	1.57 – 1.48 (m, 3 H)	0.95 (s, 3 H)

^{13}C NMR (125 MHz, CDCl$_3$)

δ 220.8	77.3	39.0	23.4
177.7	60.7	37.6	18.3
168.6	56.3	30.5	14.5
151.5	45.8	27.3	12.7
138.3	45.6	25.8	12.5
125.9	40.6	23.9	10.5
125.0	39.0	23.7	

HRMS ES calculated for C$_{29}$H$_{44}$O$_5$Na [M+Na]$^+$: 495.3087, found: 495.3102

TLC: R$_f$ = 0.40 (20% v/v ethyl acetate in hexanes)

$[\alpha]_D^{23}$ -64.8 (c = 1.0, CHCl$_3$); 97% ee
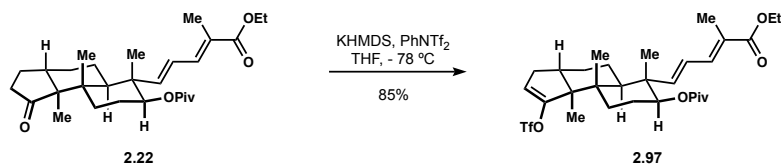
Vinyl Triflate 2.97. To a solution of ketone **2.22** (21 mg, 0.044 mmol) in THF (0.1 M) at -78 ℃ was added KHMDS (0.067 mmol) as a solution in THF (0.5 M). The reaction was stirred 15 min before adding *N*-phenyltriflimide (33 mg, 0.088 mmol) as a solution in THF (0.2 M). After stirring an additional 15 min, the reaction was quenched with methanol (0.1 mL), acetone, (0.2 mL), Et$_3$N (0.1 mL) and a spatula tip of DMAP according to a literature protocol. The solution was stirred for 1 h, quenched with 1 N aqueous HCl and the aqueous layer was extracted with diethyl ether three times (20 mL combined). The combined organic layers were washed with water (5 mL), brine (5 mL), dried over anhydrous magnesium sulfate, filtered and concentrated under reduced pressure. Purification by flash chromatography (gradient elution: 100% hexanes to 5% v/v ethyl acetate in hexanes) yielded vinyl triflate **2.101** (22.2 mg, 85% yield) as a white solid.

Vinyl triflate **2.97**
^{1}H NMR (500 MHz, CDCl$_3$)

δ 7.13 (d, *J* = 11.2 Hz, 1 H)	2.18 – 2.14 (m, 1 H)	1.29 (t, J = 7.1 Hz, 3 H)
6.23 (dd, *J* = 15.4, 11.2 Hz, 1 H)	2.02 – 1.96 (m, 1 H)	1.14 (s, 3 H)
5.74 (d, *J* = 15.4 Hz, 1 H)	1.90 (s, 3 H)	1.13 (s, 3 H)
5.56 (t, *J* = 1.4 Hz, 1 H)	1.73 – 1.68 (m, 4 H)	1.09 (s, 9 H)
4.60 (dd, *J* = 8.7, 6.9 Hz, 1 H)	1.58 – 1.56 (m, 3 H)	1.07 (s, 3 H)
4.19 (q, *J* = 7.1 Hz, 2 H)	1.45 – 1.42 (m, 1 H)	
2.28 – 2.22 (m, 1 H)	1.34 – 1.32 (m, 1 H)	

^{13}C NMR (125 MHz, CDCl$_3$)

δ 177.6	114.4	39.0	23.6
168.6	77.0	38.9	18.8
157.9	60.7	31.0	14.4
151.3	54.9	30.3	12.7
138.2	45.9	27.3	12.2
126.0	45.4	24.5	
125.1	43.0	24.4	

*Note: 2 carbon signals are missing despite multiple attempts at acquiring this spectra.

HRMS ES calculated for C$_{30}$H$_{43}$F$_3$O$_7$SNa [M+Na]$^+$: 627.2579, found: 627.2567

TLC: R$_f$ = 0.63 (20% v/v ethyl acetate in hexanes)
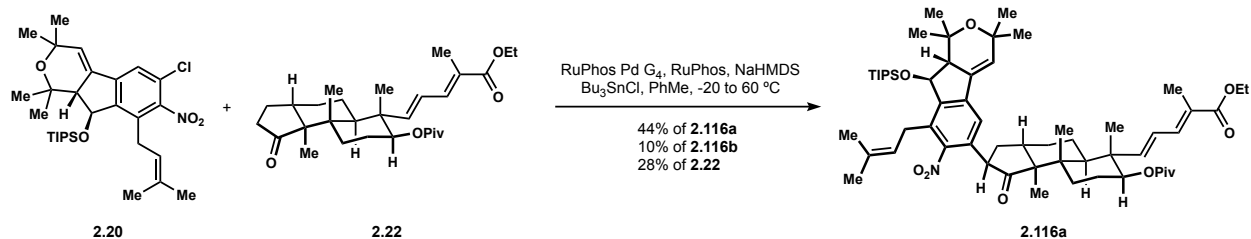
Arylketones 2.116a and 2.116b. Ketone **2.22** (72.0 mg, 0.15 mmol) and chloroarene **2.20** (92.1 mg, 0.17 mmol) were azeotropically dried with benzene in separate dram vials before being transferred into a glovebox. To the dram vial containing chloroarene **2.20** was added RuPhos Pd G4 (32.3 mg, 0.038 mmol) and RuPhos (17.7 mg, 0.038 mmol). To the dram vial containing ketone **13** was added Bu$_3$SnCl (3.04 mL, 0.05 M in toluene), which was then placed in a freezer cooled to -25 °C for 1 h. A 0.05 M solution of NaHMDS in toluene was also prepared and placed in the freezer for 1 h. NaHMDS (3.35 mL, 0.05 M) was then added to the ketone solution and placed back in the freezer for 30 min, then allowed to warm to room temperature over an additional 30 min. The tin enolate solution was next added to the vial containing arylchloride, precatalyst and ligand, cooled back down to -25 °C for 1 h and then added NaHMDS (0.76 mL, 0.05 M). The reaction was warmed back up to room temperature then heated to 50 °C in a sand bath for 17 h. The reaction mixture was removed from the glovebox, quenched with a saturated aqueous solution of NH$_4$Cl and the aqueous layer was extracted with ethyl acetate three times (30 mL combined). The combined organic layers were washed with water (20 mL), brine (20 mL), dried over anhydrous magnesium sulfate, filtered and concentrated under reduced pressure. Purification by flash chromatography (gradient elution: 100% hexanes to 8% v/v ethyl acetate in hexanes) yielded a mixture of diastereomers and starting ketone **2.22**. Further purification by preparatory TLC (15% v/v ethyl acetate in hexanes) allowed for separation of diastereomers, yielding undesired arylketone **2.116b** (16.0 mg, 10% yield) and desired arylketone **2.116a** (72.5 mg, 44% yield) and

as pale-yellow amorphous solids along with starting ketone **2.22** (19.8 mg, 28% recovery). The diastereomeric ratio was determined by analysis of crude ^{1}H NMR.
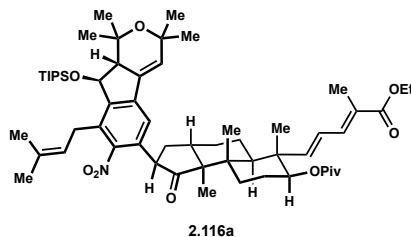
2.116a

Arylketone **2.116a**

^{1}H NMR (500 MHz, CD$_3$OD)

7.26 (s, 1 H)	1.90 (d, J = 1.2 Hz, 3 H)
7.16 (d, J = 11.4 Hz, 1 H)	1.83 – 1.74 (m, 4 H)
6.37 – 6.32 (m, 2 H)	1.70 (s, 3 H)
5.89 (d, J = 15.3 Hz, 1 H)	1.64 (s, 3 H)
5.28 (d, J = 3.1 Hz, 1 H)	1.64 – 1.53 (m, 1 H)
4.94 – 4.92 (m, 1 H)	1.51 – 1.44 (m, 6 H)
4.67 (dd, J = 11.4, 4.6 Hz, 1 H)	1.34 (s, 3 H)
4.19 (q, J = 7.0 Hz, 2 H)	1.33 (s, 3 H)
3.88 (dd, J = 15.4, 7.0 Hz, 1 H)	1.30 (t, J = 7.1 Hz, 3 H)
3.73 (dd, J = 10.5, 2.0 Hz, 1 H)	1.21 (s, 3 H)
3.35 (dd, J = 15.6, 6.8 Hz, 1 H)	1.18 (s, 3 H)
2.81 (t, J = 2.8 Hz, 1 H)	1.17 (s, 3H)
2.69 – 2.63 (m, 1 H)	1.10 (s, 9 H)
2.27 – 2.20 (m, 1 H)	1.02 – 0.99 (m, 12 H)
2.18 – 2.16 (m, 1 H)	0.93 (d, J = 6.1 Hz, 9 H)
2.06 (ddd, J = 13.5, 7.2, 2.1 Hz, 1 H)	0.86 (s, 3 H)

¹³C NMR (125 MHz, CD$_3$OD)

217.9	134.0	59.0	30.1	18.2
179.2	127.9	58.0	30.0	18.1
170.0	126.7	47.8	28.4	15.1
154.0	126.1	46.9	27.5	14.6
153.3	121.5	46.5	26.7	12.9
145.0	118.3	40.4	25.7	12.7
142.7	78.8	40.4	24.6	12.3
139.7	78.4	39.9	24.3	
137.0	76.0	33.0	22.1	
136.3	74.4	31.4	18.7	
135.1	61.8	31.3	18.6	

HRMS ES calculated for C$_{59}$H$_{89}$O$_9$SiNa [M+Na]$^+$: 1006.6204, found: 1006.6236

TLC: R$_f$ = 0.52 (20% v/v ethyl acetate in hexanes)

[α]$_D^{22}$ -115.4 (c = 1.0, CHCl$_3$)
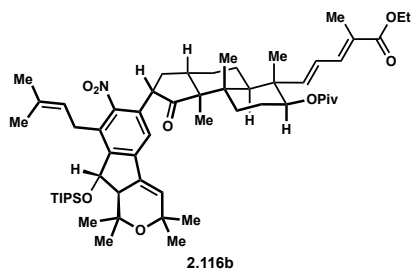
2.116b

Arylketone **2.116b**

^{1}H NMR (500 MHz, CD$_3$OD)

7.18 (s, 1 H)	1.90 (d, J = 1.2 Hz, 3 H)
7.16 (d, J = 11.2 Hz, 1 H)	1.84 – 1.75 (m, 3 H)
6.35 (dd, J = 15.4, 11.2 Hz, 1 H)	1.73 (s, 3 H)
6.29 (d, J = 2.6 Hz, 1 H)	1.71 – 1.68 (m, 2 H)
5.89 (d, J = 15.4 Hz, 1 H)	1.66 (s, 3 H)
5.28 (d, J = 3.0 Hz, 1 H)	1.52 – 1.43 (m, 6 H)
5.03 – 5.00 (m, 1 H)	1.33 (s, 3 H)
4.69 (dd, J = 11.0, 4.8 Hz, 1 H)	1.32 (s, 3 H)
4.19 (q, J = 7.1 Hz, 2 H)	1.31 – 1.28 (m, 4 H)
3.91 (dd, J = 15.3, 7.5 Hz, 1 H)	1.20 (s, 3 H)
3.35 (dd, J = 10.7, 8.1 Hz, 1 H)	1.18 (s, 3 H)
3.19 (dd, J = 15.2, 5.7 Hz, 1 H)	1.15 (s, 3 H)
2.80 (t, J = 2.8 Hz, 1 H)	1.10 (s, 9 H)
2.42 – 2.36 (m, 1 H)	1.02 – 0.97 (m, 12 H)
2.25 (ddd, J = 12.1, 8.1, 5.2 Hz, 1 H)	0.92 (d, J = 6.7 Hz, 9 H)
2.21 – 2.18 (m, 1 H)	0.86 (s, 3 H)

118

¹³C NMR (125 MHz, CD₃OD)

^{13}C NMR (125 MHz, CD$_3$OD)

219.5	133.8	58.9	30.0	18.5
179.2	128.1	58.3	30.0	18.2
170.0	126.8	54.1	28.3	15.2
154.0	126.1	47.0	27.6	14.6
153.2	121.8	46.6	25.8	12.8
145.4	118.9	40.5	25.7	12.7
142.8	78.7	40.2	24.9	10.9
139.7	78.3	39.9	24.3	
136.9	76.0	35.1	22.1	
135.0	74.4	31.6	19.1	
134.8	61.8	31.4	18.7	

HRMS ES calculated for C$_{59}$H$_{89}$O$_9$SiNa [M+Na]$^+$: 1006.6204, found: 1006.6193

TLC: R$_f$ = 0.48 (20% v/v ethyl acetate in hexanes)

$[\alpha]_D^{22}$ -52.1 (c = 1.0, CHCl$_3$)

Diastereomers **2.116a** and **2.116b** were distinguished through COSY and NOESY correlations (see below).

2.116b
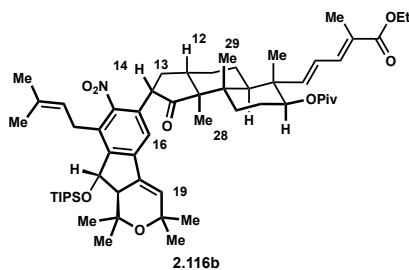
¹H (Nod C numbering)	Observed Correlations	Absent Correlations
H16 (6.99 ppm)	H13-*cis* (1.59 ppm)	H29 (1.11 ppm)
	H14 (3.32 ppm)	H12 (2.27 ppm)
	H19 (6.09 ppm)	
	H28 (1.12 ppm)	
H12 (2.27 ppm)	H29 (1.11 ppm)	

2.116a
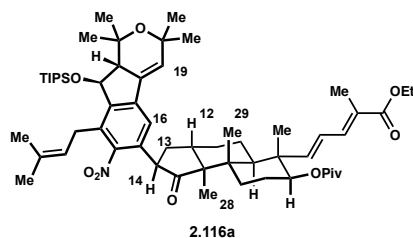
^{1}H (Nod C numbering)	Observed Correlations	Absent Correlations
H16 (7.01 ppm)	H12 (2.48 ppm)	H28 (1.12 ppm)
	H13-*cis* (2.02 ppm)	
	H14 (3.70 ppm)	
	H19 (6.02 ppm)	
	H29 (1.19 ppm)	
H12 (2.48 ppm)	H13-*cis* (2.02 ppm)	
	H29 (1.19 ppm)	

2.115a → **S2.6**

1) Zn, AcOH, EtOH, rt
2) TAS-F, DMF, 60 °C

73%, 2 steps
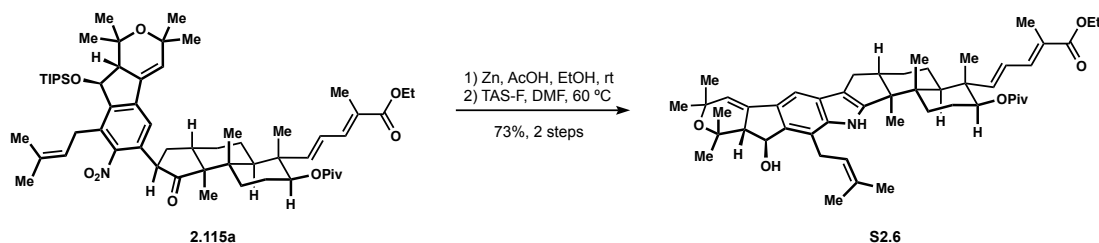
Nodulisporic acid C diester S2.6. A 1 dram vial was charged with arylketone **2.116a** (19 mg, 0.019 mmol), Zn dust (62 mg, 0.95 mmol), AcOH (54 μL, 0.95 mmol), and EtOH (1.9 mL) and stirred vigorously at room temperature for 45 min. The reaction was diluted in ethyl acetate and filtered through Celite, then concentrated under reduced pressure. The crude material was added to an oven-dried 1 dram vial, then transferred into a glovebox. The vial was charged with TAS-F and DMF, sealed with a screw cap containing a septum, and heated to 60 °C for 1 h. The reaction was quenched with saturated aqueous NH$_4$Cl and the aqueous layer was extracted twice with ethyl acetate. The combined organic layers were washed twice with water and once with brine, then dried over anhydrous sodium sulfate, filtered and concentrated under reduced pressure.

Purification on pH 7 silica (gradient elution: 10% to 15% v/v ethyl acetate in hexanes) afforded

10.5 mg (73 % yield, 2 steps) of nodulisporic acid C diester **S2.6** as a yellow solid.

Nodulisporic acid C diester **S2.6**

^{1}H NMR (600 MHz, CDCl$_3$):

δ 7.83 (s, 1 H)	2.75 – 2.70 (m, 1 H)	1.46 – 1.40 (m, 1 H)
7.40 (s, 1 H)	2.68 (dd, J = 4.8, 2.9 Hz, 1 H)	1.34 (s, 3 H)
7.16 (d, J = 11.1 Hz, 1 H)	2.64 (dd, J = 13.3, 6.4 Hz, 1 H)	1.32 – 1.30 (m, 6 H)
6.28 (dd, J = 15.4, 11.2 Hz, 1 H)	2.31 (dd, J = 13.3, 10.6 Hz, 1 H)	1.17 (s, 3 H)
5.96 (d, J = 2.9 Hz, 1 H)	2.09 – 2.04 (m, 1 H)	1.16 (s, 3 H)
5.80 (d, J = 15.3 Hz, 1 H)	1.92 (d, J = 1.2 Hz, 3 H)	1.12 (s, 9 H)
5.42 – 5.39 (m, 1 H)	1.90 – 1.86 (m, 5 H)	1.08 (s, 3 H)
5.08 (dd, J = 8.8, 5.0 Hz, 1 H)	1.80 – 1.77 (m, 1 H)	1.02 (s, 3 H)
4.67 (dd, J = 9.9, 6.4 Hz, 1 H)	1.76 (d, J = 1.0 Hz, 3 H)	
4.20 (q, J = 7.1 Hz, 2 H)	1.61 – 1.54 (m, 1 H)	
3.84 – 3.75 (m, 2 H)	1.51 – 1.49 (m, 5 H)	

^{13}C NMR (151 MHz, CDCl$_3$):

δ 177.8	133.0	118.6	53.2	30.1	23.6
168.7	131.9	107.6	49.0	30.0	22.9
152.0	126.8	77.2	45.8	27.6	19.4
151.3	126.0	76.6	45.1	27.3	18.2
141.2	125.2	74.0	39.1	27.3	14.6
138.2	123.4	72.7	39.0	25.8	14.5
136.1	121.8	60.7	33.2	25.2	12.8
135.4	120.4	60.4	33.1	24.5	12.3

HRMS (ES+) calculated for C$_{50}$H$_{69}$NO$_6$Na [M+Na]$^+$: 802.5023, found: 802.5002.

TLC: R$_f$ = 0.25 (20% v/v ethyl acetate in hexanes)

$[\alpha]_D^{22}$ -19.8 (c = 0.5, CHCl$_3$)

S2.6   (–)-nodulisporic acid C (**2.19**)

Reagents above arrow: LiOH, H$_2$O, MeOH, 1,4-dioxane, 100 °C, quant.
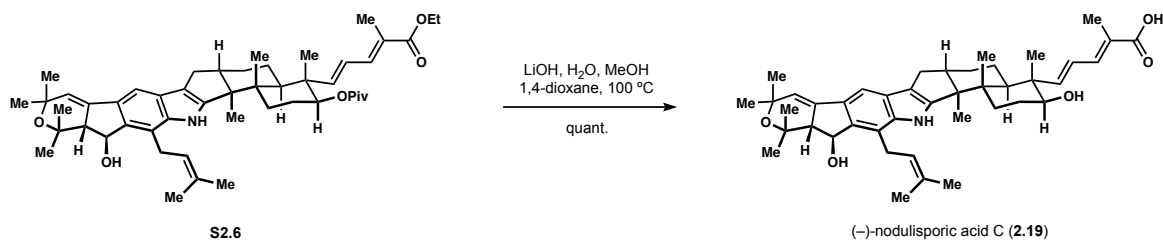
(–)-Nodulisporic acid C (2.19). A 1 dram vial was charged with **S2.6** (6 mg, 0.008 mmol) and LiOH·H$_2$O (17 mg, 0.40 mmol) and flushed with argon. Water (50 μL) that had been degassed with argon was added, followed by dioxane (0.1 mL) and MeOH (50 μL). The dram vial was again flushed with argon and sealed with a teflon-lined screw cap. The reaction was heated to 100 °C for 30 h, then cooled to room temperature. The solvents were evaporated under reduced pressure and the crude was dissolved in a mixture of AcOH (0.14 mL) and ethyl acetate (2 mL) and sonicated until homogeneous. The volatiles were evaporated under reduced pressure, re-dissolved in ethyl acetate and transferred to a round bottom flask with filtering through Celite. The solvent was again evaporated under reduced pressure to afford 5.5 mg (*ca*. 100% yield) of nodulisporic acid C as a yellow solid. The crude was dissolved in acetone-d6 and transferred to an NMR tube. After collection of spectral data, 10 μL of D$_2$O was added and new spectra were collected. 10 μL of a saturated solution of NaHCO$_3$ in D$_2$O was added and shaken thoroughly, then new spectra of the sodium salt of nodulisporic acid C were collected. During the course of our investigations we were unable to obtain an adequate spectrum of the sodium salt in the absence of water due to substantial peak broadening. Upon addition of D$_2$O, rapid exchange of the indole NH with deuterium was observed. This and the D$_2$O/(CD$_3$)$_2$CO mixture could also account for the slight differences in chemical shift of the sodium salt compared to the reported spectra. However, we found that the free acid of nodulisporic acid C matched the reported spectra well and as such was also used for comparison.
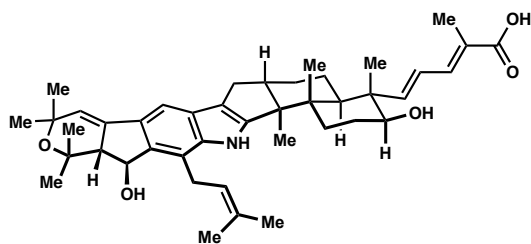
(–)-nodulisporic acid C (**2.19**)

Nodulisporic acid C (**2.19**)

^{1}H NMR (600 MHz, (CD$_3$)$_2$CO)

δ 9.04 (s, 1 H)	2.78-2.73 (m, 1 H)	1.68 (s, 3 H)
7.32 (s, 1 H)	2.69 (dd, J = 4.8, 3.0 Hz, 1 H)	1.65-1.57 (m, 2 H)
7.22 (d, J = 11.0 Hz, 1 H)	2.63 (dd, J = 12.9, 6.4 Hz, 1 H)	1.54-1.45 (m, 2 H)
6.38 (dd, J = 15.4, 11.3 Hz, 1 H)	2.30 (dd, J = 12.3, 11.7 Hz, 1 H)	1.41 (s, 3 H)
5.99-5.97 (m, 2 H)	1.92 (s, 3 H)	1.28 (s, 3 H)
5.31-5.30 (m, 1 H)	1.91-1.85 (m, 2 H)	1.26 (s, 3 H)
5.03 (d, J = 4.9 Hz, 1 H)	1.84 (s, 3 H)	1.16 (s, 3 H)
4.03 (dd, J = 15.3, 8.0 Hz, 1 H)	1.81-1.78 (m, 1 H)	1.09 (s, 3 H)
3.71 (dd, J = 15.1, 5.4 Hz, 1 H)	1.78-1.75 (m, 1 H)	1.07 (s, 3 H)
3.49 (dd, J = 10.7, 4.4 Hz, 1 H)	1.73-1.69 (m, 1 H)	1.02 (s, 3 H)

^{13}C NMR (126 MHz, (CD$_3$)$_2$CO)

δ 170.5	132.2	118.9	54.4	30.4	25.5
154.8	131.7	107.6	49.8	30.4	23.2
153.1	127.4	77.0	47.9	29.8	19.4
142.2	125.8	76.5	45.1	28.0	18.2
139.6	124.4	74.3	39.8	27.7	14.8
137.7	123.4	74.3	39.8	27.7	14.8
137.2	119.8	60.7	32.4	25.8	11.8

HRMS (ES+) calculated for C$_{43}$H$_{57}$NO$_5$Na [M+Na]$^+$: 690.4135, found: 690.4130.

TLC: R$_f$ = 0.5 (10% v/v methanol in CH$_2$Cl$_2$)

[α]$_D^{22}$ -18.9 (c = 0.4, MeOH)
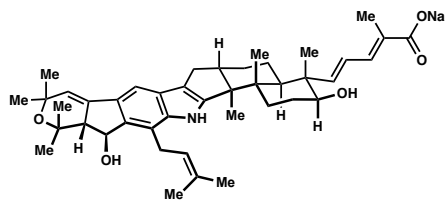
(–)-nodulisporic acid C (**2.19**) sodium salt

Nodulisporic acid C (**2.19**) sodium salt

^{1}H NMR (600 MHz, (CD$_3$)$_2$CO)

δ 9.04 (s, 1 H)	2.76-2.71 (m, 1 H)	1.63-1.55 (m, 2 H)
7.30 (s, 1 H)	2.69 (dd, J = 4.9, 3.0 Hz, 1 H)	1.54-1.49 (m, 1 H)
7.16 (d, J = 11.2 Hz, 1 H)	2.61 (dd, J = 13.1, 6.4 Hz, 1 H)	1.48-1.42 (m, 1 H)
6.34 (dd, J = 15.4, 11.2 Hz, 1 H)	2.27 (dd, J = 13.0, 10.8 Hz, 1 H)	1.40 (s, 3 H)
5.95 (d, J = 2.9 Hz, 1 H)	1.89 (s, 3 H)	1.27 (s, 3 H)
5.90 (d, J = 15.3 Hz, 1 H)	1.87-1.85 (m, 2 H)	1.26 (s, 3 H)
5.30 (t, J = 6.9 Hz, 1 H)	1.82 (s, 3 H)	1.14 (s, 3 H)
5.01 (d, J = 5.1 Hz, 1 H)	1.81-1.77 (m, 1 H)	1.07 (s, 3 H)
4.01 (dd, J = 15.0, 7.8 Hz, 1 H)	1.77-1.74 (m, 1 H)	1.05 (s, 3 H)
3.71 (dd, J = 15.0, 5.6 Hz, 1 H)	1.71-1.67 (m, 1 H)	1.00 (s, 3 H)
3.46 (dd, J = 11.1, 4.6 Hz, 1 H)	1.66 (s, 3 H)	

^{13}C NMR (126 MHz, (CD$_3$)$_2$CO)

δ 171.6	132.1	118.7	54.3	30.3	25.3
153.6	131.7	118.7	498	30.3	23.1
153.0	127.3	76.9	47.7	27.9	19.3
142.0	126.0	76.2	45.0	27.5	18.1
138.4	124.3	74.4	39.7	26.5	14.8
137.5	123.3	72.8	33.4	26.0	13.3
137.2	119.7	60.5	32.3	25.8	11.8

$[\alpha]_D^{22}$ -25.5 (c = 0.4, MeOH)

Synthetic **2.19**	Synthetic **2.19** sodium salt + D$_2$O	Natural **2.19** (ref 6c)
9.04 (brs, 1H)	9.04 (brs, 1H)	9.00 (brs, 1H)
7.32 (s, 1H)	7.30 (s, 1H)	7.31 (s, 1H)
7.22 (d, J = 11.0 Hz, 1H)	7.16 (d, J = 11.2 Hz, 1H)	7.22 (d, J = 11.5 Hz, 1H)
6.38 (dd, J = 15.4, 11.3 Hz, 1H)	6.34 (dd, J = 15.4, 11.2 Hz, 1H)	6.38 (dd, J = 15.0, 11.5 Hz, 1H)
5.99-5.97 (m, 1H)	5.95 (d, J = 2.9 Hz, 1H)	5.96 (d, J = 3.0 Hz, 1H)
	5.90 (d, J = 15.3 Hz, 1H)	5.96 (d, J = 15.0 Hz, 1H)
5.31-5.30 (m, 1H)	5.30 (t, J = 6.9 Hz, 1H)	5.30 (dd, J = 6.0, 8.0 Hz, 1H)
5.03 (d, J = 4.9 Hz, 1H)	5.01 (d, J = 5.1 Hz, 1H)	5.00 (d, J = 3.0 Hz, 1H)
4.03 (dd, J - 15.3, 8.0 Hz, 1H)	4.01 (dd, J = 15.0, 7.8 Hz, 1H)	4.00 (dd, J = 15.0, 8.0 Hz, 1H)
3.71 (dd, J = 15.1, 5.4 Hz, 1H)	3.71 (dd, J = 15.0, 5.6 Hz, 1H)	3.70 (dd, J = 15.0, 6.0 Hz, 1H)
3.49 (dd, J = 10.7, 4.4 Hz, 1H)	3.46 (dd, J = 11.1, 4.6 Hz, 1H)	3.45 (dd, J = 10.5, 4.5 Hz, 1H)
2.78-2.73 (m, 1H)	2.76-2.71 (m, 1H)	2.75 (m, 1H)
2.69 (dd, J = 4.8, 3.0 Hz, 1H)	2.69 (dd, J = 4.9, 3.0 Hz, 1H)	2.70 (dd, J = 6.0, 3.0 Hz, 1H)
2.63 (dd, J = 12.9, 6.4 Hz, 1H)	2.61 (dd, J = 13.1, 6.4 Hz, 1H)	2.60 (dd, J = 13.0, 6.5 Hz, 1H)
2.3 (dd, J = 12.3, 11.7 Hz, 1H)	2.27 (dd, J = 13.0, 10.8 Hz, 1H)	2.25 (dd, J = 13.0, 10.5 Hz, 1H)
1.92 (s, 3H)	1.89 (s, 3H)	1.90 (d, J = 1.2 Hz, 1H)
1.91-1.85 (m, 2H)	1.87-1.85 (m, 2H)	1.85 (m, 2H)
1.84 (s, 3H)	1.82 (s, 3H)	1.80 (s, 3H)
1.81-1.78 (m, 1H)	1.81-1.77 (m, 1H)	1.81 (m, 1H)
1.78-1.75 (m, 1H)	1.77-1.74 (m, 1H)	1.78 (m, 1H)
1.73-1.69 (m, 1H)	1.71-1.67 (m, 1H)	1.75 (m, 1H)
1.68 (s, 3H)	1.66 (s, 3H)	1.67 (s. 3H)
1.65-1.57 (m, 2H)	1.63-1.55 (m, 2H)	1.60 (m, 2H)
1.54-1.45 (m, 2H)	1.54-1.49 (m, 1H)	1.46 (m, 2H)
	1.48-1.42 (m, 1H)	
1.41 (s, 3H)	1.40 (s, 3H)	1.40 (s, 3H)
1.28 (s, 3H)	1.27 (s, 3H)	1.27 (s, 3H)
1.26 (s, 3H)	1.26 (s, 3H)	1.26 (s, 3H)
1.16 (s, 3H)	1.14 (s, 3H)	1.13 (s, 3H)
1.09 (s, 3H)	1.07 (s, 3H)	1.07 (s, 3H)
1.07 (s, 3H)	1.05 (s, 3H)	1.05 (s, 3H)
1.02 (s, 3H)	1.00 (s, 3H)	1.00 (s, 3H)

Synthetic **2.19**	Synthetic **2.19** sodium salt + D$_2$O	Natural **2.19** (ref 6c)
11.8	11.8	11.7
12.9	13.3	12.7
14.8	14.8	14.7
18.2	18.1	18.1
19.4	19.3	19.4
23.2	23.1	23.1
25.5	25.3	25.4
25.8	25.8	25.4
26.6	26.0	26.0
27.7	26.5	26.6
28.0	27.5	27.6
29.8	27.9	27.9
30.4	30.3	30.3
30.4	30.3	30.3
32.4	32.3	32.3
33.5	33.4	33.4
39.8	39.7	39.7
45.1	45.0	45.0
47.9	47.7	47.9
49.8	49.8	49.7
54.4	54.3	54.3
60.7	60.5	60.7
72.7	72.8	72.7
74.3	74.4	74.2
76.5	76.2	76.5
77.0	76.9	76.9
107.6	107.5	107.6
118.9	118.7	118.8
119.8	119.7	119.8
123.4	123.3	123.3
124.4	124.3	124.4
		125.4
125.8	126.0	125.6
127.4	127.3	127.4
131.7	131.7	131.7
132.2	132.1	132.2
137.3	137.2	137.1
137.7	137.5	137.2
139.6	138.4	140.1
142.2	142.0	142.1
153.1	153.0	153.0
154.8	153.6	155.2
170.5	171.6	170.0

2.4 References and Notes

1. Ondeyka, J. G.; Helms, G. L.; Hensens, O. D.; Goetz, M. A.; Zink, D. L.; Tsipouras, A.; Shoop, W. L.; Slayton, L.; Dombrowski, A. W.; Polishook, J. D.; Ostlind, D. A.; Tsou, N. N.; Ball, R. G.; Singh, S. B. *J. Am. Chem. Soc*. **1997**, *119*, 8809.

2. (a) Smith, M. M.; Warren, V. A.; Thomas, B. S.; Brochu, R. M.; Ertel, E. A.; Rohrer, S.; Schaeffer, J.; Schmatz, D.; Petuch, B. R.; Tang, Y.–S.; Meinke, P. T.; Kaczorowski, G. J.; Cohen, C. J. *Biochemistry* **2000**, *39,* 5543. (b) Ludmerer, S. W.; Warren, V. A.; Williams, B. S.; Zheng, Y.; Hunt, D. C.; Ayer, M. B.; Wallace, M. A.; Chaudhary, A. G.; Egan, M. A.; Meinke, P. T.; Dean, D. C.; Garcia, M. L.; Cully, D. F.; Smith, M. M. *Biochemistry* **2002**, *41*, 6548.

3. Meinke, P. T.; Smith, M. M.; Shoop, W. L. *Curr. Top. Med, Chem.* **2002,** *2,* 655.

4. Shoop, W. L.; Gregory, L. M.; Zakson-Aiken, M.; Michael, B. F.; Haines, H. W.; Ondeyka, J. G.; Meinke, P. T.; Schmatz, D. M. *J. Parasitol*. **2001**, *87*, 419.

5. (a) Springer, J. P.; Clardy, J.; Wells, J. M.; Cole, R. J.; Kirksey, J. W. *Tetrahedron Lett*. **1975**, *16*, 2531. (b) Knaus, H.-G.; McManus, O. B.; Lee, S. H.; Schmalhofer, W. A.; Garcia-Calvo, M.; Helms, L. M. H.; Sanchez, M.; Giangiacomo, K.; Reuben, J. P.; Smith, A. B., III.; Kaczorowski, G. J.; Garcia, M. L. *Biochemistry*, **1994**, *33*, 5819. (c) Sanchez, M.; McManus, O. B. *Neuropharmacology*, **1996**, *35*, 963.

6. (a) Hensens, O. D.; Ondeyka, J. D.; Dombrowski, A. W.; Ostlind, D. A.; Zink, D. L. *Tetrahedron Lett*. **1999**, *40*, 5455. (b) Ondeyka, J. G.; Dahl-Roshak, A. M.; Tkacz, J. S.; Zink, D. L.; Zakson-Aiken, M.; Shoop, W. L.; Goetz, M. A.; Singh, S. B. *Bioorg. Med. Chem. Lett*. **2002,** *12,* 2941. (c) Ondeyka, J. G.; Byrne, K.; Vesey, D.; Zink, D. L.; Shoop, W. L.; Goetz, M. A.; Singh, S. B. *J. Nat. Prod*. **2003,** *66,* 121. (d) Singh, S. B.; Ondeyka, J. G.; Jayasuriya, H.; Zink, D. L.; Ha, S. N.; Dahl-Roshak, A.; Greene, J.; Kim, J, A.; Smith, M. M.; Shoop, W.; Tkacz, J. S. *J. Nat. Prod.* **2004,** *67,* 1496.

7. Meinke, P. T.; Ayer, M. B.; Colletti, S. L.; Li, C.; Lim, J.; Ok, D.; Salva, S.; Schmatz, D. M.; Shih, T. L.; Shoop, W. L.; Warmke, L. M.; Wyvratt, M. J.; Zakson-Aiken, M.; Fisher, M. H. *Bioorg. Med. Chem. Lett.* **2000,** *10,* 2371.

8. Meinke, P. T.; Colletti, S. L.; Fisher, M. H.; Wyvratt, M. J.; Shih, T. L.; Ayer, M. B.; Li, C.; Lim, J.; Ok, D.; Salva, S.; Warmke, L. M.; Zakson, M.; Michael, B. F.; deMontigny, P.; Ostlind, D. A.; Fink, D.; Drag, M.; Schmatz, D. M.; Shoop, W. L. *J. Med. Chem.* **2009**, *52*, 3505.

9. Smith, A. B., III; Davulcu, A. H.; Kürti, L. *Org. Lett*. **2006**, *8*, 1665.

10. Zou, Y.; Melvin, J. E.; Gonzales, S. S.; Spafford, M. J.; Smith, A. B., III. *J. Am. Chem. Soc*. **2015**, *137*, 7095.

11. Zou, Y.; Li, X.; Yang, Y.; Berritt, S.; Melvin, J.; Gonzales, S.; Spafford, M.; Smith, A. B., III. *J. Am. Chem. Soc*. **2018**, *140*, 9502.

12. Zou, Y.; Smith, A. B., III. *J. Antibiot.* **2018**, *71*, 185.

13. (a) Smith, A. B., III.; Ishiyama, H.; Cho, Y. S.; Ohmoto, K. *Org. Lett*. **2001**, *3*, 3967. (b) Smith, A. B., III.; Davulcu, A. H.; Kürti, L. *Org. Lett*. **2006**, *8*, 1669. (c) Smith, A. B., III.; Kürti, L.; Davulcu, A. H. *Org. Lett*. **2006**, *8*, 2167. (d) Smith, A. B., III.; Kürti, L.; Davulcu, A.; Cho, Y. S.; Ohmoto, K. J. *Org. Chem*. **2007**, *72*, 4611.

14. Mewshaw, R. Smith, A. B., III. *J. Am. Chem. Soc*. **1985**, *107*, 1769.

15. (a) Lo, J. C.; Yabe, Y.; Baran, P. S. *J. Am. Chem. Soc*. **2014**, *136*, 1304. (b) Lo, J. C.; Gui, J.; Yabe, Y.; Pan, C.–M.; Baran, P. S. *Nature*, **2014**, *516*, 343. (c) Lo, J. C.; Kim, D.; Pan,

C.–M.; Edward, J. T.; Yabe, Y.; Gui, J. Qin, T.; Gutiérrez, S.; Giacoboni, J.; Smith, M. W.; Holland, P. L.; Baran, P. S. *J. Am. Chem. Soc.* **2017**, *139*, 2484. (d) Obradors, C.; Martinez, R. M.; Shenvi, R. A. *J. Am. Chem. Soc.* **2016**, *138*, 4962.

16. For selected examples of radical conjugate additions to form quaternary carbons, see: (a) Barton, D. H. R.; Crich, D. *Tetrahedron Lett.* **1985**, *26*, 757. (b) Okada, K.; Okamoto, K.; Morita, N.; Okubo, K.; Oda, M. *J. Am. Chem. Soc.* **1991**, *113*, 9401. (c) Schnermann, M. J.; Overman, L. E. *Angew. Chem., Int. Ed.* **2012**, *51*, 9576. (d) Sun, Y.; Li, R.; Zhang, W.; Li, A. *Angew. Chem., Int. Ed.* **2013**, *52*, 9201. (e) Lackner, G. L.; Quasdorf, K. W.; Overman, L. E. *J. Am. Chem. Soc.* **2013**, *135*, 15342. (f) Chu, L.; Ohta, C.; Zuo, Z.; MacMillan, D. W. C. *J. Am. Chem. Soc.* **2014**, *136*, 10886. (g) Zhou, S.; Zhang, D.; Sun, Y.; Li, R.; Zhang, W.; Li, A. *Adv. Synth. Catal.* **2014**, *356*, 2867. (h) Müller, D. S.; Untiedt, N. L.; Dieskau, A. P.; Lackner, G. L.; Overman, L. E. *J. Am. Chem. Soc.* **2015**, 137, 660. (i) Chinzei, T.; Miyazawa, K.; Yasu, Y.; Koike, T.; Akita, M. *RSC Adv.* **2015**, 5, 21297. (j) Lackner, G. L.; Quasdorf, K. W.; Pratsch, G.; Overman, L. E. J. *Org. Chem.* **2015**, *80*, 6012. (k) Pratsch, G.; Lackner, G. L.; Overman, L. E. *J. Org. Chem.* **2015**, *80*, 6025. (l) Nawrat, C. C.; Jamison, C. R.; Slutskyy, Y.; MacMillan, D. W. C.; Overman, L. E. *J. Am. Chem. Soc.* **2015**, *137*, 11270.

17. For relevant reductive aldol reaction, see: Isayama, S.; Mukaiyama, T. *Chem. Lett.* **1989**, *18*, 2005.

18. George, D. T.; Kuenstner, E. J., Pronin, S. V. *J. Am. Chem. Soc.* **2015,** *137,* 15410.

19. For recent examples of gold-catalyzed cascades in synthesis, see: (a) Yue, G.; Zhang, Y.; Fang, L.; Li, C.-c.; Luo, T.; Yang, Z. *Angew. Chem. Int. Ed.* **2014**, *53*, 1837. (b) McGee, P.; Betournay, G.; Barabé, F.; Barriault, L. *Angew. Chem. Int. Ed.* **2017**, *56*, 6280. (c) Ferrer, S.; Echavarren, A. M. *Org. Lett.* **2018**, *20*, 5784.

20. Evans, D. A.; Truesdale, L. K. *Tetrahedron Lett.* **1973**, *14*, 4929.

21. Umbreit, M. A.; Sharpless, K. B. *J. Am. Chem. Soc.* **1977**, *99*, 5526.

22. Omura, K.; Swern, D. *Tetrahedron*, **1978**, *34*, 1651.

23. Parikh, J. R.; Doering, W. e. V. *J. Am. Chem. Soc.* **1967**, *89*, 5505.

24. Anelli, P. A.; Biffi, C.; Montanari, F.; Quici, S. *J. Org. Chem.* **1987**, *52*, 2559.

25. Figerio, M.; Santagostino, M. *Tetrahedron Lett.* **1994**, *35*, 8019.

26. Dess, D. B.; Martin, J. C. *J. Am. Chem. Soc.* **1991**, *113*, 7277.

27. This experiment was conducted and data collected by D.T.G.

28. In this setting, the corresponding catalytic alkenylation proved less efficient: Holmbo, S. D.; Godfrey, N. A.; Hirner, J. J.; Pronin, S. V. *J. Am. Chem. Soc.* **2016**, *138*, 12316.

29. Stork, G.; Danheiser, R. L. *J. Org. Chem.* **1973**, *38*, 1775.

30. Evans, D. A.; Golob, D. A. *J. Am. Chem. Soc.* **1975**, *97*, 4765.

31. For reviews on asymmetric conjugate additions, see: (a) Alexakis, A.; Benheim, C. *Eur. J. Org. Chem.* **2002**, 3221. (b) Hayashi, T.; Yamasaki, K.; *Chem. Rev.* **2003**, *103*, 2829. (c) López, F.; Minnaard, A. J.; Feringa, B. L.; *Acc. Chem. Res.* **2007**, *40*, 179. (d) Alexakis, A.; Bäckvall, J. E.; Krause, N.; Pàmies, O.; Diéguez, M. *Chem. Rev.* **2008**, *108*, 2824. (e) Harutyunyan, S. R.; den Hartong, T.; Geurts, K,; Minnaard, A. J.; Feringa, B. L. *Chem. Rev.* **2008**, *108*, 2824. (f) Gutnov, A. *Eur. J. Org. Chem.* **2008**, 4547. (g) Alexakis, A.; Krause, N.; Woodward, S. (Eds.), Copper-Catalyzed Asymmetric Synthesis, Wiley-VCH, Weinheim, **2014**. (h) Maksymowicz, R. M.; Bissette, A. J.; Fletcher, S. P. *Chem. Eur. J.* **2015**, *21*, 5668.

32. Escher, I. E.; Pfaltz, A. *Tetrahedron*, **2000**, *56*, 2879.

33. Degrado, S. J.; Mizutani, H.; Hoveyda, A. H. *J. Am. Chem. Soc.* **2001**, *123*, 755.

34. Krauss, I. J.; Leighton, J. L. *Org. Lett.* **2003**, *5*, 3201.

35. (a) Germain, N.; Guénée, L.; Mauduit, M.; Alexakis, A. *Org. Lett.* **2014**, *16*, 118. (b) Germain, N.; Alexakis, A. *Chem. Eur. J.* **2015**, *21*, 8597. (c) Homs, A.; Muratore, M. E.; Echavarren, A. E. *Org. Lett.* **2015**, *17*, 461.

36. Feringa, B. L.; Badorrey, R.; Peña, D.; Harutyunyan, S. R.; Minnaard, A. *J. Proc. Natl. Acad. Sci. U.S.A.* **2004**, *101*, 5834.

37. Calvo, B. C.; Madduri, A. V. R.; Harutyunyan, S. R.; Minnaard, A. J. *Adv. Synth. Catal.* **2014**, *356*, 2061.

38. Wadsworth, W. *Org. React.* **1977**, *25*, 73.

39. (a) Nugent, W. A. *Chem. Commun.* **1999**, *35*, 1369. (b) Lurain, A. E.; Maestri, A.; Kelly, A. R.; Carroll, P. J.; Walsh, P. J. *J. Am. Chem. Soc.* **2004**, *126*, 13608.

40. Sonogashira, K. *J. Organomet. Chem.* **2002**, *653*, 46. and references therein.

41. Stille, J. K. *Pure Appl. Chem.* **1985**, *57*, 1771. and references therein.

42. (a) Barluenga, J.; Fernandez, M. A.; Aznar, F.; Valdes, C. *Chem. Eur. J.* **2005**, *11*, 2276. (b) Barluenga, J.; Valdes, C. *Chem. Commun.* **2005**, 4891.

43. (a) Wolfe, J. P.; Buchwald, S. L. *Angew. Chem. Int. Ed.* **1999**, *38*, 2413. (b) Surry, D. S.; Buchwald, S. L. *Chem. Sci.* **2011**, *2*, 27. (c) Bruno, N. C.; Tudge, M. T.; Buchwald, S. L. *Chem. Sci.* **2013**, *4*, 916. (d) Bruno, N. C.; Niljianskul, N.; Buchwald, S. L. *J. Org. Chem.* **2014**, *79*, 4161. (e) Arrechea, P. L.; Buchwald, S. L. *J. Am. Chem. Soc.* **2016**, *138*, 12486.

44. (a) Mewshaw, R. Smith, A. B., III. *J. Am. Chem. Soc.* **1985**, *107*, 1769. (b) Mewshaw, R. E.; Taylor, M. D.; Smith, A. B., III. *J. Org. Chem.* **1989**, *54*, 3449. (c) Smith, A. B., III.; Sunazuka, T.; Leenay, T.L.; Kingery-Wood, J. *J. Am. Chem. Soc.* **1990**, *112*, 8197. (d) Smith, A. B., III,; Kingery-Wood, J.; Leenay, T. L.; Nolen, E. G.; Sunazuka, T. *J. Am. Chem. Soc.* **1992**, *114*, 1438.

45. (a) Sharpe, R. J.; Johnson, J. S. *J. Am. Chem. Soc.* **2015**, *137*, 4968. (b) Sharpe, R. J.; Johnson, J. S. *J. Org. Chem.* **2015**, *137*, 15410.

46. RajanBabu, T. V.; Reddy, G. S.; Fukunaga, T. *J. Am. Chem. Soc.* **1985**, *107*, 5473.

47. Bellina, F.; Rossi, R. *Chem. Rev.* **2010**, *110*, 1082.

48. (a) Fox, J. M.; Huang, X.; Chiffi, A.; Buchwald, S. L. *J. Am. Chem. Soc.* **2000**, *122*, 1360. (b) Rutherford, J. L.; Rainka, M. P.; Buchwald, S. L. *J. Am. Chem. Soc.* **2002**, *124*, 15168.

49. (a) Kawatsura, M.; Hartwig, J. F. *J. Am. Chem. Soc.* **1999**, *121*, 1473. (b) Su, W.; Raders, S.; Verkade, J. G.; Liao, X.; Hartwig, J. F. *Angew. Chem. Int. Ed.* **2006**, *45*, 5852.

50. (a) Kuwajima, I.; Urabe, H. *J. Am. Chem. Soc.* **1982**, *104*, 6831. (b) Iwama, T.; Rawal, V. H. *Org. Lett.* **2006**, *8*, 5725.

51. See experimental section.

52. Shiina, I., Umezaki, Y., Ohashi, Y., Yamazaki, Y., Dan, S., Yamori, T. *J. Med. Chem.* **2013,** *56*, 150.

Chapter 3: Studies Toward Paxilline and Related Indole Diterpenes

3.1 Target Introductions and Synthetic Rationale

The tremorgenic indoloterpenoids carrying the paxilline-type oxidation state or higher make up a significant portion of the paxilline indoloterpenoids. While the successful synthesis of nodulisporic acid C was rewarding validation of our strategy to the terpene core, only 27 out of the >150 congeners known to us bear the paspaline-type core we constructed.[1] Expanding the utility of our key polycyclization to access the additional terpenoid frameworks would not only push the limits of our reaction, but could permit biological evaluation of these molecules. To begin proof of concept development, we targeted paxilline (**3.1**, Figure 3.1).[2] We imagined a successful approach to this framework and oxidation state would readily translate to the more complex derivatives such as penitrem A (**3.2**)[3] and lolitrem B (**3.3**).[4]

Figure 3.1 Tremorgenic Indole Diterpenes

paxilline (**3.1**)   penitrem A (**3.2**)   lolitrem B (**3.3**)
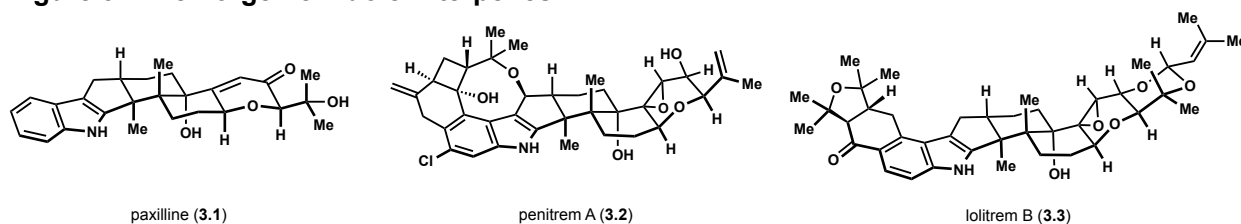
3.2 Synthetic Strategies Explored to Access Paxilline and Related Congeners

3.2.1 A Bioinspired Retro-ene Elimination

Our initial strategy was inspired by the proposed biosynthetic sequence and presumed intermediates that transform paspaline (**3.4**) into paxilline (Scheme 3.1a).[5] Of note were paspaline B (**3.5**)[6], having the C30 methyl group (paspaline numbering) oxidized to an aldehyde, as well as carboxylic derivative (**3.6,** Scheme 3.1a).[7] It is unknown if one or both C30 oxidized congeners are converted into paxilline in a biological setting. From a synthetic standpoint, we were drawn to the shared aldehyde moiety in our polycyclization product **3.7** and paspaline B (**3.5**). We believed

Figure 3.2 Biosynthetic Inspiration for Accessing Additional Paxilline Indole Diterpene Congeners

a)

paxilline (**3.1**)

paspaline (**3.4**)

paspaline B (**3.5**)

3.6

b)

paxilline (**3.1**)

3.7
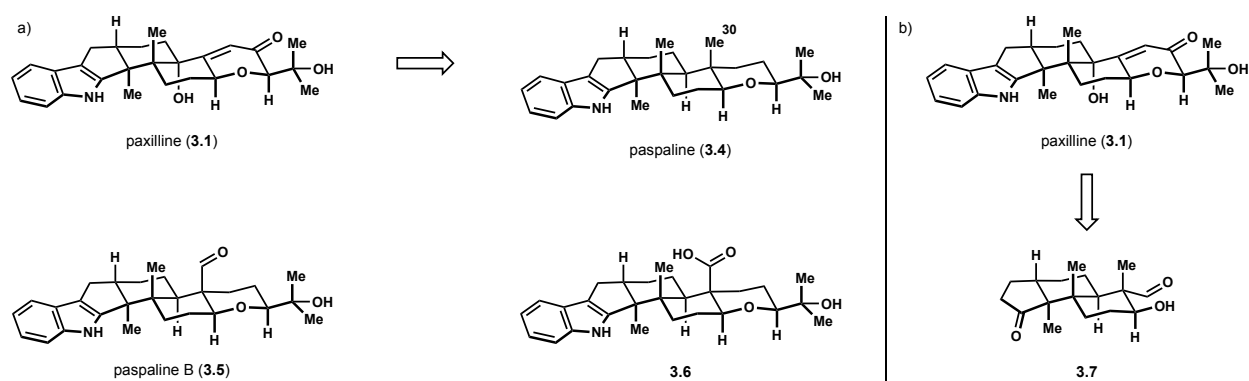
we could perform the same net transformation, using aldehyde **3.7,** and develop a unified approach to the entire paxilline indole diterpene family (Scheme 3.2b).

We established the feasibility of this transformation on protected tricycle **3.8** (Scheme 3.1). A direct dehydroformylation was considered[8], but known procedures do not lend themselves to sterically encumbered systems, such as aldehydes found on quaternary carbons. We therefore elected to employ a two-step sequence of a Baeyer–Villiger oxidation of aldehyde **3.8** followed by retro-ene elimination of formate **3.9**.[9] This transformation worked reasonably well, showing a higher propensity for alkyl over hydride migration in the oxidation step. Careful work-up to avoid hydrolysis to the tertiary alcohol permitted direct elimination to produce alkene **3.10** and provided us a handle for elaboration to the dihydropyranone found in paxilline.

Scheme 3.1 Dehydroformylation via Retro-ene Elimination

3.8

m-CPBA, NaHCO$_3$
CH$_2$Cl$_2$, 0 °C

3.9

1,2-dichlorobenzene
2,6-lutidine, 160 °C

66% over 2 steps

3.10
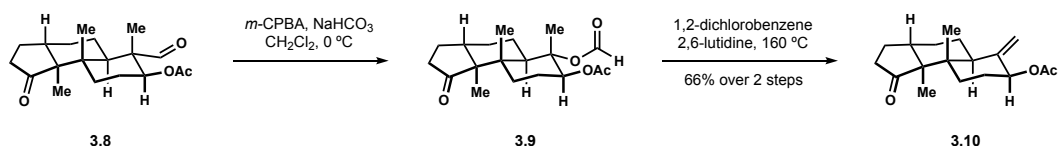
Section 3.2.2 Alkene Oxidation Attempts

The first approach we considered was Schenk-ene oxidation of the exocyclic alkene.[10] Direct oxidation of such substrates with singlet oxygen has been reported by Mihelich, who also developed conditions to induce elimination of the intermediate peroxide and produce unsaturated

131

Scheme 3.2 Attempted Schenk-ene Oxidations

a) Mihelich, 1983

b) Singlet Oxygen Schenck-ene Reaction Attempts with Tricyclic Alkene **3.14**

sensitizers screened for $^1O_2$ generation:
• TPP
• rose bengal
• methylene blue,
• fluorescein
• eosin Y

other methods for $^1O_2$ generation:
• oxone, NaHCO$_3$
• NaOCl, H$_2$O$_2$
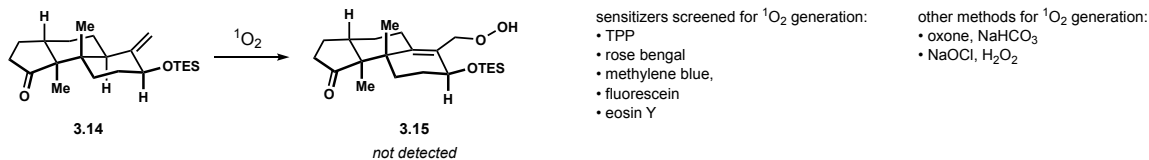
c) Ene Reaction Attempts of Alkene **3.16** with PTAD

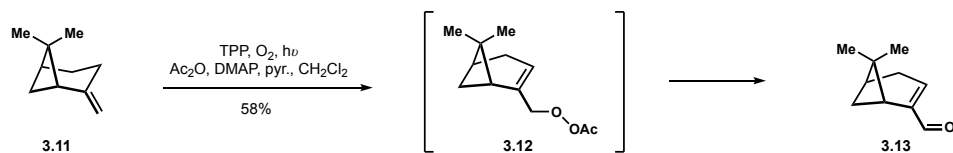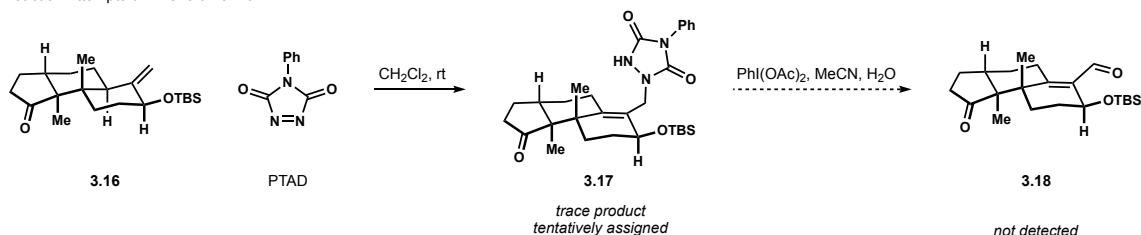carbonyls directly (Scheme 3.2a).[11] Mihelich notes the absence of 1,1-disubstituted alkenes undergoing analogous ene reactions. Provided in this report is one of the few examples in the conversion of pinene derivative **3.11** to peroxide **3.12**, which undergoes facile elimination to enal **3.13**. Decades later, examples are still sparse. The presence of an allylic acetate in our derivative **3.10** further deactivated the alkene, making our proposed Schenk-ene oxidation a rather demanding transformation.[12] After initial unsuccessful oxidations of allylic acetate **3.10**, we moved to silyl ether **3.14** hoping for a less deactivated system (Scheme 3.2b). A survey of singlet oxygen generating conditions and sensitizers did not result in any formation of the desired peroxide **3.15**.[13] We further tested ene reactivity on the more robust TBS protected allylic alcohol **3.16** by employing potent eneophile PTAD (Scheme 3.2c).[14] Product formation of adduct **3.17** appeared to be present in crude mixtures, though yields were well below 10% and pure material was difficult to separate from PTAD by-products. Attempts to oxidize the crude material and recover enal **3.18** were unsuccessful.

We elected to move away from ene reactivity and attempted electrophilic additions to the alkene. Presumably for the same electronic reasons that plagued the ene reaction, bromoselenation of the alkene **3.16** also failed to elicit a reaction (Scheme 3.3a).[15] The alkene was receptive to epoxidation as illustrated in Scheme 3.3b; however, based on simplistic stereochemical modeling, poor orbital alignment between the C–H σ-bond and C–O σ^* disfavoured base induced fragmentation of epoxide **3.21**. The lack of useful reactivity from this alkene and steady build-up of manipulations that was occurring without the introduction of a single carbon atom led us to reconsider intermolecular functionalization. Instead we surveyed strategies that would allow us to bring a reactive functionality into proximity of the alkene by exploiting the alcohol.

Scheme 3.3 Electrophilic Substitutions of Alkene 3.16

a) Attempted Bromoselenation Towards Vinyl Bromide **3.20**
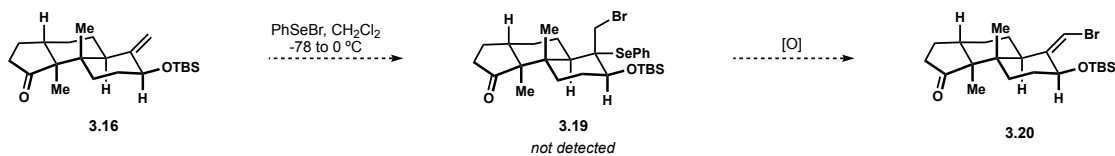
b) Epoxidation of Alkene **3.16** and Inaccessible Fragmentation Product **3.22**
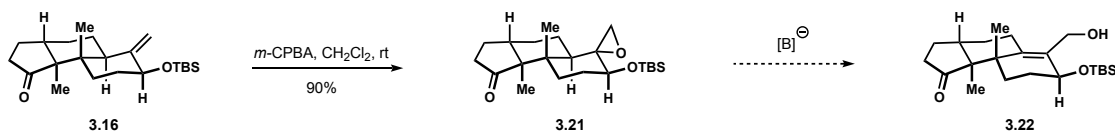
Section 3.2.3 Ring-closing Metathesis Strategy

We could easily append a variety of fragments via *O*-alkylation or formation of mixed acetals and silyl ethers. In the context of alkene functionalization, we felt the most straightforward method to productively engage the alkene was through a ring-closing metathesis (RCM).[16] The first system we assessed for alkylation of allylic alcohol **3.23** was metallocarbene insertion of 1,3-dicarbonyl **3.24**[17] (Scheme 3.4a).[18] Utilizing this sequence was enticing as it would introduce most of the oxidation present in paxilline (**3.3**), as well as an alkene for RCM. The *O*-alkylation proved to be quite efficient. Utilizing catalytic rhodium(II) acetate dimer, ketoenol **3.25** was readily prepared. Various ruthenium catalysts did not deliver 1,3-dicarbonyl **3.26**, presumably failing to

Scheme 3.4 Metallocarbene Insertion and Attempted RCM

a) Initial *O*-alkylation and RCM Attempts with Ketoenol **3.25**

b) RCM Attempt on a Methylated Ketoenol **3.28**

c) Grignard Reagent Addition to 1,3-Dicarbonyls Developed by Da

d) Attempt to Remove Presence of the Enol
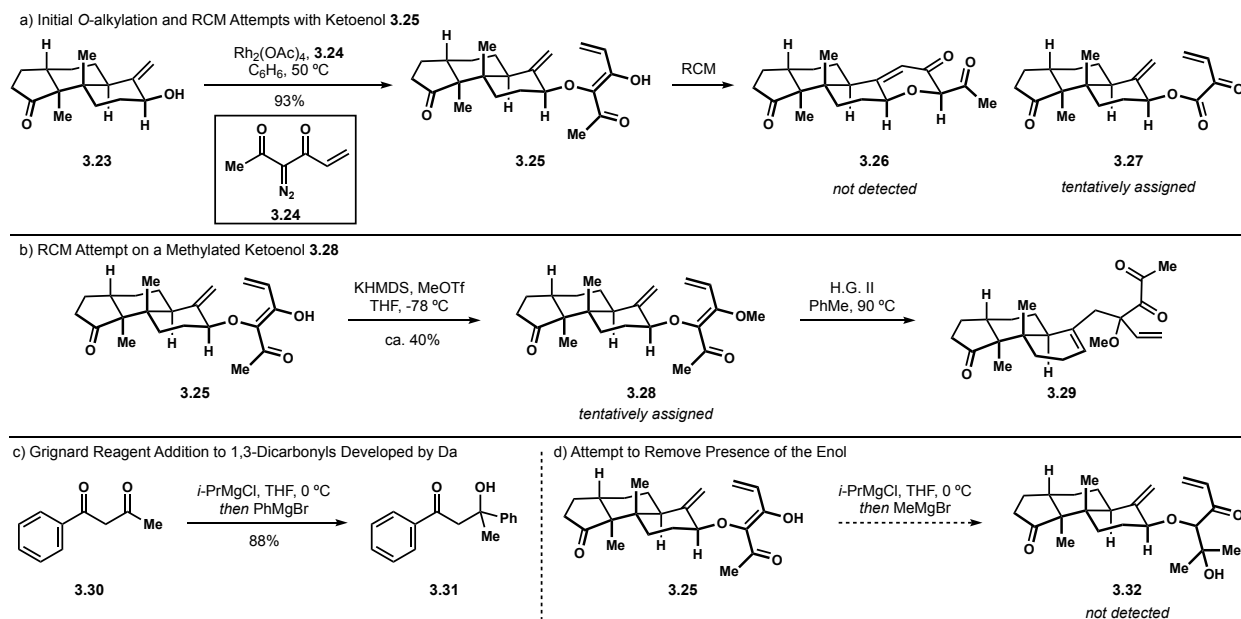
engage either alkene, whereas elevated temperatures led to oxidative degradation product **3.27**. Degassing the RCM reactions returned only starting material. Speculating the ketoenol may be interfering with reactivity by acting as a ligand, ketoenol **3.25** was methylated and enol ether **3.28** subjected to RCM conditions (Scheme 3.4b). Of note, **3.28** was isolated as the sole geometric isomer, though the alkene geometry was not confirmed. It is speculated that chelation of the intermediate potassium enolate by the adjacent ketone would have led to the depicted isomer **3.28**. As RCM reaction temperatures approached 90 ℃, the enol ether was fully consumed. However, the sole product was the Claisen rearrangement derived 1,2-dicarbonyl **3.29**, corroborating we had made the alkene regioisomer depicted, but not confirming alkene geometry. The need for elevated temperatures to achieve ring closure disqualified any RCM substrate prone to a Claisen rearrangement. To circumvent this issue, we attempted a method to deconjugate the system. A report by Da demonstrated that it is possible to selectively add an organometallic nucleophile to the ketone of dicarbonyl **3.30** over the benzylic ketone to access β-hydroxyketone **3.31** (Scheme 3.5c).[19] Adding a nucleophile to the ketone over the enone of dicarbonyl **3.25** would eliminate the

enol species and potentially encourage the RCM reactivity. Attempted nucleophilic addition did not generate tertiary alcohol **3.32** as desired and returned only starting material (Scheme 3.5d). The lack of reactivity may be due to complications from the cyclopentanone that is also enolizable, leading us to once again consider an electronically modified derivative.

Literature precedent for the formation of electron deficient ruthenium alkylidene intermediates is sparse. It is more typical for the ruthenium carbene to first engage a simple, aliphatic olefin, allowing proximity effects to promote metathesis with an enone.[20] Our system lacks this benefit, and instead possesses a 1,1-disubstituted alkene, which is more likely to be inert to metathesis catalysts. Considering the poor electronics and the steric demand of the exocyclic alkene, it appeared unlikely this would be the first to engage the catalyst. We decided to attempt bringing in an alkene we knew would engage a metallocarbene in the form of allylic alcohol **3.33** (Scheme 3.5). This approach was inspired by Smith's metalloenamine opening of an epoxide to install a similar oxidation pattern for the synthesis of penitrem D.[21] We envisioned doing so by utilizing bis-alkoxy silane intermediate **3.34** to render the metathesis intramolecular. If successful in generating diol **3.35**, displacement of the allylic pivalate would forge the tetracycle **3.36** in an oxidation state suited to the penitrems.

Scheme 3.5 Silyl Tethered RCM strategy
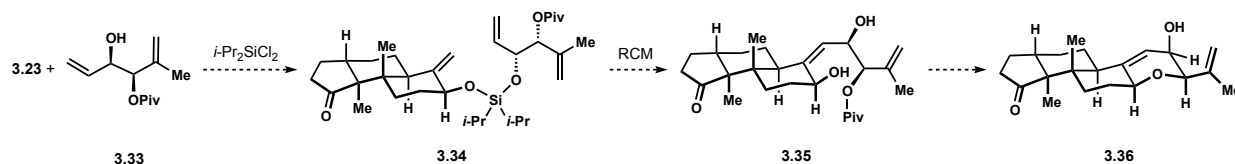

We began preparation of the requisite fragment **3.33** utilizing Smith's procedures to a similar intermediate (Scheme 3.6). Oxidative cleavage of (D)-mannitol diacetonide (**3.37**) provided aldehyde **3.38**. Smith reported addition of an isopropenyl organocopper nucleophile to this aldehyde proceeds with high levels of stereocontrol.[22] Unfortunately, the nature of the

**Scheme 3.6 Attempted Synthesis of a Functionalized RCM Coupling Partner**
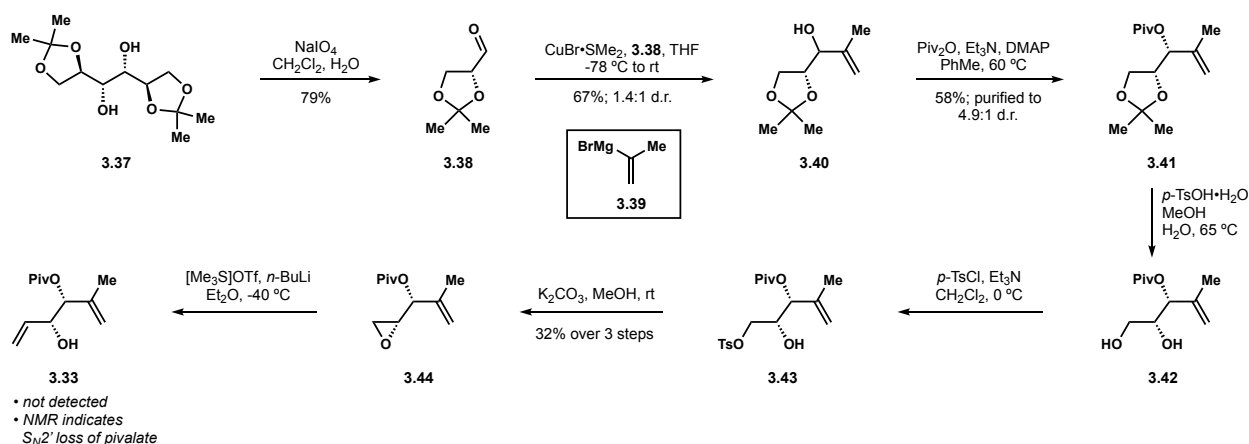
nucleophile and a detailed set of conditions are not provided in the literature. In our hands, copper(I) iodide, as reported by Smith, consistently provided a stoichiometric mixture of alcohol **3.40,** whereas copper(I) bromide dimethyl sulfide slightly favoured one diastereomer. We hypothesized the stereochemistry of alcohol **3.40** may prove inconsequential in the conversion of alcohol **3.35** to dihydropyranone **3.36** (Scheme 3.5) should the reaction proceed through an allylic cation. Nevertheless, pivalate protection of alcohol **3.40** did permit partial separation of diastereomers **3.4.** The acetonide of protected triol **3.41** was removed to provide diol **3.42,** which was converted into epoxide **3.44**. Installation of the alkene of allylic alcohol **3.33** intended for RCM was to be achieved through addition-elimination with a trimethylsulfonium anion to open the epoxide.[23] Unfortunately, crude NMR analysis indicated loss of the pivalate group as well as the vinyl protons associated with the isopropene fragment.

Proper protecting group choice would likely resolve the undesired elimination of allylic ester **3.44**, but concomitant to development of the sequence in Scheme 3.6, simpler substrates were evaluated to assess the feasibility of the RCM in general. To this end, homoallylic mixed acetal **3.45** was prepared as a mixture of diastereomers and subjected to several RCM conditions (Scheme 3.7a). This substrate failed to yield any of the desired dihydropyran **3.46** and returned only starting

Scheme 3.7 Additional RCM Substrates Assessed

a) Model RCM Attempts with Homoallylacetal **3.45**
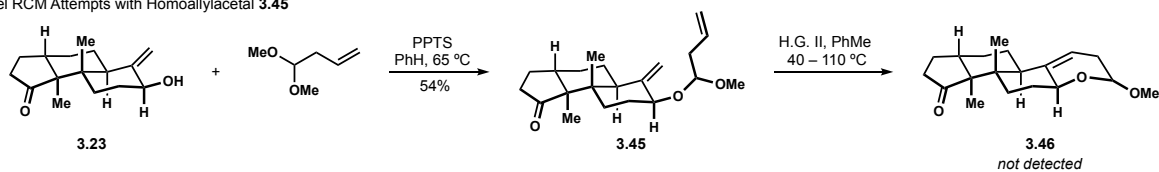
b) Saxton' Approach to Paspalicine
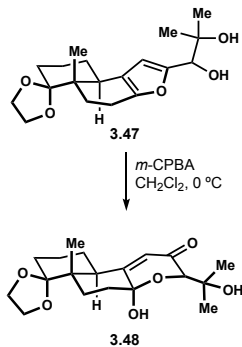
c) RCM Attempt Towards a Dihydrofuran
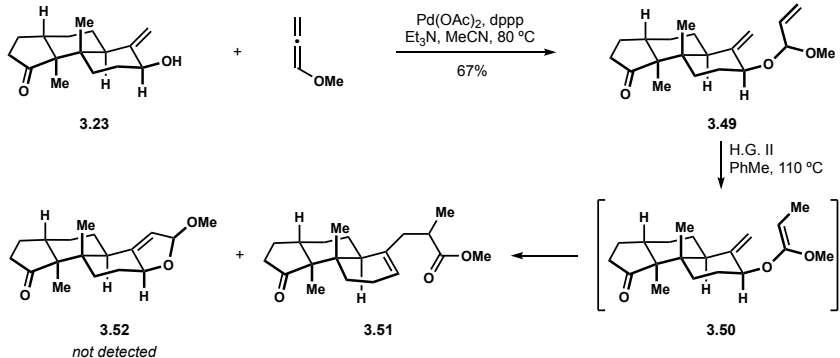
d) Attempted RCM with Acrylate Derivative **3.55**
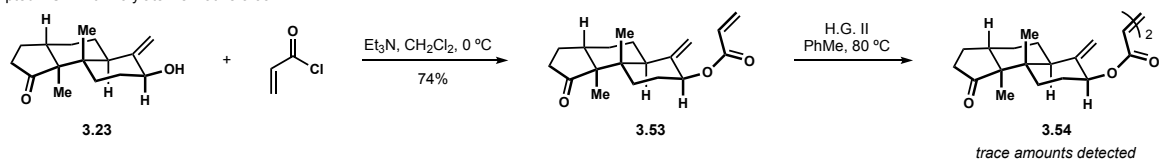
material. We were intrigued by Saxton's approach to paspalicine, whereby an Achmatowicz reaction of furan **3.47** generates the dihydropyranone motif **3.48** we were pursuing (Scheme 3.7b).[24] Reasoning we may be able to employ this strategy by preparing the appropriate furan through RCM, we prepared allyl acetal **3.49**, again as a mixture of diasteromers (Scheme 3.7c). Unfortunately, under RCM conditions we observed alkene isomerization and subsequent Ireland–Claisen rearrangement, which led to formation of ester **3.51**. Addition of 1,4-dibenzoquinone as a hydride scavenger did not promote desired reactivity and dihydrofuran **3.52** could not be accessed.[25] Lastly, an unsaturated system was revisited to determine if the initial dicarbonyl strategy illustrated in Scheme 3.4 was worth pursuing further. Acrylate derivative **3.53** was thus prepared and subjected to standard RCM conditions (Scheme 3.7d). In this instance, dimerization product **3.55** was observed, suggesting the exocyclic alkene would not partake in the metathesis reaction.

3.3 A Revised Polycyclization Approach

3.3.1 Retrosynthetic Analysis of Paxilline

The absence of reactivity intrinsic of the 1,1-disubstituted alkene necessitated a more dramatic revision of our strategy. We again revisited the biosynthetic pathway and considered the possibility of having the requisite carbons in place prior to carrying out the net dehydroformylation in a manner more analogous to the biosynthesis. Analysis of our system led us to believe we could access paxilline through alkene isomers **3.55** or **3.56** (Scheme 3.8a). This mixture of isomers would in turn arise from oxidation and formate elimination of the corresponding tetracyclic aldehyde **3.57**. It was unclear what regiochemistry the elimination would provide, though we believed either alkene would be viable precursors to paxilline based on precedent from Smith's syntheses of

Scheme 3.8 Revised Polycyclization Towards Paxilline and Previously Explored Substrates

a) Revised Retrosynthetic Analysis of Paxilline
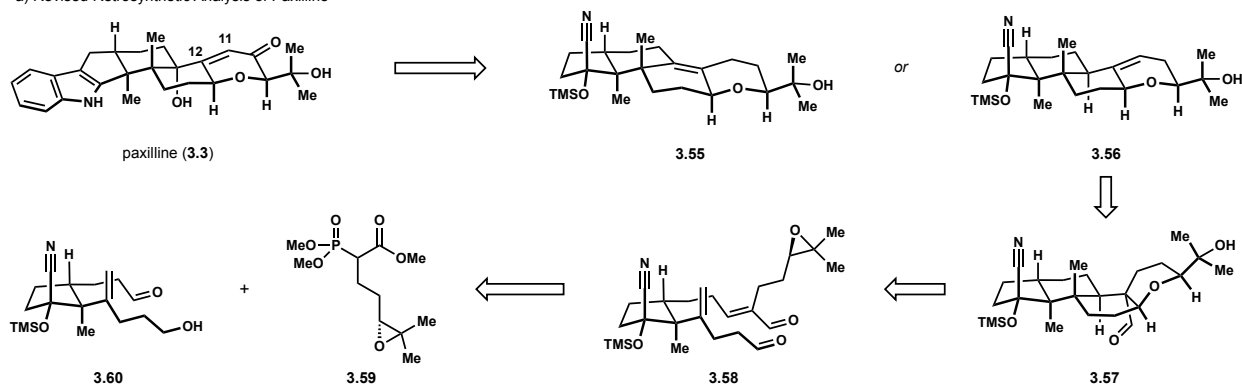
b) Previous Polycyclization Derivatives Explored in Our Lab

138
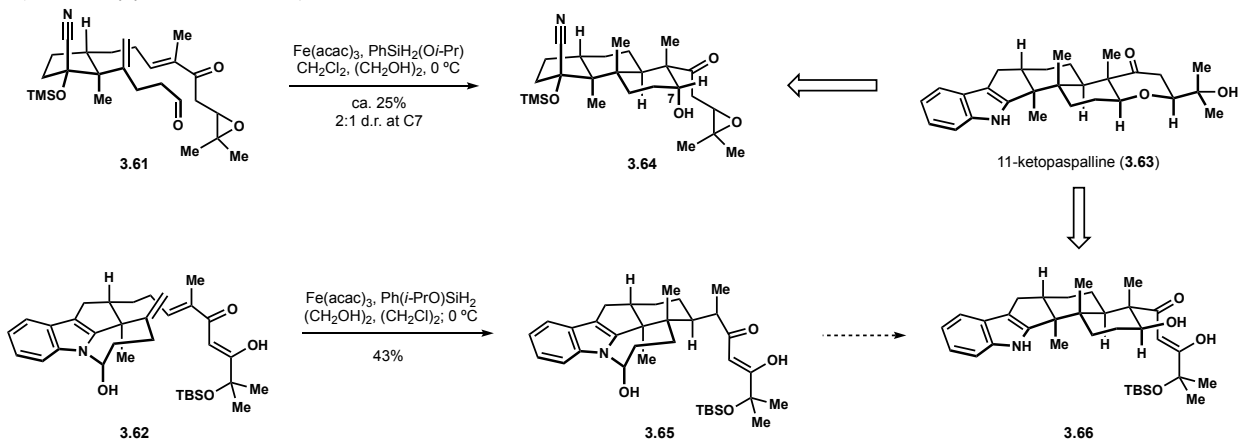
paspalicine[26] and penitrem D.[21] To apply this strategy, we revisited the polycyclization substrate altogether. By exchanging the C12 methyl group with alkyl epoxide **3.58**, all necessary carbon atoms are added without introducing extraneous complexity for the synthesis of the substrate. A Horner–Wadsworth–Emmons (HWE) reaction between enantioenriched phosphonate **3.59** and aldehyde **3.60** would readily provide access to epoxide **3.58**. It is worth noting that similar strategies were attempted within our lab on polycyclization derivatives **3.61** and **3.62** to access 11-ketopaspalline (**3.63**) (Scheme 3.8b).[27] Notably, rather than f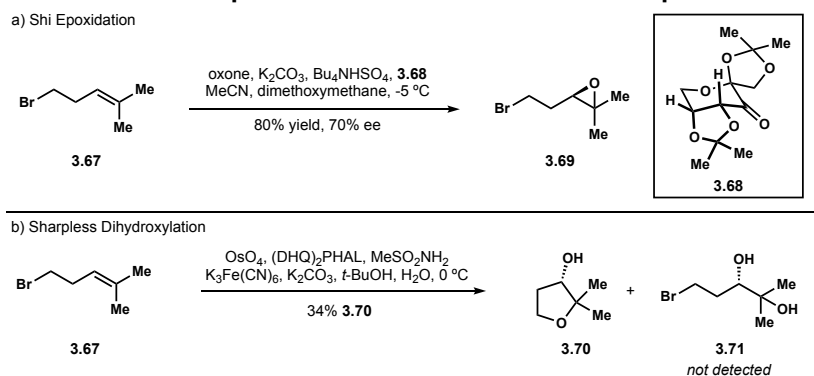unctionalizing the methyl substituent, additional complexity is added by exchanging the aldehyde for a ketone derivative. In the case of epoxyketone **3.61**, the polycyclization results in hydroxyketone **3.64** as an unfavourable mixture of diastereomers at C7. Ketoenol **3.62** did undergo the HAT initiated conjugate addition to afford intermediate **3.65**; however, attempts to induce the subsequent aldol addition failed to provide hydroxyketone **3.66**.

3.3.2 Synthesis of a New Polycyclization Substrate

The first task in applying this approach was generation of the enantioenriched phosphonate. We first assessed the Shi epoxidation of homoprenyl bromide **3.67** (Scheme 3.9a).[29] While this reaction did provide the desired epoxide **3.69** in appreciable yield, enantioenrichment was modest. This was not surprising as trisubstituted alkenes symmetrically substituted on one carbon are a limitation to this method. The low levels of enrichment were expected to be problematic in the HWE reaction. Considering the requisite aldehyde **3.60** is prepared in approximately 70% ee, combining it with a phosphonate derived from the Shi epoxidation would result in a substantial loss of material as other stereoisomers. Furthermore, the epoxidation itself is not particularly scalable. The alternative route considered for accessing this fragment was a Sharpless
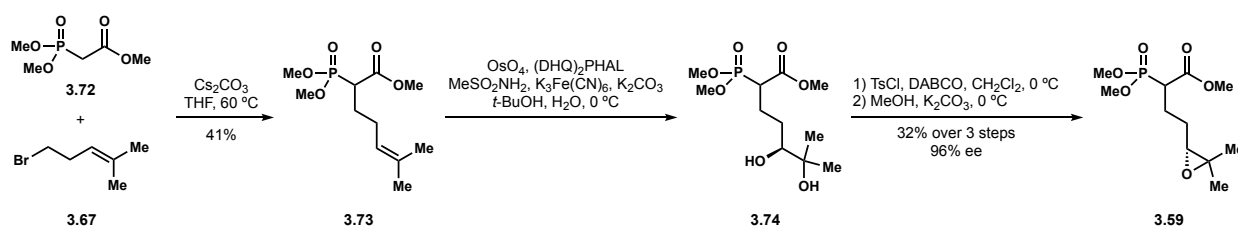
enantioselective dihydroxylation-displacement sequence to generate the epoxide **3.69** (Scheme 3.9b).[29] This sequence was quickly abandoned as dihydroxylation of homoprenyl bromide **3.67** was followed immediately by etherification to tetrahydrofuran **3.70**, which could not be mitigated for access to diol **3.71**.

Scheme 3.9 Attempts to Generate Enantioenriched Epoxide 3.69

a) Shi Epoxidation

oxone, K$_2$CO$_3$, Bu$_4$NHSO$_4$, **3.68**
MeCN, dimethoxymethane, -5 °C

80% yield, 70% ee

3.67   **3.69**   **3.68**

b) Sharpless Dihydroxylation

OsO$_4$, (DHQ)$_2$PHAL, MeSO$_2$NH$_2$
K$_3$Fe(CN)$_6$, K$_2$CO$_3$, t-BuOH, H$_2$O, 0 °C

34% **3.70**

3.67   **3.70**   **3.71**
not detected

By carrying out the alkylation of phosphonate **3.72** with bromide **3.67** first, the dihydroxylation could then be conducted successfully on the resulting phosphonate **3.67** (Scheme 3.10). There was an issue with the workup of this reaction in that the diol is quite soluble in water. Minimizing addition of aqueous solutions and thorough extraction of the aqueous layer with ethyl acetate permitted recovery of nearly all material on multigram scale. Following conversion of the secondary alcohol to the sulfonate, treatment with potassium carbonate induced intramolecular displacement and delivered the desired epoxide **3.59**. Derivatization of **3.59** with acetone permitted determination of enantioenrichment, which was a satisfactory 96% ee.

Scheme 3.10 Synthesis of Enantioenriched Epoxyphosphonate 3.59

3.72

3.67

Cs$_2$CO$_3$
THF, 60 °C

41%

3.73

OsO$_4$, (DHQ)$_2$PHAL
MeSO$_2$NH$_2$, K$_3$Fe(CN)$_6$, K$_2$CO$_3$
t-BuOH, H$_2$O, 0 °C

3.74

1) TsCl, DABCO, CH$_2$Cl$_2$, 0 °C
2) MeOH, K$_2$CO$_3$, 0 °C

32% over 3 steps
96% ee

3.59

One option to access aldehyde **3.60** would be to use an appropriate nucleophile in the enantioselective conjugate addition. The alternative was provided in a report from Nicolaou, who illustrated that following dihydroxylation of alkenes, addition of hypervalent iodine can induce cleavage to the corresponding carbonyls (Scheme 3.11a).[30] Due to the challenges associated with developing enantioselective conjugate additions, we felt use of this oxidative cleavage would expedite access to aldehyde **3.60** directly from the trisubstituted alkene **3.77** (Scheme 3.11b). Although our substrate **3.77** contains two alkenes, the rate of dihydroxylation proved to be substantially greater for the trisubstituted alkene. Minor adjustments to the reaction conditions resulted in high yields of desired aldehyde **3.60**. Treatment of phosphonate **3.59** with LiHMDS followed by addition of aldehyde **3.60** successfully produced ester **3.78** as a 1:1 mixture of alkene isomers. Reduction of the esters to the corresponding alcohols **3.79** and double oxidation with DMP of the resulting diol afforded a mixture of aldehydes **3.59a** and **3.59b**.
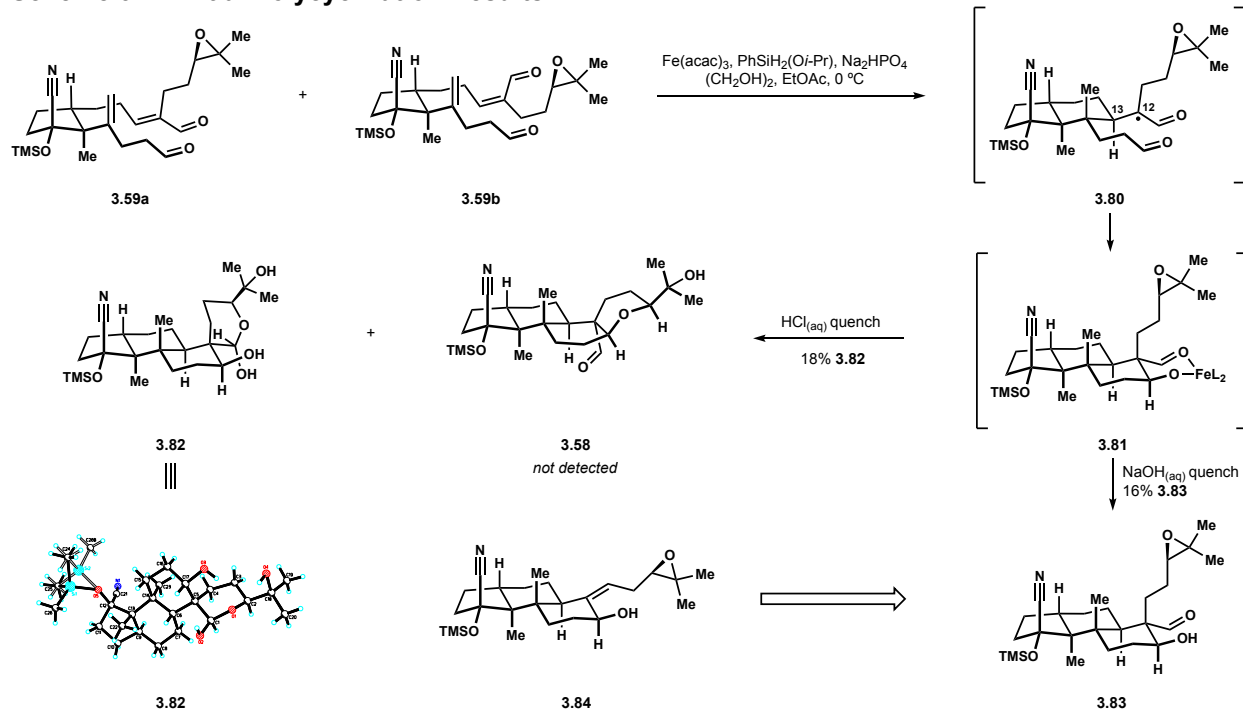
Scheme 3.11 Synthesis of a Polycyclization Precursor for Paxilline
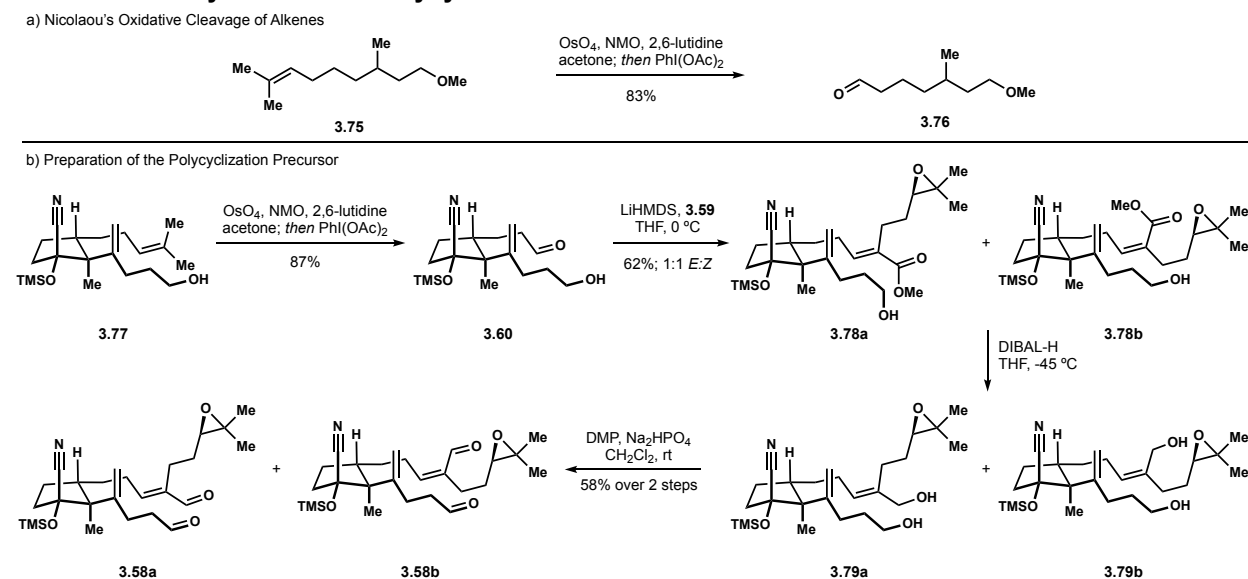
3.3.3 Development of a New Polycyclization

We reasoned that the mixture of alkene isomers **3.59a** and **3.59b** would be inconsequential. HAT and the subsequent conjugate addition results in the same intermediate **3.80**, which is free to

141

Scheme 3.12 Initial Polycyclization Results

rotate about the C12–C13 bond at a rate that should far exceed reduction and aldol addition (Scheme 3.12).[31] Subjecting the dialdehyde to conditions optimized in the nodulisporic acid C[1b,32] sequence appeared very promising qualitatively by TLC analysis prior to quenching. Typically, this reaction is quenched with acid with no change to the TLC appearance. Unexpectedly, the suspected product was completely converted into a more polar compound following addition of dilute hydrochloric acid. Isolation of this material was challenging for a multitude of reasons. First, there are additional diastereomers due to the olefination of a modestly enantioenriched aldehyde with the nearly enantiopure phosphonate. Prior to the polycyclization, all intermediates are oils, eliminating the possibility of recrystallization before subjecting the dialdehyde to the HAT conditions. Second, there are several products being formed and co-elution complicated NMR analysis even further. Diagnostic peaks corresponding to an aldehyde and two protons adjacent to an oxygen atom were present following isolation, leading us to believe there may be facile generation of the tetrahydropyran **3.58**. To our surprise and dismay, recrystallization provided X-

ray quality crystals and unambiguously determined that we instead opened the epoxide with the aldehyde, coinciding with the addition of an equivalent of water to produce hemiacetal **3.82**. Evidently, the aldehyde observed in the NMR belongs to a compound yet to be identified. Quenching the reaction with water alone led to visibly less hemiacetal, while a basic workup and isolation on deactivated silica permitted collection of polycyclization product **3.83** with the epoxide intact. This provided us the opportunity to induce dehydroformylation prior to tetrahydropyran formation and access alkene **3.84**.

The epoxyaldehyde **3.83** was expected to proceed through the oxidation-elimination sequence with relative ease as the system is more analogous to the unfunctionalized derivative **3.10** (Scheme 3.1). However, a new risk is presented the possibility of two geometric alkene isomers being formed from the elimination step. We hoped that the decalin system would bias the reaction towards formation of the Z alkene **3.84**. In the initial attempt, epoxyaldehyde **3.83** was subjected to the Baeyer–Villiger reaction successfully based on crude NMR analysis (Scheme 3.13). The tetrahydropyran was unintentionally formed upon exposure to silica gel, but provided the opportunity to determine which alkene may arise from the formate elimination. Remarkably, prolonged heating returned starting material with no evidence for the formation of cyclic alkenes

Scheme 3.13 Efforts to Eliminate the Formate on Tetrahydropyran 3.86


143
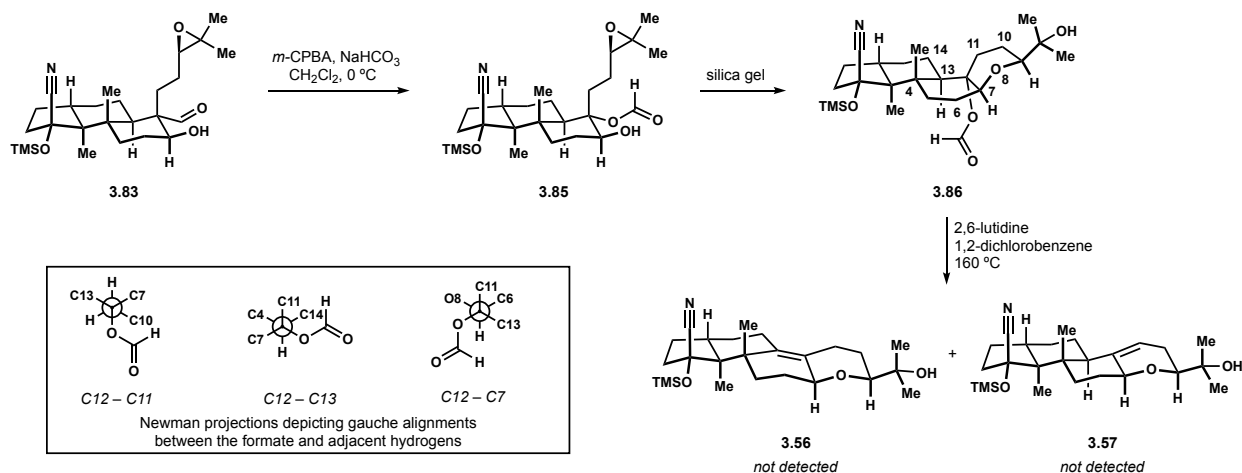
3.56 or **3.57**. Based on stereochemical modelling, it appears orbital overlap between the formate and any adjacent hydrogen is inadequate, only aligning in gauche relationships. A conformational ring flip of the tetrahydropyran also appears unlikely, rendering the reaction energetically inaccessible from **3.86**.

It was now clear that to access the desired unsaturation, the epoxide must remain intact until the alkene is installed. To this end, studies are incomplete, though preliminary results demonstrated promising outcomes. Performing the deformylation on tricyclic intermediate **3.85** was complicated due to acid sensitivity already discussed. Subjecting **3.85** to the elimination conditions as crude material again led to tetrahydropyran **3.86** with the formate still present. This was likely caused by formation of the tetrahydropyran prior to elimination, catalyzed by trace 2-iodobenzoic acid from the prior Baeyer–Villiger oxidation. Material that was sufficiently pure appeared to provide the desired dihydropyran **3.57** in the elimination reaction (Scheme 3.14). While the scale was too small for full characterization, there was a distinct vinyl C-H peak in the proton NMR and two downfield methine signals corresponding to the two ethereal protons of the dihydropyran. This result also indicates formation of the desired geometric alkene **3.91** as an intermediate, though we have yet to determine the selectivity ratio. With the milligram of material held, we explored further reactivity by attempting an allylic oxidation. Treatment of alkene **3.57**

Scheme 3.14 Construction of the Desoxy-paxilline Core

144
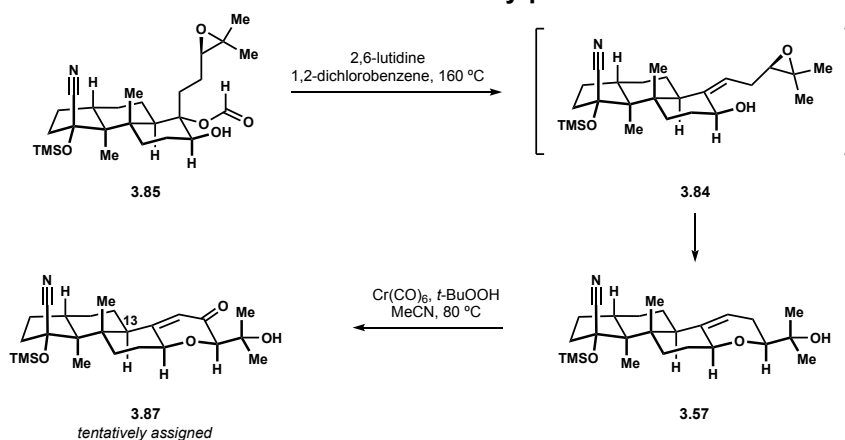
with chromium(0) hexacarbonyl and *tert*-butylhydroperoxide[33] cleanly converted the material into a new compound that was UV active by TLC analysis, indicative of conversion to an enone. Analysis of the proton NMR sprectra supported oxidation to enone **3.92** with the observation of a downfield shift of the vinyl proton. It should be noted that peaks in this spectrum are exceptionally small and proper assignment was not possible. Nevertheless, the crude product was collected and submitted for high-resolution mass spectrometry, which supported presence of the desired enone **3.87**.

3.3.4 Conclusions and Outlook

In summary, our key transformation in the synthesis of nodulisporic acid C has been generalized, allowing us to access the oxidation pattern found in paxilline and many other PIDs. With further optimization of this foundational approach, it is not beyond reason to believe paxilline and other complex indole diterpenes will be accessed using this chemistry. Outstanding challenges to this project include C-H oxidation of enone **3.87** at C13 (Scheme 3.14) along with further optimization of the tetrahydropyran generating sequence. Careful handling of intermediates appears to be a straightforward solution to the latter. Additionally, a general solution for enantioselective conjugate additions to 2-methylcyclopent-2-en-1-one stands to benefit our lab and the broader synthetic chemistry community.

3.4 Experimental Section

3.4.1 General Experimental Details

All reactions were carried out in flame-dried glassware under positive pressure of dry nitrogen unless otherwise noted. Reaction solvents (Fisher, HPLC grade) including tetrahydrofuran (THF), diethyl ether (Et$_2$O), dichloromethane (CH$_2$Cl$_2$), and toluene (PhMe) were dried by percolation through a column packed with neutral alumina and a column packed with a supported copper catalyst for scavenging oxygen (Q5) under positive pressure of argon. Methyl *tert*-butyl ether (MTBE, Millipore Sigma, ACS grade) was distilled from sodium diphenylketyl under positive pressure of nitrogen. Anhydrous 1,2-dichloroethane (DCE, Fisher, ACS Grade) and anhydrous triethylamine (Et$_3$N, Oakwood Chemical) were distilled from calcium hydride (10% w/v) under positive pressure of nitrogen. Anhydrous hexamethylphosphoramide (HMPA, Oakwood Chemical) was distilled from calcium hydride (10% w/v) under vacuum (*ca*. 0.1 torr). Solvents for extraction, thin layer chromatography (TLC), and flash column chromatography were purchased from Fischer (ACS Grade) and VWR (ACS Grade) and used without further purification. Chloroform-d, benzene-d$_6$, acetone-d$_6$ and methanol-d$_4$ for ^{1}H and ^{13}C NMR analysis were purchased from Cambridge Isotope Laboratories and used without further purification. Commercially available reagents were used without further purification unless otherwise noted. Reactions were monitored by thin layer chromatography (TLC) using precoated silica gel plates (EMD Chemicals, Silica gel 60 F$_{254}$). Flash column chromatography was performed over silica gel (Acros Organics, 60 Å, particle size 0.04-0.063 mm). GC/FID analysis was performed on Agilent 7820A system with helium as carrier gas. HPLC analysis was performed on an Agilent 1100 series. Optical rotation readings were obtained using JASCO P-1010 polarimeter. ^{1}H NMR and ^{13}C NMR spectra were recorded on Bruker DRX-500 (BBO probe), Bruker DRX-500 (TCI cryoprobe),

Bruker AVANCE600 (TBI probe), and Bruker AVANCE600 (BBFO cryoprobe) spectrometers using residual solvent peaks as internal standards (CHCl$_3$ @ 7.26 ppm ^{1}H NMR, 77.16 ppm ^{13}C NMR; C$_6$H$_6$ @ 7.16 ppm ^{1}H NMR, 128.00 ppm ^{13}C NMR; MeOH @ 3.31 ppm ^{1}H NMR, 49.00 ppm ^{13}C NMR; (CH$_3$)$_2$CO @ 2.05 ppm ^{1}H NMR, 29.84 ppm ^{13}C NMR). High-resolution mass spectra (HRMS) were recorded on Waters LCT Premier TOF spectrometer with ESI and CI sources.

3.4.2 Experimental Procedures

3.7 → **3.8**

Ac$_2$O, Et$_3$N, DMAP
PhMe, rt
79%
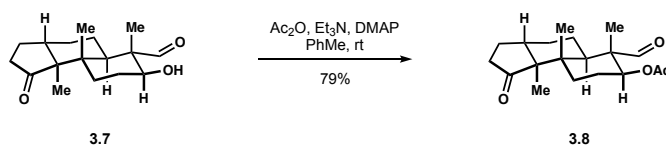
Acetate 3.8. To a solution of alcohol **3.7** (0.334 g, 1.2 mmol) in toluene (0.5 M) at room temperature was added acetic anhydride (0.45 mL, 4.8 mmol), Et$_3$N (0.84 mL, 6.0 mmol) andthen DMAP (0.015 g, 0.12 mmol). The reaction mixture was stirred 2 h and quenched with 1 N aqueous HCl. The layers were separated and the aqueous layer extracted twice with diethyl ether (40 mL combined). The organic layers were combined and washed with 1 N aqueous HCl (10 mL), H$_2$O (10 mL), brine (10 mL), dried over anhydrous magnesium sulfate, filtered and concentrated under reduced pressure. Purification by flash chromatography (gradient elution: 100% hexanes to 5% v/v ethyl acetate in hexanes) afforded acetate **3.8** (0.304 g, 79% yield) as a white solid.

^{1}H NMR (500 MHz, CDCl$_3$)

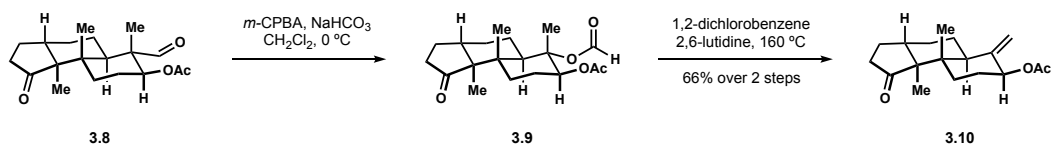|		
δ 9.26 (s, 1 H)	1.96 (s, 3 H)	1.46 – 1.38 (m, 2 H)
4.94 (dd, J = 10.9, 5.1 Hz, 1 H)	1.91 – 1.88 (m, 1 H)	1.09 (s, 3 H)
2.34 (dd, J = 19.3, 8.5 Hz, 1 H)	1.86 – 1.77 (m, 3 H)	1.05 (s, 3 H)
2.26 – 2.16 (m, 2 H)	1.75 – 1.67 (m, 2 H)	0.99 (s, 3 H)
2.06 – 1.98 (m, 1 H)	1.55 – 1.51 (m, 1 H)	

^{13}C NMR (126 MHz, CDCl$_3$)

δ 220.3	54.3	30.3	21.2
204.1	40.3	25.5	17.6
170.4	39.8	24.4	10.5
73.5	38.4	23.8	9.2
55.8	37.3	22.8	

HRMS (ESI) calculated for C$_{19}$H$_{28}$O$_4$Na [M+Na]$^+$: 343.1885, found 343.1894.

TLC: R$_i$ = 0.75 (50% EtOAc in hexanes)

Allylic acetate 3.10. A round bottom flask was charged with aldehyde **3.8** (0.27 g, 0.84 mmol),

NaHCO$_3$ (0.57 g, 6.7 mmol) and CH$_2$Cl$_2$ (0.1 M). Dry *m*-CPBA[34] (0.58 g, 3.4 mmol) was added

and the reaction mixture stirred vigorously for 1 h. The reaction was quenched with H$_2$O, then 2

N aqueous NaOH and diluted with CH$_2$Cl$_2$. The layers were separated and the aqueous layer

extracted twice with CH$_2$Cl$_2$ (40 mL combined). The organic layers were combined and washed

with 2 N aqueous NaOH (10 mL), H$_2$O (10 mL), brine (10 mL), dried over anhydrous magnesium

sulfate, filtered and concentrated under reduced pressure. Crude formate **3.9** was used without

further purification. Formate **3.9** (0.84 mmol) was transferred to a scintillation vial and to the vial

was added 1,2-dichlorobenzene (4.2 mL) and 2,6-lutidine (0.29 mL, 2.5 mmol). The vial was

sealed with a teflon lined cap and the reaction mixture heated to 160 ºC with vigorous stirring for

24 h. The heat was removed and the reaction allowed to cool to room temperature before quenching

with 1 N aqueous HCl. The layers were separated and the aqueous layer extracted twice with

diethyl ether (40 mL combined). The organic layers were combined and washed with 1 N aqueous

HCl (10 mL), H$_2$O (10 mL), brine (10 mL), dried over anhydrous magnesium sulfate, filtered and

concentrated under reduced pressure. Purification by flash chromatography (gradient elution: 100% hexanes to 5% v/v ethyl acetate in hexanes) afforded allylic acetate **3.10** (0.16 g, 66% yield over two steps) as a white solid.

Allylic acetate **3.10**

^{1}H NMR (500 MHz, CDCl$_3$)

δ 5.08 – 5.05 (m, 1 H)	2.12 (m, 3 H)	1.65 – 1.58 (m, 3 H)
4.90 – 4.89 (m, 1 H)	2.07 – 2.00 (m, 1 H)	1.49 – 1.42 (m, 2 H)
4.62 (s, 1 H)	1.96 – 1.92 (m, 1 H)	1.00 (s, 3 H)
2.33 (ddd, 1 H, J = 19.3, 8.6, 1.1 Hz)	1.88 – 1.82 (m, 1 H)	0.82 (s, 3 H)
2.22 – 2.16 (m, 3 H)	1.75 – 1.66 (m, 2 H)	

^{13}C NMR (126 MHz, CDCl$_3$)

δ 220.5	43.7	25.7
170.3	40.7	25.2
147.5	40.5	23.7
104.4	37.2	21.3
74.8	30.9	14.2
54.2	29.3	10.7

HRMS (ES+) calculated for C$_{18}$H$_{26}$O$_3$Na [M+Na]$^+$: 313.1780, found 313.1774

TLC: R$_f$ = 0.67 (20% v/v ethyl acetate in hexanes)

S3.1   S3.2   3.14
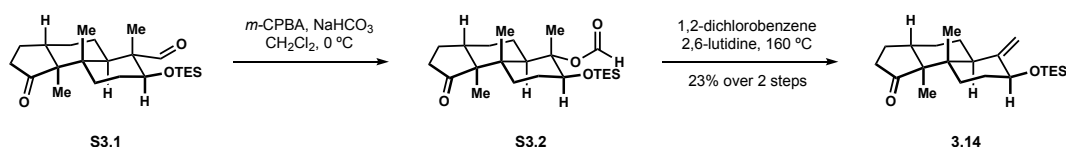
Triethyl silyl ether 3.14. Aldehyde **S3.1** was prepared from alcohol **3.7** according to the literature.[35] Aldehyde **S3.1** (0.225 g, 0.57 mmol) was subjected to the conditions reported above for aldehyde **3.10**, affording triethyl silyl ether **3.14** (48 mg, 23% over two steps) as a white solid.
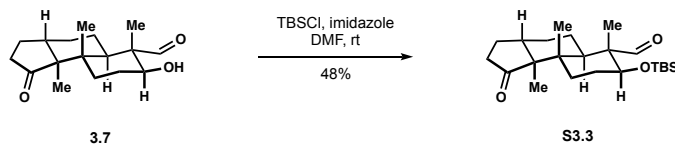
Triethyl silyl ether **3.14**

^{1}H NMR (500 MHz, CDCl$_3$)

δ 5.18 (app q, 1 H, J = 1.7 Hz)   2.14 – 2.11 (m, 1 H)   1.50 – 1.41 (m, 2 H)

4.61 (app q, 1 H, J = 1.7 Hz)   2.06 – 1.99 (m, 2 H)   0.99 (s, 3 H)

3.89 – 3.86 (m, 1 H)   1.87 – 1.81 (m, 2 H)   0.96 (t, 9 H, J = 8.0 Hz)

2.32 (ddd, 1 H, J = 19.3, 8.6, 1.0 Hz)   1.72 – 1.69 (m, 1 H)   0.79 (s, 3 H)

2.23 – 2.17 (m, 1 H)   1.65 – 1.55 (m, 5 H)   0.61 (q, 6 H, J = 8.1 Hz)

^{13}C NMR (126 MHz, CDCl$_3$)

δ 220.7	40.7	25.3
151.7	40.6	23.8
104.6	37.2	14.3
74.0	33.7	10.8
54.3	31.2	7.1
43.6	26.0	5.0

TLC: R$_f$ = 0.47 (20% v/v ethyl acetate in hexanes)

TBS Ether S3.3. To a solution of alcohol 3.7 (0.159 g, 0.57 mmol) in DMF (0.5 M) at room temperature was added imidazole (0.117 g, 1.71 mmol) and TBSCl (0.172 g, 1.14 mmol). The reaction mixture was stirred overnight (20 h) and quenched with H$_2$O and diluted with diethyl ether. The layers were separated and the aqueous layer extracted twice with diethyl ether (40 mL combined). The organic layers were combined and washed with 1 N aqueous HCl (10 mL), twice with H$_2$O (20 mL combined), brine (10 mL), dried over anhydrous magnesium sulfate, filtered and concentrated under reduced pressure. Purification by flash chromatography (gradient elution:
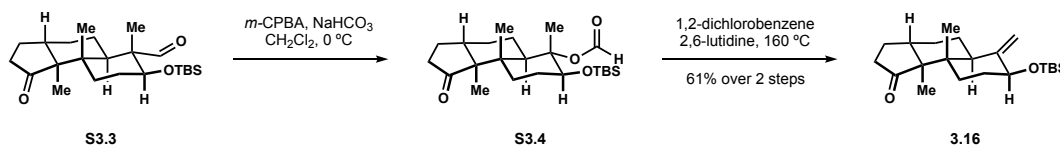
100% hexanes to 5% v/v ethyl acetate in hexanes) afforded TBS ether **S3.3** (0.107 g, 48% yield) as a white solid.

TBS ether **S3.3**
^{1}H NMR (500 MHz, CDCl$_3$)

δ 9.30 (s, 1 H)	1.74 – 1.59 (m, 4 H)	0.97 (s, 3 H)
3.72 (dd, 1 H, J = 11.3, 4.8 Hz)	1.54 – 1.51 (m, 1 H)	0.81 (s, 9 H)
2.32 (dd, 1 H, J = 20.1, 8.5 Hz)	1.43 – 1.35 (m, 2 H)	0.03 (s, 3 H)
2.21 – 2.15 (m, 2 H)	1.07 (s, 3 H)	– 0.04 (s, 3 H)
2.01 (dt, 1 H, J = 19.3, 9.6 Hz)	1.05 – 1.04 (m, 1 H)	
1.84 – 1.78 (m, 2 H)	1.03 (s, 3 H)	

TLC: R$_f$ = 0.14 (10% v/v ethyl acetate in hexanes)

Allylic TBS ether 3.16. Aldehyde **S3.3** (96 mg, 0.24 mmol) was subjected to the conditions reported for aldehyde **3.10**, affording allylic TBS ether **3.16** (46 mg, 61% over two steps) as a white solid.

Allylic TBS ether **3.16**
^{1}H NMR (500 MHz, CDCl$_3$)

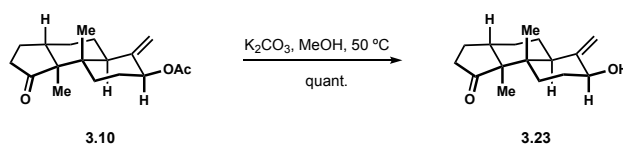|		
δ 5.15 (app q, 1 H, J = 1.7 Hz)	2.06 – 1.99 (m, 2H)	0.79 (s, 3 H)
4.61 – 4.60 (m, 1 H)	1.72 – 1.69 (m, 1 H)	0.06 (s, 3 H)
3.88 – 3.85 (m, 1 H)	1.62 – 1.55 (m, 4 H)	0.06 (s, 3 H)
2.32 (ddd, 1 H, J = 19.2, 8.6, 0.9 Hz)	1.50 – 1.41 (m, 2 H)	
2.24 – 2.18 (m, 1 H)	1.00 (s, 3 H)	
2.14 – 2.11 (m, 1 H)	0.92 (s, 9 H)	

¹³C NMR (126 MHz, CDCl₃)

δ 220.7	43.6	31.2	18.6
151.8	40.8	26.1	14.3
104.7	40.6	26.0	10.8
74.4	37.3	25.3	− 4.7
54.3	33.5	23.8	− 4.8

TLC: R_f = 0.39 (10% v/v ethyl acetate in hexanes)

Allylic alcohol 3.23. A 10 mL round bottom flask was charged with allylic acetate **3.10** (0.125 g, 0.43 mmol), anhydrous potassium carbonate (6 mg, 0.043 mmol) and dry methanol (0.1 M). The reaction mixture was stirred at 50 °C for 1 h, quenched with 1 N aqueous HCl and diluted with diethyl ether. The layers were separated and the aqueous layer extracted twice with diethyl ether (20 mL combined). The organic layers were combined and washed with H₂O (10 mL), brine (10 mL), dried over anhydrous magnesium sulfate, filtered and concentrated under reduced pressure. Purification by flash chromatography (gradient elution: 100% hexanes to 5% v/v ethyl acetate in hexanes) afforded allylic alcohol **3.23** (0.107 g, quantitative yield) as a white solid.

Allylic alcohol **3.23.**
¹H NMR (500 MHz, CDCl₃)

δ 5.10 (s, 1 H)	2.22 – 2.15 (m, 2 H)	1.70 – 1.57 (m, 5 H)
4.67 (s, 1 H)	2.10 – 2.10 (m, 3 H)	1.54 – 1.42 (m, 3 H)
3.93 (dd, 1 H, J = 11.1, 5.3 Hz)	1.88 – 1.82 (m, 1 H)	1.00 (s, 3 H)
2.33 (dd, 1 H, J = 19.2, 8.6 Hz)	1.74 – 1.71 (m, 1 H)	0.80 (s, 3 H)

TLC: R_f = 0.56 (50% v/v ethyl acetate in hexanes)
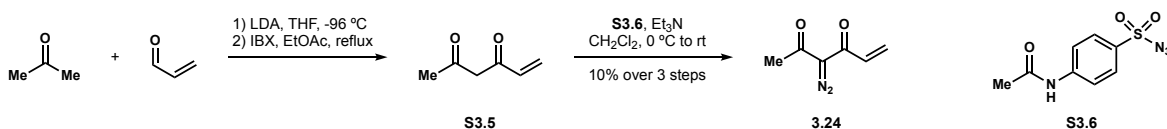
Diazodicarbonyl 3.24. To a solution of LDA in THF (11 mmol, 0.25 M) at -96 ºC was added

acetone (0.74 mL, 10 mmol) dropwise. The solution of enolate was stirred 30 min before adding

acrolein (0.67 mL, 10 mmol) quickly as a solution in THF (2 M). The reaction mixture was stirred

5 min and quenched with saturated aqueous NH_4Cl. The layers were separated and the aqueous

layer extracted twice with diethyl ether (100 mL combined). The organic layers were combined

and washed with H_2O (20 mL), brine (20 mL), dried over anhydrous magnesium sulfate, filtered

and concentrated under reduced pressure. In a 100 mL round-bottom flask, the crude aldol adduct

(0.66 g) was dissolved in ethyl acetate (0.2 M) and then added IBX (2.43 g, 8.7 mmol). The flask

was fitted with a reflux condenser and the reaction mixture heated to reflux with vigorous stirring

for 2 h. The reaction mixture was cooled to room temperature, filtered through a pad of silica gel

with diethyl ether (50 mL) and concentrated under reduced pressure.

Crude 1,3-dicarbonyl **S3.5** was dissolved in CH_2Cl_2 (0.2 M) and cooled to 0 ºC. To the solution

was added Et_3N (1.6 mL, 11.6 mmol) followed by 4-acetamidobenzenesulfonyl azide (1.32 g, 5.5

mmol). The reaction mixture was warmed to room temperature, stirred 2h and quenched with

saturated aqueous NH_4Cl. The layers were separated and the aqueous layer extracted twice with

CH_2Cl_2 (50 mL combined). The organic layers were combined and washed with H_2O (10 mL),

brine (10 mL), dried over anhydrous magnesium sulfate, filtered and concentrated under reduced

pressure. Purification by flash chromatography (gradient elution: 100% hexanes to 10% v/v ethyl

acetate in hexanes) afforded diazodicarbonyl **3.24** (0.140 g, 10% yield over three steps) as a yellow

oil.

Diazodicarbonyl **3.24**

^{1}H NMR (500 MHz, CDCl$_3$)

 δ 6.99 (dd, 1 H, J = 16.8, 10.3 Hz)

 6.46 (dd, 1 H, J = 16.8, 1.5 Hz)

 5.81 (dd, 1 H, J = 10.4, 1.6 Hz)

 2.49 (s, 3 H)

^{13}C NMR (126 MHz, CDCl$_3$)*
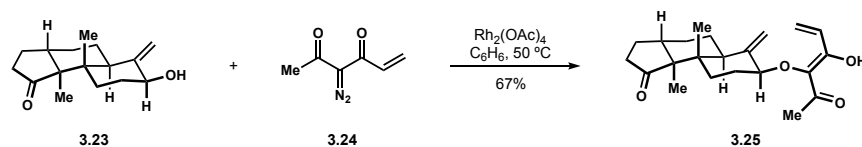
 δ 131.5

 129.6

 28.9

*Multiple runs of the ^{13}C NMR with additional scans acquired were attempted. The carbonyl and diazo ^{13}C signals were consistently absent.

TLC: R$_f$ = 0.21 (20% v/v ethyl acetate in hexanes)

Ketoenol 3.25. A flame dried 5 mL Schlenk flask was charged with allylic alcohol **3.23** (23 mg, 0.09 mmol), rhodium(II) acetate dimer (4.1 mg, 0.009 mmol), benzene (1 M) and heated to 50 ºC. Diazodicarbonyl **3.24** (37.3 mg, 0.27 mmol) was then added as a solution in benzene (0.1 M) over the course of 1 h with a syringe pump. Once addition of **3.24** was complete, the reaction mixture was removed from heat and filtered through a plug of Celite eluted with diethyl ether and concentrated under reduced pressure. Purification by flash chromatography (gradient elution: 100% hexanes to 10% v/v ethyl acetate in hexanes) afforded ketoenol **3.25** (21.3 mg, 93% yield) as a colourless thin film.
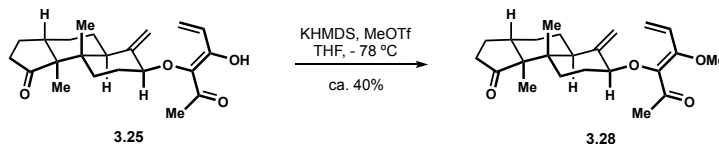
Ketoenol **3.25**

^{1}H NMR (500 MHz, CDCl$_3$)

δ 13.95 (s, 1 H)	3.71 – 3.67 (m, 1 H)	1.88 – 1.83 (m, 1 H)
6.68 (dd, 1 H, J = 17.3, 10.7 Hz)	2.32 (dd, 1 H, J = 19.3, 8.6 Hz)	1.76 – 1.73 (m, 1 H)
6.22 (dd, 1 H, J = 17.3, 1.7 Hz)	2.23 (s, 3 H)	1.65 –1.58 (m, 2 H)
5.66 (dd, 1 H, J = 10.7, 1.8 Hz)	2.22 – 2.19 (m, 2 H)	1.53 – 1.42 (m, 4 H)
5.41 (s, 1 H)	2.07 – 2.00 (mm 2 H)	0.97 (s, 3 H)
4.78 (s, 1 H)	1.96 – 1.93 (m, 1 H)	0.85 (s, 3 H)

^{13}C NMR (126 MHz, CDCl$_3$)

δ 220.4	127.7	44.0	29.2	14.3
199.8	125.0	40.8	25.7	10.6
166.2	105.8	40.5	25.2	
148.4	85.8	37.1	24.3	
134.1	54.2	30.9	23.7	

TLC: R$_f$ = 0.37 (20% v/v ethyl acetate in hexanes)

Methyl enol ether 3.28. To a solution of ketoenol **3.25** (10 mg, 0.028 mmol) in CH$_2$Cl$_2$ (0.1 M) at -78 ºC was added KHMDS (0.042 mmol, 0.5 M in THF). The enolate solution was stirred 15 min before adding methyl trifluormethanesulfonate (12 µL, 0.11 mmol) at -78 ºC then warming the reaction mixture to room temperature and stirring until the yellow colour of the potassium enolate dissipated. The reaction was quenched with saturated aqueous NaHCO$_3$, the layers separated and the aqueous layer was extracted twice with CH$_2$Cl$_2$ (20 mL combined). The organic layers were combined and washed with H$_2$O (5 mL), brine (5 mL), dried over anhydrous

magnesium sulfate, filtered and concentrated under reduced pressure. Purification by flash chromatography (gradient elution: 100% hexanes to 5% v/v ethyl acetate in hexanes) afforded methyl enol ether **3.28** (4.5 mg, 43% yield) as a thin film.

Methyl enol ether **3.28**

^{1}H NMR (500 MHz, CDCl$_3$)

|		
δ 6.74 (dd, 1 H, J = 17.6, 11.0 Hz)	2.41 (s, 3 H)	1.64 – 1.60 (m, 2 H)
5.73 (dd, 1 H, J = 17.6, 1.6 Hz)	2.32 (dd, 1 H, J = 19.1, 8.6 Hz)	1.53 – 1.41 (m, 5 H)
5.46 (dd, 1 H, J = 11.0, 1.6 Hz)	2.24 – 2.14 (m, 2 H)	0.96 (s, 3 H)
5.34 (s, 1 H)	2.08 – 1.99 (m, 2 H)	0.82 (s, 3 H)
4.74 (s, 1 H)	1.87 – 1.82 (m, 2 H)	
3.74 (s, 3 H)	1.74 – 1.71 (m, 1 H	

TLC: R$_f$ = 0.31 (20% v/v ethyl acetate in hexanes)
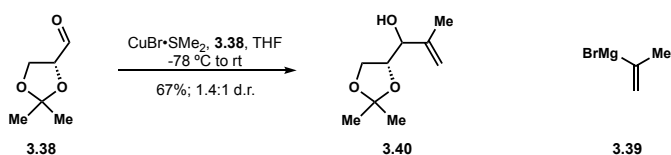
Allylic Alcohol 3.40. A flame-dried Schlenck flask was charged with copper(I) bromide dimethyl sulfide (0.247 g, 1.2 mmol) and THF (1 mL). The suspension of copper was cooled to -78 ºC before adding isopropenylmagnesium bromide (28.7 mmol, 0.24 M in THF) dropwise then aldehyde **3.38** (3.12 g, 24 mmol) as a solution in THF (1 M). The reaction mixture was warmed to room temperature and stirred 1 h then quenched with a 3:1 (v/v) mixture of saturated aqueous NH$_4$Cl and 28% (v/v) aqueous NH$_3$ (50 mL). The layers were separated and the aqueous layer extracted twice with diethyl ether (200 mL combined). The organic layers were combined and washed twice with the NH$_4$Cl/NH$_3$ solution (50 mL combined), H$_2$O (50 mL), brine (50 mL), dried over

anhydrous magnesium sulfate, filtered and concentrated under reduced pressure. Purification by flash chromatography (gradient elution: 100% hexanes to 20% v/v ethyl acetate in hexanes) afforded allylic alcohol **3.40** (2.77 g, 67% yield) as a colourless oil and 1.4:1 mixture of diastereomers that were taken forward together. Spectral Data math that provided in the literature.[36]
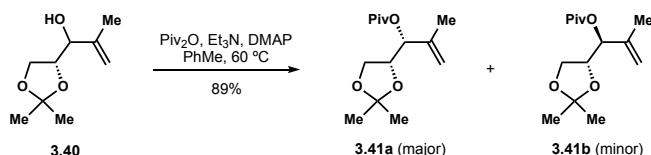
Allylic Pivalates 3.41a and 3.41b. To a solution of allylic alcohol **3.40** (0.80 g, 4.6 mmol) in toluene (2 M) was added trimethylacetic anhydride (1.4 mL, 7.0 mmol) followed by Et$_3$N (1.3 mL, 9.2 mmol) and DMAP (0.056 g, 0.46 mmol). The reaction mixture was heated to 50 º C, stirred overnight (20 h) and quenched with 1 N aqueous HCl. The layers were separated and the aqueous layer was extracted twice with CH$_2$Cl$_2$ (40 mL combined). The organic layers were combined and washed with 2 N aqueous NaOH (20 mL), H$_2$O (10 mL), brine (10 mL), dried over anhydrous magnesium sulfate, filtered and concentrated under reduced pressure. Purification by flash chromatography (gradient elution: 100% hexanes to 5% v/v ethyl acetate in hexanes) afforded allylic pivalates **3.41a** and **3.41b** (1.05 g, 89% yield combined) as a colourless oils. Pure fractions of the major and minor diastereomers were collected for characterization. Major diastereomer **3.41a** (0.68 g, 58% yield) was advanced as a 4.9:1 ratio of diastereomers.
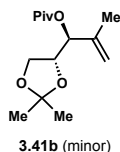
157

3.41a (major)
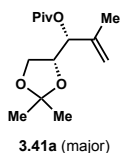
¹H NMR (500 MHz, CDCl₃)

δ 5.18 (d, 1 H, J = 5.9 Hz)   3.73 (dd, 1 H, J = 8.6, 6.0 Hz)

5.03 (m, 1 H)   1.77 (s, 3 H)

4.99 – 4.98 (m, 1 H)   1.43, (s, 3 H)

4.31 (q, 1 H, J = 6.2 Hz)   1.35 (s, 3 H)

3.98 (dd, 1 H, J = 8.6, 6.6 Hz)   1.24 (s, 9 H)

¹³C NMR (126 MHz, CDCl₃)

δ 177.8	110.0	66.0	26.7
141.1	76.7	39.1	25.6
114.6	76.1	27.3	19.3

TLC: R_f = 0.57 (20% v/v ethyl acetate in hexanes)

3.41b (minor)

¹H NMR (500 MHz, CDCl₃)

δ 5.17 (d, 1 H, J = 6.4 Hz)   3.85 (dd, 1 H, J = 8.4, 6.2 Hz)

5.02 (m, 1 H)   1.79 (s, 3 H)

4.99 – 4.98 (m, 1 H)   1.42, (s, 3 H)

4.25 (q, 1 H, J = 6.3 Hz)   1.35 (s, 3 H)

4.01 (dd, 1 H, J = 8.4, 6.4 Hz)   1.22 (s, 9 H)

¹³C NMR (126 MHz, CDCl₃)

δ 177.2	109.8	66.2	26.7
141.5	76.1	39.0	25.4
114.1	75.9	27.3	19.4

TLC: R_f = 0.62 (20% v/v ethyl acetate in hexanes)
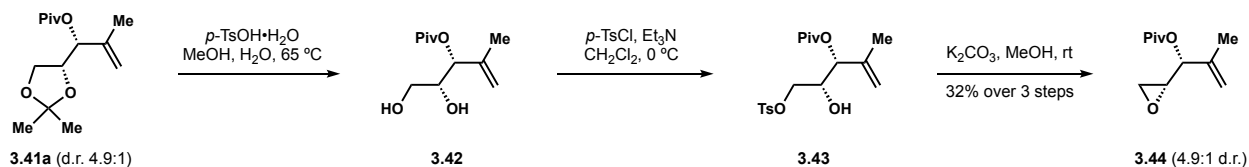
Epoxide 3.44. To a solution of acetonide **3.41a** (0.68 g, 2.6 mmol; 4.9:1 d.r.) in 3:1 MeOH:H$_2$O (0.2 M) was added *p*-toluenesulfonic acid monohydrate (0.025 g, 0.13 mmol). The reaction mixture was heated to 65 ºC and stirred overnight (17 h). The reaction was quenched with saturated aqueous NaHCO$_3$ and diluted with ethyl acetate. The layers were separated and the aqueous layer was extracted three times with ethyl acetate (100 mL combined). The organic layers were combined and washed with H$_2$O (10 mL), brine (10 mL), dried over anhydrous magnesium sulfate, filtered and concentrated under reduced pressure. The crude diol **3.42** was then dissolved in CH$_2$Cl$_2$ (0.5 M) and cooled to 0 ºC before adding Et$_3$N (3.7 mL, 26.5 mmol) followed by *p*-toluenesulfonyl chloride (0.50 g, 2.6 mmol). The reaction mixture was stirred vigorously at 0 ºC for 1 h and quenched with 1 N aqueous HCl. The layers were separated and the aqueous layer was extracted twice with CH$_2$Cl$_2$ (100 mL combined). The organic layers were combined and washed with H$_2$O (20 mL), brine (20 mL), dried over anhydrous magnesium sulfate, filtered through a plug of silica (elution with ethyl acetate) and concentrated under reduced pressure. To a solution of tosylate **3.43** in MeOH (0.2 M) was added anhydrous potassium carbonate (0.349 g, 2.52 mmol) at room temperature. The reaction mixture was stirred vigorously for 2 h and quenched with 1 N aqueous HCl and diluted with diethyl ether. The layers were separated and the aqueous layer was extracted twice with diethyl ether (100 mL combined). The organic layers were combined and washed with H$_2$O (20 mL), brine (20 mL), dried over anhydrous magnesium sulfate, filtered and concentrated under reduced pressure. Purification by flash chromatography (gradient elution: 100% hexanes to 5% v/v ethyl acetate in hexanes) afforded epoxide **3.44** (0.168 g, 32% yield over three steps) as a colourless oil in a 3.9:1 diastereomeric ratio.

Epoxide **3.44**

^{1}H NMR (500 MHz, CDCl$_3$)

  δ 5.05 (s, 1 H)

  4.98 (s, 1 H)

  4.93 (d, 1 H, J = 6.2 Hz)

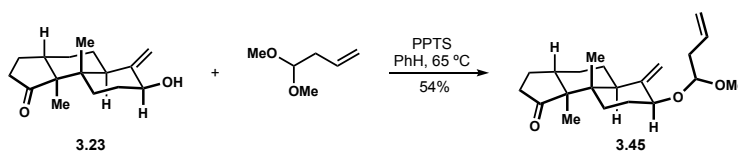 3.17 – 3.14 (m, 1 H)

  2.84 (dd, J = 4.8, 4.2 Hz)

  2.66 (dd, J = 5.0, 2.6 Hz)

  1.81 (s, 3 H)

  1.24 (s, 9 H)

TLC: R$_f$ = 0.54 (20% v/v ethyl acetate in hexanes)

Mixed Acetal 3.46. To a solution of allylic alcohol **3.23** (20 mg, 0.08 mmol) and 4,4-dimethoxybut-1-ene (*Chem. Ber*. **1996**, *119*, 1725.) (28 mg, 0.24 mmol) in benzene (0.1 M) was added one crystal of PPTS (~2 mg). The reaction mixture was heated to 60 ºC, stirred 2 h and quenched with saturated aqueous NaHCO$_3$. The biphasic mixture was diluted with diethyl ether and the layers separated. The layers were separated and the aqueous layer was extracted twice with diethyl ether (20 mL combined). The organic layers were combined and washed with H$_2$O (5 mL), brine (5 mL), dried over anhydrous magnesium sulfate, filtered and concentrated under reduced pressure. Purification by flash chromatography (gradient elution: 100% hexanes to 5% v/v ethyl acetate in hexanes) afforded mixed acetal **3.45** (14 mg, 54% yield) as a mixture of diastereomers.

Mixed acetal **3.45**

^{1}H NMR (500 MHz, CDCl$_3$)

δ 5.87 – 5.78 (m, 1 H)	2.33 (dd, 1 H, J = 19.5, 8.1 Hz)	1.67 – 1.60 (m, 3 H)
5.29 – 5.06 (m, 3 H)	2.22 – 2.16 (m, 2 H)	1.53 – 1.41 (m, 3 H)
4.66 – 4.56 (m, 2 H)	2.12 – 2.01 (m, 2 H)	0.99 (s, 3 H)
3.87 – 3.85 (m, 1 H)	2.07 – 2.01 (m, 1 H)	0.81, 0.80 (s, 3 H, diast.)
3.31 (s, 3 H)	1.87 – 1.82 (m, 1 H)	
2.48 – 2.43 (m, 2 H)	1.73 – 1.70 (m, 1 H)	

TLC: R$_f$ = 0.42 (20% v/v ethyl acetate in hexanes)
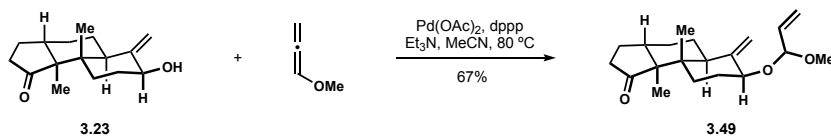
Allyl Acetal 3.49. A flame-dried 5 mL Schlenk flask was charged with allylic alcohol **3.23** (26 mg, 0.10 mmol), palladium(II)acetate (1.2 mg, 0.005 mmol), 1,3-bis(diphenylphosphino)propane (2.2 mg, 0.005 mmol) and the atmosphere exchanged three times with nitrogen. MeCN (0.1 M) and Et$_3$N (22 μL, 0.15 mmol) were added and the solution heated in an oil bath at 80 ºC with stirring to ligate the palladium. The mixture was removed from heat and methoxyallene (27 μL, 0.31 mmol) was added. The reaction mixture was returned to the oil bath, stirred at 80 ºC for 18 h, and quenched with 1 N aqueous HCl and diluted with diethyl ether. The layers were separated and the aqueous layer was extracted twice with diethyl (20 mL combined). The organic layers were combined and washed with H$_2$O (5 mL), brine (5 mL), dried over anhydrous magnesium sulfate, filtered and concentrated under reduced pressure. Purification by flash chromatography (gradient elution: 100% hexanes to 5% v/v ethyl acetate in hexanes) afforded allyl acetal **3.49** (21 mg, 67% yield) as a white solid.

Allyl Acetal **3.49**

^{1}H NMR (500 MHz, C$_6$D$_6$)

δ 5.96 (m, 1 H)	3.25, 3.12 (s, 3 H, diast.)	1.38 – 1.21 (m, 4 H)
5.65 – 5.37 (m, 2 H)	2.41 – 2.35 (m, 1 H)	1.16 – 1.03 (m, 2 H)
5.17 – 5.08 (m, 2 H)	2.06 – 1.97 (m, 2 H)	0.86, 0.84 (s, 3 H, diast.)
4.76, 4.69 (s, 1 H, diast.)	1.82 – 1.65 (m, 4 H)	0.63, 0.63 (s, 3 H, diast.)
3.98 (td, 1 H, J = 11.6, 5.5 Hz)	1.52 – 1.40 (m, 1 H)	

TLC: R$_f$ = 0.57 (20% v/v ethyl acetate in hexanes)
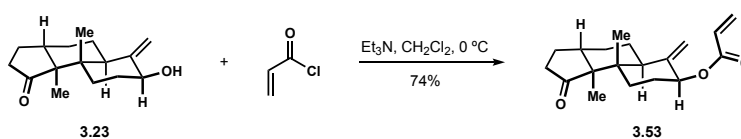
Acrylate 3.53. To a solution of allylic alcohol **3.23** (11 mg, 0.044 mmol) in CH$_2$Cl$_2$ (0.1 M) at 0 °C was added Et$_3$N (19 μL, 0.13 mmol) followed by acryloyl chloride (7 μL, 0.09 mmol). The reaction mixture was stirred at 0 °C for 1 h and quenched with saturated aqueous NaHCO$_3$. The layers were separated and the aqueous layer was extracted twice with CH$_2$Cl$_2$ (20 mL combined). The organic layers were combined and washed with H$_2$O (5 mL), brine (5 mL), dried over anhydrous magnesium sulfate, filtered and concentrated under reduced pressure. Purification by flash chromatography (gradient elution: 100% hexanes to 5% v/v ethyl acetate in hexanes) afforded acrylate **3.53** (9.9 mg, 74% yield) as a thin film.

Acrylate **3.53**

^{1}H NMR (500 MHz, CDCl$_3$)

δ 6.46 (dd, 1 H, J = 17.4, 1.4 Hz)	2.34 (dd, 1 H, J = 19.3, 8.6 Hz)	1.63 – 1.59 (m, 2 H)
6.19 (dd, 1 H, J = 17.3, 10.4 Hz)	2.24 – 2.19 (m, 3 H)	1.50 – 1.43 (m, 2 H)
5.86 (dd, 1 H, J = 10.4, 1.4 Hz)	2.08 – 2.02 (m, 1 H)	1.02 (s, 3 H)
5.17 – 5.13 (m, 1 H)	2.00 – 1.97 (m, 1 H)	0.84 (s, 3 H)
4.91 (s, 1 H)	1.88 – 1.83 (m, 1 H)	
4.63 (s, 1 H)	1.78 – 1.67 (m, 3 H)	

^{13}C NMR (126 MHz, CDCl$_3$)

δ 220.5	104.5	40.5	25.2
165.4	74.9	37.2	23.8
147.3	54.3	30.87	14.2
131.0	43.7	29.3	10.7
128.8	40.7	25.7	

TLC: R_f = 0.48 (20% v/v ethyl acetate in hexanes)
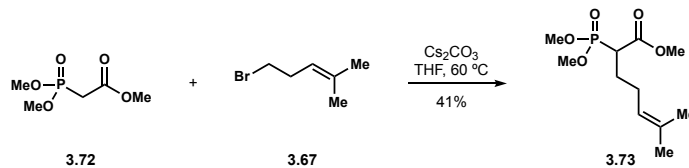
Phosphonate 3.73. To a solution of bromide **3.67** (13.4 g, 82.4 mmol) and Cs$_2$CO$_3$ (29.5 g, 90.6 mmol) in THF (1 M) was added phosphonate **3.72** (15.0 g, 82.4 mmol). The reaction mixture was heated to 60 ºC, stirred 24 h and quenched with saturated aqueous NH$_4$Cl. The layers were separated and the aqueous layer was extracted three times with ethyl acetate (1 L combined). The organic layers were combined and washed with H$_2$O (100 mL), brine (100 mL), dried over anhydrous magnesium sulfate, filtered and concentrated under reduced pressure. Purification by flash chromatography (gradient elution: 100% hexanes to 50% v/v ethyl acetate in hexanes)

afforded phosphonate **3.73** (8.92 g, 41% yield) as a colourless oil. Spectral data match that found in the literature.[37]

3.73 → **3.74** → **3.59**

OsO$_4$, (DHQ)$_2$PHAL
MeSO$_2$NH$_2$, K$_3$Fe(CN)$_6$, K$_2$CO$_3$
t-BuOH, H$_2$O, 0 °C

1) TsCl, DABCO, CH$_2$Cl$_2$, 0 °C
2) MeOH, K$_2$CO$_3$, 0 °C

32% over 3 steps
96% ee
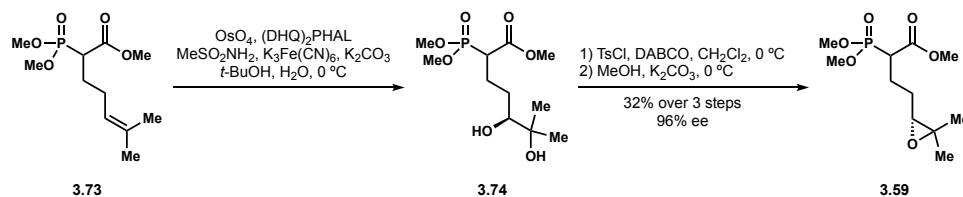
Epoxide 3.59. A 1 L round-bottom flask was charged with phosphonate **3.73** (10.24 g, 38.7 mmol), sodium bicarbonate (9.75 g, 116.1 mmol), anhydrous potassium carbonate (16.0 g, 116.1 mmol), potassium ferricyanide (38.2 g, 116.1 mmol), methanesulfonamide (3.68 g, 38.7 mmol), (DHQ)$_2$PHAL (0.301 g, 0.39 mmol), *tert*-butyl alcohol (100 mL) and H$_2$O (100 mL) and a large stir bar. The heterogeneous mixture was cooled in an ice bath to 0 °C while stirring. Osmium tetroxide (0.050 g, 0.2 mmol) was then added and the flask transferred to the refrigerator with a stir plate. The reaction mixture was stirred 36 h at 4 °C and diluted with ethyl acetate (500 mL). The layers were separated and the aqueous layer extracted with ethyl acetate (200 mL) until diol **3.74** was no longer visible by TLC in the extracts. The organic layers were dried with anhydrous magnesium sulfate, filtered and concentrated under reduced pressure. The concentrated mixture still containing H$_2$O was dissolved in 200 mL of ethyl acetate and the aqueous layer removed. The organic layer was dried over anhydrous magnesium sulfate, filtered and concentrated again.

The crude diol **3.74** was dissolved in CH$_2$Cl$_2$ (0.5 M), cooled to 0 °C and then added DABCO (9.36 g, 96.7 mmol) followed by *p*-toluenesulfonyl chloride (14.8 g, 77.4 mmol). The reaction mixture was stirred 1 h at 0 °C and quenched with 1 N aqueous HCl. The layers were separated and the aqueous layer extracted with ethyl acetate four times (1 L combined). The organic layers were

164

combined and washed with 1 N aqueous HCl (100 mL), brine (100 mL), dried over anhydrous magnesium sulfate, filtered and concentrated under reduced pressure.

The crude tosylate was dissolved in MeOH (0.5 M) and to the solution was added anhydrous potassium carbonate (10.7 g, 77.4 mmol). The reaction mixture was stirred 1 h and quenched with saturated aqueous NH$_4$Cl and diluted with ethyl acetate. The layers were separated and the aqueous layer extracted with ethyl acetate in 100 mL portions until the TLC of an extract showed no phosphonate present. The organic layers were combined and washed with 2 N aqueous NaOH (50 mL), brine (50 mL), dried over anhydrous magnesium sulfate, filtered and concentrated under reduced pressure. Purification by flash chromatography (gradient elution: 100% hexanes to 100% v/v ethyl acetate in hexanes) afforded epoxide **3.59** (3.47 g, 32% yield over three steps) as a colourless oil along with phosphonate **3.73** (2.36 g, 23% recovery). Enantiopurity was assessed by conducting an olefination of acetone (see following compound **S3.7**).

Phosphonate **3.73**
^{1}H NMR (500 MHz, CDCl$_3$)

δ 3.82 – 3.77 (m, 9 H)   1.68 – 1.59 (m, 2 H)

3.11 – 3.00 (m, 1 H)   1.30 (app d, 3 H, J = 2.7 Hz)

2.71 – 2.68 (m, 1 H)   1.24 (s, 3 H)

2.18 – 1.97 (m, 2 H)

HRMS (ES+) calculated for C$_{11}$H$_{21}$O$_6$PNa [M+Na]$^+$: 303.0974, found 303.0972
TLC: R$_f$ = 0.28 (100% ethyl acetate)
96% ee
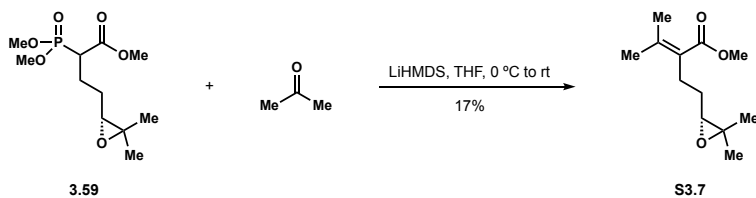
α,β-Unsaturated Ester S3.7. To a solution of phophonate **3.59** (50 mg, 0.18 mmol) in THF (1 M) at 0 °C was added LiHMDS (0.36 mL, 0.5 M in THF). The solution was stirred for 30 min at 0 °C and then added anhydrous acetone (0.66 mL, 8.9 mmol). The reaction mixture was warmed to room temperature, stirred 24 h and quenched with 1 N aqueous HCl. The layers were separated and the aqueous layer extracted twice with diethyl ether (20 mL combined). The organic layers were combined and washed with H_2O (5 mL), brine (5 mL), dried over anhydrous magnesium sulfate, filtered and concentrated under reduced pressure. Purification by flash chromatography (gradient elution: 100% hexanes to 10% v/v ethyl acetate in hexanes) afforded α,β-unsaturated ester **S3.7** (6.5 mg, 17% yield) as a colourless oil.

α,β-Unsaturated ester **S3.7**
^{1}H NMR (500 MHz, CDCl$_3$)

δ 3.72 (s, 3 H)	1.84 (s, 3 H)
2.71 (t, 1 H, J = 6.4 Hz)	1.66 – 1.59 (m, 2 H)
2.51 – 2.41 (m, 2 H)	1.29 (s, 3 H)
2.00 (s, 3 H)	1.24 (s, 3 H)

^{13}C NMR (126 MHz, CDCl$_3$)

δ 169.9	58.6	25.0
144.2	51.4	23.3
126.7	28.5	22.2
63.9	26.7	18.8

TLC: R_f = 0.83 (50% v/v ethyl acetate in hexanes

Enantiopurity was assessed on a GC/FID (HP – Chiral – 20B; 6.88 psi; 0.5 mL/min; initial column temperature 50 ºC, then 10 °C/min to 105 °C, hold for 200 min, then 10 °C/min to 200 °C, hold for 10 min): tR = 204.22, 207.07 min.

3.77   **3.60**
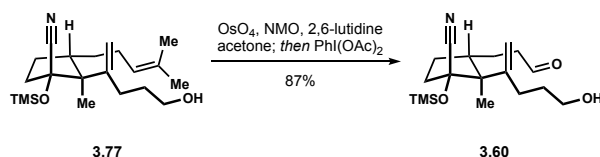
Aldehyde 3.60. To a solution of alkene **3.77** (0.50 g, 1.4 mmol) in acetone and H_2O (10:1 v/v; 0.1 M) at 0 ºC was added NMO (0.242 g, 2.1 mmol), 2,6-lutidine (0.24 mL, 2.1 mmol) and osmium tetroxide (~7 mg, 0.028 mmol). The reaction mixture was brought to room temperature and stirred vigorously until complete consumption of alkene **3.77** was observed by TLC analysis (Note: occasionally an additional crystal of osmium tetroxide was added on a case by case basis when the reaction appeared to stall). (Diacetoxyiodo)benzene (0.68 g, 2.1 mmol) was then added to the reaction mixture and stirring continued for an addition 2 h, or until the triol had been fully consumed by TLC analysis. The reaction was quenched with saturated aqueous $Na_2S_2O_3$ and diluted with diethyl ether. The layers were separated and the aqueous layer extracted twice with diethyl ether (100 mL combined). The organic layers were combined and washed with H_2O (20 mL), 1 N aqueous HCL (20 mL), brine (20 mL), dried over anhydrous magnesium sulfate, filtered and concentrated under reduced pressure. Purification by flash chromatography (gradient elution: 100% hexanes to 20% v/v ethyl acetate in hexanes) afforded aldehyde **3.60** (0.41 g, 87% yield) as a pale-yellow oil.

Aldehyde **3.60**

^{1}H NMR (500 MHz, CDCl$_3$)

δ 9.79 (t, 1 H, J = 1.3 Hz)	2.38 – 2.21 (m, 4 H)	1.44 – 1.39 (m, 2 H)
5.11 (s, 1 H)	2.04 – 2.00 (m 1 H)	1.01 (s, 3 H)
5.01 (s, 1 H)	1.96 – 1.90 (m, 2 H)	0.22 (s, 9 H)
3.74 – 3.66 (m, 2 H)	1.80 – 1.77 (m, 2 H)	
2.49 –2.45 (m, 2 H)	1.53 – 1.49 (br s, 2 H)	

HRMS (ES+) calculated for C$_{18}$H$_{31}$NO$_3$Na [M+Na]$^+$: 360.1971, found 360.1956

TLC: R$_f$ = 0.19 (30% v/v ethyl acetate in hexanes)
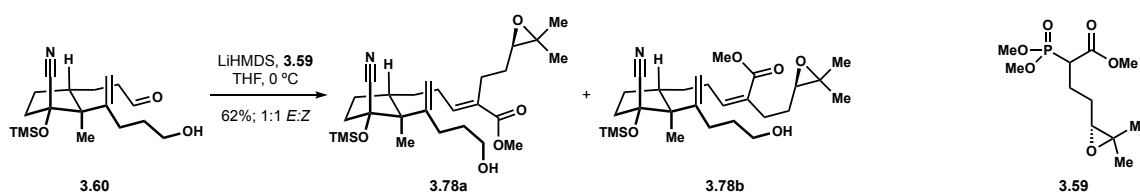
α,β-Unsaturated Esters 3.78a and 3.78b. To a solution of phosphonate **2.59** (0.525 g, 1.9 mmol) in THF (1 M) at -78 ºC was added LiHMDS (1.8 mL, 1 M). The mixture was stirred 30 min before adding aldehyde **3.60** (0.575 g, 1.7 mmol) as a solution in THF (0.1). The reaction mixture was brought to room temperature, stirred 1 h and quenched with 1 N aqueous HCl. The layers were separated and the aqueous layer extracted twice with diethyl ether (100 mL combined). The organic layers were combined and washed with H$_2$O (20 mL), brine (20 mL), dried over anhydrous magnesium sulfate, filtered and concentrated under reduced pressure. Purification by flash chromatography (gradient elution: 100% hexanes to 20% v/v ethyl acetate in hexanes) afforded α,β-unsaturated esters **3.78a** and **3.78b** (0.58 g, 62 % yield) as a colourless oil and inseparable 1:1 mixture of E and Z alkene isomers.

α,β-Unsaturated esters **3.78a** and **3.78b**

^{1}H NMR (500 MHz, CDCl$_3$)

δ 6.78, 5.95 (t, 1 H, J = 7.6 Hz)	2.49 – 2.33 (m, 5 H)	1.51 – 1.45 (m, 2 H)
5.07 (s, 1 H)	2.28 – 2.20 (m, 3 H)	1.28 (s, 3 H)
4.98, 4.96 (s, 1 H)	2.09 – 2.05 (m, 1 H)	1.24 – 1.23 (m, 4 H)
3.74, 3.73 (s, 3 H)	1.94 – 1.88 (m, 1 H)	0.96 (s, 3 H)
3.70 – 3.67 (m, 2 H)	1.80 – 1.74 (m, 2 H)	0.21 (s, 9 H)
2.71 – 2.69 (m, 1 H)	1.66 – 1.60 (m, 3 H)	

^{13}C NMR (126 MHz, CDCl$_3$)

δ 168.1	82.6	40.7	28.3	13.0
149.6	77.4	40.7	27.8	1.2
149.5	63.8	37.0	27.7	
142.9	63.8	37.0	27.2	
142.8	62.9	31.7	25.4	
131.6	62.9	31.7	25.4	
131.4	58.6	31.6	25.0	
122.1	58.6	31.2	25.0	
122.0	56.2	30.7	23.7	
111.2	56.2	30.7	18.8	
111.2	51.9	28.7	18.8	
82.7	51.5	28.6	13.0	

HRMS (ES+) calculated for C$_{27}$H$_{45}$NO$_5$SiNa [M+Na]$^+$: 514.2964, found 514.2961

TLC: R$_f$ = 0.26 (30% v/v ethyl acetate in hexanes)
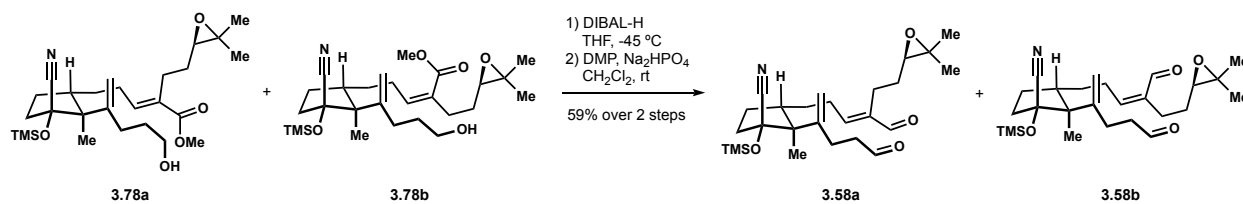
Dialdehydes 3.58a and 3.58b. To a solution of α,β-unsaturated esters **3.78a** and **3.78b** (0.457 g, 0.93 mmol) in THF (0.1 M) at -45 ºC was added DIBAL-H (3.7 mL, 1 M in toluene) over the course of 1 h with a syringe pump. After DIBAL-H addition was complete, the reaction mixture was stirred 2 h and quenched with 1 N aqueous HCl. The heterogeneous mixture was diluted with 1 N aqueous HCl until homogeneous. The layers were separated and the aqueous layer extracted twice with diethyl ether (200 mL combined). The organic layers were combined, washed with H₂O (20 mL), brine (20 mL), dried over anhydrous magnesium sulfate, filtered and concentrated under reduced pressure to afford a crude mixture of diols.

The crude diols **3.79a and 3.79b** were dissolved in CH₂Cl₂ (0.1 M) and to the solution was added dibasic sodium phosphate (0.53 g, 3.7 mmol) followed by Dess–Martin periodinane (1.58 g, 3.7 mmol). The hetereogeneous reaction mixture was stirred vigorously for 3 h and quenched with saturated aqueous NaHCO₃. The layers were separated and the aqueous layer extracted twice with CH₂Cl₂ (200 mL combined). The organic layers were combined and washed twice with 2 N aqueous NaOH (100 mL combined), H₂O (20 mL), brine (20 mL), dried over anhydrous magnesium sulfate, filtered and concentrated under reduced pressure. Purification by flash chromatography (gradient elution: 100% hexanes to 20% v/v ethyl acetate in hexanes) afforded dialdehydes **3.58a** and **3.58b** (0.254 g, 58% yield over two steps) as a colourless oil and inseparable 1:1 mixture of *E* and *Z* alkene isomers.

Dialdehydes **3.58a** and **3.58b**

^{1}H NMR (500 MHz, CDCl$_3$)

δ 10.12, 9.38 (s, 1 H)	2.44 – 2.32 (m, 6 H)	1.28 (s, 3 H)
9.79 (s, 1 H)	2.13 – 2.05 (m, 1 H)	1.23 (s, 3 H)
6.53 – 6.47 (m, 1 H)	1.98 – 1.91 (m, 1 H)	1.01 (s, 3 H)
4.99 – 4.96 (m, 2 H)	1.74 – 1.58 (m, 3 H)	0.22 (s, 9 H)
2.69 – 2.57 (m, 5 H)	1.52 – 1.47 (m, 2 H)	

TLC: R$_f$ = 0.36 (30% v/v ethyl acetate in hexanes)
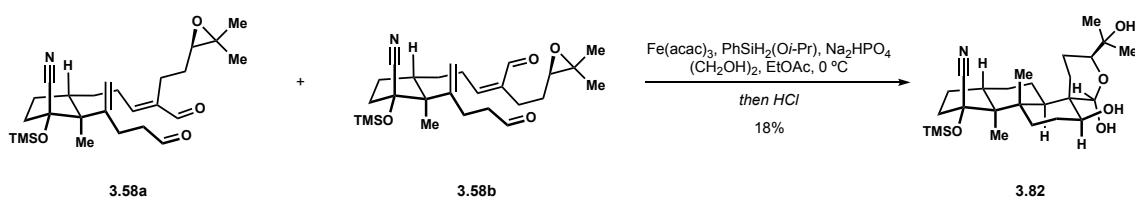
Hemiacetal 3.82. A Schlenk flask was charged with iron(III) acetylacetonate (0.142 g, 0.40 mmol), anhydrous ethylene glycol (55 μL, 0.99 mmol), dibasic sodium phosphate (0.047 g, 0.33 mmol), dialdehydes **3.58a** and **3.58b** (0.152 g, 0.33 mmol) and ethyl acetate (4.0 mL). The mixture was degassed using a freeze-pump-thaw technique (3 cycles) and cooled to 0 ºC. Over 15 min, isopropoxyphenylsilane (0.165 g, 0.99 mmol) in degassed (sparged with argon) ethyl acetate (0.40 mL) were added via syringe pump. Following addition, the reaction mixture was stirred vigorously for 1 h, then quenched with degassed (sparged with argon) 1 N aqueous HCl (5 mL). The layers were separated and the aqueous layer extracted twice with ethylacetate (40 mL combined). The organic layers were combined, washed with 1 N aqueous HCl (10 mL), H$_2$O (10 mL), brine (10 mL), dried over anhydrous sodium sulfate, filtered and concentrated under reduced pressure. Purification by flash chromatography (gradient elution: 100% hexanes to 5% v/v ethyl acetate in hexanes) afforded impure hemiacetal **3.82** (38.7 mg) as an amorphous solid. The impure product was dissolved in boiling hexanes (ca. 2 mL), cooled to room temperature and allowed to slowly

evaporate to approximately one quarter of the volume. The mother liquor was decanted and the precipitated material was dried under vacuum to afford hemiacetal **3.82** (0.028 g, 18% yield) as a white solid. X-ray quality crystals were obtained by suspending the solid in hot CH_2Cl_2 (2 mL) and adding diethyl ether to the boiling solution until the precipitate fully dissolved. The supernatant was filtered through a Kimwipe into a scintillation vial, fitted with a septum pierced with a syringe needle, cooled to room temperature and slowly evaporated overnight.

3.82
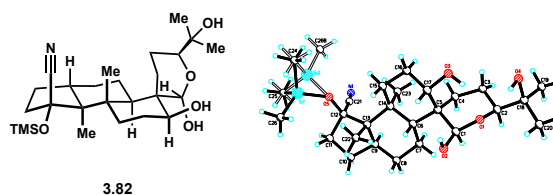
Hemiacetal **3.82**

^{1}H NMR (500 MHz, CDCl$_3$)

δ 4.96 (s, 1 H)	2.33 – 2.24 (m, 3 H)	1.43 (s, 3 H)
4.05 (dd, 1 H, J = 11.5, 3.6 Hz)	2.04 – 1.93 (m, 2 H)	1.36 – 1.22 (m, 3 H)
3.89 (br s, 1 H)	1.89 – 1.86 (m, 1 H)	1.18 (s, 3 H)
3.51 (br s, 1 H)	1.82 – 1.76 (m, 2 H)	1.15 (s, 3 H)
3.43 (dd, 1 H, J = 12.5, 2.8 Hz)	1.68 – 1.62 (m, 5 H)	0.96 (s, 3 H)
2.47 (br s, 1H)	1.54 – 1.48 (m, 2 H)	0.23 (s, 9 H)

TLC: R$_f$ = 0.36 (30% v/v ethyl acetate in hexanes)
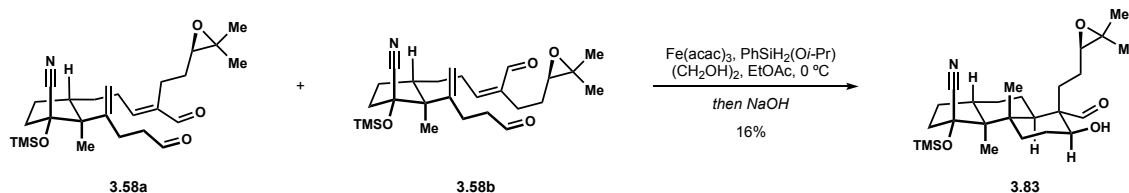
Hydroxyaldehyde 3.83. A Schlenk flask was charged with iron(III) acetylacetonate (72.8 mg, 0.40 mmol), anhydrous ethylene glycol (29 μL, 0.57 mmol), dialdehydes **3.58a** and **3.58b** (79 mg, 0.17 mmol) and ethyl acetate (2.3 mL). The mixture was degassed using a freeze-pump-thaw

technique (3 cycles) and cooled to 0 ºC. Over 1 h, isopropoxyphenylsilane (86 mg, 0.52 mmol) in

degassed (sparged with argon) ethyl acetate (0.80 mL) were added via syringe pump. Following

addition, the reaction mixture was stirred vigorously for 1 h, then quenched with degassed (sparged

with argon) 2 N aqueous NaOH (5 mL). The layers were separated and the aqueous layer extracted

twice with ethyl acetate (40 mL combined). The organic layers were combined, washed with 2 N

aqueous NaOH (10 mL), brine (10 mL), dried over anhydrous sodium sulfate, filtered and

concentrated under reduced pressure. Purification by flash chromatography on Et$_3$N-treated silica

(gradient elution: 100% hexanes to 10% v/v ethyl acetate in hexanes) afforded impure

hydroxyaldehyde **3.83** (12.4 mg, ca. 16% yield) as an amorphous solid. Analytically pure

hydroxyaldehyde **3.83** has yet to be obtained. A ^{1}H NMR spectra is included in the appendix with

diagnostic peaks identified.
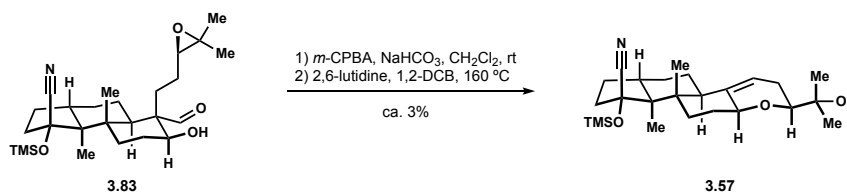
Dihydropyran 3.57. To a solution of aldehyde 3.83 (49 mg, 0.11 mmol) in CH$_2$Cl$_2$ (0.1 M) at

room temperature was added NaHCO$_3$ (84 mg, 1.0 mmol) followed by anhydrous *m*-CPBA (86

mg, 0.5 mmol). The reaction mixture was stirred 2 h and quenched with H$_2$O. The layers were

separated and the aqueous layer extracted twice with CH$_2$Cl$_2$ (20 mL combined). The organic

layers were combined, washed twice with 2 N aqueous NaOH (10 mL combined), brine (10 mL),

dried over anhydrous sodium sulfate, filtered and concentrated under reduced pressure.

The crude formate was transferred to a 1 dram vial with a stir bar and to the vial was added 1,2-dichlorobenzene (0.2 M) and 2,6-lutidine (50 μL, 0.55 mmol). The vial was sealed with a teflon lined cap and heated at 160 ºC with stirring for 18h. The reaction mixture was removed from heat and quenched with 1 N aqueous HCl. The layers were separated and the aqueous layer extracted twice with CH_2Cl_2 (20 mL combined). The organic layers were combined and washed with H_2O (5 mL), brine (5 mL), dried over anhydrous magnesium sulfate, filtered and concentrated under reduced pressure. Purification by flash chromatography (gradient elution: 100% hexanes to 20% v/v ethyl acetate in hexanes) afforded dihydropyran (1.2 mg, ca. 3% yield) as a thin film. Analytically pure dihydropyran **3.57** has yet to be obtained. A ^{1}H NMR spectra is included in the appendix with diagnostic peaks identified.

3.5 References and Notes

1. (a) See Chapter 2. (b) George, D. T.; Kuenstner, E. J., Pronin, S. V. *J. Am. Chem. Soc.* **2015,** *137,* 15410. (c) Godfrey, N. A.; Schatz, D. J.; Pronin, S. V. *J. Am. Chem. Soc.* **2018,** *140,* 12770.

2. (a) Springer, J. P.; Clardy, J.; Wells, J. M.; Cole, R. J.; Kirksey, J. W. *Tetrahedron Lett.* **1975**, *16*, 2531. (b) Knaus, H.-G.; McManus, O. B.; Lee, S. H.; Schmalhofer, W. A.; Garcia-Calvo, M.; Helms, L. M. H.; Sanchez, M.; Giangiacomo, K.; Reuben, J. P.; Smith, A. B., III.; Kaczorowski, G. J.; Garcia, M. L. *Biochemistry*, **1994**, *33*, 5819. (c) Sanchez, M.; McManus, O. B. *Neuropharmacology*, **1996**, *35*, 963.

3. For isolation and structure determination of the penitrems, see: (a) Wilson, B. J.; Wilson, C. H.; Hayes, A. W. *Nature*, **1968**, *220*, 77. (b) De Jesus, A. E.; Steyn, P. S.; Van Heerden, F R.; Vleggaar, R.; Wessels, P. L. *J. Chem. Soc., Chem. Commun.* **1981**, 289. (c) De Jesus, A. E.; Steyn, P. S.; Van Heerden, F R.; Vleggaar, R.; Wessels, P. L. *J. Chem. Soc. Perkin Trans. 1,* **1983**, 1847. (d) De Jesus, A. E.; Steyn, P. S.; Van Heerden, F R.; Vleggaar, R.; Wessels, P. L. *J. Chem. Soc. Perkin Trans. 1,* **1983**, 1857. (e) González, M. C.; Lull, C.; Moya, P.; Ayala, I.; Primo, J.; Yúfera, E. P. *J. Agric. Food. Chem.* **2003**, *51*, 2156.

4. For isolation and structure determination of the lolitrems, see: (a) Gallagher, R. T.; Hawkes, A. D.; Steyn, P. S.; Vleggaar, R. *J. Chem. Soc., Chem. Commun.* **1984**, 614. (b) Miles, C. O.; Munday, S. C.; Wilkins, A. L.; Ede, R. M.; Towers, N. R. *J. Agric. Food Chem.* **1994**, *42*, 1488. (c) Munday-Finch, S. C.; Miles, C. O.; Wilkins, A. L.; Hawkes, A. D. *J. Agric. Food Chem.* **1995**, *43*, 1283. (d) Munday-Finch, S. C.; Wilkins, A. L.; Miles, C. O.; Ede, R. M.; Thomson, R. A. *J. Agric. Food Chem.* **1996**, *44*, 2782.

5. (a) Tagami, K.; Liu, C.; Minami, A.; Noike, M.; Isaka, T.; Fueki, S.; Shichio, Y.; Toshima, H.; Gomi, K.; Dairi, T.; Oikawa, H. *J. Am. Chem. Soc.* **2013**, *135*, 1260. (b) Reddy, P.; Guthridge, K.; Vassiliadis, S.; Hemsworth, J.; Hettiarachchige, I.; Spangenberg, G.; Rochfort, S. *Toxins*, **2019**, *11*, 302.

6. (a) Munday-Finch, S. MC.; Wilkins, A. L.; Miles, C. O. *Phytochemistry*, **1996**, *41*, 327. (b) Saikia, S.; Nicholson, M. J.; Young, C.; Parker, E. J.; Scott, B. *Mycol. Res.* **2008**, *112*, 184.

7. Fan, Y.; Wang, Y.; Liu, P.; Fu, P.; Zhu, T.; Wang, W.; Zhu, W. *J. Nat. Prod.* **2013**, *76*, 1328.

8. Murphy, S. K.; Park, J.-W.; Cruz, F. A.; Dong, V. M. *Science*, **2015**, *347*, 56.

9. Barrero, A. F.; Alvarez-Manzaneda, E. J.; Alvarez-Manzaneda, R.; Chahboun, R.; Meneses, R.; Aparicio B., M. *Synlett.* **1999**, 713.

10. Prein, M.; Adam, W. *Angew. Chem. Int. Ed.* **1996**, *35*, 477.

11. Mihelich, E. D.; Eickhoff, D. J. *J. Org. Chem.* **1983**, *48*, 4135.

12. Stephenson, L. M. *Acc. Chem. Res.* **1980**, *13*, 419.

13. (a) Foote, C. S.; Wexler, S.; Ando, W.; Higgins, R. *J. Am. Chem. Soc.* **1968**, *90*, 975. (b) Carreno, M. C.; Gonzalez-Lopez, M.; Urbano, A. *Angew. Chem., Int. Ed.* **2006**, *45*, 2737−2741. (c) Ghogare, A. A.; Greer, A. *Chem. Rev.* **2016**, *116*, 9994. and references therin.

14. Orfanopoulos, M.; Smonou, I.; Foote, C. S. *J. Am. Chem. Soc.* **1990**, *112*, 3607.

15. Crimmin, M. J.; O'Hanlon, P. J.; Rogers, N. H. *J. Chem. Soc. Perkin Trans. 1,* **1985**, 541.

16. Bassetti, M.; Annibale, A. D.; Fanfoni, A.; Minissi, F. *Org. Lett.* **2005**, *7*, 1805.

17. See experimental section for preparation.

18. Hunter, A. C.; Schlitzer, S. C.; Sharma, I. *Chem. Eur. J.* **2016**, *22*, 16062.

19. Yuan, R.; Zhao, D.; Zhang, L.-Y.; Pan, X.; Yang, Y.; Wang, P.; Li, H.-F.; Da, C.-S. *Org. Biomol. Chem.* **2016**, *14*, 724.

20. Chatterjee, A. K.; Choi, T.-L.; Sanders, D. P.; Grubbs, R. H. *J. Am. Chem. Soc.* **2003**, *125*, 11360.

21. Smith, A. B., III; Kanoh, N.; Ishiyama, H.; Hartz, R. A. *J. Am. Chem. Soc.* **2000**, *122*, 11254.

22. Smith, A. B., III; Ohta, M.; Clark, W. M.; Leahy, J. W. *Tetrahedron Lett.* **1993**, *34*, 3033.

23. Bode, J. W.; Carreira, E. M. *J. Org. Chem.* **2001**, *66*, 6410.

24. (a) Ali, A.; Saxton, J. E. *Tetrahedron Lett.* **1989**, *30*, 3197. (b) Ali, A.; Guile, S. D.; Saxton, J. E.; Thornton-Pett, M. *Tetrahedron*, **1991**, *47*, 6407.

25. Hong, S. H.; Sanders, D. P.; Lee, C. W.; Grubbs, R. H. *J. Am. Chem. Soc.* **2005**, *127*, 17160.

26. (a) Smith, A. B., III; Sunazuka, T.; Leenay, T. L.; Kingery-Wood, J. *J. Am. Chem. Soc.* **1990**, *112*, 8197. (b) Smith, A. B., III; Kingery-Wood, J.; Leenay, T. L.; Nolen, E. G.; Sunazuka, T. *J. Am. Chem. Soc.* **1992**, *114*, 1438.

27. Ketoaldehyde **3.61** was prepared and studied by Dr. David T. George and hemiaminal **3.62** was prepared and studied by Dr. Eric J. Kuenstner.

28. Wang, Z.-X.; Tu, Y.; Frohn, M.; Zhang, J.-R.; Shi, Y. *J. Am. Chem. Soc.* **1997**, *119*, 11224.

29. (a) Sharpless, K. B.; Amberg, W.; Bennani, Y. L.; Crispino, G. A.; Hartung, J.; Jeong, K.-S.; Kwong, H.-L.; Morikawa, K.; Wang, Z.-M.; Xu, D.; Zhang, X.-L. *J. Org. Chem.* **1992**, *57*, 2768. (b) Vanhessche, K. P. M.; Wang, Z.-M.; Sharpless, K. B. *Tetrahedron Lett.* **1994**, *35*, 3469.

30. Nicolaou, K. C.; Adsool, V. A.; Hale, C. R. H. *Org. Lett.* **2010**, *12*, 1552.

31. Kim, D.; Rahaman, S. M. W.; Mercado, B. Q.; Poli, R.; Holland, P. *J. Am. Chem. Soc.* **2019**, *141*, 7473.

32. Obradors, C.; Martinez, R. M.; Shenvi, R. A. *J. Am. Chem. Soc.* **2016**, *138*, 4962.

33. Pearson, A. J.; Chen, Y.-S.; Han, G. R.; Hsu, S.-Y.; Ray, T. *J. Chem. Soc. Perkin Trans. 1,* **1985**, 267.

34. Schwartz, Nelson. N.; Blumbergs, J. H. *J. Org. Chem.* **1964**, *29*, 1976.

35. Zou, Y.; Melvin, J. E.; Gonzales, S. S.; Spafford, M. J.; Smith, A. B., III. *J. Am. Chem. Soc.* **2015**, *137*, 7095.

36. Mulzer, J.; Funk, G. *Synthesis*, **1994** *1994*, 101.

37. Álvarez-Méndez, S. J.; Saad, J. R.; Tonn, C. E.; Martín, V. S.; García, C. *Arabian J. Chem.* **2019**, *12*, 3764.

Chapter 4: Radical-Polar Crossover Annulations

4.1 Introduction

4.1.1 Advent of Reductive Alkene Coupling

The origin of the radical-polar crossover reaction utilized in our lab's syntheses of (±)-eindole SB[1] and (–)-nodulisporic acid C[2] lies within a relatively new, but increasingly rich field of radical and metal hydride chemistry. Beginning with Mukaiyama's hydration[3] utilizing cobalt acetylacetone catalysts and silane reductants, this new branch of metal hydride chemistry has grown rapidly as it enables mild hydrofunctionalization of unactivated alkenes (**4.1**, Scheme 4.1). Intimate mechanistic understanding of the reaction and reactive intermediates has allowed many groups to expand the breadth of hydrofunctionalizations possible.[4] The power of this transformation lies in the ability to generate the nucleophilic alkyl radical intermediate **4.2** in Markovnikov fashion through hydrogen atom transfer (HAT).[5] HAT reactions are complementary to direct protonation of alkenes that would generate high-energy carbocations such as **4.3**. Such intermediates are of course limited to attack by a nucleophile and are also prone to detrimental elimination pathways or hydride and alkyl migrations. The first-row transition metals known to facilitate HAT to alkenes are generally unable to oxidize the radical **4.2**, permitting extended lifetimes of this intermediate which preserves nucleophilic character.

Scheme 4.1 Mechanistic Advantage of HAT
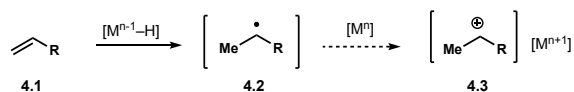
In 2014, Baran and co-workers recognized that iron(III) hydrides chemoselectively reduce electron rich alkenes preferentially to electron deficient ones.[6] This reactivity profile has had profound consequences for exploiting HAT processes in the context of C–C bond forming processes. In his initial report, Baran demonstrated very efficient generation of alkyl radicals

mediated by iron, which then underwent Giese reactions with electron deficient alkenes. The radical process permitted efficient intramolecular conjugate additions to form highly congested systems such as **4.5** (Scheme 4.2a) and the iron(III) hydride chemoselectivity meant only a moderate excess of electron rich alkene was needed for intermolecular coupling as demonstrated in Scheme 4.2b. Baran expanded upon this methodology to include functionalized alkenes, developing umpolung reactions to access oxidation patterns such as the one found in γ-hydroxyketone **4.7** that would be considered challenging by other means (Scheme 4.2c).[7] Notably, three component coupling variants were demonstrated more recently, whereby the resulting enolate radical is reduced and employed in an intermolecular aldol addition to generate β-hydroxy esters such as **4.8**.[8]

Scheme 4.2 Select Examples from Baran's Seminal Reductive Alkene Coupling Reports

a) Access to Congested Systems

b) Intermolecular Coupling

c) Polarity Reversal (Umpolung Reactivity)

d) Three Component Reaction
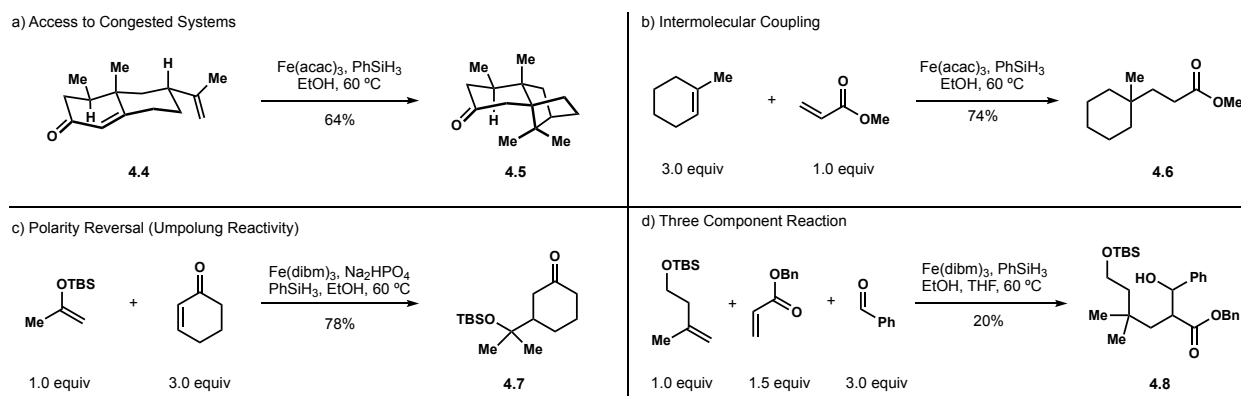
4.1.2 Recent Applications in Total Synthesis

The ability to access nucleophilic, alkyl radicals is a powerful method for constructing otherwise challenging carbon-carbon bond disconnections.[9] While radical reactivity has been exploited for decades in total synthesis,[10] use of metal hydrides to couple alkenes is still in its infancy. Nonetheless, chemists have already begun to recognize powerful disconnections for streamlining syntheses of complex molecules with highly congested cores. Liu and co-workers applied Baran's conditions *en route* to hispidanin A (**4.9**, Scheme 4.3a).[11] Notably, the feat was

accomplished with an impressive polarity inverted polyene cyclization.[12] Selectively engaging the 1,1-disubstituted alkene of **4.10** initiated a conjugate addition cascade that led to production of *trans*-decalin **4.11** in reasonable efficiency. This reaction also illustrates how the enolate radical formed from the initial conjugate addition can be persuaded into performing additional reactions. Li has more recently applied the reductive coupling in the very complex setting that is aplysiasecosterol A (**4.12,** Scheme 4.3b).[13] With enone **4.13** being prepared in a convergent fashion, HAT initiated conjugate addition led to diastereoselective formation of cyclopentane **4.14**, requiring only two additional manipulations to access the natural product. This transformation is remarkable in that it constructs the most stereochemically complex portion of the molecule at the very end of the synthesis and highlights how powerful this chemistry can be.

Scheme 4.3 Application of Reductive Alkene Coupling in Total Synthesis

a) Liu's Polyene Cyclization en route to Hispidanin A
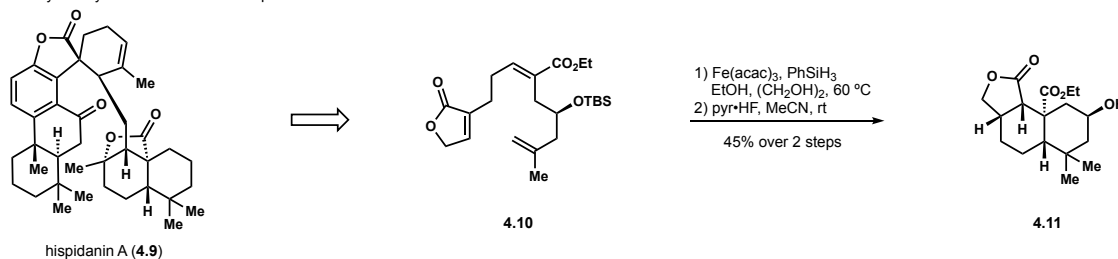
b) Li's Diastereoselective Conjogate Addition for the Synthesis of Aplysiasecosterol A
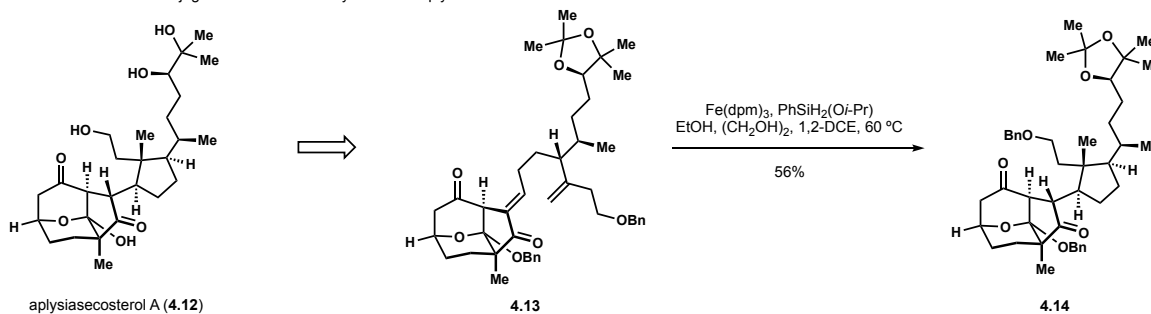
4.2 Development of a Radical-Polar Crossover Annulation

4.2.1 Rational for Developing an Annulative Process

Discussed in detail in Chapter 2, we have capitalized on both the chemoselectivity of iron(III) hydrides and resulting enolate radical.[14] Applying a HAT to dicarbonyl **4.15** initiated the

179

intramolecular conjugate addition and saw the resulting enolate radical reduced and engage the aldehyde in aldol fashion (Scheme 4.4a). This sequence constructed two ring systems with high levels of stereocontrol to provide facile access to *trans*-decalin **4.16**. A logical extension to this methodology was to examine whether an intermolecular variant with simple unsaturated carbonyls **4.17** and **4.18** was feasible (Scheme 4.4b). Doing so held the potential to become a powerful method for annulative assembly of complex molecules.[15] From a more general viewpoint, the method would construct highly functionalized cyclohexanes bearing multiple stereocenters, two of which are quaternary. Furthermore, we recognized the molecular skeletons we hoped to construct would be highly complementary to traditional Diels–Alder disconnections.[16] The requirement for the 1,3-diene to adopt an s-*cis* geometry for concerted cycloaddition to occur severely limits the employment of terminally di-substituted alkenes in Diels–Alder reactions.[17] Thus, generation of quaternary carbons via biomolecular cycloadditions to access connectivity patterns found in **4.19** are rare.[18] Furthermore, the saturated cyclohexanes bearing geminal dimethyl substitution map particularly well onto labdane and scalarane natural products,[19] providing the impetus to develop this chemistry.

Scheme 4.4 Radical-Polar Crossover Cyclizations

a) Intramolecular Polycyclization Applied to Nodulisporic Acid C

b) Unexplored Potential of Radical-Polar Crossover Reactivity
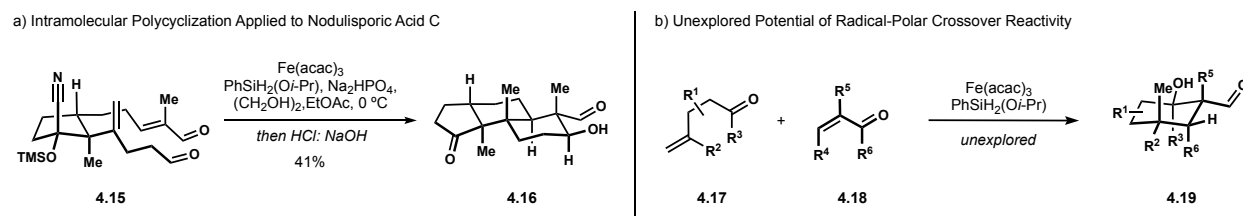
4.2.2 Reaction Optimization

The feasibility of a bimolecular reaction was initially demonstrated by former group member Dr. David T. George on scalereolide derived enal **4.20 (**Scheme 4.5). Subjecting this substrate and methacrolein to conditions used in Baran's reductive alkene coupling provided a

mixture of the desired cyclopentanol **4.21** and a considerable amount of 1,4-reductive aldol side product **4.22**.

Scheme 4.5 Initial Attempt of a Radical-Polar Crossover Annulation

| | **4.20** | | | **4.21** | | | **4.22** |
| | | | | 25% | | | 47%; 3:1 d.r. |
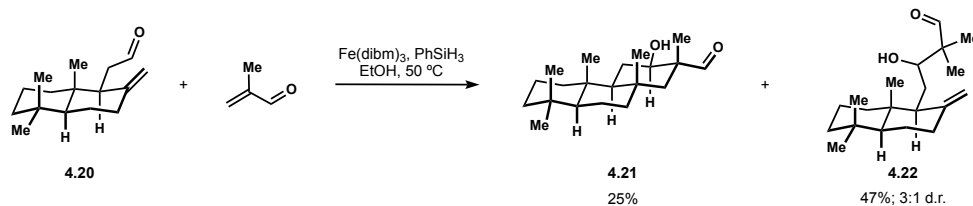
Another colleague, William P. Thomas further developed this reactivity, optimizing the stoichiometry of carbonyls and catalyst loading on a simpler system utilizing γ,δ-unsaturated enal **4.23,** methacrolein and (isopropoxy)phenylsilane.[20] Initially, the yield of cyclohexanol **4.24** was limited to 35%, with a substantial quantity of reductive aldol product **4.25** also being formed. In comparison to the scalerolide derivative **4.20**, the ratio of product distribution was effectively switched to now favour production of the cyclohexanol. From his efforts to further improve on this ratio, W.P.T. discovered that the method of methacrolein and silane addition had a dramatic effect. By changing the rate of addition of silane and methacrolein from a single portion to slow addition as a solution over the course of an hour, formation of the undesired product **4.25** was completely mitigated. Further optimization using this procedure led to an appreciable 60% yield of cyclohexanol **4.24** as a single diastereomer.[21]

Scheme 4.6 Key Developments in Reaction Engineering

	% Yield **4.24**	% Yield **4.25**
single addition of silane:	35%	9%
slow addition of silane:	54%	< 1%

4.23		
2.0 equiv	1.0 equiv	
		4.24	**4.25**
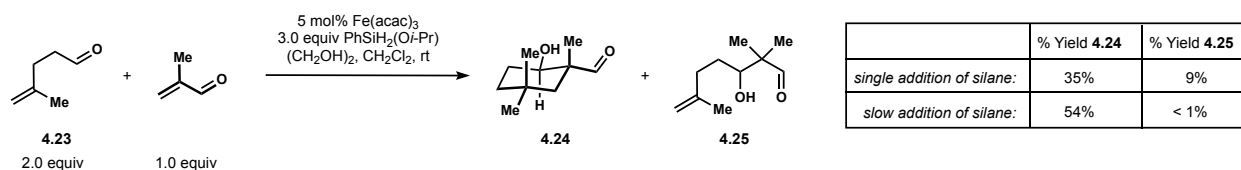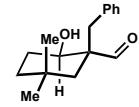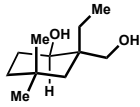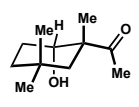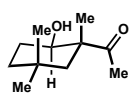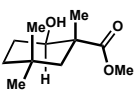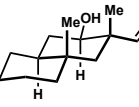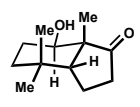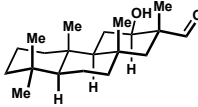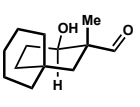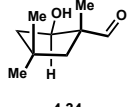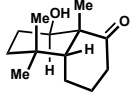
4.2.3 Substrate Scope

Once we were satisfied with the performance of the annulation, we explored additional substrates (Table 4.1a). The α-substitution of the α,β-unsaturated aldehyde proved crucial, as

acrolein could not be employed in the reaction. Other α-substituted acroleins however, did undergo

diastereoselective annulations to provide cyclohexanols **4.26** and **4.27**. When the α,β-unsaturated

aldehyde was replaced with isopropenyl methyl ketone, the diastereoselectivity was completely

lost, presumably due to a mixture of E and Z isomers in the iron enolate intermediate, affording a

mixture of β-hydroxyketones **4.28** and **4.29**. The reaction tolerated more complex γ,δ-unsaturated

aldehydes, permitting diastereoselective formation of decalin **4.30**. 2-methylcyclopen-2-en-1-one

was also receptive to conjugate addition-aldol cascade to afford *cis* hydrindane **4.31** in high

diastereoselectivity and reasonable yield. Application of our newly optimized conditions to the

original system explored by D.T.G. provided a modest improvement to the initial yield of tricyclic

product **4.22**. Other systems such as spirocycle **4.32** were explored with less success. The

methodology is currently limited to α,β-unsaturated aldehydes and ketones, as ester **4.33** was not

observed (Table 4.1b), likely owing to the difference is pKa with the ester being more prone to

quenching with ethylene glycol in solution. Additionally, the formation of cyclopentanol **4.34** was

unsuccessful, as was the attempted annulation with 2-methylcyclohex-2-en-1-one to form decalin

4.35.

Table 4.1 Radical-Polar Crossover Annnulation of *α,β*- and *γ,δ*-Unsaturated Carbonyls

a) Successfully Annulated Substrates[a]

4.26
62%; d.r. >10:1[b,c]

4.27
46%; d.r. >10:1[b,d]

4.28 and **4.29**
54%; d.r. 1.2:1 (**4.28:4.29**)[e]

4.30
58%; d.r. 5.8:1[b,c]

4.31
42%; d.r.>10:1[b]

4.22
37%; d.r.>10:1[b]

4.32
35%; d.r. >10:1[b,f]

b) Current Substrate Limitations

4.33

4.34

4.35

[a]Diastereomeric ratios determined by ^{1}H NMR analysis of crude product mixtures. [b]Yield for analytically pure isomer. [c]Structure confirmed by X-ray crystallographic analysis. [d]Isolated after reduction. [e]Individual isomers isolated and characterized. [f]NMR yield using mesitylene as an internal standard.

We next looked to expand further upon the carbonyl species we could employ. When γ,δ-unsaturated ketone **4.36** was first subjected to the standard conditions, a significant amount of what appeared to be ketoaldehyde **4.37** was present along with desired cyclohexanol **4.38** (Table 4.2a). By lowering the equivalents of ethylene glycol in the reaction from three to one, the uncyclized product was fully converted into **4.38**, which could be isolated in high yield as silyl ether **4.39** (Table 4.1b). Derivatization of **4.38** and other tertiary alcohol products proved necessary to avoid decomposition through retro-aldol pathways during isolation. We revisited the parent system from Scheme 4.6 and lowered the equivalents of glycol to one, only to find trace product formation. This remains a difficult result to rationalize, but it certainly appears that the intermediate enolate and its ability to undergo aldol addition is quite sensitive to the protic solvent. The ethylene glycol modification did translate successfully to the ethyl and *n*-propyl derivatives **4.40** and **4.41** in reasonable yield, but diminished further for the phenyl derivative **4.42**, which began to show the uncyclized ketoaldehyde once again. The fact that the reaction does not suffer from retro-aldol pathways highlight how mild the conditions are. To further test the limits of enolate reactivity, we briefly examined α,β-unsaturated carbonyls bearing leaving groups at the saturated β-position. Incredibly, silyl ether **4.43**, acetate **4.44** and thioether **4.45** were all successfully formed. While the yield of each product was modest, the success of the aldol addition may have profound mechanistic implications.[8,22] It is generally believed that the enolate radical is reduced prior to aldol addition. If this were the case, one would expect facile elimination of β-leaving groups, especially an acetate. While we have not thoroughly analyzed the product mixture to confirm this has not occurred, the products of aldol addition suggest the reduction may occur after the C–C bond formation.

Table 4.2 Annulations of γ,δ-Unsaturated Ketones and Functionalized Methacroleins

a) Reaction Optimization for γ,δ-Unsaturated Ketones

	4.37	**4.38**
3 equiv. (CH₂OH):	28%	41%
1 equiv. (CH₂OH):	0%	75%
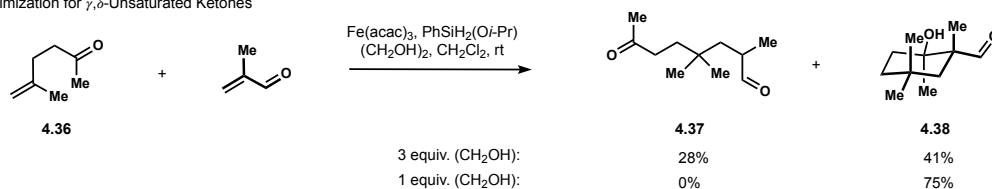
b) Annulations Derivatives Prone to Decomposition

4.39	**4.40**	**4.41**	**4.42**	**4.43**	**4.44**	**4.45**
72%; d.r. >10:1[a, b]	52%; d.r.>10:1[a,c]	40%; d.r.>10:1[a,d]	35%; d.r.>10:1[a,d]	45%; d.r. 4.1:1[a,e]	26%[a,d]	28%; d.r. >10:1[a,d]
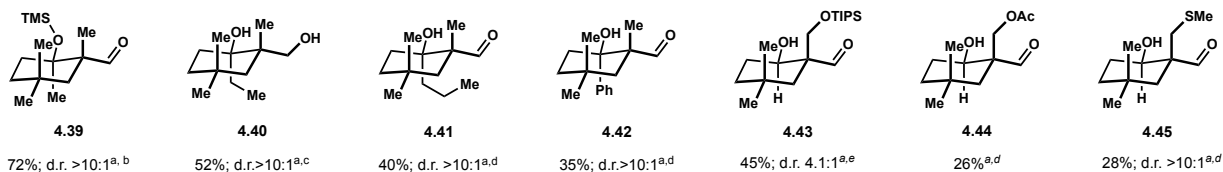
[a]Diastereomeric ratios determined by ¹H NMR analysis of crude product mixtures. [b]Isolated after TMS protection. [c]Isolated after reduction. [d]NMR yield using mesitylene as an internal standard. [e]Isolated as a mixture of diastereomers.

4.2.4 Application Towards a Total Synthesis of Forskolin

With a functioning method at hand, we looked to apply the annulation in the context of a total synthesis. As previously alluded to, the scaffolds we can construct map particularly well onto labdane diterpenes.[23] Thus, W.P.T. embarked on a synthesis of forskolin[24] (**4.46**, Scheme 4.7). Utilizing the parent γ,δ-unsaturated aldehyde **4.23**, annulation with enone **4.47** proceeded with high efficiency. Unfortunately, a near stoichiometric mixture of hydroxyl ketones **4.48** and **4.49** are produced. Though **4.47** can be quickly converted into the desired epimer **4.48**. Furthermore, enone **4.47** can be prepared asymmetrically through use of Corey's oxazaborolidine catalyst[25] system. Taken together, forskolin (**4.46**) was prepared in an expedient 14 step process.[26]

Scheme 4.7 Application of the Radical-Polar Crossover Annulation Towards Forskolin
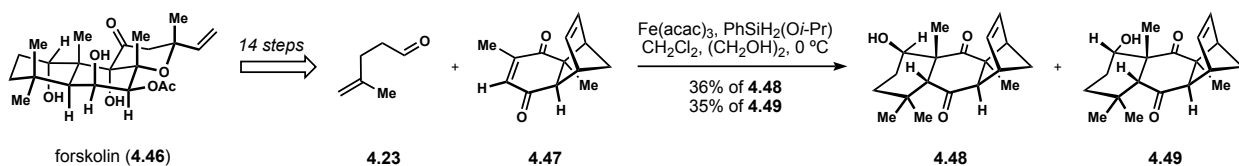
4.2.5 Conclusions and Outlook

In summary, we developed a new annulation method to access decorated cyclohexanols with high levels of stereocontrol. The reaction provides an alternative to the Diels-Alder cycloaddition to access such motifs. The utility of this method was demonstrated by W.P.T. with a successful total synthesis of the labdane diterpene forskolin. Efforts to apply this chemistry to complex targets requiring more elaborate unsaturated carbonyl precursors are underway within our lab.

4.3 Experimental Section

4.3.1 General Experimental Details

All reactions were carried out in flame-dried glassware under positive pressure of dry nitrogen unless otherwise noted. Reaction solvents (Fisher, HPLC grade) including tetrahydrofuran (THF), diethyl ether (Et$_2$O), dichloromethane (CH$_2$Cl$_2$), and toluene (PhMe) were dried by percolation through a column packed with neutral alumina and a column packed with a supported copper catalyst for scavenging oxygen (Q5) under positive pressure of argon. Methyl *tert*-butyl ether (MTBE, Millipore Sigma, ACS grade) was distilled from sodium diphenylketyl under positive pressure of nitrogen. Anhydrous 1,2-dichloroethane (DCE, Fisher, ACS Grade) and anhydrous triethylamine (Et$_3$N, Oakwood Chemical) were distilled from calcium hydride (10% w/v) under positive pressure of nitrogen. Anhydrous hexamethylphosphoramide (HMPA, Oakwood Chemical) was distilled from calcium hydride (10% w/v) under vacuum (*ca*. 0.1 torr). Solvents for extraction, thin layer chromatography (TLC), and flash column chromatography were purchased from Fischer (ACS Grade) and VWR (ACS Grade) and used without further purification. Chloroform-d, benzene-d$_6$, acetone-d$_6$ and methanol-d$_4$ for ^{1}H and ^{13}C NMR analysis were purchased from Cambridge Isotope Laboratories and used without further purification. Commercially available reagents were used without further purification unless otherwise noted. Reactions were monitored by thin layer chromatography (TLC) using precoated silica gel plates (EMD Chemicals, Silica gel 60 F$_{254}$). Flash column chromatography was performed over silica gel (Acros Organics, 60 Å, particle size 0.04-0.063 mm). GC/FID analysis was performed on Agilent 7820A system with helium as carrier gas. HPLC analysis was performed on an Agilent 1100 series. Optical rotation readings were obtained using JASCO P-1010 polarimeter. ^{1}H NMR and ^{13}C NMR spectra were recorded on Bruker DRX-500 (BBO probe), Bruker DRX-500 (TCI cryoprobe),

Bruker AVANCE600 (TBI probe), and Bruker AVANCE600 (BBFO cryoprobe) spectrometers using residual solvent peaks as internal standards (CHCl$_3$ @ 7.26 ppm ^{1}H NMR, 77.16 ppm ^{13}C NMR; C$_6$H$_6$ @ 7.16 ppm ^{1}H NMR, 128.00 ppm ^{13}C NMR; MeOH @ 3.31 ppm ^{1}H NMR, 49.00 ppm ^{13}C NMR; (CH$_3$)$_2$CO @ 2.05 ppm ^{1}H NMR, 29.84 ppm ^{13}C NMR). High-resolution mass spectra (HRMS) were recorded on Waters LCT Premier TOF spectrometer with ESI and CI sources.

4.3.2 Experimental Procedures
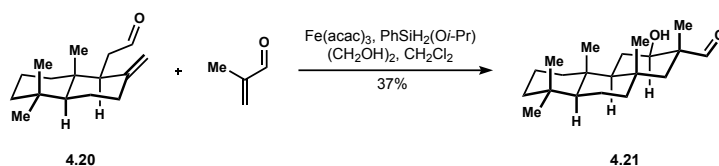
Perhydrophenanthrene 4.21. A Schlenk flask was charged with iron(III) acetylacetonate (3.5 mg, 0.01 mmol), anhydrous ethylene glycol (34 μL, 0.6 mmol), γ,δ-unsaturated aldehyde **4.20**[27] (93.8 mg, 0.4 mmol) and 1,2-dichloroethane (0.40 mL). The mixture was degassed using a freeze-pump-thaw technique (3 cycles). Over 1 h, methacrolein (17 μL, 97% pure, 0.2 mmol) and isopropoxyphenylsilane (100 mg, 0.6 mmol) in degassed (sparged with argon) 1,2-dichloroethane (0.20 mL) were added via syringe pump. Following addition, the reaction mixture was stirred vigorously for 1 h, then quenched with degassed (sparged with argon) 1 N aqueous HCl (2 mL). The layers were separated and the aqueous layer extracted twice with CH$_2$Cl$_2$ (20 mL combined). The organic layers were combined, washed with 1 N aqueous HCl (10 mL), H$_2$O (10 mL), brine (10 mL), dried over anhydrous sodium sulfate, filtered and concentrated under reduced pressure. Purification by flash chromatography (gradient elution: 100% hexanes to 5% v/v ethyl acetate in hexanes) afforded perhydrophenanthrene **4.21** (22.6 mg, 37% yield) as a white solid.

Perhydrophenanthrene **4.21**

^{1}H NMR (500 MHz, C$_6$D$_6$)

δ 9.28 (s, 1 H)	1.25 – 1.09 (m, 7 H)	0.78 (s, 3 H)
3.60 (dd, 1 H, J = 11.1, 3.4 Hz)	0.95 (d, 1 H, J = 13.4 Hz)	0.68 (s, 3 H)
1.59 – 1.48 (m, 3 H)	0.86 (s, 3 H)	0.61 – 0.59 (m, 2 H)
1.40 – 1.32 (m, 5 H)	0.79 (s, 3 H)	0.50 (d, 2 H, J = 12.5 Hz)

^{13}C NMR (126 MHz, C$_6$D$_6$)

δ 205.0	49.1	34.9	21.5
73.4	43.4	33.5	18.9
56.6	42.5	33.4	18.4
56.4	39.8	26.4	16.2
51.5	37.3	23.0	14.6

HRMS (ES+) calculated for C$_{20}$H$_{34}$O$_2$Na [M+Na]$^+$: 329.2456, found 329.2457

TLC: R$_f$ = 0.28 (20% v/v ethyl acetate in hexanes)
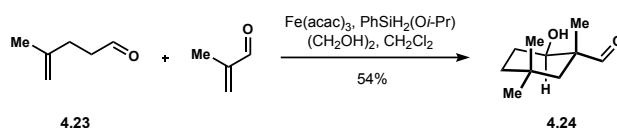
Cyclohexanol 4.24. A Schlenk flask was charged with iron(III) acetylacetonate (3.5 mg, 0.01 mmol), anhydrous ethylene glycol (34 μL, 0.6 mmol), γ,δ-unsaturated aldehyde **4.23**[28] (39.3 mg, 0.4 mmol) and CH$_2$Cl$_2$ (0.80 mL). The mixture was degassed using a freeze-pump-thaw technique (3 cycles). Over 1 h, methacrolein (17 μL, 97% pure, 0.2 mmol) and isopropoxyphenylsilane (100 mg, 0.6 mmol) in degassed (sparged with argon) CH$_2$Cl$_2$ (0.40 mL) were added via syringe pump. Following addition, the reaction mixture was stirred vigorously for 1 h, then quenched with degassed (sparged with argon) 1 N aqueous HCl (2 mL). The layers were separated and the aqueous layer extracted twice with CH$_2$Cl$_2$ (20 mL combined). The organic layers were combined, washed with 1 N aqueous HCl (10 mL), H$_2$O (10 mL), brine (10 mL), dried over anhydrous sodium

sulfate, filtered and concentrated under reduced pressure. Purification by flash chromatography (gradient elution: 100% hexanes to 5% v/v ethyl acetate in hexanes) afforded cyclohexanol **4.24** (18.5 mg, 54% yield) as a colorless oil.

Cyclohexanol **4.24**

^{1}H NMR (500 MHz, CDCl$_3$)

δ 9.44 (s, 1 H)	1.57 (br s, 1 H)	1.10 (s, 3 H)
4.00 (dd, 1 H, J = 10.2, 3.5 Hz)	1.46 (s, 1 H)	0.99 (s, 3 H)
1.80 – 1.74 (m, 1 H)	1.44 (s, 1 H)	0.85 (s, 3 H)
1.70 – 1.63 (m, 1 H)	1.23 – 1.18 (m, 1 H)	

^{13}C NMR (126 MHz, CDCl$_3$)

δ 205.9	31.0
69.6	30.7
50.9	29.2
43.1	27.0
34.2	17.8

HRMS CI calculated for C$_{10}$H$_{18}$O$_2$NH$_4$ [M+NH$_4$]$^+$: 188.1651, found 188.1652

TLC: R$_f$ = 0.32 (20% v/v ethyl acetate in hexanes)
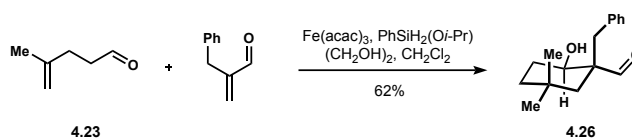
Cyclohexanol 4.26. A Schlenk flask was charged with iron(III) acetylacetonate (3.5 mg, 0.01 mmol), anhydrous ethylene glycol (34 μL, 0.6 mmol), γ,δ-unsaturated aldehyde **4.23**[28] (39.3 mg, 0.4 mmol) and CH$_2$Cl$_2$ (0.80 mL). The mixture was degassed using a freeze-pump-thaw technique (3 cycles). Over 1 h, α-methylene-benzenepropanal[29] (29.2 mg, 0.2 mmol) and isopropoxyphenylsilane (100 mg, 0.6 mmol) in degassed (sparged with argon) CH$_2$Cl$_2$ (0.40 mL)

were added via syringe pump. Following addition, the reaction mixture was stirred vigorously for 1 h, then quenched with degassed (sparged with argon) 1 N aqueous HCl (2 mL). The layers were separated and the aqueous layer extracted twice with CH$_2$Cl$_2$ (20 mL combined). The organic layers were combined, washed with 1 N aqueous HCl (10 mL), H$_2$O (10 mL), brine (10 mL), dried over anhydrous sodium sulfate, filtered and concentrated under reduced pressure. Purification by flash chromatography (gradient elution: 100% hexanes to 5% v/v ethyl acetate in hexanes) provided impure cyclohexanol **4.26**, which was recrystallized by dissolving in boiling hexanes (1.5 mL) and slowly cooling to 0 ºC. The supernatant was decanted to afford pure cyclohexanol **4.26** (30.1 mg, 62% yield) as a white solid.

Cyclohexanol **4.26**
^{1}H NMR (500 MHz, CDCl$_3$)

δ 9.52 (s, 1 H)	2.99 (d, 1 H, J = 13.7 Hz)	1.43 (br s, 1 H)
7.27 – 7.24 (m, 2 H)	2.78 (d, 1 H, J = 13.7 Hz)	1.18 – 1.14 (m, 1 H)
7.22 – 7.18 (m, 1 H)	1.81 – 1.74 (m, 1 H)	1.00 (s, 3 H)
7.16 – 7.14 (m, 2 H)	1.67 (s, 2 H)	0.77 (s, 3 H)
4.02 (app t, 1 H, J = 2.5 Hz)	1.62 – 1.55 (m, 2 H)	

^{13}C NMR (126 MHz, CDCl$_3$)

δ 206.6	65.8	32.0
135.8	55.1	31.0
130.6	42.3	27.1
128.3	41.1	26.1
126.8	33.6	

HRMS (ES+) calculated for C$_{16}$H$_{22}$O$_2$Na [M+Na]$^+$: 269.1518, found 269.1519
TLC: R$_f$ = 0.37 (20% v/v ethyl acetate in hexanes)

Cyclohexanol **4.26** was crystallized by dissolving in distilled hexanes in a dram vial fitted with a septum and allowing slow evaporation of the solvent. Crystallographic analysis revealed that the product was oxidized by air to form the carboxylic acid **S4.1**.

S4.1

4.23   **4.27**
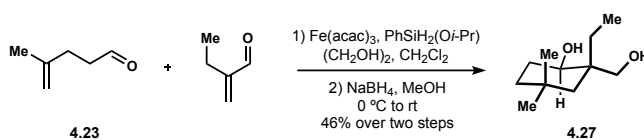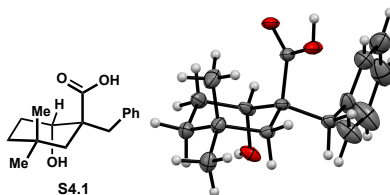
Diol 4.27. A Schlenk flask was charged with iron(III) acetylacetonate (3.5 mg, 0.01 mmol), anhydrous ethylene glycol (34 μL, 0.6 mmol), γ,δ-unsaturated aldehyde **4.23**[28] (39.3 mg, 0.4 mmol) and CH_2Cl_2 (0.80 mL). The mixture was degassed using a freeze-pump-thaw technique (3 cycles). Over 1 h, 2-ethylacrolein (20 μL, 90% pure, 0.2 mmol) and isopropoxyphenylsilane (100 mg, 0.6 mmol) in degassed (sparged with argon) CH_2Cl_2 (0.40 mL) were added via syringe pump. Following addition, the reaction mixture was stirred vigorously for 1 h, then quenched with degassed (sparged with argon) 1 N aqueous HCl (2 mL). The layers were separated and the aqueous layer extracted twice with CH_2Cl_2 (20 mL combined). The organic layers were combined, washed with 1 N aqueous HCl (10 mL), H_2O (10 mL), brine (10 mL), dried over anhydrous sodium sulfate, filtered and concentrated under reduced pressure.

The crude mixture was then dissolved in 2.0 mL of MeOH and cooled to 0 °C before adding $NaBH_4$ (38 mg, 1.0 mmol). The reaction mixture was warmed to room temperature over 30 min and quenched with 1 N aqueous HCl (5 mL). The layers were separated and the aqueous layer extracted twice with Et_2O (20 mL combined). The organic layers were combined, washed with H_2O (10 mL),

brine (10 mL), dried over anhydrous sodium sulfate, filtered and concentrated under reduced pressure. The crude was again dissolved in Et$_2$O (2.0 mL) and treated with 49% aqueous HF (0.10 mL) for 15 minutes then quenched with a slurry of CaCO$_3$ and diluted with H$_2$O (10 mL). The layers were separated and the aqueous layer extracted twice with Et$_2$O (20 mL combined). The organic layers were combined, washed with H$_2$O (10 mL), brine (10 mL), dried over anhydrous sodium sulfate, filtered and concentrated under reduced pressure. Purification by flash chromatography (gradient elution: 100% hexanes to 20% v/v ethyl acetate in hexanes) afforded 20.6 mg of a mixture of the desired diol and the reductive aldol side product. Diol **4.27** was recrystallized by dissolving in boiling hexanes (1.5 mL) and slowly cooling to 0 ºC. The supernatant was decanted to afford pure diol **4.27** (17.0 mg, 46% yield over two steps) as a white solid.

Diol **4.27**

^{1}H NMR (500 MHz, CDCl$_3$)

δ 3.64 (dd, 1 H, J = 11.5, 4.1 Hz)	1.42 (dq, 1 H, J = 13.4, 3.1 Hz)
3.54 (d, 1 H, J = 10.6 Hz)	1.34 (dd, 1 H, J = 14.4, 2.5 Hz)
3.25 (d, 1 H, J = 10.5 Hz)	1.25 – 1.19 (m, 1 H)
2.90 – 2.59 (br m, 2 H)	1.03 (s, 3H)
1.87 – 1.80 (m, 1 H)	0.90 – 0.87 (m, 6 H)
1.74 – 1.66 (m, 1 H)	0.60 (d, 1 H, J = 14.3 Hz)
1.63 – 1.53 (m, 2 H)	

^{13}C NMR (126 MHz, CDCl$_3$)

δ 80.2	38.0	26.9
71.9	34.7	17.5
41.7	30.5	7.6
40.0	27.4	

HRMS (ES+) calculated for C$_{11}$H$_{22}$O$_2$Na [M+Na]$^+$: 209.1517, found 209.1519

TLC: $R_f = 0.50$ (50% v/v ethyl acetate in hexanes)
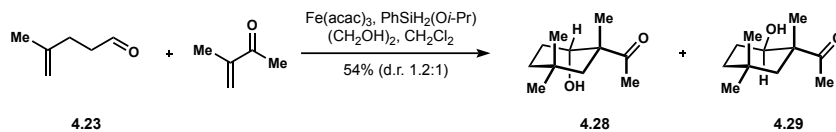
Hydroxyketones 4.28 and 4.29. A Schlenk flask was charged with iron(III) acetylacetonate (7.1 mg, 0.02 mmol), anhydrous ethylene glycol (34 μL, 0.6 mmol), γ,δ-unsaturated aldehyde **4.23**[28] (39.3 mg, 0.4 mmol) and CH_2Cl_2 (0.80 mL). The mixture was degassed using a freeze-pump-thaw technique (3 cycles). Over 1 h, 3-methyl-3-buten-2-one (20.5 μL, 95% pure, 0.2 mmol) and isopropoxyphenylsilane (100 mg, 0.6 mmol) in degassed (sparged with argon) CH_2Cl_2 (0.40 mL) were added via syringe pump. Following addition, the reaction mixture was stirred vigorously for 1 h, then quenched with degassed (sparged with argon) 1 N aqueous HCl (2 mL). The layers were separated and the aqueous layer extracted twice with CH_2Cl_2 (20 mL combined). The organic layers were combined, washed with 1 N aqueous HCl (10 mL), H_2O (10 mL), brine (10 mL), dried over anhydrous sodium sulfate, filtered and concentrated under reduced pressure. Purification by flash chromatography (gradient elution: 100% hexanes to 5% v/v ethyl acetate in hexanes) afforded hydroxyketone **4.28** (10.9 mg, 30% yield) and **4.29** (8.7 mg, 24% yield) as colorless oils.

4.28
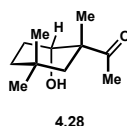
Hydroxyketone **4.28**
^{1}H NMR (500 MHz, CDCl$_3$)

δ 3.54 (d, 1 H, $J = 11.1$ Hz)	1.79 –1.74 (m, 1 H)
3.17 (td, 1 H, $J = 11.3, 4.3$ Hz)	1.46 (dq, 1 H, $J = 13.5, 3.5$ Hz)
2.16 (s, 3 H)	1.31 – 1.27 (m, 5 H)
1.98 (dd, 1 H, $J = 14.6, 2.8$ Hz)	0.92 (s, 3 H)
1.92 – 1.84 (m, 1 H)	0.84 (s, 3 H)

^{13}C NMR (126 MHz, CDCl$_3$)

δ 217.8	38.7	26.2
78.6	32.8	25.7
52.0	31.7	25.6
49.4	28.9	

HRMS (ES+) calculated for C$_{11}$H$_{20}$O$_2$Na [M+Na]$^+$: 207.1361, found 207.1360

TLC: R$_f$ = 0.41 (20% v/v ethyl acetate in hexanes)
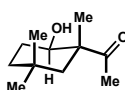
4.29

Hydroxyketone **4.29**

^{1}H NMR (500 MHz, CDCl$_3$)

δ 3.99 (dd, 1 H, J = 9.7, 3.9 Hz)	1.50 – 1.45 (m, 1 H)
2.13 (s, 3 H)	1.38 (d, 1 H, J = 13.9 Hz)
1.77 – 1.72 (m, 1 H)	1.23 – 1.19 (m, 4 H)
1.67 – 1.62 (m, 1 H)	1.03 (s, 3 H)
1.58 (dd, 1 H, J = 13.8, 1.9 Hz)	0.88 (s, 3 H)

^{13}C NMR (126 MHz, CDCl$_3$)

δ 215.3	36.4	26.4
71.6	32.2	24.9
52.5	31.5	18.5
45.4	29.2	

HRMS (ES+) calculated for C$_{11}$H$_{20}$O$_2$Na [M+Na]$^+$: 207.1361, found 207.1367

TLC: R$_f$ = 0.29 (20% v/v ethyl acetate in hexanes)

Diastereomers **4.28** and **4.29** were assigned based on nOe correlations.

4.28
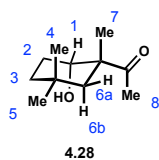
^{1}H (arbitrary numbering)	Key correlations	Absent Correlations
H1 (3.17 ppm)	H7 (1.27 ppm)	H6b (1.36 ppm)
H6a (1.98 ppm)	H4 (0.92 ppm)	
	H5 (0.84 ppm)	
	H6b (1.27 – 1.23 ppm)	
	H7 (1.27 ppm)	
	H8 (2.16 ppm)	

4.29
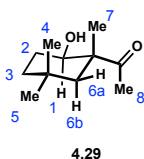
^{1}H (arbitrary numbering)	Key correlations	Absent Correlations
H1 (3.99 ppm)	H6b (1.38 ppm)	H7 (1.23 ppm)
H6a (1.58 ppm)	H4 (1.03 ppm)	
	H5 (0.88 ppm)	
	H7 (1.23 ppm)	
	H8 (2.13 ppm)	
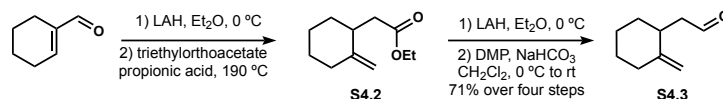
γ,δ-unsaturated aldehyde S4.3. A 50 mL round bottom flask was charged with lithium aluminum hydride (86.0 mg, 2.27 mmol) and diethyl ether (10 mL). The suspension was cooled 0 °C and 1-cyclohexene-1-carboxaldehdye (0.40 mL, 3.50 mmol) was added in diethyl ether (5 mL) over 10 min. The flask was warmed to room temperature. After 2.5 h the flask was cooled to 0 °C and water (0.08 mL), MeOH (0.16 mL), and water (0.24 mL) were added sequentially. The solution was stirred for 15 min at room temperature and filtered. The filtrate was dried over anhydrous sodium sulfate, filtered and concentrated under reduced pressure. A 30 mL microwave vial was

charged with the crude alcohol, triethylorthoacetate (9.0 mL, 49 mmol) and propionic acid (13 μL, 0.18 mmol). The vial was sealed and brought to 190 °C for 5 min. The flask was cooled to room temperature and diluted with diethyl ether (10 mL) and washed with 1 N aqueous HCl (5 mL). The aqueous layer was extracted twice with diethyl ether (20 mL combined). The organic layers were combined and washed with saturated aqueous $NaHCO_3$ (5 mL). The organic layer was dried over anhydrous magnesium sulfate, filtered and concentrated under reduced pressure. Purification by flash chromatography (elution with 2% v/v diethyl ether in pentane) afforded γ,δ-unsaturated ester **S4.2**. ^{1}H and ^{13}C NMR data match that provided in the literature.[30]

γ,δ-unsaturated ester **S4.2** was dissolved in diethyl ether (5 mL) and added to a suspension of lithium aluminum hydride (0.21 g, 5.7 mmol) in diethyl ether (15 mL) at 0 °C. The reaction mixture was then warmed to room temperature. After 1 h the flask was cooled to 0 °C and water (0.2 mL), MeOH (0.4 mL), and water (0.6 mL) were added sequentially. The solution was stirred for 15 min at room temperature and filtered. The filtrate was dried over anhydrous sodium sulfate. Then filtered and concentrated under reduced pressure. A solution of the crude alcohol in CH_2Cl_2 (5 mL) was added to a suspension of Dess–Martin periodinane (1.91 g, 4.50 mmol) in CH_2Cl_2 (25 mL) at 0 °C and then warmed to room temperature. After 1.5 h Dess–Martin periodinane (0.50 g, 1.1 mmol) and $NaHCO_3$ (0.75 g, 8.9 mmol) were added. After 1 h the mixture was concentrated under reduced pressure and diluted with diethyl ether (20 mL). The organic layer was washed with saturated aqueous $NaHCO_3$ (5 mL), saturated aqueous sodium thiosulfate (5 mL), and water (5 mL). The layers were separated and the aqueous layer was extracted twice with diethyl ether (20 mL combined). The organic layers were combined and washed with brine (5 mL), dried over anhydrous magnesium sulfate, filtered and concentrated under reduced pressure. Purification by

flash chromatography (elution with 5% v/v diethyl ether in pentane) afforded γ,δ-unsaturated aldehyde **S4.3** as a colorless oil (0.36 g, 71% over four steps). ^{1}H NMR data matched that provided in the literature.[31]
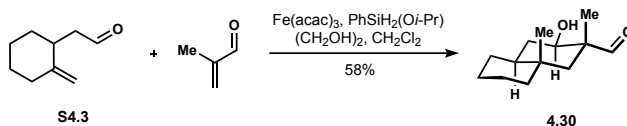
Decalin 4.30. A Schlenk flask was charged with iron(III) acetylacetonate (7.1 mg, 0.02 mmol), anhydrous ethylene glycol (34 μL, 0.6 mmol), γ,δ-unsaturated aldehyde **S4.3** (55.3 mg, 0.4 mmol) and CH_2Cl_2 (0.80 mL). The mixture was degassed using a freeze-pump-thaw technique (3 cycles). Over 1 h, methacrolein (17 μL, 97% pure, 0.2 mmol) and isopropoxyphenylsilane (100 mg, 0.6 mmol) in degassed (sparged with argon) CH_2Cl_2 (0.40 mL) were added via syringe pump. Following addition, the reaction mixture was stirred vigorously for 1 h, then quenched with degassed (sparged with argon) 1 N aqueous HCl (2 mL). The layers were separated and the aqueous layer extracted twice with CH_2Cl_2 (20 mL combined). The organic layers were combined, washed with 1 N aqueous HCl (10 mL), H_2O (10 mL), brine (10 mL), dried over anhydrous sodium sulfate, filtered and concentrated under reduced pressure. Purification by flash chromatography (gradient elution: 100% hexanes to 5% v/v ethyl acetate in hexanes) afforded decalin **4.30** (24.4 mg, 58% yield) as a colorless oil.

Decalin **4.30**
^{1}H NMR (500 MHz, CDCl$_3$)

δ 9.41 (s, 1 H)	1.56 – 1.44 (m, 6 H)	1.02 – 0.98 (m, 1 H)
3.95 – 3.92 (m, 1 H)	1.36 (d, 1 H, J = 13.8 Hz)	0.97 (s, 3 H)
1.73 – 1.70 (m, 2 H)	1.23, 1.13 (m, 7 H)	

¹³C NMR (126 MHz, CDCl₃)

^{13}C NMR (126 MHz, CDCl$_3$)

δ 206.1	41.3	21.3
72.3	34.1	18.3
51.7	33.5	14.9
46.2	28.0	
44.5	26.6	

HRMS (ES+) calculated for C$_{13}$H$_{22}$O$_2$Na [M+Na]$^+$: 233.1517, found 233.1528

TLC: R$_f$ = 0.26 (20% v/v ethyl acetate in hexanes)

Decalin **4.30** was crystallized by dissolving the compound in a 10:1 v/v mixture of CH$_2$Cl$_2$:diethyl ether in a dram vial fitted with a septum and allowing slow evaporation of the solvent. Crystallographic analysis revealed that the product had dimerized to form the acetal **S4.4**.
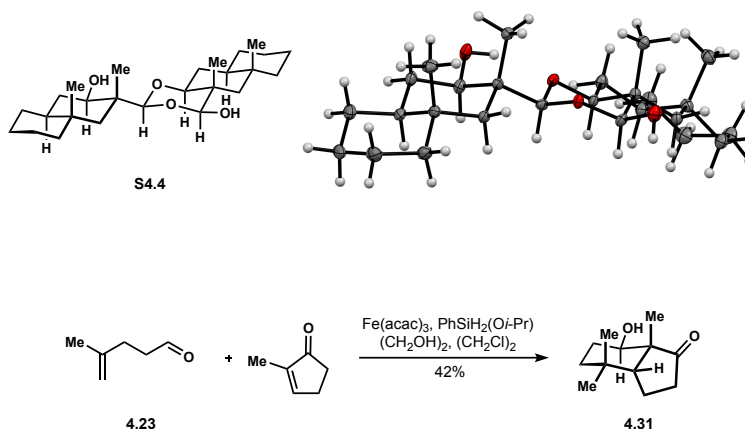
Hexahydroindanone 4.31. A Schlenk flask was charged with iron(III) acetylacetonate (35 mg, 0.1 mmol), anhydrous ethylene glycol (34 μL, 0.15 mmol), γ,δ-unsaturated aldehyde **4.23**[28] (39.3 mg, 0.4 mmol), 2-methyl-2-cyclopentenone (20 μL, 0.2 mmol) and 1,2-dichloroethane (0.40 mL). The mixture was degassed using a freeze-pump-thaw technique (3 cycles). Over 1 h, isopropoxyphenylsilane (100 mg, 0.6 mmol) in degassed (sparged with argon) 1,2-dichloroethane (0.20 mL) were added via syringe pump. Following addition, the reaction mixture was stirred vigorously for 18 h, then quenched with dropwise addition of 49% aqueous HF (0.10 mL) and

diluted with H_2O (10 mL). The layers were separated and the aqueous layer extracted twice with CH_2Cl_2 (20 mL combined). The organic layers were combined, washed with H_2O (10 mL), brine (10 mL), dried over anhydrous sodium sulfate, filtered and concentrated under reduced pressure. Purification by flash chromatography (gradient elution: 100% hexanes to 5% v/v ethyl acetate in hexanes) afforded 19.6 mg of impure product. A second column (gradient elution: 100% CH_2Cl_2 to 1% v/v acetone in CH_2Cl_2) yielded pure hexahydroindanone **4.31** (16.9 mg, 43% yield) as a colorless oil. ^1H and ^{13}C NMR data match that provided in the literature.[32]

Hexahydroindanone **4.31**
^1H NMR (500 MHz, $CDCl_3$)

δ 3.53 – 3.50 (m, 1 H)	1.73 – 1.64 (m, 3 H)
2.50 (ddd, 1 H, J = 19.1, 8.2, 0.65 Hz)	1.59 – 1.53 (m, 1 H)
2.22 (ddd, 1 H, J = 19.1, 11.6, 9.4 Hz)	1.37 (dtd, 1 H, J = 13.6, 3.4, 1.5 Hz)
2.14 (br s, 1 H)	1.21 (s, 3 H)
1.95 – 1.90 (m, 1 H)	1.11 (s, 3 H)
1.85 – 1.81 (m, 1 H)	0.93 (s, 3 H)

^{13}C NMR (126 MHz, $CDCl_3$)

δ 223.6	36.9	29.1
68.0	34.0	25.3
55.1	31.7	22.5
52.6	29.6	17.1

HRMS (ES+) calculated for $C_{12}H_{20}O_2Na$ $[M+Na]^+$: 219.1361, found 219.1362
TLC: R_f = 0.10 (20% v/v ethyl acetate in hexanes)
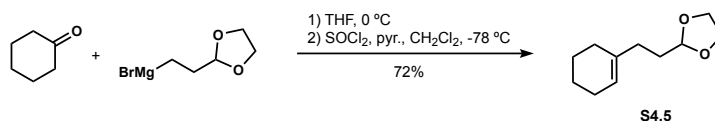
Cyclohexene S4.5. A flame-dried round bottom flask was charged with cyclohexanone (0.47 g, 4.8 mmol), THF (0.2 M) and cooled to 0 ℃. Bromo[2-(1,3-dioxolan-2-yl)ethyl]magnesium was added dropwise to the solution of ketone. The reaction was stirred 1h at 0 ℃, quenched with 1N aqueous HCl and diluted with diethyl ether. The layers were separated and the aqueous layer extracted twice with diethyl ether (40 mL combined). The organic layers were combined, washed with water (10 mL), brine (10 mL) dried over anhydrous magnesium sulfate, filtered and concentrated under reduced pressure. The crude tertiary alcohol was used without purification.

To a solution of crude alcohol in dichloromethane (0.1 M) at -78 ℃ was added thionyl chloride (1.1 mL, 14.4 mmol) followed by pyridine (1.9 mL, 24 mmol). The reaction was stirred 1h, quenched with saturated aqueous NaHCO$_3$ and warmed to room temperature. The layers were separated and the aqueous layer extracted twice with CH$_2$Cl$_2$ (40 mL combined). The organic layers were combined, washed with H$_2$O (10 mL), brine (10 mL), dried over anhydrous sodium sulfate, filtered and concentrated under reduced pressure. Purification by flash chromatography (gradient elution: 100% hexanes to 5% v/v ethyl acetate in hexanes) afforded cyclohexene **S4.5** (0.63 g, 72% yield over two steps) as a colourless oil.

Cyclohexene **S4.5**

^{1}H NMR (500 MHz, CDCl$_3$)

δ 5.44 – 5.41 (m, 1 H)	1.99 – 1.96 (m, 2 H)
4.86 (t, 1 H, J = 4.8 Hz)	1.94 – 1.91 (m, 2 H)
3.98 – 3.95 (m, 2 H)	1.77 – 1.73 (m, 2 H)
3.86 – 3.84 (m, 2 H)	1.62 – 1.60 (m, 2 H)
2.05 (t, 2 H, J = 8.1 Hz)	1.54 – 1.53 (m, 2 H)

TLC: R$_f$ = 0.39 (10% v/v ethyl acetate in hexanes)
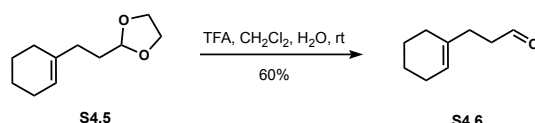
γ,δ-unsaturated aldehyde S4.6. To a solution of acetal **S4.5** (0.32 g, 1.7 mmol) in CH$_2$Cl$_2$ (0.5 M) was added trifluoroacetic acid (2.6 mL; 50% v/v in water). The reaction mixture was stirred until starting material had been consumed by TLC analysis and quenched with saturated aqueous NaHCO$_3$. The layers were separated and the aqueous layer extracted twice with CH$_2$Cl$_2$ (40 mL combined). The organic layers were combined, washed with H$_2$O (10 mL), brine (10 mL), dried over anhydrous sodium sulfate, filtered and concentrated under reduced pressure. Purification by flash chromatography (gradient elution: 100% hexanes to 5% v/v ethyl acetate in hexanes) afforded γ,δ-unsaturated aldehyde **S4.6** (0.14 g, 60% yield) as a colourless oil. Spectral data match that reported in the literature.[33]
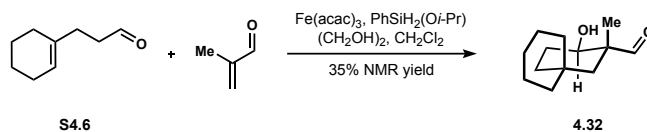
Spirocycle 4.32. A Schlenk flask was charged with iron(III) acetylacetonate (3.5 mg, 0.01 mmol), anhydrous ethylene glycol (34 μL, 0.6 mmol), γ,δ-unsaturated aldehyde **S4.6** (44.8 mg, 0.4 mmol) and CH_2Cl_2 (0.80 mL). The mixture was degassed using a freeze-pump-thaw technique (3 cycles). Over 1 h, methacrolein (17 μL, 97% pure, 0.2 mmol) and isopropoxyphenylsilane (100 mg, 0.6 mmol) in degassed (sparged with argon) CH_2Cl_2 (0.40 mL) were added via syringe pump. Following addition, the reaction mixture was stirred vigorously for 1 h, then quenched with degassed (sparged with argon) 1 N aqueous HCl (2 mL). The layers were separated and the aqueous layer extracted twice with CH_2Cl_2 (20 mL combined). The organic layers were combined, washed with 1 N aqueous HCl (10 mL), H_2O (10 mL), brine (10 mL), dried over anhydrous sodium sulfate, filtered and concentrated under reduced pressure. Purification attempted with column chromatography resulted in decomposition. A yield of spirocycle **4.32** was determined to be 36% by addition of mesitylene as an internal standard to the crude mixture. The crude spectra with the diagnostic aldehyde peak at δ 9.44 integrated is included in the appendix.
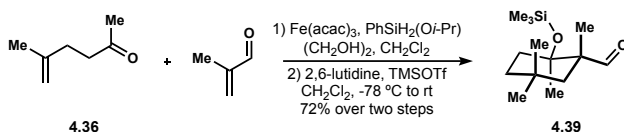
Silylether 4.39. A Schlenk flask was charged with iron(III) acetylacetonate (14.1 mg, 0.04 mmol), anhydrous ethylene glycol (1 μL, 0.2 mmol), γ,δ-unsaturated ketone **4.36**[34,35] (44.8 mg, 0.4 mmol) and CH_2Cl_2 (0.80 mL). The mixture was degassed using a freeze-pump-thaw technique (3 cycles). Over 1 h, methacrolein (17 μL, 97% pure, 0.2 mmol) and isopropoxyphenylsilane (100 mg, 0.6 mmol) in degassed (sparged with argon) CH_2Cl_2 (0.40 mL) were added via syringe pump.

Following addition, the reaction mixture was stirred vigorously for 1 h, then quenched with 1 N aqueous HCl (2 mL). The layers were separated and the aqueous layer extracted twice with CH_2Cl_2 (20 mL combined). The organic layers were combined, washed with 1 N aqueous HCl (10 mL), H_2O (10 mL), brine (10 mL), dried over anhydrous sodium sulfate, filtered and concentrated under reduced pressure. The crude hydroxyaldehyde was then dissolved in CH_2Cl_2 (1 mL) and cooled to -78 °C. To the solution was added 2,6-lutidine (0.12 mL, 1.0 mmol) and TMSOTf (0.14 mL, 0.8 mmol). The reaction was warmed to room temperature over 30 minutes before being quenched with saturated aqueous $NaHCO_3$ (5 mL). The layers were separated and the aqueous layer extracted twice with CH_2Cl_2 (20 mL combined). The organic layers were combined, washed with 1 N aqueous HCl (10 mL), H_2O (10 mL), brine (10 mL), dried over anhydrous sodium sulfate, filtered and concentrated under reduced pressure. Purification by flash chromatography (gradient elution: 100% hexanes to 1% v/v CH_2Cl_2 in hexanes) afforded silylether **4.39** (37.0 mg, 72% yield over two steps) as a colorless oil.

Silylether **4.39**
^{1}H NMR (500 MHz, CDCl$_3$)

δ 9.61 (s, 1 H)	1.18 – 1.13 (m, 1 H)
1.79 – 1.73 (m, 1 H)	1.01 (s, 3 H)
1.62 – 1.53 (m, 3 H)	0.92 (s, 3 H)
1.42 (dd, 1 H, J = 14.0, 1.8 Hz)	0.80 (s, 3 H)
1.35 (s, 3 H)	0.12 (s, 9 H)

^{13}C NMR (126 MHz, CDCl$_3$)

δ 206.2	34.6	28.4
75.0	33.9	24.9
53.9	32.8	18.2
45.1	30.7	2.6

HRMS (ES+) calculated for $C_{14}H_{28}O_2SiNa$ [M+Na]$^+$: 279.1756, found 279.1753

TLC: $R_f = 0.41$ (5% v/v ethyl acetate in hexanes)
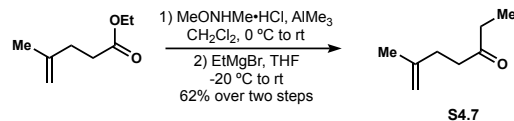
γ,δ-unsaturated ketone S4.7. A flame dried 100 mL Schlenk flask was charged with *N,O*-dimethylhydroxylamine hydrochloride (0.82 g, 8.4 mmol), CH_2Cl_2 (20 mL) and cooled to 0 ºC. Trimethylaluminum (4.3 mL of 2.0 M solution in hexanes, 8.6 mmol) was added dropwise and the solution warmed to room temperature. After stirring for 30 min at room temperature, ethyl 4-methyl-4-pentenoate was added dropwise as a solution in CH_2Cl_2 (10 mL) and the reaction mixture was stirred overnight (16 h). The reaction was quenched slowly with aqueous 2 M H_2SO_4 (20 mL) and the aqueous layer extracted with CH_2Cl_2 twice (50 mL combined). The combined organic layers were washed with H_2O (20 mL), brine (20 mL), dried over anhydrous magnesium sulfate, filtered and concentrated under reduced pressure. The crude Weinreb amide was used in the subsequent step without further purification.

To a solution of Weinreb amide in THF (4.2 mL) at -20 ºC was added ethylmagnesium bromide (6.5 mL of a 0.70 M solution in THF, 4.6 mmol). The solution was warmed to room temperature and stirred until complete by TLC analysis. The reaction was quenched with 1 N aqueous HCl (20 mL) and the aqueous layer extracted with diethyl ether twice (50 mL combined). The combined organic layers were washed with H_2O (20 mL), brine (20 mL), dried over anhydrous magnesium sulfate, filtered and concentrated under reduced pressure. Purification by flash chromatography (gradient elution: 100% pentanes to 1% v/v diethyl ether in pentanes) afforded γ,δ-unsaturated

ketone **S4.7** (0.33 g, 62% yield over two steps) as a colorless oil. ^{1}H and ^{13}C NMR data match that provided in the literature.[35]
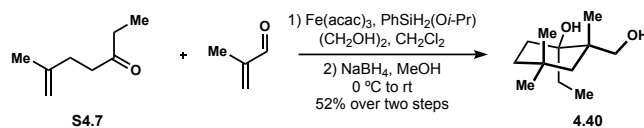
Diol 4.40. A Schlenk flask was charged with iron(III) acetylacetonate (3.5 mg, 0.01 mmol), anhydrous ethylene glycol (34 μL, 0.6 mmol), γ,δ-unsaturated ketone **S4.7** (50.5 mg, 0.4 mmol) and CH$_2$Cl$_2$ (0.80 mL). The mixture was degassed using a freeze-pump-thaw technique (3 cycles). Over 1 h, methacrolein (17 μL, 96% pure, 0.2 mmol) and isopropoxyphenylsilane (100 mg, 0.6 mmol) in degassed (sparged with argon) CH$_2$Cl$_2$ (0.40 mL) were added via syringe pump. Following addition, the reaction mixture was stirred vigorously for 1 h, then quenched with degassed (sparged with argon) 1 N aqueous HCl (2 mL). The layers were separated and the aqueous layer extracted twice with CH$_2$Cl$_2$ (20 mL combined). The organic layers were combined, washed with 1 N aqueous HCl (10 mL), H$_2$O (10 mL), brine (10 mL), dried over anhydrous sodium sulfate, filtered and concentrated under reduced pressure. The crude mixture was then dissolved in 2.0 mL of MeOH and cooled to 0 ºC before adding NaBH$_4$ (38 mg, 1.0 mmol). The reaction mixture was warmed to room temperature over 30 min and quenched with 1 N aqueous HCl (5 mL). The layers were separated and the aqueous layer extracted twice with Et$_2$O (20 mL combined). The organic layers were combined, washed with H$_2$O (10 mL), brine (10 mL), dried over anhydrous sodium sulfate, filtered and concentrated under reduced pressure.

The crude was again dissolved in Et$_2$O (2.0 mL) and treated with 49% aqueous HF (0.10 mL) for 15 minutes then quenched with a slurry of CaCO$_3$ and diluted with H$_2$O (10 mL). The layers were separated and the aqueous layer extracted twice with Et$_2$O (20 mL combined). The organic layers

were combined, washed with H_2O (10 mL), brine (10 mL), dried over anhydrous sodium sulfate, filtered and concentrated under reduced pressure. Purification by flash chromatography (gradient elution: 100% hexanes to 10% v/v ethyl acetate in hexanes) afforded diol **4.40** (20.9 mg, 52% yield) as a colorless oil.

Diol **4.40**

^{1}H NMR (500 MHz, CDCl$_3$)

δ 3.67 (d, 1 H, J = 10.4 Hz)	1.65 – 1.56 (m, 2 H)	1.10 (d, 1 H, J = 14.2 Hz)
3.17 (d, 1 H, J = 10.5 Hz)	1.49 (dt, 1 H, J = 13.8, 4.0 Hz)	1.05 (s, 3 H)
2.66 – 2.45 (br s, 1 H)	1.34 – 1.30 (m, 1H)	1.02 – 0.96 (m, 1 H)
2.35 – 2.23 (br s, 1 H)	1.24 (s, 3 H)	0.91 (t, 3 H, J = 7.4 Hz)
1.76 – 1.69 (m, 1 H)	1.17 – 1.14 (m, 1 H)	0.89 (s, 3 H)

^{13}C NMR (126 MHz, CDCl$_3$)

δ 76.8	36.1	27.4
70.9	34.3	25.7
46.1	30.5	20.4
42.0	29.0	7.4

HRMS (ES+) calculated for $C_{12}H_{24}O_2Na$ [M+Na]$^+$: 223.1674, found 223.1678

TLC: R_f = 0.65 (50% v/v ethyl acetate in hexanes)

Relative configuration of diol **4.40** was assigned based on nOe correlations.
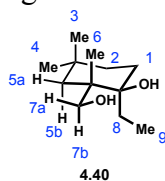
^{1}H (arbitrary numbering)	Key correlations
H7a (3.17 ppm)	H5a (1.02 – 0.96 ppm)
	H8 (1.76 – 1.69ppm and 1.65 – 1.56 ppm)
H7b (3.67 ppm)	H5b (1.10 ppm)
	H8 (1.76 – 1.69ppm and 1.65 – 1.56 ppm)
H5b (1.10 ppm)	H8 (1.76 – 1.69 ppm)
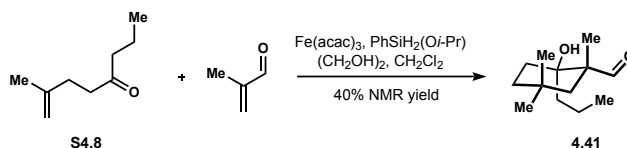
Cyclohexanol 4.41. A Schlenk flask was charged with iron(III) acetylacetonate (14.1 mg, 0.04 mmol), anhydrous ethylene glycol (34 μL, 0.6 mmol), γ,δ-unsaturated aldehyde **S4.8**[35] (56 mg, 0.4 mmol) and CH_2Cl_2 (0.80 mL). The mixture was degassed using a freeze-pump-thaw technique (3 cycles). Over 1 h, methacrolein (17 μL, 97% pure, 0.2 mmol) and isopropoxyphenylsilane (100 mg, 0.6 mmol) in degassed (sparged with argon) CH_2Cl_2 (0.40 mL) were added via syringe pump. Following addition, the reaction mixture was stirred vigorously for 1 h, then quenched with degassed (sparged with argon) 1 N aqueous HCl (2 mL). The layers were separated and the aqueous layer extracted twice with CH_2Cl_2 (20 mL combined). The organic layers were combined, washed with 1 N aqueous HCl (10 mL), H_2O (10 mL), brine (10 mL), dried over anhydrous sodium sulfate, filtered and concentrated under reduced pressure. Purification attempted with column chromatography resulted in decomposition. A yield of cyclohexanol **4.41** was determined to be 40% by addition of mesitylene as an internal standard to the crude mixture. The crude spectra with the diagnostic aldehyde peak at δ 9.69 integrated is included in the appendix.
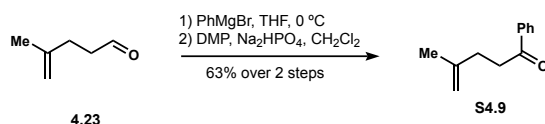
γ,δ-unsaturated ketone S4.9. To a solution of γ,δ-unsaturated aldehyde **4.23**[28] (0.20 g, 2.0 mmol) in THF (0.2 M) at 0 °C was added phenylmagnesiumbromide (2.6 mL, 0.85 M in THF). The reaction mixture was warmed to room temperature, stirred 1 h and quenched with 1 N aqueous HCl. The layers were separated and the aqueous layer extracted twice with diethyl ether (40 mL combined). The organic layers were combined, washed with H_2O (10 mL), brine (10 mL), dried over anhydrous magnesium sulfate, filtered and concentrated under reduced pressure. The alcohol

was taken forward without further purification. To a solution of alcohol in CH_2Cl_2 (0.1 M) was added Na_2HPO_4 (0.57 g, 4.0 mmol) and Dess–Martin periodinane (1.7 g, 4.0 mmol). The reaction mixture was stirred at room temperature for 2 h and quenched with saturated aqueous $NaHCO_3$. The layers were separated and the aqueous layer extracted twice with CH_2Cl_2 (40 mL combined). The organic layers were combined, washed with saturated aqueous $Na_2S_2O_8$ (10 mL), saturated aqueous $NaHCO_3$ (10 mL), H_2O (10 mL), brine (10 mL), dried over anhydrous magnesium sulfate, filtered and concentrated under reduced pressure. Purification by flash chromatography (gradient elution: 100% hexanes to 10% v/v ethyl acetate in hexanes) afforded γ,δ-unsaturated ketone **S4.9** (0.22 g, 63% yield over two steps) as a colorless oil. Spectral data match that found in the literature.[36]
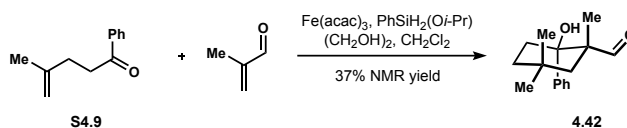
Cyclohexanol 4.42. A Schlenk flask was charged with iron(III) acetylacetonate (14.1 mg, 0.04 mmol), anhydrous ethylene glycol (34 μL, 0.6 mmol), γ,δ-unsaturated aldehyde **S4.9** (70 mg, 0.4 mmol) and CH_2Cl_2 (0.80 mL). The mixture was degassed using a freeze-pump-thaw technique (3 cycles). Over 1 h, methacrolein (17 μL, 97% pure, 0.2 mmol) and isopropoxyphenylsilane (100 mg, 0.6 mmol) in degassed (sparged with argon) CH_2Cl_2 (0.40 mL) were added via syringe pump. Following addition, the reaction mixture was stirred vigorously for 1 h, then quenched with degassed (sparged with argon) 1 N aqueous HCl (2 mL). The layers were separated and the aqueous layer extracted twice with CH_2Cl_2 (20 mL combined). The organic layers were combined, washed with 1 N aqueous HCl (10 mL), H_2O (10 mL), brine (10 mL), dried over anhydrous sodium sulfate, filtered and concentrated under reduced pressure. Purification attempted with column chromatography resulted in decomposition. A yield of cyclohexanol **4.42** was determined to be

37% by addition of mesitylene as an internal standard to the crude mixture. The crude spectra with the diagnostic aldehyde peak at δ 9.86 integrated is included in the appendix.
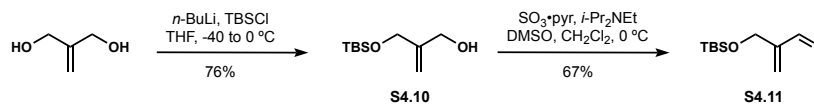
α,β-unsaturated aldehyde S4.11. To a solution of 2-methylene-1,3-propanediol (0.25 g, 2.8 mmol) in THF (1 M) at -40 ºC was added *n*-butyl lithium (2.8 mmol, 1.9 M in hexanes). The reaction mixture was stirred 30 min before adding TBSCl (0.43 g, 2.8 mmol). The reaction mixture was warmed to room temperature and left to stir overnight (18 h) and quenched with 1 N aqueous HCl. The layers were separated and the aqueous layer extracted twice with CH_2Cl_2 (40 mL combined). The organic layers were combined, washed with 1 N aqueous HCl (10 mL), H_2O (10 mL), brine (10 mL), dried over anhydrous sodium sulfate, filtered and concentrated under reduced pressure to afford crude alcohol **S4.10** (0.44 g, 76% yield) that was deemed analytically pure. Spectral data match that found in the literature.[37]

To a solution of alcohol **S4.10** (0.20 g, 0.99 mmol) in CH_2Cl_2 (0.1 M) at -78 ºC was added *i*-Pr$_2$NEt (0.86 mL, 4.9 mmol) followed by SO_3•pyr (0.46 g, 3.0 mmol) in DMSO (4 mL). The reaction mixture was stirred 30 min at -78 ºC and quenched with 1 N aqueous HCl. The layers were separated and the aqueous layer extracted twice with CH_2Cl_2 (40 mL combined). The organic layers were combined, washed with 1 N aqueous HCl (10 mL), twice with H_2O (20 mL combined), brine (10 mL), dried over anhydrous magnesium sulfate, filtered and concentrated under reduced pressure. Purification by flash chromatography (gradient elution: 100% hexanes to 2% v/v ethyl acetate in hexanes) afforded α,β-unsaturated aldehyde **S4.11** (0.13 g, 67% yield) as a colorless oil. Spectral data match that found in the literature.[37]
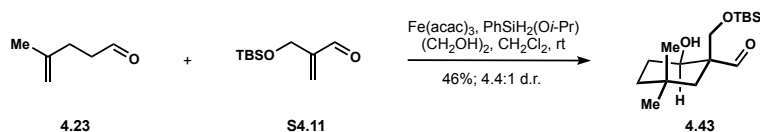
Cyclohexanol 4.43. A Schlenk flask was charged with iron(III) acetylacetonate (3.5 mg, 0.01 mmol), anhydrous ethylene glycol (34 μL, 0.6 mmol), γ,δ-unsaturated aldehyde **4.23**[28] (39.3 mg, 0.4 mmol) and CH_2Cl_2 (0.80 mL). The mixture was degassed using a freeze-pump-thaw technique (3 cycles). Over 1 h, α,β-unsaturated aldehyde **S4.11** (40 mg, 0.2 mmol) and isopropoxyphenylsilane (100 mg, 0.6 mmol) in degassed (sparged with argon) CH_2Cl_2 (0.40 mL) were added via syringe pump. Following addition, the reaction mixture was stirred vigorously for 1 h, then quenched with degassed (sparged with argon) 1 N aqueous HCl (2 mL). The layers were separated and the aqueous layer extracted twice with CH_2Cl_2 (20 mL combined). The organic layers were combined, washed with 1 N aqueous HCl (10 mL), H_2O (10 mL), brine (10 mL), dried over anhydrous sodium sulfate, filtered and concentrated under reduced pressure. Purification by flash chromatography (gradient elution: 100% hexanes to 5% v/v ethyl acetate in hexanes) afforded cyclohexanol **4.43** in a 4.4:1 mixture of diastereomers (27.7 mg, 46% yield) as a white solid.

Cyclohexanol **4.43**
^{1}H NMR (500 MHz, CDCl$_3$)*

δ 9.55 (s, 1 H)	1.79 – 1.68 (m, 2 H)	0.96 (s, 3 H)
4.32 (dd, 1 H, J = 4.8, 3.1 Hz)	1.55 (dt, 1 H, J = 12.7, 3.9 Hz)	0.86 (s, 9 H)
3.81 (d, 1 H, 10.2 Hz)	1.45 (d, 1 H, J = 14.0 Hz)	0.80 (s, 3 H)
3.70 (d, 1 H, 10.2 Hz)	1.39 (d, 1 H, J =14.2 Hz)	0.04 (s, 3 H)
1.79 – 1.68 (m, 2 H)	1.25 – 1.15 (m, 1 H)	0.04 (s, 3 H)

*Peaks integrated correspond to the major diastereomer.

γ,δ-unsaturated aldehydes S4.13 and S4.14. To a solution of alcohol **S4.10** (0.235 g, 1.16 mmol) in CH_2Cl_2 (1 M) at 0 °C was added acetic anhydride (0.44 mL, 4.6 mmol), followed by Et_3N (0.81 mL, 5.8 mmol) and DMAP (14.2 mg, 0.12 mmol). The reaction mixture was warmed to room temperature, stirred 2 h and quenched with 1 N aqueous HCl. The layers were separated and the aqueous layer extracted twice with CH_2Cl_2 (20 mL combined). The organic layers were combined, washed with 1 N aqueous HCl (10 mL), saturated aqueous $NaHCO_3$ (10 mL), brine (10 mL), dried over anhydrous magnesium sulfate, filtered and concentrated under reduced pressure.

The crude protected diol was re-dissolved in CH_2Cl_2 (0.1 M) and added to the solution was a few drops of 1 M methanolic HCl at room temperature. The reaction mixture was stirred overnight (20 h) and quenched with saturated aqueous $NaHCO_3$. The layers were separated and the aqueous layer extracted twice with CH_2Cl_2 (20 mL combined). The organic layers were combined, washed with H_2O (10 mL), brine (10 mL), dried over anhydrous magnesium sulfate, filtered and concentrated under reduced pressure. Spectral data match that found in the literature.[38]

The crude alcohol **S4.12** was dissolved in CH_2Cl_2 (0.25 M) cooled to -78 °C and then added *i*-Pr_2NEt (0.87 mL, 5 mmol) followed by $SO_3\cdot pyr$ (0.48 g, 3 mmol) as a solution in DMSO (5 mL). The reaction mixture was stirred 30 min and quenched with 1 N HCl. The layers were separated and the aqueous layer extracted twice with pentane (20 mL combined). The organic layers were combined, washed with 1 N aqueous HCl (10 mL), twice with H_2O (20 mL combined), brine (10 mL), dried over anhydrous magnesium sulfate, filtered and concentrated under reduced pressure.

Purification by flash chromatography (gradient elution: 100% pentane to 10% v/v diethyl ether in pentanes) afforded acetate **S4.13** (42 mg, 33% yield over three steps) and thioether **S4.14** (35 mg, 30% yield over three steps) as colourless oils.
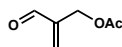
S4.13

Spectral data of **S4.13** match that found in the literature.[39]

Thioether **S4.14**

^{1}H NMR (500 MHz, CDCl$_3$)

δ 9.60 (s, 1 H)

6.37 (s, 1 H)

6.12 (s, 1 H)

3.31 (s, 2 H)

2.05 (s, 3 H)

TLC: R$_f$ = 0.20 (20% v/v ethyl acetate in hexanes); KMnO$_4$ stain required
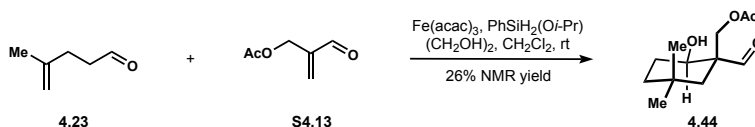
Cyclohexanol 4.44. A Schlenk flask was charged with iron(III) acetylacetonate (3.5 mg, 0.01 mmol), anhydrous ethylene glycol (34 μL, 0.6 mmol), γ,δ-unsaturated aldehyde **4.23**[28] (39.3 mg, 0.4 mmol) and CH$_2$Cl$_2$ (0.80 mL). The mixture was degassed using a freeze-pump-thaw technique (3 cycles). Over 1 h, α,β-aldehyde **S4.13** (25.6 mg, 0.2 mmol) and isopropoxyphenylsilane (100 mg, 0.6 mmol) in degassed (sparged with argon) CH$_2$Cl$_2$ (0.40 mL) were added via syringe pump. Following addition, the reaction mixture was stirred vigorously for 1 h, then quenched with degassed (sparged with argon) 1 N aqueous HCl (2 mL). The layers were separated and the

aqueous layer extracted twice with CH_2Cl_2 (20 mL combined). The organic layers were combined, washed with 1 N aqueous HCl (10 mL), H_2O (10 mL), brine (10 mL), dried over anhydrous sodium sulfate, filtered and concentrated under reduced pressure. A yield of cyclohexanol **4.44** was determined to be 26% by addition of mesitylene as an internal standard to the crude mixture. The crude spectra with the diagnostic aldehyde peak at δ 9.59 integrated is included in the appendix.
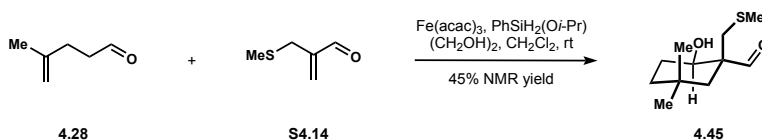
Cyclohexanol 4.45. A Schlenk flask was charged with iron(III) acetylacetonate (3.5 mg, 0.01 mmol), anhydrous ethylene glycol (34 μL, 0.6 mmol), γ,δ-unsaturated aldehyde **4.23**[27] (39.3 mg, 0.4 mmol) and CH_2Cl_2 (0.80 mL). The mixture was degassed using a freeze-pump-thaw technique (3 cycles). Over 1 h, α,β-unsaturated aldehyde **S4.14** (25.6 mg, 0.2 mmol) and isopropoxyphenylsilane (100 mg, 0.6 mmol) in degassed (sparged with argon) CH_2Cl_2 (0.40 mL) were added via syringe pump. Following addition, the reaction mixture was stirred vigorously for 1 h, then quenched with degassed (sparged with argon) 1 N aqueous HCl (2 mL). The layers were separated and the aqueous layer extracted twice with CH_2Cl_2 (20 mL combined). The organic layers were combined, washed with 1 N aqueous HCl (10 mL), H_2O (10 mL), brine (10 mL), dried over anhydrous sodium sulfate, filtered and concentrated under reduced pressure. A yield of cyclohexanol **4.45** was determined to be 26% by addition of mesitylene as an internal standard to the crude mixture. The crude spectra with the diagnostic aldehyde peak at δ 9.58 integrated is included in the appendix.
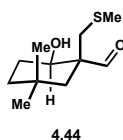
HRMS (ES+) calculated for $C_{11}H_{20}O_2SNa$ [M+Na]$^+$: 239.1082, found 239.1087

4.4 References and Notes

1. George, D. T.; Kuenstner, E. J., Pronin, S. V. *J. Am. Chem. Soc.* **2015,** *137,* 15410.
2. Godfrey, N. A.; Schatz, D. J.; Pronin, S. V. *J. Am. Chem. Soc.* **2018,** *140,* 12770.
3. Isayama, S.; Mukaiyama, T. *Chem. Lett.* **1989,** *18,* 1071.
4. For seminal reports of various hydrofunctionalizations, see: (a) Kato, K. Mukaiyama, T. *Chem. Lett.* **1992,** *21,* 1137. (b) Magnus, P.; Waring, M. J.; Scott, D. A. *Tetrahedron Lett.* **2000,** *41,* 9731. (c) Waser, J.; Gaspar, G.; Nambu, H.; Carreira, E. M. *J. Am. Chem. Soc.* **2006,** *128,* 11693. (d) Gaspar, G.; Carreira, E. M. *Angew. Chem., Int. Ed.* **2008,** *47,* 5758. (e) Girijavallabhan, V.; Alvarez, C.; Njoroge, F. G. *J. Org. Chem.* **2011,** *76,* 6442. (f) Barker, T. J.; Boger, D. L. *J. Am. Chem. Soc.* **2012,** *134,* 13588. (g) Shigehisa, H.; Aoki, T.; Yamaguchi, S.; Shimizu, N.; Hiroya, K. *J. Am. Chem. Soc.* **2013,** *135,* 10306. (h) King, S. M.; Ma, X.; Herzon, S. B. *J. Am. Chem. Soc.* **2014,** *136,* 6884. (i) Green, S. A.; Huffman, T. R.; McCourt, R. O.; van der Puyl, V.; Shenvi, R. A. *J. Am. Chem. Soc.* **2019,** *141,* 7709.
5. For recent reviews of HAT processes, see: (a) Crossley, S. W. M.; Martinez, R. M.; Obradors, C.; Shenvi, R. *Chem. Rev.* **2016,** *116,* 8912. (b) Matos, J. L.; Green, S. A.; Shenvi, R. A. *Organic Reactions,* **2019,** *100,* 383.
6. Lo, J. C.; Yabe, Y.; Baran, P. S. *J. Am. Chem. Soc.* **2014,** *136,* 1304.
7. Lo, J. C.; Gui, J.; Yabe, Y.; Pan, C.–M.; Baran, P. S. *Nature,* **2014,** *516,* 343.
8. Lo, J. C.; Kim, D.; Pan, C.–M.; Edward, J. T.; Yabe, Y.; Gui, J. Qin, T.; Gutiérrez, S.; Giacoboni, J.; Smith, M. W.; Holland, P. L.; Baran, P. S. *J. Am. Chem. Soc.* **2017,** *139,* 2484.
9. For selected examples of radical conjugate additions to form quaternary carbons, see: (a) Barton, D. H. R.; Crich, D. *Tetrahedron Lett.* **1985,** *26,* 757. (b) Okada, K.; Okamoto, K.; Morita, N.; Okubo, K.; Oda, M. *J. Am. Chem. Soc.* **1991,** *113,* 9401. (c) Schnermann, M. J.; Overman, L. E. *Angew. Chem., Int. Ed.* **2012,** *51,* 9576. (d) Sun, Y.; Li, R.; Zhang, W.; Li, A. *Angew. Chem., Int. Ed.* **2013,** *52,* 9201. (e) Lackner, G. L.; Quasdorf, K. W.; Overman, L. E. *J. Am. Chem. Soc.* **2013,** *135,* 15342. (f) Chu, L.; Ohta, C.; Zuo, Z.; MacMillan, D. W. C. *J. Am. Chem. Soc.* **2014,** *136,* 10886. (g) Zhou, S.; Zhang, D.; Sun, Y.; Li, R.; Zhang, W.; Li, A. *Adv. Synth. Catal.* **2014,** *356,* 2867. (h) Müller, D. S.; Untiedt, N. L.; Dieskau, A. P.; Lackner, G. L.; Overman, L. E. *J. Am. Chem. Soc.* **2015,** 137, 660. (i) Chinzei, T.; Miyazawa, K.; Yasu, Y.; Koike, T.; Akita, M. *RSC Adv.* **2015,** 5, 21297. (j) Lackner, G. L.; Quasdorf, K. W.; Pratsch, G.; Overman, L. E. J. *Org. Chem.* **2015,** *80,* 6012. (k) Pratsch, G.; Lackner, G. L.; Overman, L. E. *J. Org. Chem.* **2015,** *80,* 6025. (l) Nawrat, C. C.; Jamison, C. R.; Slutskyy, Y.; MacMillan, D. W. C.; Overman, L. E. *J. Am. Chem. Soc.* **2015,** *137,* 11270.
10. For recent reviews of radical reactions in total synthesis, see: (a) Jasperse, C. P.; Curran, D. P.; Fevig, T. L. *Chem. Rev.* **1991,** *91,* 1237. (b) Romero, K. J.; Galliher, M. S.; Pratt, D. A.; Stephenson, C. R. *Chem. Soc. Rev.* **2018,** *47,* 7851. (c) Pitre, S. P.; Weires, N. A.; Overman, L. E. *J. Am. Chem. Soc.* **2019,** *141,* 2800.
11. Deng, H.; Cao, W.; Liu, R.; Zhang, Y.; Liu, B. *Angew. Chem. Int. Ed.* **2017,** *56,* 5849.
12. For recent development of the HAT initiated polyene cyclization, see: Vrubliauskas, D.; Vanderwal, C. D. *Angew. Chem., Int. Ed.* **2020,** *59,* 6115.
13. Lu, Z.; Zhang, X.; Guo, Z.; Chen, Y.; Mu, T.; Li, A. *J. Am. Chem. Soc.* **2018,** *140,* 9211.
14. For relevant reductive aldol reaction, see: Isayama, S.; Mukaiyama, T. *Chem. Lett.* **1989,** *18,* 2005.

15. For selected reviews, see: (a) Jung, M. E. *Tetrahedron* **1976**, *32*, 3. (b) Trost, B. M. *Angew. Chem.* **1986**, *98*, 1. (c) Posner, G. H. *Chem. Rev.* **1986**, *86*, 831. (d) Larock, R. C. *J. Organomet. Chem.* **1999**, *576*, 111. (e) Molander, G. A. *Acc. Chem. Res.* **1998**, *31*, 603. (f) Dötz, K. H.; Tomuschat, P. *Chem. Soc. Rev.* **1999**, *28*, 187. (g) Rheault, T. R.; Sibi, M. P. *Synthesis* **2003**, *2003*, 0803. (h) Mal, D.; Pahari, P. *Chem. Rev.* **2007**, *107*, 1892.

16. For selected reviews, see: (a) Boger, D. L. *Chem. Rev.* **1986**, *86*, 781. (b) Winkler, J. D. *Chem. Rev.* **1996**, *96*, 167. (c) Corey, E. J. *Angew. Chem., Int. Ed.* **2002**, *41*, 1650. (d) Nicolaou, K. C.; Snyder, S. A.; Montagnon, T.; Vassilikogiannakis, G. *Angew. Chem., Int. Ed.* **2002**, *41*, 1668. (e) Takao, K.; Munakata, R.; Tadano, K. *Chem. Rev.* **2005**, *105*, 4779.

17. For selected examples of bimolecular Diels−Alder reactions with highly substituted 1,3-dienes and relevant discussions, see: (a) Roush, W. R.; Limberakis, C.; Kunz, R. K.; Barda, D. A. *Org. Lett.* **2002**, *4*, 1543. (b) Du, X.; Chu, H. V.; Kwon, O. *Tetrahedron Lett.* **2004**, *45*, 8843. (c) Usuda, H.; Kuramochi, A.; Kanai, M.; Shibasaki, M. *Org. Lett.* **2004**, *6*, 4387. (d) Jung, M. E.; Ho, D.; Chu, H. V. *Org. Lett.* **2005**, *7*, 1649. (e) Jung, M. E.; Guzaev, M. *Org. Lett.* **2012**, *14*, 5169. (f) Huwyler, N.; Carreira, E. M. *Angew. Chem. Int. Ed.* **2012**, *51*, 13066. (g) Ishihaara, Y.; Mendoza, A.; Baran, P. S. *Tetrahedron*, **2013**, *69*, 5685.

18. For solutions to this problem, see: (a) Zutterman, F.; Krief, A. *J. Org. Chem.* **1983**, *48*, 1135. (b) Kienzle, F.; Stadlwieser, J.; Mergelsherg, I. *Helv. Chim. Acta* **1989**, *72*, 348. (c) Stork, G.; Chan, T. Y. *J. Am. Chem. Soc.* **1995**, *117*, 6595.

19. For selected examples, see: (a) Kazlauskas, R.; Murphy, P. T.; Quinn, R. J.; Wells, R. J. *Tetrahedron Lett.* **1976**, *17*, 2631. (b) Cimino, G.; De Stefano, S.; Minale, L.; Trivellone, E. *J. Chem. Soc., Perkin Trans. 1,* **1977**, 1587. (c) Bhat, S. V.; Bajwa, B. S.; Dornauer, H. de Souza, N. J.; Fehlhaber, H.−W. *Tetrahedron Lett.* **1977**, *18*, 1669. (d) Walker, R. P.; Thompson, J. E.; Faulkner, D. *J. Org. Chem.* **1980**, *45*, 4976. (e) Crews, P.; Bescansa, P. *J. Nat. Prod.* **1986**, *49*, 1041.

20. Obradors, C.; Martinez, R. M.; Shenvi, R. A. *J. Am. Chem. Soc.* **2016**, *138*, 4962.

21. Initial optimization efforts were highly collaborative between D.T.G., W.P.T. and D.J.S. and full optimization efforts are not included to avoid confusion over contributions or inclusion of incomplete tables consisting of a single researcher's findings. All data included in the remainder of the chapter was obtained by D.J.S. unless otherwise specified.

22. Kim, D.; Rahaman, S. M. W.; Mercado, B. Q.; Poli, R.; Holland, P. *J. Am. Chem. Soc.* **2019**, *141*, 7473.

23. For selected examples, see: (a) Kazlauskas, R.; Murphy, P. T.; Quinn, R. J.; Wells, R. J. *Tetrahedron Lett.* **1976**, *17*, 2631. (b) Cimino, G.; De Stefano, S.; Minale, L.; Trivellone, E. *J. Chem. Soc., Perkin Trans. 1* **1977**, 1587. (c) Walker, R. P.; Thompson, J. E.; Faulkner, D. J. *J. Org. Chem.* **1980**, *45*, 4976. (d) Crews, P.; Bescansa, P. *J. Nat. Prod.* **1986**, *49*, 1041.

24. Bhat, S. V.; Bajwa, B. S.; Dornauer, H.; de Souza, N. J.; Fehlhaber, H.-W. *Tetrahedron Lett.* **1977**, *18*, 1669.

25. Liu, D.; Canales, E.; Corey, E. J. *J. Am. Chem. Soc.* **2007**, *129*, 1498.

26. Thomas, W. P.; Schatz, D. J.; George, D. T.; Pronin, S. V. *J. Am. Chem. Soc.* **2019**, *141*, 12246.

27. Yip, K.T.; Yang, D. *Org. Lett.* **2011**, *138*, 2134.

28. Qian, H.; Han, X.; Widenhoefer, R. A. *J. Am. Chem. Soc.* **2004**, *126*, 9536.

29. Erkkilä, A.; Pihko, P. M. *Eur. J. Org. Chem.* **2007**, 4205.

30. Kimura, M.; Shimizu, M.; Tanaka, S.; Tamaru, Y.; *Tetrahedron*, **2005**, *61*, 3709.

31. Mehl, F.; Bombarda, I.; Franklin, C.; Gaydou, E. *Synthetic Comm.* **2010**, *40*, 462.
32. Fernández-Mateos, A.; Coca, G. P.; González, R. R.; Hernández, R. R. *J. Org. Chem.* **1996**, *61*, 9097.
33. Klein, J. E. M. N.; Müller-Bunz, H.; Evans, P. *Org. Biomol. Chem.* **2009,** *7,* 986.
34. Baig, M. A.; Banthorpe, D. V.; Carr, G.; Whittaker, D. *J. Chem. Soc. Perkin Trans 2*, **1989**, 1981.
35. Šmit, B. M.; Pavlović, R. Z. *Tetrahedron*, **2015**, *71*, 1101.
36. Suresh, R.; Simlandy, A. K.; Mukherjee, S.; *Org. Lett.* **2018**, *20*, 1300.
37. Senter, T. J.; Fadeyi, O. O.; Lindsley, C. W. *Org. Lett.* **2012**, *14*, 1869.
38. Katsina, T.; Sharma, S. P.; Buccafusca, R.; Quin, D. J. Moody, T. S.; Arseniyadis, S. *Org. Lett.* **2019**, *21*, 9348.
39. Kano, T.; Tanaka, Y.; Osawa, K.; Yurino, T.; Maruoka, K. *Chem. Commun.* **2009**, 1956

Appendix A: NMR Spectra for Chapter 2
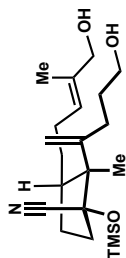
2.26 (¹H NMR, 500 MHz, CDCl₃)

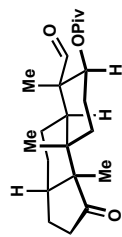DS-1-105 1 1 /Users/devonschatz/Documents/NMR
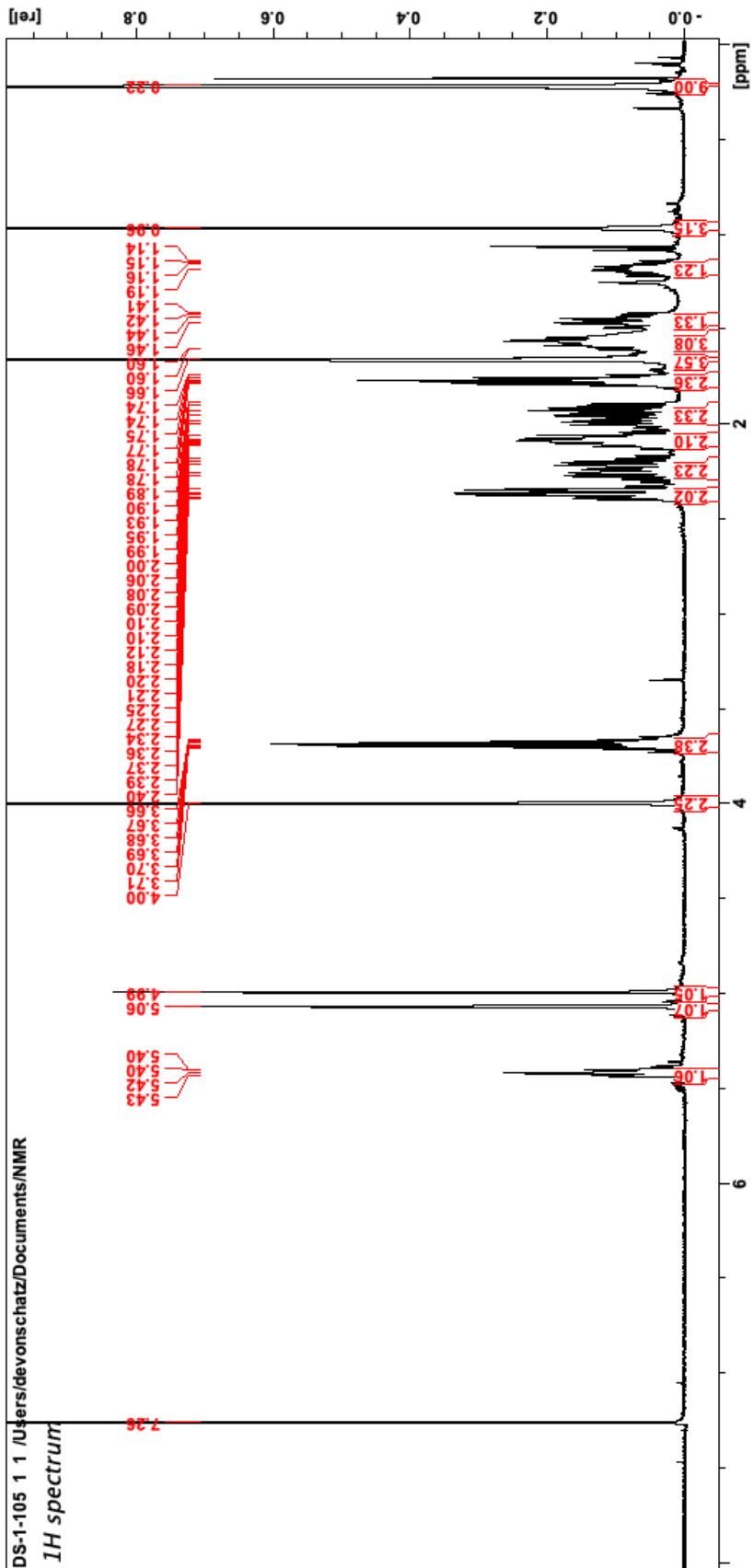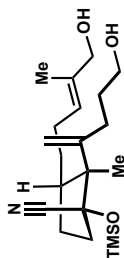
1H spectrum

2.26 (^{13}C NMR, 126 MHz, CDCl$_3$)

DS-1-24 8 1 /Users/devonschatz/Documents/NMR

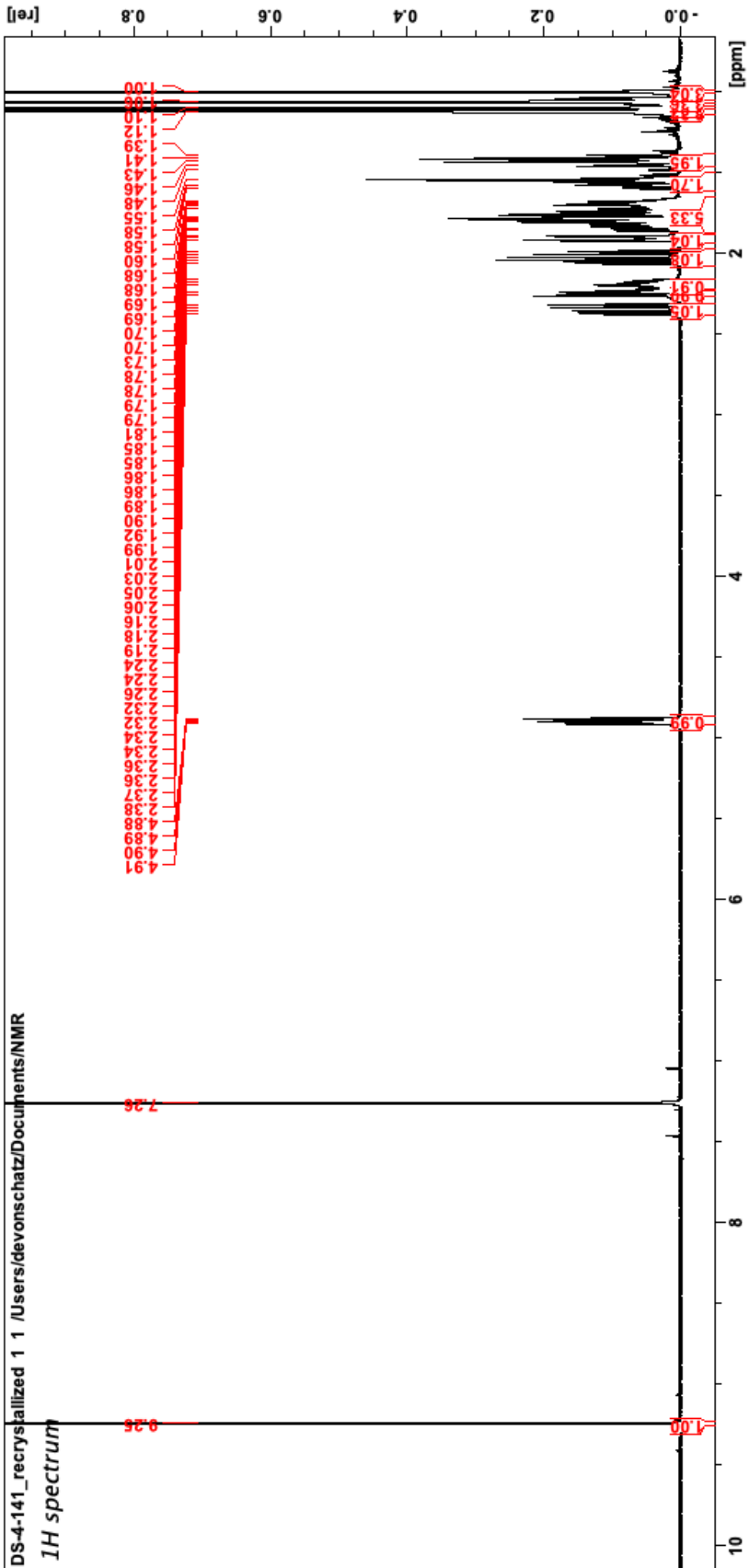*Z–restored spin–echo 13C spectrum with 1H decoupling*
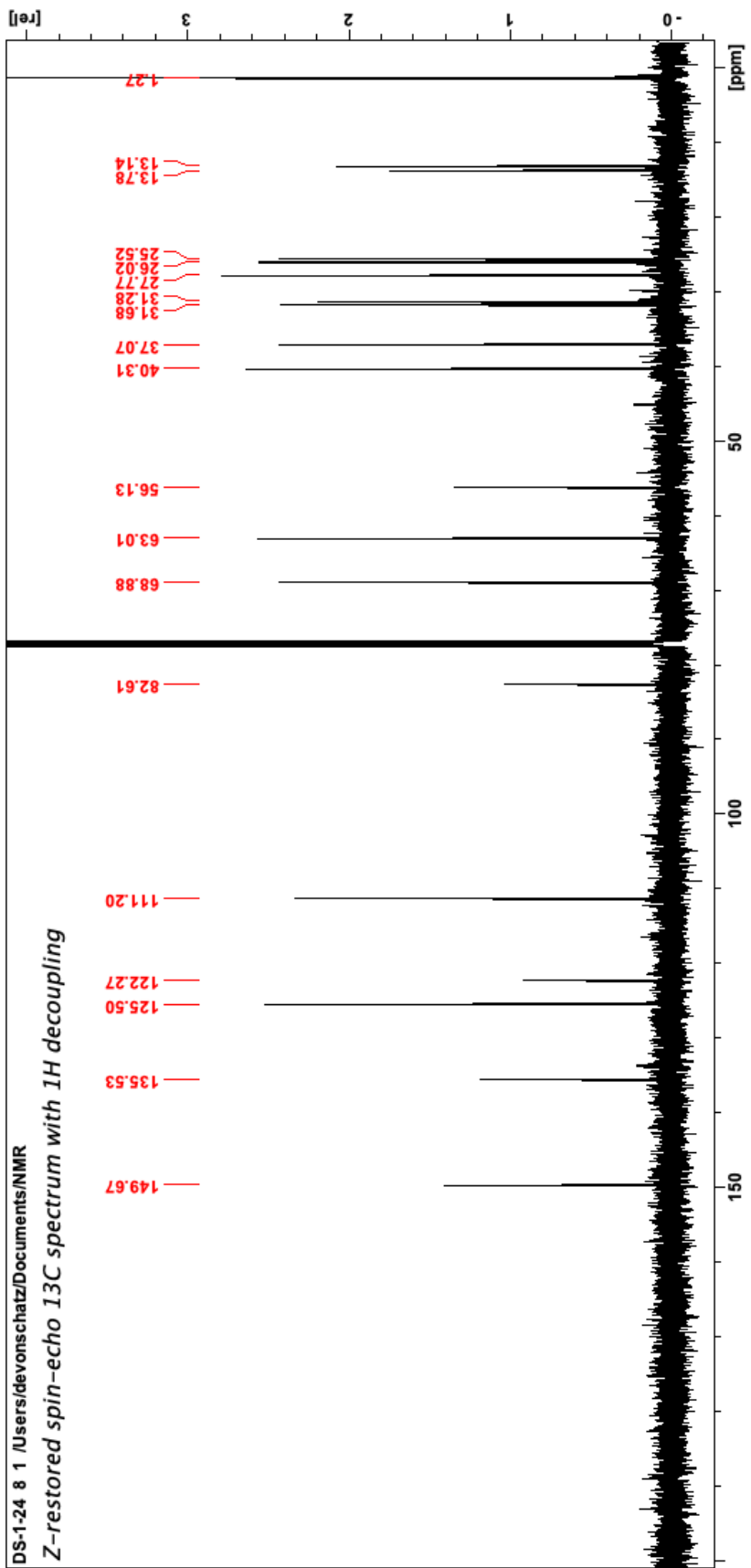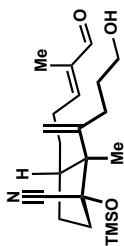
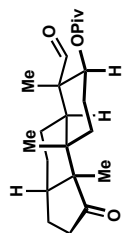2.31 (¹H NMR, 500 MHz, CDCl₃)

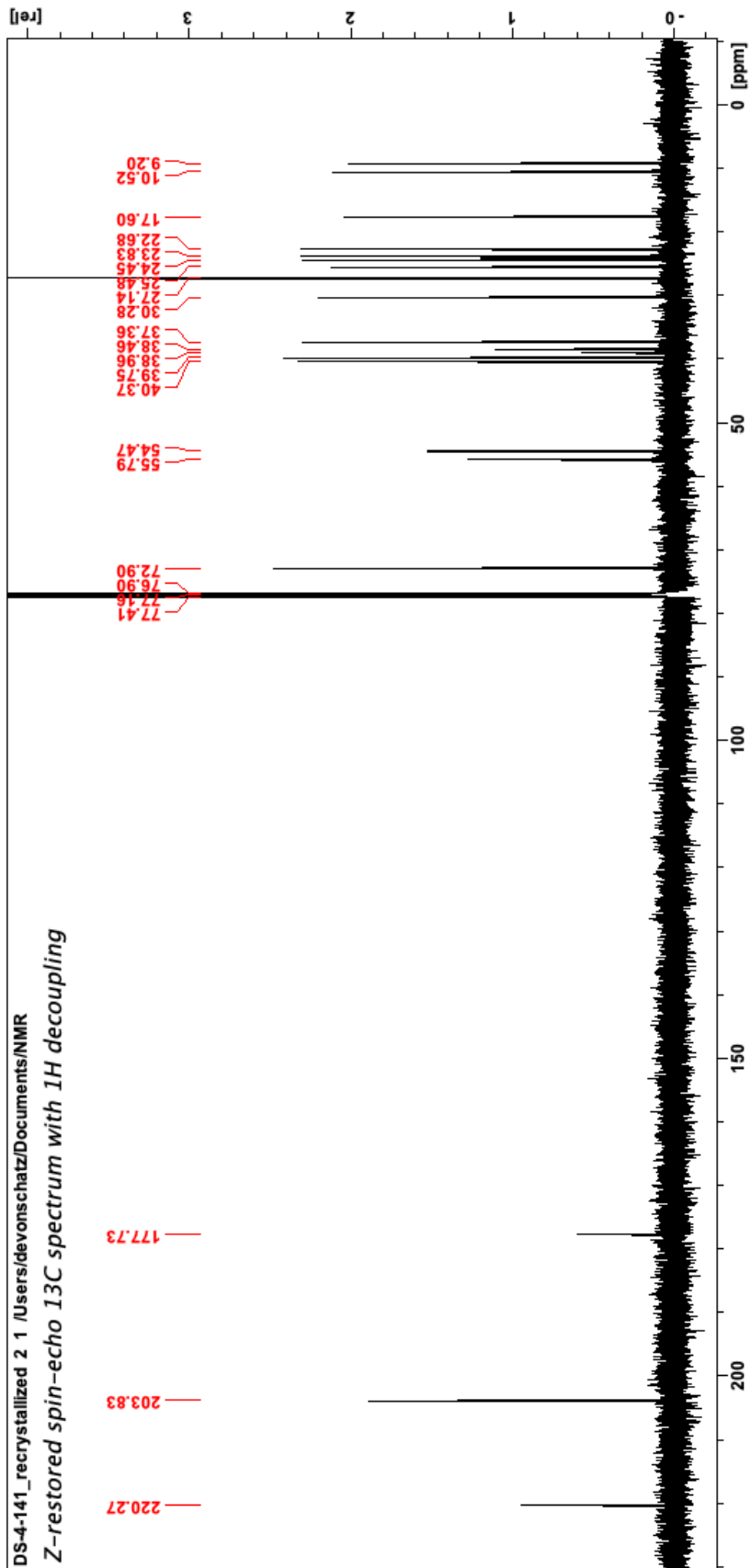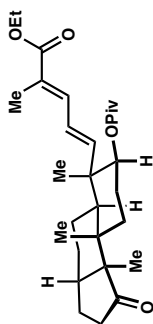DS-4-138_hydroxyaldehyde 3 1 /Users/devonschatz/Documents/NMR
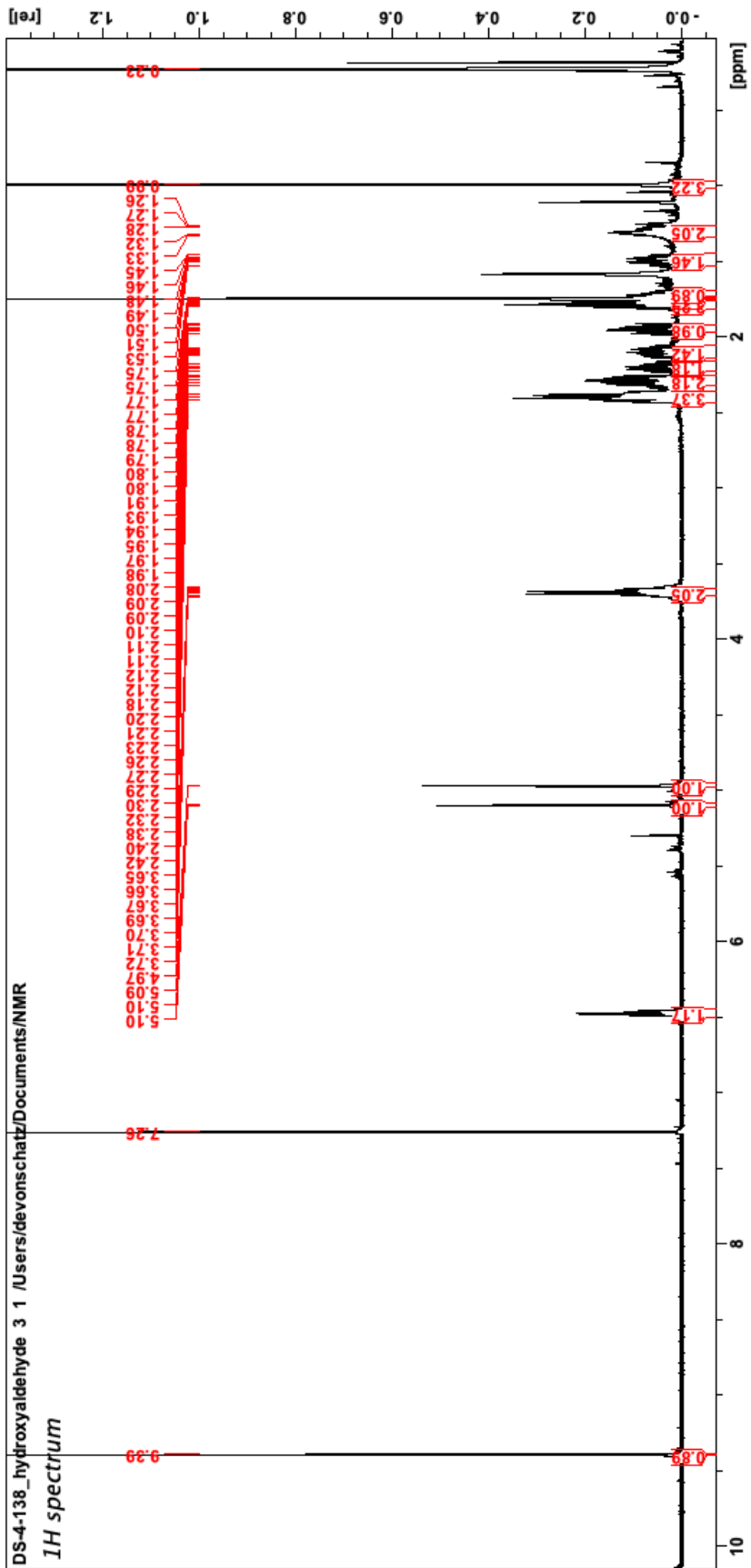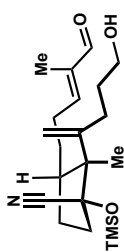
1H spectrum

2.31 (^{13}C NMR, 126 MHz, CDCl$_3$)

DS-4-138_hydroxyaldehyde 2 1 /Users/devonschatz/Documents/NMR

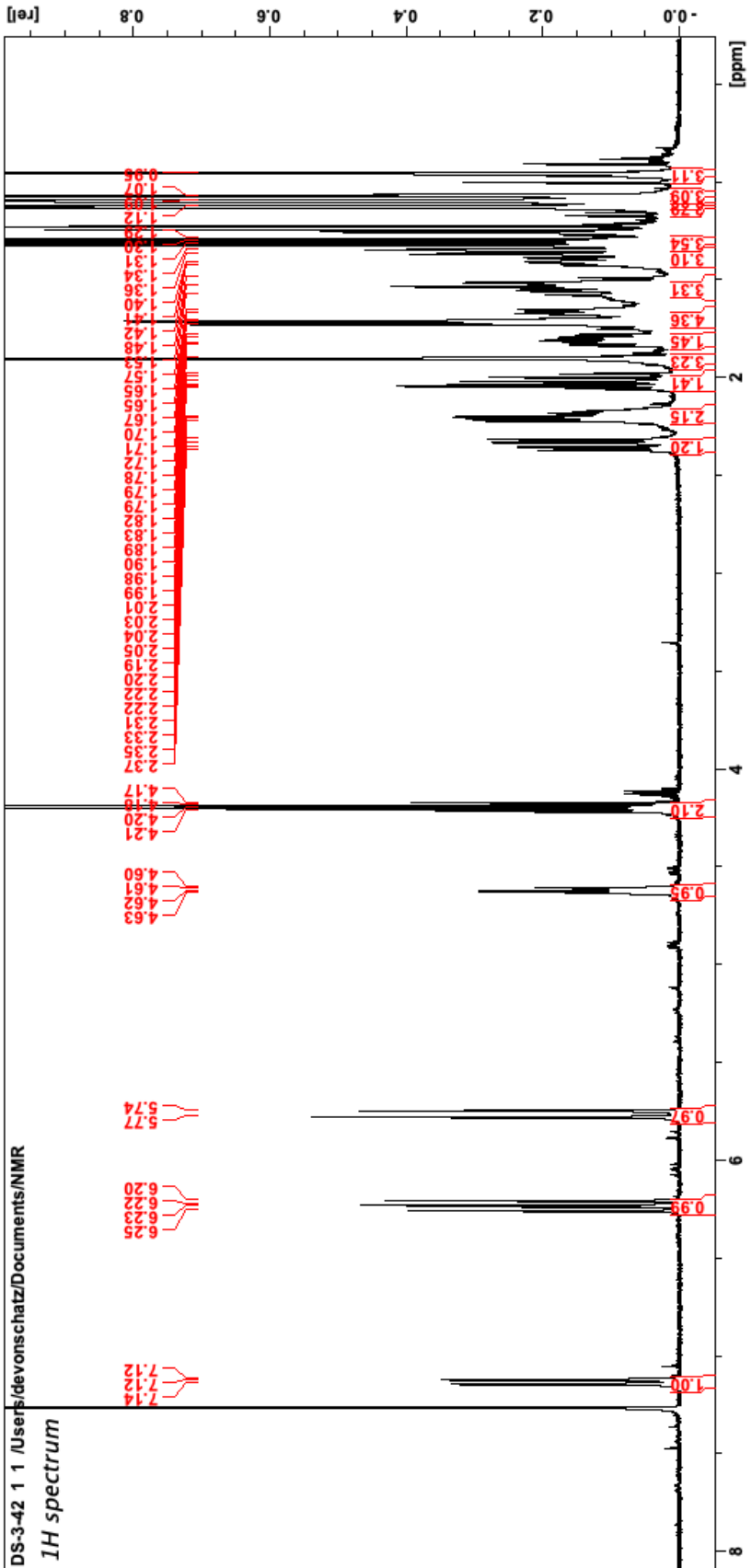*Z-restored spin-echo 13C spectrum with 1H decoupling*
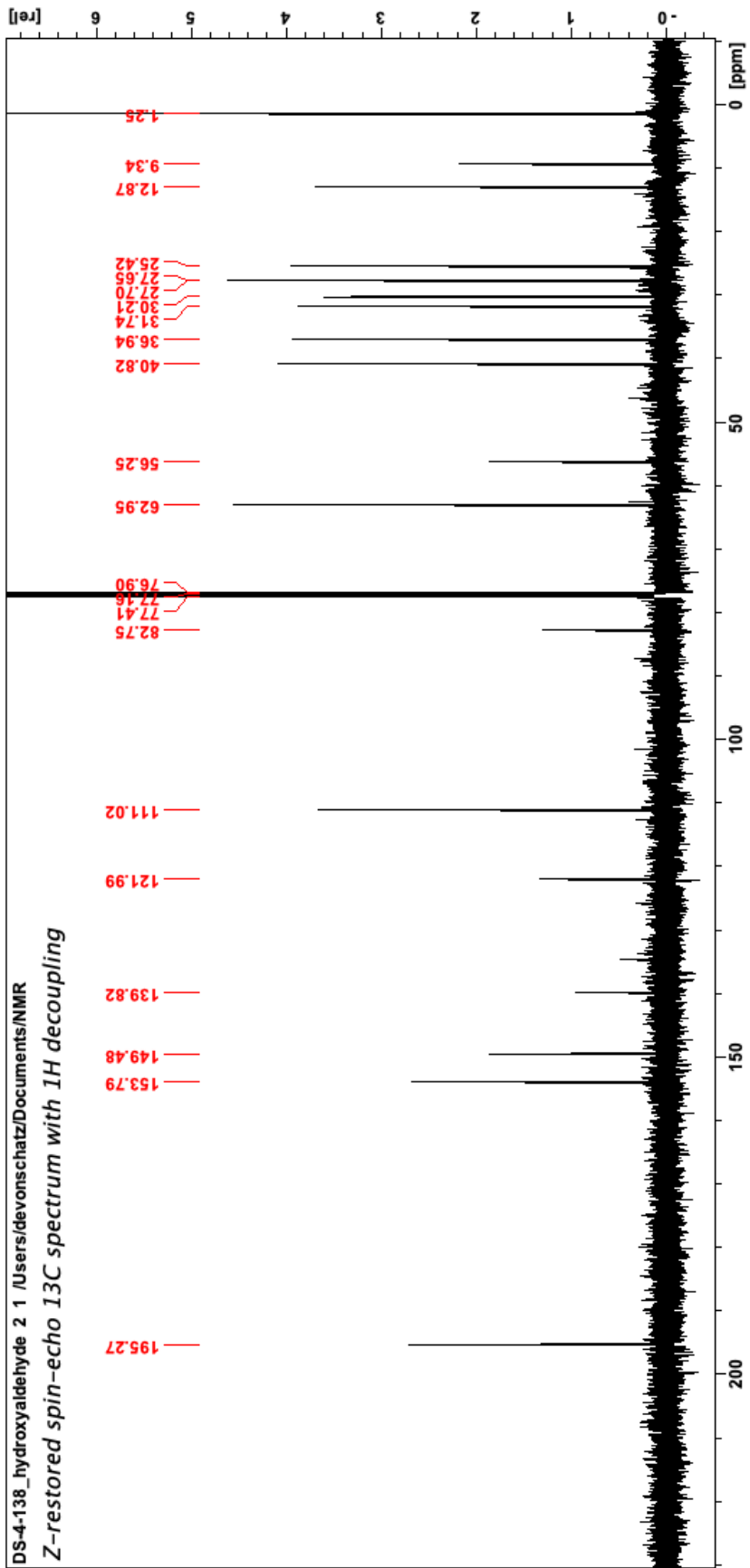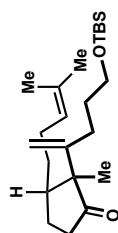
S2.1 (1H NMR, 500 MHz, CDCl$_3$)

DS-1-11 4 1 /Users/devonschatz/Documents/NMR

1H spectrum

222
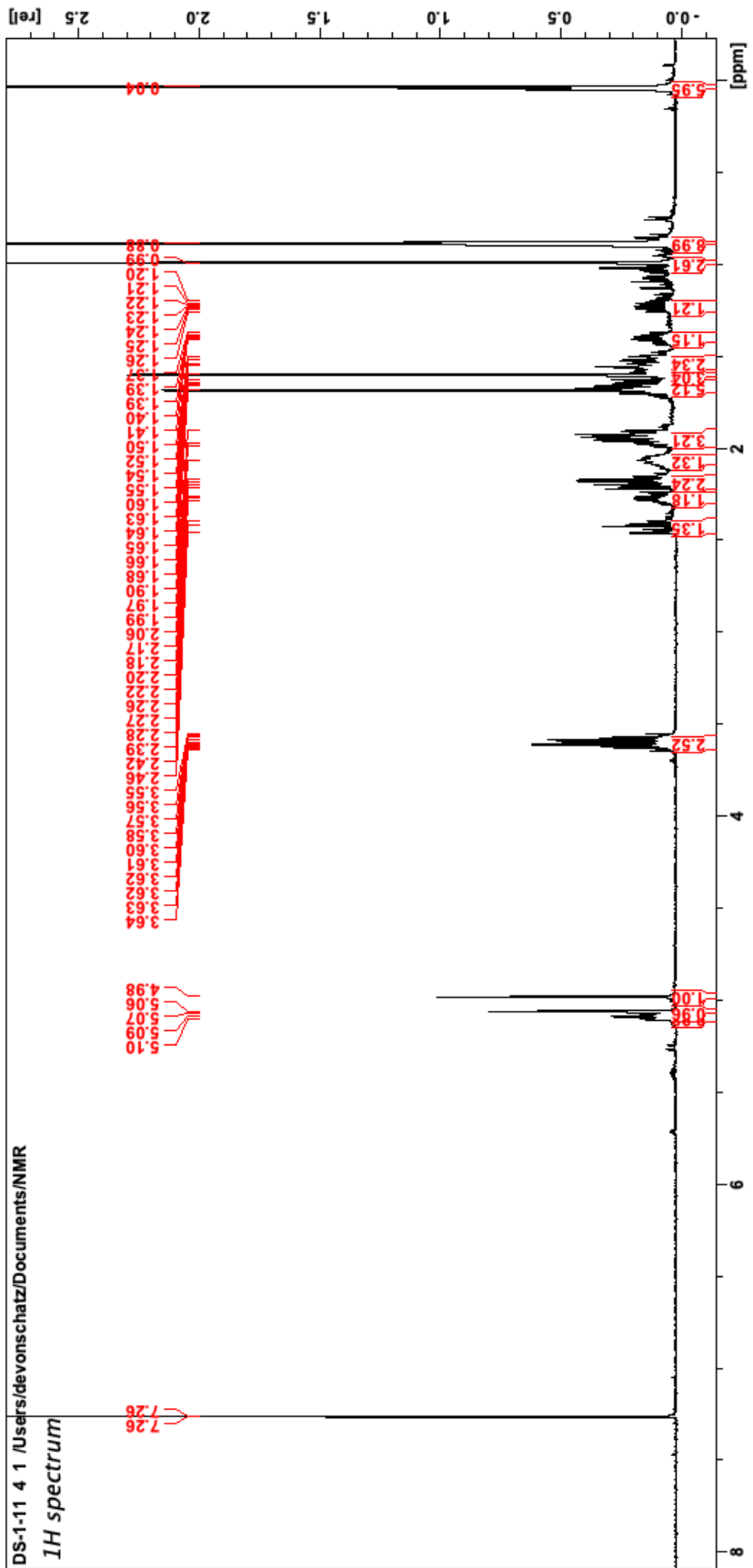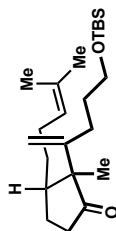
S2.1 (^{13}C NMR, 126 MHz, CDCl$_3$)

DS-1-11 3 1 /Users/devonschatz/Documents/NMR

Z-restored spin-echo 13C spectrum with 1H decoupling

221.92

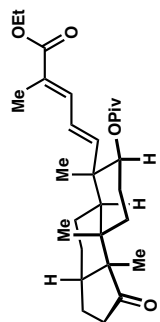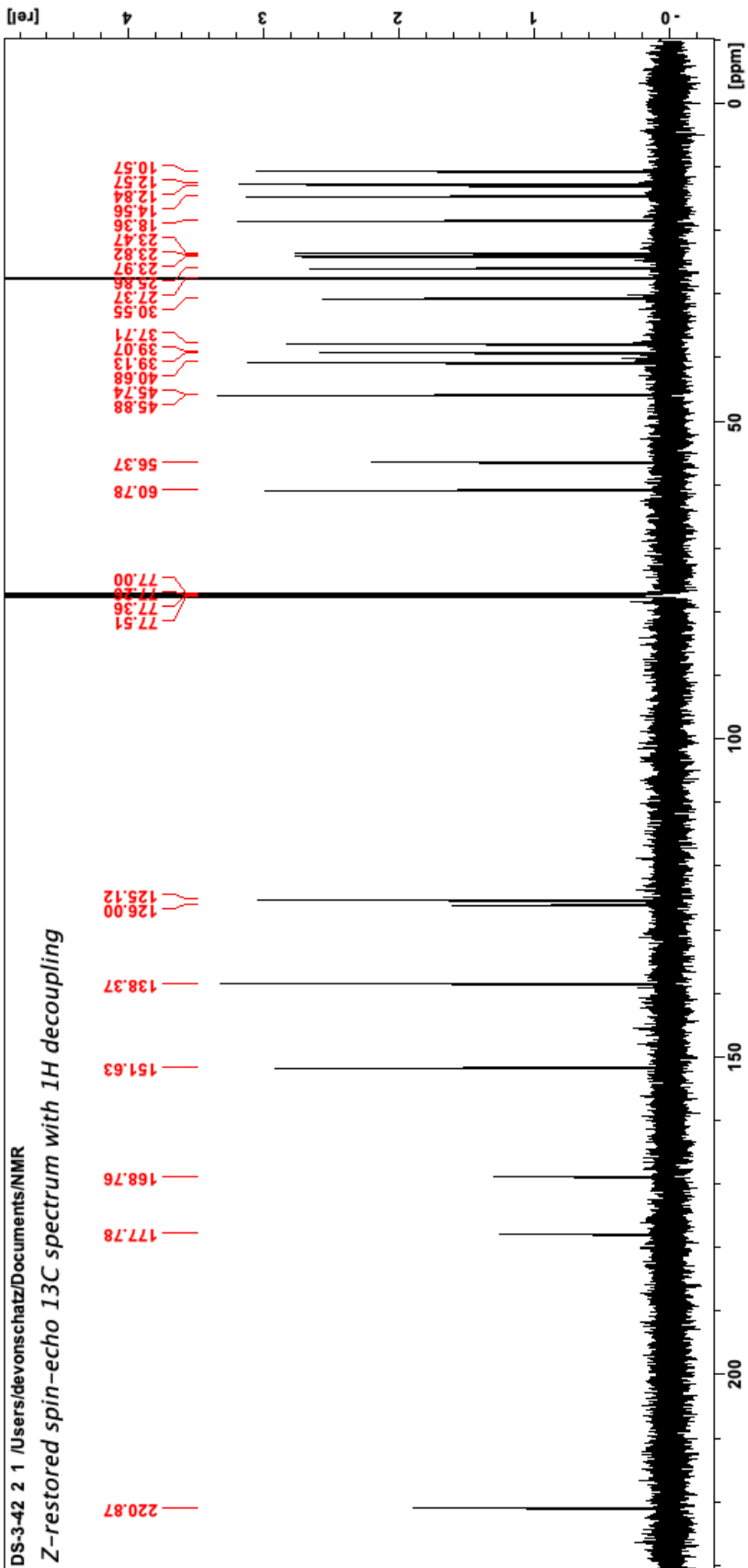149.37

132.03

124.42

112.07

77.41
77.15
76.90

62.98

58.84

43.23

38.01
32.15
29.82
29.18
26.15
26.08
25.84
25.39
18.43
17.82
15.06

−5.13

[rel]

4

3

2

1

0

0   50   100   150   200   [ppm]
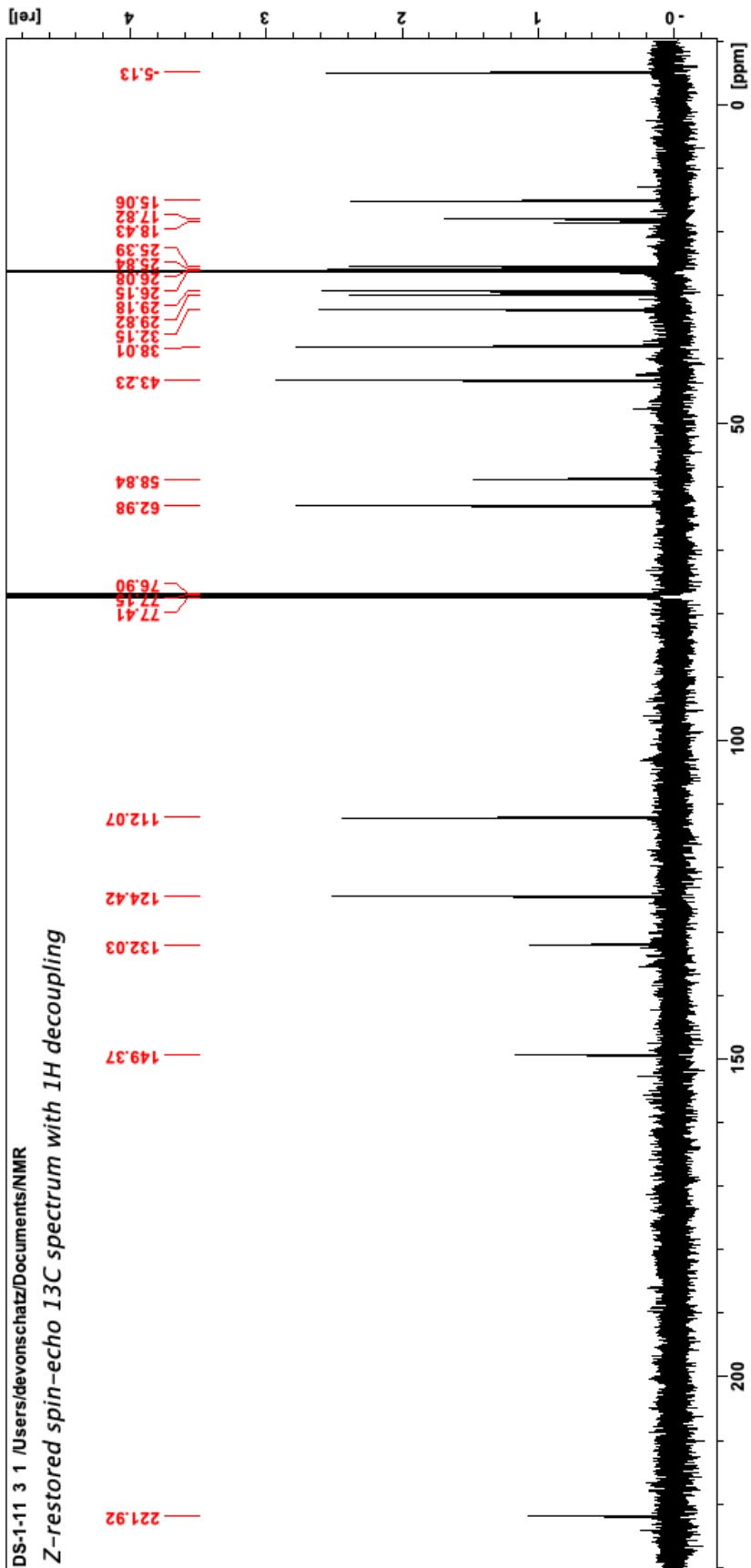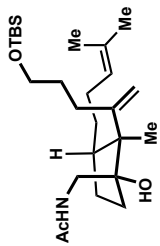
2.30 (1H NMR, 500 MHz, CDCl₃)

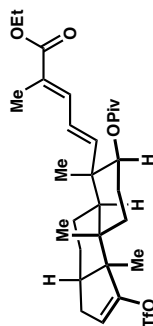DS-1-17 2 1 /Users/devonschatz/Documents/NMR

1H spectrum

224
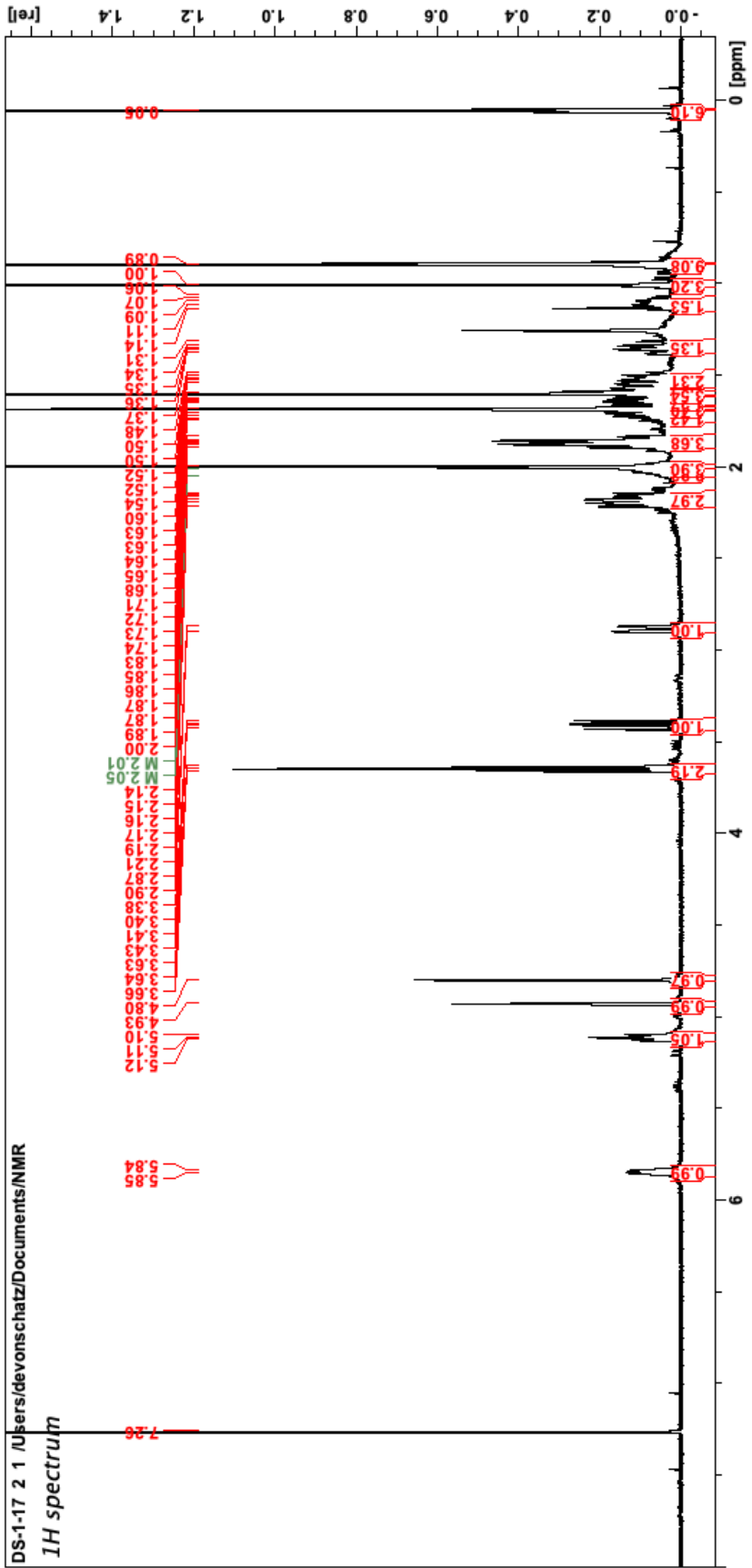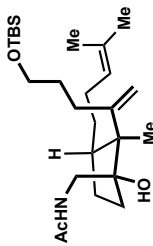
2.30 (^{13}C NMR, 126 MHz, CDCl$_3$)

DS-1-17 3 1 /Users/devonschatz/Documents/NMR

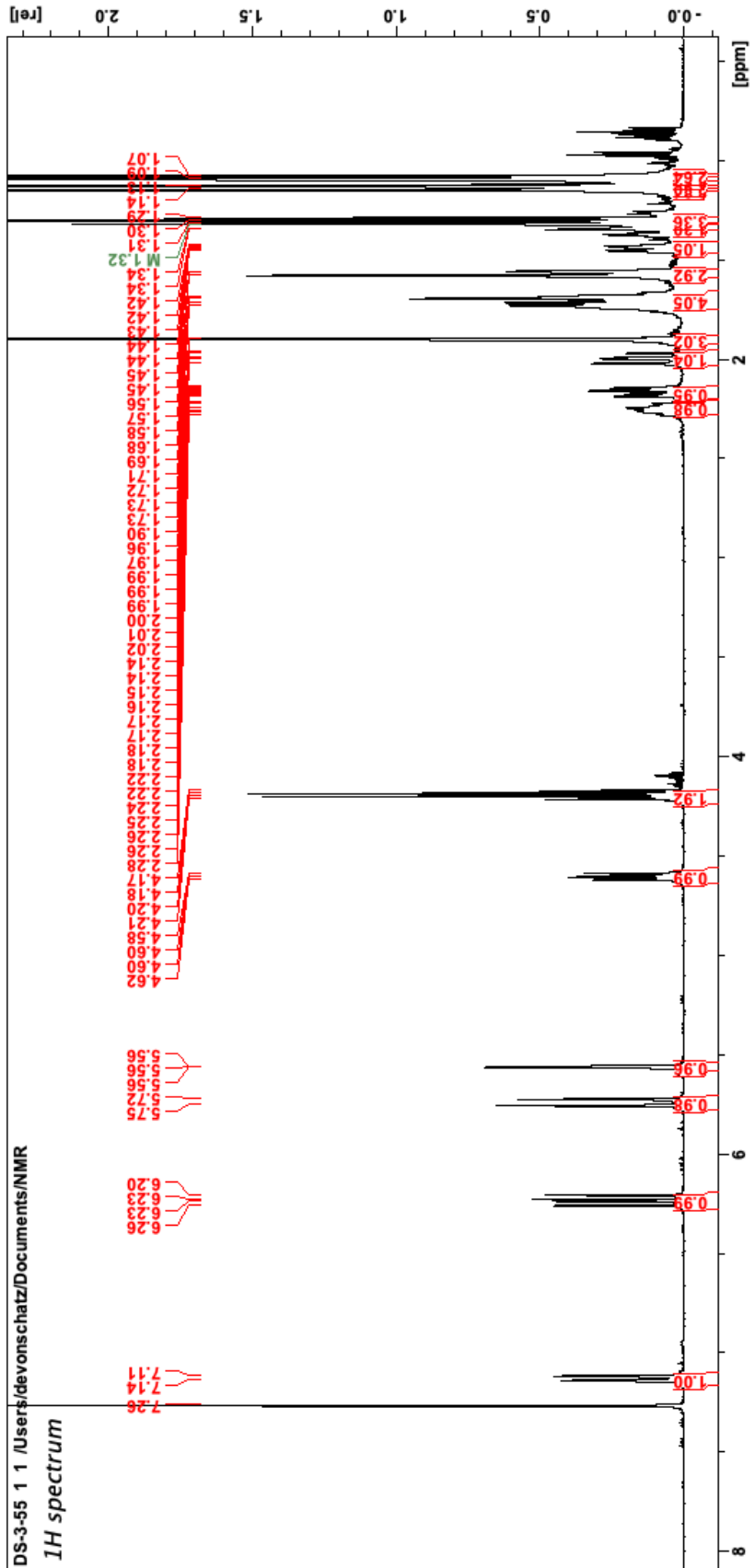Z-restored spin-echo 13C spectrum with 1H decoupling

225
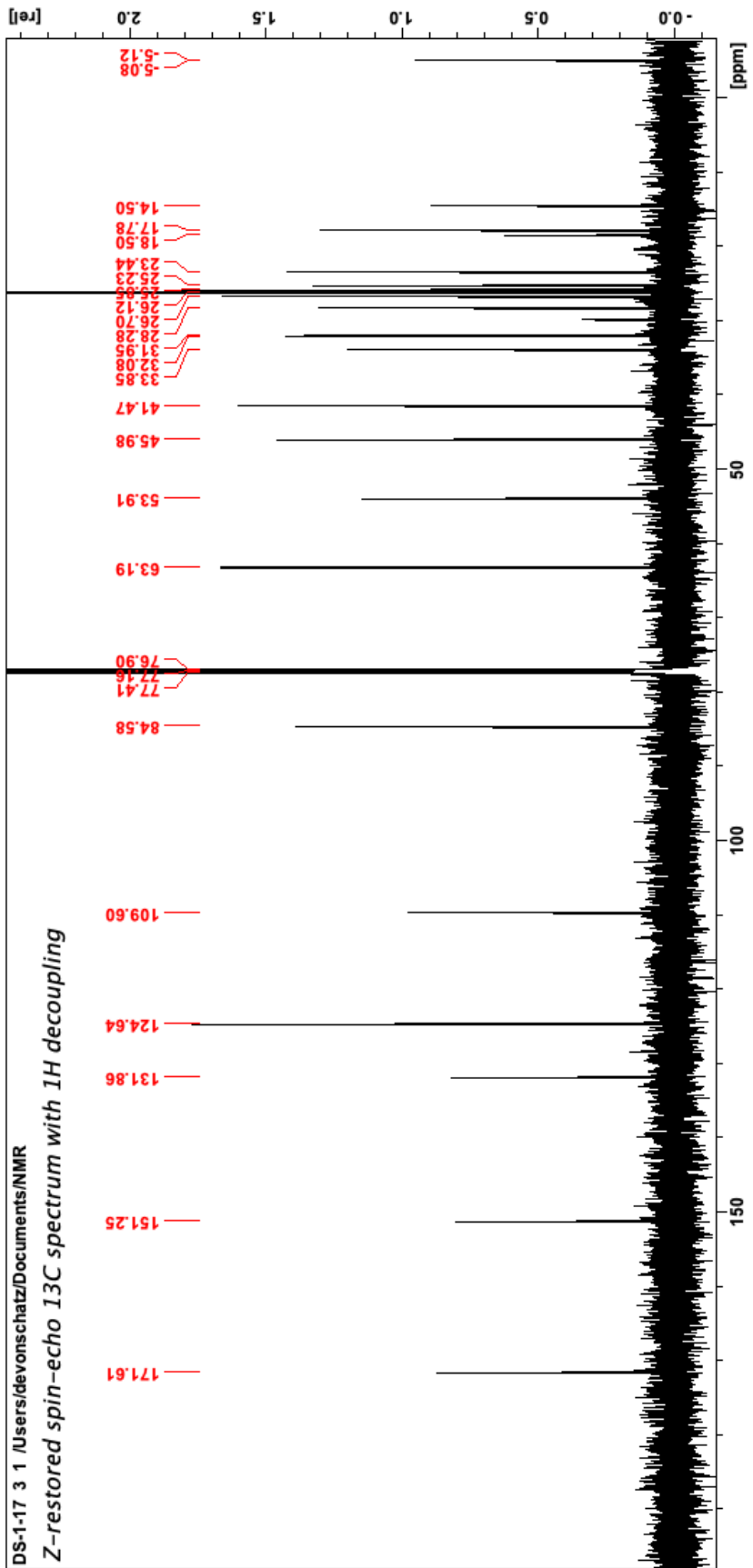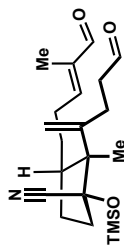
2.32 (^{1}H NMR, 500 MHz, CDCl$_3$)
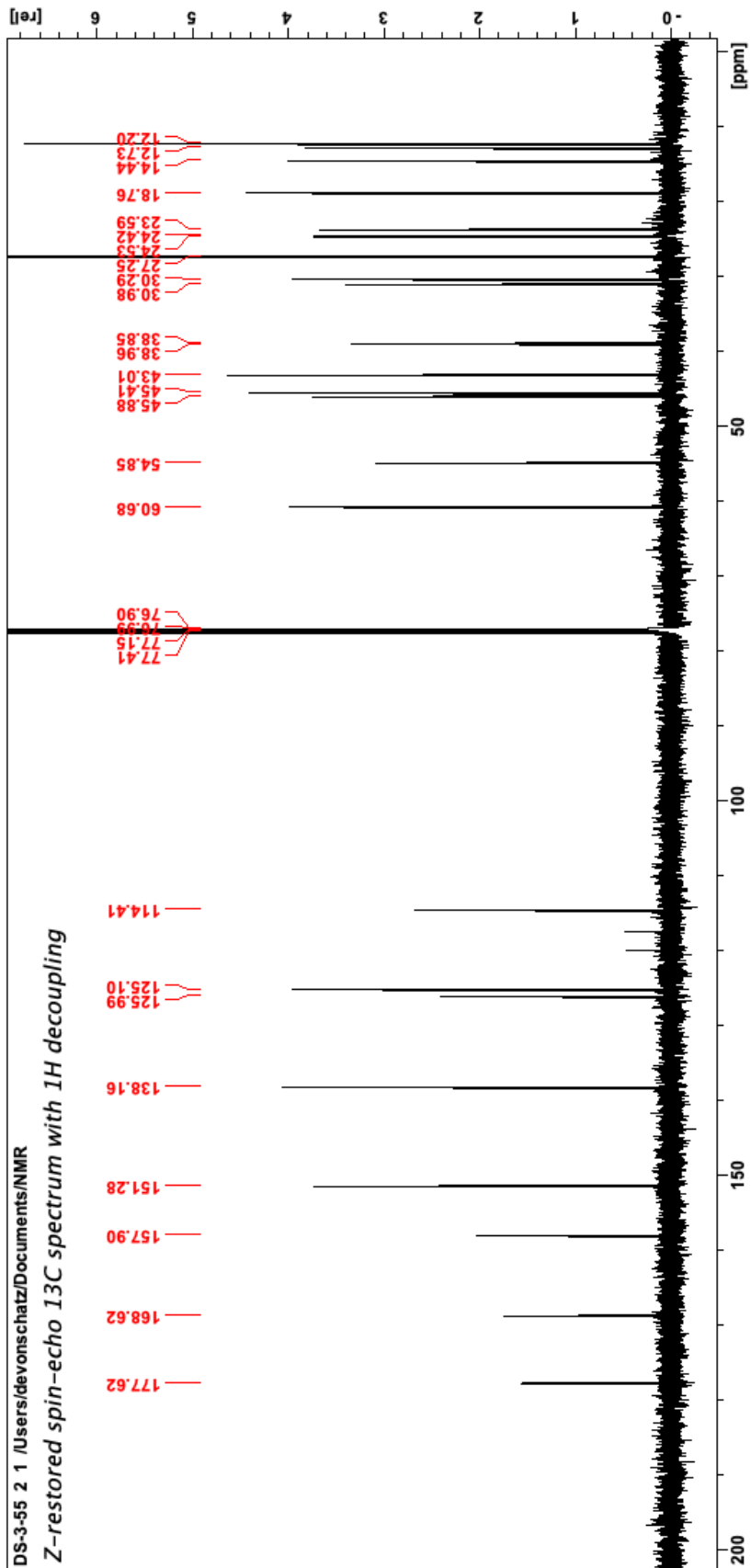
DS-1-97 1 1 /Users/devonschatz/Documents/NMR

1H spectrum

226
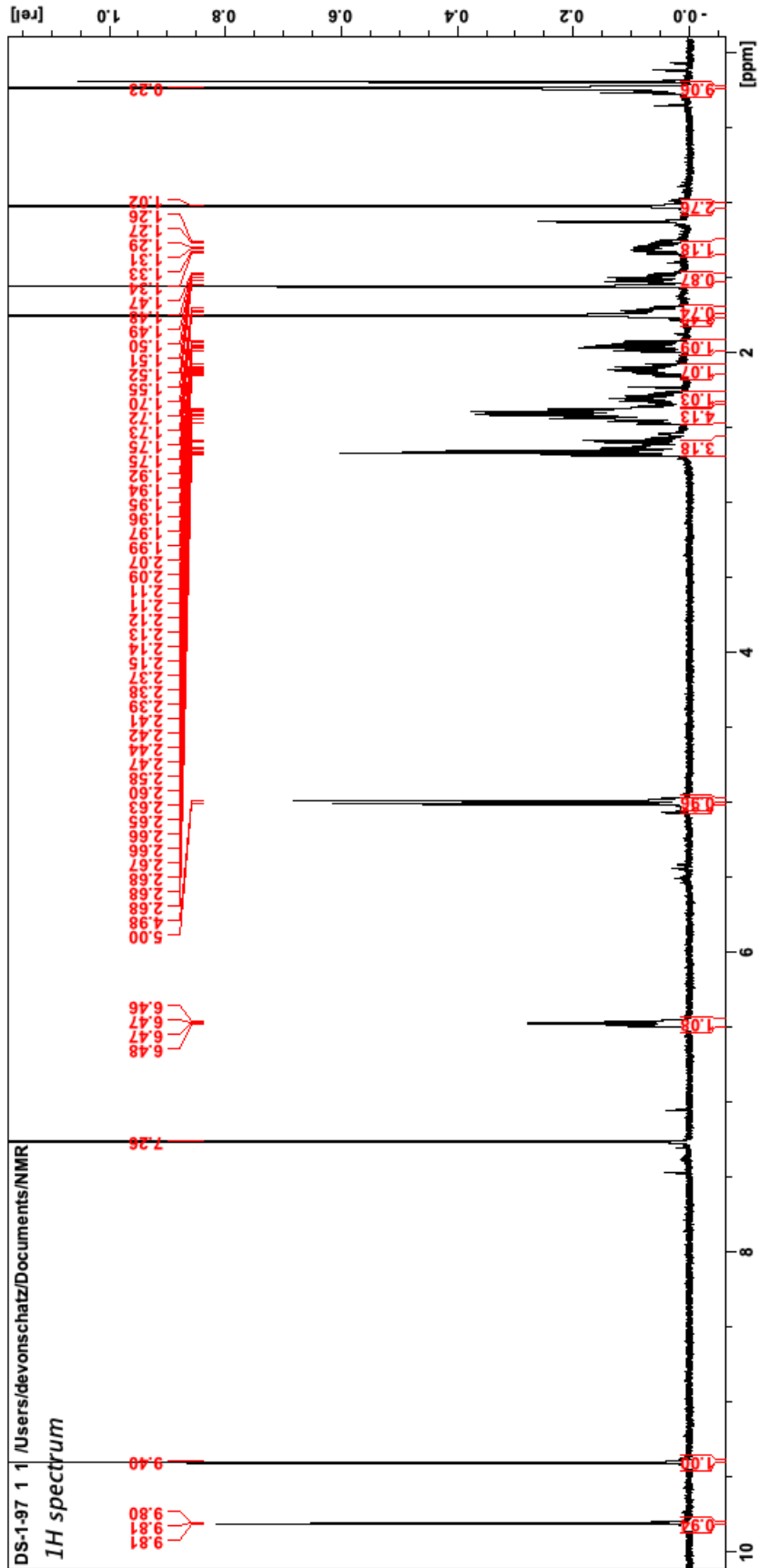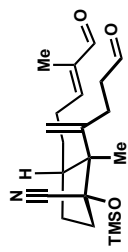
2.32 (^{13}C NMR, 126 MHz, CDCl$_3$)

DS-1-65 3 1 /Users/devonschatz/Documents/NMR

Z–restored spin–echo 13C spectrum with 1H decoupling

202.14
195.26
153.63
148.49
139.86
121.82
111.47
82.71
77.41
77.16
76.90
56.24
42.84
40.79
36.71
30.13
27.60
25.39
23.81
12.81
9.36
1.24
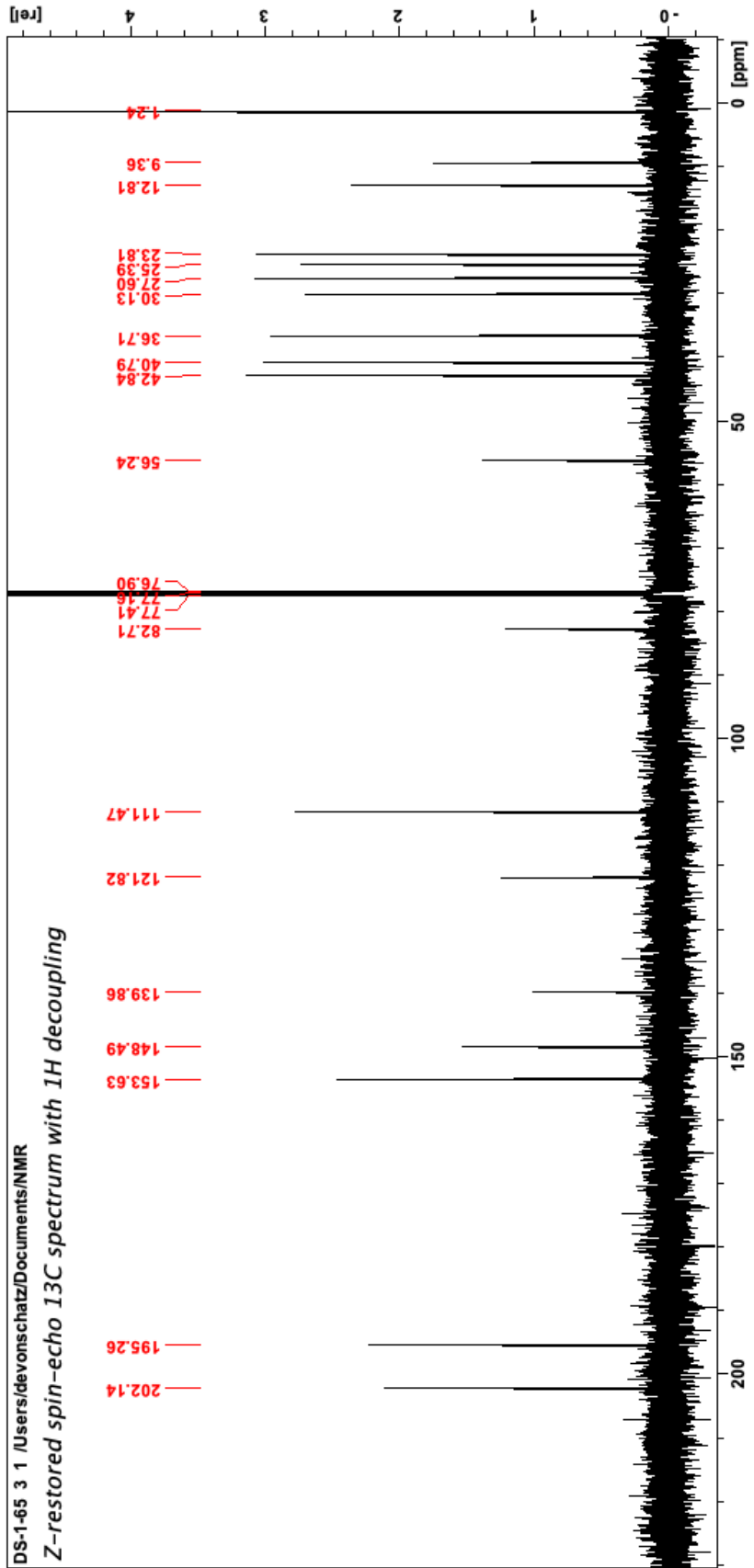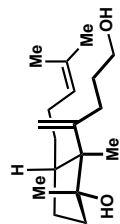
S2.2 (^{1}H NMR, 500 MHz, CDCl$_3$)

DS-4-148 2 1 /Users/devonschatz/Documents/NMR
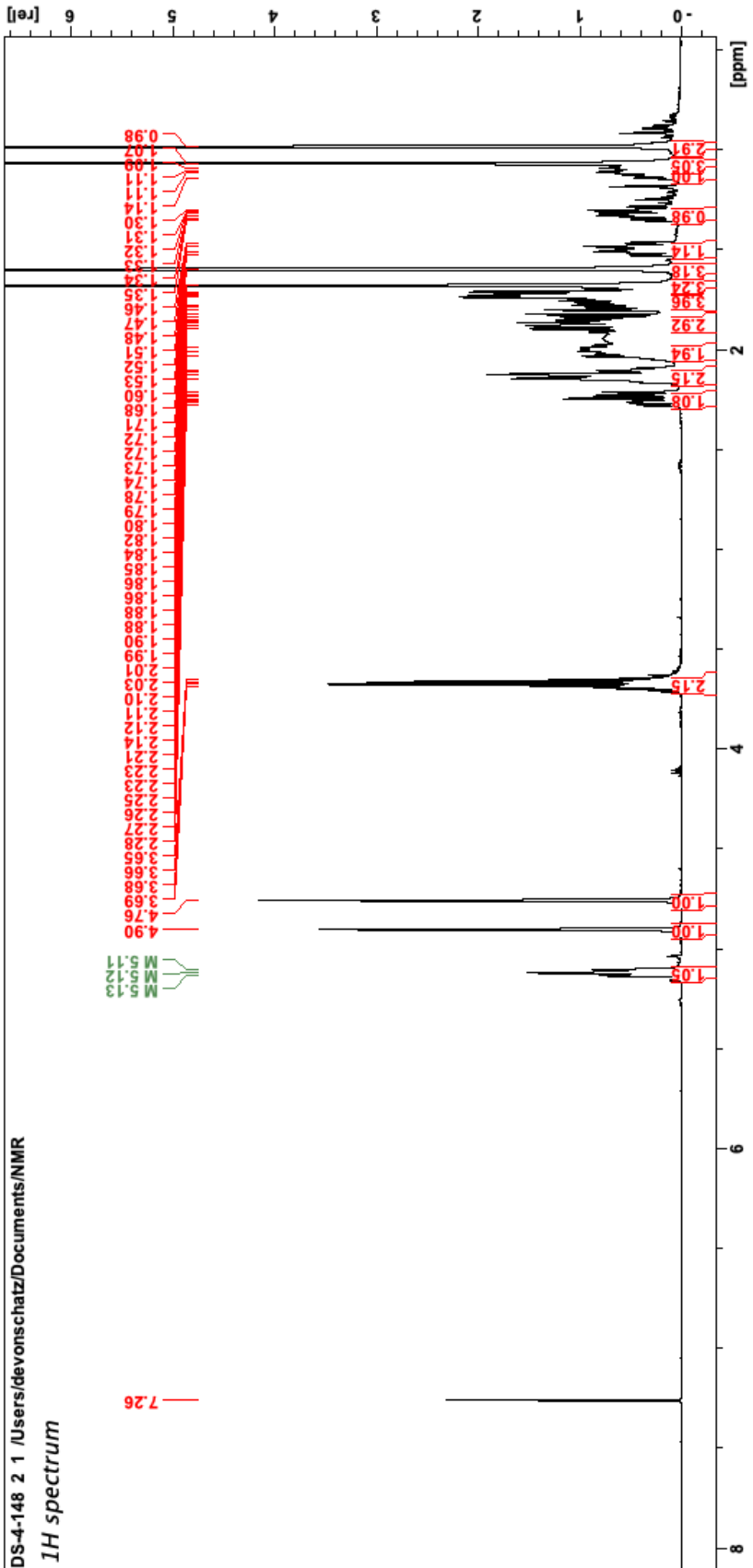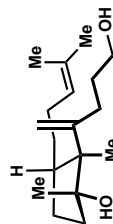
1H spectrum

S2.2 (^{13}C NMR, 126 MHz, CDCl$_3$)

DS-4-148 4 1 /Users/devonschatz/Documents/NMR

Z–restored spin–echo 13C spectrum with 1H decoupling

14.42
17.73
25.35
25.82
26.56
26.76
27.88
31.64
32.22
38.58
41.55
54.37
62.70
76.91
77.16
77.41
82.14
108.92
124.82
131.64
151.58

229
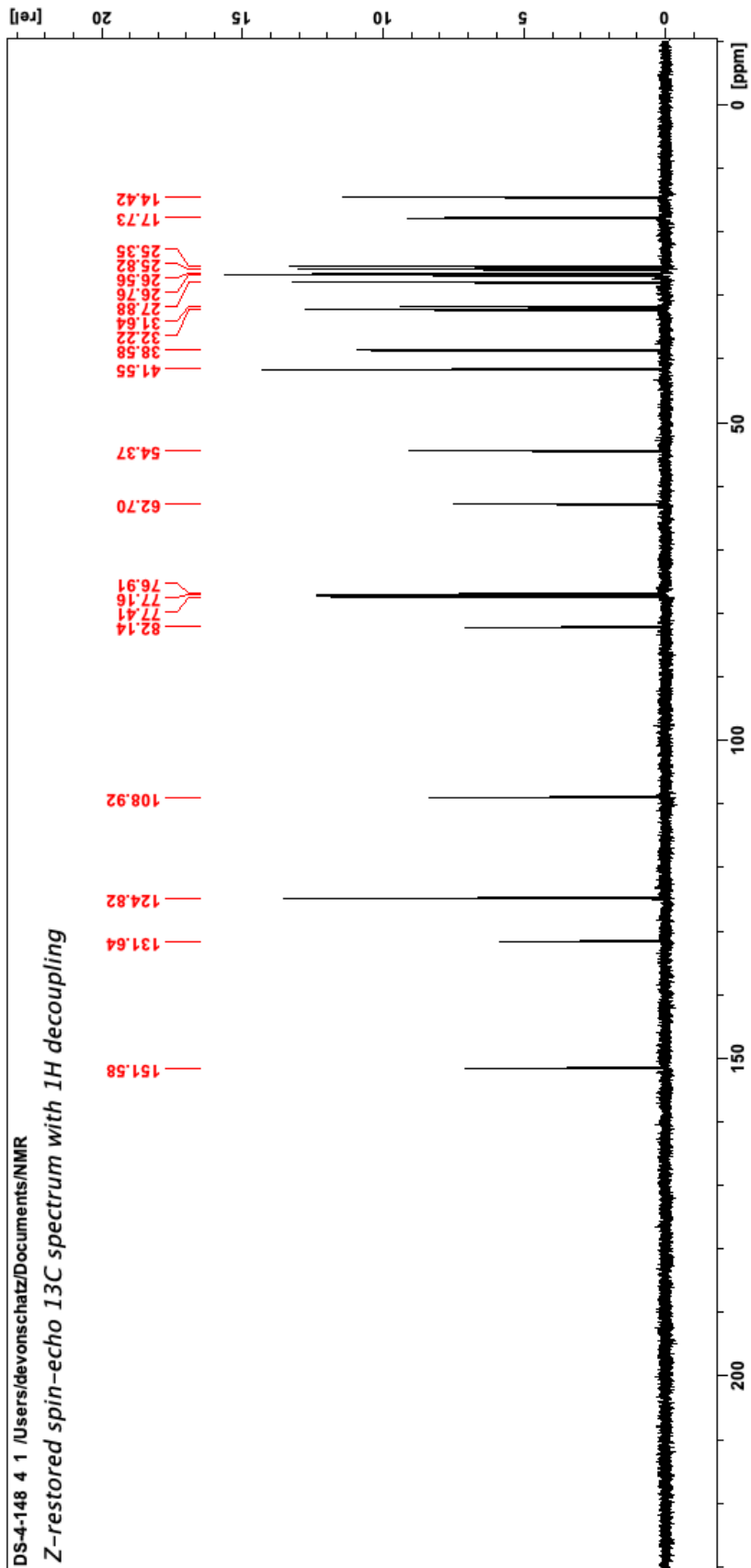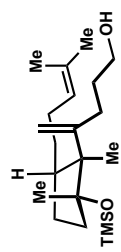
S2.3 (1H NMR, 500 MHz, CDCl₃)

DS-4-180 1 1 /Users/devonschatz/Documents/NMR
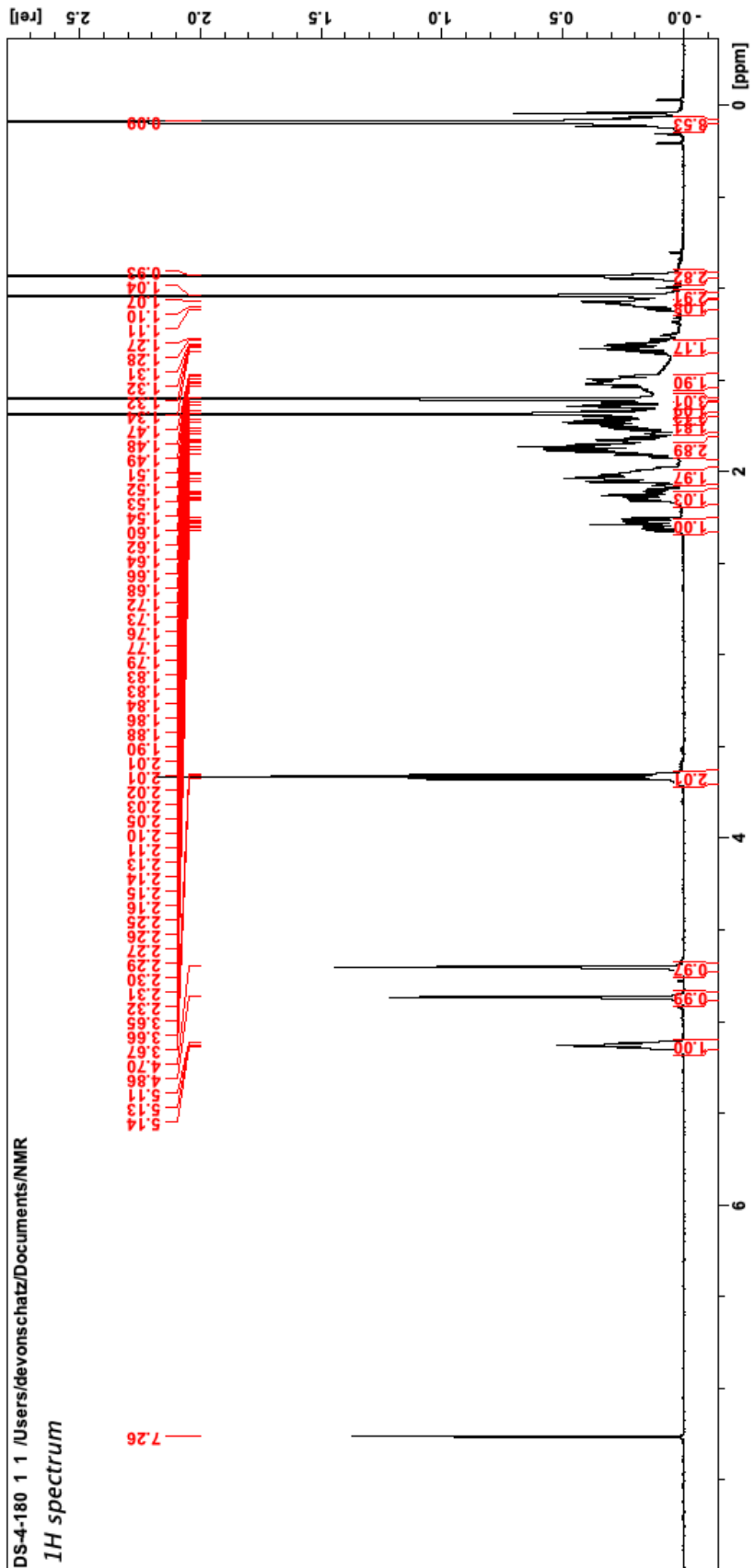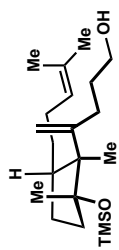
1H spectrum

S2.3 (^{13}C NMR, 126 MHz, CDCl$_3$)

DS-4-180 2 1 /Users/devonschatz/Documents/NMR

Z–restored spin–echo 13C spectrum with 1H decoupling

Peaks: 2.40, 14.90, 17.74, 25.83, 25.90, 26.88, 27.21, 27.35, 32.02, 32.33, 37.88, 40.35, 55.30, 63.38, 76.90, 77.16, 77.41, 84.29, 108.36, 124.97, 131.54, 152.28
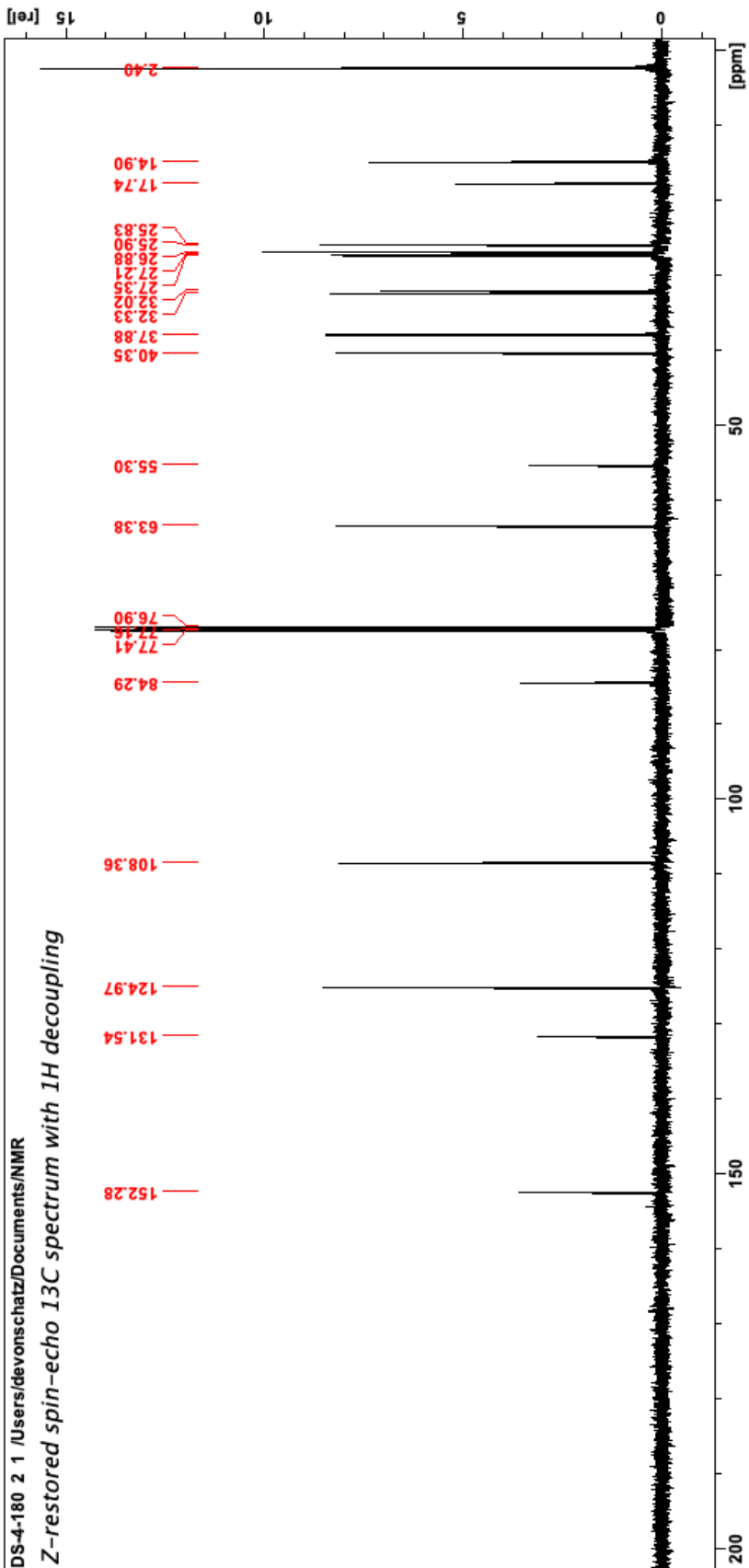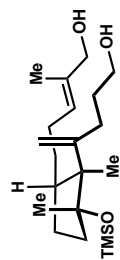
S2.4 (¹H NMR, 500 MHz, CDCl₃)

DS-4-155 1 1 /Users/devonschatz/Documents/NMR
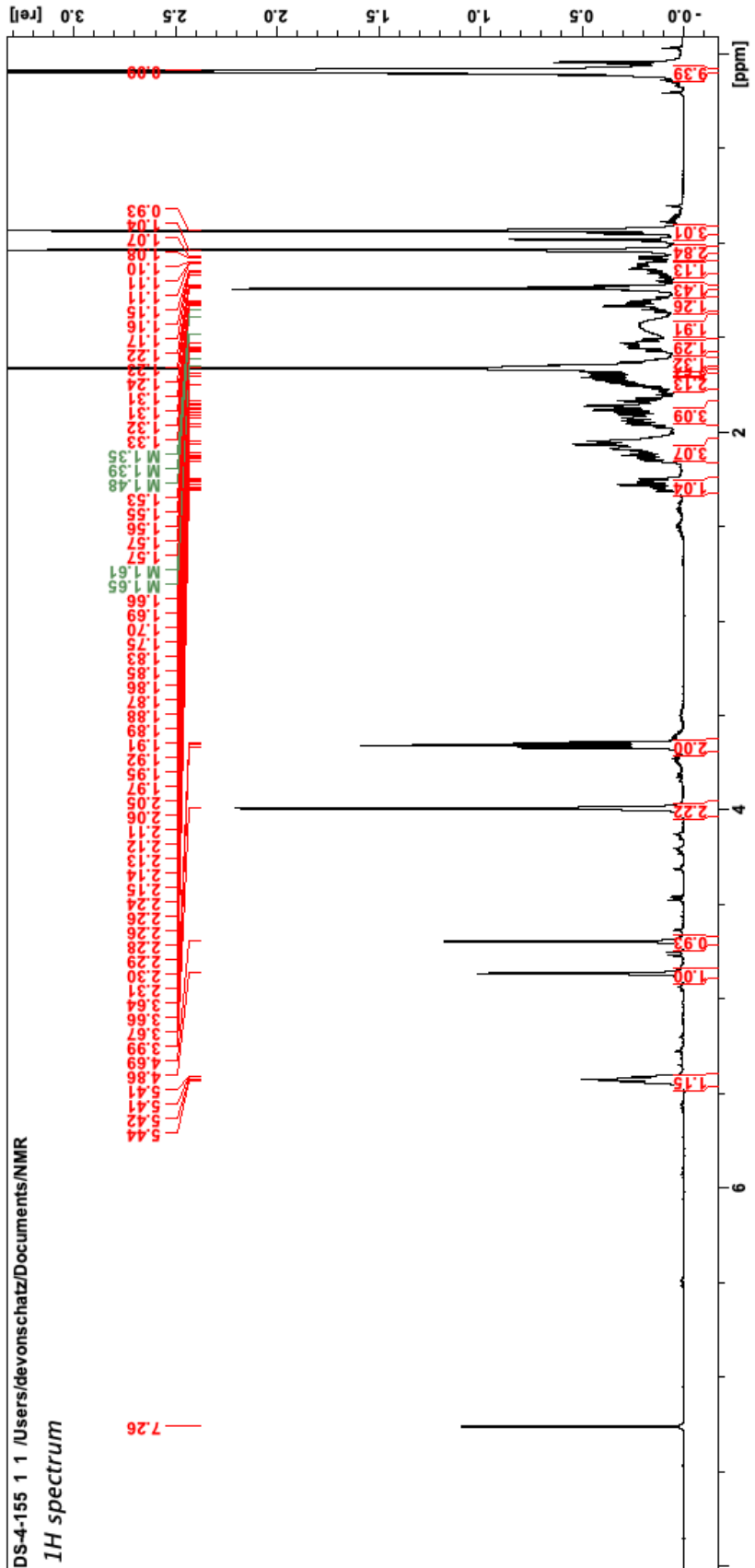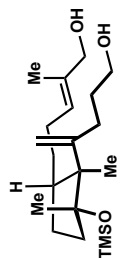
1H spectrum

S2.4 (^{13}C NMR, 126 MHz, CDCl$_3$)

DS-4-155 2 1 /Users/devonschatz/Documents/NMR

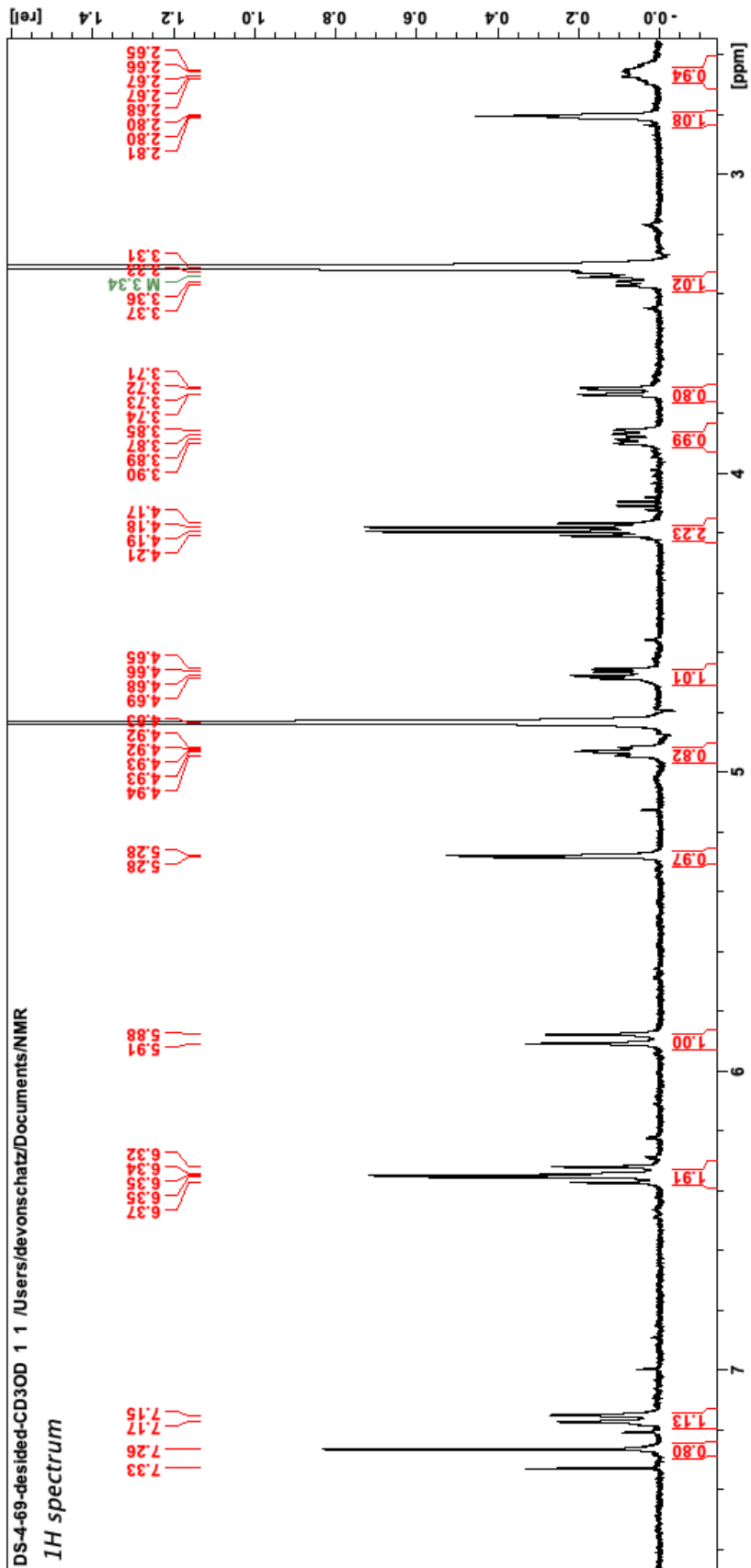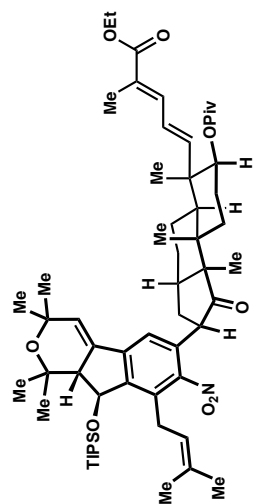*Z-restored spin-echo 13C spectrum with 1H decoupling*
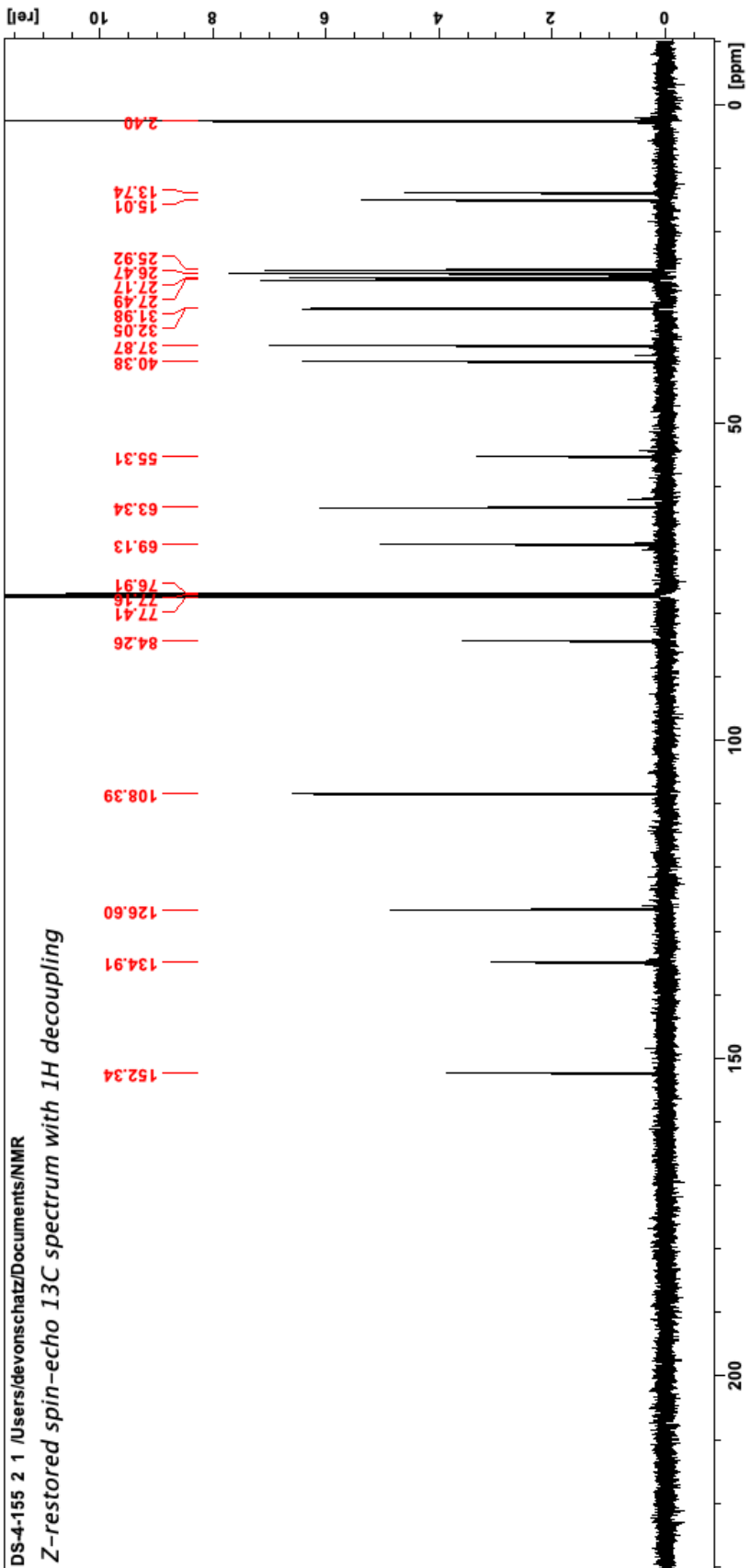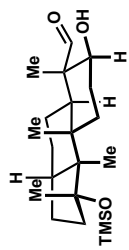
2.36 (¹H NMR, 500 MHz, CDCl₃)

DS-4-185 2 1 /Users/devonschatz/Documents/NMR

1H spectrum

234
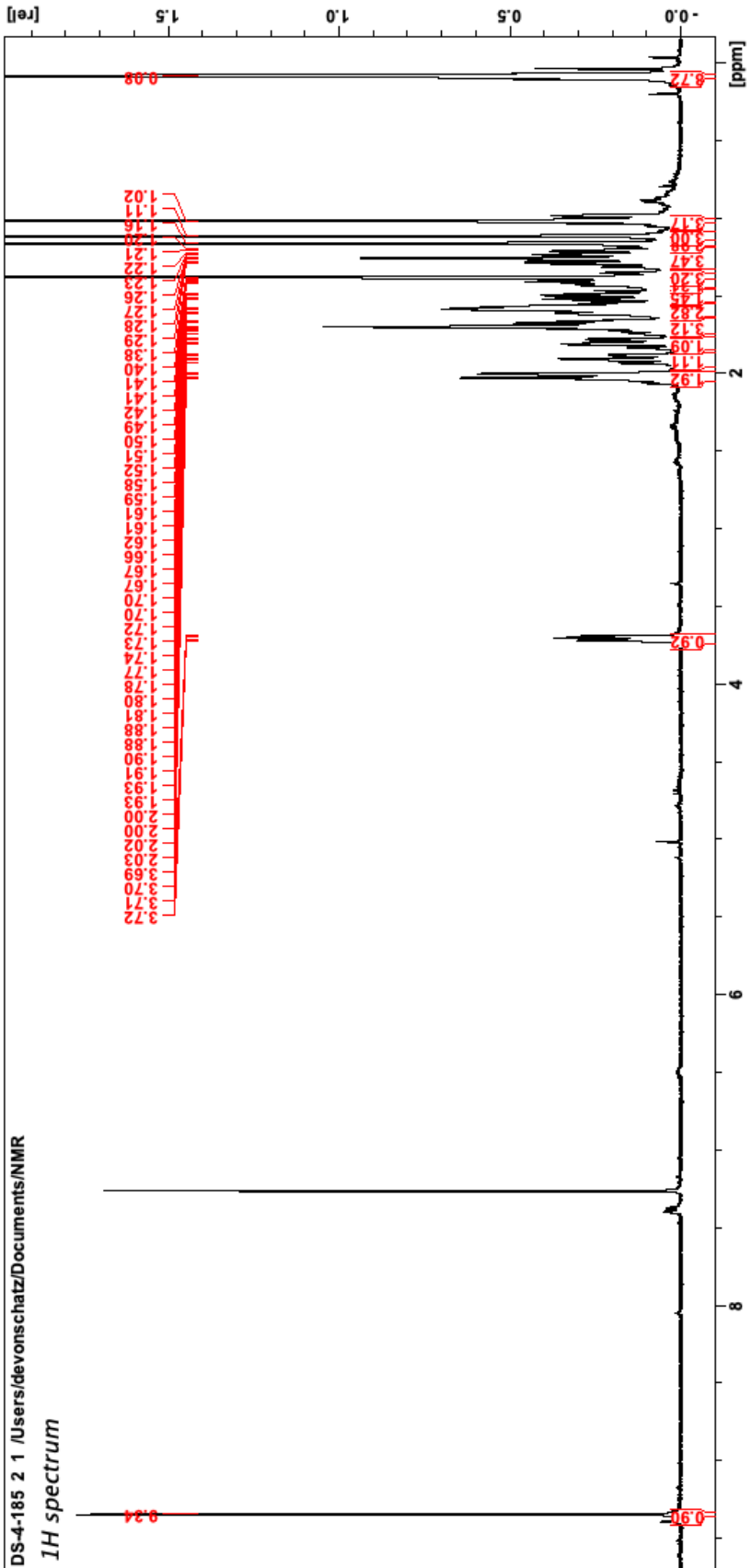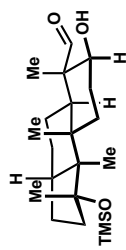
2.36 (^{13}C NMR, 126 MHz, CDCl$_3$)

DS-4-185 3 1 /Users/devonschatz/Documents/NMR

Z-restored spin-echo 13C spectrum with 1H decoupling

206.86

86.97

77.41
77.16
76.91
72.33

55.06
54.01

41.59
41.25
39.94
37.27
32.00
31.70
27.44
26.55
25.56
24.18

19.30

13.05

9.64

2.53

235
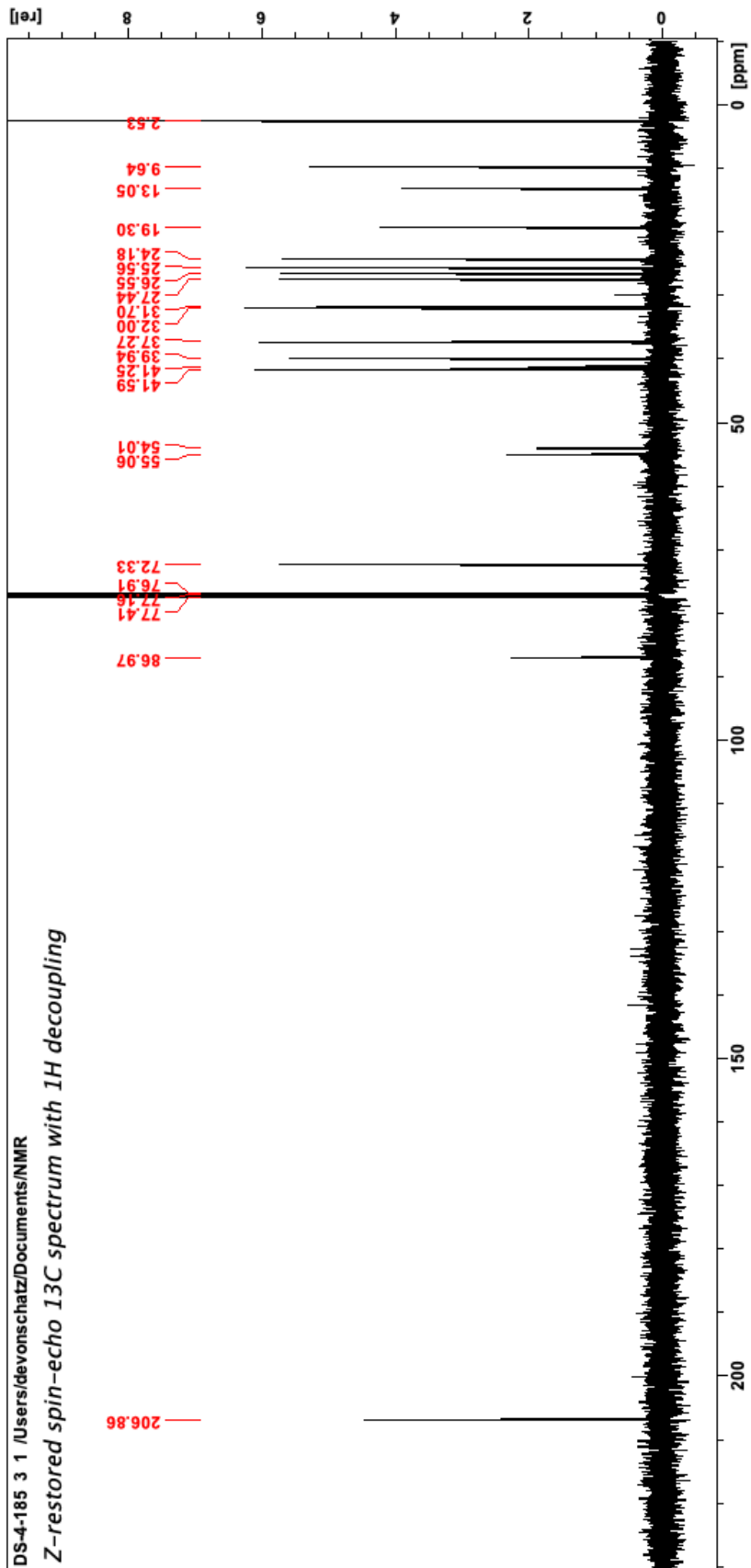
2.82 (^{1}H NMR, 500 MHz, CDCl$_3$)

DS-4-141_recrystallized 1 1 /Users/devonschatz/Documents/NMR

1H spectrum

236

2.82 (^{13}C NMR, 126 MHz, CDCl$_3$)

DS-4-141_recrystallized 2 1 /Users/devonschatz/Documents/NMR

Z–restored spin–echo 13C spectrum with 1H decoupling

237

DS-3-42 1 1 /Users/devonschatz/Documents/NMR

1H spectrum

2.22 (¹H NMR, 500 MHz, CDCl₃)

238

2.22 (^{13}C NMR, 126 MHz, CDCl$_3$)

DS-3-42 2 1 /Users/devonschatz/Documents/NMR

Z-restored spin-echo 13C spectrum with 1H decoupling

239

Me
OEt
O
OPiv
Me
H
H
Me
Me
H
Me
H
TfO

2.97 (¹H NMR, 500 MHz, CDCl₃)

DS-3-55 1 1 /Users/devonschatz/Documents/NMR

1H spectrum

[rel]

2.0   1.5   1.0   0.5   0.0   [ppm]

1.07
1.09
1.11
1.14
1.29
1.30
1.31
M 1.32
1.34
1.34
1.42
1.42
1.43
1.43
1.44
1.44
1.45
1.56
1.57
1.58
1.68
1.69
1.71
1.72
1.73
1.73
1.90
1.96
1.97
1.99
1.99
2.00
2.01
2.02
2.14
2.14
2.15
2.16
2.17
2.17
2.18
2.18
2.22
2.22
2.22
2.24
2.25
2.26
2.27
2.28
2.28
4.17
4.18
4.20
4.21
4.58
4.60
4.60
4.62

5.55
5.56
5.56
5.72
5.75

6.20
6.23
6.23
6.26

7.11
7.14
7.26

3.47
3.48
3.16
3.36
3.66
1.05
2.92
4.05
3.02
1.04
0.99
0.98
1.92
0.99
0.96
0.96
0.96
1.00

2.97 (^{13}C NMR, 126 MHz, CDCl$_3$)

DS-3-55 2 1 /Users/devonschatz/Documents/NMR

Z-restored spin-echo 13C spectrum with 1H decoupling

177.62
168.62
157.90
151.28
138.16
125.99
125.10
114.41
77.41
77.15
76.99
76.90
60.68
54.85
45.88
45.41
43.01
38.96
38.85
30.98
30.29
27.25
24.55
24.42
23.59
18.76
14.44
12.73
12.20

241

DS-4-69-desided-CD3OD 1 1 /Users/devonschatz/Documents/NMR

2.116a (^{1}H NMR, 500 MHz, CD$_3$OD)

1H spectrum

DS-4-69-desided-CD3OD 1 1 /Users/devonschatz/Documents/NMR

2.116a (¹H NMR, 500 MHz, CD₃OD)

1H spectrum

DS-4-69-desided-CD3OD 1 1 /Users/devonschatz/Documents/NMR

2.116a (¹H NMR, 500 MHz, CD₃OD)

1H spectrum

244

2.116a (^{13}C NMR, 126 MHz, CD$_3$OD)

DS-4-69-desided-CD3OD 2 1 /Users/devonschatz/Documents/NMR

Z–restored spin–echo 13C spectrum with 1H decoupling

245

DS-4-69-desired 4 1 "C:\Users\Nicole\Desktop\Pronin Lab\NMRs"
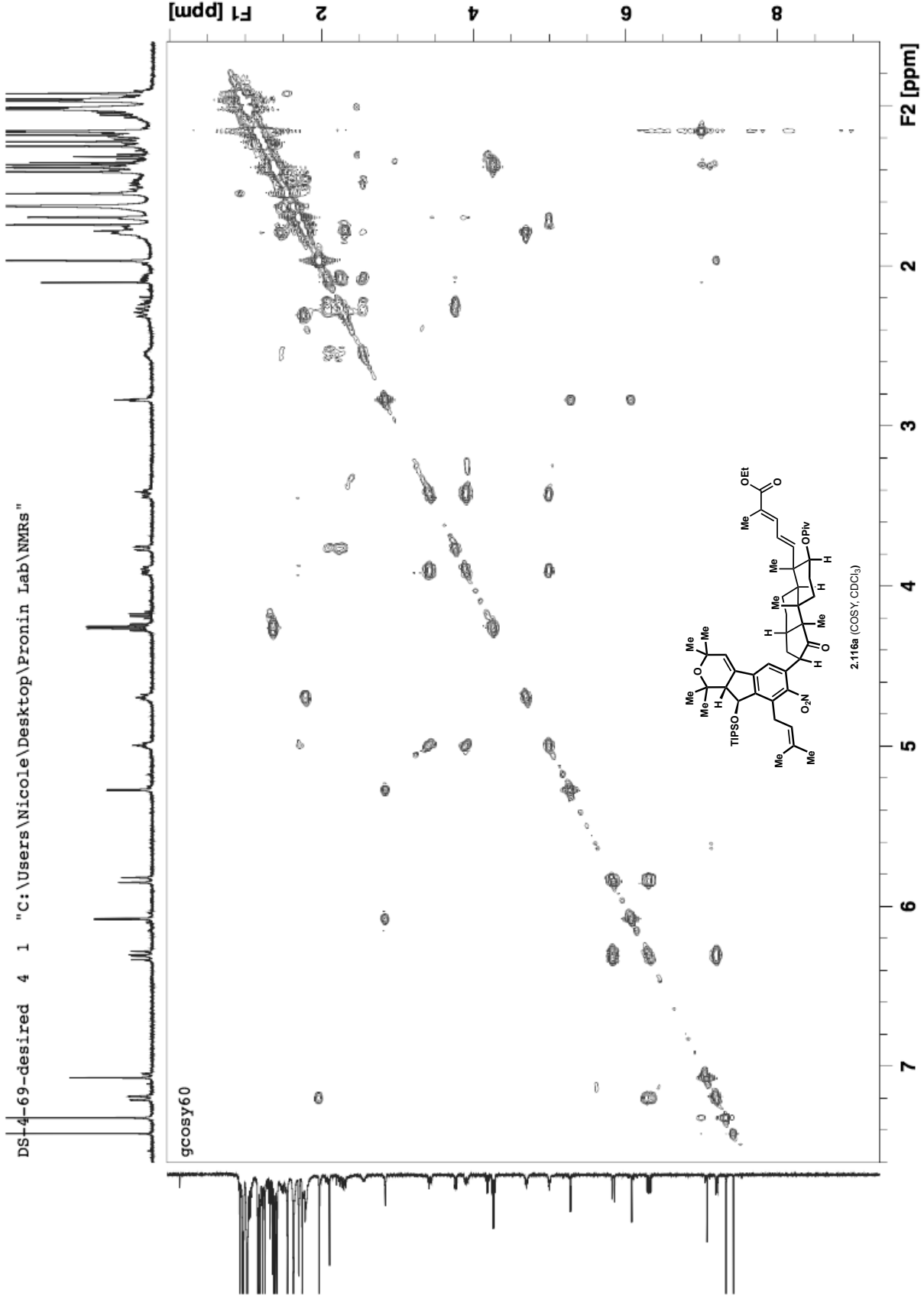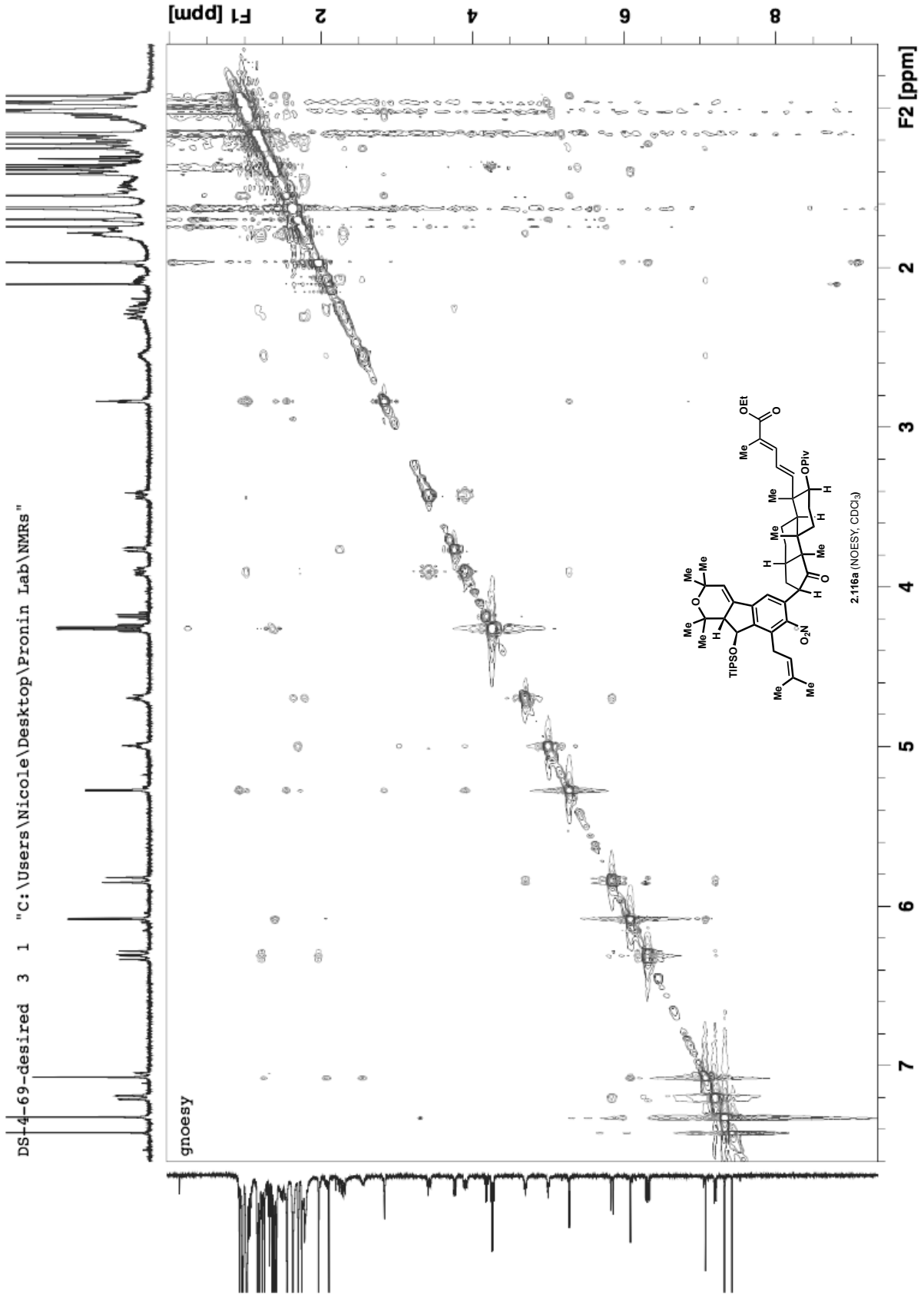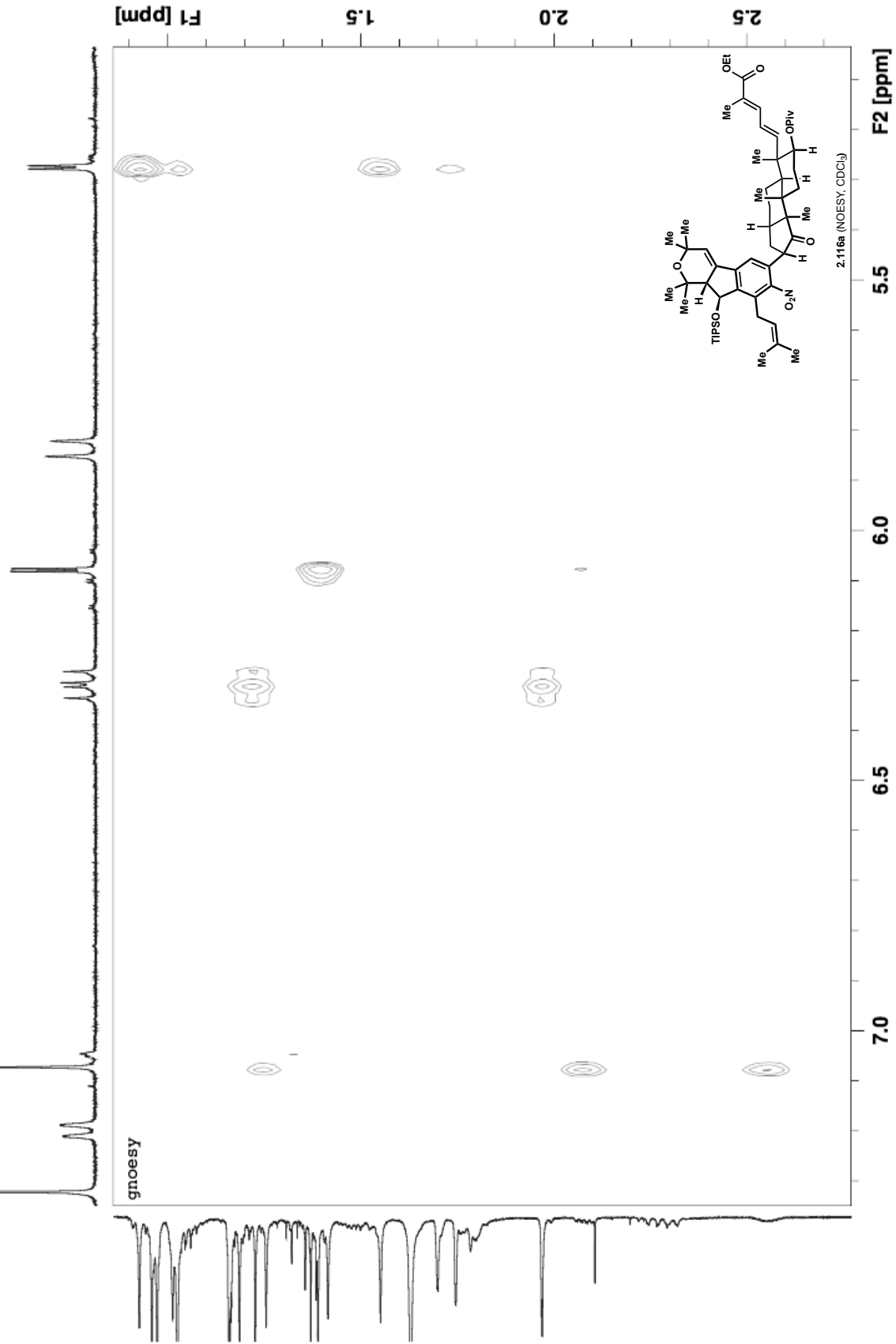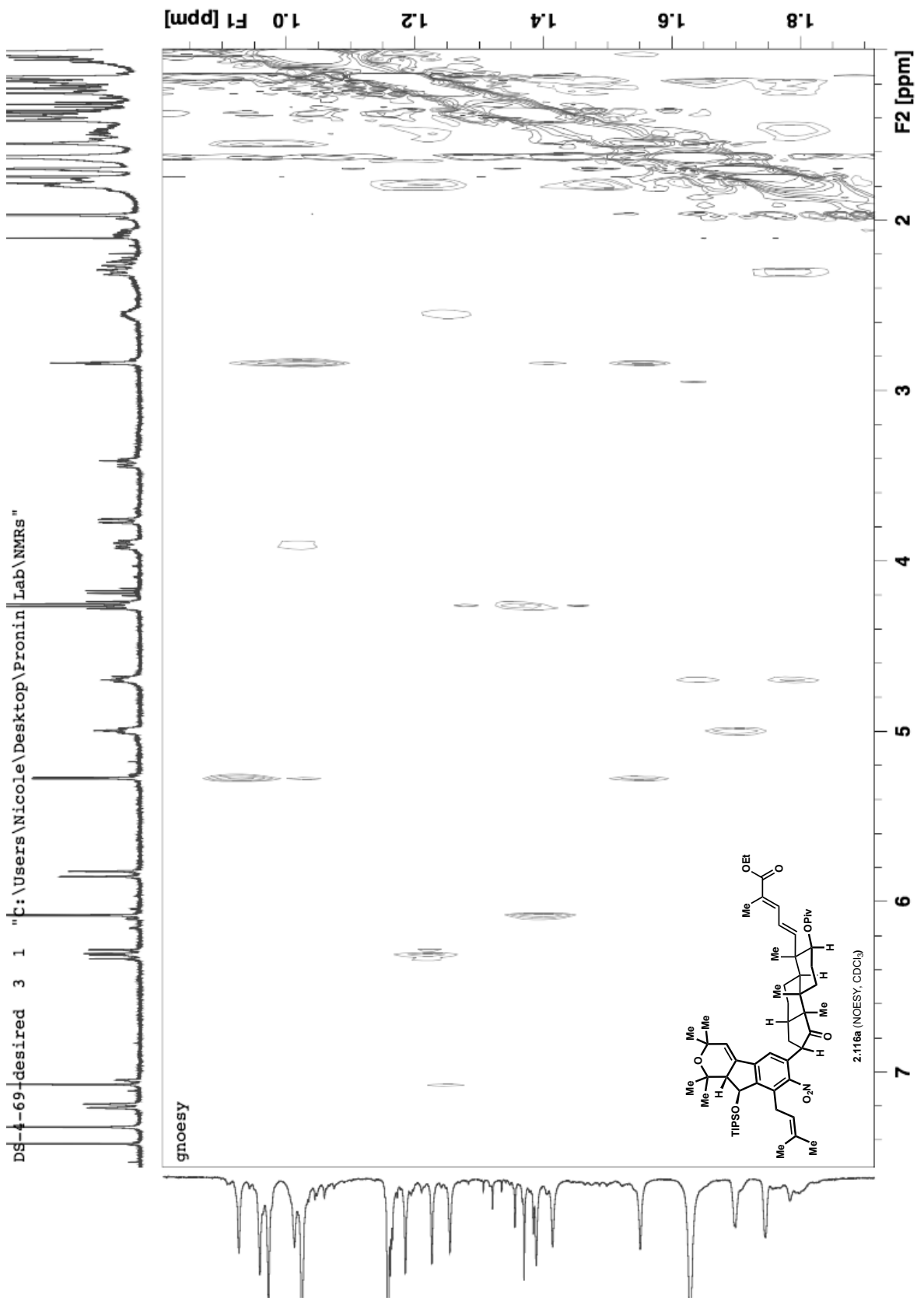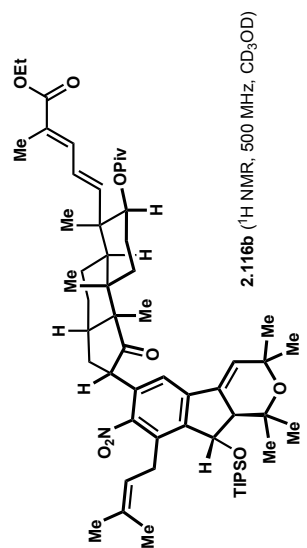
gcosy60

2.116a (COSY, CDCl₃)

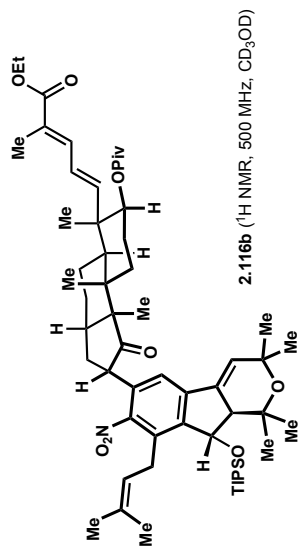2.116a (NOESY, CDCl₃)

2.116a (NOESY, CDCl₃)
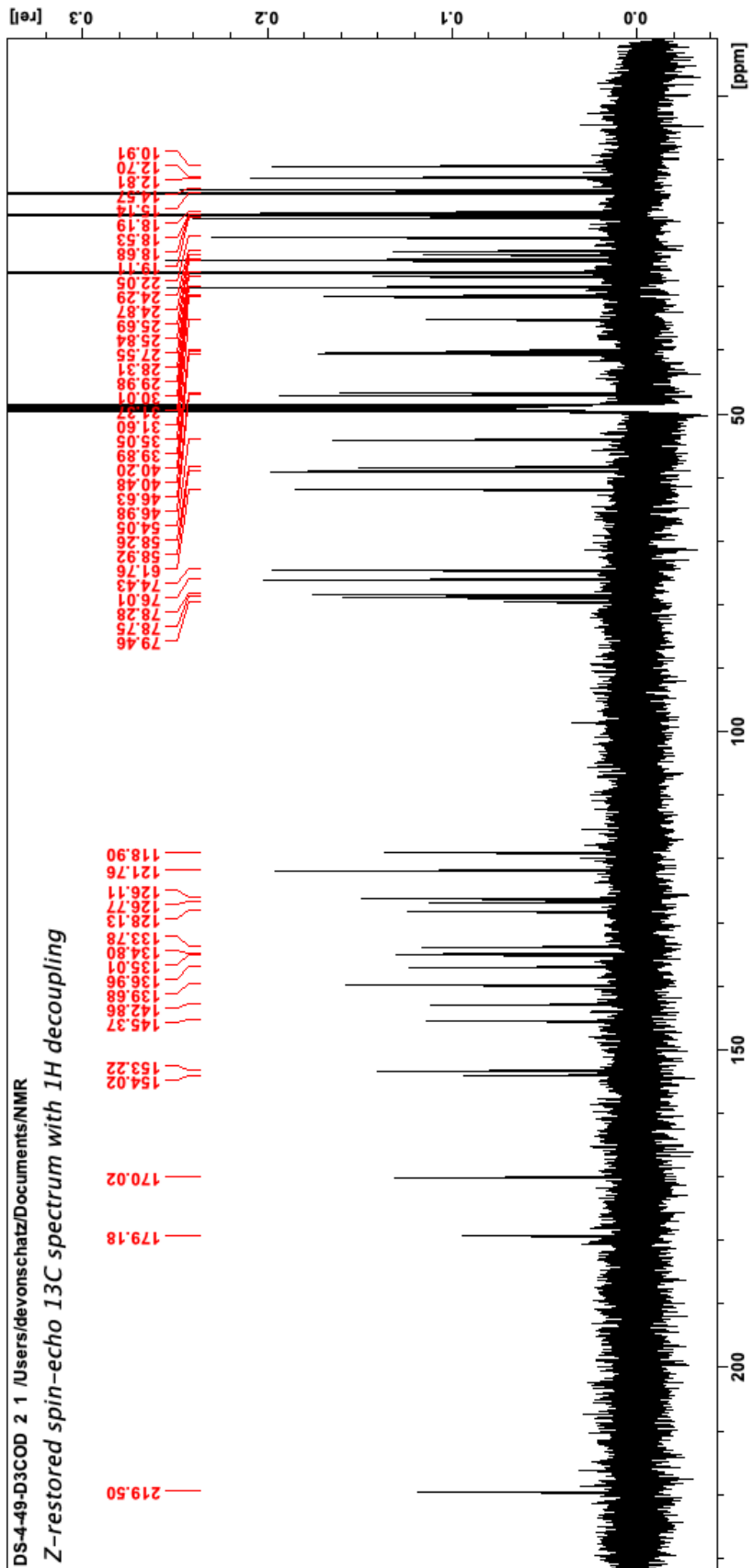
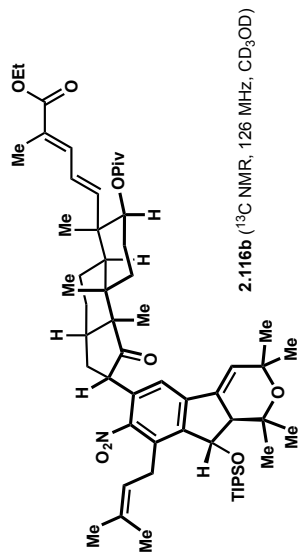DS-4-49-D3COD 1 1 /Users/devonschatz/Documents/NMR

1H spectrum

2.116b (1H NMR, 500 MHz, CD₃OD)

250

DS-4-49-D3COD 1 1 /Users/devonschatz/Documents/NMR

1H spectrum

2.116b (¹H NMR, 500 MHz, CD₃OD)

251

DS-4-49-D3COD 1 1 /Users/devonschatz/Documents/NMR

1H spectrum

2.116b (1H NMR, 500 MHz, CD₃OD)

252

DS-4-49-D3COD 2 1 /Users/devonschatz/Documents/NMR
Z-restored spin-echo 13C spectrum with 1H decoupling
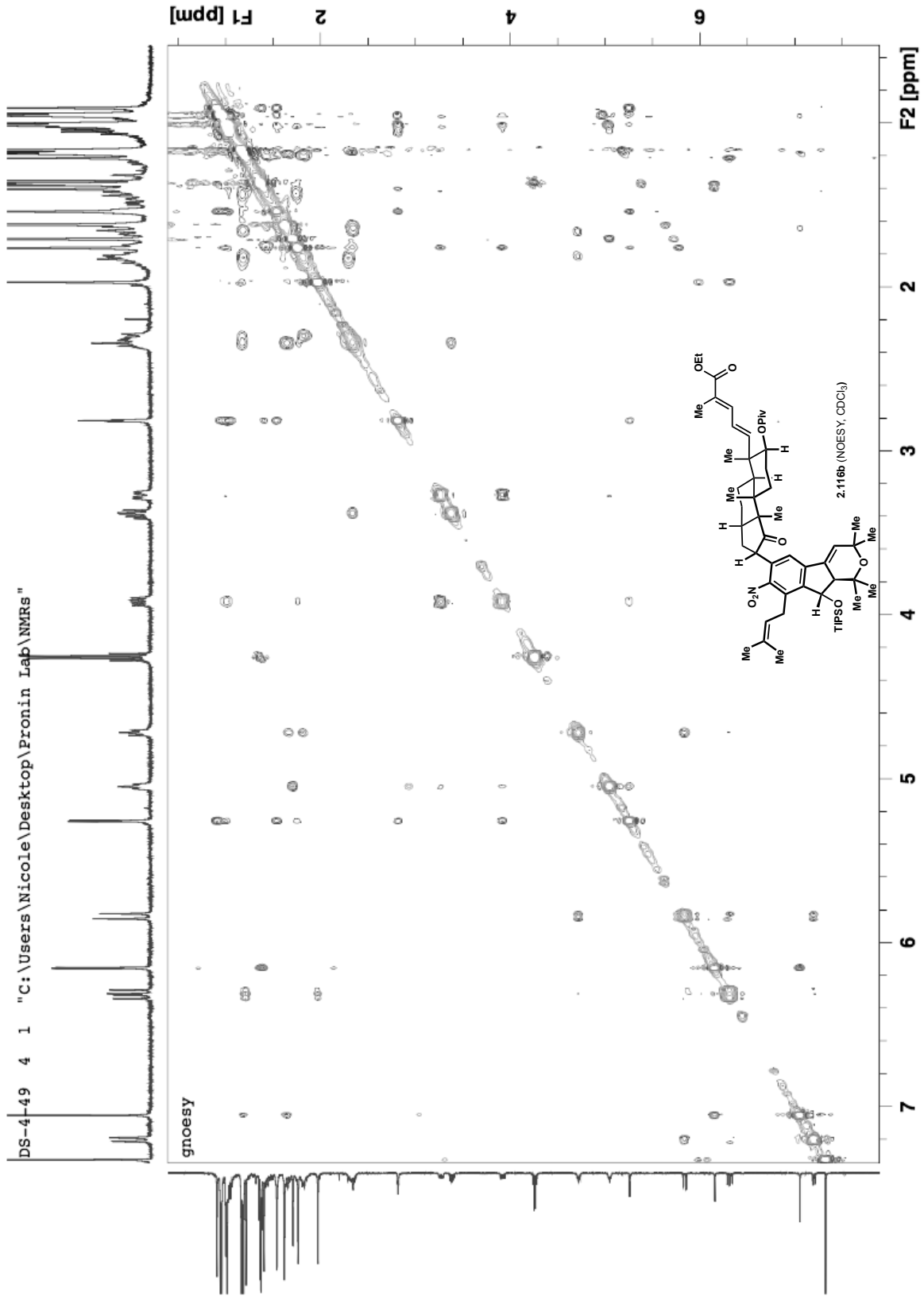
2.116b (^{13}C NMR, 126 MHz, CD$_3$OD)

2.116b (COSY, CDCl₃)

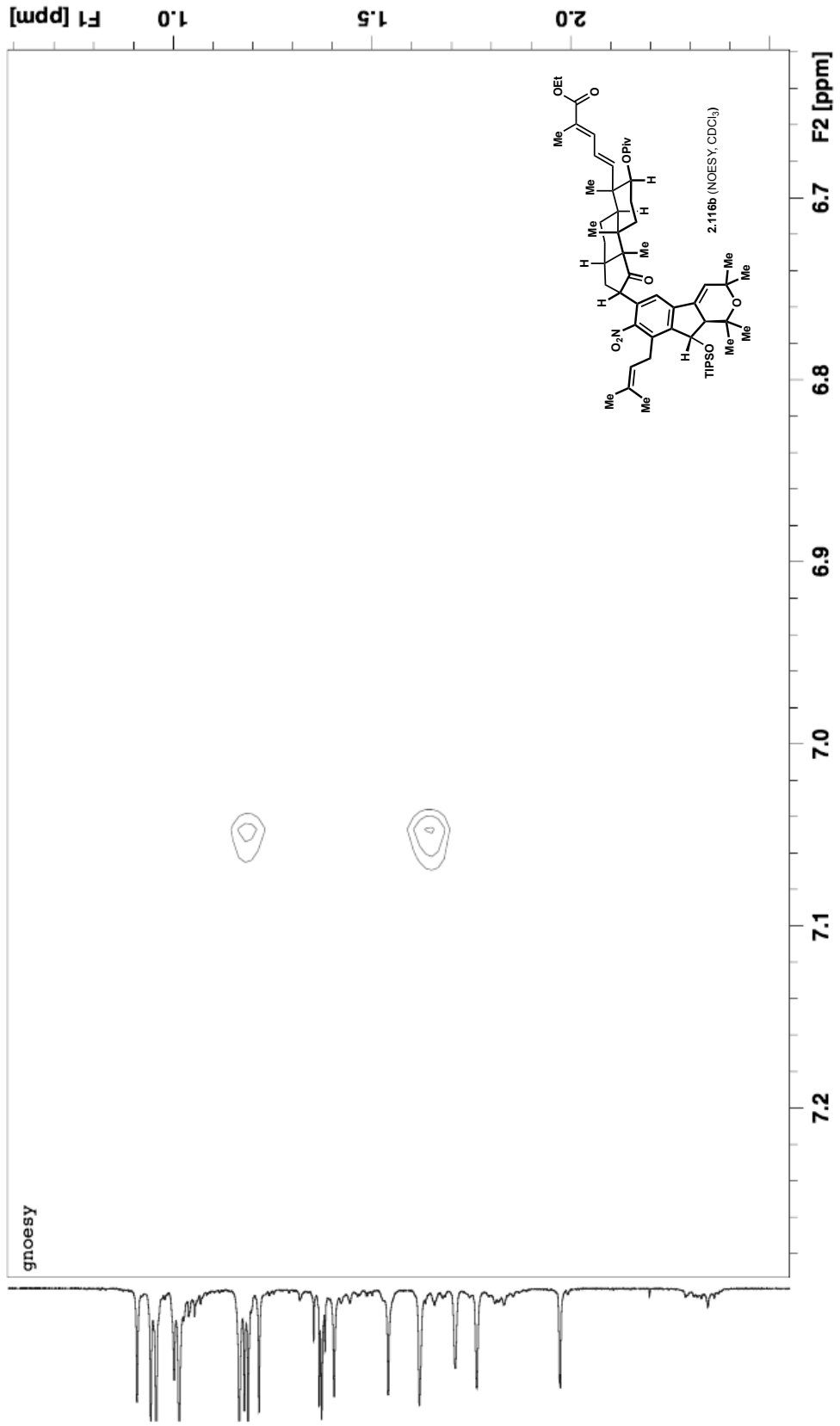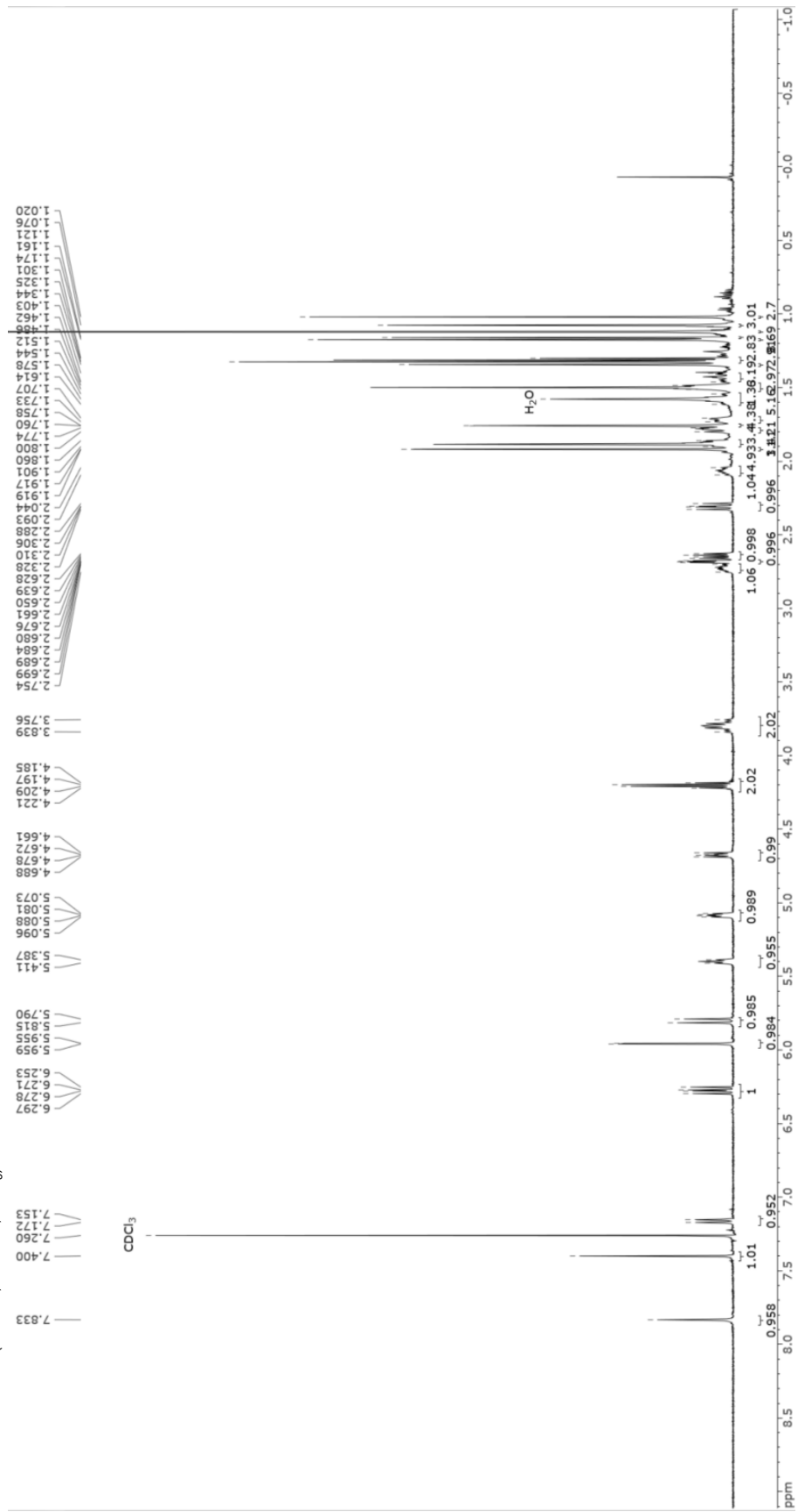DS-4-49   5   1   "C:\Users\Nicole\Desktop\Pronin Lab\NMRs"

gcosy60

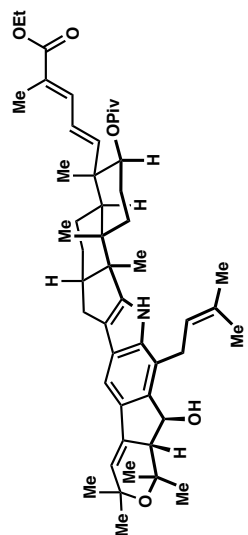2.116b (NOESY, CDCl₃)

DS-4-49 4 1 "C:\Users\Nicole\Desktop\Pronin Lab\NMRs"

gnoesy

2.116b (NOESY, CDCl$_3$)
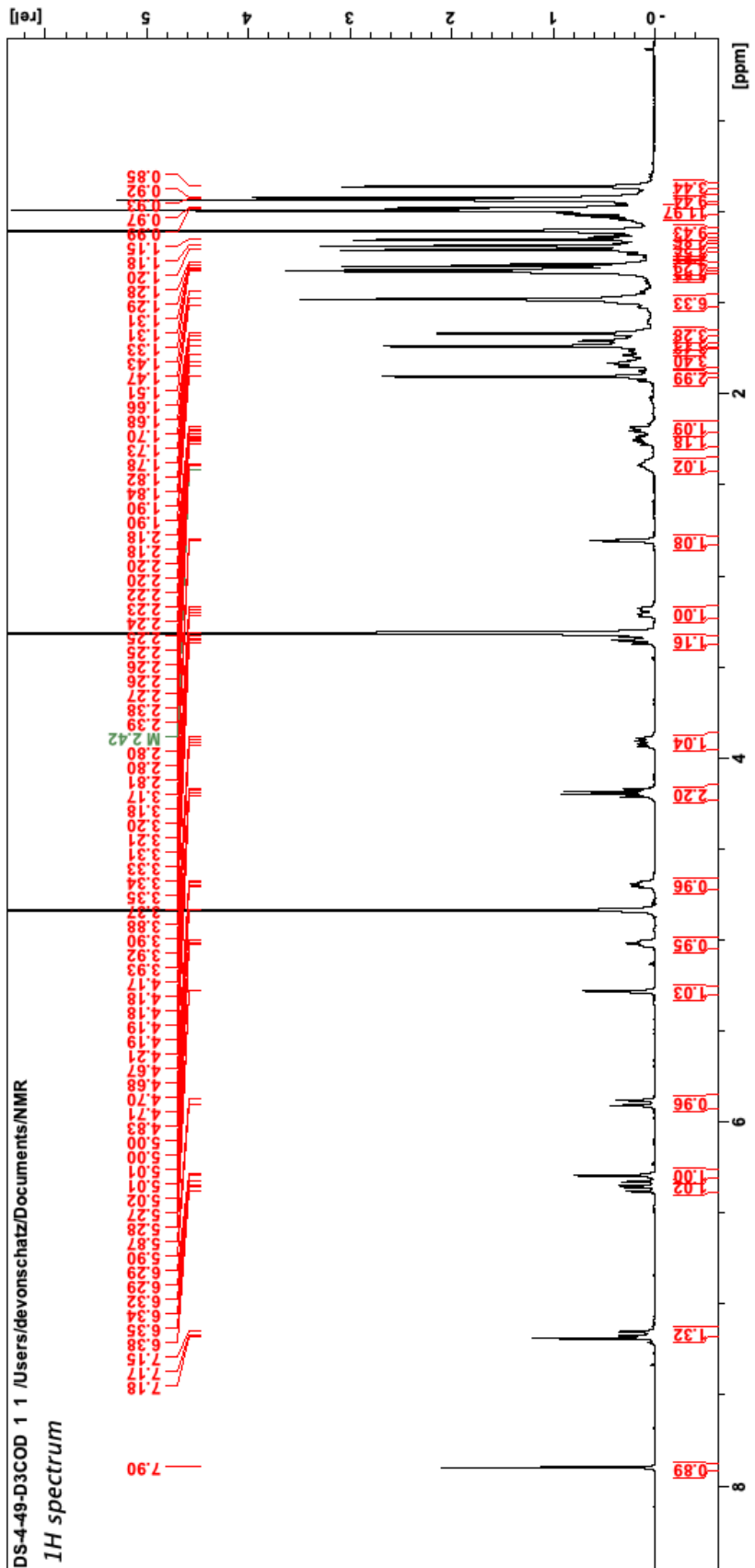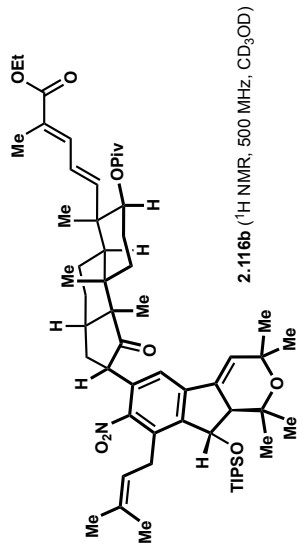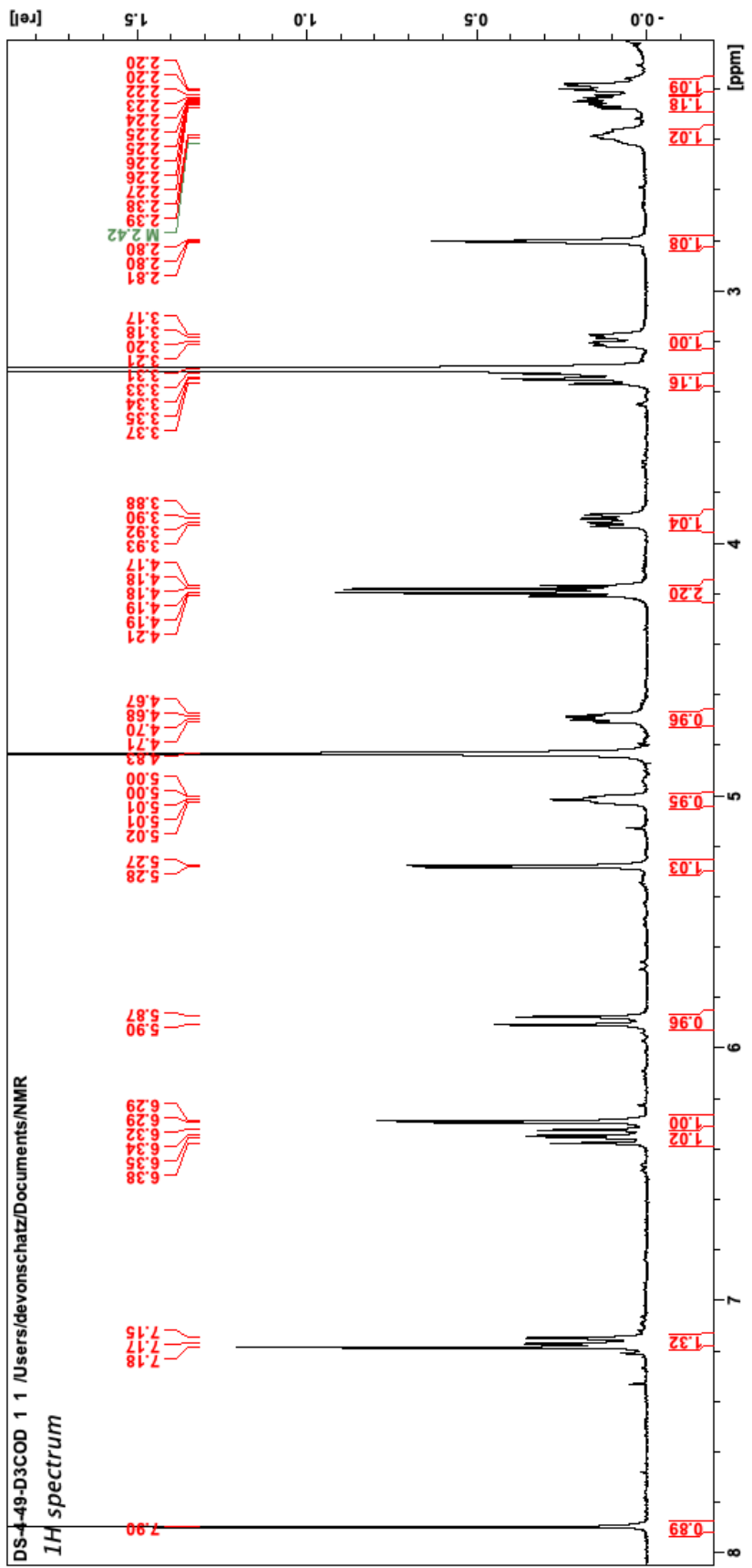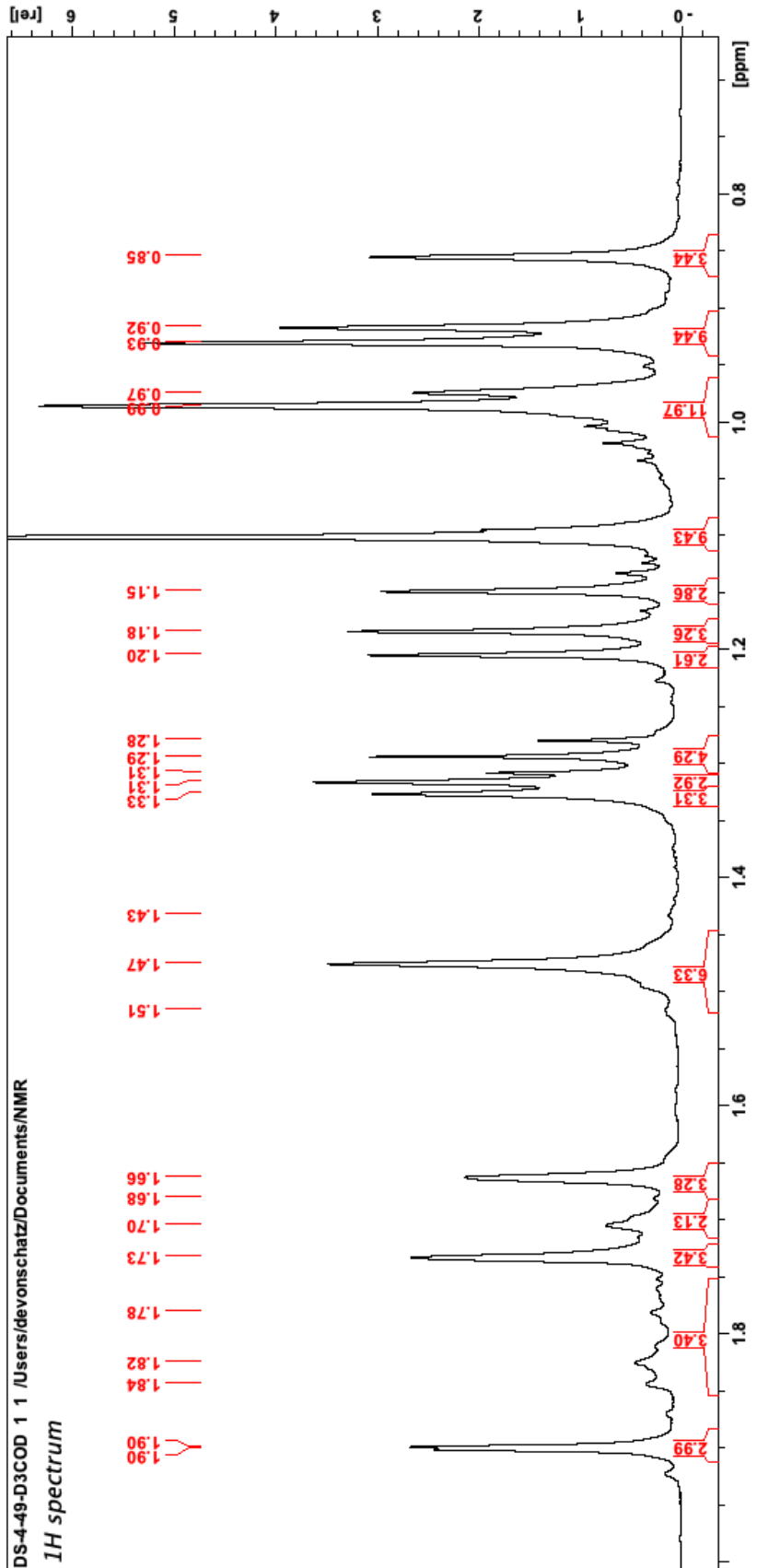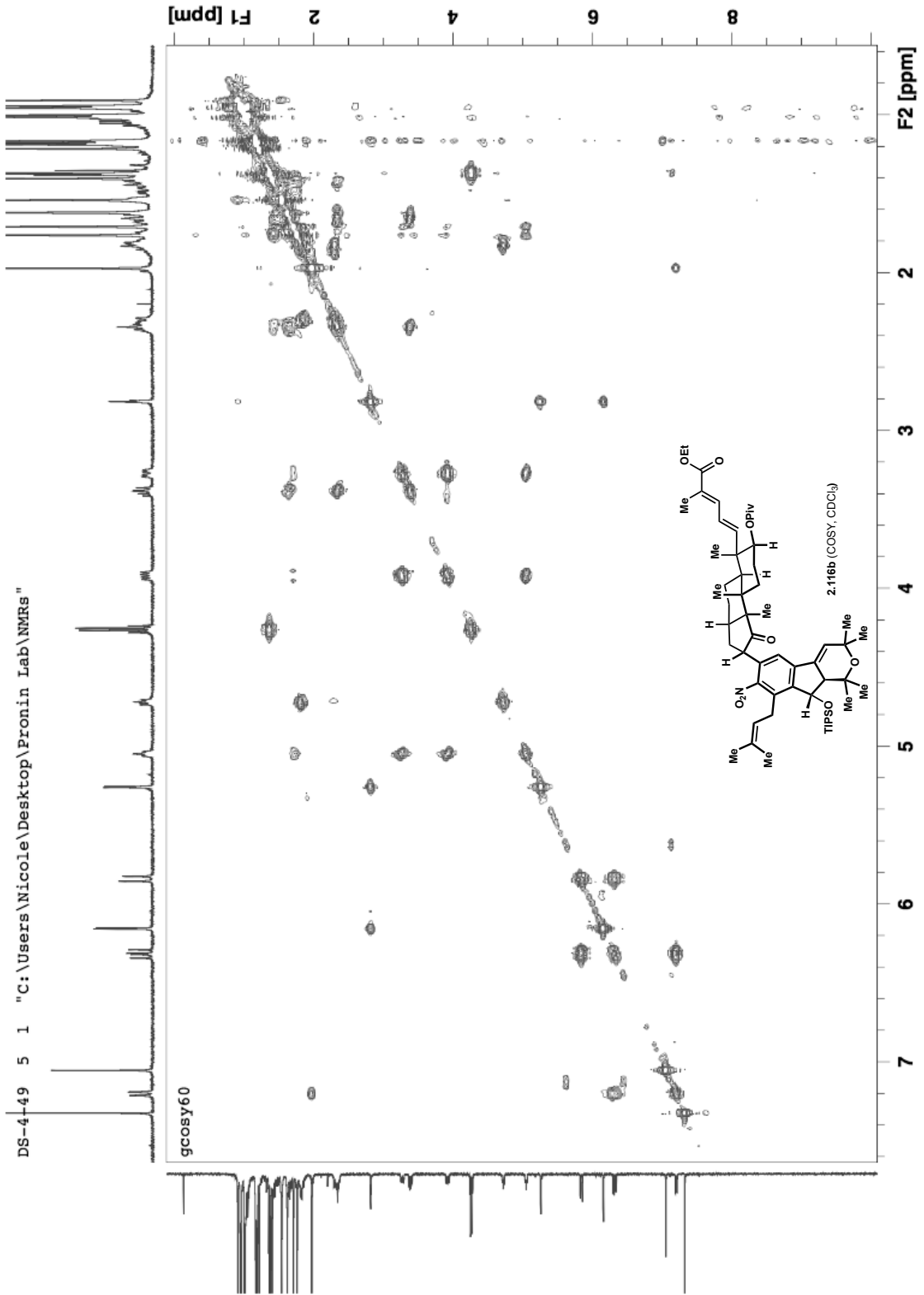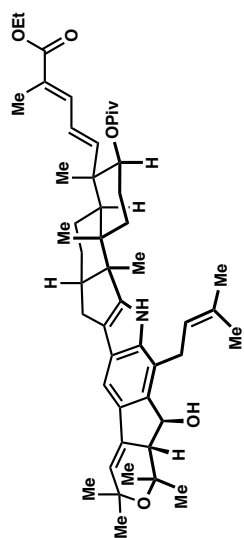
S2.6 (^{1}H NMR, 500 MHz, CDCl$_3$)

S2.6 (^{1}H NMR, 500 MHz, CDCl$_3$)

258

S2.6 (^{13}C NMR, 126 MHz, CDCl$_3$)

12.262
12.776
14.476
14.565
18.219
19.347
22.895
23.649
24.510
25.231
25.769
27.249
27.291
27.560
30.005
30.066
32.073
33.117
39.034
39.090
45.100
45.767
48.983

53.174

60.361
60.717

72.700
73.945
76.560
76.948
77.160
77.221
77.372

CDCl$_3$

107.604

118.644
120.453
121.852
123.362
125.207
125.971
126.762
131.931
132.997
135.437
136.111
138.228
141.181

151.341
151.950

168.663

177.813
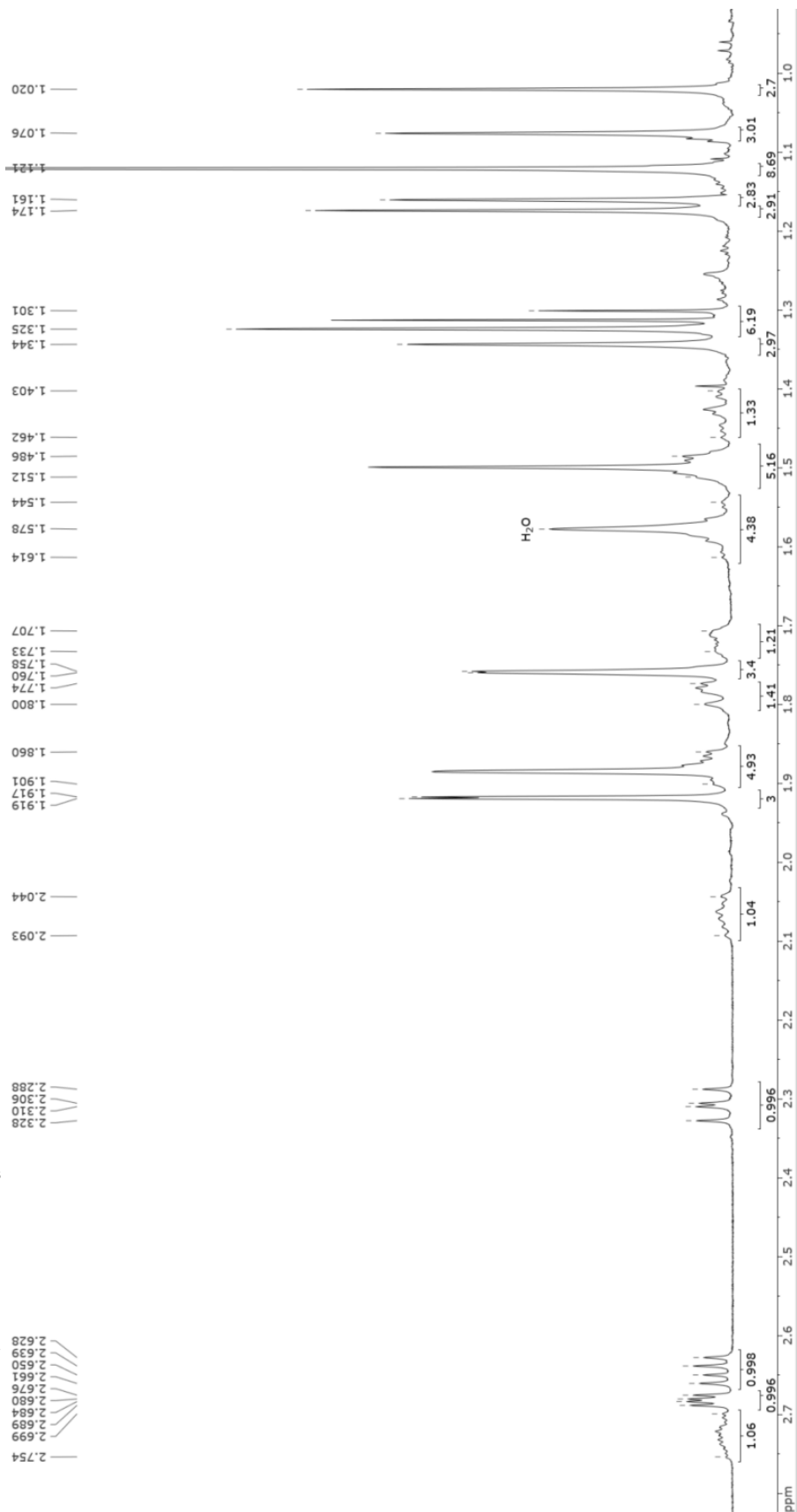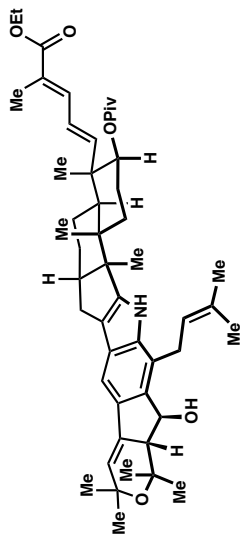
(–)-nodulisporic acid C (**2.19**) (^{1}H NMR, 500 MHz, CDCl$_3$)

S2.6 (^{13}C NMR, 126 MHz, CDCl$_3$)

261

(–)-nodulisporic acid C (**2.19**) (^{13}C NMR, 126 MHz, CDCl$_3$)

206.129

(CD$_3$)$_2$CO

170.537

AcOH

153.086
154.814

142.230
139.641
137.717
137.269

132.259
131.721

127.429
125.782
124.402
123.361
119.824
118.879

107.575

76.997
76.502
74.283
72.738

60.743

54.384

49.843
47.935
45.079

39.797
33.460
32.415
30.440
30.428
29.840
30.043
27.693
26.640
26.098
25.832
25.474
23.202
19.365
18.170
14.811
12.941
11.795

(CD$_3$)$_2$CO

PivOH

AcOH

262

(−)-nodulisporic acid C (**2.19**) (^{13}C NMR, 126 MHz, CDCl$_3$)

11.795
12.941
14.811
18.170
19.365
23.202
25.474
25.832
26.098
26.640
27.693
28.012
29.840
30.428
30.440
32.415
33.460

AcOH

PivOH

(CD$_3$)$_2$CO

263

(−)-nodulisporic acid C (**2.19**) sodium salt (^{1}H NMR, 500 MHz, CDCl$_3$)

(–)-nodulisporic acid C (**2.19**) sodium salt (^{1}H NMR, 500 MHz, CDCl$_3$)

265

(−)-nodulisporic acid C (**2.19**) sodium salt (^{13}C NMR, 126 MHz, CDCl$_3$)

11.794
13.267
14.755
18.138
19.304
23.120
25.341
25.788
26.023
26.585
27.501
27.936
30.324
33.202
33.400
39.721
45.005
47.202
49.789
54.318
60.496
72.825
74.399
76.253
76.953
107.478
118.728
119.705
123.317
124.327
125.997
127.316
131.700
132.147
137.187
137.516
138.389
142.044
152.961
153.559
171.590

(CD$_3$)$_2$CO
(CD$_3$)$_2$CO

+PivONa+

(–)-nodulisporic acid C (**2.19**) sodium salt (^{13}C NMR, 126 MHz, CDCl$_3$)

11.794

13.267

14.755

18.138

19.304

23.120

25.341
25.788
26.023
26.585
27.501
27.936

(CD$_3$)$_2$CO

+PivONa

30.324

32.302

33.400

ppm
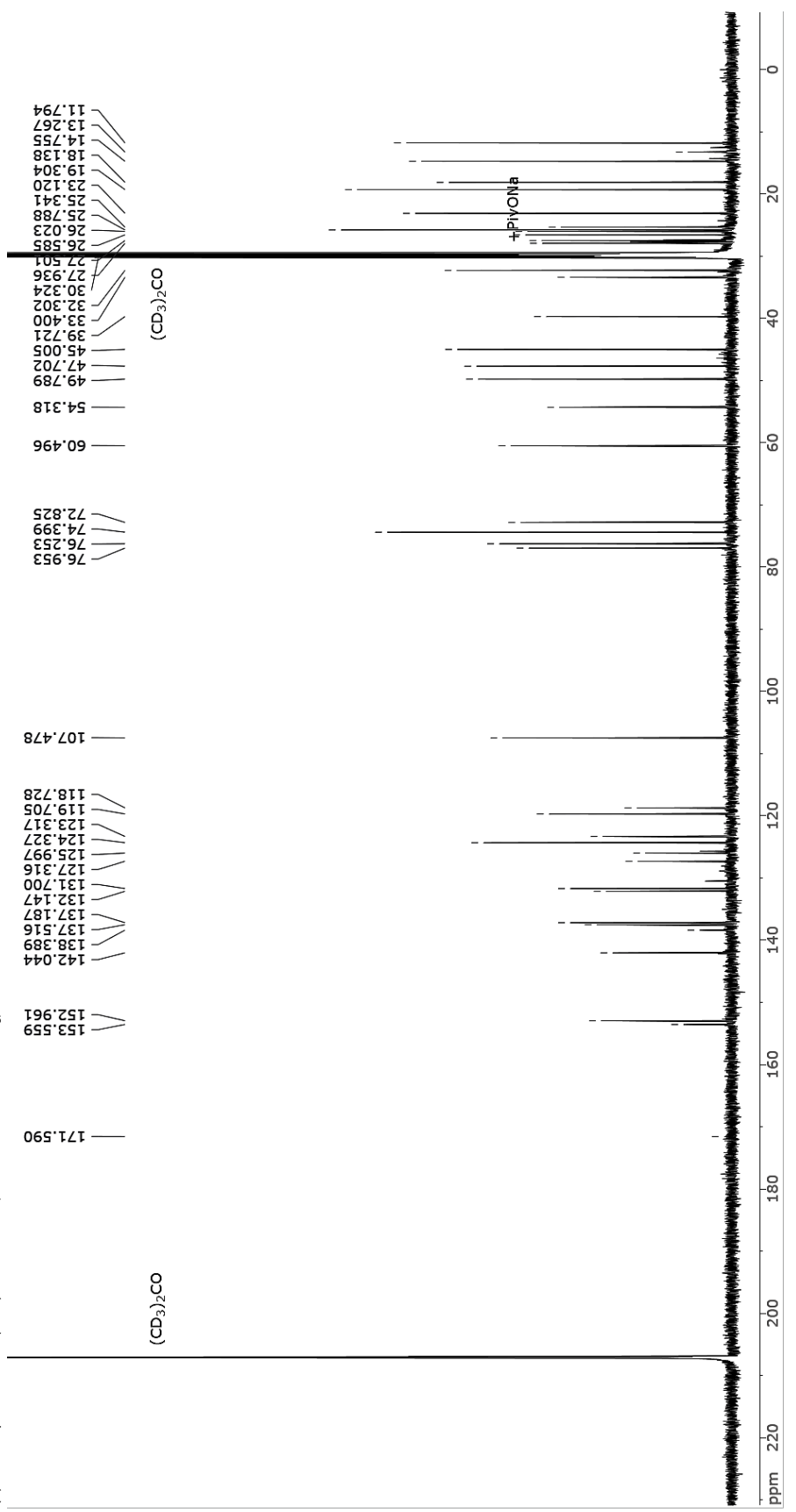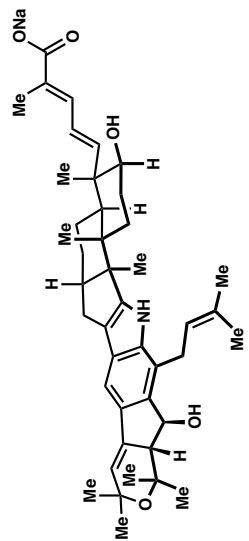
Appendix B: NMR Spectra for Chapter 3
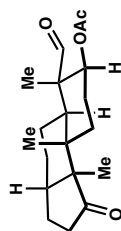
3.8 (^{1}H NMR, 500 MHz, CDCl$_3$)

DS-4-301F1 1 1 /Users/devonschatz/Documents/NMR
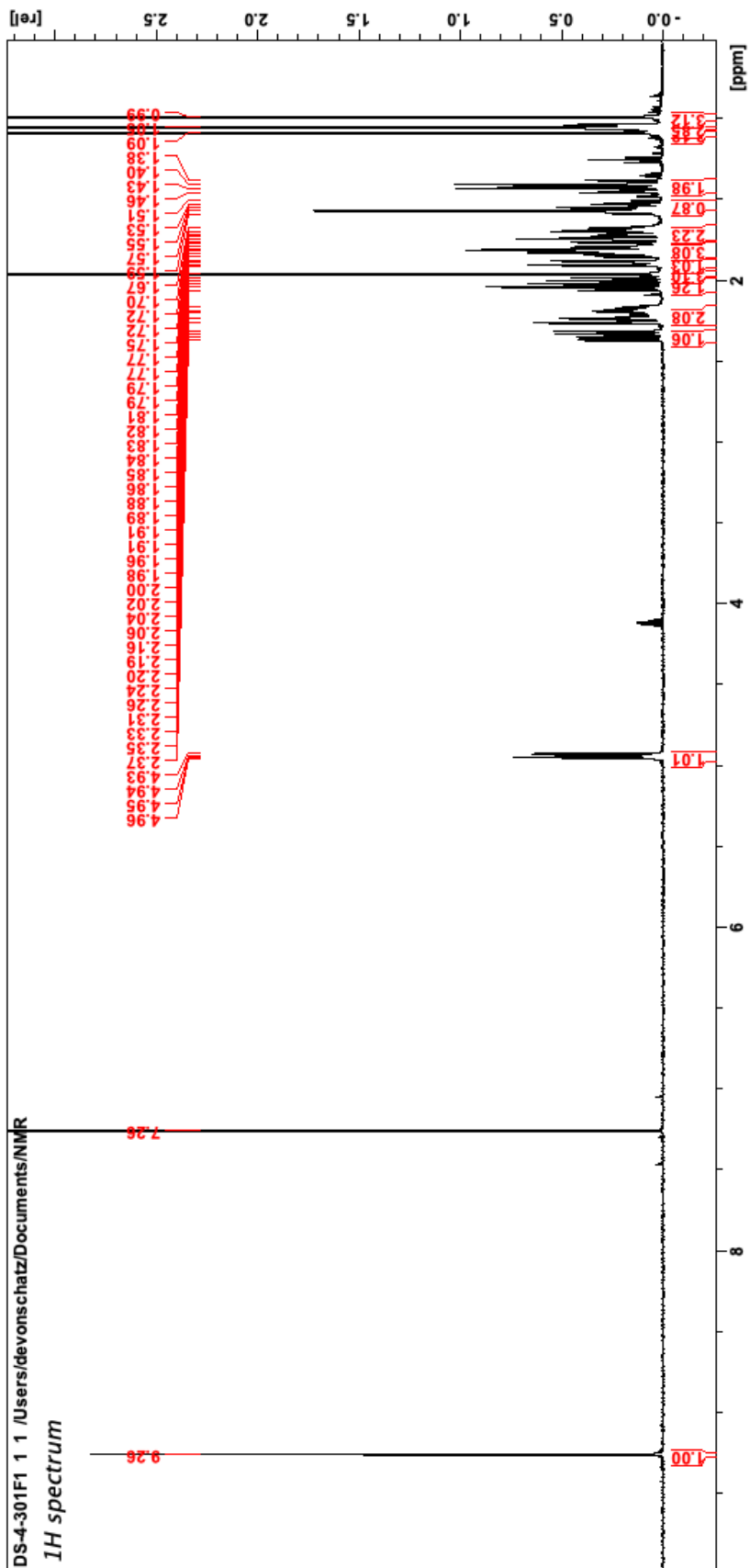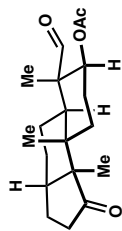
1H spectrum

3.8 (^{13}C NMR, 126 MHz, CDCl$_3$)

DS-1-247 5 1 /Users/devonschatz/Documents/NMR

Z–restored spin–echo 13C spectrum with 1H decoupling
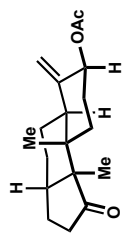
3.10 (^{1}H NMR, 500 MHz, CDCl$_3$)

DS-4-290 2 1 /Users/devonschatz/Documents/NMR
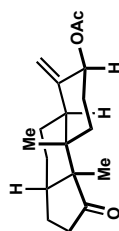
1H spectrum

3.10 (^{13}C NMR, 126 MHz, CDCl$_3$)

DS-4-290 3 1 /Users/devonschatz/Documents/NMR

Z-restored spin-echo 13C spectrum with 1H decoupling

Peaks: 10.69, 14.18, 21.30, 23.74, 25.15, 25.67, 29.28, 30.86, 37.17, 40.51, 40.67, 43.71, 54.23, 74.77, 76.91, 77.16, 77.41, 104.35, 147.37, 170.30, 220.48

272
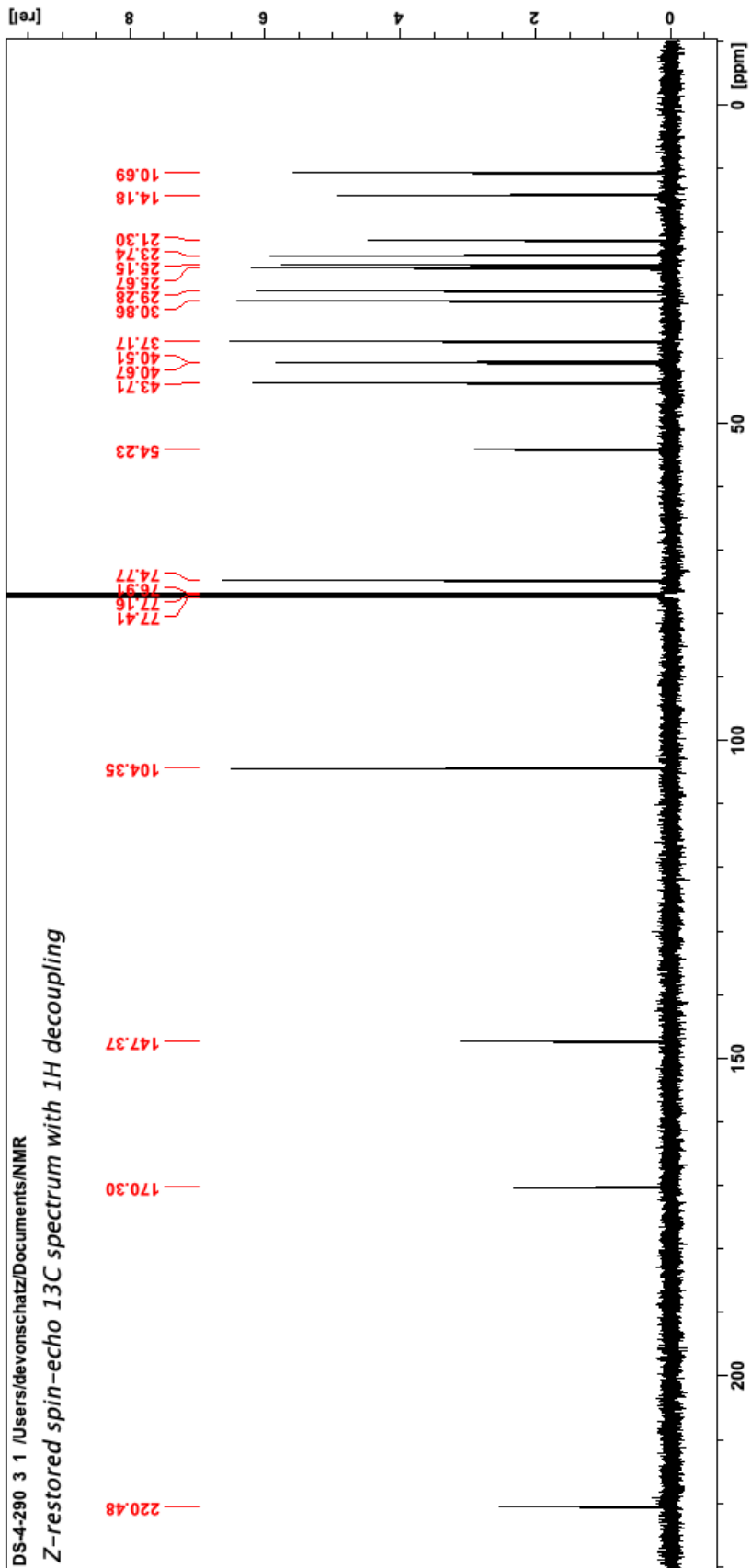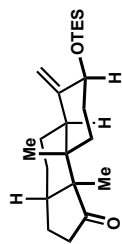
3.14 (¹H NMR, 500 MHz, CDCl₃)

DS-4-222_F1 1 1 /Users/devonschatz/Documents/NMR
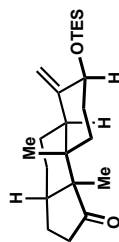
1H spectrum

3.14 (^{13}C NMR, 126 MHz, CDCl$_3$)

DS-4-222_F1 2 1 /Users/devonschatz/Documents/NMR

Z-restored spin-echo 13C spectrum with 1H decoupling

Peaks (ppm): 5.02, 7.08, 10.76, 14.31, 23.80, 25.30, 25.95, 31.21, 33.66, 37.24, 40.56, 40.74, 43.61, 54.31, 74.01, 76.90, 77.16, 77.41, 104.60, 151.71, 220.67

S3.3 (^{1}H NMR, 500 MHz, CDCl$_3$)

DS-4-268 1 1 /Users/devonschatz/Documents/NMR

1H spectrum

275

3.16 (^{1}H NMR, 500 MHz, CDCl$_3$)

DS-4-291 2 1 /Users/devonschatz/Documents/NMR
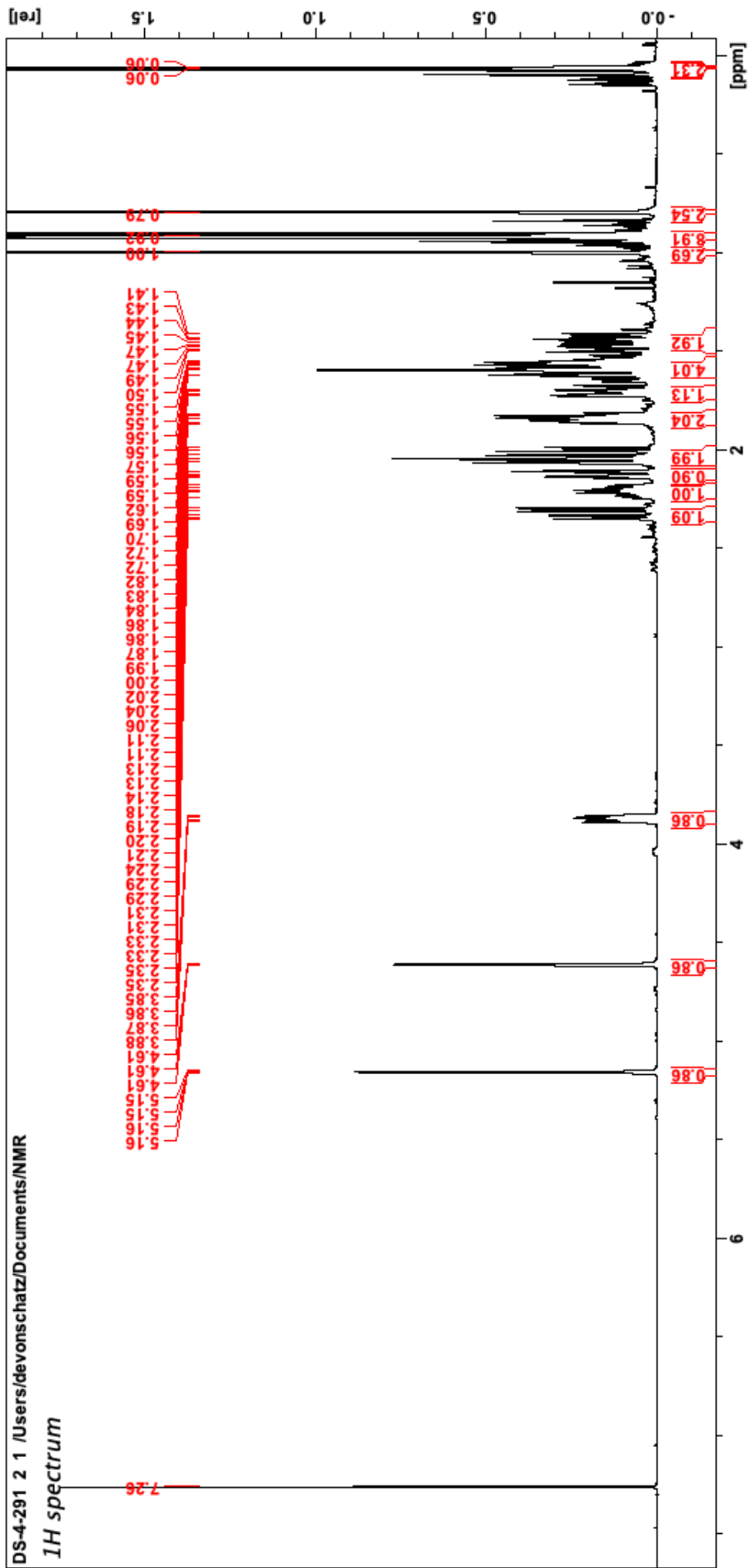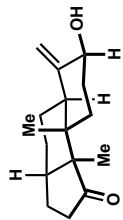
1H spectrum

3.23 (^{1}H NMR, 500 MHz, CDCl$_3$)

DS-5-39 1 1 /Users/devonschatz/Documents/NMR
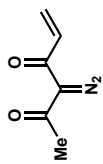
1H spectrum

3.24 (^{1}H NMR, 500 MHz, CDCl$_3$)

DS-5-38 1 1 /Users/devonschatz/Documents/NMR
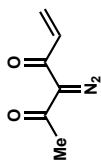
1H spectrum

3.24 (^{13}C NMR, 126 MHz, CDCl$_3$)

DS-5-38 2 1 /Users/devonschatz/Documents/NMR

Z–restored spin–echo 13C spectrum with 1H decoupling

DS-6-32 1 1 /Users/devonschatz/Documents/NMR

1H spectrum

3.25 (1H NMR, 500 MHz, CDCl₃)

3.25 (^{13}C NMR, 126 MHz, CDCl$_3$)

DS-6-32 2 1 /Users/devonschatz/Documents/NMR

Z–restored spin–echo 13C spectrum with 1H decoupling

DS-6-53 2 1 /Users/devonschatz/Documents/NMR

3.28 (^{1}H NMR, 500 MHz, CDCl$_3$)
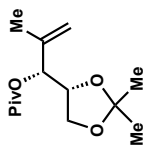
1H spectrum

3.41a (¹H NMR, 500 MHz, CDCl₃)

"DS-5-268 F2 pure" 1 1 /Users/devonschatz/Documents/NMR
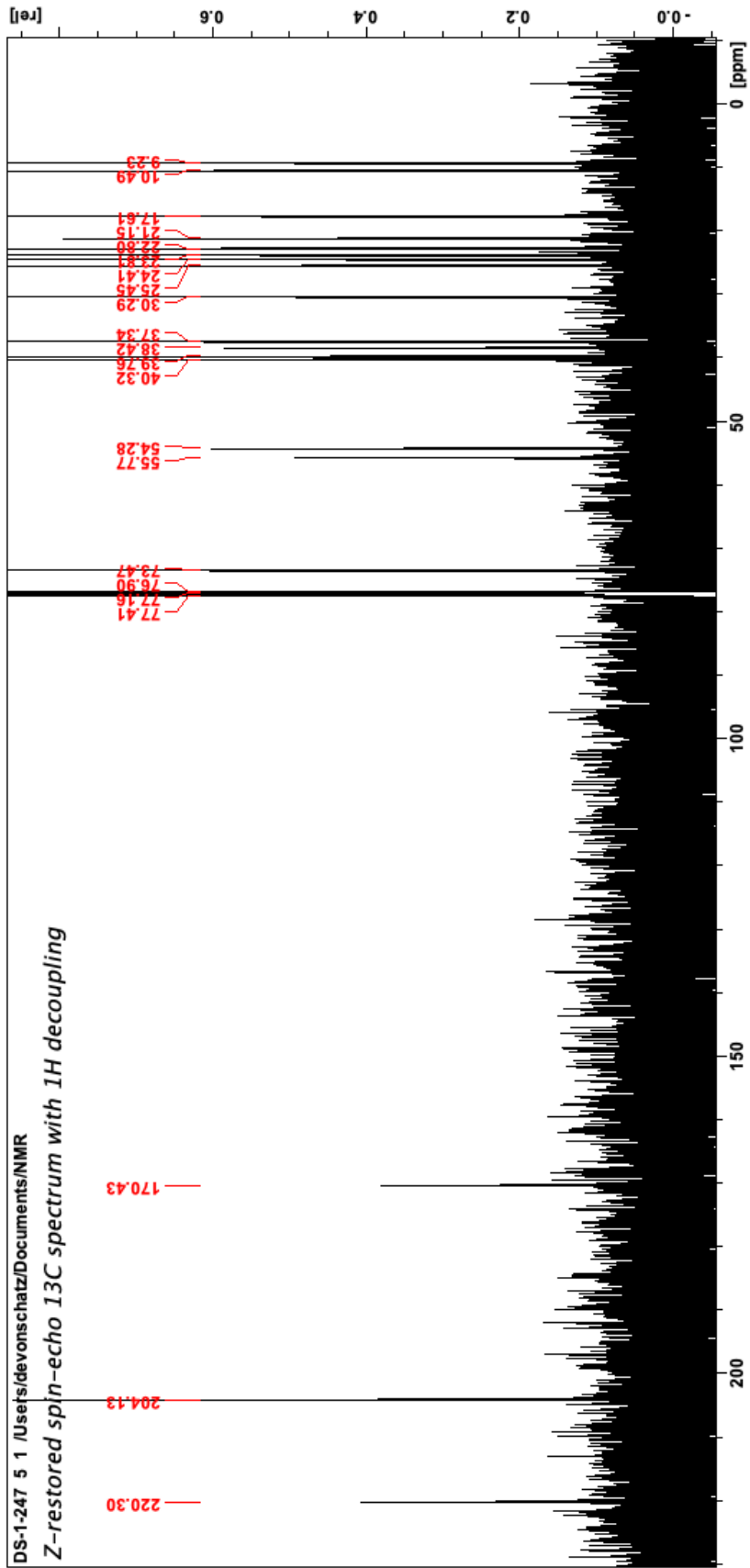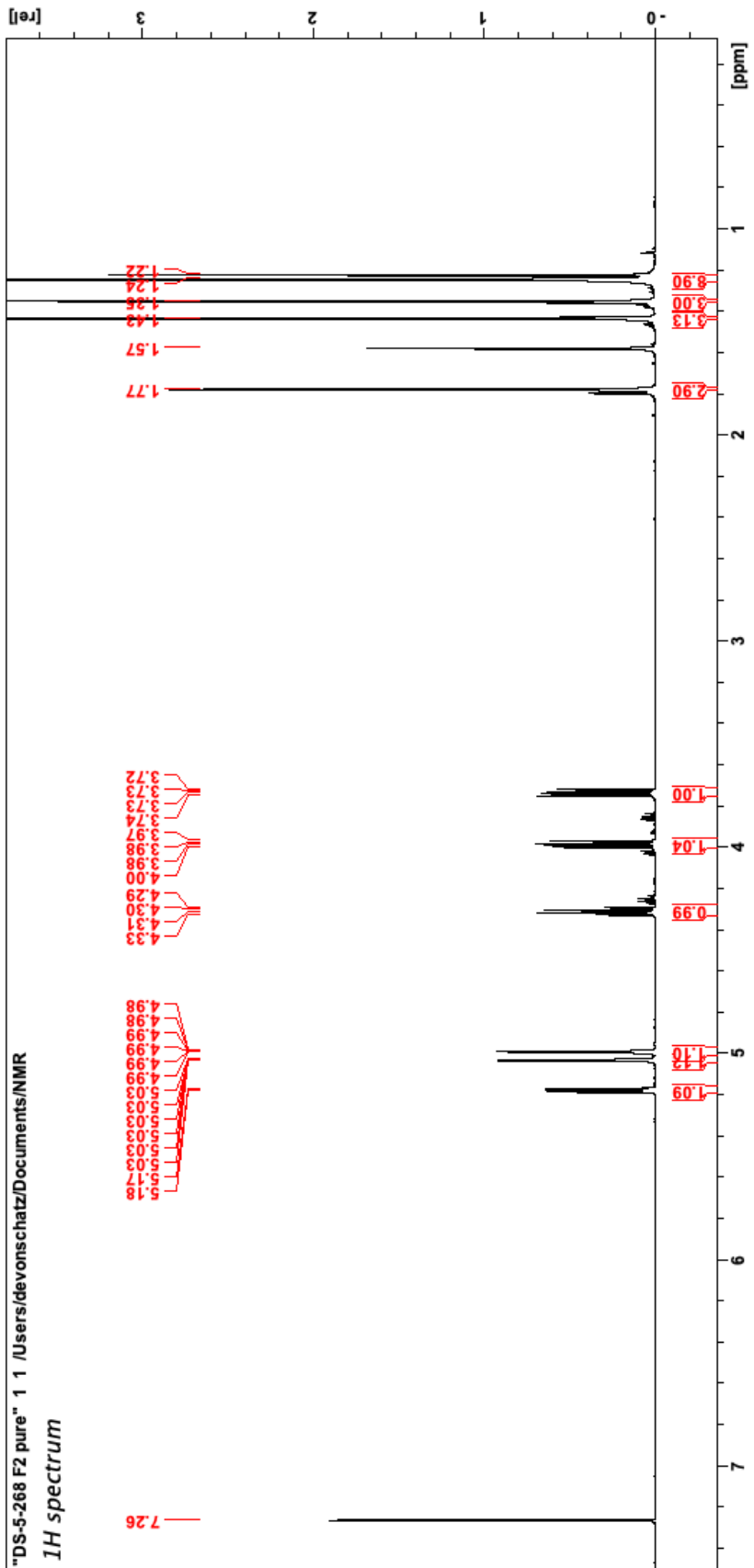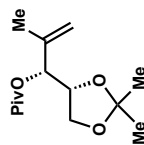
1H spectrum

3.41a (^{13}C NMR, 126 MHz, CDCl$_3$)

"DS-5-268 F2 pure" 2 1 /Users/devonschatz/Documents/NMR

Z-restored spin-echo 13C spectrum with 1H decoupling

177.75

141.06

114.63
110.02

77.41
77.16
76.90
76.67
76.07

65.96

39.11

27.30
26.89
26.69
25.58

19.32

3.41b (¹H NMR, 500 MHz, CDCl₃)

"DS-5-268 F1 Pure" 1 1 /Users/devonschatz/Documents/NMR
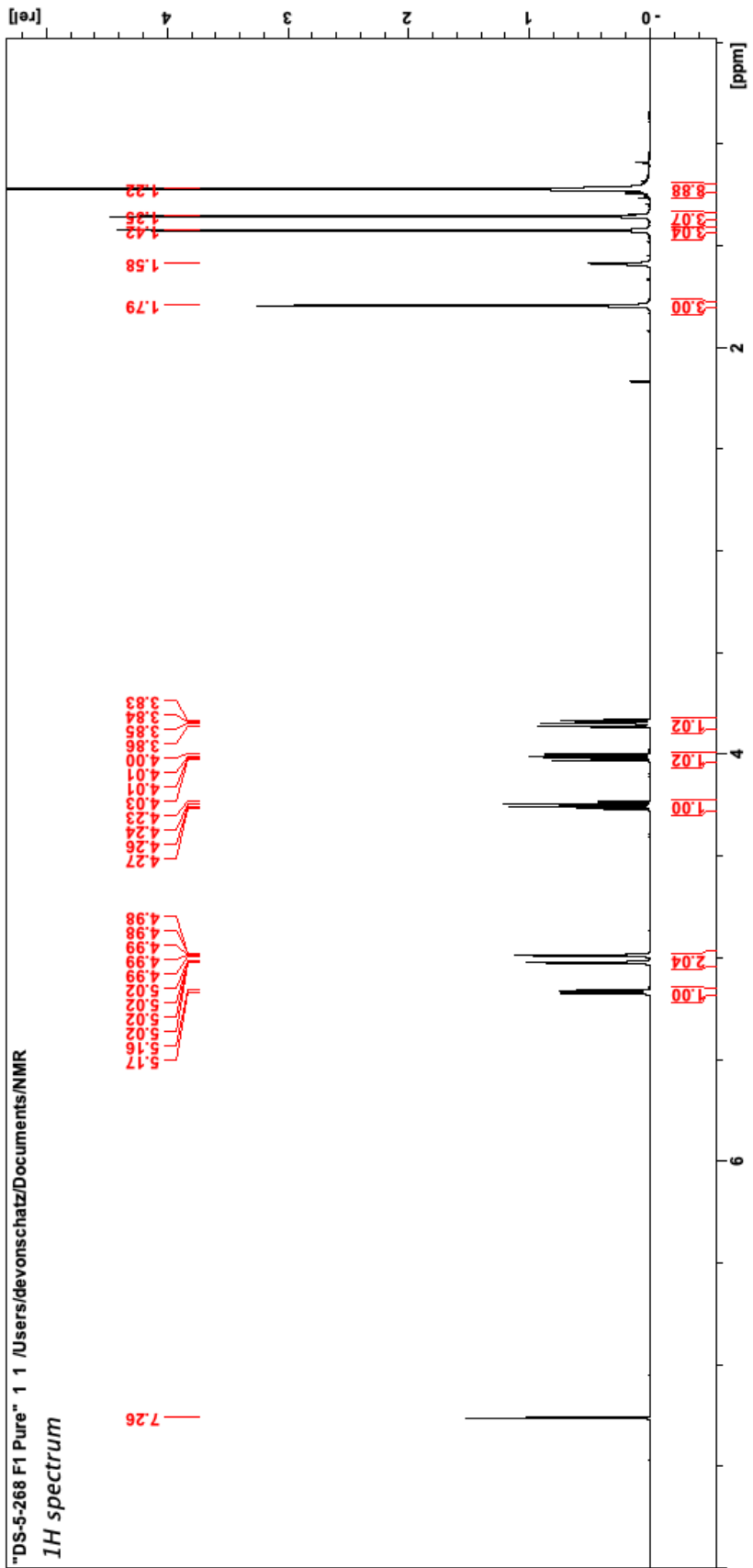
1H spectrum

3.41b (^{13}C NMR, 126 MHz, CDCl$_3$)

"DS-5-268 F1 Pure" 2 1 /Users/devonschatz/Documents/NMR

Z–restored spin–echo 13C spectrum with 1H decoupling

177.15
141.48
114.14
109.84
77.41
77.16
76.90
76.08
75.87
66.21
39.04
27.28
26.12
25.44
19.38

286

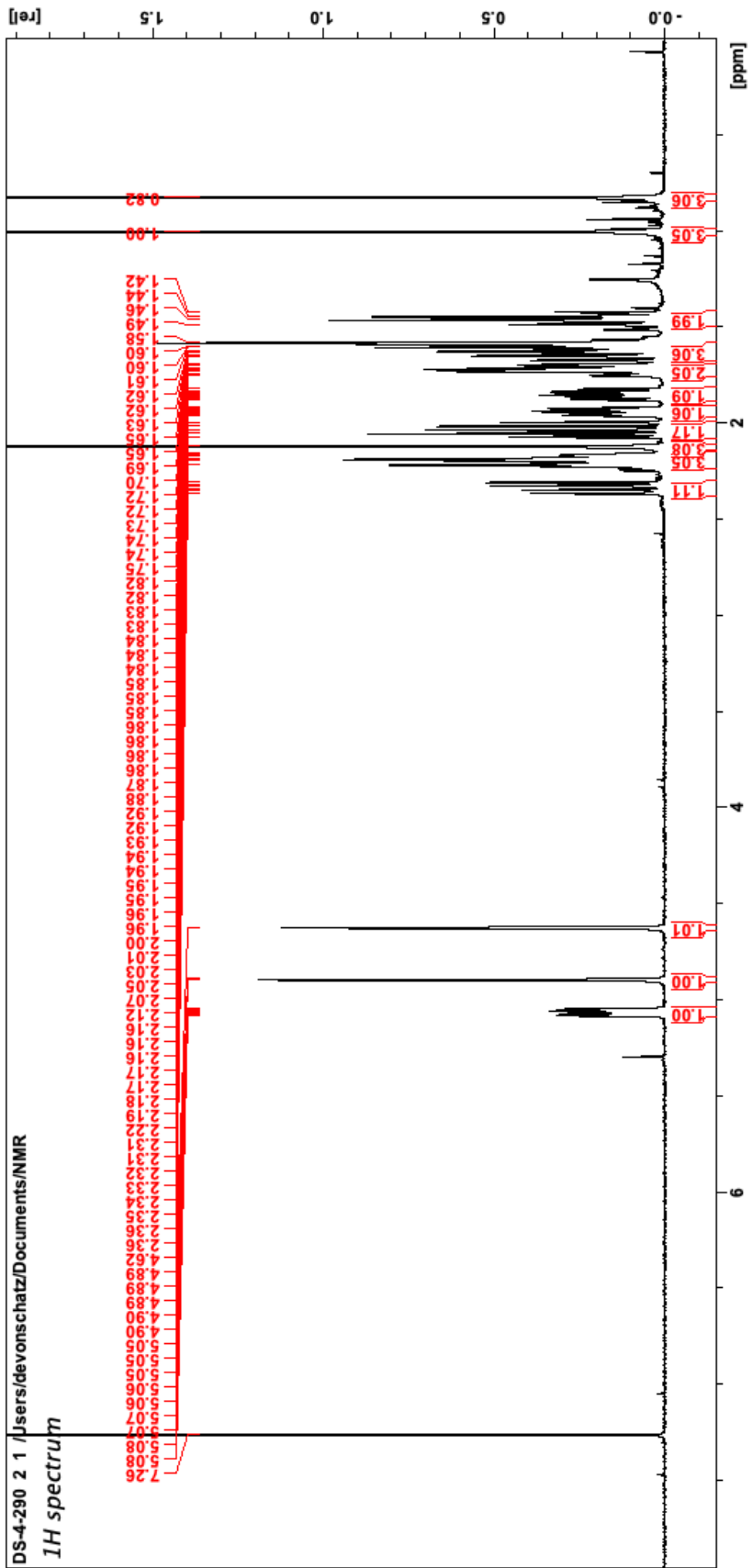3.44 (4.9:1 d.r.) (^{1}H NMR, 500 MHz, CDCl$_3$)

DS-5-279 2 1 /Users/devonschatz/Documents/NMR
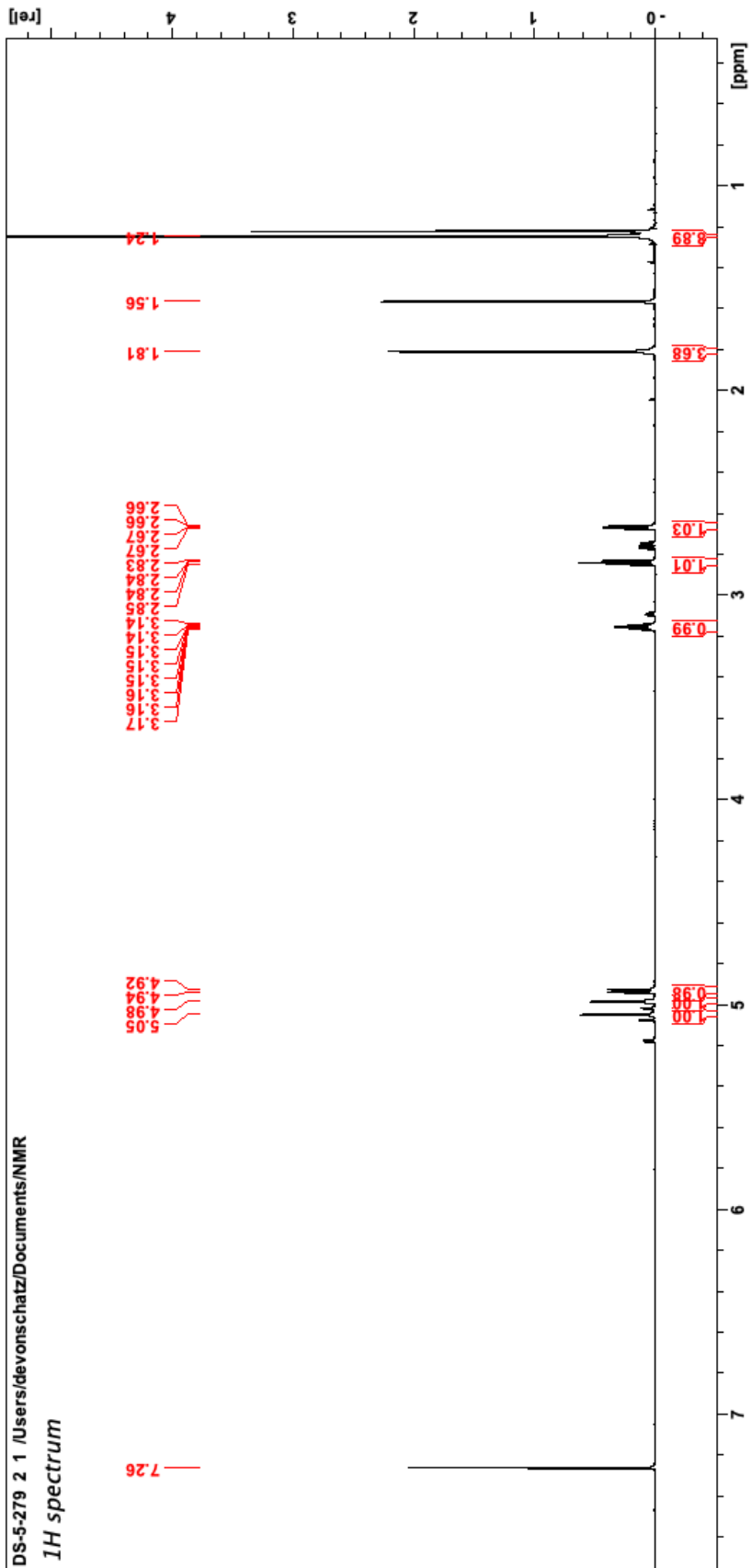
1H spectrum

3.45 (^{1}H NMR, 500 MHz, CDCl$_3$)

DS-6-123 2 1 /Users/devonschatz/Documents/NMR

1H spectrum

288
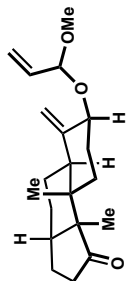
3.49 (1H NMR, 500 MHz, CDCl₃)

"DS6-179 c6d6" 1 1 /Users/devonschatz/Documents/NMR
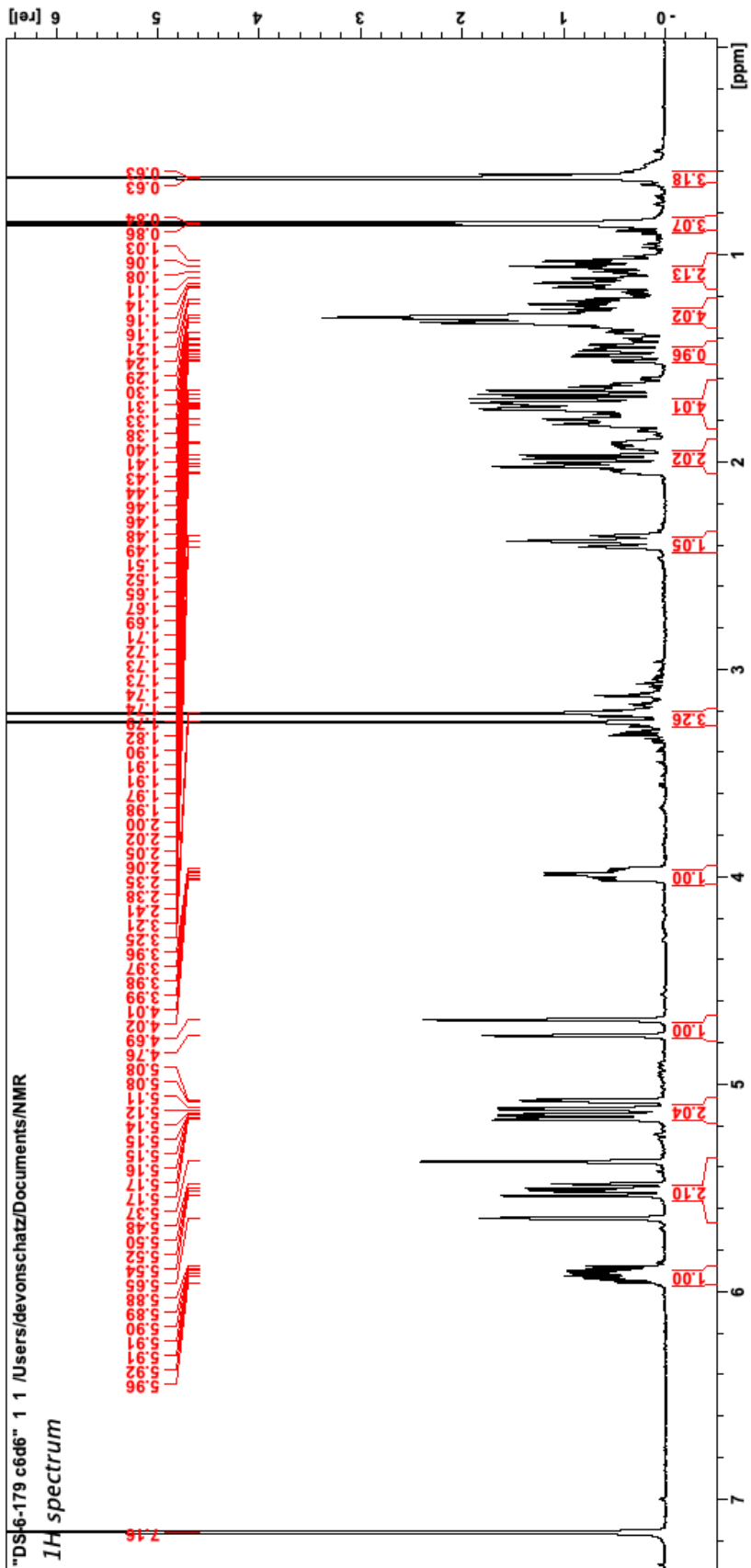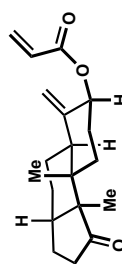
1H spectrum

DS-6-136 2 1 /Users/devonschatz/Documents/NMR

1H spectrum

3.53 (¹H NMR, 500 MHz, CDCl₃)
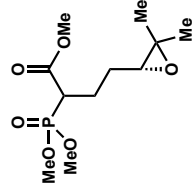
3.59 (^{1}H NMR, 500 MHz, CDCl$_3$)
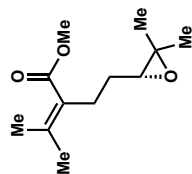
DS-7-19 2 1 /Users/devonschatz/Documents/NMR

1H spectrum

S3.7 (^{1}H NMR, 500 MHz, CDCl$_3$)
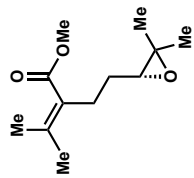
DS-7-19 2 1 /Users/devonschatz/Documents/NMR

1H spectrum

292

S3.7 (^{13}C NMR, 126 MHz, CDCl$_3$)

DS-7-75 2 1 /Users/devonschatz/Documents/NMR

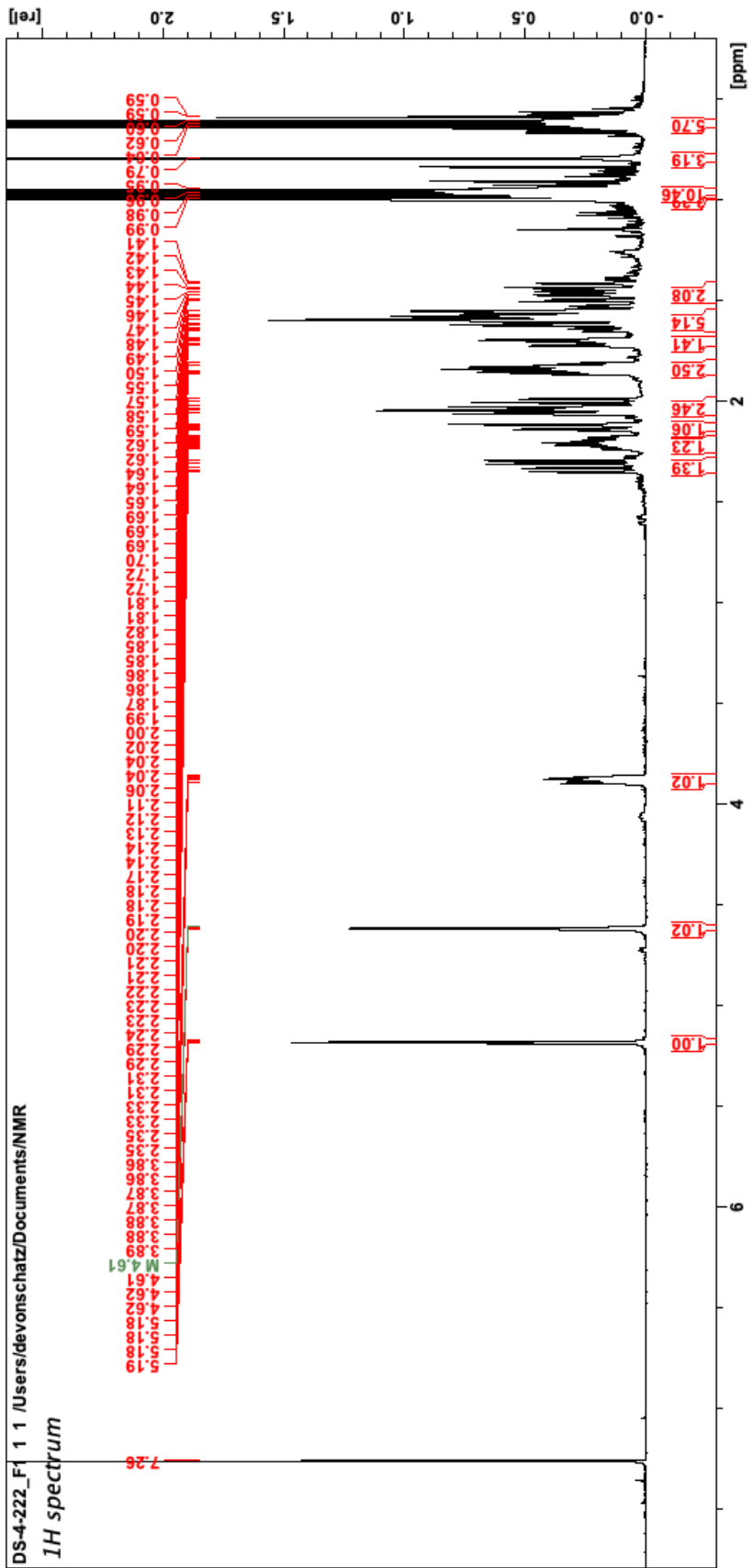*Z–restored spin–echo 13C spectrum with 1H decoupling*

18.77
22.22
23.26
23.26
25.00
26.73
28.52
51.37
58.62
63.93
76.90
77.16
77.41
126.70
144.22
169.85

293
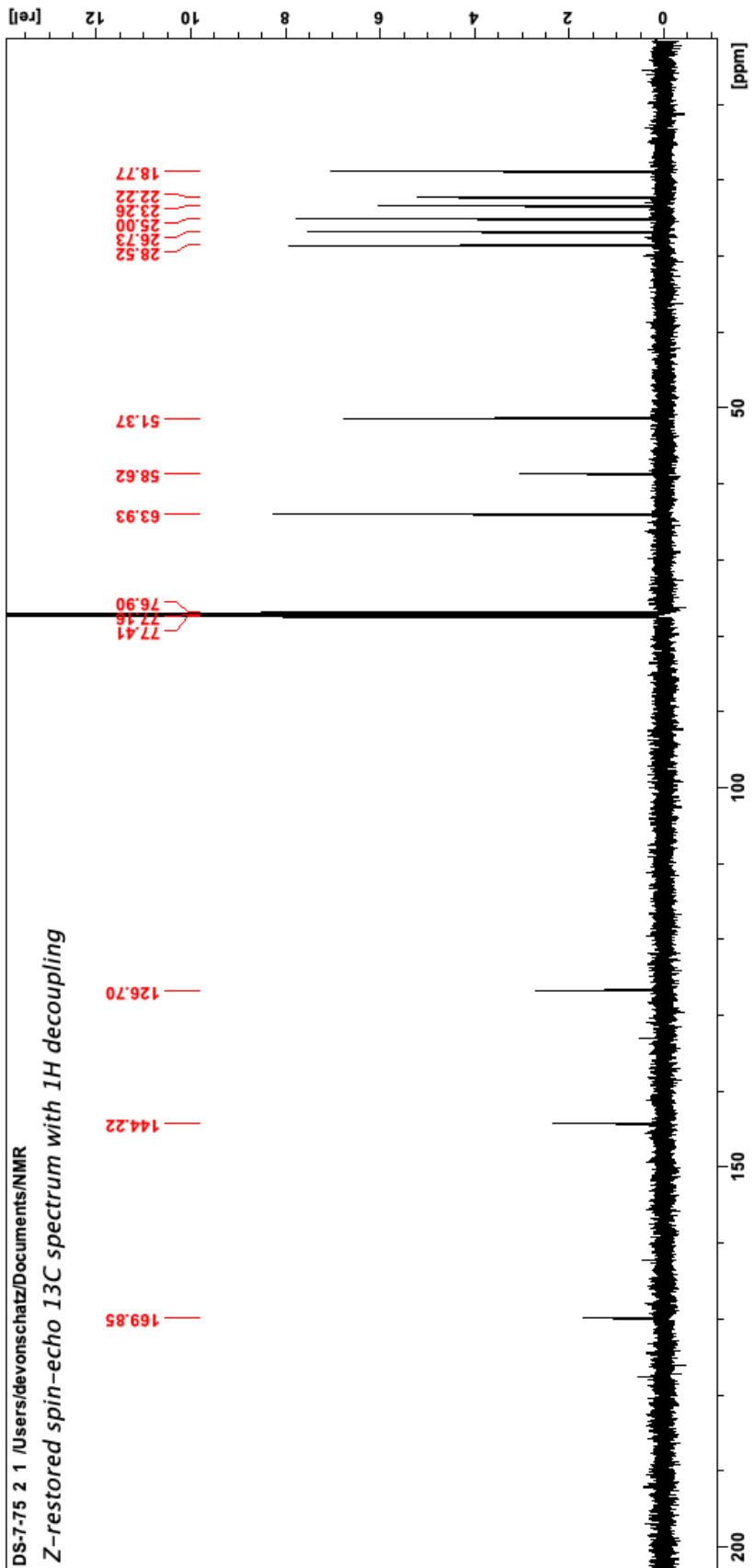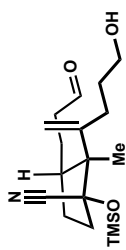
3.60 (^{1}H NMR, 500 MHz, CDCl$_3$)

DS-6-211 2 1 /Users/devonschatz/Documents/NMR

1H spectrum

294

3.78a

3.78b
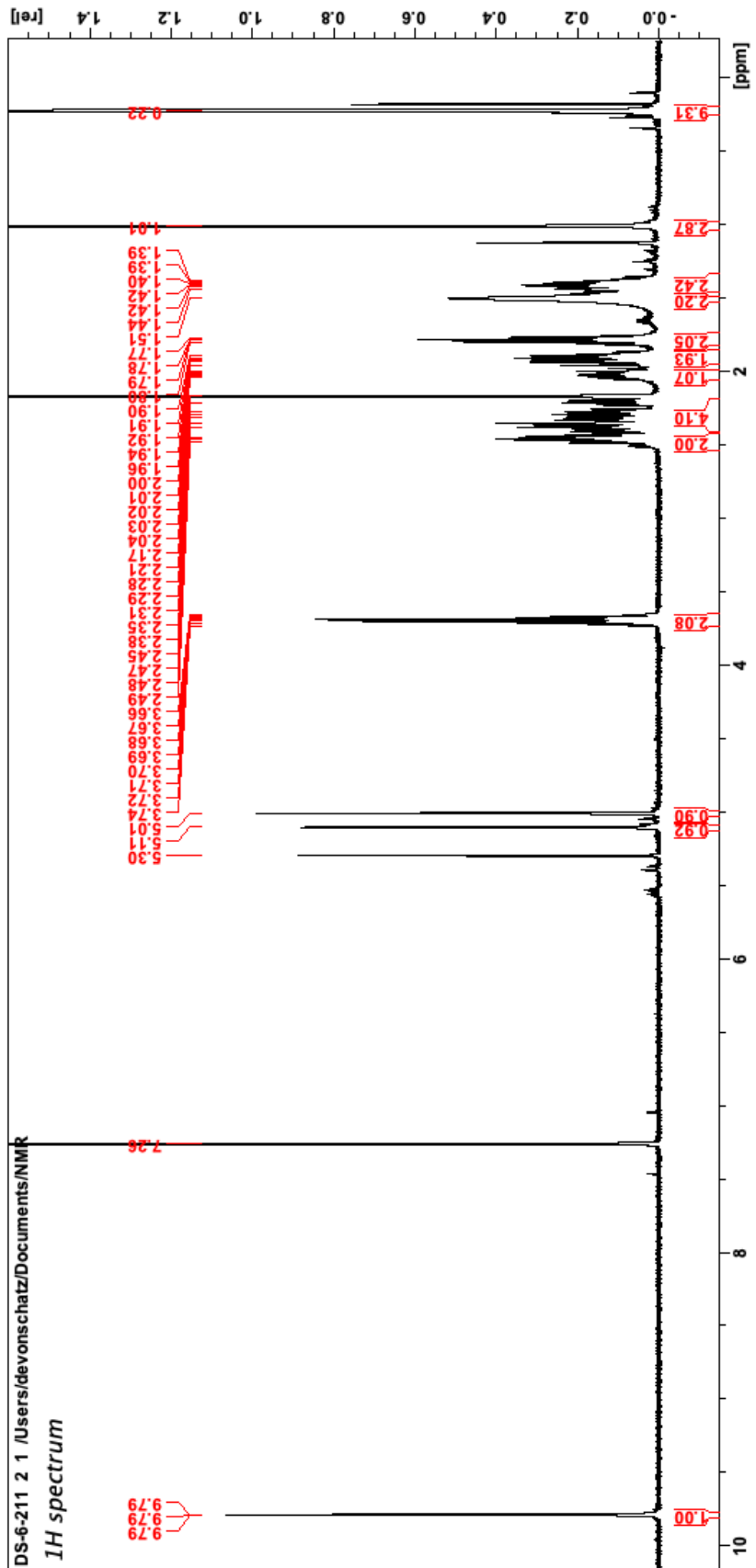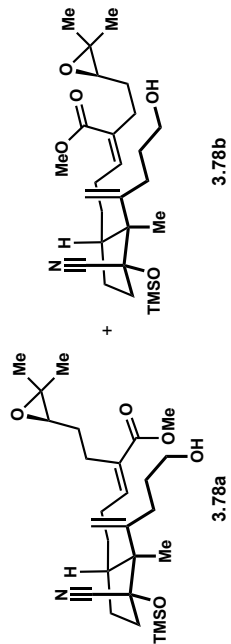
(¹H NMR, 500 MHz, CDCl₃)

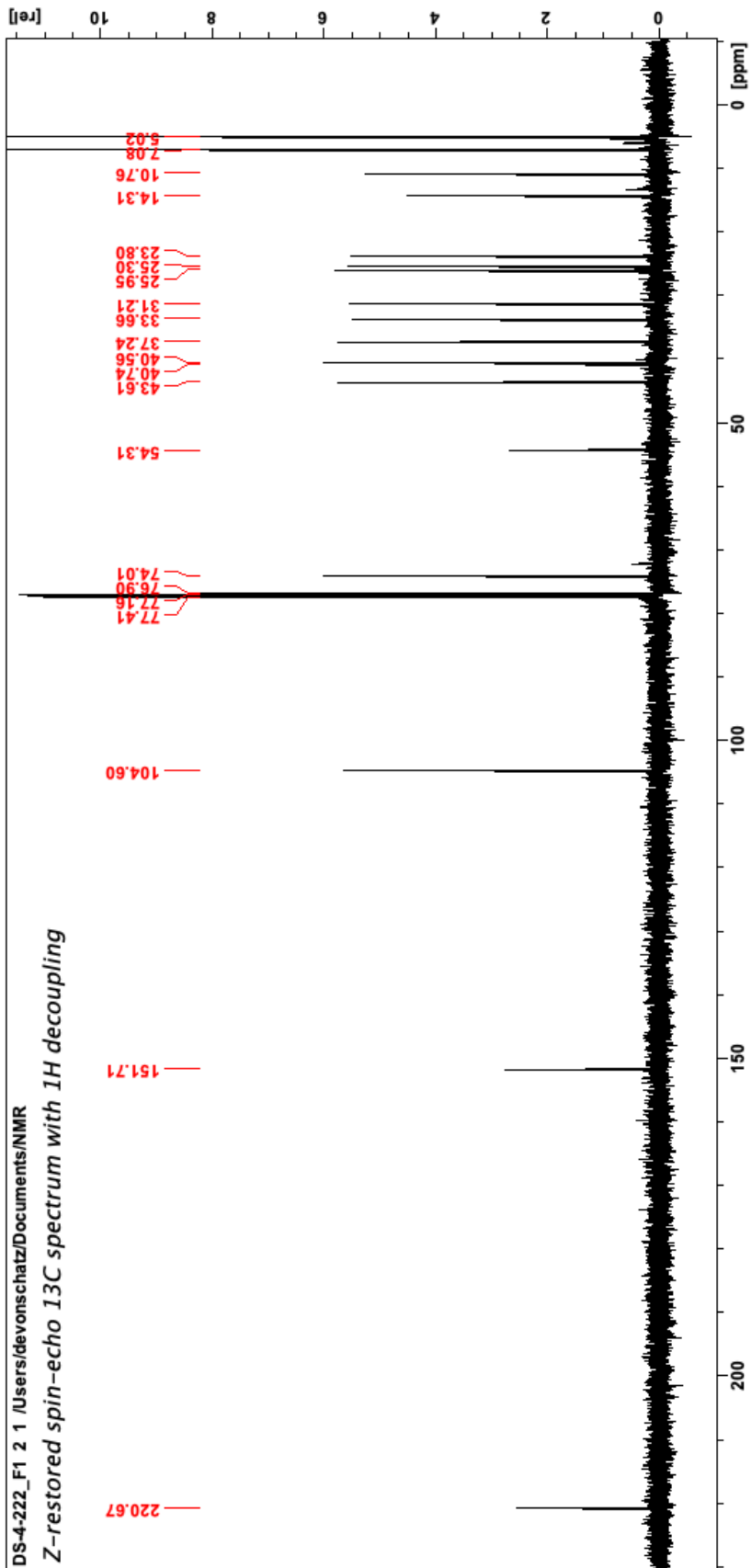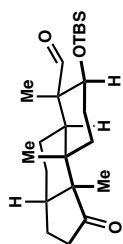DS-7-26 2 1 /Users/devonschatz/Documents/NMR

1H spectrum

3.78b

3.78a

(¹³C NMR, 126 MHz, CDCl₃)

DS-7-26 3 1 /Users/devonschatz/Documents/NMR
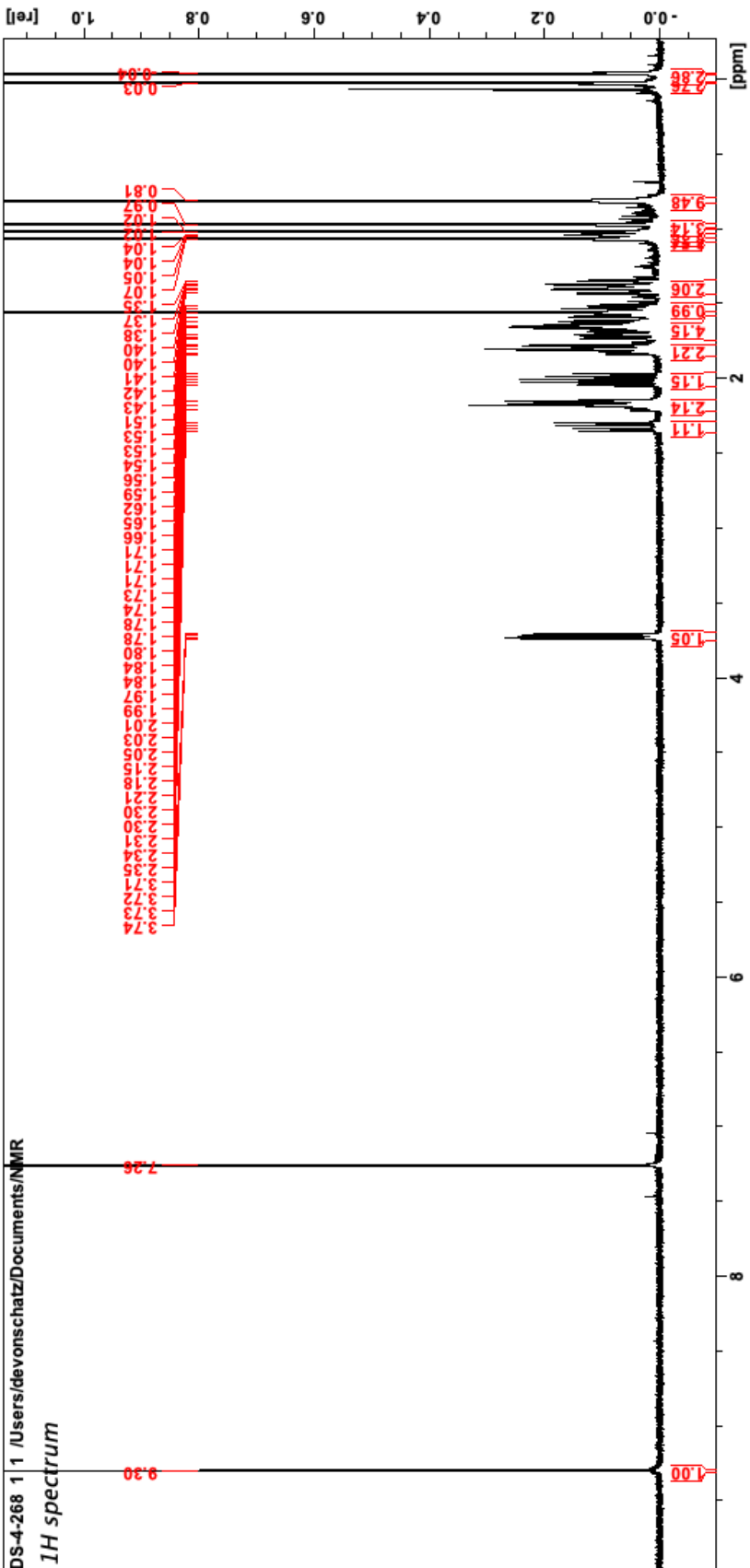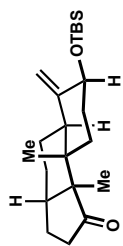
Z-restored spin-echo 13C spectrum with 1H decoupling

1.32

12.96
13.01

18.81
18.83
23.72
24.96
25.01
25.39
25.43
27.13
27.72
27.75
28.29
28.59
28.72
30.68
30.73
31.18
31.64
31.67
31.74
37.01
37.03
40.68
40.70
51.46
51.88
56.18
56.21
58.56
58.62
62.88
62.93
63.82
63.84
76.90
77.16
77.36
77.41
82.64
82.69

111.10
111.15

122.03
122.13

131.43
131.64

142.76
142.94

149.45
149.60

168.11

296

Me
Me
O

Me
Me
O

3.58a   +   **3.58b**
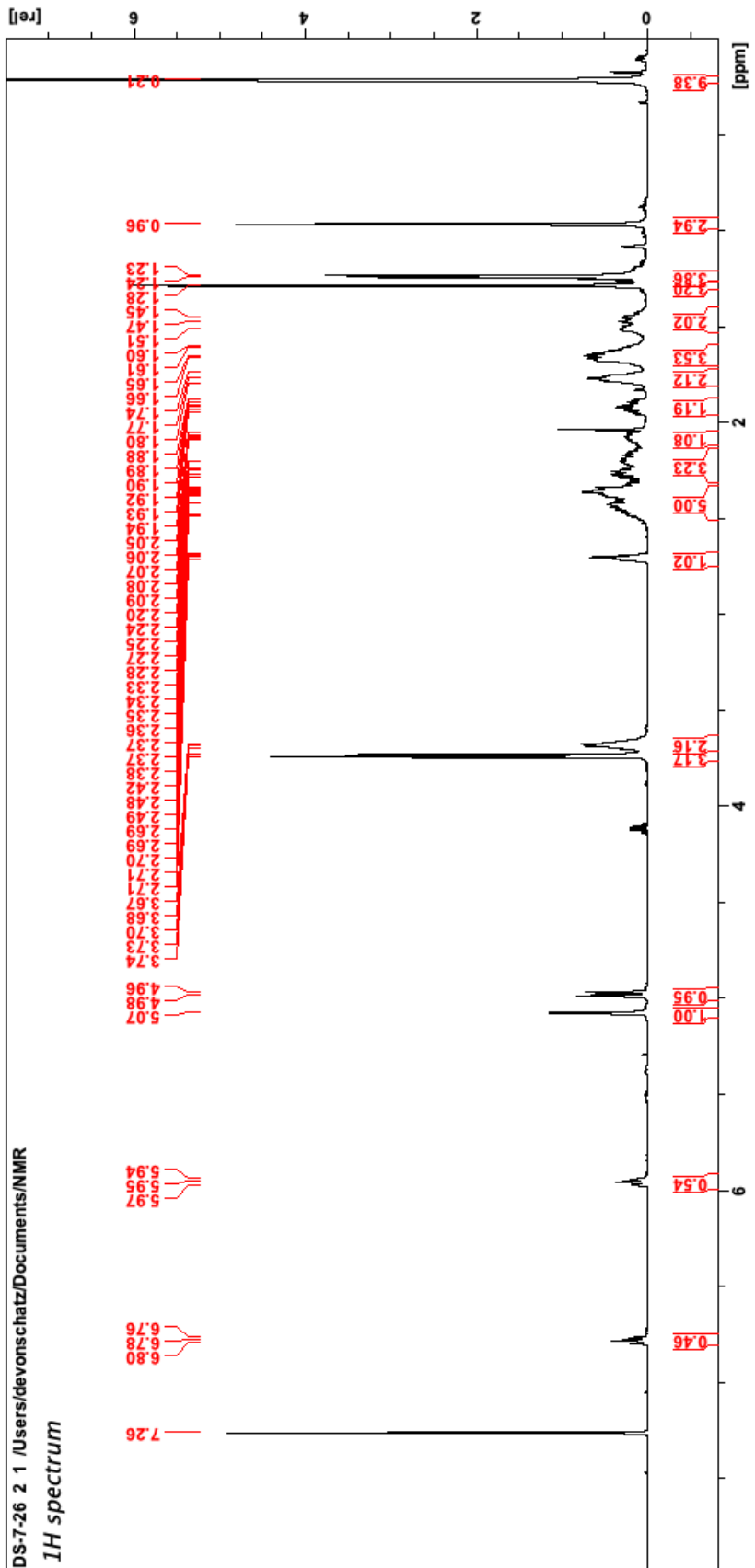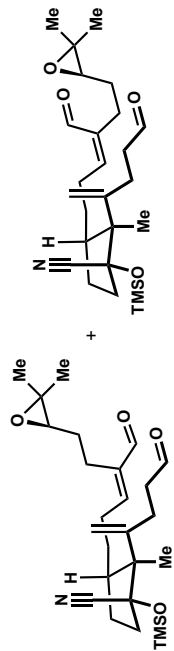
(^{1}H NMR, 500 MHz, CDCl$_3$)

DS-7-25 2 1 /Users/devonschatz/Documents/NMR

1H spectrum

TMSO   Me   N   H
TMSO   Me   N   H

0.33

1.01
1.23
1.28
1.47
1.50
1.51
1.52
1.58
1.59
1.60
1.61
1.65
1.66
1.67
1.74
1.91
1.92
1.94
1.95
1.98
2.05
2.07
2.12
2.13
2.33
2.33
2.40
2.41
2.44
2.57
2.62
2.63
2.65
2.67
2.69

4.96
4.98
4.99

6.47
6.48
6.50
6.51
6.53

9.38

9.79

10.12

9.49
2.73
3.59
2.03
3.13
1.19
1.16
6.08
5.18
1.93
1.00
0.53
1.05
0.40

9
5
4
3
2
1
0
[rel]
[ppm]
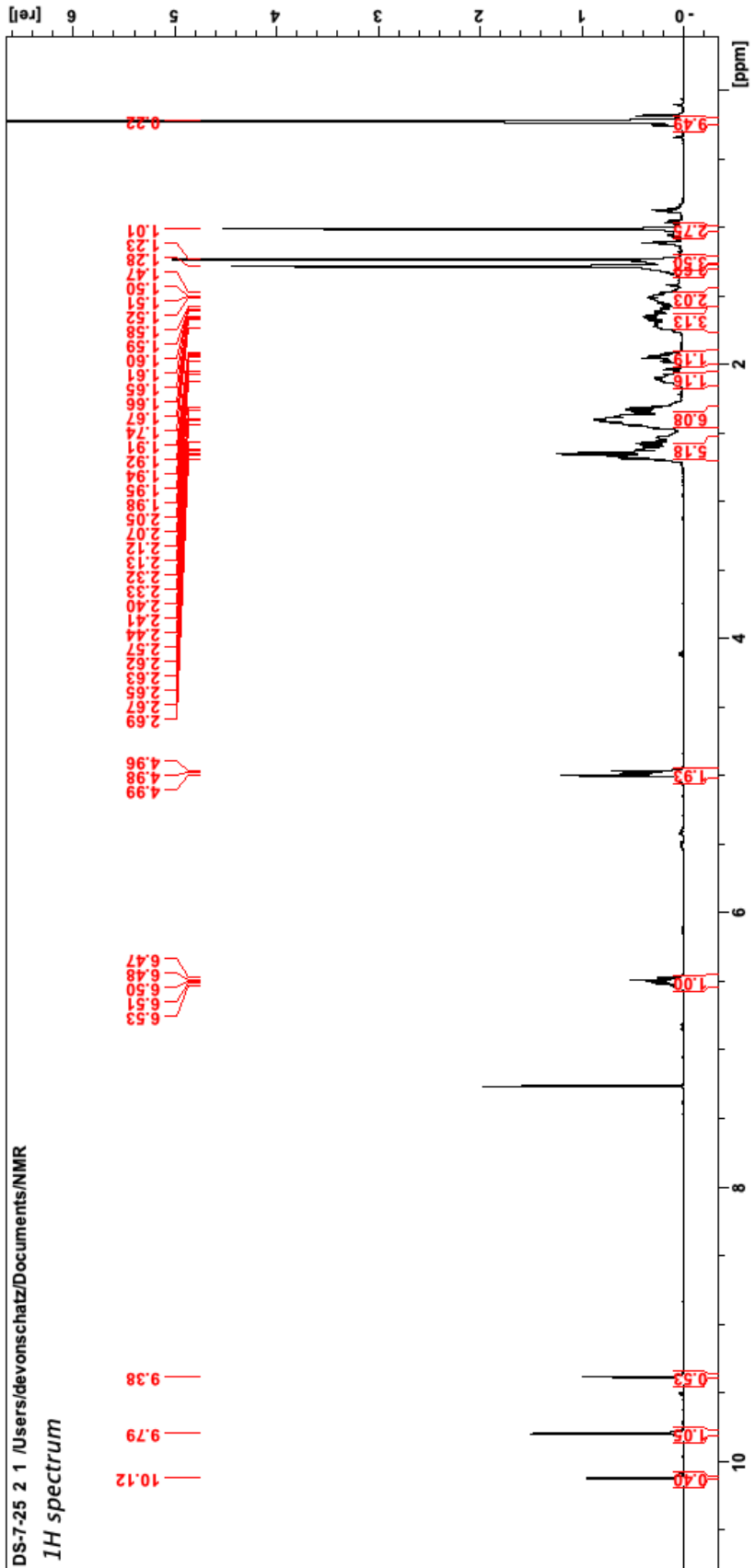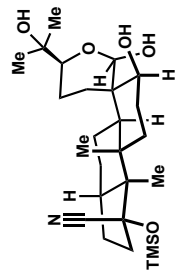
3.82 (^{1}H NMR, 500 MHz, CDCl$_3$)

"DS-7-129 recrystallized" 1 1 /Users/devonschatz/Documents/NMR

1H spectrum

298
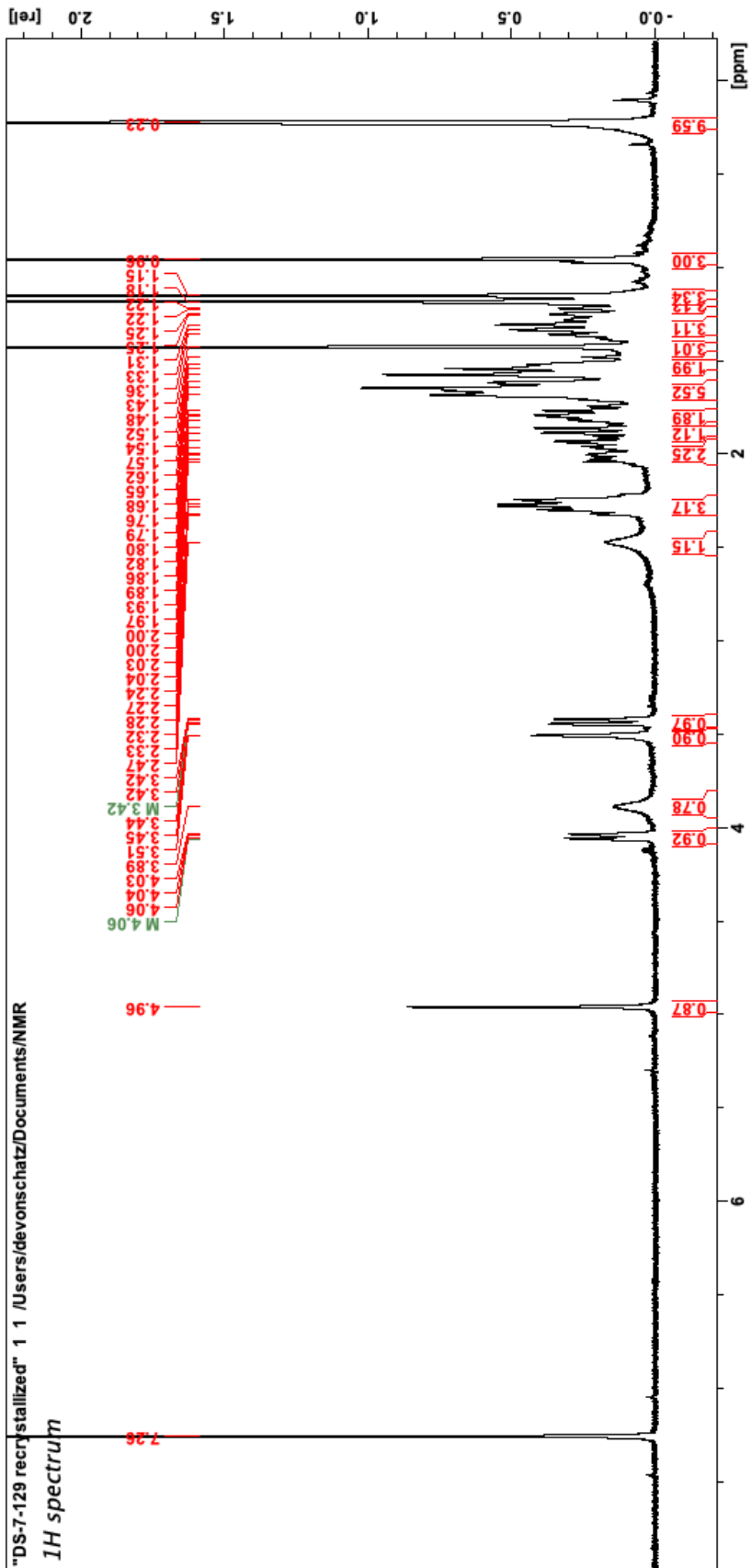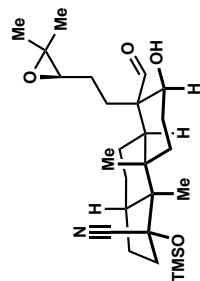
3.83 (^{1}H NMR, 500 MHz, CDCl$_3$)

DS-7-138 1 1 /Users/devonschatz/Documents/NMR
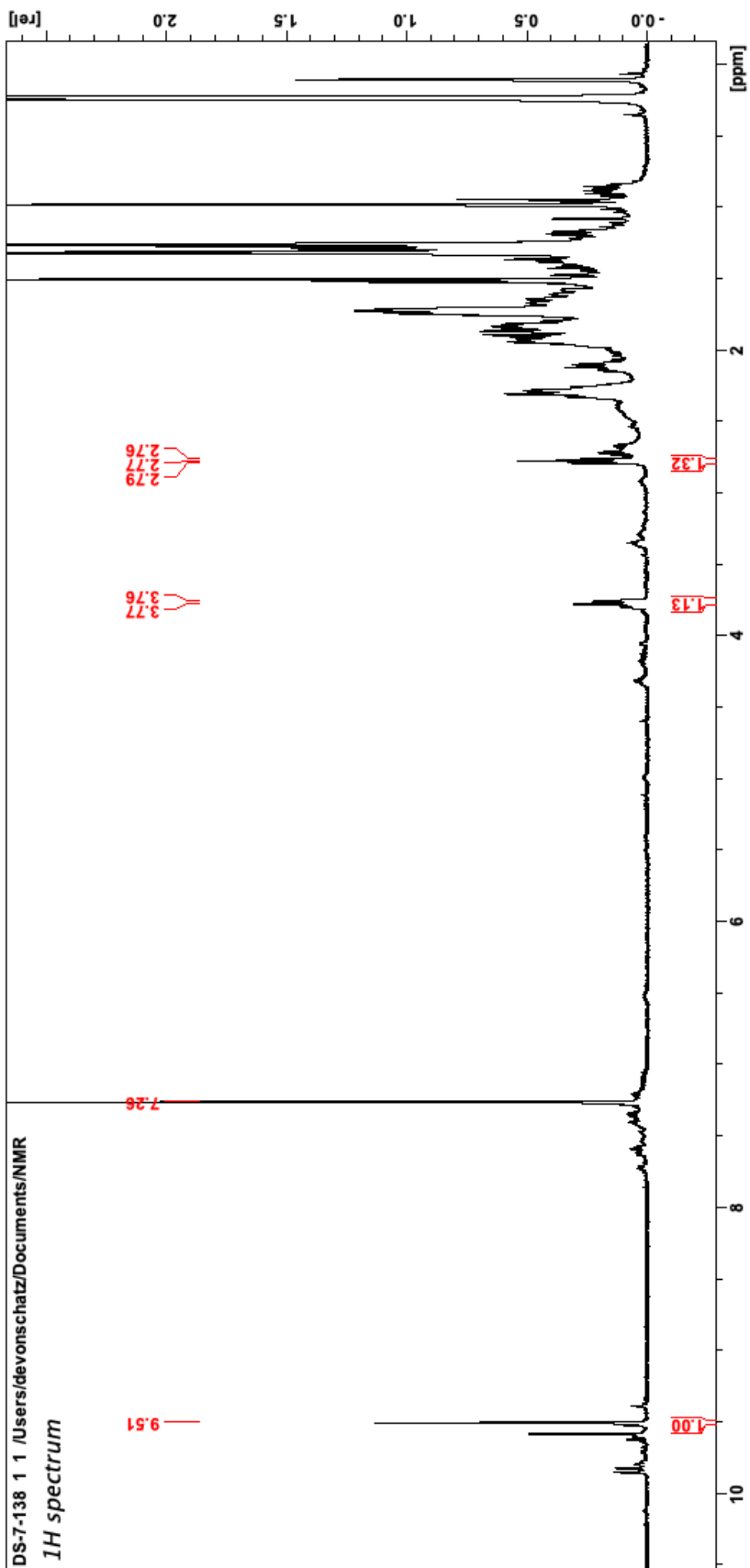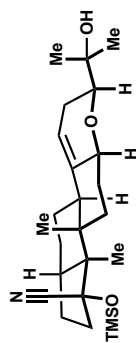
1H spectrum

3.57 (¹H NMR, 500 MHz, CDCl₃)

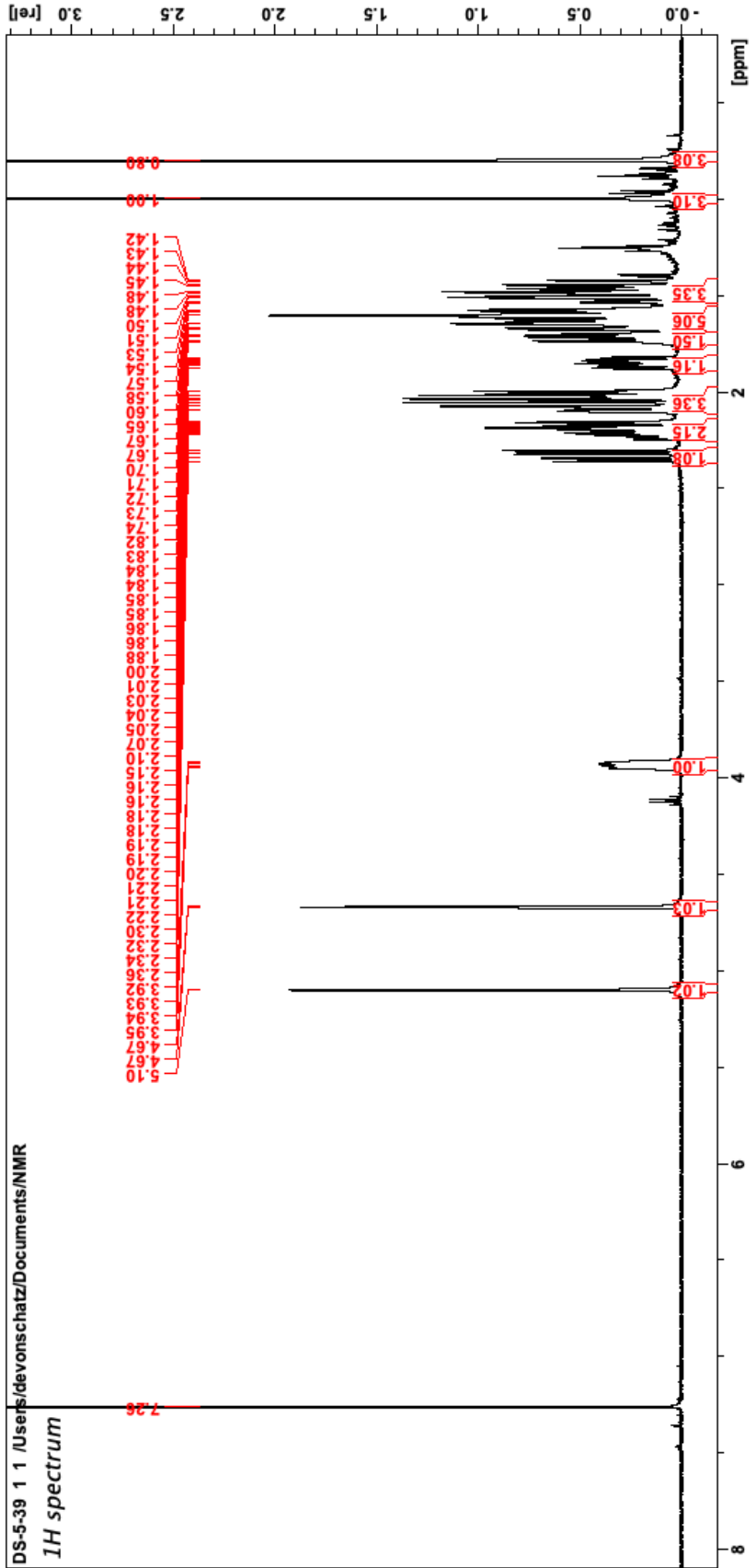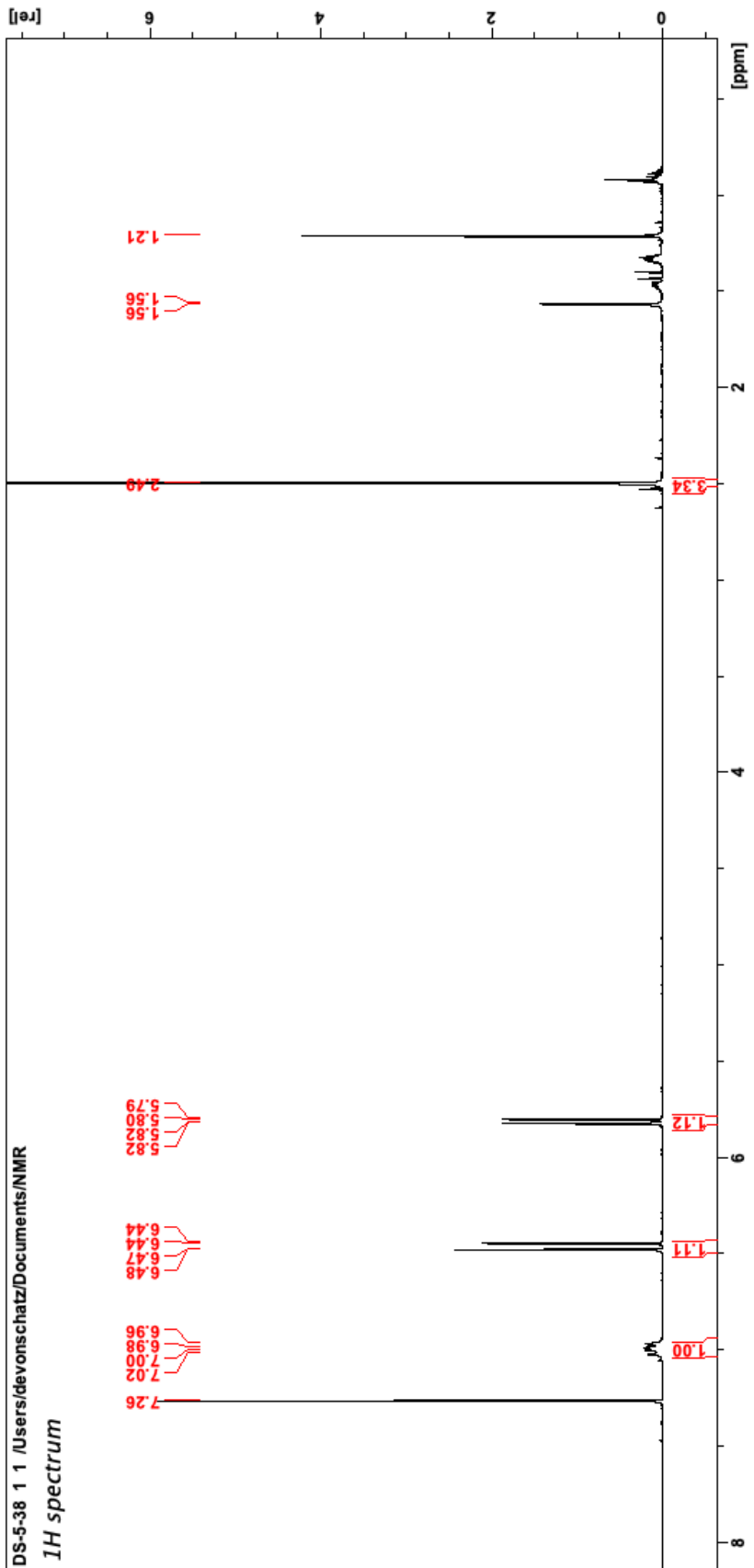"DS-7-120 F2" 1 1 /Users/devonschatz/Documents/NMR
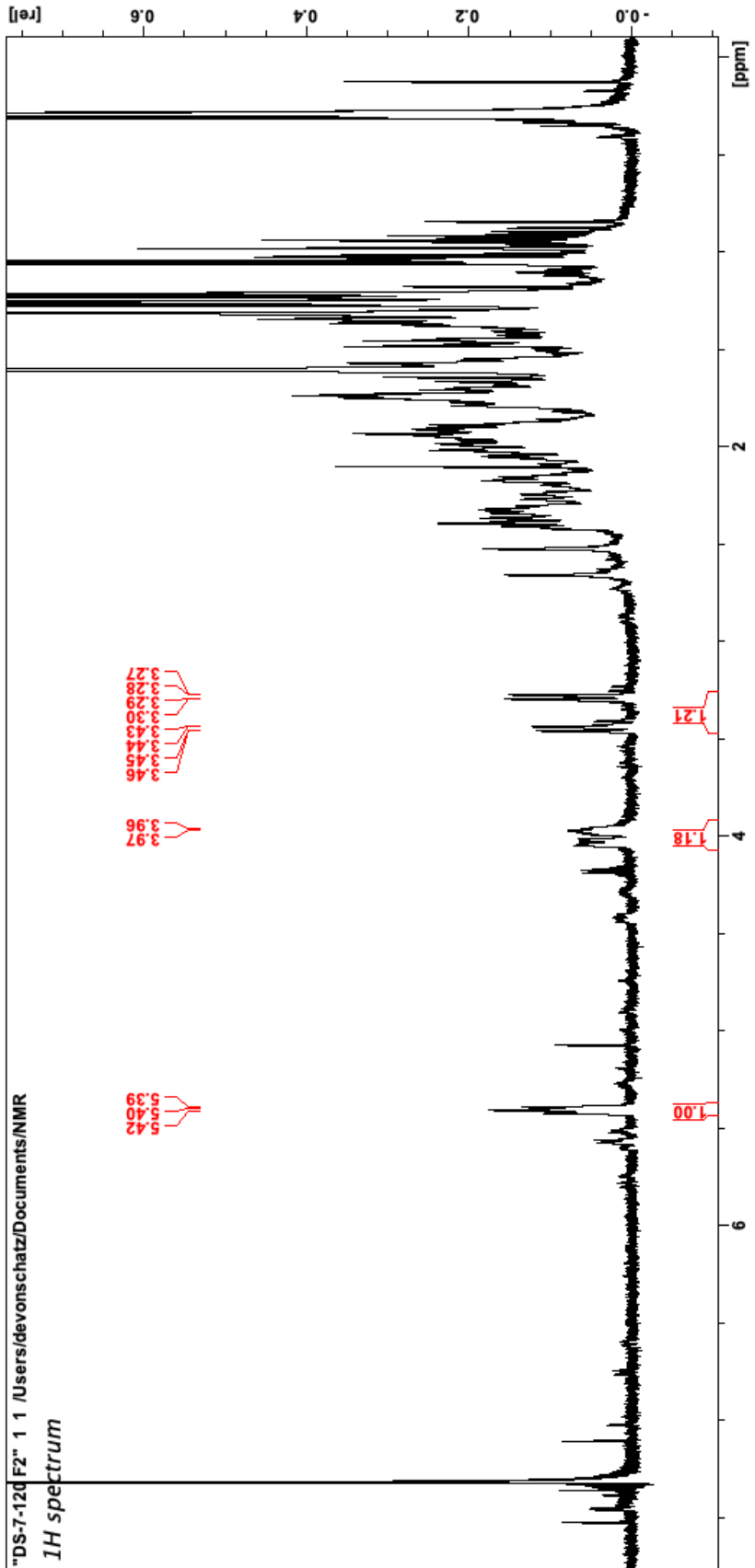
1H spectrum

Appendix C: NMR Spectra for Chapter 4
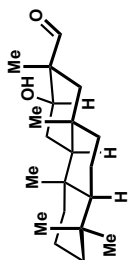
4.21 (^{1}H NMR, 500 MHz, C_6D_6)

"DS-6-106 C6D6" 3 1 /Users/devonschatz/Documents/NMR
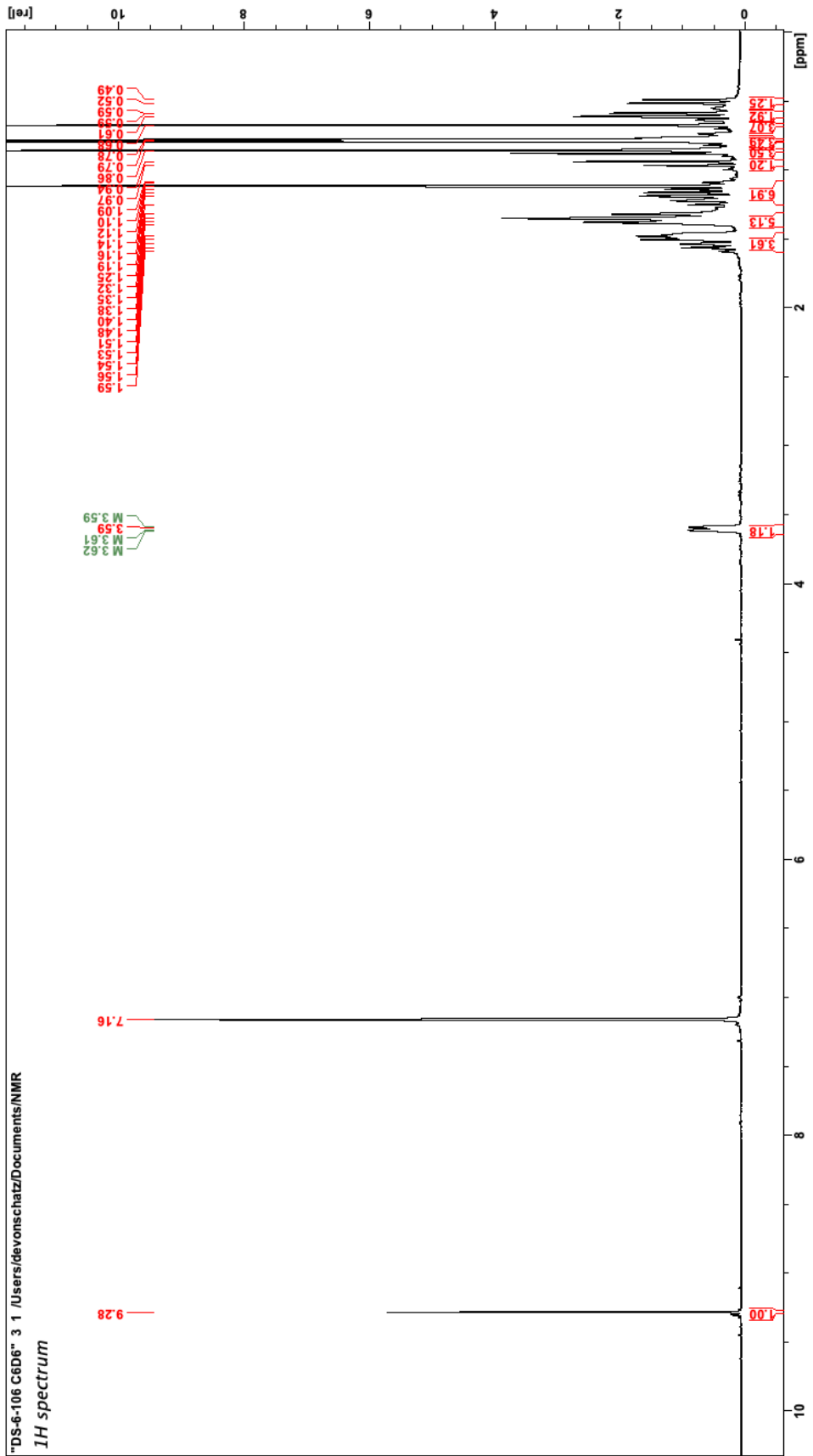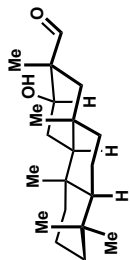
1H spectrum

4.21 (^{1}H NMR, 500 MHz, C$_6$D$_6$)

"DS-6-106 C6D6" 3 1 /Users/devonschatz/Documents/NMR
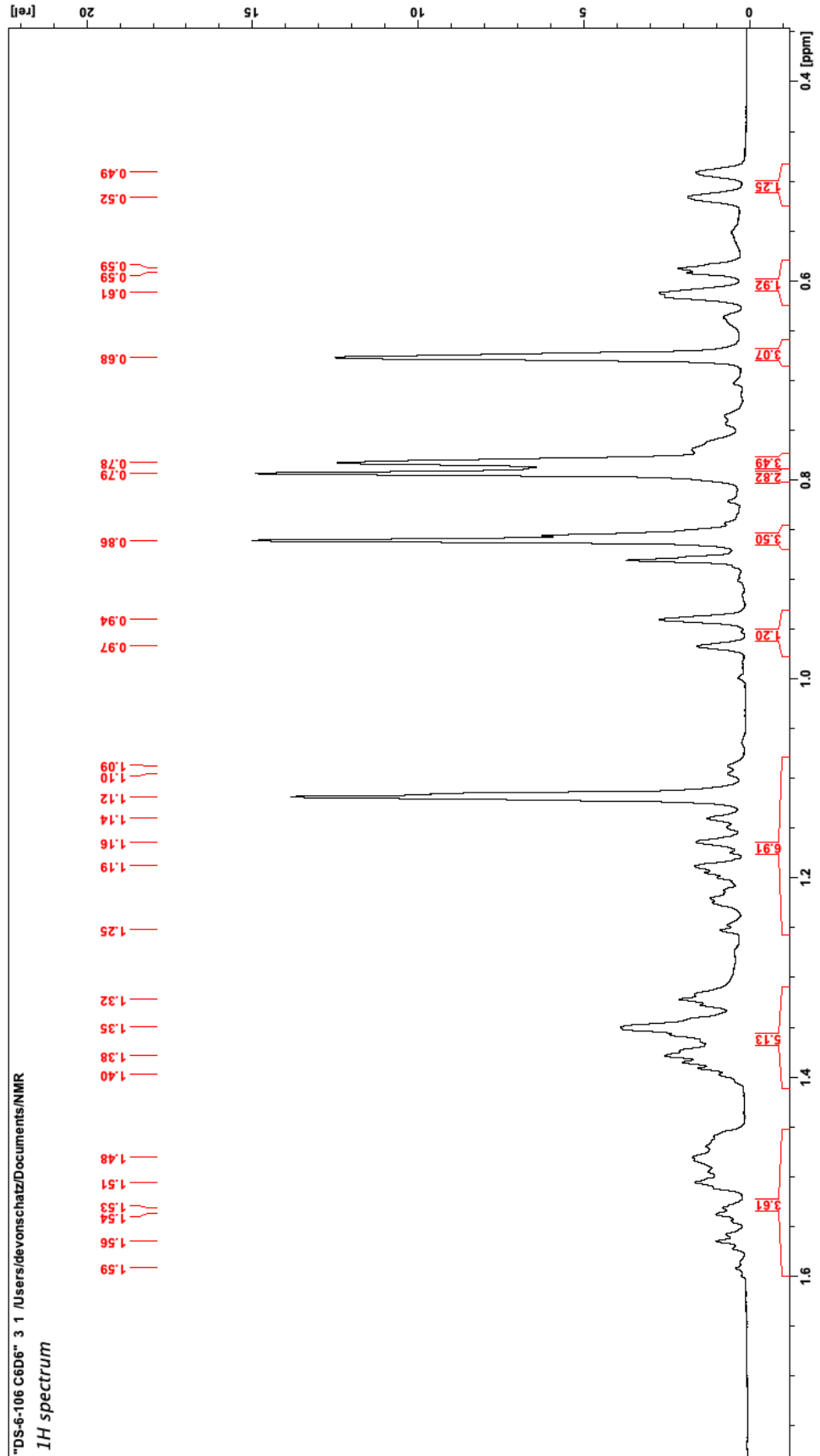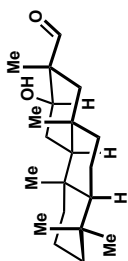
1H spectrum

4.21 (^{13}C NMR, 126 MHz, C$_6$D$_6$)

"DS-6-106 C6D6" 4 1 /Users/devonschatz/Documents/NMR

Z-restored spin-echo 13C spectrum with 1H decoupling

205.01

127.86
128.06
128.25

73.35

56.42
56.59

51.50
49.08

43.43
42.45
39.78
37.32
34.92
33.53
33.44

26.43
22.99
21.53
18.91
18.35
16.23
14.63
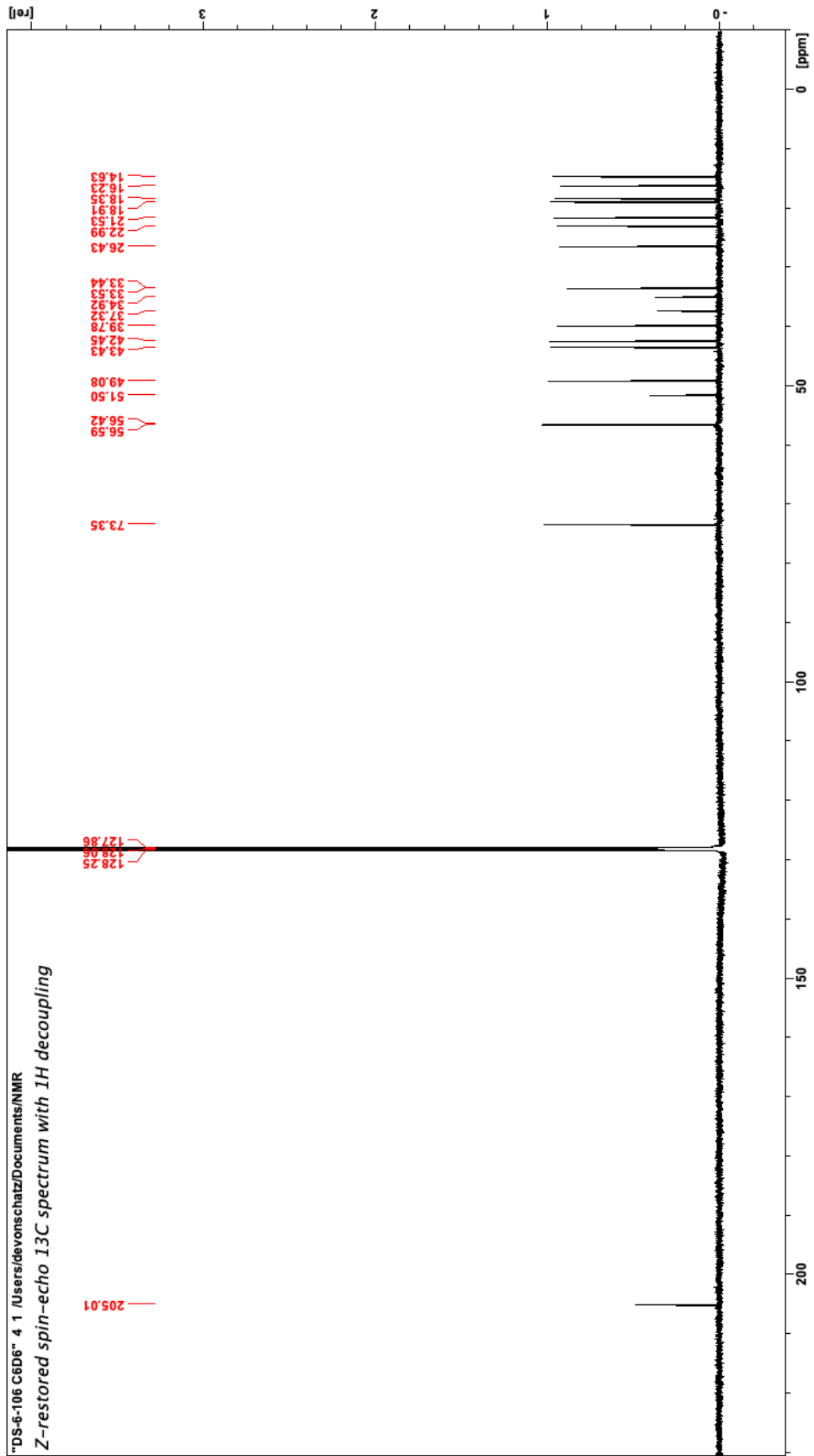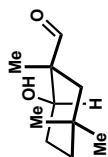
4.24 (^{1}H NMR, 500 MHz, CDCl$_3$)

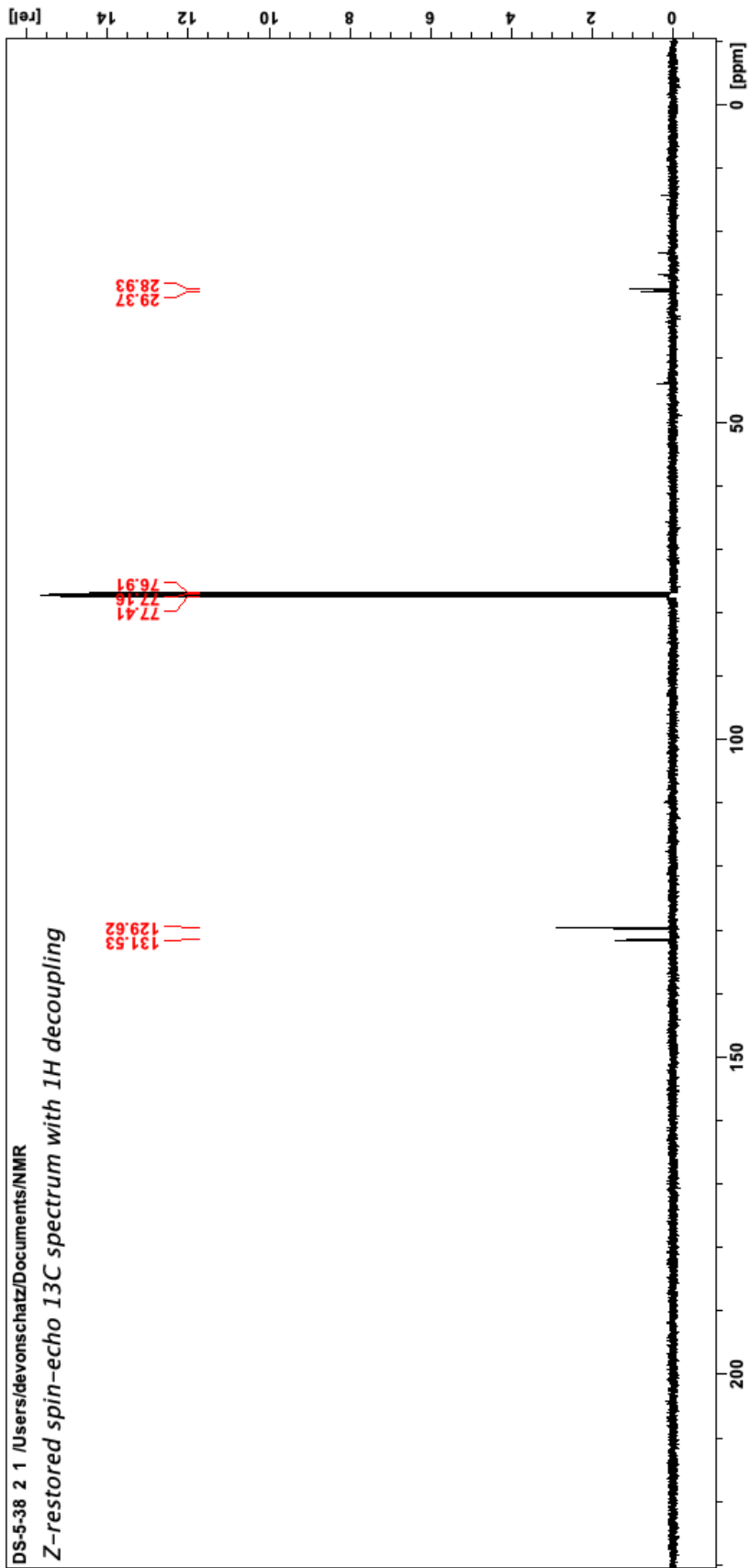DS-5-131 3 1 /Users/devonschatz/Documents/NMR
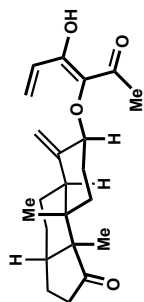*1H spectrum*

305
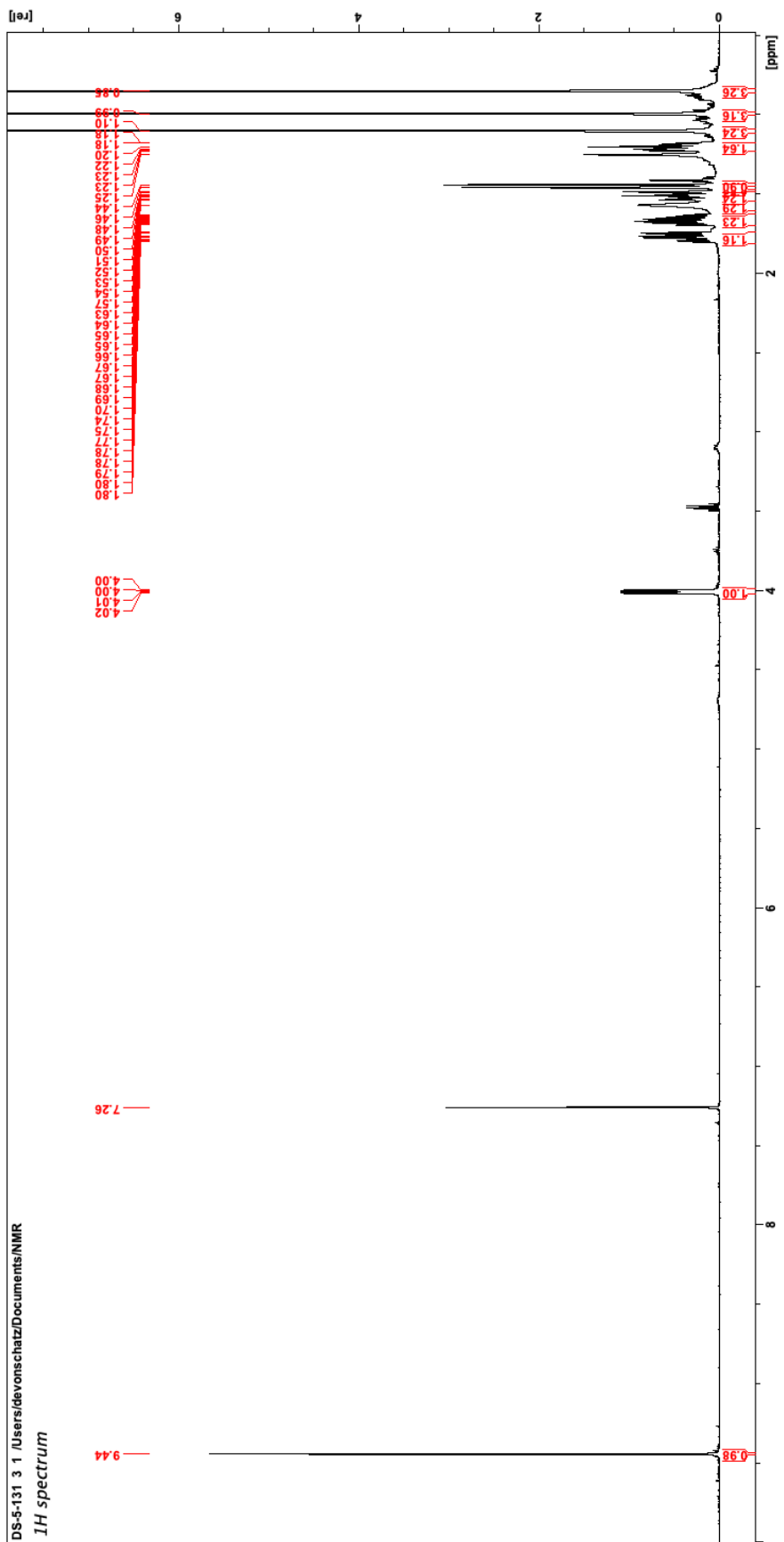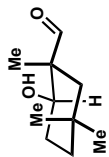
4.24 (^{13}C NMR, 126 MHz, CDCl$_3$)

DS-5-131 5 1 /Users/devonschatz/Documents/NMR

Z-restored spin-echo 13C spectrum with 1H decoupling
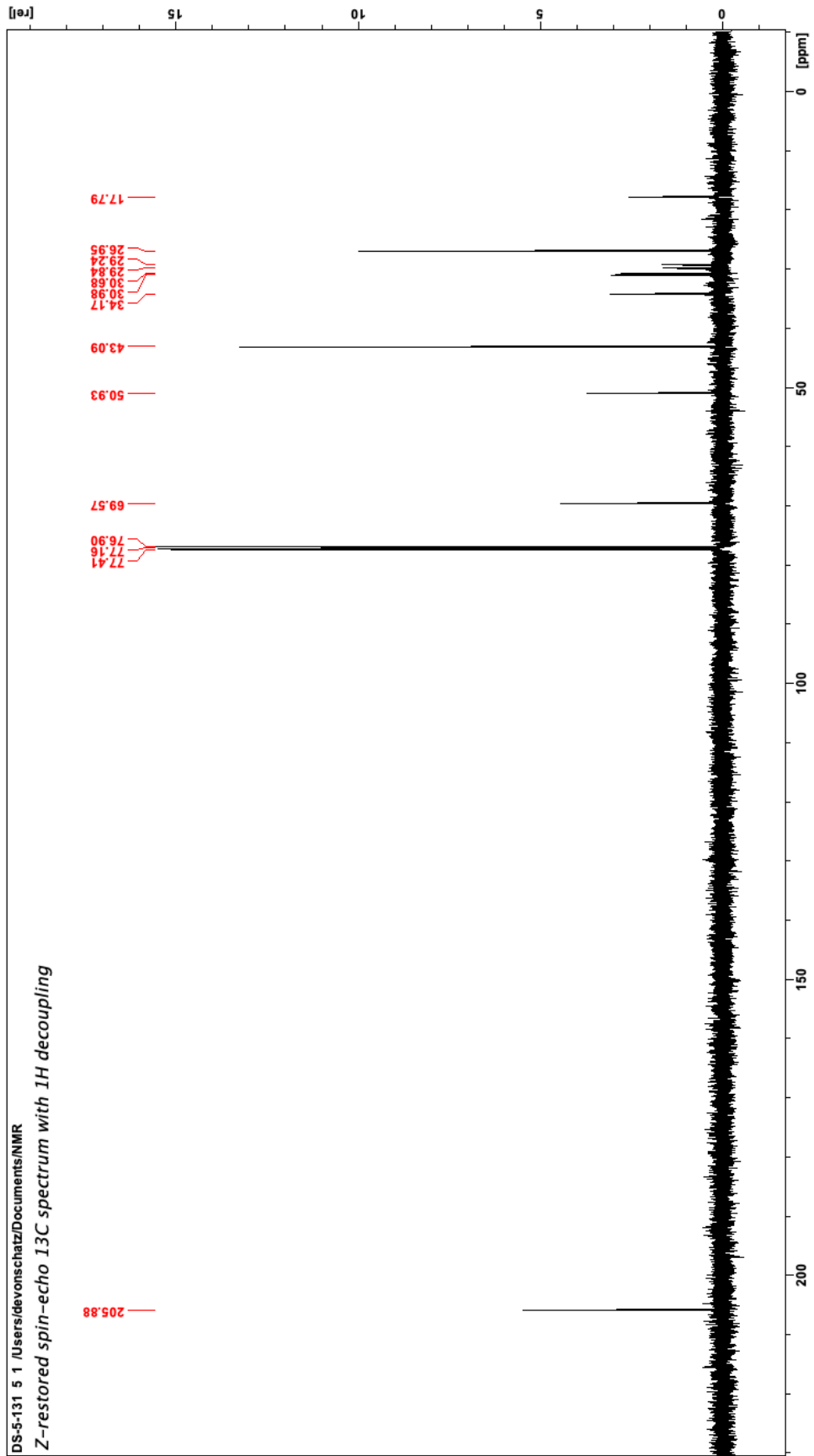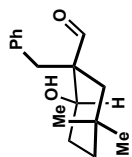
4.26 (^{1}H NMR, 500 MHz, CDCl$_3$)

DS-5-142 3 1 /Users/devonschatz/Documents/NMR
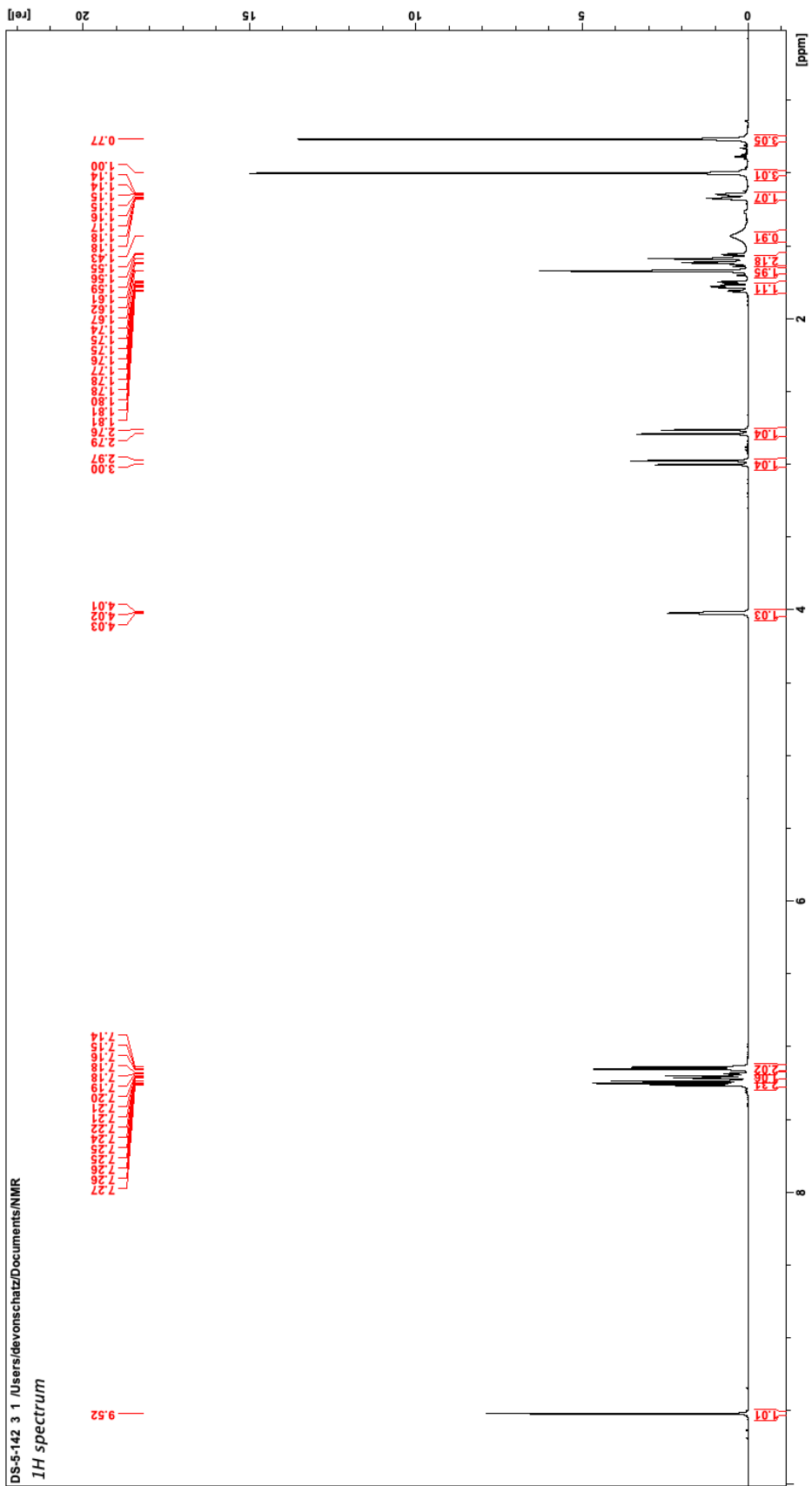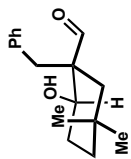
1H spectrum

4.26 (^{13}C NMR, 126 MHz, CDCl$_3$)

DS-5-142 4 1 /Users/devonschatz/Documents/NMR
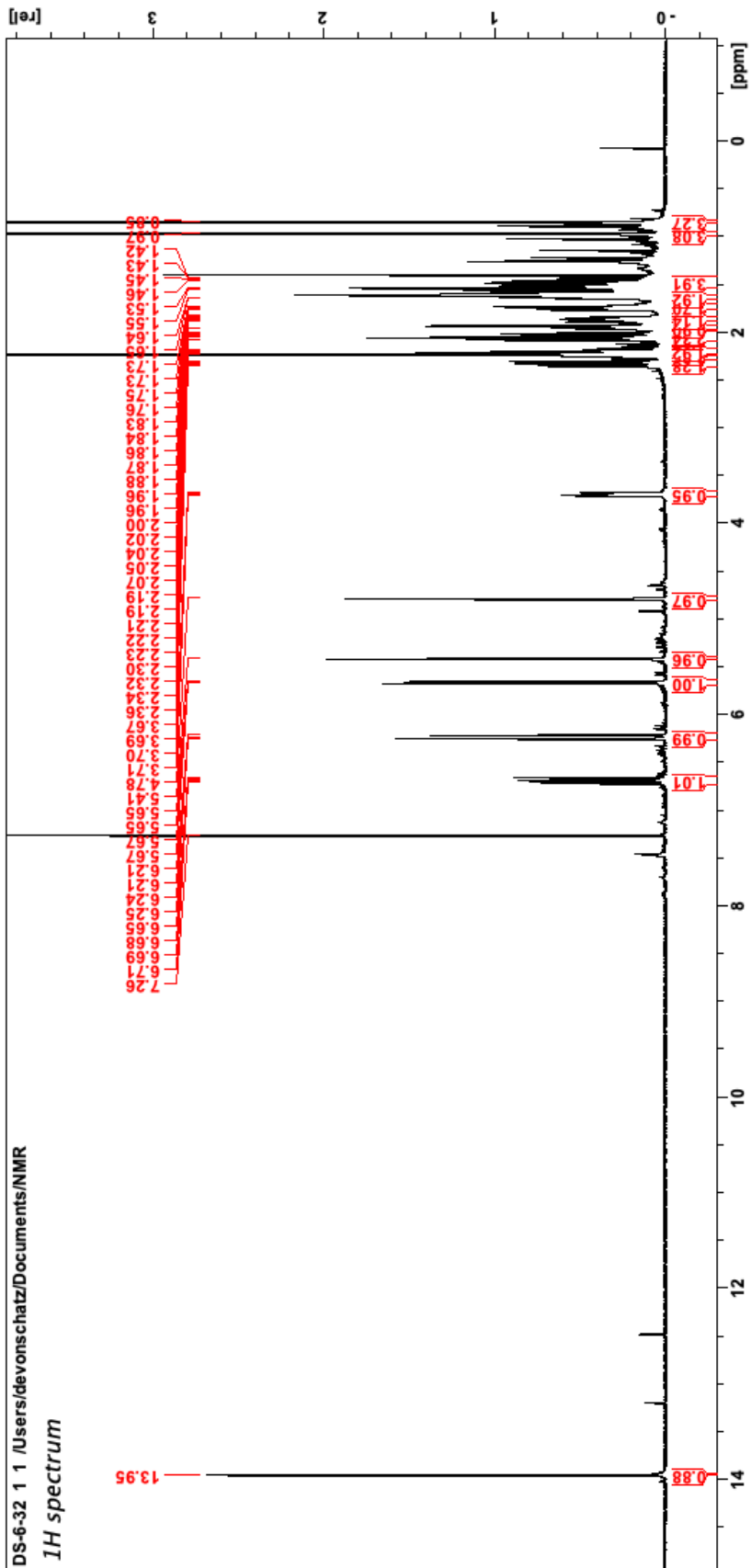
Z–restored spin–echo 13C spectrum with 1H decoupling
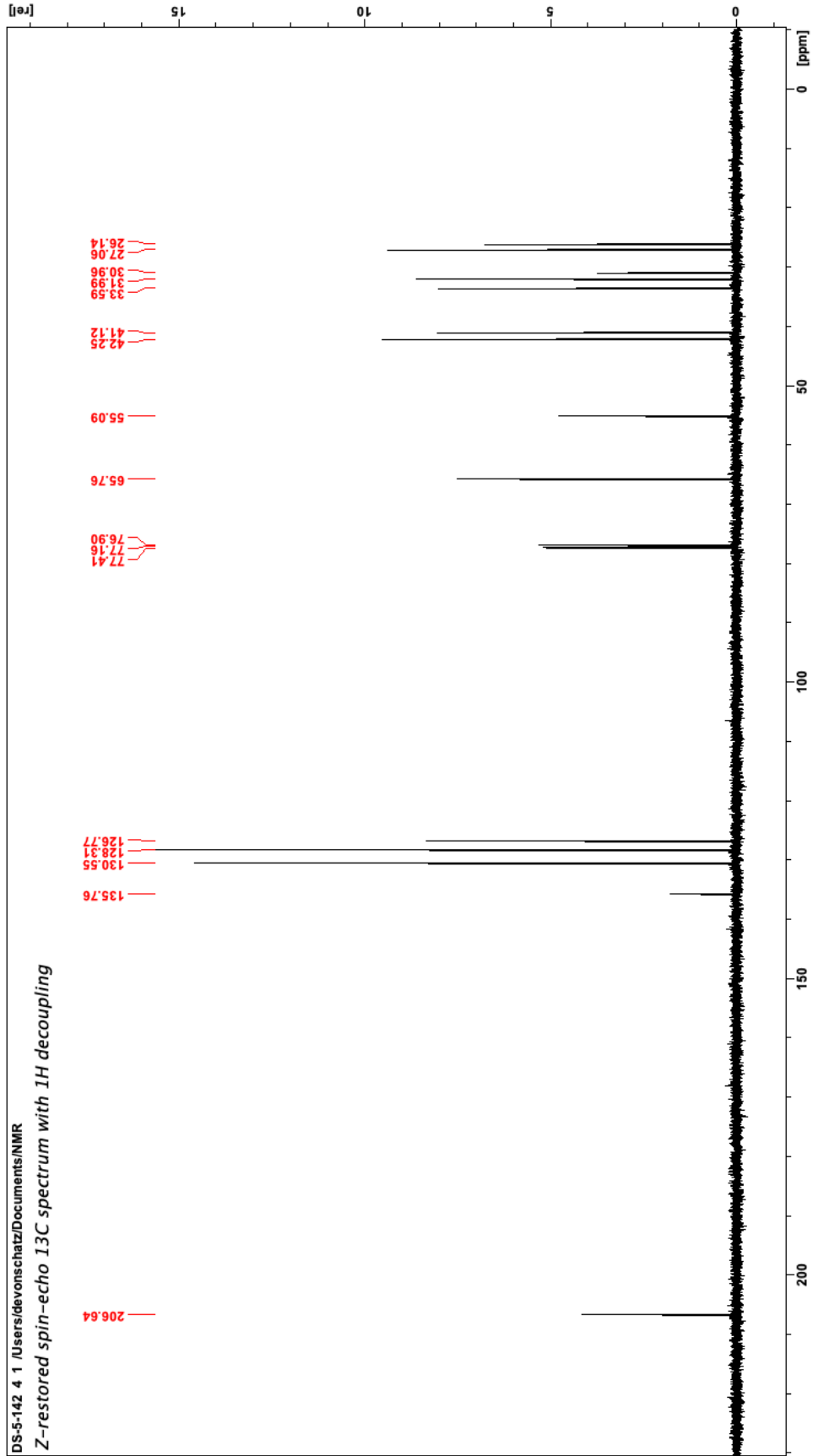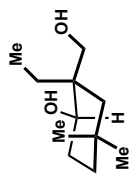
4.27 (¹H NMR, 500 MHz, CDCl₃)

DS-6-111 2 1 /Users/devonschatz/Documents/NMR
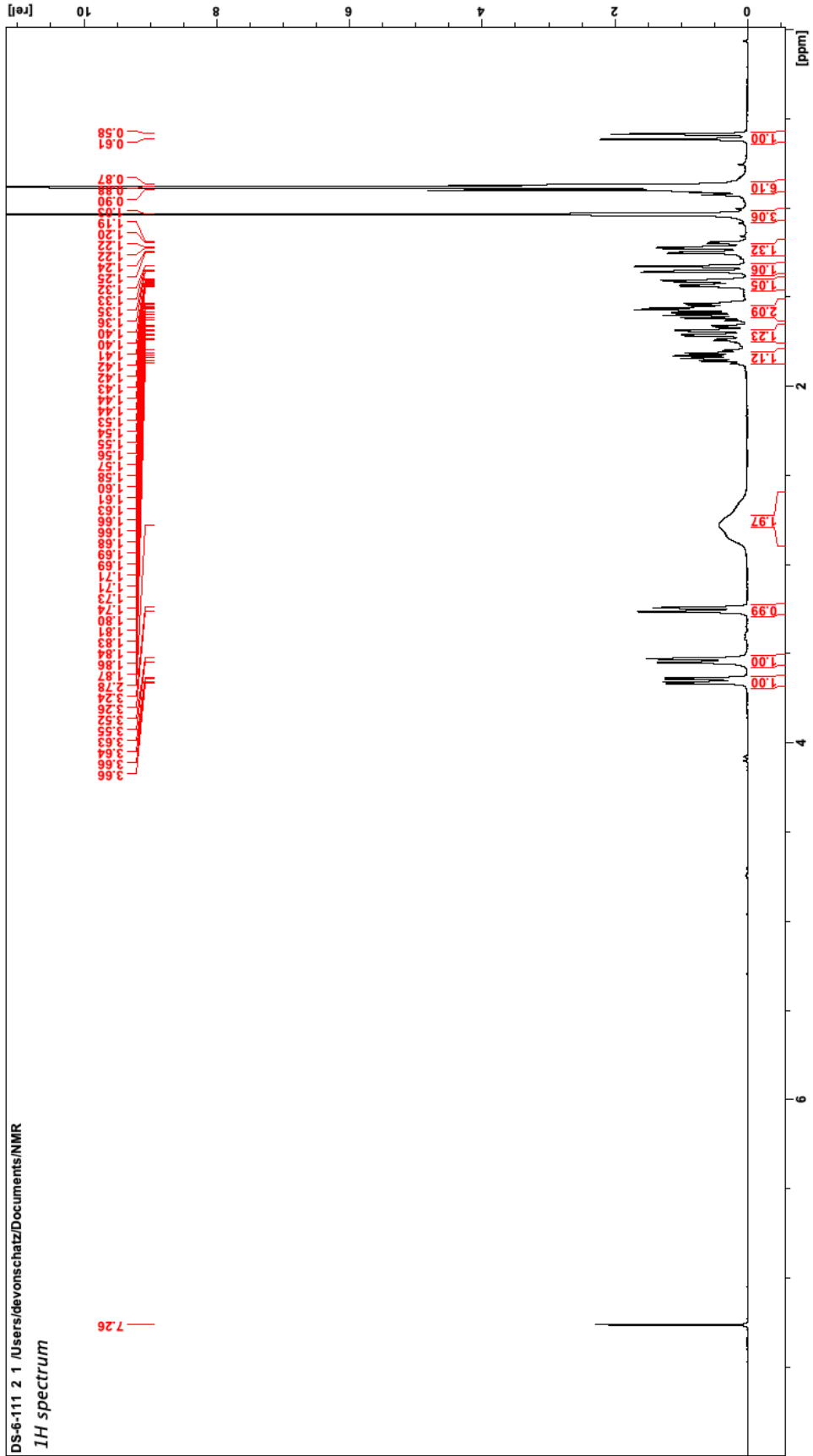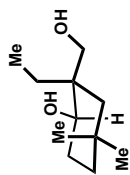
1H spectrum

4.27 (^{13}C NMR, 126 MHz, CDCl$_3$)

DS-6-111 4 1 /Users/devonschatz/Documents/NMR
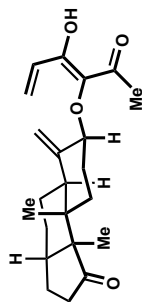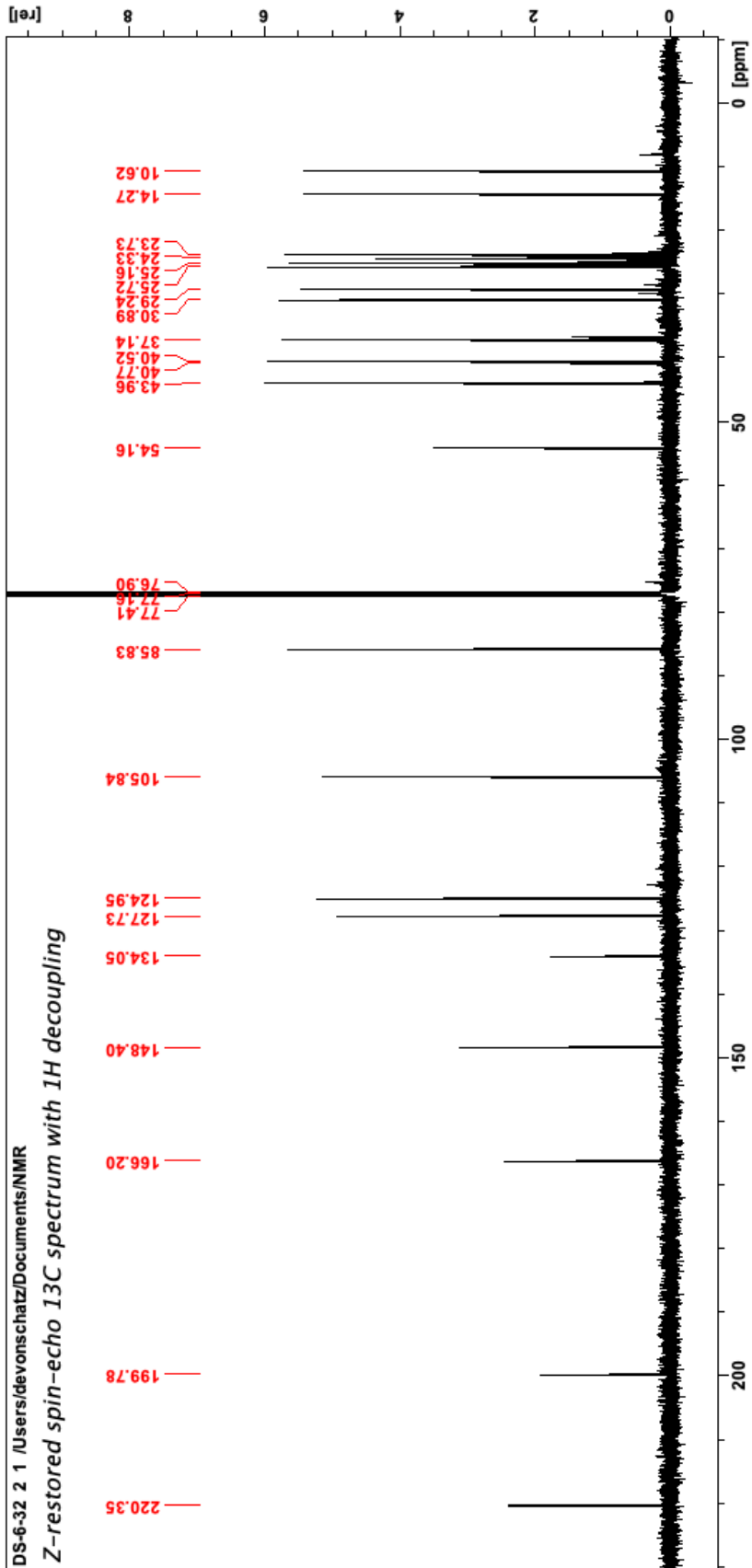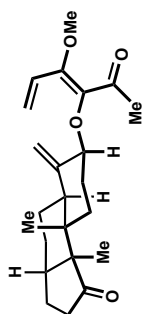
Z-restored spin-echo 13C spectrum with 1H decoupling

310
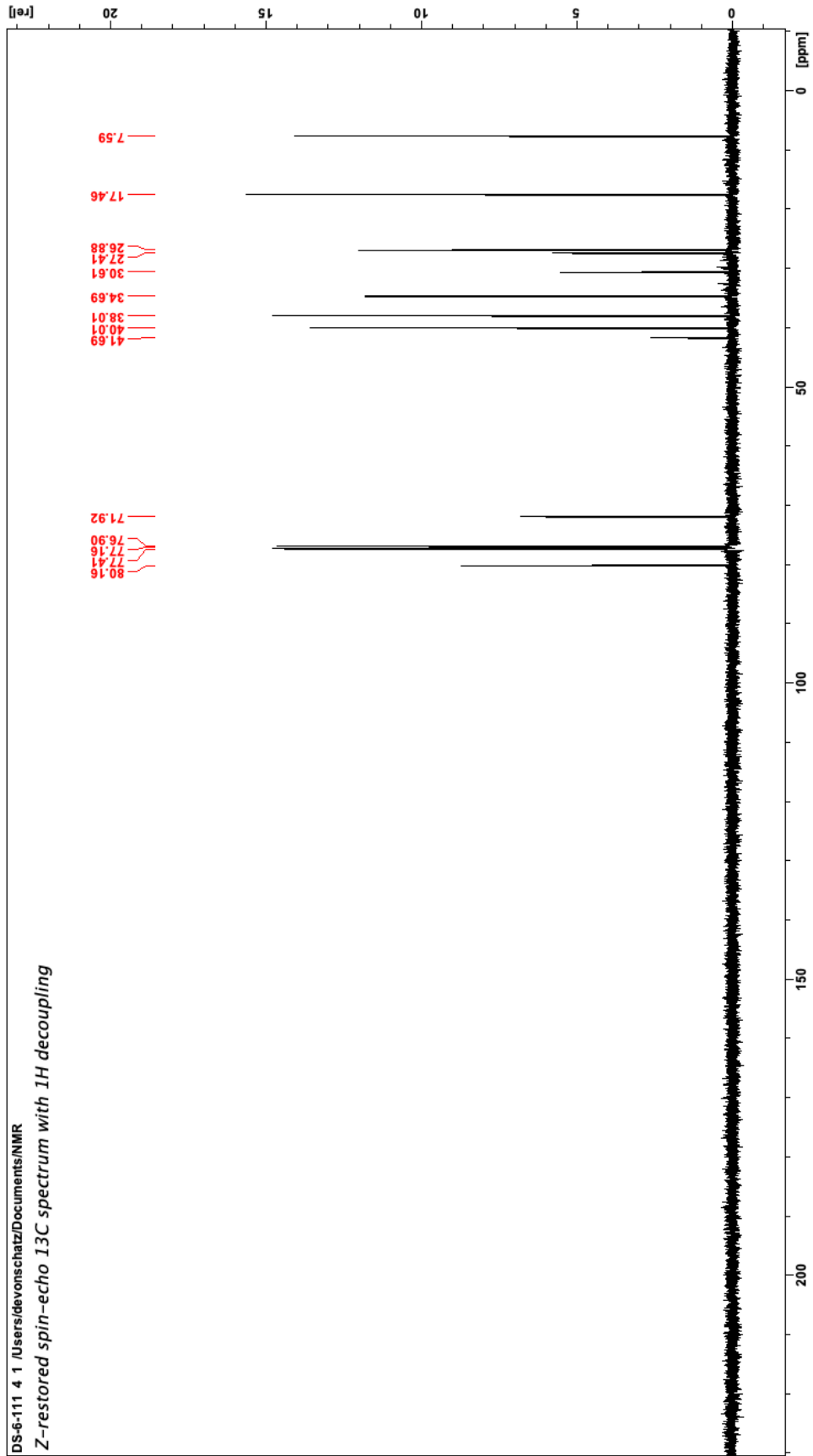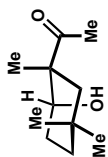
4.28 (¹H NMR, 500 MHz, CDCl₃)

"DS-5-119 F2 rerun" 1 1 /Users/devonschatz/Documents/NMR
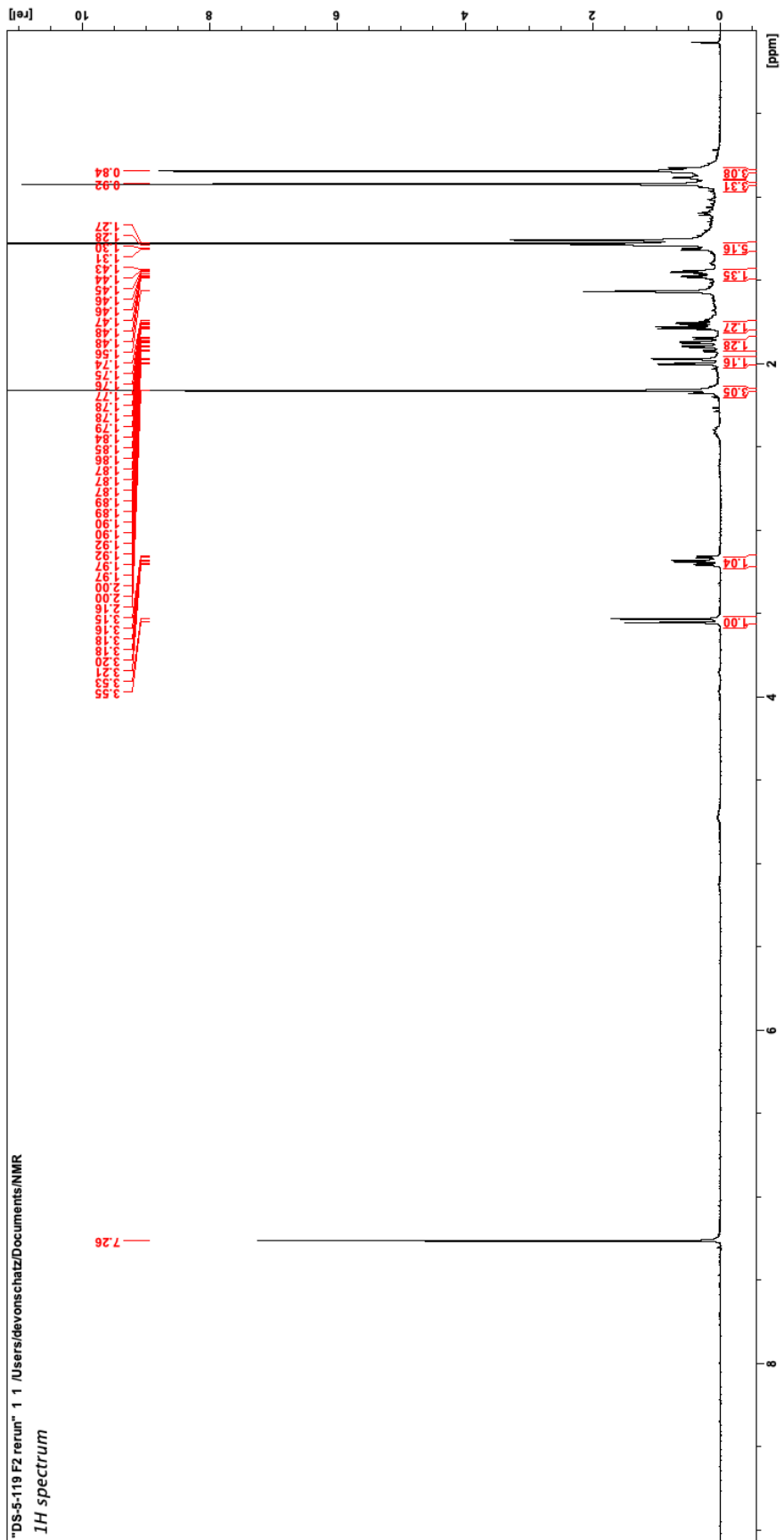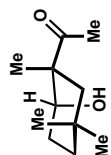
1H spectrum

4.28 (^{13}C NMR, 126 MHz, CDCl$_3$)

"DS-5-119 F2 rerun" 5 1 /Users/devonschatz/Documents/NMR

Z-restored spin-echo 13C spectrum with 1H decoupling

4.28 (COSY, CDCl$_3$)

"DS-5-119 F2 cosy" 2 1 /Users/devonschatz/Documents/NMR

gcosy60

313

4.28 (NOESY, CDCl$_3$)

"DS-5-119 F2 noesy" 2 1 /Users/devonschatz/Documents/NMR
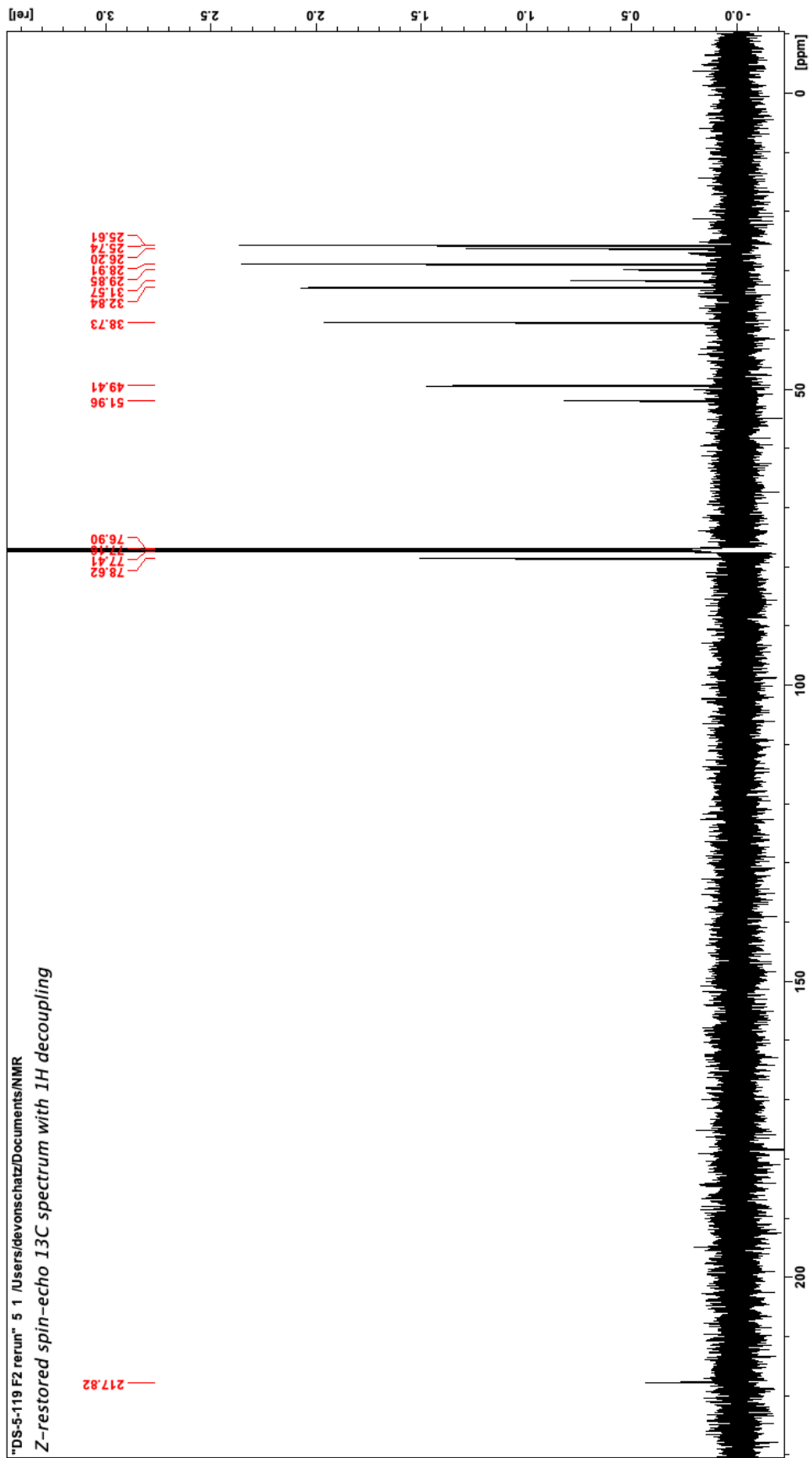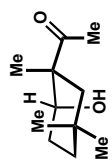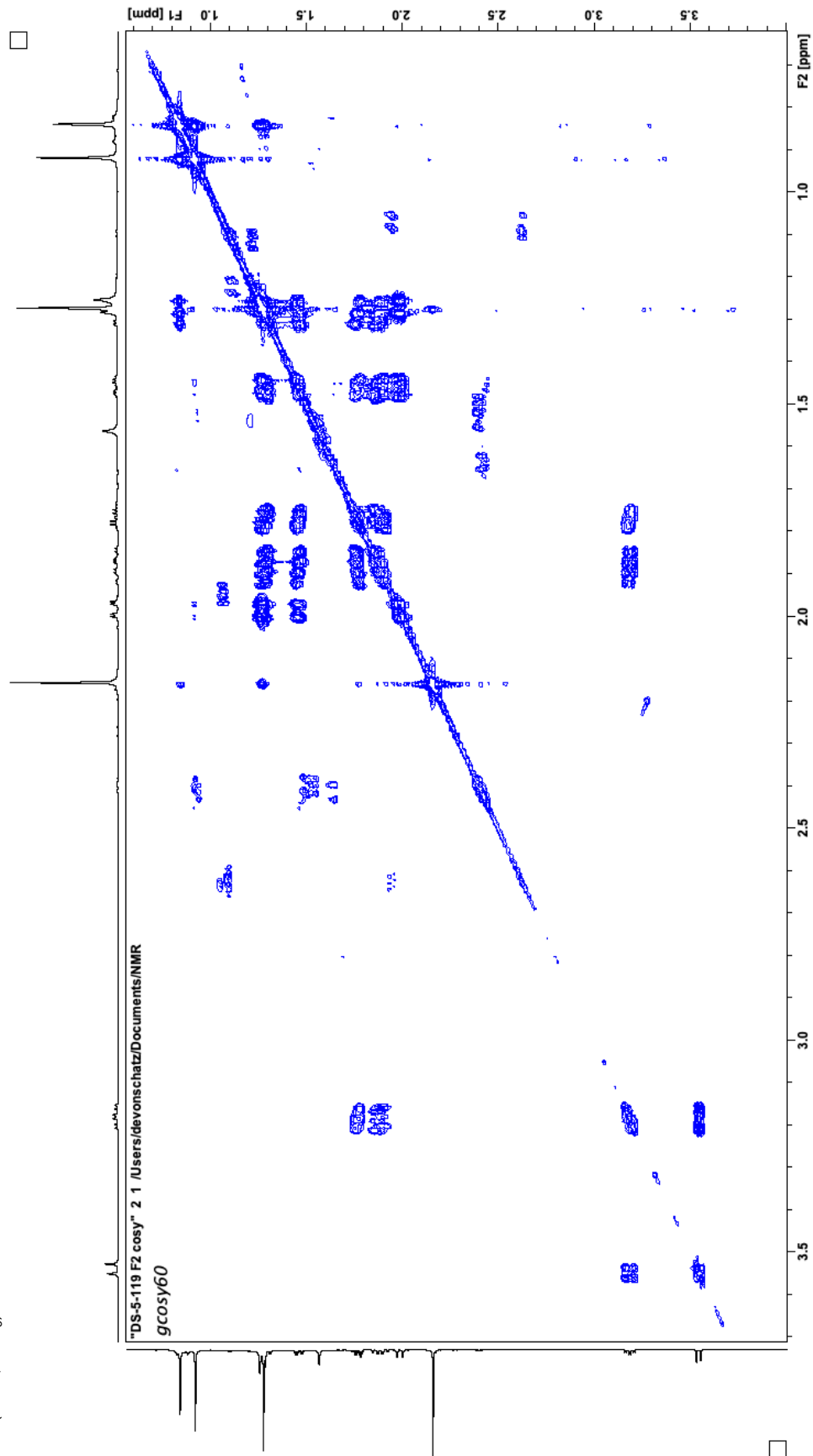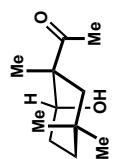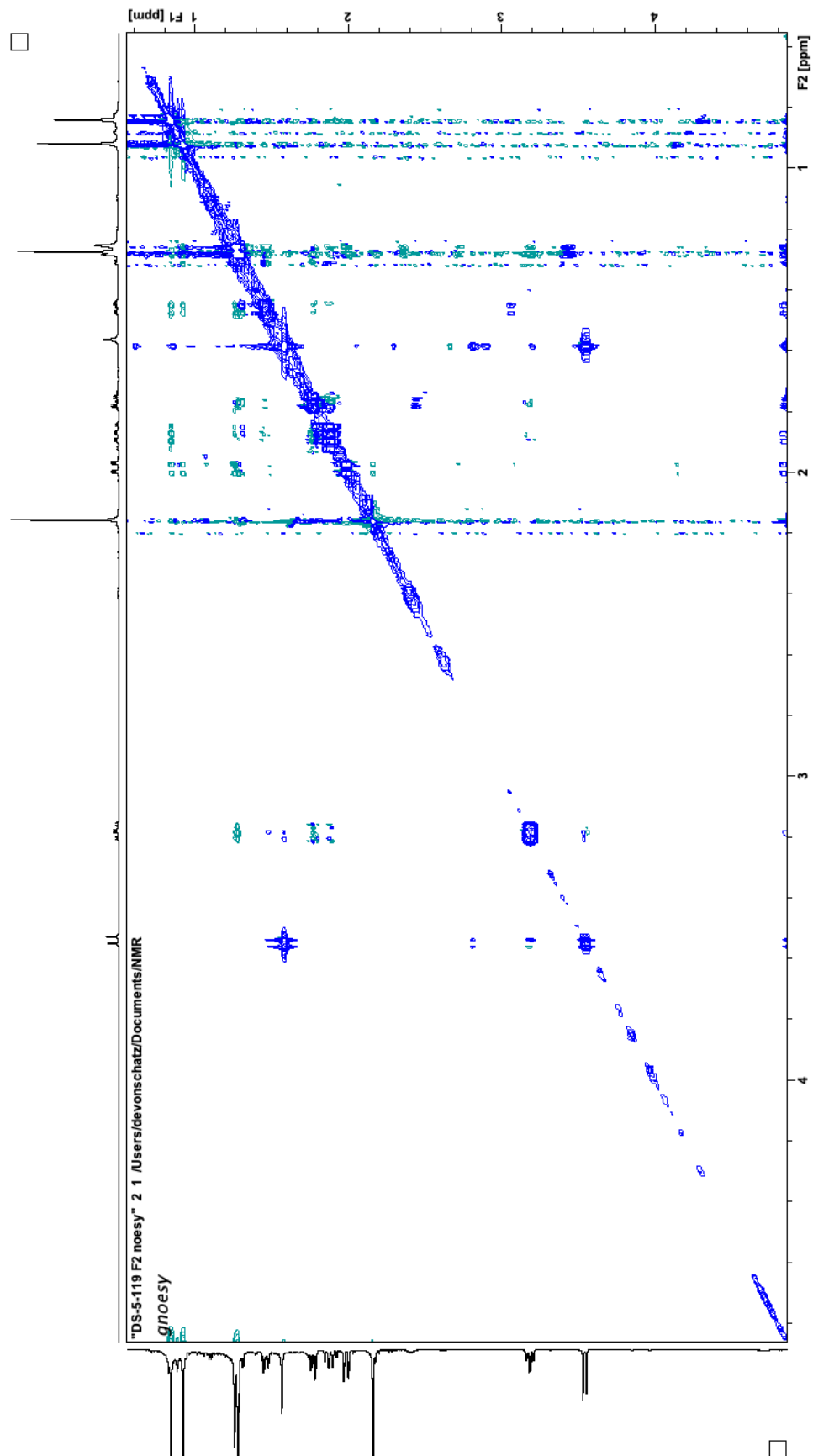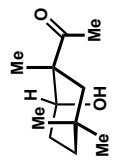
gnoesy

4.28 (NOESY, CDCl$_3$)

4.28 (NOESY, CDCl₃)

316
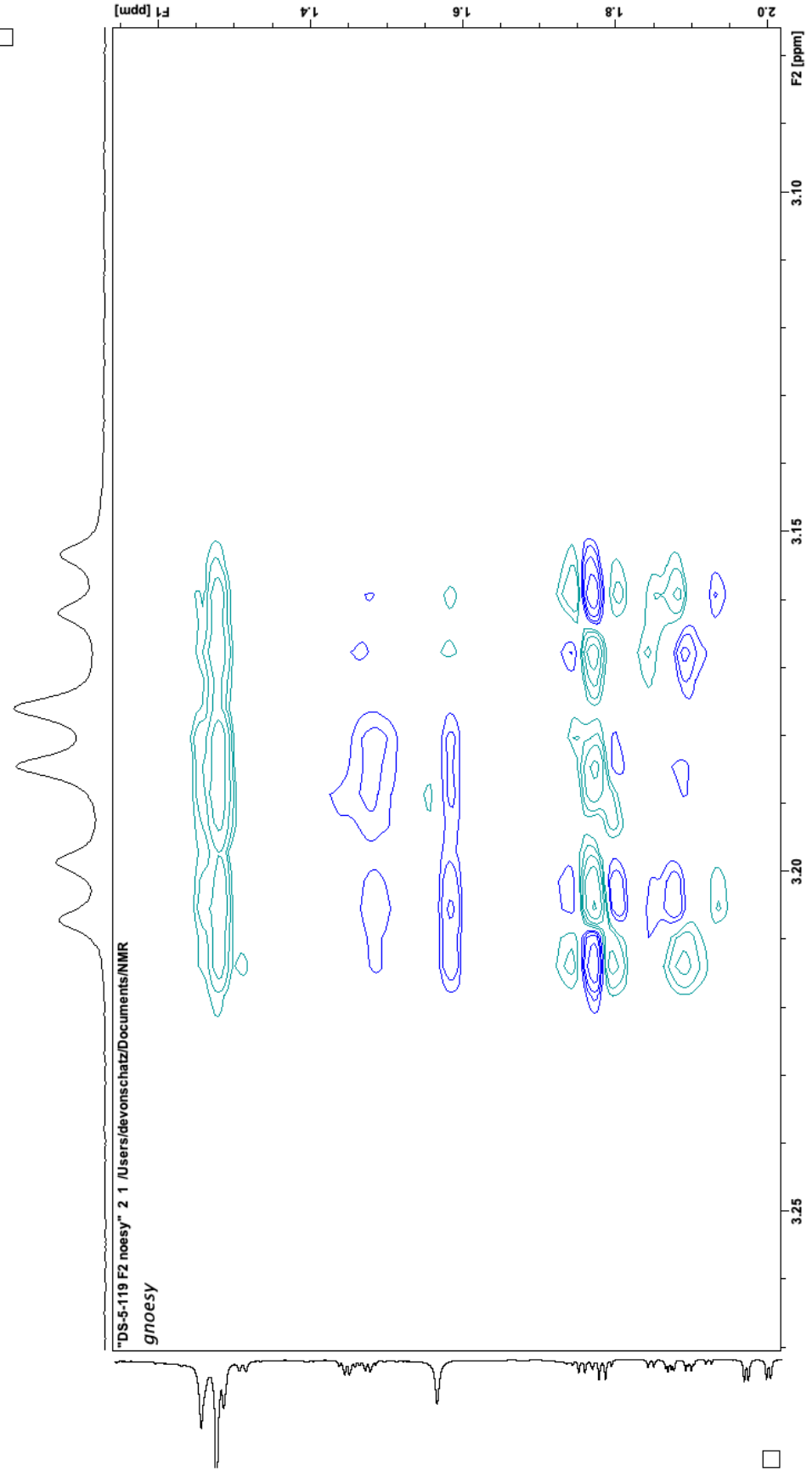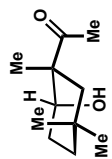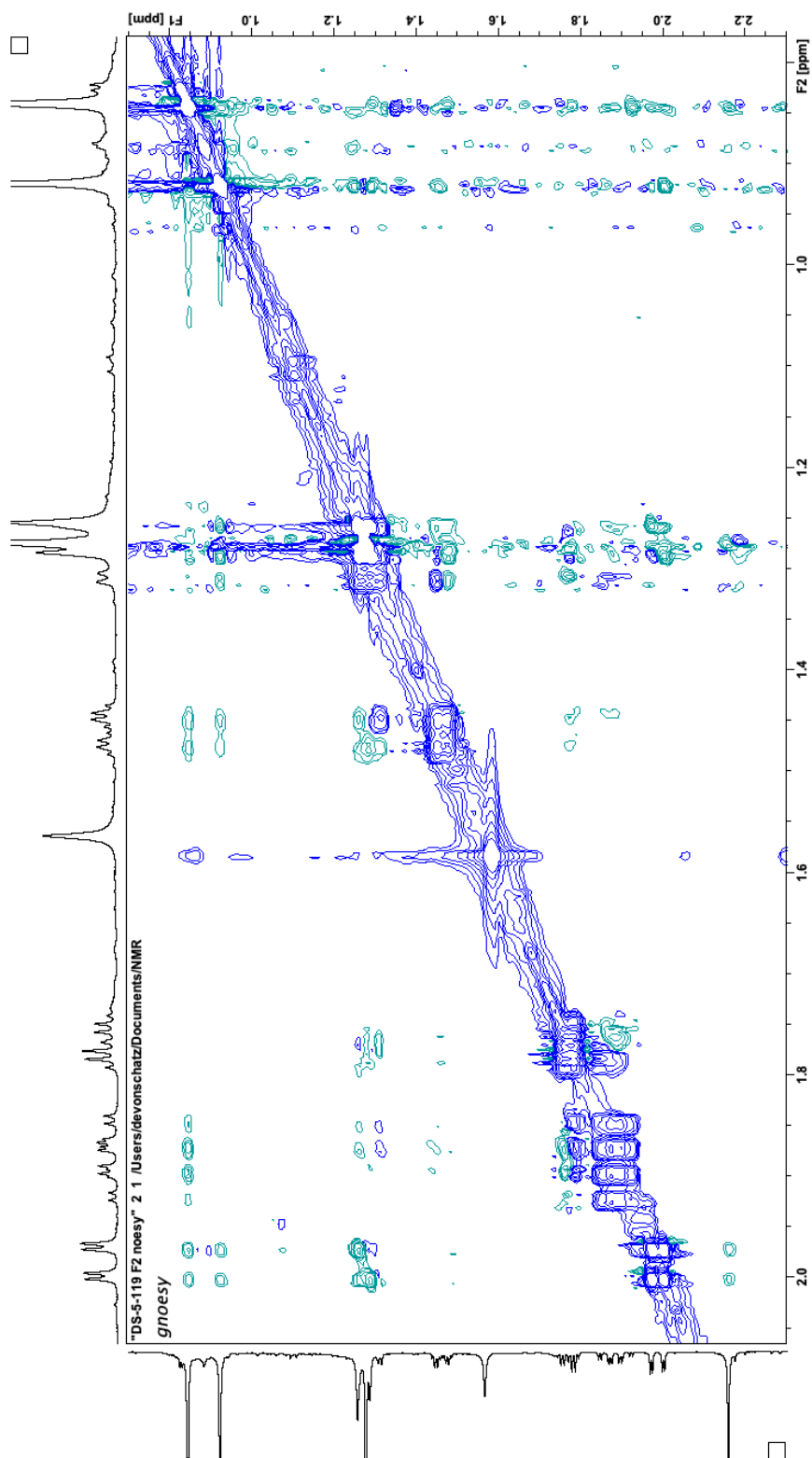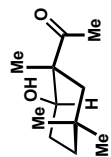
4.29 (^{1}H NMR, 500 MHz, CDCl$_3$)

"DS-5-119 F3" 4 1 /Users/devonschatz/Documents/NMR
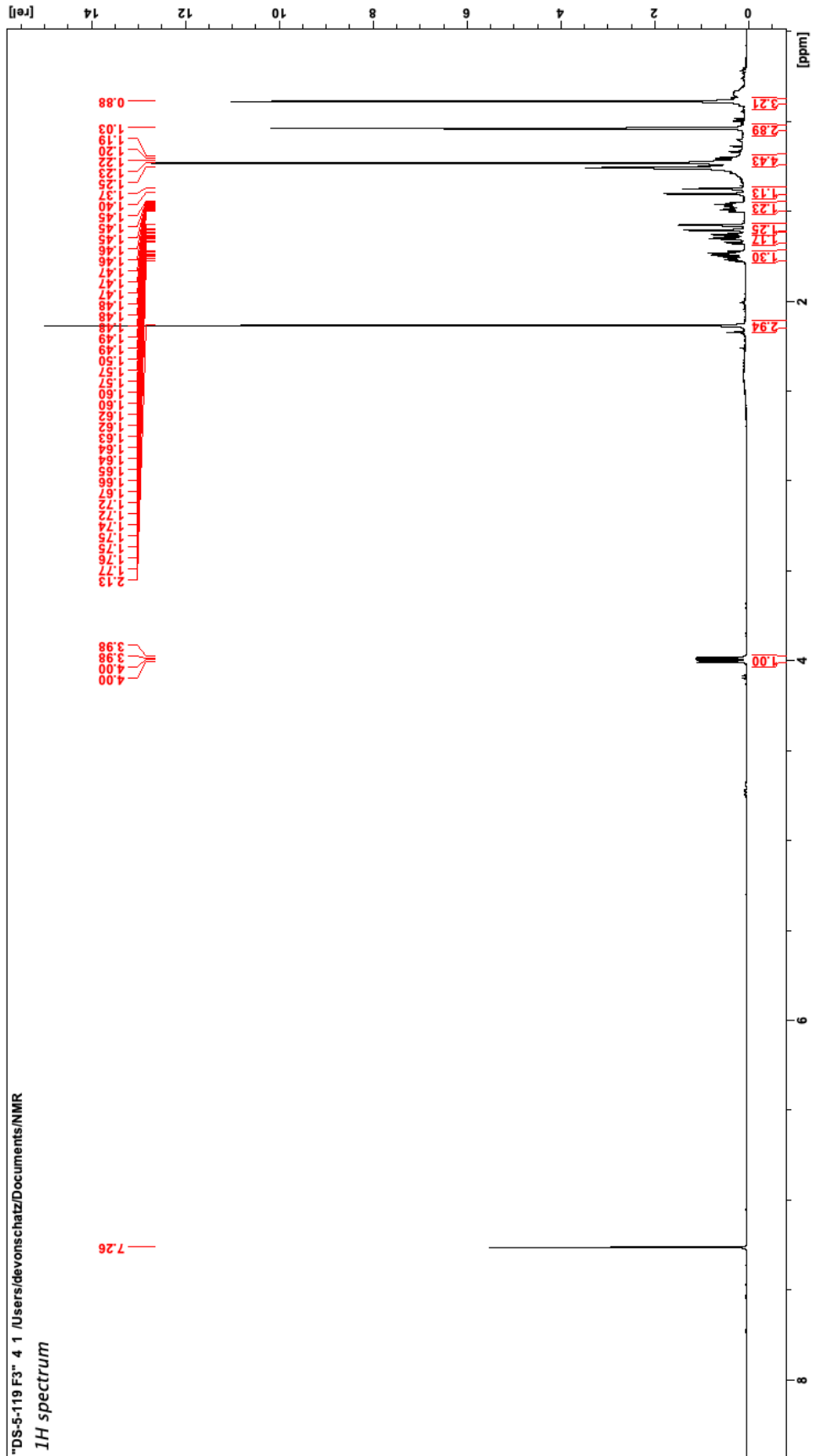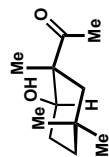
1H spectrum

4.29 (^{13}C NMR, 126 MHz, CDCl$_3$)

"DS-5-119 F3" 7 1 /Users/devonschatz/Documents/NMR

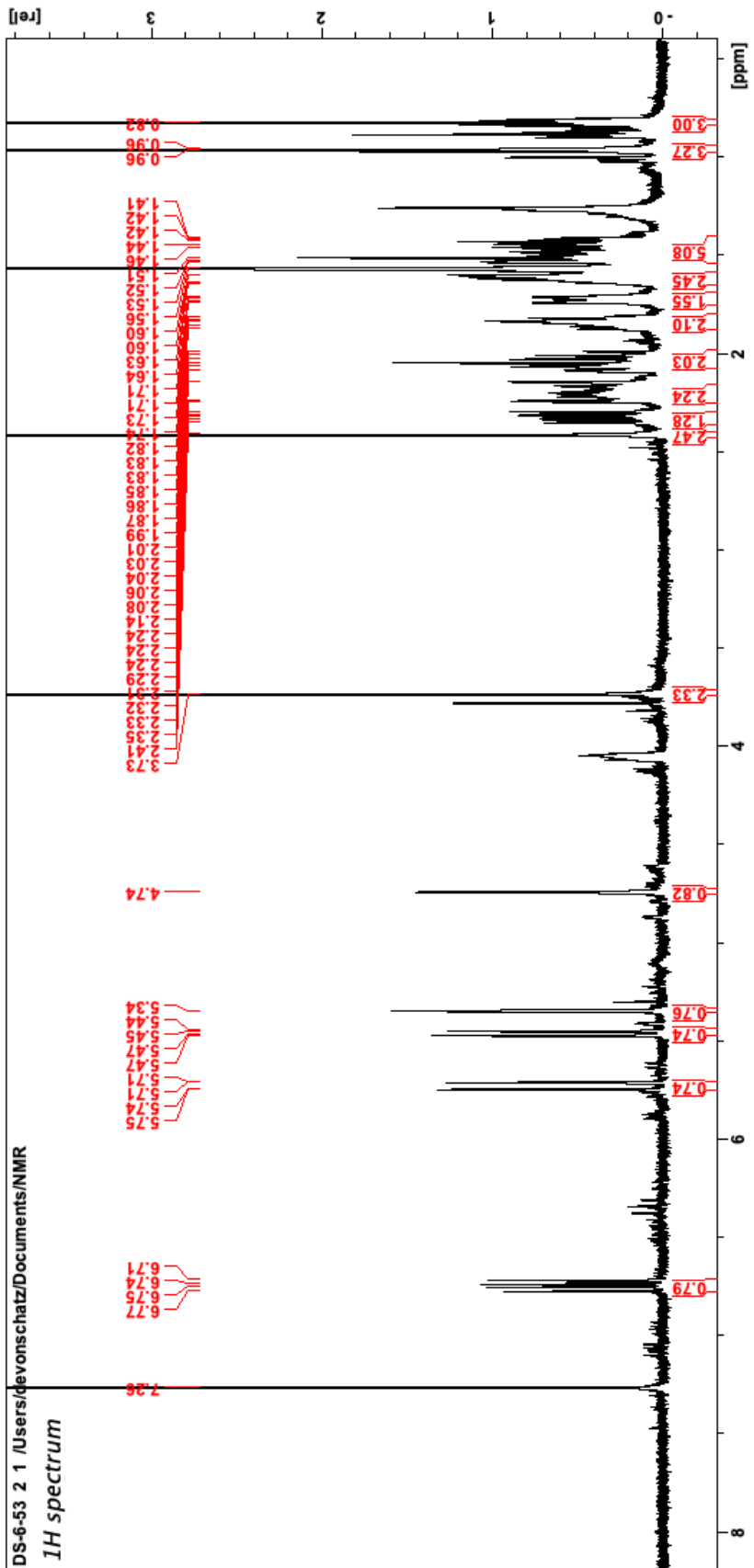*Z-restored spin-echo 13C spectrum with 1H decoupling*

215.33

77.41
76.91
76.16
71.60

52.46

45.35

36.37
32.19
31.52
29.85
29.23
26.35
24.94

18.50
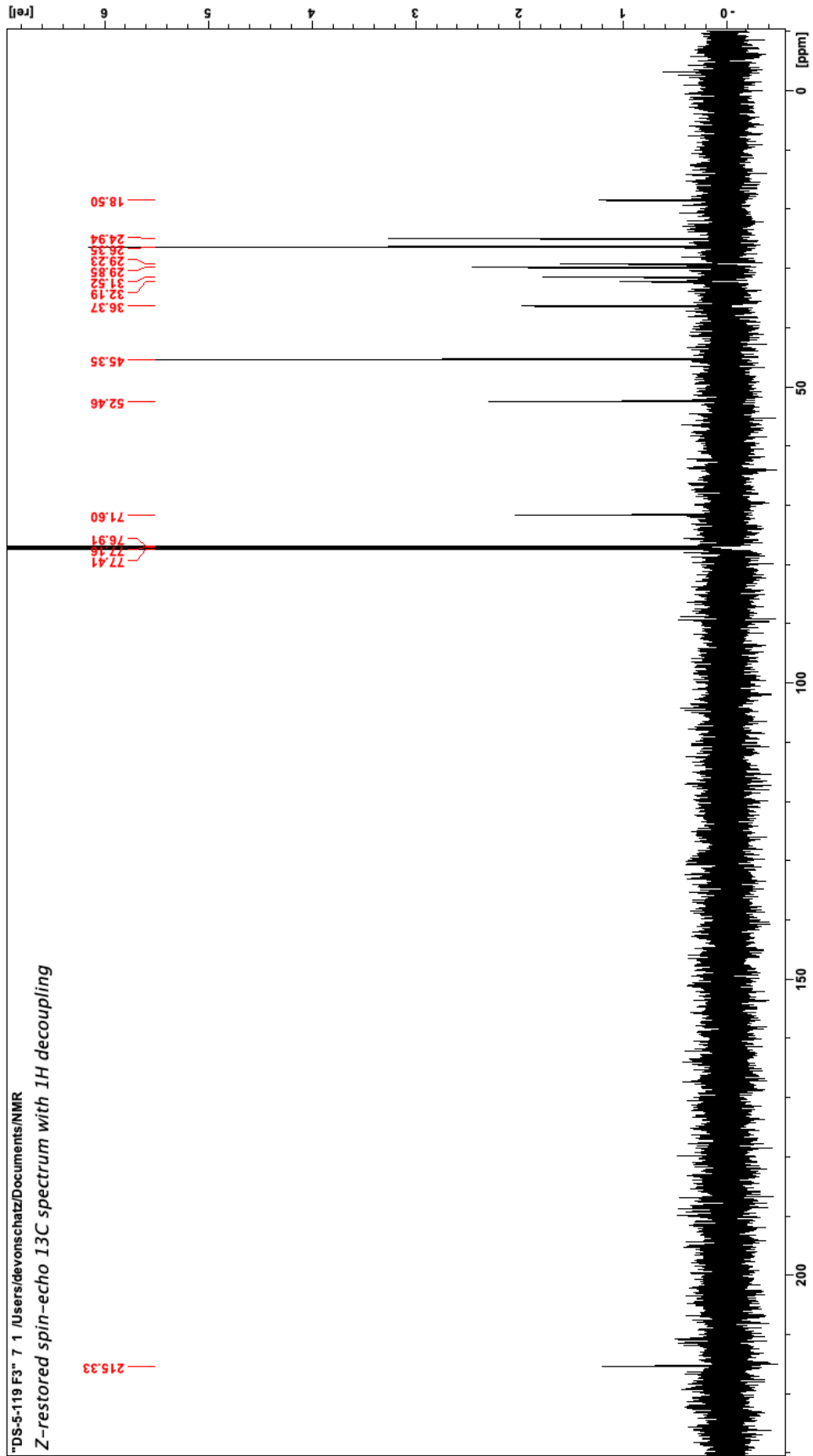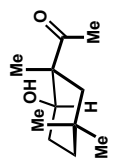
4.29 (COSY, CDCl$_3$)

4.29 (COSY, CDCl₃)

"DS-5-119 F3 cosy" 2 1 /Users/devonschatz/Documents/NMR

gcosy60

320

4.29 (NOESY, CDCl₃)

321

4.29 (NOESY, CDCl$_3$)

"DS-5-119 F3" 6 1 /Users/devonschatz/Documents/NMR
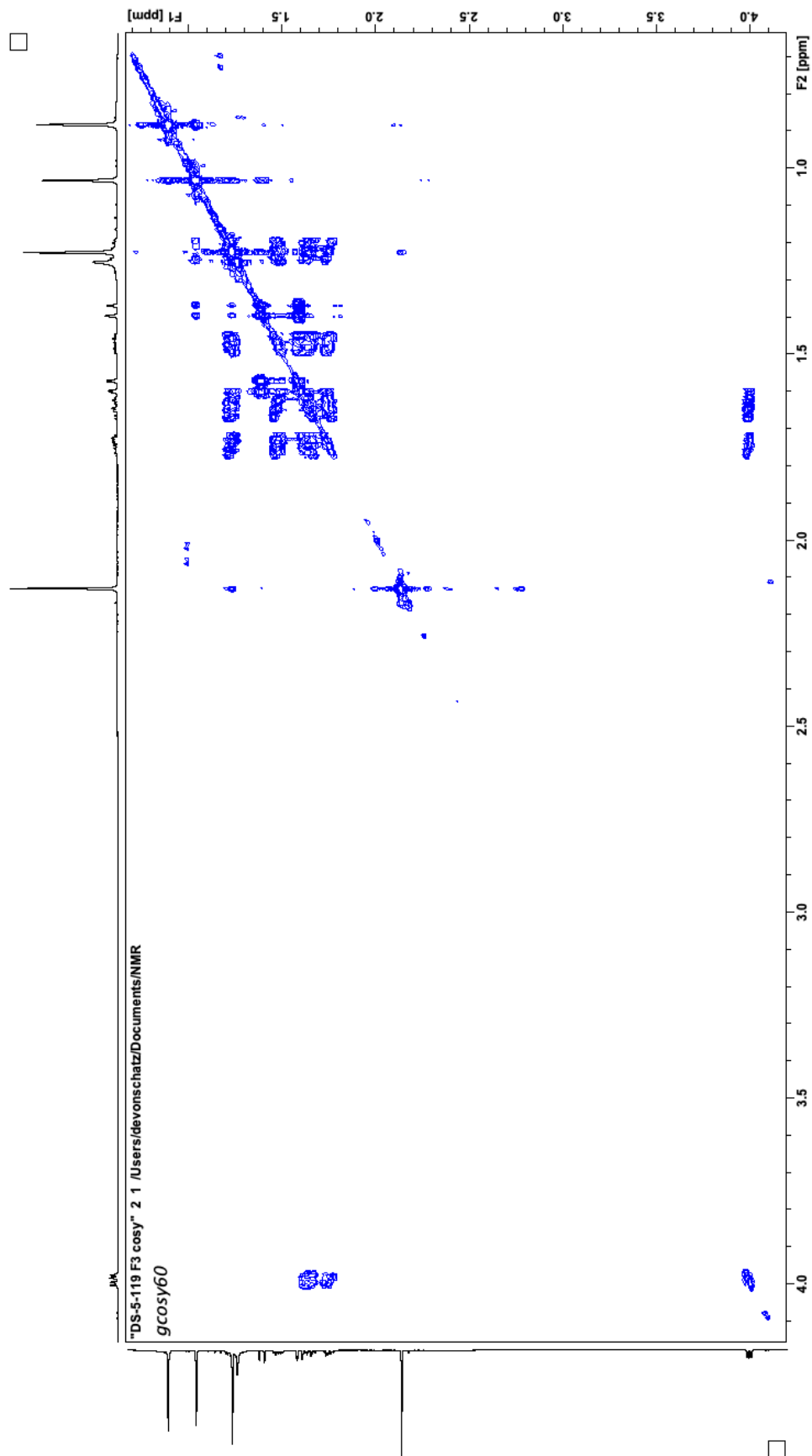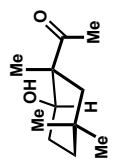
gnoesy

4.29 (NOESY, CDCl$_3$)
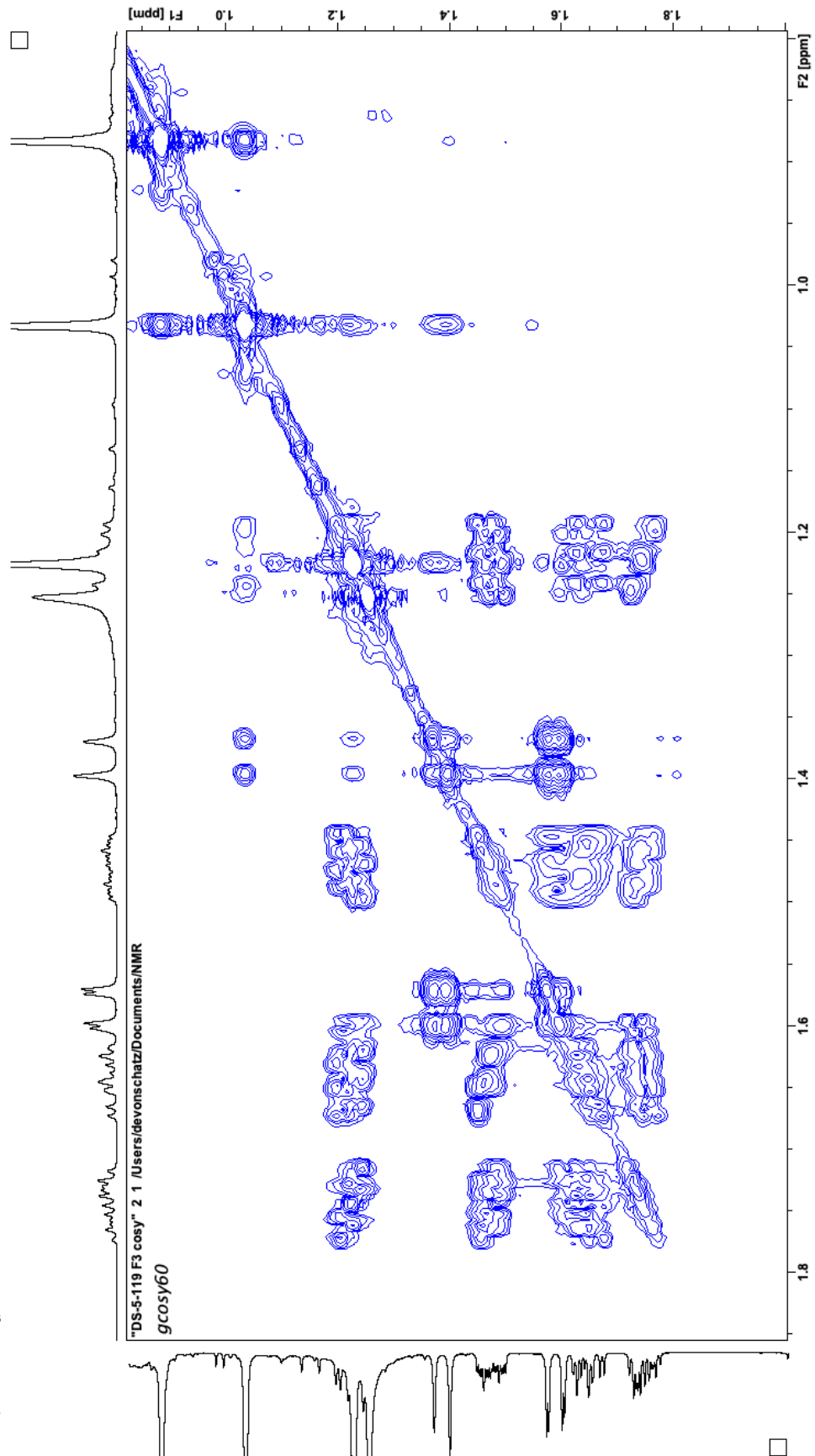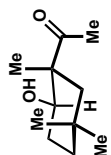
"DS-5-119 F3" 6 1 /Users/devonschatz/Documents/NMR
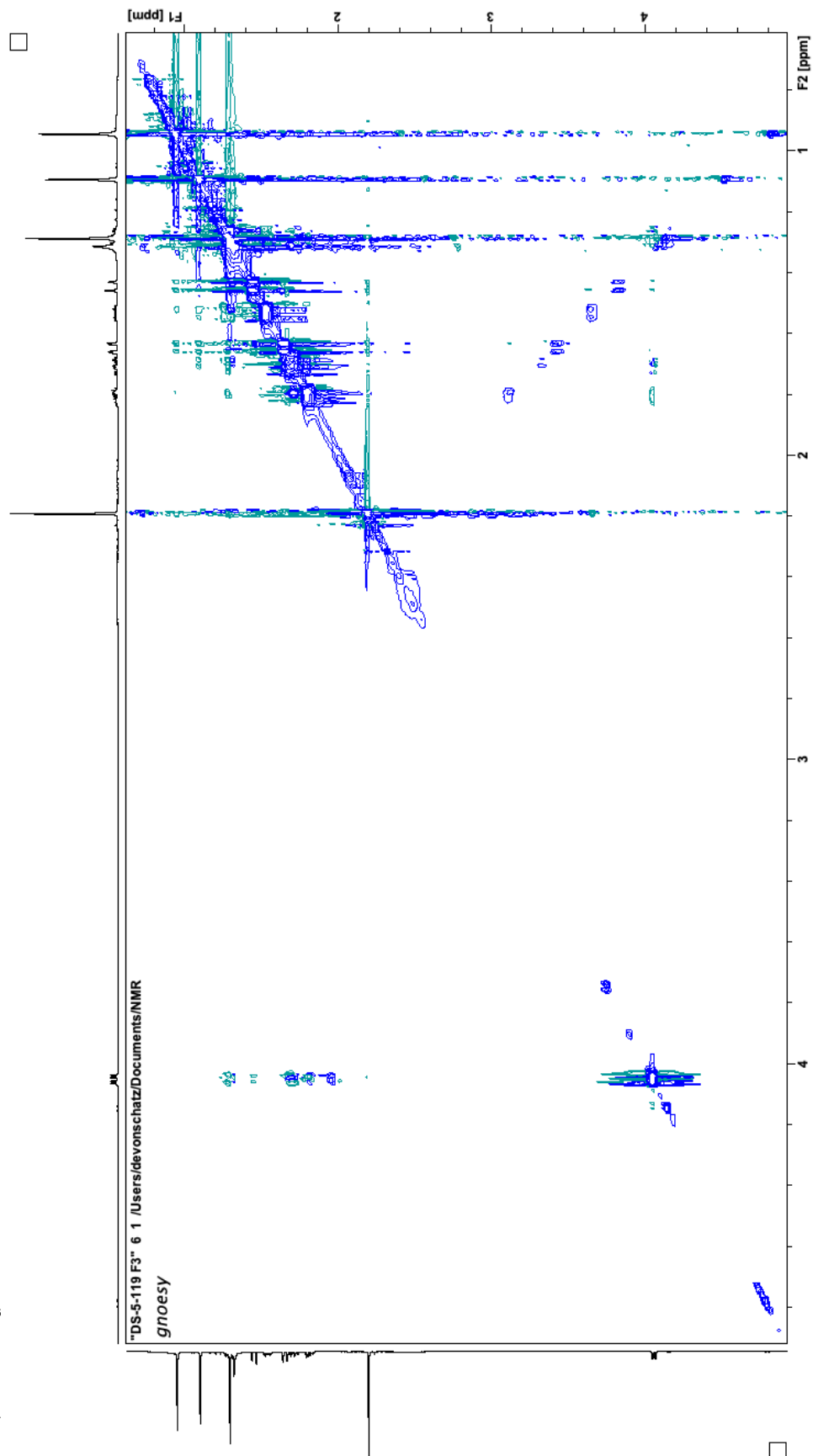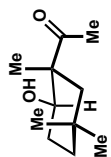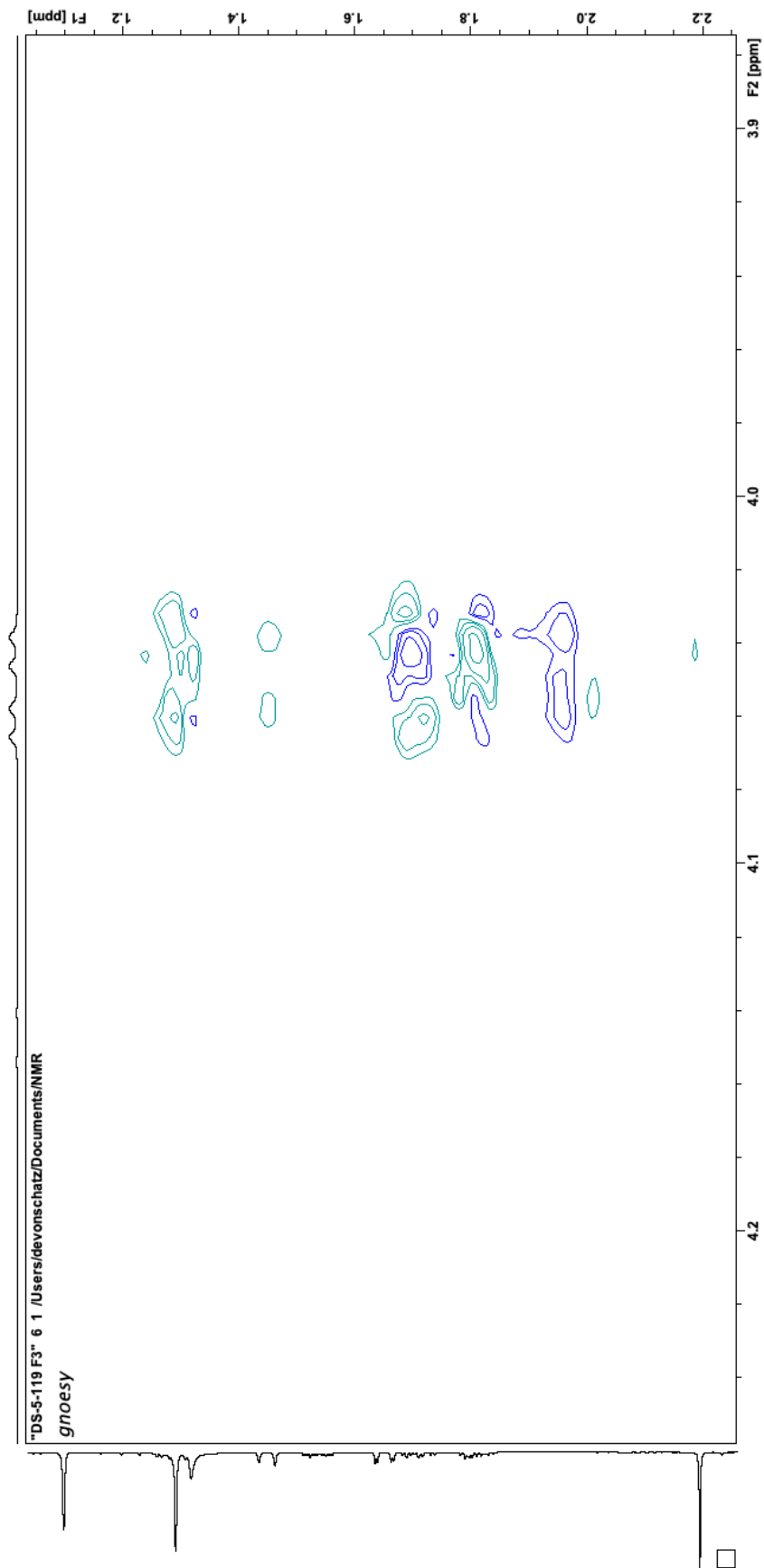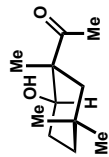
gnoesy

323
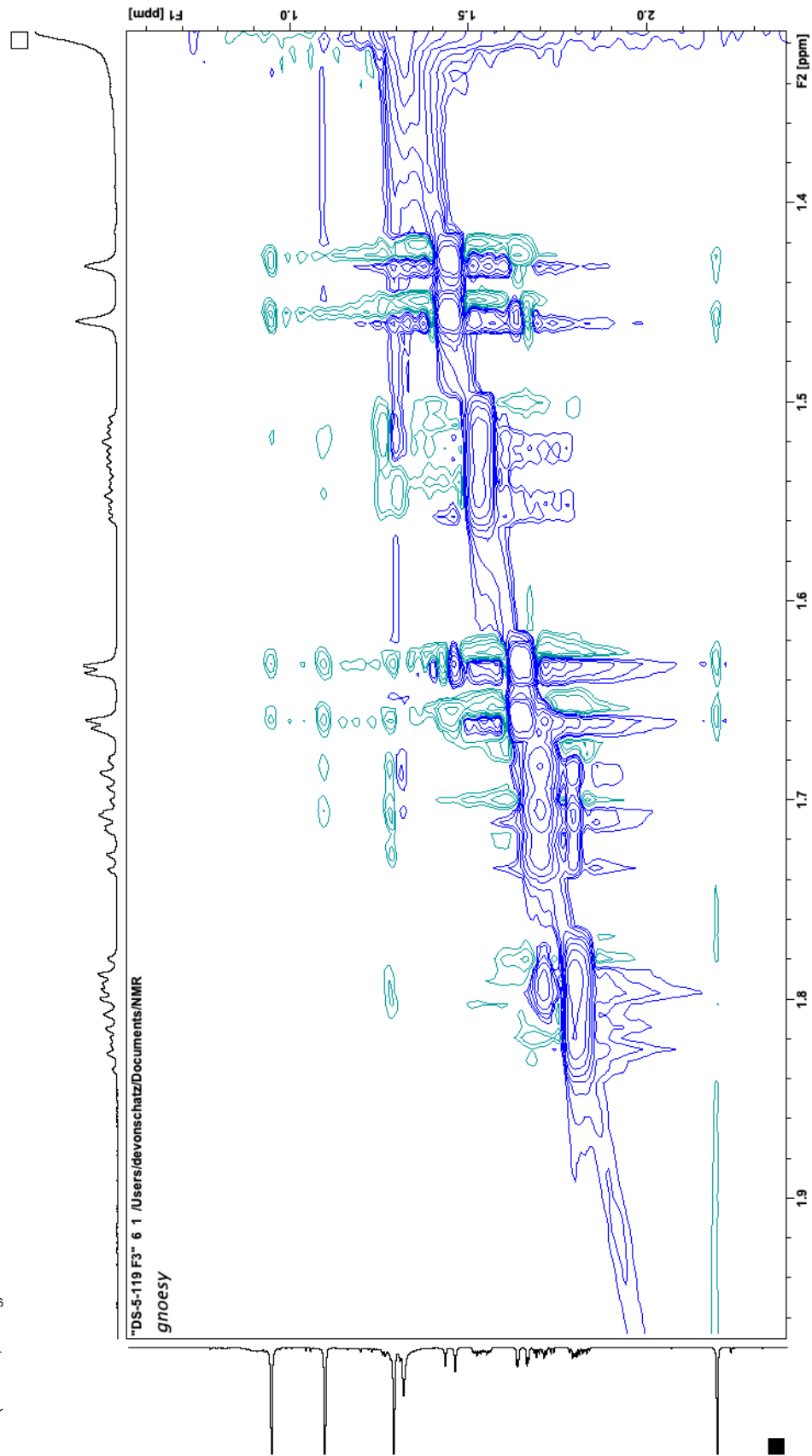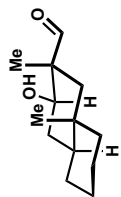
4.30 (^{1}H NMR, 500 MHz, CDCl$_3$)

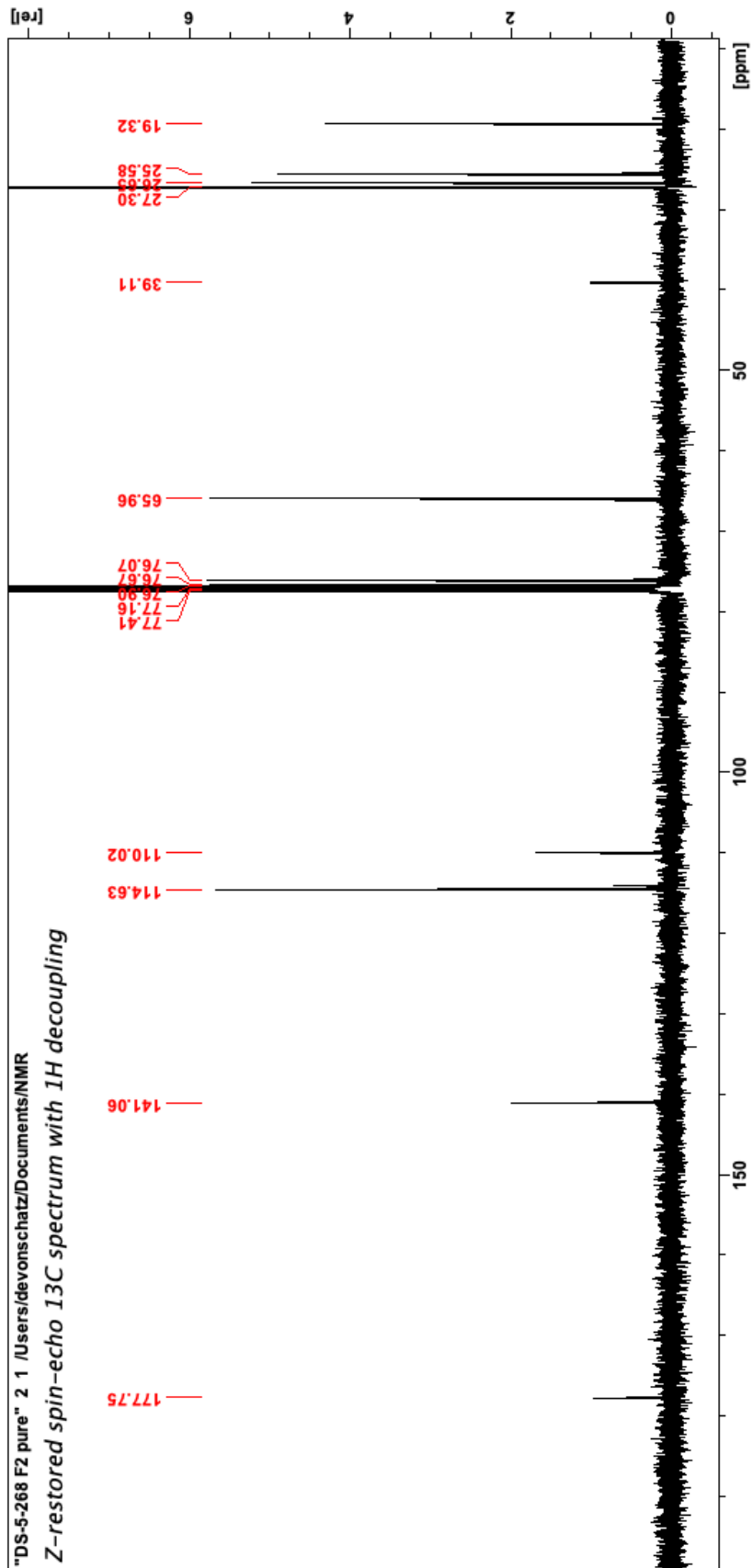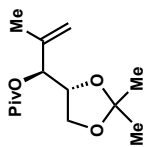"DS-5-118 major" 5 1 /Users/devonschatz/Documents/NMR
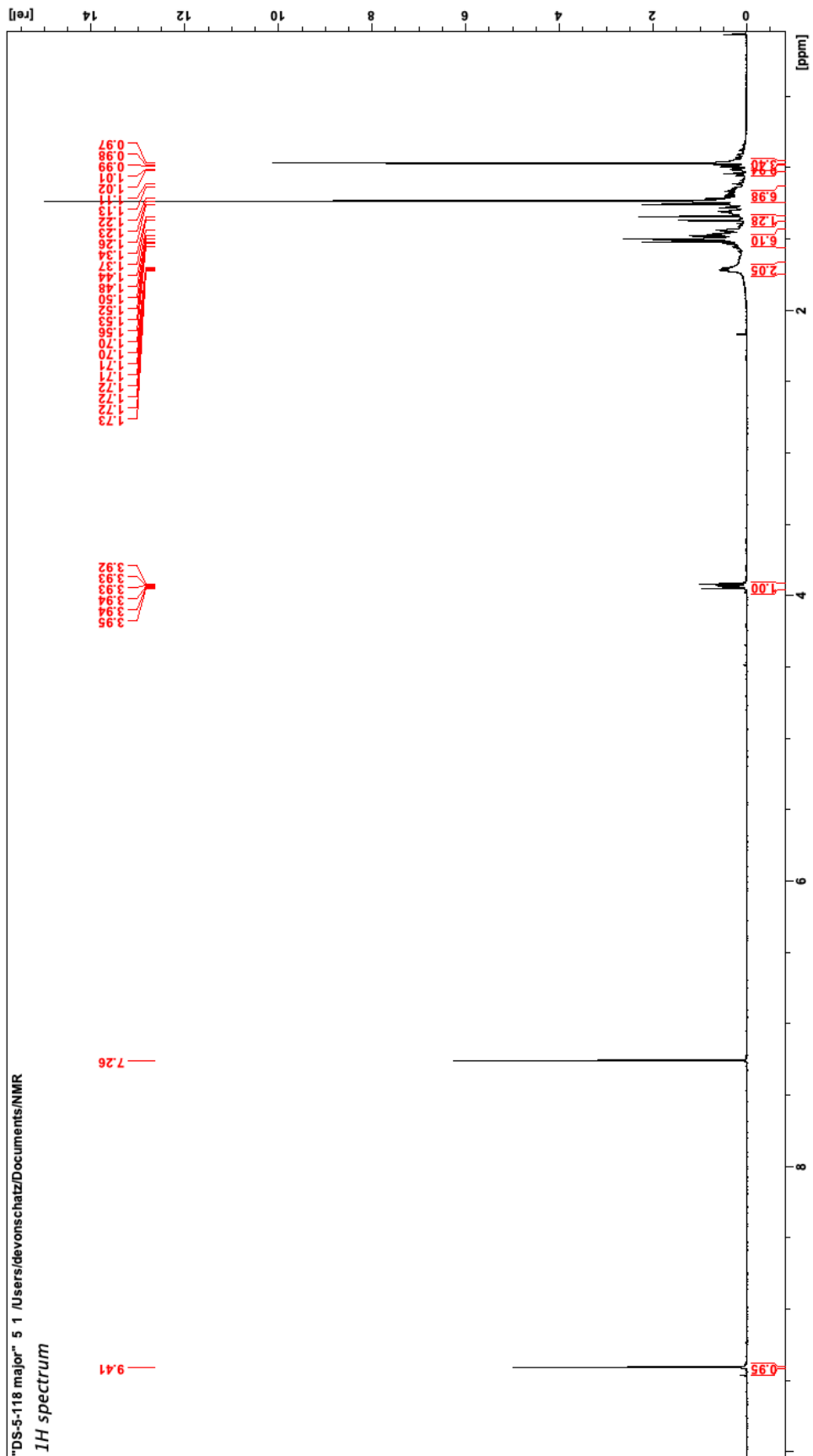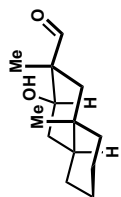
1H spectrum

4.30 (^{13}C NMR, 126 MHz, CDCl$_3$)

"DS-5-118 major" 2 1 /Users/devonschatz/Documents/NMR

Z-restored spin-echo 13C spectrum with 1H decoupling

14.92
18.30
21.29
26.60
28.00
33.51
34.13
41.30
44.50
46.24
51.65
72.32
76.90
77.16
77.41
206.08
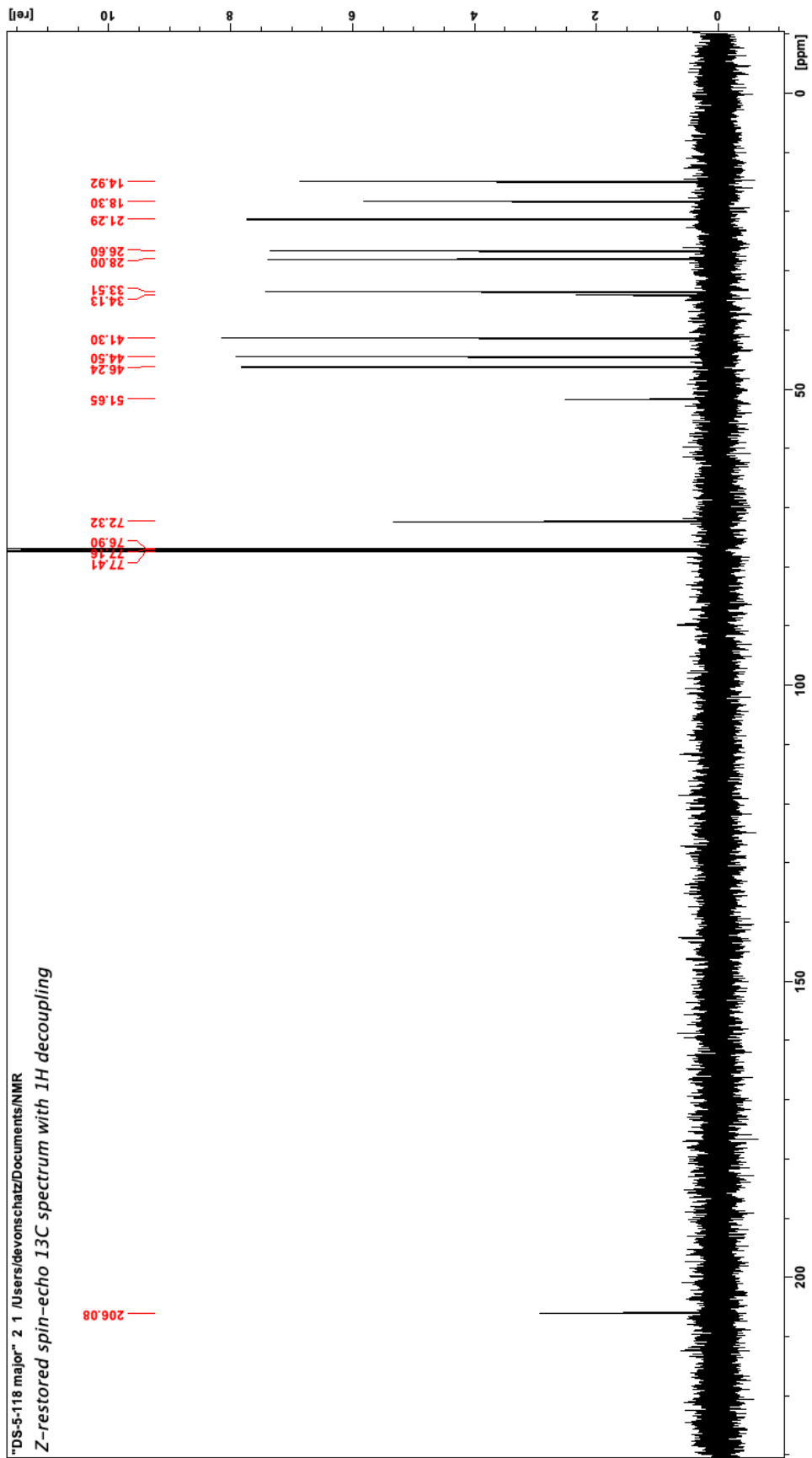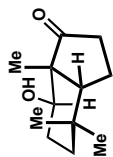
4.31 (^{1}H NMR, 500 MHz, CDCl$_3$)

"DS-5-139 column 2" 1 1 /Users/devonschatz/Documents/NMR
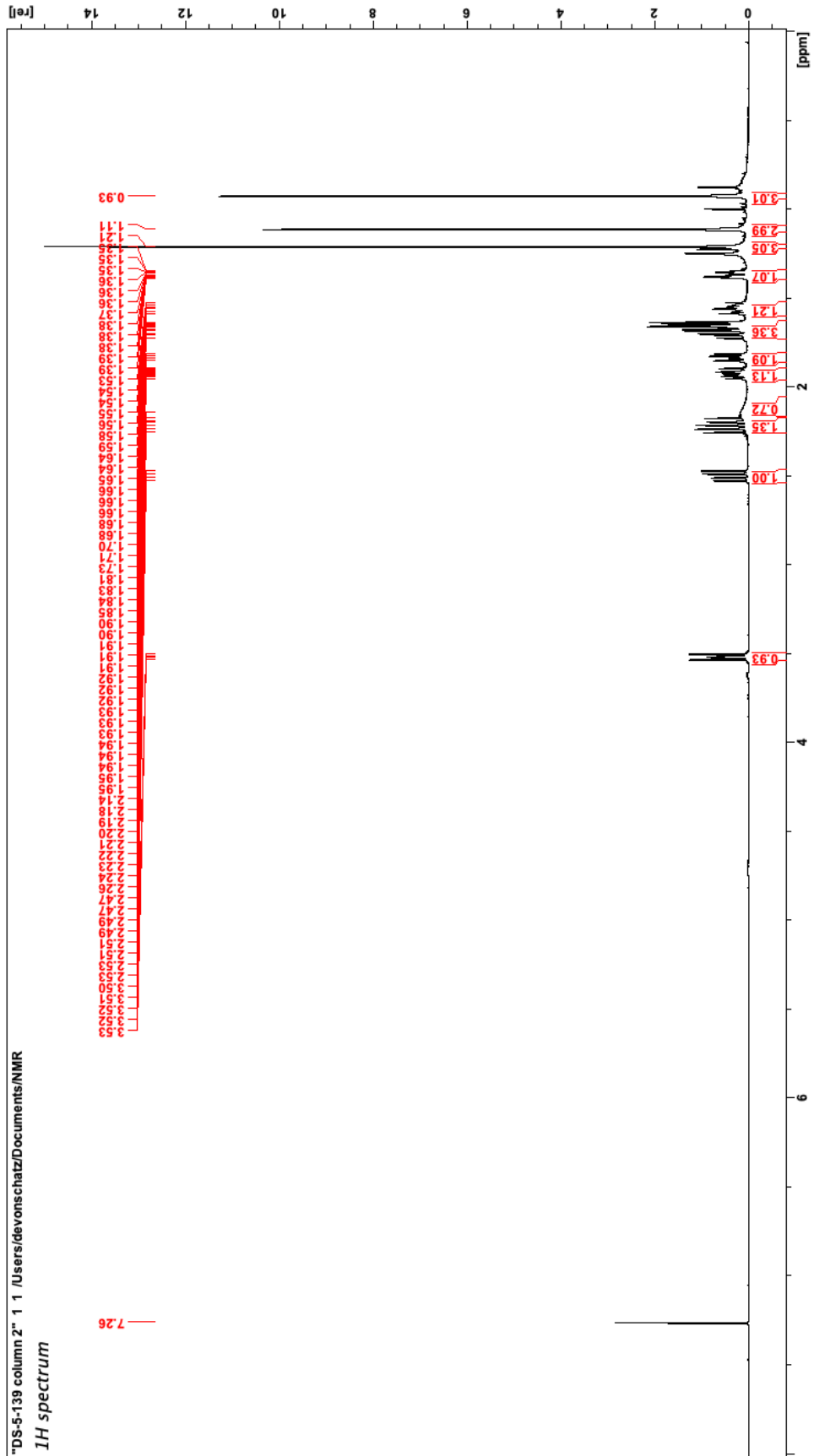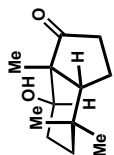
1H spectrum

4.31 (^{13}C NMR, 126 MHz, CDCl$_3$)

"DS-5-139 column 2" 2 1 /Users/devonschatz/Documents/NMR
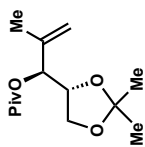
Z-restored spin-echo 13C spectrum with 1H decoupling

17.05
22.47
25.29
29.06
29.55
31.71
33.99
36.88
52.57
55.11
68.02
76.90
77.16
77.41
223.64
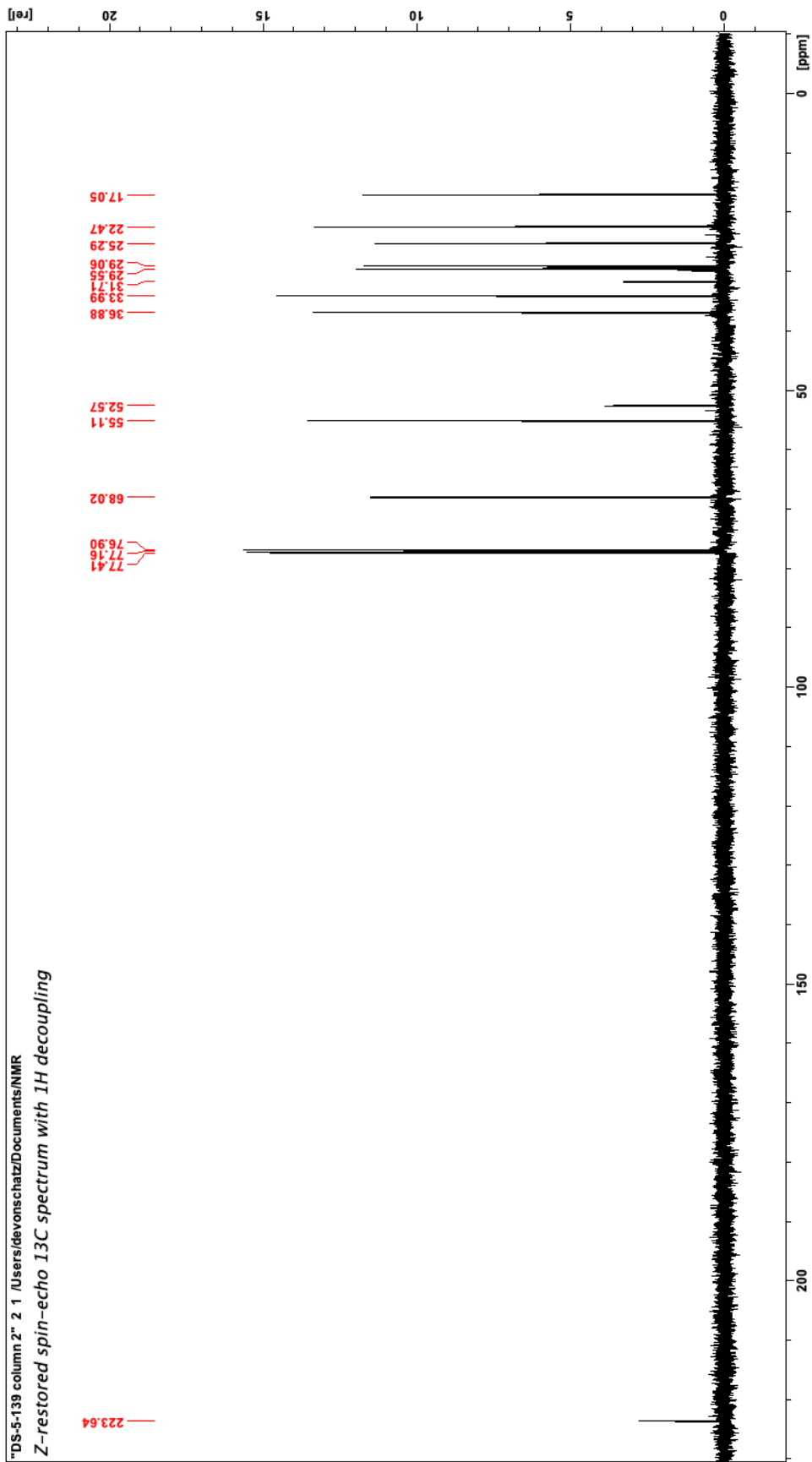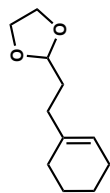
S4.5 (¹H NMR, 500 MHz, CDCl₃)

DS-5-180 2 1 /Users/devonschatz/Documents/NMR
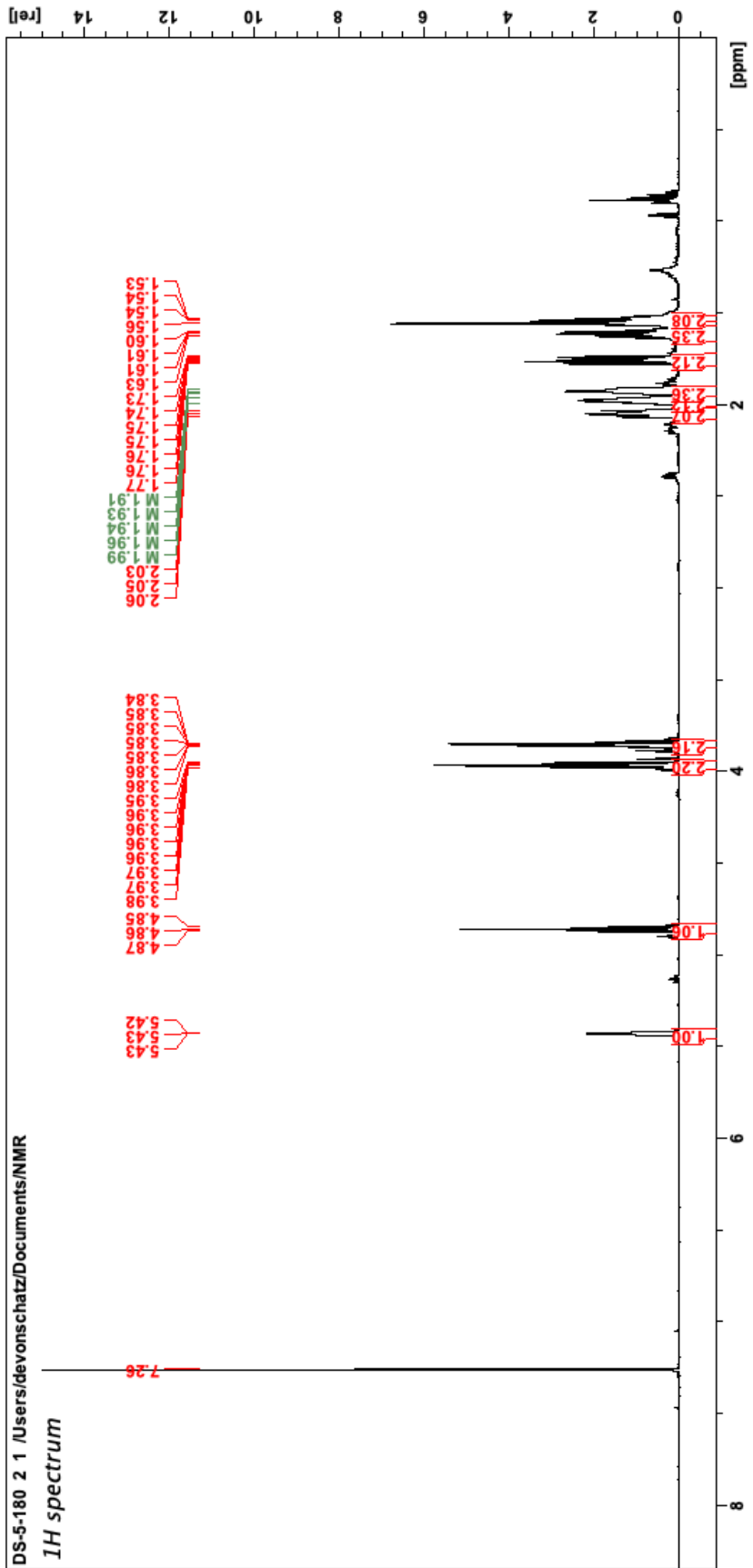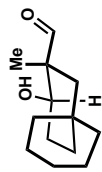
1H spectrum

4.32 (^{1}H NMR, 500 MHz, CDCl$_3$)

DS-5-185 1 1 /Users/devonschatz/Documents/NMR
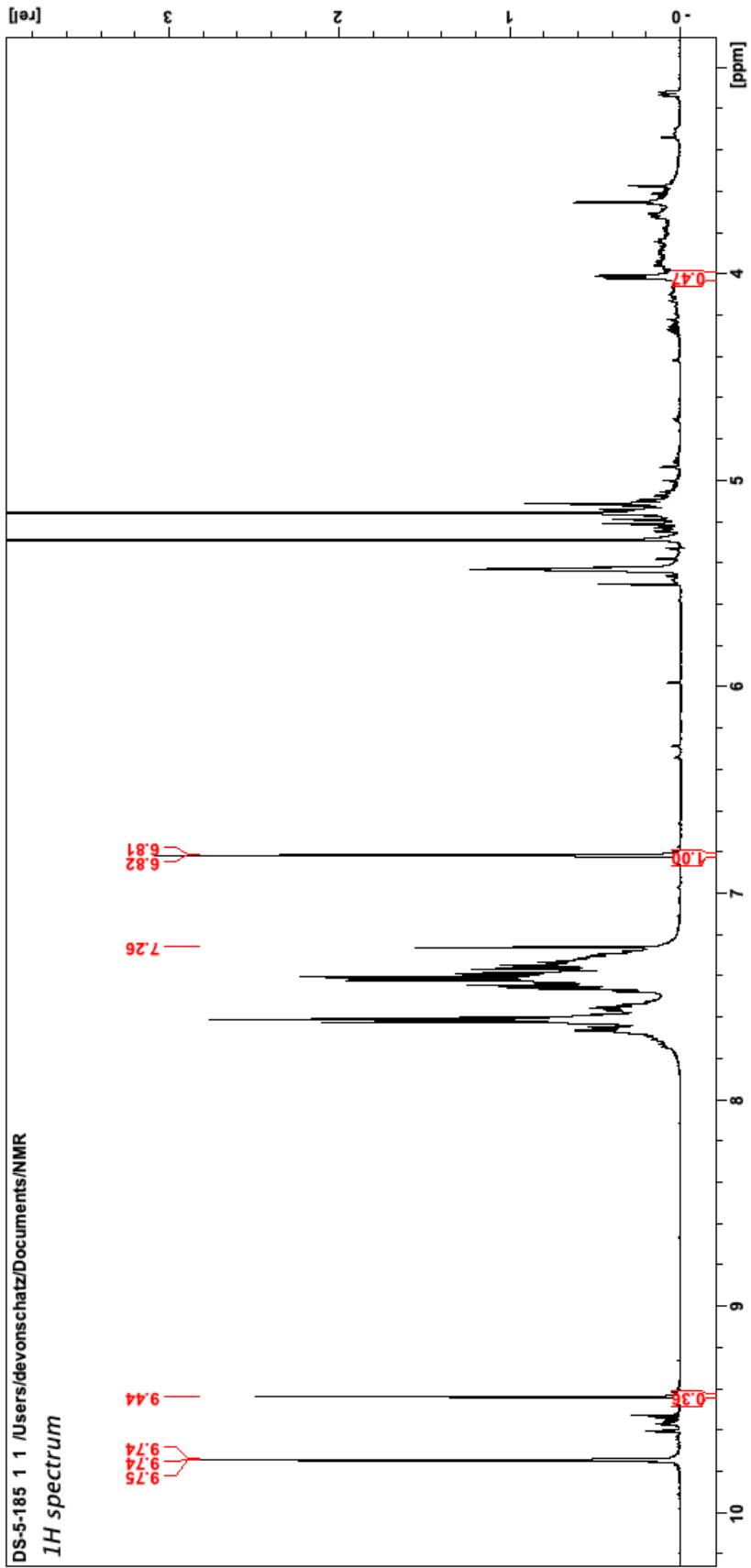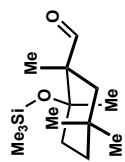
1H spectrum

4.39 (^{1}H NMR, 500 MHz, CDCl$_3$)
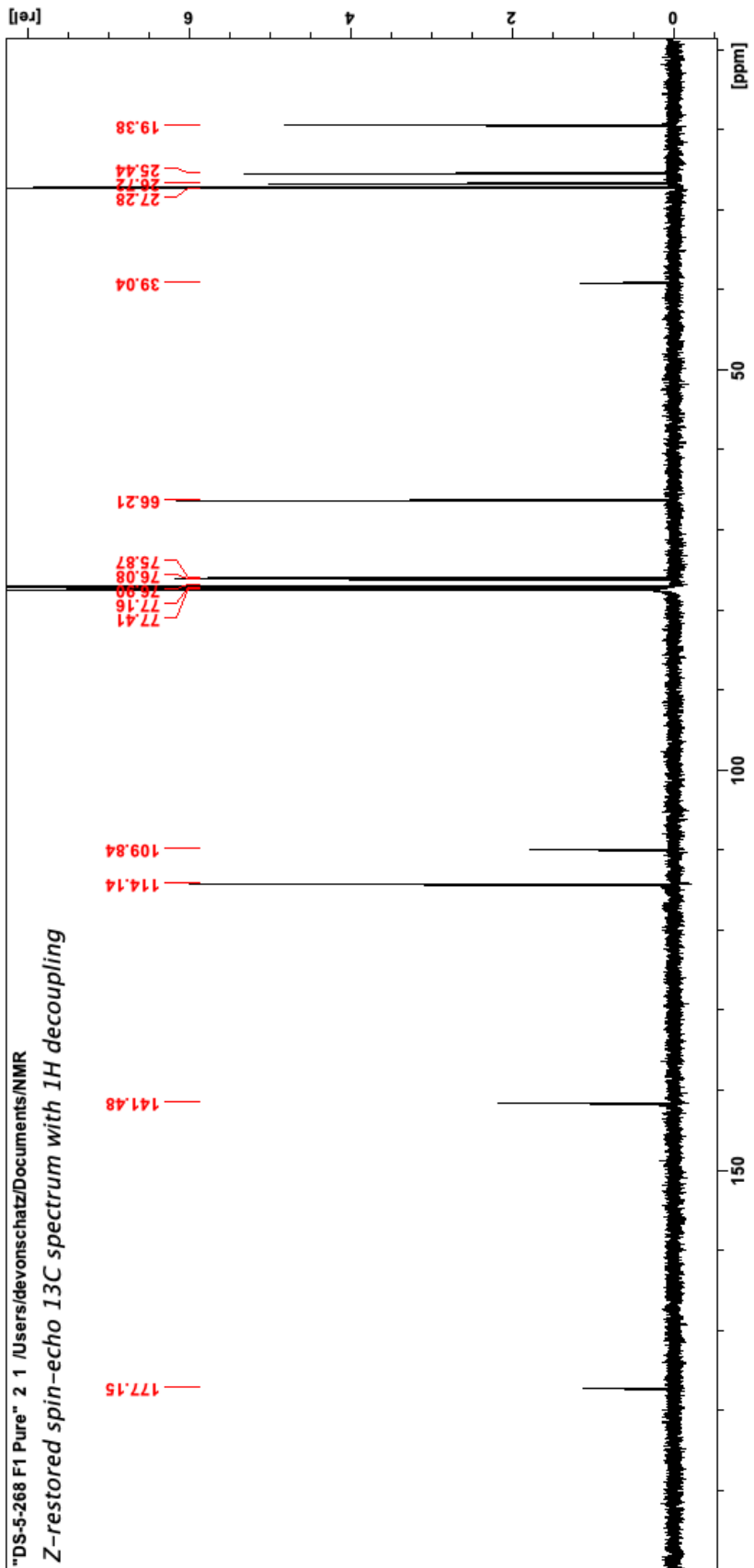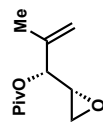
DS-5-211 1 1 /Users/devonschatz/Documents/NMR

1H spectrum

330
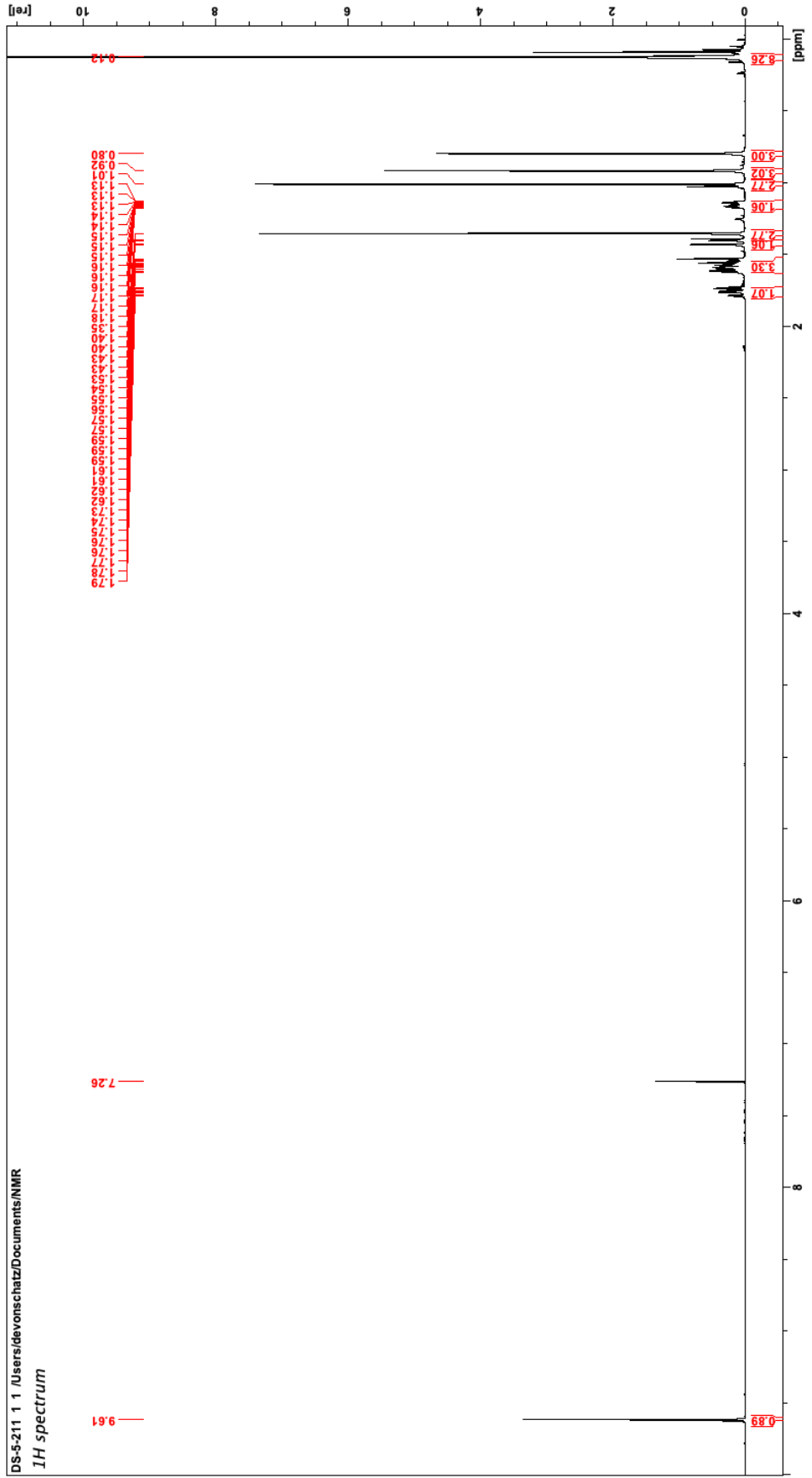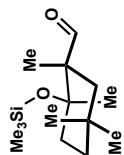
4.39 (^{13}C NMR, 126 MHz, CDCl$_3$)

DS-5-211 4 1 /Users/devonschatz/Documents/NMR

Z–restored spin–echo 13C spectrum with 1H decoupling

206.24

77.41
77.16
76.90
74.99

53.87

45.14

34.61
33.94
32.83
30.65
28.38
24.88

18.20

2.55

15

10

5

0

[rel]

0

50

100

150

200

[ppm]
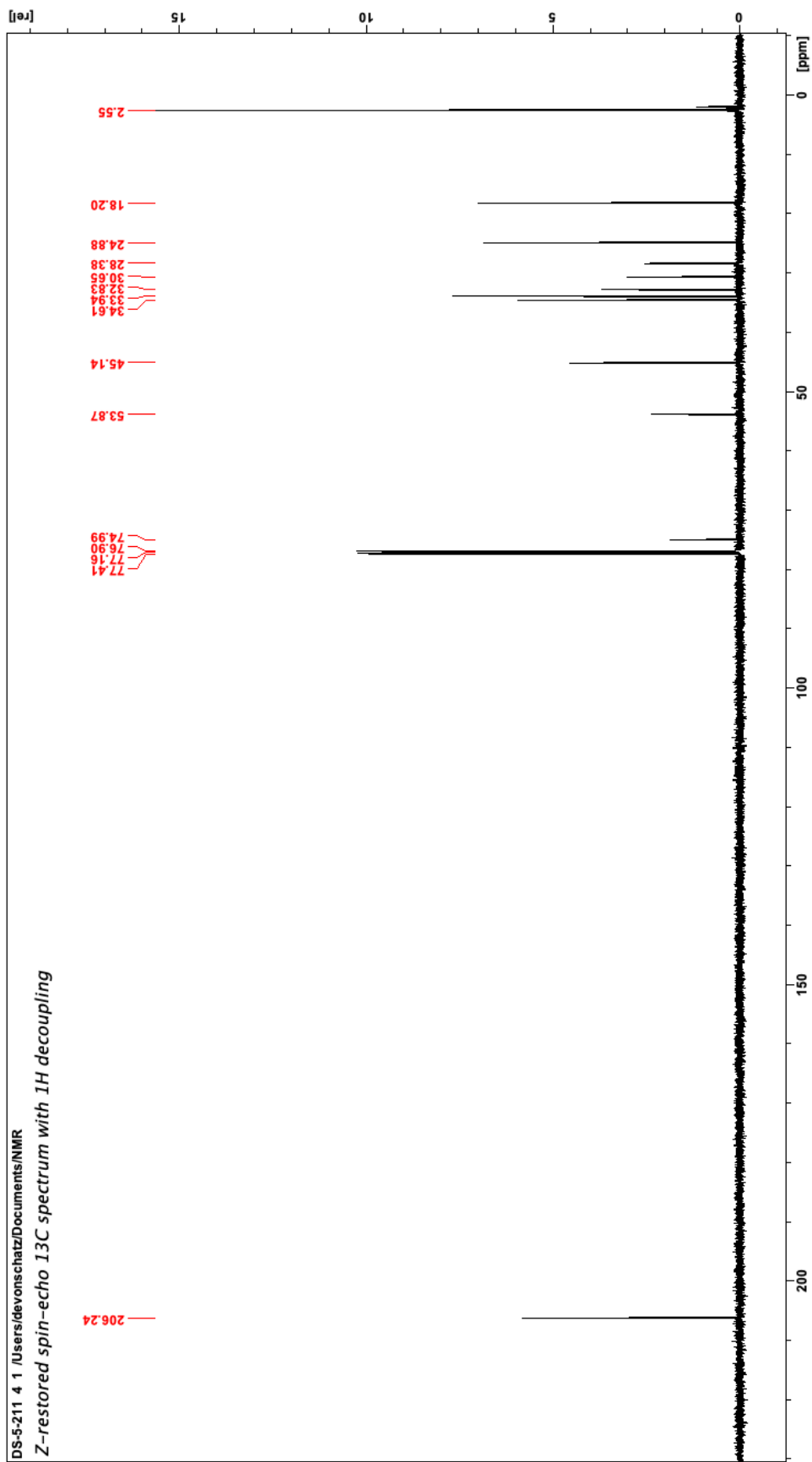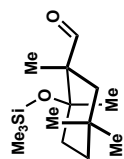
4.39 (NOESY, CDCl₃)

4.39 (NOESY, CDCl₃)

DS-6-30 3 1 /Users/devonschatz/Documents/NMR
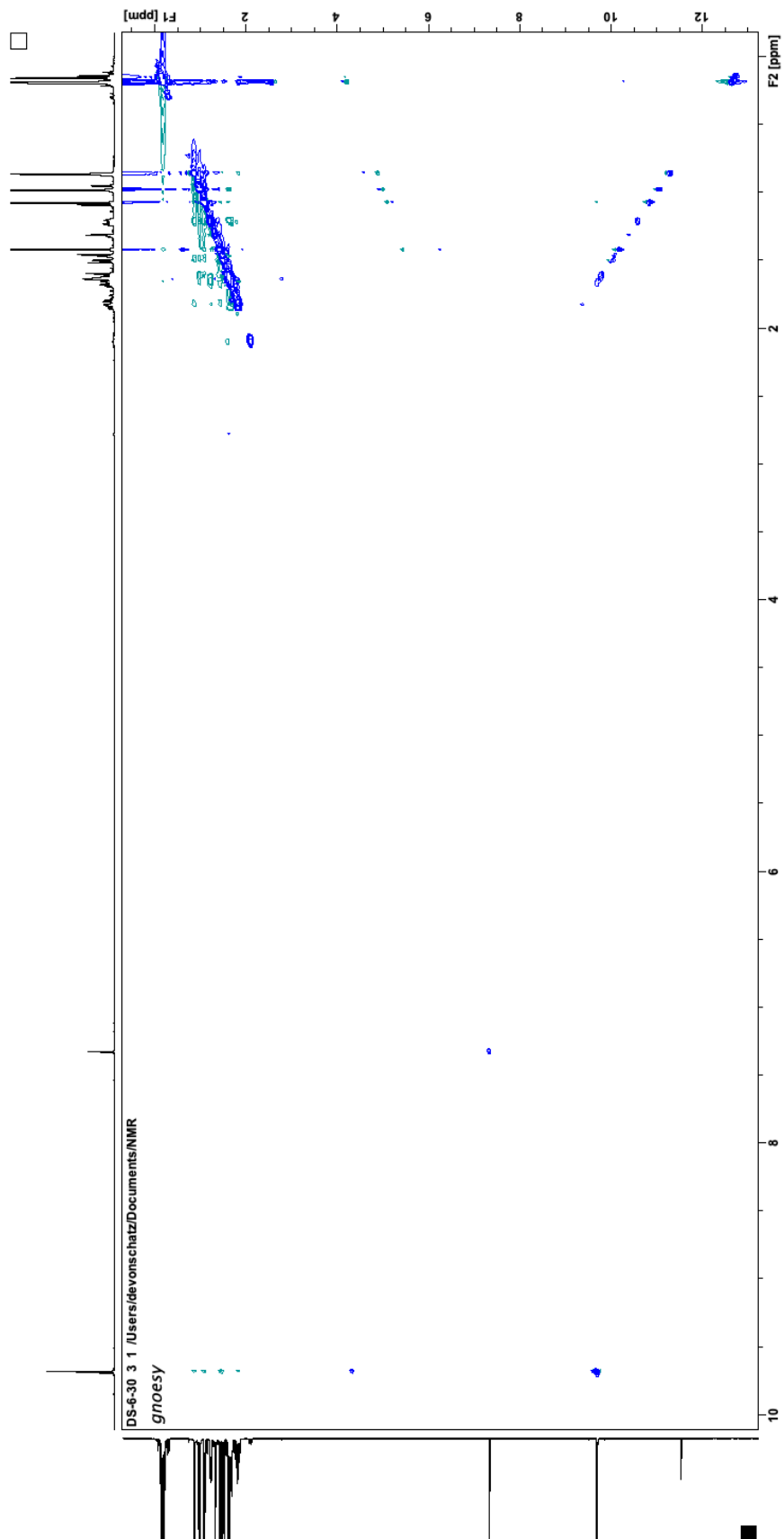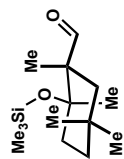
gnoesy

333
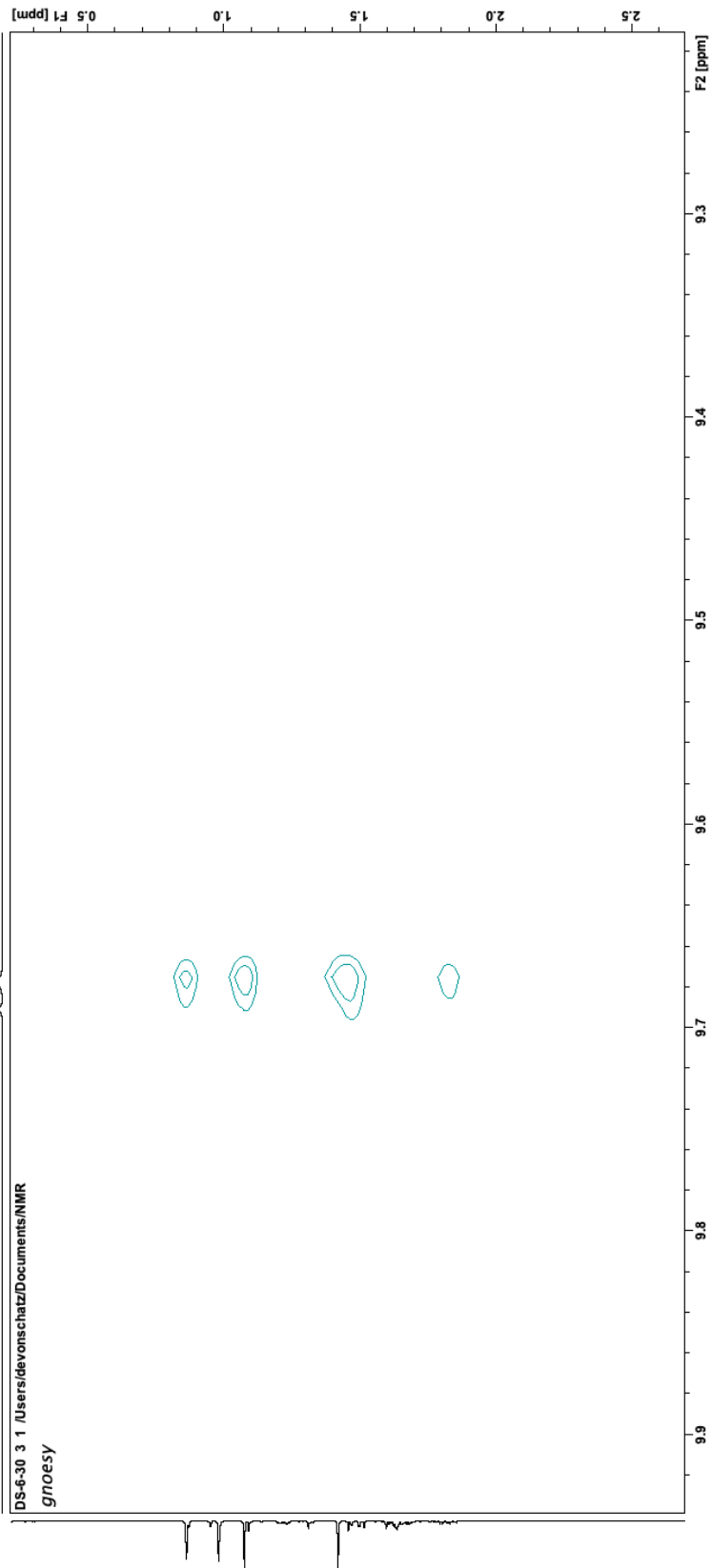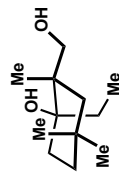
4.40 (^{1}H NMR, 500 MHz, CDCl$_3$)

DS-6-113 1 1 /Users/devonschatz/Documents/NMR

1H spectrum

4.40 (^{1}H NMR, 500 MHz, CDCl$_3$)
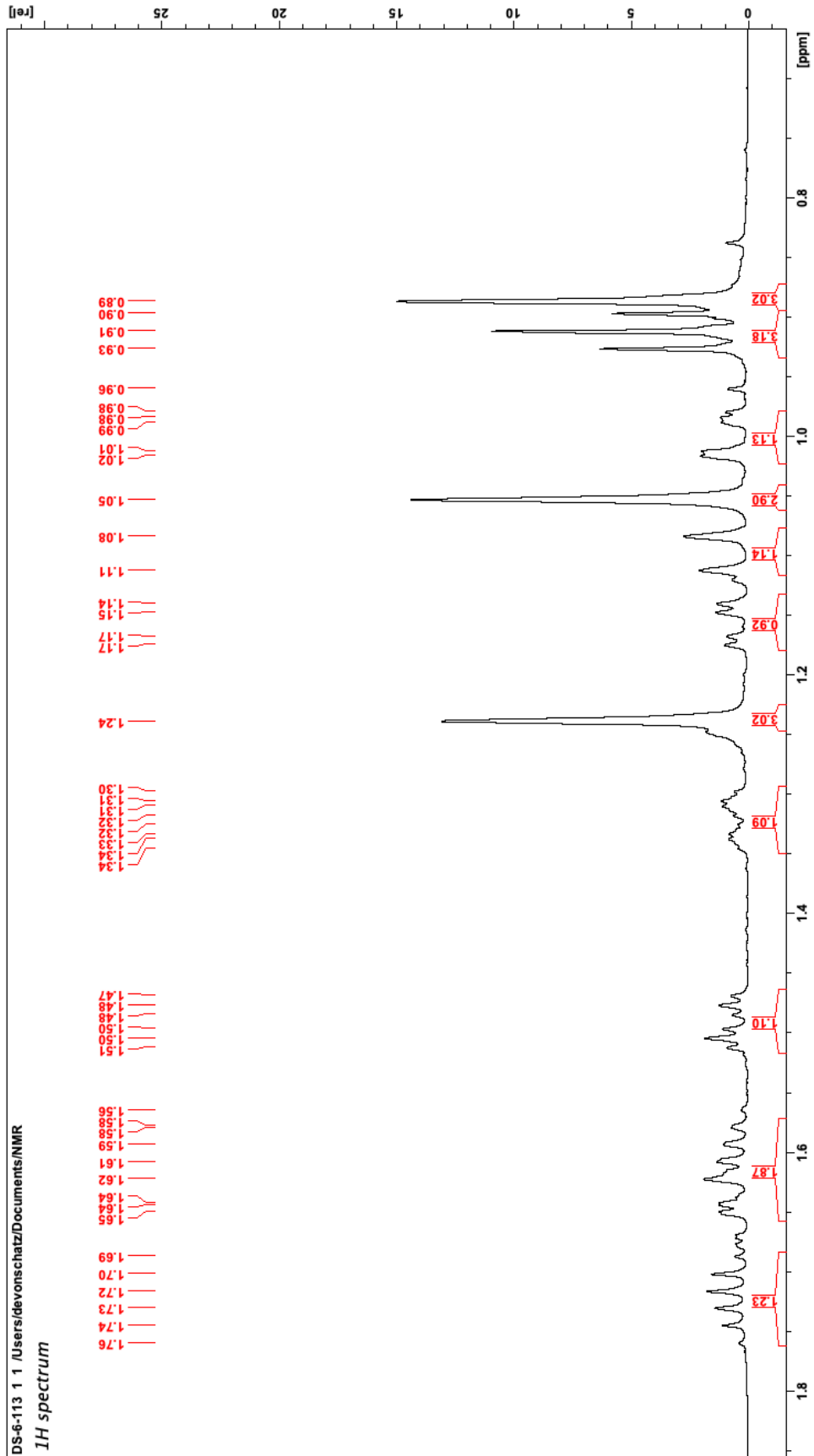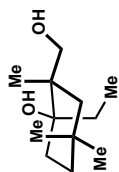
DS-6-113 1 1 /Users/devonschatz/Documents/NMR

1H spectrum

335

4.40 (^{13}C NMR, 126 MHz, CDCl$_3$)

DS-6-113 2 1 /Users/devonschatz/Documents/NMR
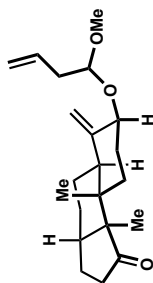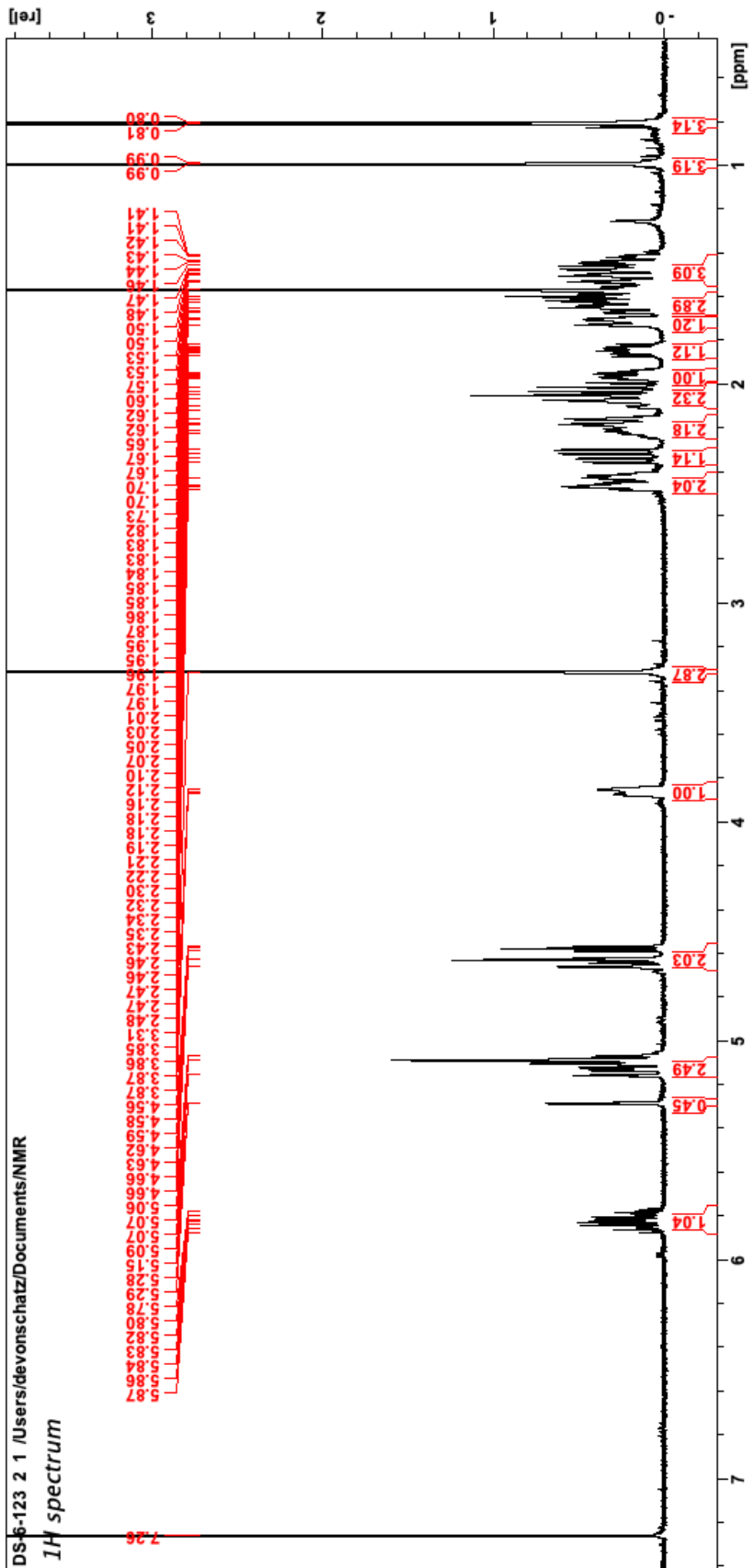
Z-restored spin-echo 13C spectrum with 1H decoupling

4.40 (^{13}C NMR, 126 MHz, CDCl$_3$)

DS-6-113 2 1 /Users/devonschatz/Documents/NMR

Z-restored spin-echo 13C spectrum with 1H decoupling

337

4.40 (COSY, CDCl$_3$)

DS-6-113 5 1 /Users/devonschatz/Documents/NMR

gcosy60
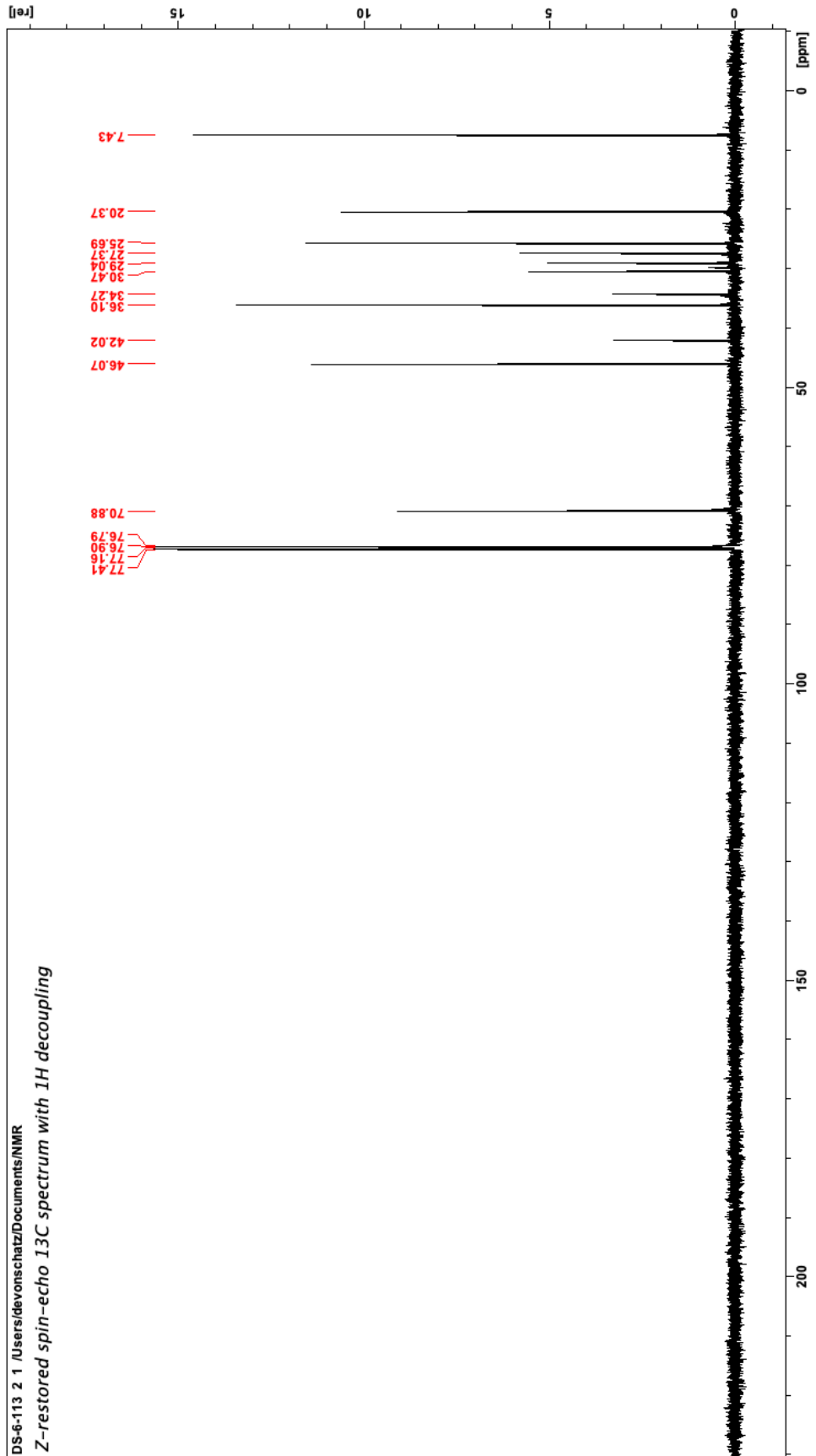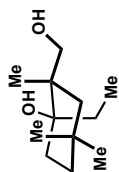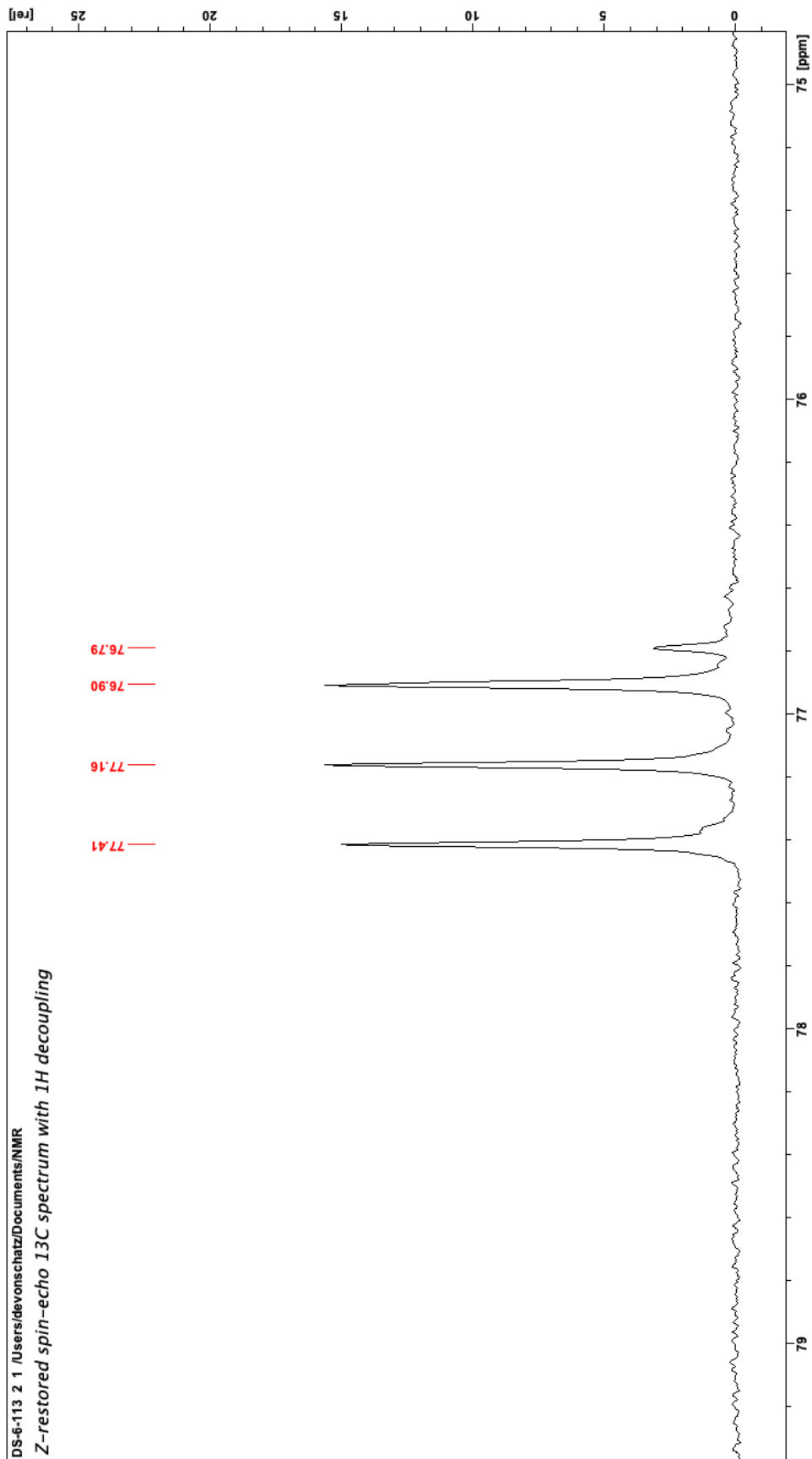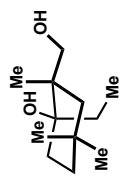
4.40 (NOESY, CDCl₃)

4.40 (NOESY, CDCl$_3$)

4.40 (NOESY, CDCl₃)

DS-6-113 4 1 /Users/devonschatz/Documents/NMR
noesygptp

341
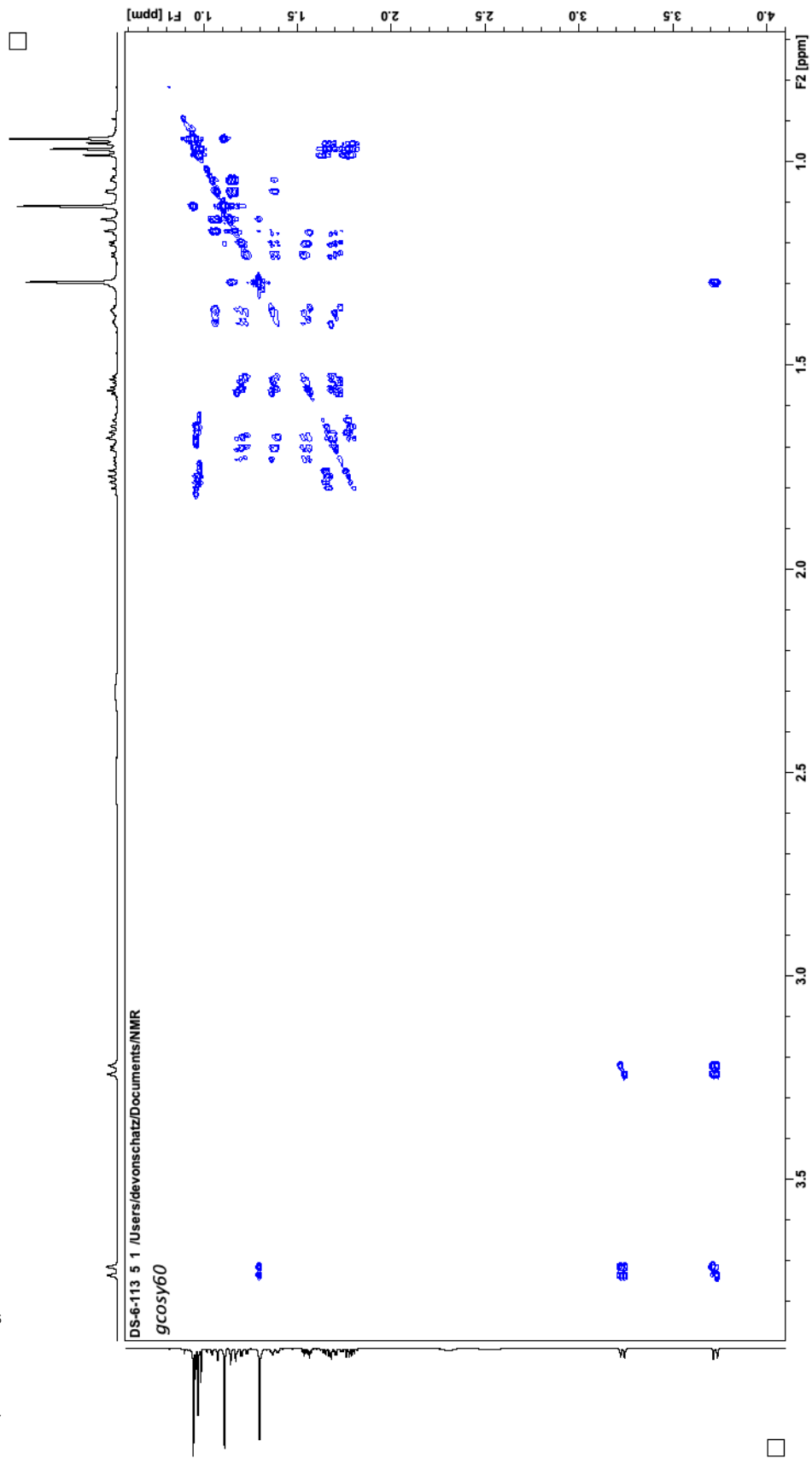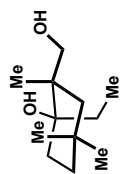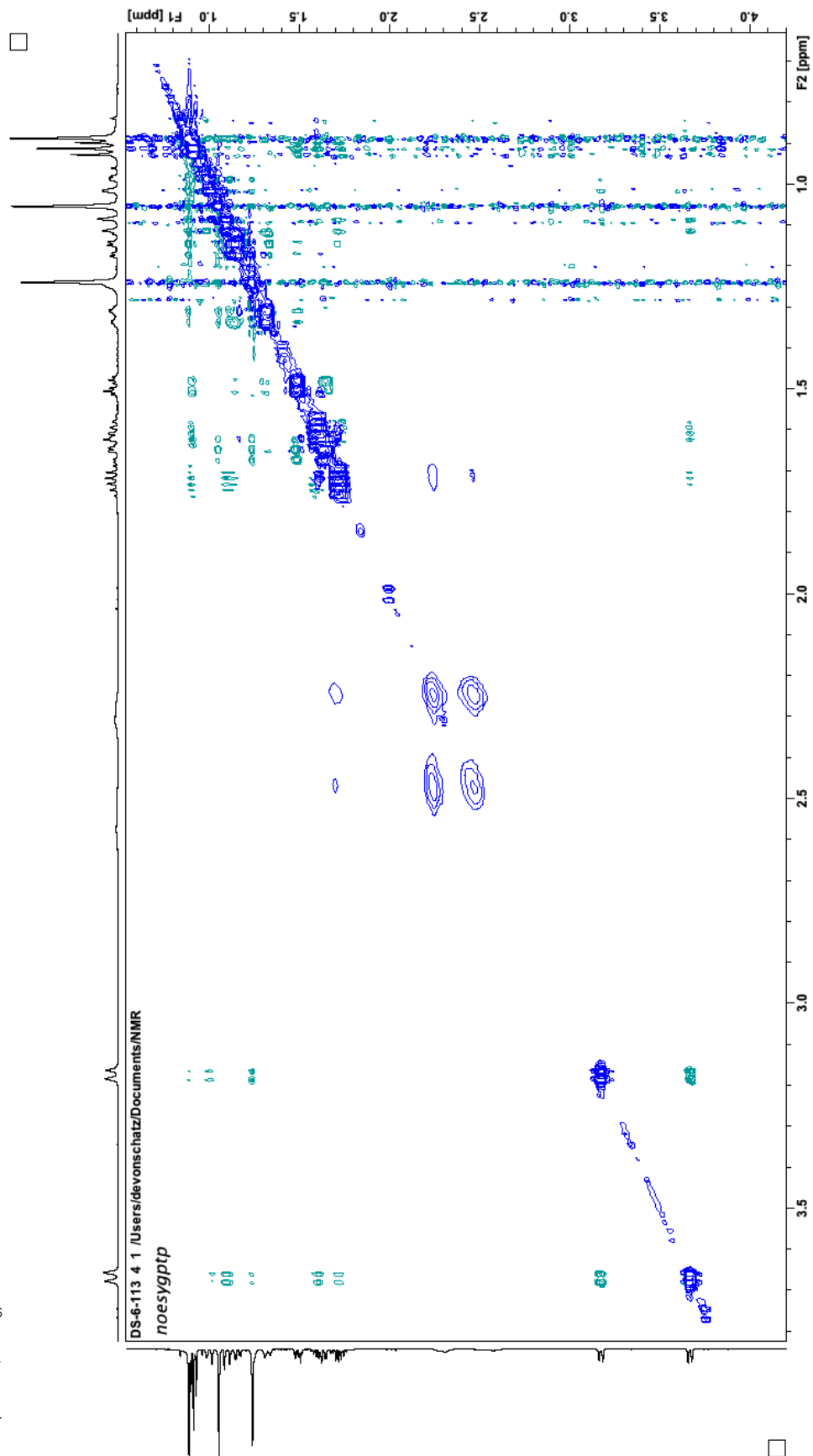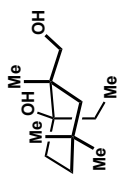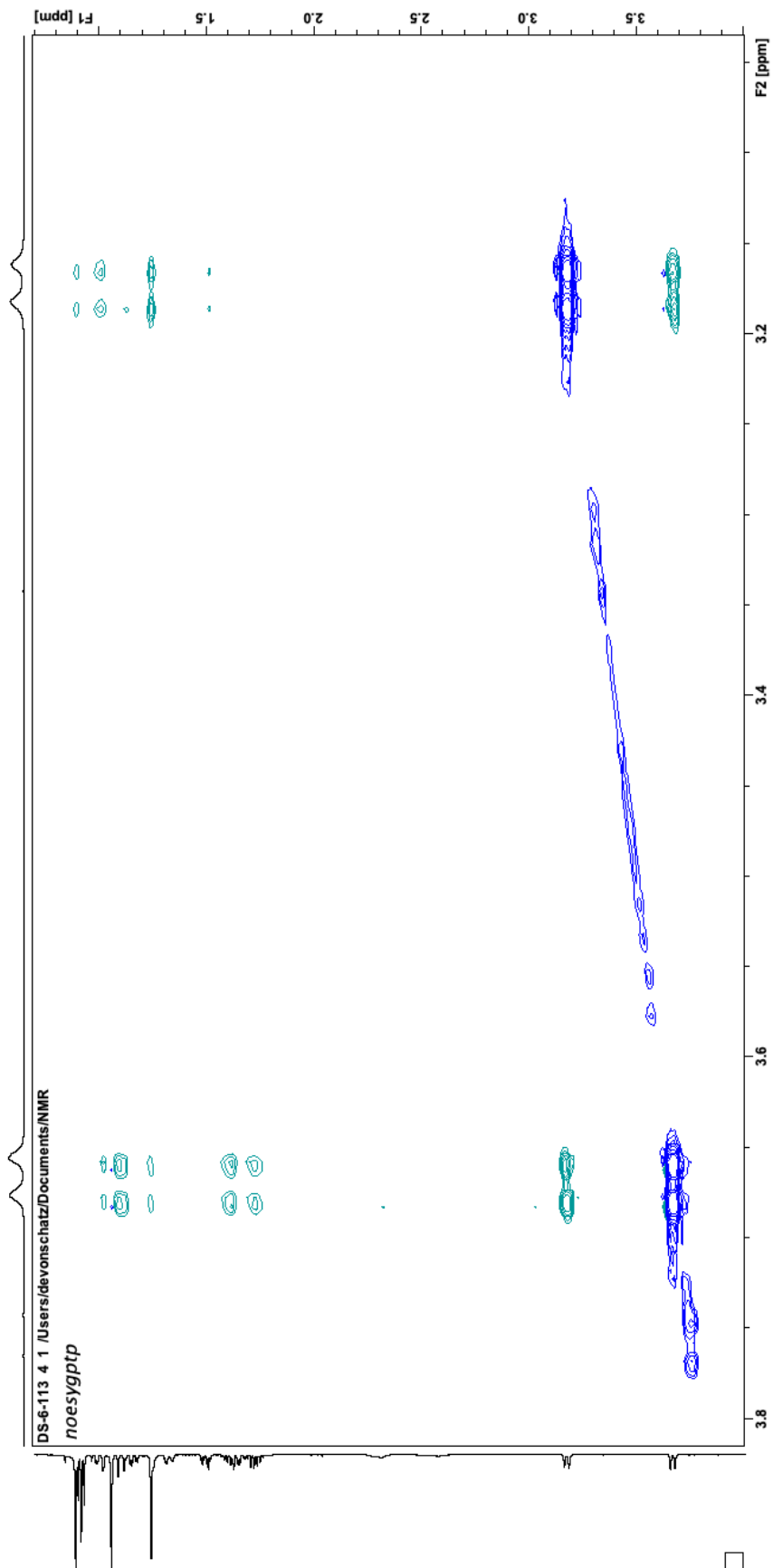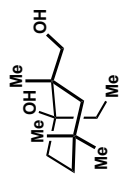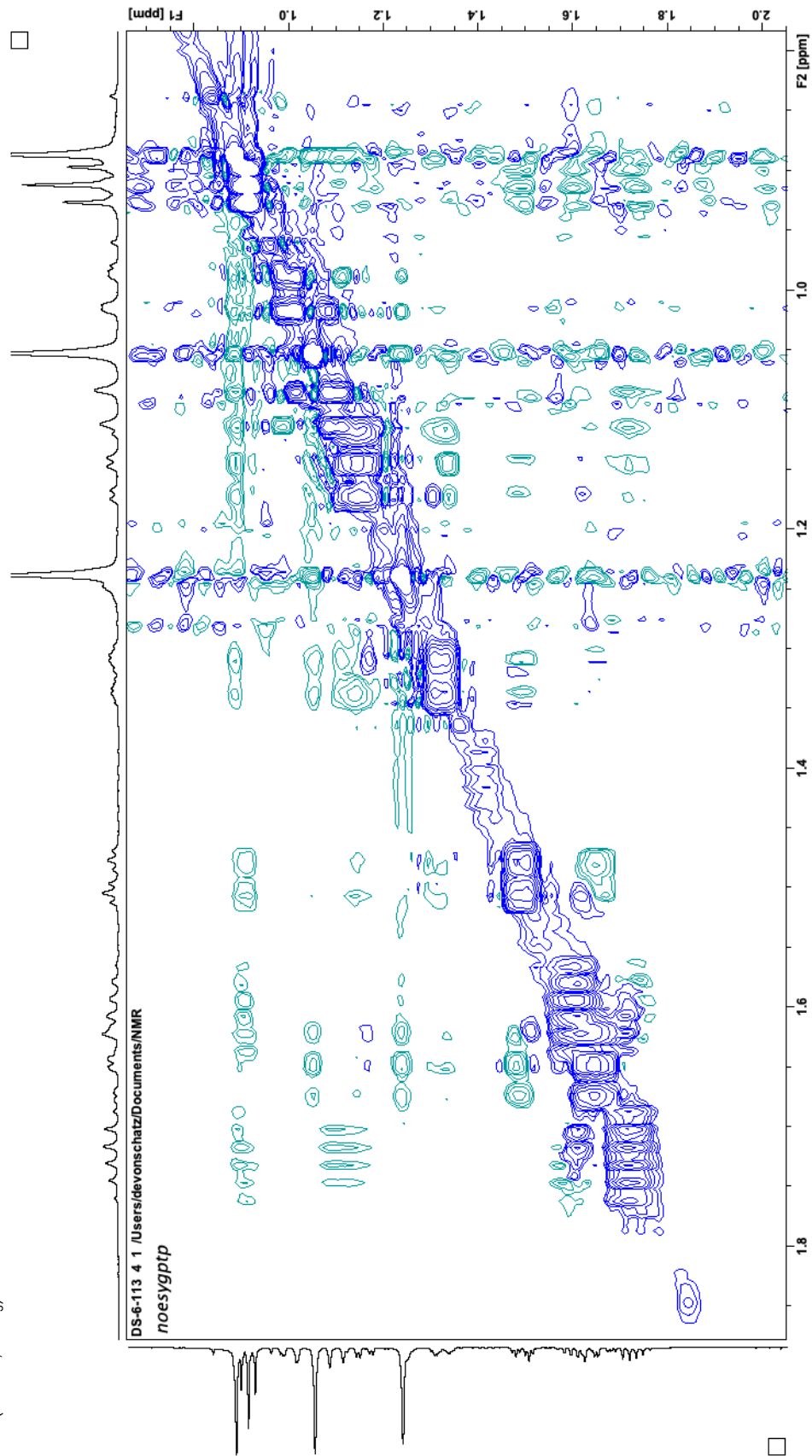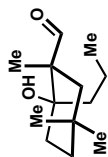
4.41 (^{1}H NMR, 500 MHz, CDCl$_3$)

DS-6-88 1 1 /Users/devonschatz/Documents/NMR

1H spectrum

DS-6-76 1 1 /Users/devonschatz/Documents/NMR
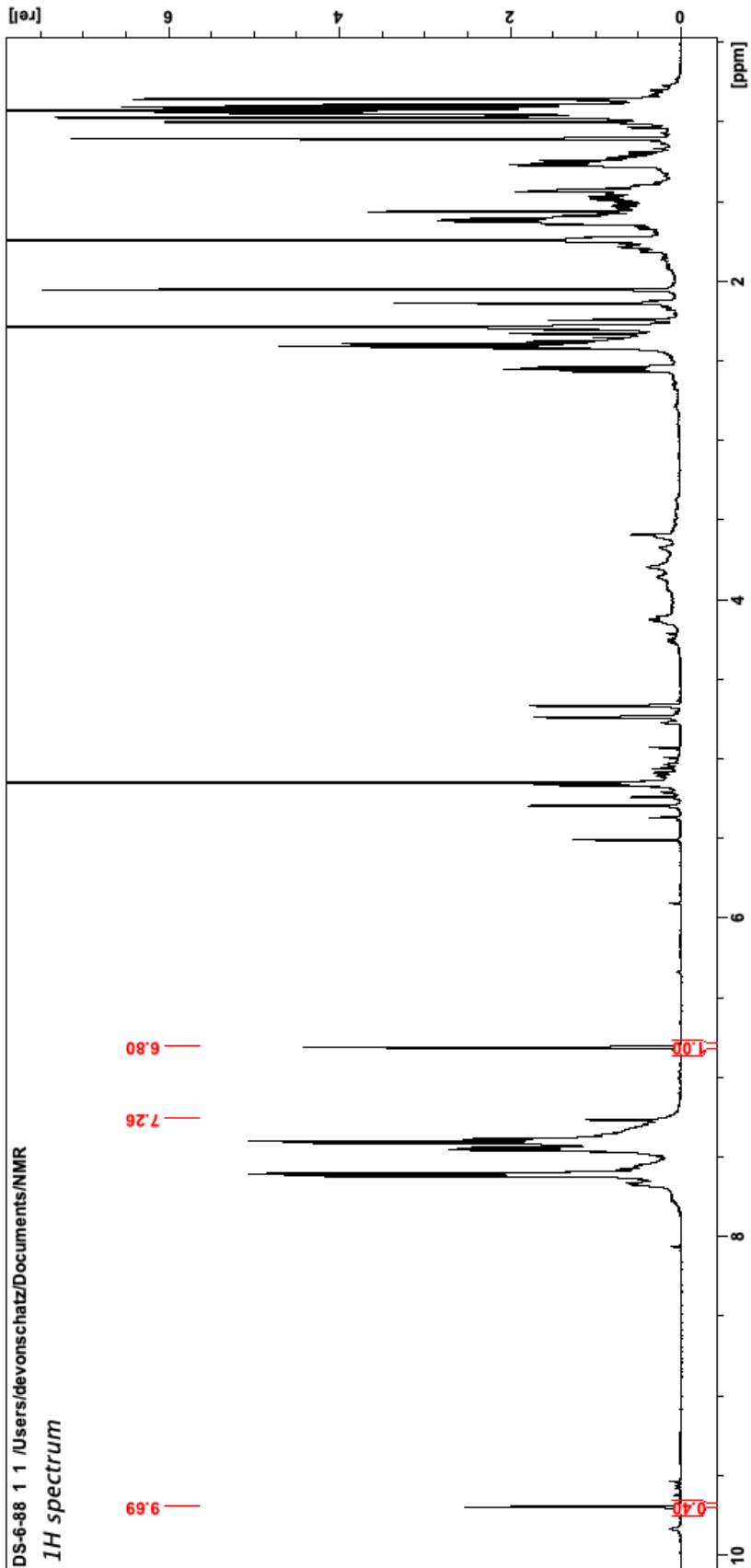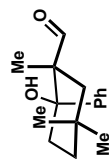
4.42 (^{1}H NMR, 500 MHz, CDCl$_3$)

1H spectrum

9.86

9.60
9.61

7.26

6.82
6.82
6.82
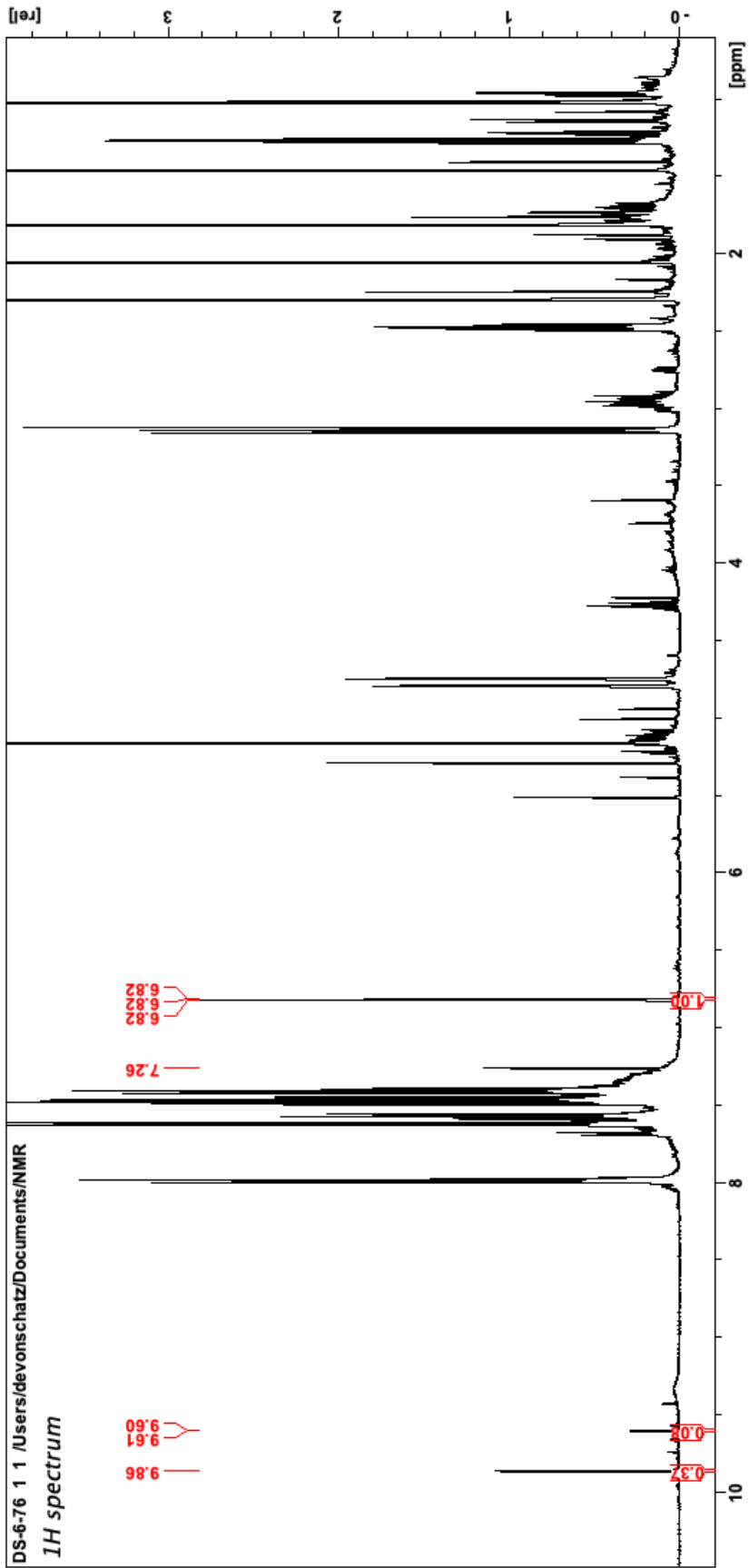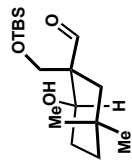
DS-6-171 2 1 /Users/devonschatz/Documents/NMR
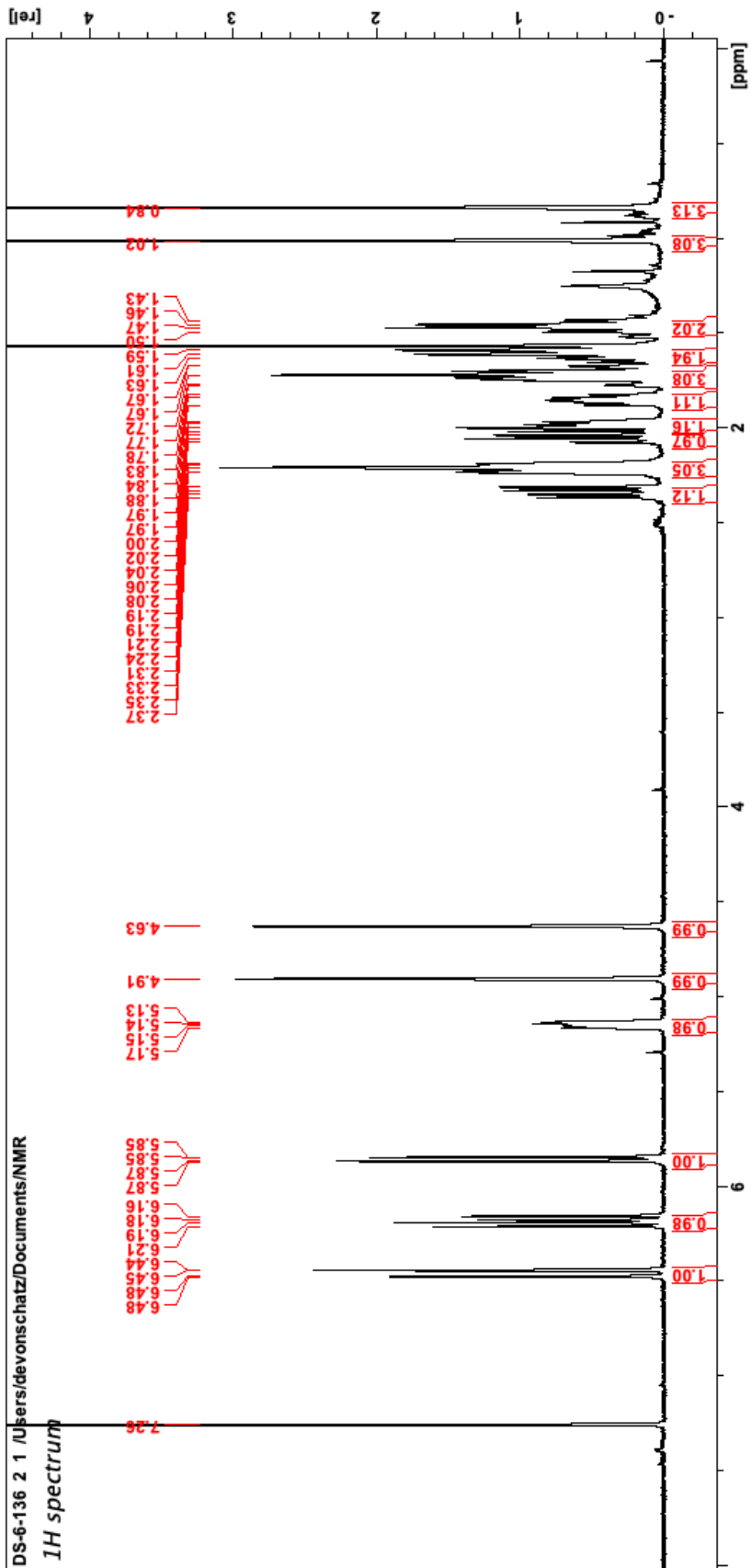
1H spectrum

4.43 (¹H NMR, 500 MHz, CDCl₃)
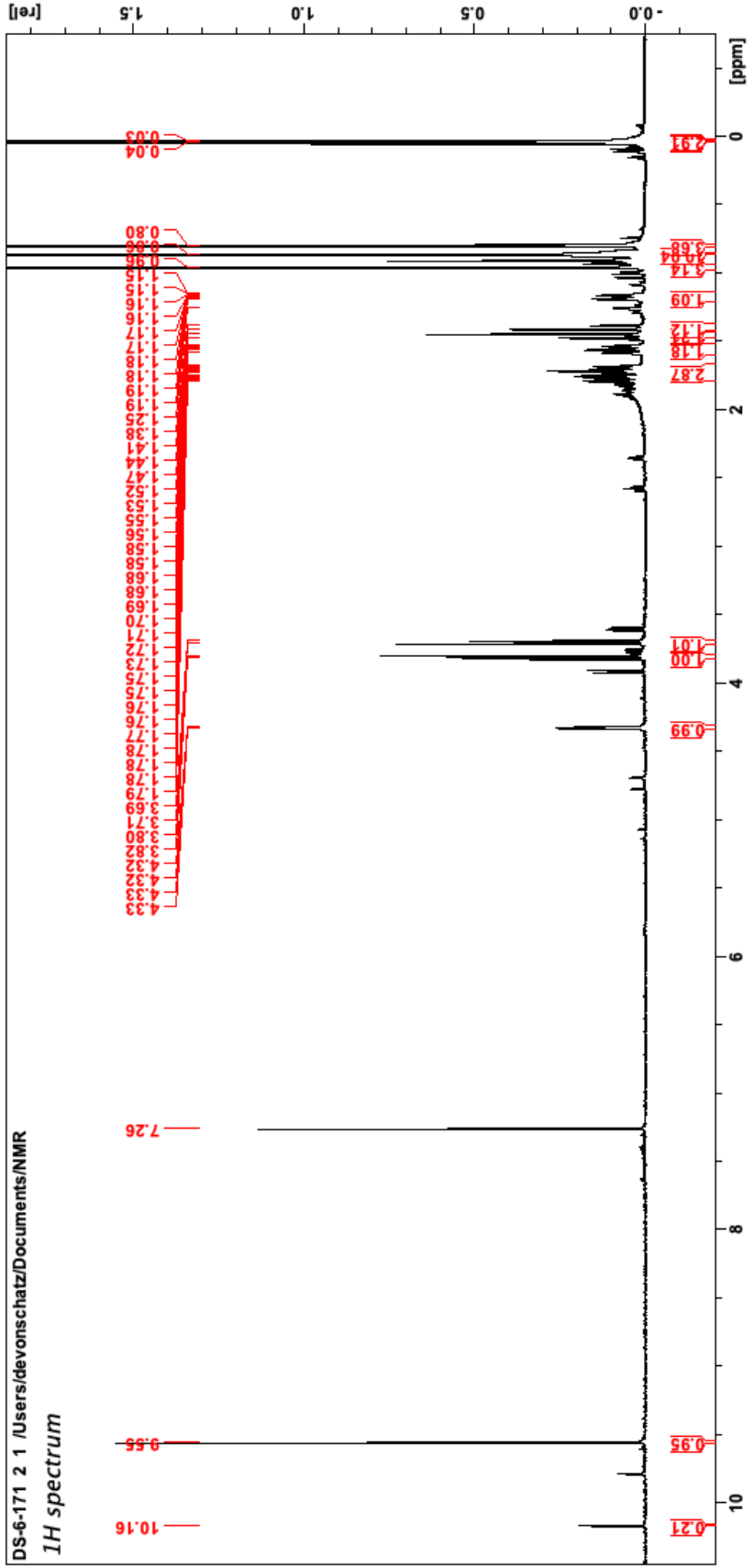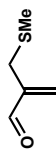
S4.14 (^{1}H NMR, 500 MHz, CDCl$_3$)

DS-6-196 2 1 /Users/devonschatz/Documents/NMR
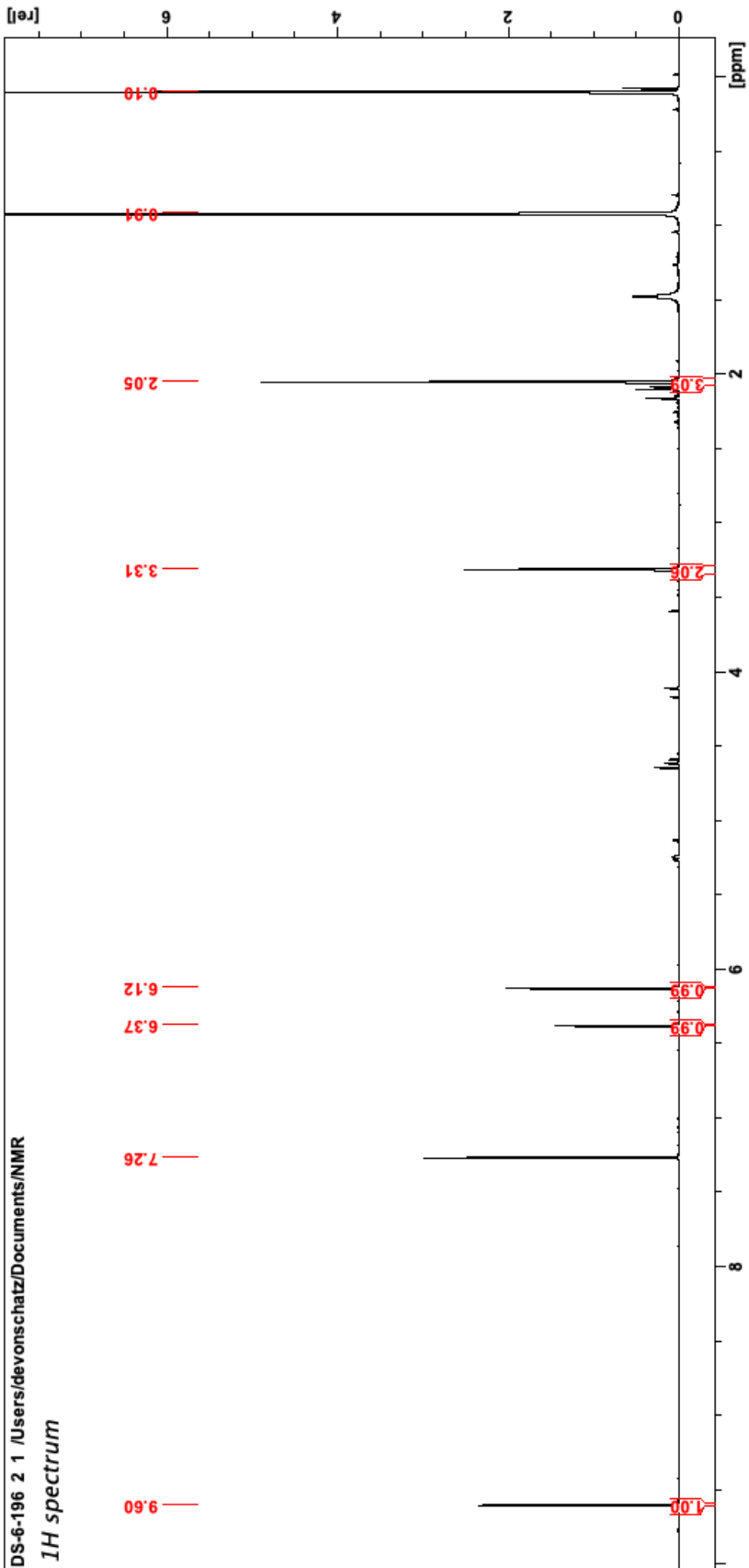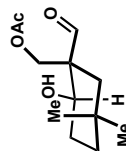
1H spectrum

DS-6-201 1 1 /Users/devonschatz/Documents/NMR
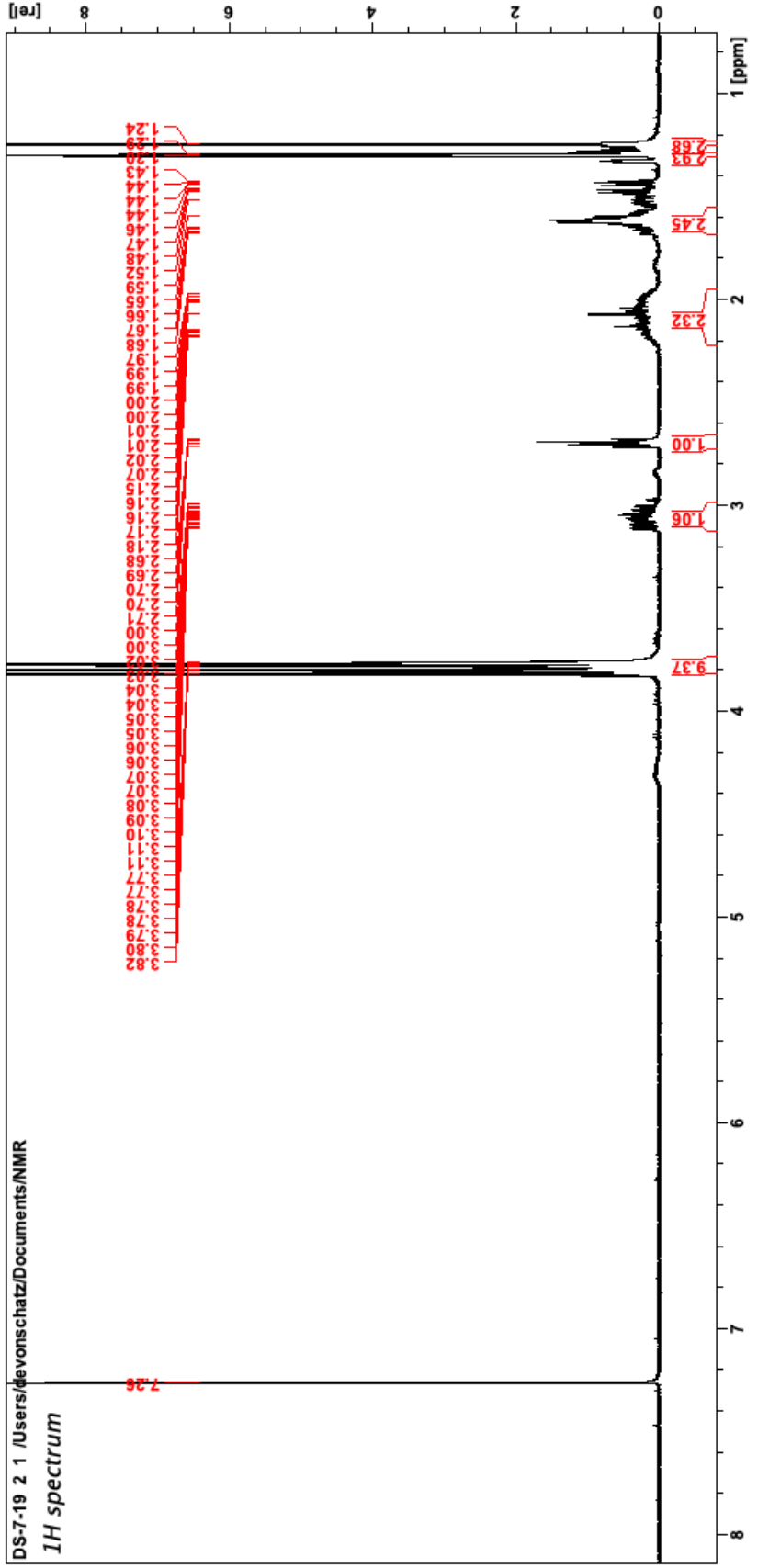
1H spectrum

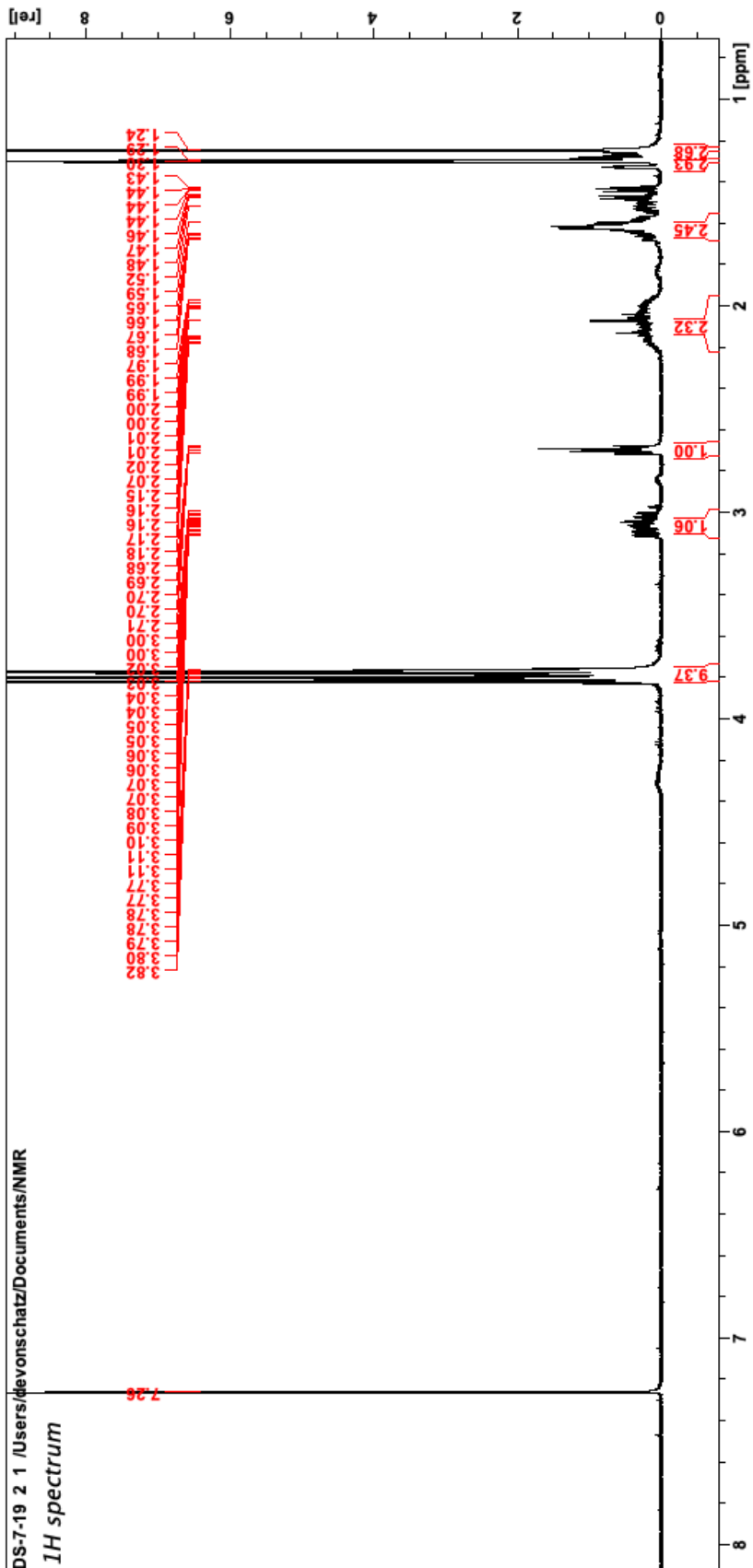4.44 (¹H NMR, 500 MHz, CDCl₃)
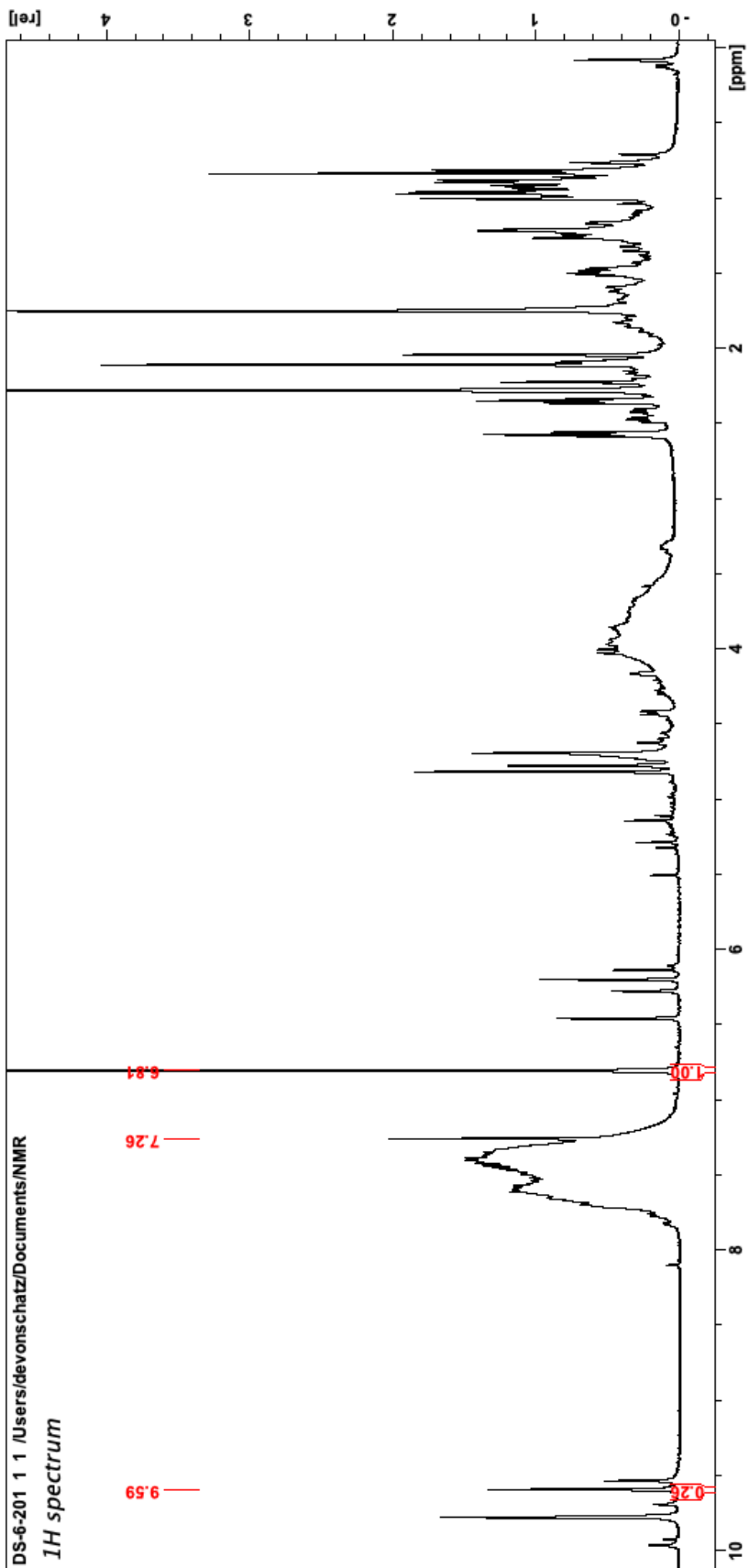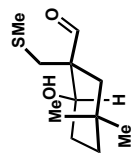
4.45 (^{1}H NMR, 500 MHz, CDCl$_3$)

DS-6-200 1 1 /Users/devonschatz/Documents/NMR

1H spectrum
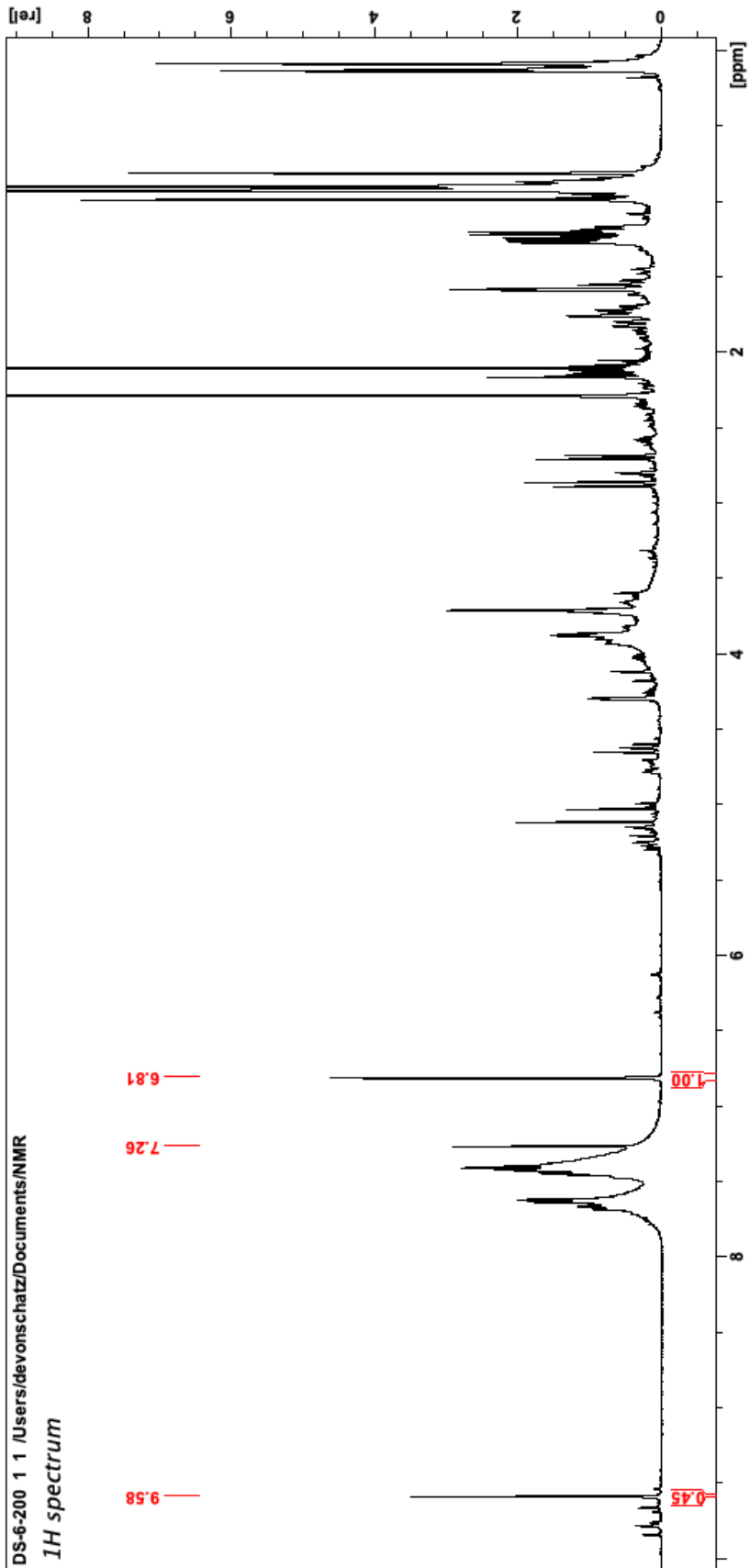
Appendix D: GC Data of S2.5 and S3.7

File   :D:\MassHunter\GCMS\1\data\DJS\DS-4-188_method 14.D
Operator   :
Acquired   : 13 Aug 2018 18:56   using AcqMethod Homoprenyl CA_ketone 14.M
Instrument :   Chiral GC
Sample Name:
Misc Info   :
Vial Number: 5
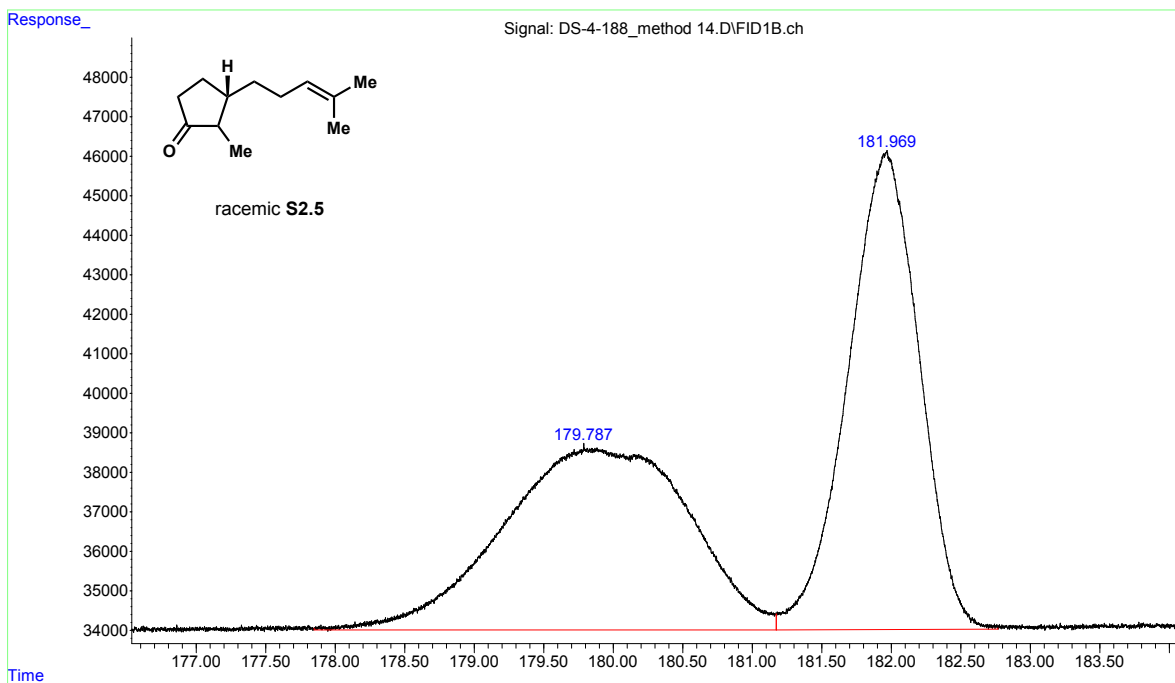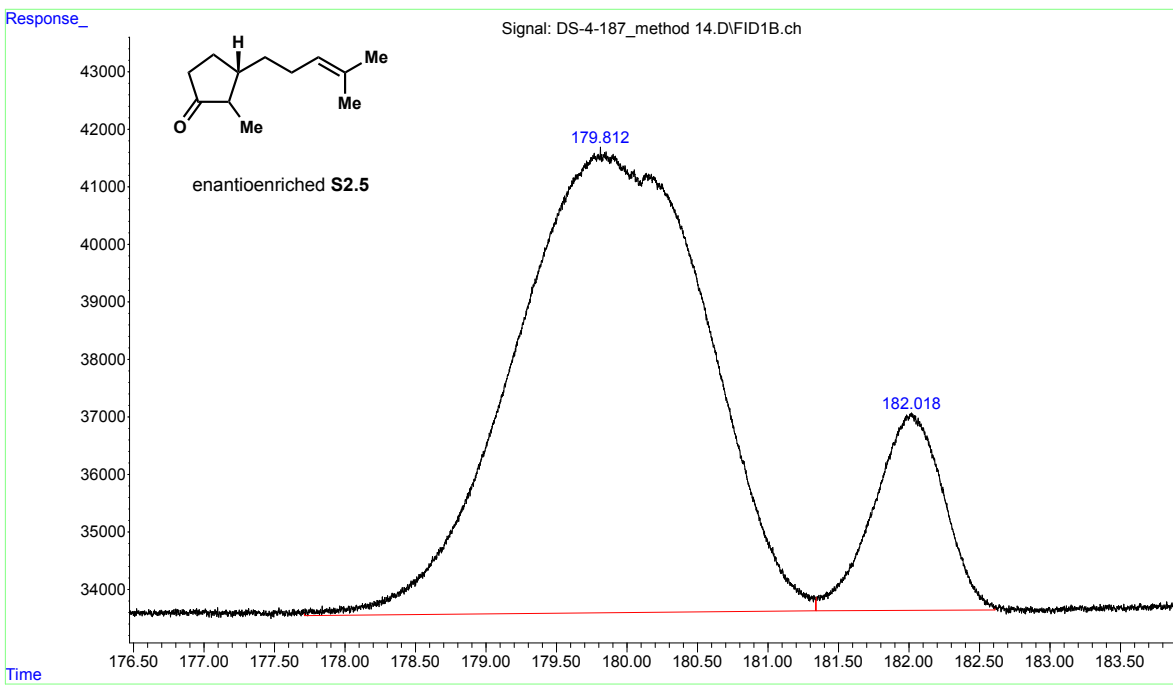
Area Percent Report

    Data Path : D:\MassHunter\GCMS\1\data\DJS\
    Data File : DS-4-188_method 14.D
    Signal(s) : FID1B.ch
    Acq On   : 13 Aug 2018 18:56
    Sample   :
    Misc   :
    ALS Vial : 5   Sample Multiplier: 1

    Integration File: autoint1.e

    Method   : D:\MassHunter\GCMS\1\methods\Homoprenyl CA_ketone 14.M
    Title   :

    Signal   : FID1B.ch

peak   R.T.   Start   End   PK peak   peak   peak   % of
 #   min   min   min   TY height   area   % max.   total
---   -----   -----   ----   --- -------   -------   ------   ------
  1 179.787 177.848 181.172   M   4724   4320516   99.96%   49.991%
  2 181.969 181.172 182.766   M   12132   4322140 100.00%   50.009%
                    Sum of corrected areas: 8642656

Thu Aug 30 17:23:15 2018

Area Percent Report

```
peak  R.T.    Start    End   PK  peak      peak      peak    % of
 #    min     min      min   TY height     area      % max.   total
---  -----   -----    ----  --- -------   -------   ------  ------
 1179.812 177.712 181.337    M   8095    7560612 100.00% 86.580%
 2182.018 181.342 182.609    M   3431    1171915  15.50% 13.420%
                   Sum of corrected areas:     8732527
```

Thu Aug 30 17:20:17 2018

350

File   :D:\MassHunter\GCMS\1\data\DJS\DS-7-75 RUN 9 - METHOD 8.D
Operator   :
Acquired : 29 Jan 2020 09:52   using AcqMethod HWE OLEFINATION OF ACETONE METHOD 8.M
Instrument :   Chiral GC
Sample Name:
Misc Info :
Vial Number: 1
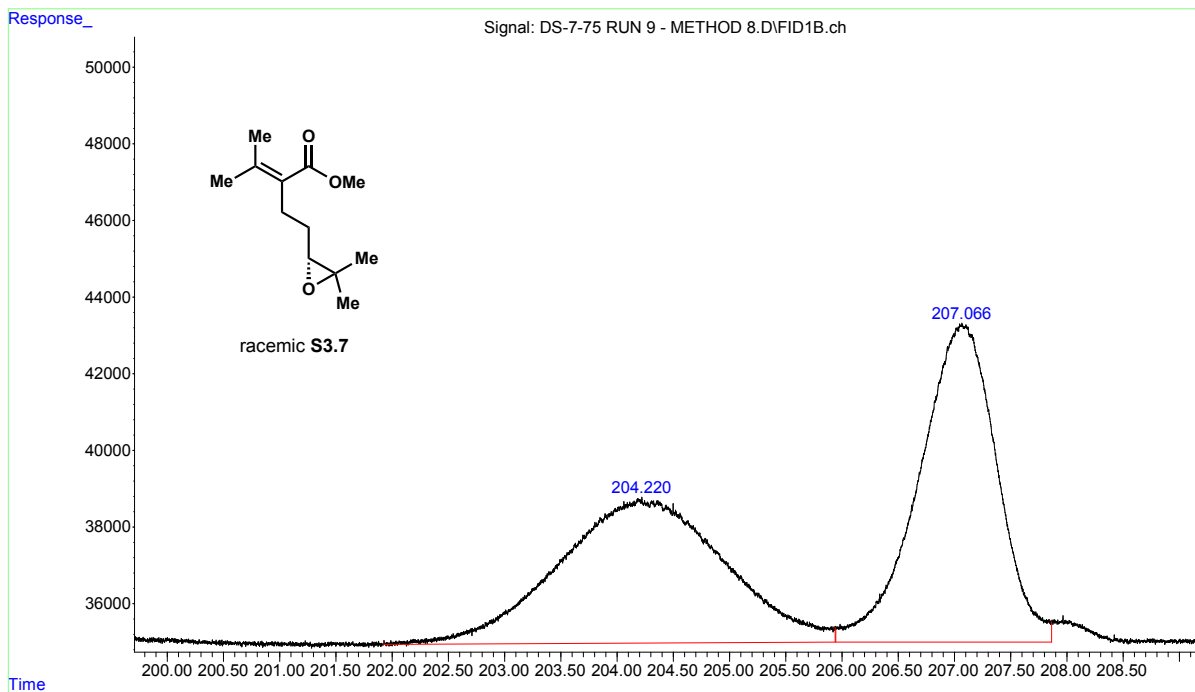
Area Percent Report

Data Path : D:\MassHunter\GCMS\1\data\DJS\
Data File : DS-7-75 RUN 9 - METHOD 8.D
Signal(s) : FID1B.ch
Acq On   : 29 Jan 2020 09:52
Sample   :
Misc   :
ALS Vial : 1   Sample Multiplier: 1

Integration File: autoint1.e

Method   : D:\MassHunter\GCMS\1\data\DJS\DS-2-217_method 10.D\AcqData\Homoprenyl CA_ketone 10.M
Title   :

Signal   : FID1B.ch

```
peak  R.T.    Start    End   PK  peak      peak     peak    % of
 #    min      min     min   TY height     area    % max.   total
---  -----    -----   ----  --- -------   -------   ------  ------
 1204.220 201.926 205.938    M    3814   3834284   96.19% 49.030%
 2207.066 205.944 207.863    M    8322   3985969  100.00% 50.970%
                  Sum of corrected areas:      7820253
```

Homoprenyl CA_ketone 10.M Sat May 09 14:12:59 2020

File   :D:\MassHunter\GCMS\1\data\DJS\DS-7-95.D
Operator :
Acquired : 08 Feb 2020 17:54   using AcqMethod HWE OLEFINATION OF ACETONE METHOD 8.M
Instrument :   Chiral GC
Sample Name:
Misc Info :
Vial Number: 7

Signal: DS-7-95.D\FID1B.ch

enantioenriched **S3.7**
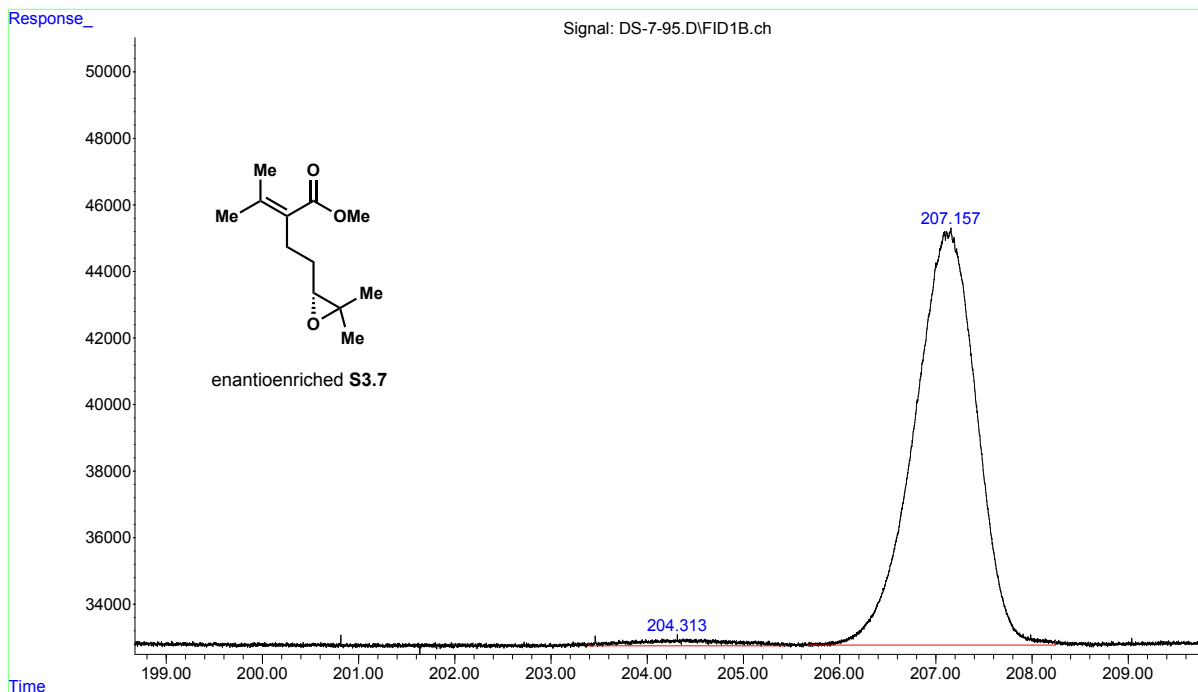
Data Path : D:\MassHunter\GCMS\1\data\DJS\
Data File : DS-7-95.D
Signal(s) : FID1B.ch
Acq On   : 08 Feb 2020 17:54
Sample   :
Misc   :
ALS Vial : 7   Sample Multiplier: 1

Integration File: autoint1.e

Method   : D:\MassHunter\GCMS\1\data\DJS\DS-2-217_method 10.D\AcqData\Homoprenyl CA_ketone 10.M
Title   :

Signal   : FID1B.ch

peak #	R.T. min	Start min	End min	PK TY	peak height	peak area	peak % max.	% of total
1	204.313	203.393	205.438	M	338	128613	2.29%	2.236%
2	207.157	205.671	208.242	M	12537	5622532	100.00%	97.764%
					Sum of corrected areas:	5751146		

Homoprenyl CA_ketone 10.M Sat May 09 14:19:20 2020

352

Appendix E: HPLC Data of 2.22
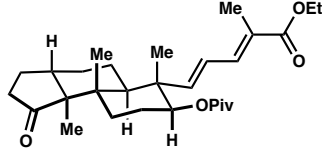
2.22 (racemic)

Data File C:\HPCHEM\1\DATA\ALEXB\DS4-111A.D   Sample Name: DS-4-111-A

Chiralcel AS-H (w/o guard); 1 ml/min; 1% iPrOH in Hexan
es, 10 ul injection

===
Injection Date : 6/8/2018 4:09:43 PM
Sample Name   : DS-4-111-A   Location : Vial 23
Acq. Operator   : ALEXB
                                                    Inj Volume : 10 µl
Acq. Method   : C:\HPCHEM\1\METHODS\ALEXB.M
Last changed   : 6/8/2018 3:34:21 PM by ALEXB
                  (modified after loading)
Analysis Method : C:\HPCHEM\1\METHODS\ALEXB.M
Last changed   : 6/5/2018 5:42:00 PM by ALEXB
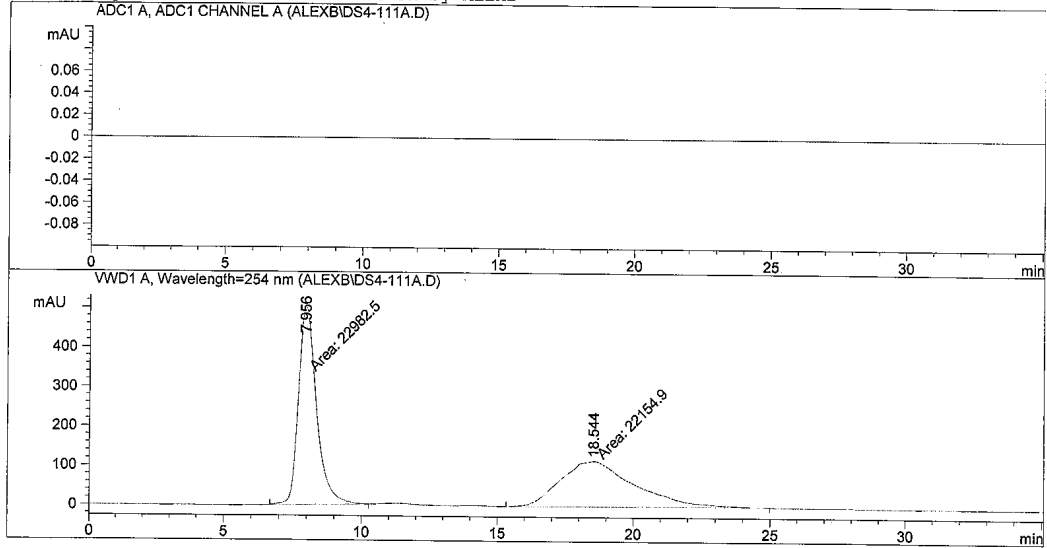
===
                      Area Percent Report
===

Sorted By   :   Signal
Multiplier   :   1.0000
Dilution   :   1.0000
Sample Amount   :   1.00000 [ng/ul]   (not used in calc.)
Use Multiplier & Dilution Factor with ISTDs

Signal 1: ADC1 A, ADC1 CHANNEL A

Signal 2: VWD1 A, Wavelength=254 nm

Peak RetTime Type Width   Area   Height   Area
 #   [min]   [min]   mAU   *s   [mAU   ]   %
----|-------|----|-------|----------|----------|--------|
  1   7.956 MM   0.7596 2.29825e4   504.26511   50.9167
  2 18.544 MM   3.1733 2.21549e4   116.36196   49.0833

Totals :   4.51374e4   620.62707

 Results obtained with enhanced integrator!
===
                    *** End of Report ***
1100 LC 6/8/2018 4:46:25 PM ALEXB   Page 1 of 1

354

(−)-2.22
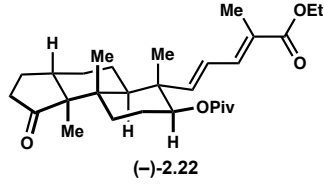
Chiralpak AS-H (w/o guard); 1.0 ml/min; 1% iPrOH in Hex
anes, 10 ul injection

==

Injection Date : 7/12/2018 5:59:41 PM
Sample Name   : DS-4-146-A   Location : Vial 61
Acq. Operator   : ALEXB
                                                Inj Volume : 10 µl
Acq. Method   : C:\HPCHEM\1\METHODS\ALEXB.M
Last changed   : 7/12/2018 5:58:00 PM by ALEXB
                  (modified after loading)
Analysis Method : C:\HPCHEM\1\METHODS\ALEXB.M
Last changed   : 7/12/2018 4:12:13 PM by ALEXB
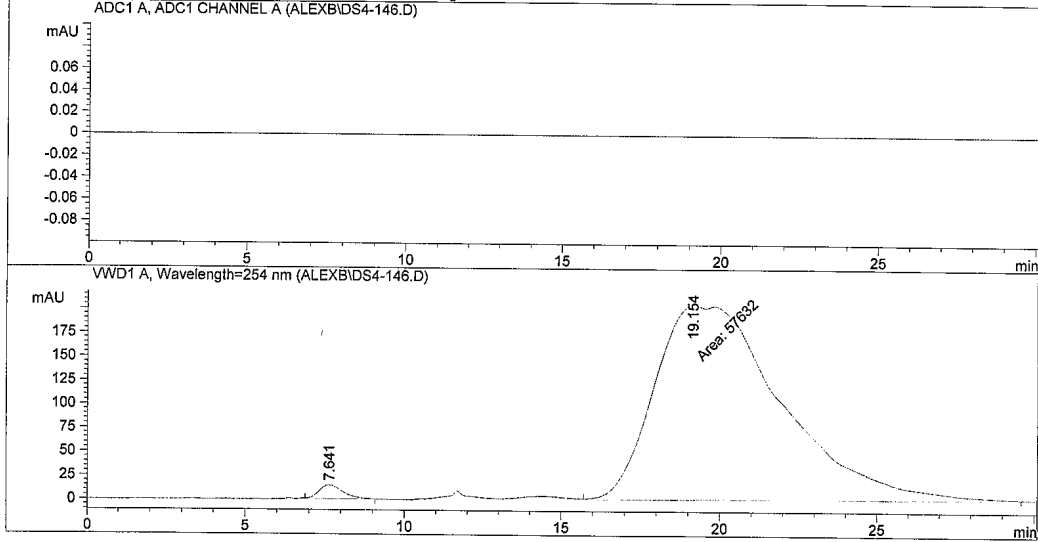
==
                      Area Percent Report
==

Sorted By   :   Signal
Multiplier   :   1.0000
Dilution   :   1.0000
Sample Amount   :   1.00000   [ng/ul]   (not used in calc.)
Use Multiplier & Dilution Factor with ISTDs

Signal 1: ADC1 A, ADC1 CHANNEL A

Signal 2: VWD1 A, Wavelength=254 nm

Peak RetTime Type Width   Area   Height   Area
  #   [min]   [min]   mAU *s   [mAU   ]   %
----|-------|----|-------|----------|----------|--------|
  1   7.641 VB 0.8207 783.72424   14.71781 1.3416
  2 19.154 MM 4.6765 5.76320e4   205.39664 98.6584

Totals :   5.84157e4   220.11445

Results obtained with enhanced integrator!
==
                    *** End of Report ***

1100 LC 7/12/2018 6:31:36 PM ALEXB   Page 1 of 1

355

Appendix F: X-ray Crystallographic Data of 3.82, S4.1 and S4.4

Table 1a. Crystal data and structure refinement for 3.82.

Identification code	svp25 (Devon Schatz)
Empirical formula	$C_{26} H_{45} N O_5 Si$
Formula weight	479.72
Temperature	93(2) K
Wavelength	0.71073 Å
Crystal system	Orthorhombic
Space group	$P2_12_12_1$
Unit cell dimensions	a = 7.0577(5) Å $\qquad$ $\alpha = 90°$.
	b = 16.6418(12) Å $\qquad$ $\beta = 90°$.
	c = 21.9763(16) Å $\qquad$ $\gamma = 90°$.
Volume	2581.2(3) $Å^3$
Z	4
Density (calculated)	1.234 Mg/m^3
Absorption coefficient	0.127 mm^{-1}
F(000)	1048
Crystal color	colorless
Crystal size	0.179 x 0.068 x 0.066 mm^3
Theta range for data collection	1.535 to 26.394°
Index ranges	$-8 \leq h \leq 8, -18 \leq k \leq 20, -22 \leq l \leq 27$
Reflections collected	22744
Independent reflections	5292 [R(int) = 0.0720]
Completeness to theta = 25.500°	100.0 %
Absorption correction	Semi-empirical from equivalents
Max. and min. transmission	0.8620 and 0.7819
Refinement method	Full-matrix least-squares on F^2
Data / restraints / parameters	5292 / 0 / 334
Goodness-of-fit on F^2	1.066
Final R indices [I>2sigma(I) = 4490 data]	R1 = 0.0577, wR2 = 0.1165
R indices (all data, 0.80 Å)	R1 = 0.0733, wR2 = 0.1234
Largest diff. peak and hole	0.302 and -0.283 e.$Å^{-3}$

Table 2a. Atomic coordinates (x 10^4) and equivalent isotropic displacement parameters (Å^2 x 10^3) for svp25. U(eq) is defined as one third of the trace of the orthogonalized U^{ij} tensor.

	x	y	z	U(eq)
Si(1)	7834(3)	2948(1)	3790(1)	15(1)
Si(2)	5984(3)	3013(1)	3814(1)	13(1)
O(1)	8396(4)	8688(2)	4182(1)	11(1)
O(2)	10678(4)	7807(2)	3860(1)	12(1)
O(3)	6879(4)	7580(2)	4968(1)	14(1)
O(4)	6545(4)	9588(2)	5047(1)	26(1)
O(5)	7198(4)	3880(2)	3604(1)	20(1)
N(1)	3778(5)	4123(2)	2585(2)	24(1)
C(1)	8798(5)	8039(2)	3771(2)	11(1)
C(2)	6731(5)	9132(2)	3994(2)	12(1)
C(3)	5020(5)	8579(2)	4004(2)	12(1)
C(4)	5381(5)	7766(2)	3691(2)	12(1)
C(5)	7299(5)	7359(2)	3849(2)	9(1)
C(6)	7885(5)	6646(2)	3417(2)	10(1)
C(7)	7988(6)	6875(2)	2735(2)	14(1)
C(8)	9036(6)	6228(2)	2365(2)	16(1)
C(9)	8095(5)	5420(2)	2452(2)	12(1)
C(10)	9005(5)	4690(2)	2134(2)	15(1)
C(11)	8474(6)	3955(2)	2532(2)	16(1)
C(12)	7192(6)	4302(2)	3048(2)	14(1)
C(13)	7986(5)	5176(2)	3128(2)	11(1)
C(14)	6848(5)	5818(2)	3510(2)	10(1)
C(15)	6879(6)	5599(2)	4191(2)	13(1)
C(16)	6178(5)	6279(2)	4594(2)	14(1)
C(17)	7412(5)	7018(2)	4501(2)	10(1)
C(18)	6628(6)	9863(2)	4421(2)	17(1)
C(19)	4790(6)	10323(3)	4317(2)	26(1)
C(20)	8334(6)	10402(2)	4329(2)	26(1)
C(21)	5226(6)	4255(2)	2798(2)	14(1)
C(22)	10008(5)	5054(2)	3397(2)	17(1)
C(23)	4755(5)	5853(2)	3308(2)	13(1)

C(24)	6871(7)	2844(3)	4564(2)	29(1)
C(25)	6668(7)	2228(2)	3253(2)	24(1)
C(26)	10453(11)	2791(5)	3846(4)	24(2)
C(26B)	3359(12)	3121(6)	3876(4)	21(2)

Table 3a. Bond lengths [Å] and angles [°] for svp25.

_____

Si(1)-O(5)	1.665(3)
Si(1)-C(24)	1.839(5)
Si(1)-C(26)	1.871(8)
Si(1)-C(25)	1.872(5)
Si(2)-O(5)	1.740(4)
Si(2)-C(24)	1.785(5)
Si(2)-C(25)	1.860(5)
Si(2)-C(26B)	1.866(8)
O(1)-C(1)	1.437(4)
O(1)-C(2)	1.448(4)
O(2)-C(1)	1.396(4)
O(3)-C(17)	1.439(4)
O(4)-C(18)	1.451(5)
O(5)-C(12)	1.409(4)
N(1)-C(21)	1.145(5)
C(1)-C(5)	1.559(5)
C(2)-C(3)	1.518(5)
C(2)-C(18)	1.538(5)
C(3)-C(4)	1.539(5)
C(4)-C(5)	1.554(5)
C(5)-C(17)	1.543(5)
C(5)-C(6)	1.574(5)
C(6)-C(7)	1.548(5)
C(6)-C(14)	1.575(5)
C(7)-C(8)	1.538(5)
C(8)-C(9)	1.512(5)
C(9)-C(10)	1.541(5)
C(9)-C(13)	1.543(5)
C(10)-C(11)	1.550(6)
C(11)-C(12)	1.562(5)
C(12)-C(21)	1.494(6)
C(12)-C(13)	1.568(5)
C(13)-C(22)	1.558(5)
C(13)-C(14)	1.578(5)

C(14)-C(15)	1.541(5)
C(14)-C(23)	1.544(5)
C(15)-C(16)	1.520(5)
C(16)-C(17)	1.521(5)
C(18)-C(20)	1.516(6)
C(18)-C(19)	1.523(6)
O(5)-Si(1)-C(24)	102.4(2)
O(5)-Si(1)-C(26)	114.4(3)
C(24)-Si(1)-C(26)	106.9(3)
O(5)-Si(1)-C(25)	108.8(2)
C(24)-Si(1)-C(25)	111.1(2)
C(26)-Si(1)-C(25)	112.7(3)
O(5)-Si(2)-C(24)	101.7(2)
O(5)-Si(2)-C(25)	106.2(2)
C(24)-Si(2)-C(25)	114.2(2)
O(5)-Si(2)-C(26B)	115.4(3)
C(24)-Si(2)-C(26B)	107.2(3)
C(25)-Si(2)-C(26B)	111.9(4)
C(1)-O(1)-C(2)	111.3(3)
C(12)-O(5)-Si(1)	132.8(2)
C(12)-O(5)-Si(2)	129.9(3)
O(2)-C(1)-O(1)	107.9(3)
O(2)-C(1)-C(5)	115.4(3)
O(1)-C(1)-C(5)	110.0(3)
O(1)-C(2)-C(3)	109.4(3)
O(1)-C(2)-C(18)	105.5(3)
C(3)-C(2)-C(18)	115.6(3)
C(2)-C(3)-C(4)	113.2(3)
C(3)-C(4)-C(5)	115.3(3)
C(17)-C(5)-C(4)	114.4(3)
C(17)-C(5)-C(1)	109.6(3)
C(4)-C(5)-C(1)	104.5(3)
C(17)-C(5)-C(6)	105.6(3)
C(4)-C(5)-C(6)	115.0(3)
C(1)-C(5)-C(6)	107.6(3)

C(7)-C(6)-C(5)	114.3(3)
C(7)-C(6)-C(14)	111.3(3)
C(5)-C(6)-C(14)	117.4(3)
C(8)-C(7)-C(6)	111.3(3)
C(9)-C(8)-C(7)	110.1(3)
C(8)-C(9)-C(10)	117.5(3)
C(8)-C(9)-C(13)	112.2(3)
C(10)-C(9)-C(13)	104.4(3)
C(9)-C(10)-C(11)	105.5(3)
C(10)-C(11)-C(12)	104.9(3)
O(5)-C(12)-C(21)	107.2(3)
O(5)-C(12)-C(11)	116.3(3)
C(21)-C(12)-C(11)	104.5(3)
O(5)-C(12)-C(13)	111.4(3)
C(21)-C(12)-C(13)	114.9(3)
C(11)-C(12)-C(13)	102.6(3)
C(9)-C(13)-C(22)	110.7(3)
C(9)-C(13)-C(12)	98.9(3)
C(22)-C(13)-C(12)	104.4(3)
C(9)-C(13)-C(14)	111.1(3)
C(22)-C(13)-C(14)	110.7(3)
C(12)-C(13)-C(14)	120.3(3)
C(15)-C(14)-C(23)	107.6(3)
C(15)-C(14)-C(6)	109.1(3)
C(23)-C(14)-C(6)	111.9(3)
C(15)-C(14)-C(13)	110.4(3)
C(23)-C(14)-C(13)	111.1(3)
C(6)-C(14)-C(13)	106.7(3)
C(16)-C(15)-C(14)	112.6(3)
C(15)-C(16)-C(17)	109.8(3)
O(3)-C(17)-C(16)	106.2(3)
O(3)-C(17)-C(5)	114.3(3)
C(16)-C(17)-C(5)	113.1(3)
O(4)-C(18)-C(20)	110.2(3)
O(4)-C(18)-C(19)	105.5(3)
C(20)-C(18)-C(19)	111.0(3)

O(4)-C(18)-C(2)	109.3(3)
C(20)-C(18)-C(2)	110.4(3)
C(19)-C(18)-C(2)	110.2(3)
N(1)-C(21)-C(12)	171.4(4)

_____

Table 4a. Anisotropic displacement parameters (Å² x 10³) for svp25. The anisotropic displacement factor exponent takes the form: -2π²[h² a*²U¹¹ + ... + 2 h k a* b* U¹²]

	U^{11}	U^{22}	U^{33}	U^{23}	U^{13}	U^{12}
Si(1)	18(1)	13(1)	14(1)	-1(1)	-2(1)	3(1)
Si(2)	17(1)	10(1)	13(1)	3(1)	-2(1)	0(1)
O(1)	12(1)	10(1)	11(1)	-1(1)	1(1)	1(1)
O(2)	10(1)	18(2)	9(2)	-1(1)	2(1)	0(1)
O(3)	19(1)	10(1)	11(1)	-2(1)	4(1)	0(1)
O(4)	28(2)	33(2)	16(2)	-5(1)	1(1)	3(1)
O(5)	38(2)	12(1)	9(1)	0(1)	-3(1)	4(1)
N(1)	20(2)	25(2)	25(2)	-15(2)	6(2)	-4(2)
C(1)	12(2)	12(2)	10(2)	-1(2)	-2(2)	1(1)
C(2)	12(2)	12(2)	12(2)	4(2)	-1(2)	2(2)
C(3)	12(2)	13(2)	13(2)	1(2)	0(2)	2(2)
C(4)	10(2)	13(2)	12(2)	1(2)	0(2)	1(2)
C(5)	8(2)	8(2)	10(2)	1(2)	2(1)	1(1)
C(6)	7(2)	13(2)	9(2)	1(1)	0(2)	1(2)
C(7)	16(2)	14(2)	12(2)	-3(2)	3(2)	-2(2)
C(8)	16(2)	22(2)	10(2)	-4(2)	5(2)	-6(2)
C(9)	8(2)	16(2)	12(2)	-1(2)	0(2)	2(2)
C(10)	10(2)	22(2)	12(2)	-5(2)	-1(2)	2(2)
C(11)	15(2)	17(2)	17(2)	-5(2)	-3(2)	4(2)
C(12)	23(2)	11(2)	9(2)	1(2)	-3(2)	2(2)
C(13)	11(2)	10(2)	10(2)	0(1)	1(2)	4(2)
C(14)	10(2)	11(2)	10(2)	0(2)	1(2)	0(2)
C(15)	18(2)	10(2)	11(2)	-2(1)	3(2)	-1(2)
C(16)	19(2)	13(2)	10(2)	3(2)	5(2)	1(2)
C(17)	13(2)	10(2)	9(2)	-2(2)	1(1)	3(1)
C(18)	20(2)	15(2)	16(2)	-3(2)	3(2)	0(2)
C(19)	26(2)	18(2)	34(3)	-8(2)	3(2)	7(2)
C(20)	24(2)	12(2)	42(3)	-8(2)	8(2)	-2(2)
C(21)	21(2)	11(2)	11(2)	-4(2)	9(2)	-1(2)
C(22)	16(2)	21(2)	16(2)	-9(2)	-5(2)	6(2)
C(23)	11(2)	13(2)	16(2)	-2(2)	0(2)	1(2)

364

C(24)	40(3)	25(2)	22(2)	6(2)	4(2)	-3(2)
C(25)	30(2)	18(2)	26(2)	-6(2)	-5(2)	0(2)
C(26)	19(4)	35(5)	19(4)	-6(4)	-11(3)	13(3)
C(26B)	7(4)	38(5)	17(5)	9(4)	6(4)	4(4)

Table 5a. Hydrogen coordinates (x 10⁴) and isotropic displacement parameters (Å² x 10³) for svp25.

	x	y	z	U(eq)
H(2)	10890(60)	7730(30)	4220(20)	14(12)
H(3)	7290(80)	8040(30)	4870(30)	54(19)
H(4)	7810(90)	9440(40)	5150(30)	70(20)
H(1A)	8684	8251	3346	14
H(2A)	6927	9327	3568	14
H(3A)	3948	8851	3799	15
H(3B)	4647	8481	4432	15
H(4A)	5324	7847	3245	14
H(4B)	4343	7394	3803	14
H(6A)	9231	6532	3530	11
H(7A)	6688	6940	2573	17
H(7B)	8654	7395	2691	17
H(8A)	9022	6374	1928	19
H(8B)	10373	6198	2499	19
H(9A)	6766	5468	2298	14
H(10A)	10397	4754	2111	18
H(10B)	8499	4628	1717	18
H(11A)	9623	3701	2705	20
H(11B)	7777	3550	2290	20
H(15A)	6074	5120	4258	16
H(15B)	8190	5458	4311	16
H(16A)	6224	6112	5026	17
H(16B)	4847	6408	4490	17
H(17A)	8756	6857	4577	12
H(19A)	4691	10471	3886	39
H(19B)	4787	10810	4567	39
H(19C)	3712	9983	4429	39
H(20A)	8307	10626	3916	39
H(20B)	9497	10089	4384	39
H(20C)	8301	10841	4626	39

H(22A)	9953	4663	3731	26
H(22B)	10487	5567	3552	26
H(22C)	10857	4853	3078	26
H(23A)	4691	5934	2867	20
H(23B)	4120	6301	3514	20
H(23C)	4123	5348	3415	20
H(24A)	7168	2308	4722	44
H(24B)	7439	3252	4829	44
H(24C)	5494	2918	4554	44
H(24D)	6279	2362	4735	44
H(24E)	8248	2770	4547	44
H(24F)	6573	3308	4821	44
H(25A)	7032	1678	3359	37
H(25B)	5288	2284	3284	37
H(25C)	7071	2347	2836	37
H(25D)	6018	1725	3352	37
H(25E)	6304	2403	2844	37
H(25F)	8041	2145	3269	37
H(26A)	10708	2265	4030	37
H(26B)	11011	3214	4099	37
H(26C)	11013	2811	3438	37
H(26D)	2819	2626	4045	31
H(26E)	2822	3219	3472	31
H(26F)	3057	3574	4145	31

Table 6a. Torsion angles [°] for svp25.

C(24)-Si(1)-O(5)-C(12)	-167.7(4)
C(26)-Si(1)-O(5)-C(12)	77.0(5)
C(25)-Si(1)-O(5)-C(12)	-50.0(4)
C(24)-Si(2)-O(5)-C(12)	176.7(3)
C(25)-Si(2)-O(5)-C(12)	57.0(4)
C(26B)-Si(2)-O(5)-C(12)	-67.7(5)
C(2)-O(1)-C(1)-O(2)	161.5(3)
C(2)-O(1)-C(1)-C(5)	-71.8(3)
C(1)-O(1)-C(2)-C(3)	62.2(4)
C(1)-O(1)-C(2)-C(18)	-172.8(3)
O(1)-C(2)-C(3)-C(4)	-47.5(4)
C(18)-C(2)-C(3)-C(4)	-166.4(3)
C(2)-C(3)-C(4)-C(5)	44.3(4)
C(3)-C(4)-C(5)-C(17)	71.6(4)
C(3)-C(4)-C(5)-C(1)	-48.2(4)
C(3)-C(4)-C(5)-C(6)	-165.9(3)
O(2)-C(1)-C(5)-C(17)	60.1(4)
O(1)-C(1)-C(5)-C(17)	-62.2(4)
O(2)-C(1)-C(5)-C(4)	-176.9(3)
O(1)-C(1)-C(5)-C(4)	60.8(4)
O(2)-C(1)-C(5)-C(6)	-54.3(4)
O(1)-C(1)-C(5)-C(6)	-176.6(3)
C(17)-C(5)-C(6)-C(7)	-176.4(3)
C(4)-C(5)-C(6)-C(7)	56.4(4)
C(1)-C(5)-C(6)-C(7)	-59.5(4)
C(17)-C(5)-C(6)-C(14)	50.7(4)
C(4)-C(5)-C(6)-C(14)	-76.5(4)
C(1)-C(5)-C(6)-C(14)	167.6(3)
C(5)-C(6)-C(7)-C(8)	165.6(3)
C(14)-C(6)-C(7)-C(8)	-58.6(4)
C(6)-C(7)-C(8)-C(9)	56.3(4)
C(7)-C(8)-C(9)-C(10)	-177.6(3)
C(7)-C(8)-C(9)-C(13)	-56.6(4)
C(8)-C(9)-C(10)-C(11)	152.2(3)

C(13)-C(9)-C(10)-C(11)	27.2(4)
C(9)-C(10)-C(11)-C(12)	2.5(4)
Si(1)-O(5)-C(12)-C(21)	97.4(4)
Si(2)-O(5)-C(12)-C(21)	35.9(4)
Si(1)-O(5)-C(12)-C(11)	-19.0(5)
Si(2)-O(5)-C(12)-C(11)	-80.6(4)
Si(1)-O(5)-C(12)-C(13)	-136.0(3)
Si(2)-O(5)-C(12)-C(13)	162.4(3)
C(10)-C(11)-C(12)-O(5)	-152.4(3)
C(10)-C(11)-C(12)-C(21)	89.6(4)
C(10)-C(11)-C(12)-C(13)	-30.7(4)
C(8)-C(9)-C(13)-C(22)	-64.5(4)
C(10)-C(9)-C(13)-C(22)	63.7(4)
C(8)-C(9)-C(13)-C(12)	-173.7(3)
C(10)-C(9)-C(13)-C(12)	-45.4(3)
C(8)-C(9)-C(13)-C(14)	58.8(4)
C(10)-C(9)-C(13)-C(14)	-172.9(3)
O(5)-C(12)-C(13)-C(9)	171.5(3)
C(21)-C(12)-C(13)-C(9)	-66.3(4)
C(11)-C(12)-C(13)-C(9)	46.4(3)
O(5)-C(12)-C(13)-C(22)	57.3(4)
C(21)-C(12)-C(13)-C(22)	179.5(3)
C(11)-C(12)-C(13)-C(22)	-67.8(3)
O(5)-C(12)-C(13)-C(14)	-67.6(4)
C(21)-C(12)-C(13)-C(14)	54.5(4)
C(11)-C(12)-C(13)-C(14)	167.3(3)
C(7)-C(6)-C(14)-C(15)	177.0(3)
C(5)-C(6)-C(14)-C(15)	-48.7(4)
C(7)-C(6)-C(14)-C(23)	-64.0(4)
C(5)-C(6)-C(14)-C(23)	70.2(4)
C(7)-C(6)-C(14)-C(13)	57.7(4)
C(5)-C(6)-C(14)-C(13)	-168.0(3)
C(9)-C(13)-C(14)-C(15)	-175.7(3)
C(22)-C(13)-C(14)-C(15)	-52.3(4)
C(12)-C(13)-C(14)-C(15)	69.6(4)
C(9)-C(13)-C(14)-C(23)	64.9(4)

C(22)-C(13)-C(14)-C(23)	-171.7(3)
C(12)-C(13)-C(14)-C(23)	-49.7(4)
C(9)-C(13)-C(14)-C(6)	-57.3(4)
C(22)-C(13)-C(14)-C(6)	66.1(4)
C(12)-C(13)-C(14)-C(6)	-172.0(3)
C(23)-C(14)-C(15)-C(16)	-70.8(4)
C(6)-C(14)-C(15)-C(16)	50.8(4)
C(13)-C(14)-C(15)-C(16)	167.7(3)
C(14)-C(15)-C(16)-C(17)	-59.3(4)
C(15)-C(16)-C(17)-O(3)	-170.1(3)
C(15)-C(16)-C(17)-C(5)	63.8(4)
C(4)-C(5)-C(17)-O(3)	-51.1(4)
C(1)-C(5)-C(17)-O(3)	65.8(4)
C(6)-C(5)-C(17)-O(3)	-178.6(3)
C(4)-C(5)-C(17)-C(16)	70.6(4)
C(1)-C(5)-C(17)-C(16)	-172.5(3)
C(6)-C(5)-C(17)-C(16)	-56.9(4)
O(1)-C(2)-C(18)-O(4)	-57.6(4)
C(3)-C(2)-C(18)-O(4)	63.5(4)
O(1)-C(2)-C(18)-C(20)	63.9(4)
C(3)-C(2)-C(18)-C(20)	-175.1(3)
O(1)-C(2)-C(18)-C(19)	-173.1(3)
C(3)-C(2)-C(18)-C(19)	-52.1(4)

Table 7a. Hydrogen bonds for svp25 [Å and °].

D-H...A	d(D-H)	d(H...A)	d(D...A)	<(DHA)
O(2)-H(2)...O(3)#1	0.81(4)	1.99(5)	2.787(4)	168(4)
O(3)-H(3)...O(1)	0.85(6)	2.01(6)	2.745(4)	145(5)
O(3)-H(3)...O(4)	0.85(6)	2.66(5)	3.355(4)	140(5)

Symmetry transformations used to generate equivalent atoms:

#1 x+1/2,-y+3/2,-z+1

Table 1b. Crystal data and structure refinement for S4.1.

Identification code	svp13 (Devon Schatz)
Empirical formula	$C_{16} H_{22} O_3$
Formula weight	262.33
Temperature	133(2) K
Wavelength	0.71073 Å
Crystal system	Triclinic
Space group	$P\bar{1}$
Unit cell dimensions	a = 12.1239(8) Å α = 87.3040(9)°.
	b = 13.1282(9) Å β = 75.4289(9)°.
	c = 14.4151(10) Å γ = 76.0963(9)°.
Volume	2155.3(3) Å^3
Z	6
Density (calculated)	1.213 Mg/m^3
Absorption coefficient	0.082 mm^{-1}
F(000)	852
Crystal color	colorless
Crystal size	0.410 x 0.276 x 0.230 mm^3
Theta range for data collection	1.598 to 28.299°
Index ranges	$-16 \leq h \leq 16, -17 \leq k \leq 17, -18 \leq l \leq 19$
Reflections collected	25547
Independent reflections	10157 [R(int) = 0.0273]
Completeness to theta = 25.500°	99.6 %
Absorption correction	Semi-empirical from equivalents
Max. and min. transmission	0.8621 and 0.8090
Refinement method	Full-matrix least-squares on F^2
Data / restraints / parameters	10157 / 0 / 564
Goodness-of-fit on F^2	1.023
Final R indices [I>2sigma(I) = 7437 data]	R1 = 0.0622, wR2 = 0.1582
R indices (all data, 0.75 Å)	R1 = 0.0882, wR2 = 0.1758
Largest diff. peak and hole	1.192 and -0.406 e.Å^{-3}

Table 2b. Atomic coordinates (x 10^4) and equivalent isotropic displacement parameters ($Å^2$ x 10^3) for svp13. U(eq) is defined as one third of the trace of the orthogonalized U^{ij} tensor.

	x	y	z	U(eq)
O(1)	9451(1)	2400(1)	1092(1)	23(1)
O(2)	9884(1)	3773(1)	240(1)	24(1)
O(3)	7494(1)	5928(1)	2123(1)	22(1)
C(1)	8337(2)	4111(1)	1689(1)	15(1)
C(2)	7178(2)	3760(1)	1917(1)	18(1)
C(3)	6503(2)	3941(2)	1125(1)	22(1)
C(4)	6353(2)	5093(2)	819(2)	26(1)
C(5)	7522(2)	5423(2)	520(1)	22(1)
C(6)	8163(2)	5244(1)	1316(1)	17(1)
C(7)	9270(2)	3352(1)	967(1)	17(1)
C(8)	8809(2)	4002(2)	2611(1)	19(1)
C(9)	9965(2)	4304(2)	2484(1)	20(1)
C(10)	9992(2)	5342(2)	2618(2)	30(1)
C(11)	11049(2)	5636(2)	2460(2)	37(1)
C(12)	12099(2)	4896(2)	2179(2)	33(1)
C(13)	12089(2)	3862(2)	2063(2)	32(1)
C(14)	11028(2)	3570(2)	2210(2)	26(1)
C(15)	7119(2)	3210(2)	253(2)	29(1)
C(16)	5296(2)	3716(2)	1552(2)	33(1)
O(4)	11422(1)	2348(1)	-982(1)	26(1)
O(5)	10904(2)	999(1)	-130(1)	31(1)
O(6)	13532(1)	397(1)	-3229(1)	28(1)
C(17)	12163(2)	589(1)	-1683(1)	21(1)
C(18)	11399(2)	-126(1)	-1882(1)	21(1)
C(19)	10444(2)	380(2)	-2410(2)	26(1)
C(20)	11014(2)	923(2)	-3313(2)	29(1)
C(21)	11698(2)	1687(2)	-3102(2)	31(1)
C(22)	12643(2)	1161(2)	-2600(1)	26(1)
C(23)	11460(2)	1404(2)	-907(1)	24(1)
C(24)	13176(2)	-105(2)	-1286(1)	23(1)
C(25)	14131(2)	413(2)	-1164(2)	35(1)

373

C(26)	13965(3)	1120(2)	-438(2)	43(1)
C(27)	14860(3)	1602(2)	-350(2)	50(1)
C(28)	15951(3)	1317(2)	-987(2)	56(1)
C(29)	16154(3)	588(3)	-1703(2)	59(1)
C(30)	15260(3)	142(2)	-1801(2)	48(1)
C(31)	9969(2)	-500(2)	-2714(2)	33(1)
C(32)	9417(2)	1161(2)	-1765(2)	36(1)
O(7)	4819(2)	9027(2)	4750(2)	24(1)
O(7B)	5844(3)	7642(3)	3569(2)	28(1)
O(8)	3491(2)	8565(1)	6097(1)	38(1)
O(9)	5776(1)	5924(1)	3797(1)	27(1)
C(33)	4566(2)	7200(2)	4977(1)	21(1)
C(34)	3471(2)	6766(2)	5063(1)	27(1)
C(35)	2708(2)	7212(2)	4361(2)	27(1)
C(36)	3446(3)	6984(2)	3325(2)	49(1)
C(37)	4662(3)	7441(3)	3198(2)	23(1)
C(37B)	3290(4)	8880(4)	4503(4)	29(1)
C(38)	5390(2)	6991(2)	3978(1)	22(1)
C(39)	4233(2)	8378(2)	5202(2)	38(1)
C(40)	5228(2)	6644(2)	5730(1)	24(1)
C(41)	6342(2)	6970(2)	5722(2)	26(1)
C(42)	6319(2)	7868(2)	6208(2)	37(1)
C(43)	7351(2)	8171(2)	6181(2)	46(1)
C(44)	8417(2)	7582(2)	5687(2)	40(1)
C(45)	8462(2)	6677(2)	5217(2)	38(1)
C(46)	7434(2)	6381(2)	5226(2)	33(1)
C(47)	1690(2)	6679(2)	4559(2)	42(1)
C(48)	2202(2)	8394(2)	4513(2)	34(1)

Table 3b. Bond lengths [Å] and angles [°] for svp13.

_____

O(1)-C(7)	1.228(2)
O(2)-C(7)	1.307(2)
O(3)-C(6)	1.446(2)
C(1)-C(7)	1.524(2)
C(1)-C(2)	1.536(2)
C(1)-C(6)	1.542(2)
C(1)-C(8)	1.562(2)
C(2)-C(3)	1.542(3)
C(3)-C(16)	1.531(3)
C(3)-C(15)	1.536(3)
C(3)-C(4)	1.537(3)
C(4)-C(5)	1.533(3)
C(5)-C(6)	1.521(3)
C(8)-C(9)	1.512(3)
C(9)-C(14)	1.389(3)
C(9)-C(10)	1.395(3)
C(10)-C(11)	1.386(3)
C(11)-C(12)	1.383(3)
C(12)-C(13)	1.378(3)
C(13)-C(14)	1.393(3)
O(4)-C(23)	1.231(2)
O(5)-C(23)	1.314(2)
O(6)-C(22)	1.436(3)
C(17)-C(23)	1.522(3)
C(17)-C(22)	1.543(3)
C(17)-C(18)	1.548(3)
C(17)-C(24)	1.560(3)
C(18)-C(19)	1.545(3)
C(19)-C(31)	1.534(3)
C(19)-C(32)	1.537(3)
C(19)-C(20)	1.543(3)
C(20)-C(21)	1.529(3)
C(21)-C(22)	1.518(3)
C(24)-C(25)	1.526(3)

C(25)-C(26)	1.375(3)
C(25)-C(30)	1.417(4)
C(26)-C(27)	1.415(4)
C(27)-C(28)	1.384(5)
C(28)-C(29)	1.376(4)
C(29)-C(30)	1.388(4)
O(7)-C(39)	1.289(3)
O(7B)-C(38)	1.182(4)
O(8)-C(39)	1.369(3)
O(9)-C(38)	1.381(2)
C(33)-C(38)	1.525(3)
C(33)-C(39)	1.530(3)
C(33)-C(34)	1.542(3)
C(33)-C(40)	1.562(3)
C(34)-C(35)	1.542(3)
C(35)-C(47)	1.521(3)
C(35)-C(48)	1.530(3)
C(35)-C(36)	1.537(3)
C(36)-C(37)	1.687(5)
C(37)-C(38)	1.606(4)
C(37B)-C(48)	1.595(5)
C(37B)-C(39)	1.706(6)
C(40)-C(41)	1.510(3)
C(41)-C(42)	1.390(3)
C(41)-C(46)	1.394(3)
C(42)-C(43)	1.392(3)
C(43)-C(44)	1.372(4)
C(44)-C(45)	1.378(4)
C(45)-C(46)	1.388(3)
C(7)-C(1)-C(2)	109.80(14)
C(7)-C(1)-C(6)	111.24(14)
C(2)-C(1)-C(6)	110.73(14)
C(7)-C(1)-C(8)	104.49(14)
C(2)-C(1)-C(8)	108.73(14)
C(6)-C(1)-C(8)	111.65(14)

C(1)-C(2)-C(3)	116.03(15)
C(16)-C(3)-C(15)	108.06(17)
C(16)-C(3)-C(4)	109.53(17)
C(15)-C(3)-C(4)	110.18(17)
C(16)-C(3)-C(2)	107.67(16)
C(15)-C(3)-C(2)	112.61(17)
C(4)-C(3)-C(2)	108.72(16)
C(5)-C(4)-C(3)	112.65(16)
C(6)-C(5)-C(4)	111.61(16)
O(3)-C(6)-C(5)	109.53(15)
O(3)-C(6)-C(1)	106.96(14)
C(5)-C(6)-C(1)	113.09(15)
O(1)-C(7)-O(2)	122.76(16)
O(1)-C(7)-C(1)	120.87(16)
O(2)-C(7)-C(1)	116.32(15)
C(9)-C(8)-C(1)	114.44(14)
C(14)-C(9)-C(10)	117.97(18)
C(14)-C(9)-C(8)	121.45(17)
C(10)-C(9)-C(8)	120.56(17)
C(11)-C(10)-C(9)	120.9(2)
C(12)-C(11)-C(10)	120.3(2)
C(13)-C(12)-C(11)	119.5(2)
C(12)-C(13)-C(14)	120.2(2)
C(9)-C(14)-C(13)	121.02(19)
C(23)-C(17)-C(22)	108.78(15)
C(23)-C(17)-C(18)	110.98(16)
C(22)-C(17)-C(18)	110.85(16)
C(23)-C(17)-C(24)	106.53(16)
C(22)-C(17)-C(24)	111.42(17)
C(18)-C(17)-C(24)	108.20(15)
C(19)-C(18)-C(17)	116.48(16)
C(31)-C(19)-C(32)	108.32(19)
C(31)-C(19)-C(20)	109.09(18)
C(32)-C(19)-C(20)	110.89(17)
C(31)-C(19)-C(18)	107.90(16)
C(32)-C(19)-C(18)	112.04(18)

377

C(20)-C(19)-C(18)	108.52(17)
C(21)-C(20)-C(19)	113.20(17)
C(22)-C(21)-C(20)	112.28(17)
O(6)-C(22)-C(21)	110.06(16)
O(6)-C(22)-C(17)	107.49(15)
C(21)-C(22)-C(17)	112.67(18)
O(4)-C(23)-O(5)	122.55(18)
O(4)-C(23)-C(17)	124.08(18)
O(5)-C(23)-C(17)	113.37(16)
C(25)-C(24)-C(17)	117.02(16)
C(26)-C(25)-C(30)	117.3(2)
C(26)-C(25)-C(24)	123.2(2)
C(30)-C(25)-C(24)	119.5(2)
C(25)-C(26)-C(27)	122.0(3)
C(28)-C(27)-C(26)	118.9(3)
C(29)-C(28)-C(27)	120.4(3)
C(28)-C(29)-C(30)	120.2(3)
C(29)-C(30)-C(25)	121.1(3)
C(38)-C(33)-C(39)	109.48(16)
C(38)-C(33)-C(34)	111.17(16)
C(39)-C(33)-C(34)	111.48(18)
C(38)-C(33)-C(40)	108.89(16)
C(39)-C(33)-C(40)	107.26(17)
C(34)-C(33)-C(40)	108.44(15)
C(33)-C(34)-C(35)	116.18(17)
C(47)-C(35)-C(48)	108.06(18)
C(47)-C(35)-C(36)	110.3(2)
C(48)-C(35)-C(36)	109.74(19)
C(47)-C(35)-C(34)	107.77(18)
C(48)-C(35)-C(34)	111.40(18)
C(36)-C(35)-C(34)	109.53(18)
C(35)-C(36)-C(37)	108.1(2)
C(38)-C(37)-C(36)	113.3(2)
C(48)-C(37B)-C(39)	121.0(3)
O(7B)-C(38)-O(9)	125.6(2)
O(7B)-C(38)-C(33)	121.3(2)

378

O(9)-C(38)-C(33)	110.12(16)
O(9)-C(38)-C(37)	105.42(19)
C(33)-C(38)-C(37)	108.77(18)
O(7)-C(39)-O(8)	124.1(2)
O(7)-C(39)-C(33)	123.5(2)
O(8)-C(39)-C(33)	109.47(18)
O(8)-C(39)-C(37B)	100.7(2)
C(33)-C(39)-C(37B)	103.6(2)
C(41)-C(40)-C(33)	114.90(16)
C(42)-C(41)-C(46)	117.5(2)
C(42)-C(41)-C(40)	121.29(19)
C(46)-C(41)-C(40)	121.2(2)
C(41)-C(42)-C(43)	120.8(2)
C(44)-C(43)-C(42)	120.8(2)
C(43)-C(44)-C(45)	119.3(2)
C(44)-C(45)-C(46)	120.1(2)
C(45)-C(46)-C(41)	121.4(2)
C(35)-C(48)-C(37B)	105.6(2)

Table 4b. Anisotropic displacement parameters ($Å^2$ x 10^3) for svp13. The anisotropic displacement factor exponent takes the form: $-2\pi^2[\, h^2\, a^{*2}U^{11} + ... + 2\, h\, k\, a^*\, b^*\, U^{12}\,]$

	U^{11}	U^{22}	U^{33}	U^{23}	U^{13}	U^{12}
O(1)	29(1)	16(1)	21(1)	-1(1)	0(1)	-3(1)
O(2)	27(1)	18(1)	20(1)	-2(1)	6(1)	-5(1)
O(3)	22(1)	17(1)	21(1)	-5(1)	1(1)	-2(1)
C(1)	16(1)	16(1)	13(1)	0(1)	-1(1)	-4(1)
C(2)	18(1)	20(1)	16(1)	1(1)	-2(1)	-7(1)
C(3)	21(1)	28(1)	21(1)	1(1)	-6(1)	-10(1)
C(4)	24(1)	30(1)	25(1)	4(1)	-10(1)	-6(1)
C(5)	26(1)	20(1)	21(1)	3(1)	-6(1)	-5(1)
C(6)	17(1)	16(1)	15(1)	-1(1)	1(1)	-4(1)
C(7)	18(1)	18(1)	14(1)	-2(1)	-2(1)	-5(1)
C(8)	19(1)	21(1)	14(1)	0(1)	-1(1)	-4(1)
C(9)	22(1)	26(1)	14(1)	1(1)	-6(1)	-6(1)
C(10)	27(1)	27(1)	39(1)	-8(1)	-15(1)	-3(1)
C(11)	38(1)	31(1)	50(2)	-2(1)	-23(1)	-13(1)
C(12)	28(1)	46(1)	33(1)	4(1)	-14(1)	-16(1)
C(13)	22(1)	40(1)	31(1)	-3(1)	-7(1)	-3(1)
C(14)	23(1)	27(1)	27(1)	-2(1)	-7(1)	-4(1)
C(15)	36(1)	33(1)	24(1)	-2(1)	-9(1)	-15(1)
C(16)	25(1)	47(1)	33(1)	7(1)	-11(1)	-17(1)
O(4)	37(1)	15(1)	22(1)	-4(1)	-2(1)	-3(1)
O(5)	48(1)	18(1)	19(1)	-2(1)	3(1)	-2(1)
O(6)	34(1)	34(1)	18(1)	-5(1)	2(1)	-19(1)
C(17)	32(1)	13(1)	17(1)	-2(1)	-2(1)	-4(1)
C(18)	26(1)	14(1)	20(1)	-1(1)	-2(1)	-4(1)
C(19)	30(1)	21(1)	26(1)	3(1)	-7(1)	-2(1)
C(20)	37(1)	24(1)	25(1)	3(1)	-10(1)	-6(1)
C(21)	53(1)	19(1)	23(1)	4(1)	-10(1)	-10(1)
C(22)	46(1)	17(1)	17(1)	-1(1)	-6(1)	-14(1)
C(23)	34(1)	16(1)	18(1)	-1(1)	-5(1)	-2(1)
C(24)	31(1)	16(1)	21(1)	-1(1)	-5(1)	-7(1)
C(25)	56(2)	27(1)	34(1)	11(1)	-24(1)	-19(1)

C(26)	51(2)	38(1)	41(1)	-6(1)	-20(1)	-4(1)
C(27)	58(2)	36(1)	68(2)	0(1)	-35(2)	-13(1)
C(28)	80(2)	60(2)	49(2)	12(1)	-30(2)	-44(2)
C(29)	61(2)	90(2)	38(2)	-1(2)	-7(1)	-46(2)
C(30)	50(2)	67(2)	33(1)	-7(1)	-4(1)	-32(1)
C(31)	35(1)	32(1)	38(1)	7(1)	-16(1)	-11(1)
C(32)	33(1)	34(1)	36(1)	6(1)	-7(1)	2(1)
O(7)	23(1)	20(1)	22(1)	-2(1)	3(1)	0(1)
O(7B)	29(2)	27(2)	24(2)	-1(1)	5(1)	-11(1)
O(8)	47(1)	34(1)	24(1)	-14(1)	-5(1)	7(1)
O(9)	26(1)	24(1)	23(1)	-7(1)	6(1)	-2(1)
C(33)	22(1)	20(1)	16(1)	-1(1)	0(1)	-1(1)
C(34)	19(1)	37(1)	19(1)	4(1)	2(1)	-6(1)
C(35)	24(1)	32(1)	23(1)	-1(1)	-4(1)	-3(1)
C(36)	74(2)	37(1)	21(1)	-2(1)	-3(1)	8(1)
C(37)	24(2)	26(2)	12(2)	-1(1)	4(1)	0(1)
C(37B)	31(2)	21(2)	35(3)	-1(2)	-6(2)	-8(2)
C(38)	20(1)	20(1)	23(1)	-4(1)	3(1)	-4(1)
C(39)	59(2)	22(1)	17(1)	-3(1)	6(1)	4(1)
C(40)	27(1)	24(1)	19(1)	2(1)	-4(1)	-6(1)
C(41)	28(1)	28(1)	23(1)	7(1)	-7(1)	-8(1)
C(42)	31(1)	39(1)	40(1)	-5(1)	-3(1)	-11(1)
C(43)	42(1)	45(2)	55(2)	-5(1)	-9(1)	-21(1)
C(44)	32(1)	54(2)	39(1)	15(1)	-14(1)	-20(1)
C(45)	26(1)	52(2)	34(1)	11(1)	-9(1)	-4(1)
C(46)	30(1)	35(1)	32(1)	6(1)	-12(1)	-2(1)
C(47)	41(1)	47(1)	47(2)	5(1)	-21(1)	-17(1)
C(48)	25(1)	36(1)	36(1)	-5(1)	-1(1)	-3(1)

Table 5b. Hydrogen coordinates (x 10⁴) and isotropic displacement parameters (Å² x 10³) for svp13.

	x	y	z	U(eq)
H(2)	10470(30)	3230(30)	-170(20)	63(9)
H(3)	7510(20)	6550(20)	1970(20)	43(8)
H(2A)	6658	4136	2505	22
H(2B)	7346	3002	2061	22
H(4A)	5977	5200	276	31
H(4B)	5826	5549	1358	31
H(5A)	8023	5016	-58	27
H(5B)	7372	6176	353	27
H(6A)	8947	5412	1074	20
H(8A)	8217	4447	3127	22
H(8B)	8903	3264	2824	22
H(10A)	9277	5856	2821	36
H(11A)	11051	6348	2544	44
H(12A)	12822	5099	2066	40
H(13A)	12808	3348	1884	38
H(14A)	11032	2856	2120	31
H(15A)	6625	3312	-203	44
H(15B)	7252	2479	462	44
H(15C)	7873	3373	-58	44
H(16A)	4887	4173	2113	50
H(16B)	5392	2981	1745	50
H(16C)	4835	3851	1070	50
H(5)	10470(30)	1500(20)	290(20)	46(8)
H(6)	13930(30)	700(30)	-3620(20)	58(10)
H(18A)	11925	-740	-2265	25
H(18B)	11012	-390	-1261	25
H(20A)	11553	381	-3776	34
H(20B)	10394	1310	-3619	34
H(21A)	12064	1987	-3711	38
H(21B)	11146	2271	-2693	38

H(22A)	13010	1707	-2426	31
H(24A)	12824	-374	-655	27
H(24B)	13554	-720	-1722	27
H(26A)	13228	1290	17	51
H(27A)	14715	2114	139	60
H(28A)	16564	1626	-930	67
H(29A)	16908	389	-2132	71
H(30A)	15407	-353	-2304	57
H(31A)	9420	-209	-3108	50
H(31B)	9563	-820	-2142	50
H(31C)	10622	-1034	-3086	50
H(32A)	9687	1767	-1619	54
H(32B)	9119	818	-1167	54
H(32C)	8789	1396	-2097	54
H(8)	3490(30)	9180(30)	6270(20)	61(10)
H(9)	6230(30)	5860(20)	3280(20)	52(9)
H(34A)	2974	6904	5725	32
H(34B)	3729	5995	4968	32
H(36A)	2990	7336	2870	59
H(36B)	3665	6219	3190	59
H(37A)	5176	7250	2549	28
H(37B)	4433	8216	3250	28
H(37C)	2972	9633	4676	35
H(37D)	3764	8845	3832	35
H(38A)	6030(30)	7300(20)	3890(20)	27
H(40A)	4692	6788	6377	28
H(40B)	5422	5876	5614	28
H(42A)	5591	8279	6563	44
H(43A)	7317	8794	6508	55
H(44A)	9117	7796	5669	48
H(45A)	9197	6255	4887	46
H(46A)	7475	5764	4888	39
H(47A)	1268	6777	5236	63
H(47B)	1990	5928	4410	63
H(47C)	1154	6990	4158	63
H(48A)	2844	8754	4389	51

H(48B)	1702	8650	4072	51
H(48C)	1735	8536	5175	51

Table 6b. Torsion angles [°] for svp13.

C(7)-C(1)-C(2)-C(3)	-73.4(2)
C(6)-C(1)-C(2)-C(3)	49.8(2)
C(8)-C(1)-C(2)-C(3)	172.83(15)
C(1)-C(2)-C(3)-C(16)	-170.61(16)
C(1)-C(2)-C(3)-C(15)	70.4(2)
C(1)-C(2)-C(3)-C(4)	-52.0(2)
C(16)-C(3)-C(4)-C(5)	171.72(17)
C(15)-C(3)-C(4)-C(5)	-69.5(2)
C(2)-C(3)-C(4)-C(5)	54.3(2)
C(3)-C(4)-C(5)-C(6)	-57.0(2)
C(4)-C(5)-C(6)-O(3)	-65.4(2)
C(4)-C(5)-C(6)-C(1)	53.8(2)
C(7)-C(1)-C(6)-O(3)	-166.30(14)
C(2)-C(1)-C(6)-O(3)	71.31(18)
C(8)-C(1)-C(6)-O(3)	-50.00(18)
C(7)-C(1)-C(6)-C(5)	73.05(19)
C(2)-C(1)-C(6)-C(5)	-49.34(19)
C(8)-C(1)-C(6)-C(5)	-170.66(15)
C(2)-C(1)-C(7)-O(1)	-49.8(2)
C(6)-C(1)-C(7)-O(1)	-172.76(17)
C(8)-C(1)-C(7)-O(1)	66.6(2)
C(2)-C(1)-C(7)-O(2)	132.68(17)
C(6)-C(1)-C(7)-O(2)	9.8(2)
C(8)-C(1)-C(7)-O(2)	-110.86(17)
C(7)-C(1)-C(8)-C(9)	61.75(19)
C(2)-C(1)-C(8)-C(9)	178.95(15)
C(6)-C(1)-C(8)-C(9)	-58.6(2)
C(1)-C(8)-C(9)-C(14)	-90.7(2)
C(1)-C(8)-C(9)-C(10)	87.6(2)
C(14)-C(9)-C(10)-C(11)	1.5(3)
C(8)-C(9)-C(10)-C(11)	-176.9(2)
C(9)-C(10)-C(11)-C(12)	-1.0(4)
C(10)-C(11)-C(12)-C(13)	-0.4(4)
C(11)-C(12)-C(13)-C(14)	1.3(3)

C(10)-C(9)-C(14)-C(13)	-0.5(3)
C(8)-C(9)-C(14)-C(13)	177.83(19)
C(12)-C(13)-C(14)-C(9)	-0.8(3)
C(23)-C(17)-C(18)-C(19)	71.6(2)
C(22)-C(17)-C(18)-C(19)	-49.4(2)
C(24)-C(17)-C(18)-C(19)	-171.85(16)
C(17)-C(18)-C(19)-C(31)	168.61(17)
C(17)-C(18)-C(19)-C(32)	-72.2(2)
C(17)-C(18)-C(19)-C(20)	50.5(2)
C(31)-C(19)-C(20)-C(21)	-170.21(18)
C(32)-C(19)-C(20)-C(21)	70.6(2)
C(18)-C(19)-C(20)-C(21)	-52.9(2)
C(19)-C(20)-C(21)-C(22)	56.7(2)
C(20)-C(21)-C(22)-O(6)	66.0(2)
C(20)-C(21)-C(22)-C(17)	-54.0(2)
C(23)-C(17)-C(22)-O(6)	165.55(16)
C(18)-C(17)-C(22)-O(6)	-72.2(2)
C(24)-C(17)-C(22)-O(6)	48.4(2)
C(23)-C(17)-C(22)-C(21)	-73.0(2)
C(18)-C(17)-C(22)-C(21)	49.3(2)
C(24)-C(17)-C(22)-C(21)	169.83(16)
C(22)-C(17)-C(23)-O(4)	-8.3(3)
C(18)-C(17)-C(23)-O(4)	-130.5(2)
C(24)-C(17)-C(23)-O(4)	111.9(2)
C(22)-C(17)-C(23)-O(5)	172.83(18)
C(18)-C(17)-C(23)-O(5)	50.6(2)
C(24)-C(17)-C(23)-O(5)	-67.0(2)
C(23)-C(17)-C(24)-C(25)	-68.4(2)
C(22)-C(17)-C(24)-C(25)	50.1(2)
C(18)-C(17)-C(24)-C(25)	172.24(17)
C(17)-C(24)-C(25)-C(26)	74.2(3)
C(17)-C(24)-C(25)-C(30)	-107.8(2)
C(30)-C(25)-C(26)-C(27)	3.0(4)
C(24)-C(25)-C(26)-C(27)	-179.0(2)
C(25)-C(26)-C(27)-C(28)	-3.0(4)
C(26)-C(27)-C(28)-C(29)	1.0(4)

C(27)-C(28)-C(29)-C(30)	0.9(5)
C(28)-C(29)-C(30)-C(25)	-0.9(5)
C(26)-C(25)-C(30)-C(29)	-1.0(4)
C(24)-C(25)-C(30)-C(29)	-179.1(3)
C(38)-C(33)-C(34)-C(35)	-59.4(2)
C(39)-C(33)-C(34)-C(35)	63.0(2)
C(40)-C(33)-C(34)-C(35)	-179.10(17)
C(33)-C(34)-C(35)-C(47)	179.56(18)
C(33)-C(34)-C(35)-C(48)	-62.1(2)
C(33)-C(34)-C(35)-C(36)	59.5(2)
C(47)-C(35)-C(36)-C(37)	-171.9(2)
C(48)-C(35)-C(36)-C(37)	69.2(2)
C(34)-C(35)-C(36)-C(37)	-53.4(3)
C(35)-C(36)-C(37)-C(38)	54.2(3)
C(39)-C(33)-C(38)-O(7B)	13.4(4)
C(34)-C(33)-C(38)-O(7B)	137.0(3)
C(40)-C(33)-C(38)-O(7B)	-103.6(3)
C(39)-C(33)-C(38)-O(9)	174.96(18)
C(34)-C(33)-C(38)-O(9)	-61.4(2)
C(40)-C(33)-C(38)-O(9)	58.0(2)
C(39)-C(33)-C(38)-C(37)	-70.0(2)
C(34)-C(33)-C(38)-C(37)	53.6(2)
C(40)-C(33)-C(38)-C(37)	173.04(19)
C(36)-C(37)-C(38)-O(9)	64.5(3)
C(36)-C(37)-C(38)-C(33)	-53.6(3)
C(38)-C(33)-C(39)-O(7)	-18.6(3)
C(34)-C(33)-C(39)-O(7)	-142.1(3)
C(40)-C(33)-C(39)-O(7)	99.4(3)
C(38)-C(33)-C(39)-O(8)	179.84(19)
C(34)-C(33)-C(39)-O(8)	56.4(3)
C(40)-C(33)-C(39)-O(8)	-62.2(2)
C(38)-C(33)-C(39)-C(37B)	73.1(3)
C(34)-C(33)-C(39)-C(37B)	-50.3(3)
C(40)-C(33)-C(39)-C(37B)	-168.9(2)
C(48)-C(37B)-C(39)-O(8)	-62.6(4)
C(48)-C(37B)-C(39)-C(33)	50.7(4)

C(38)-C(33)-C(40)-C(41)	57.7(2)
C(39)-C(33)-C(40)-C(41)	-60.7(2)
C(34)-C(33)-C(40)-C(41)	178.78(16)
C(33)-C(40)-C(41)-C(42)	83.3(2)
C(33)-C(40)-C(41)-C(46)	-96.7(2)
C(46)-C(41)-C(42)-C(43)	1.3(4)
C(40)-C(41)-C(42)-C(43)	-178.8(2)
C(41)-C(42)-C(43)-C(44)	-1.1(4)
C(42)-C(43)-C(44)-C(45)	-0.3(4)
C(43)-C(44)-C(45)-C(46)	1.5(4)
C(44)-C(45)-C(46)-C(41)	-1.4(3)
C(42)-C(41)-C(46)-C(45)	0.0(3)
C(40)-C(41)-C(46)-C(45)	-179.9(2)
C(47)-C(35)-C(48)-C(37B)	169.0(2)
C(36)-C(35)-C(48)-C(37B)	-70.7(3)
C(34)-C(35)-C(48)-C(37B)	50.8(3)
C(39)-C(37B)-C(48)-C(35)	-50.6(4)

Table 7b. Hydrogen bonds for svp13 [Å and °].

D-H...A	d(D-H)	d(H...A)	d(D...A)	<(DHA)
O(2)-H(2)...O(4)	0.97(3)	1.69(3)	2.6568(19)	174(3)
O(3)-H(3)...O(4)#1	0.84(3)	2.36(3)	3.090(2)	146(2)
C(6)-H(6A)...O(2)#1	1.00	2.43	3.290(2)	143.2
O(5)-H(5)...O(1)	0.89(3)	1.72(3)	2.603(2)	171(3)
O(6)-H(6)...O(7)#1	0.80(3)	2.01(3)	2.782(3)	161(3)
O(6)-H(6)...O(7B)#1	0.80(3)	2.27(3)	2.841(4)	129(3)
O(8)-H(8)...O(6)#2	0.85(3)	1.81(3)	2.652(2)	173(3)
O(9)-H(9)...O(3)	0.80(3)	1.98(3)	2.763(2)	167(3)

Symmetry transformations used to generate equivalent atoms:

#1 -x+2,-y+1,-z   #2 x-1,y+1,z+1

Table 1c. Crystal data and structure refinement for S4.4.

Identification code	svp16 (Devon Schatz)
Empirical formula	C27 H46 Cl2 O4
Formula weight	505.54
Temperature	88(2) K
Wavelength	0.71073 Å
Crystal system	Monoclinic
Space group	$P2_1/n$
Unit cell dimensions	a = 6.1836(4) Å $\quad$ $\alpha = 90°$.
	b = 31.5163(19) Å $\quad$ $\beta = 97.1381(8)°$.
	c = 15.3756(9) Å $\quad$ $\gamma = 90°$.
Volume	2973.2(3) Å^3
Z	4
Density (calculated)	1.129 Mg/m^3
Absorption coefficient	0.246 mm^{-1}
F(000)	1096
Crystal color	colorless
Crystal size	0.254 x 0.198 x 0.152 mm^3
Theta range for data collection	1.292 to 26.372°
Index ranges	$-7 \leq h \leq 7, -39 \leq k \leq 39, -19 \leq l \leq 19$
Reflections collected	28304
Independent reflections	6077 [R(int) = 0.0468]
Completeness to theta = 25.500°	100.0 %
Absorption correction	Semi-empirical from equivalents
Max. and min. transmission	0.8620 and 0.8096
Refinement method	Full-matrix least-squares on F^2
Data / restraints / parameters	6077 / 2 / 310
Goodness-of-fit on F^2	1.062
Final R indices [I>2sigma(I) = 4755 data]	R1 = 0.0621, wR2 = 0.1346
R indices (all data, 0.80 Å)	R1 = 0.0828, wR2 = 0.1438
Largest diff. peak and hole	0.867 and -0.722 e.Å^{-3}

Table 2c. Atomic coordinates (x 10⁴) and equivalent isotropic displacement parameters (Å² x 10³) for svp16. U(eq) is defined as one third of the trace of the orthogonalized U^{ij} tensor.

	x	y	z	U(eq)
O(1)	7104(3)	2889(1)	2573(1)	14(1)
O(2)	7607(3)	2921(1)	5221(1)	21(1)
O(3)	7506(3)	2554(1)	3936(1)	14(1)
O(4)	6291(3)	2415(1)	1133(1)	19(1)
C(1)	7984(4)	3278(1)	2961(2)	13(1)
C(2)	7381(4)	3656(1)	2369(2)	16(1)
C(3)	8616(4)	4041(1)	2783(2)	16(1)
C(4)	8470(5)	4435(1)	2199(2)	21(1)
C(5)	10024(5)	4778(1)	2606(2)	23(1)
C(6)	9640(5)	4882(1)	3549(2)	23(1)
C(7)	9631(4)	4482(1)	4118(2)	20(1)
C(8)	8020(4)	4141(1)	3715(2)	16(1)
C(9)	8349(4)	3736(1)	4283(2)	15(1)
C(10)	7284(4)	3327(1)	3882(2)	12(1)
C(11)	8267(4)	2939(1)	4392(2)	15(1)
C(12)	8033(4)	2538(1)	3071(2)	13(1)
C(13)	7162(4)	2124(1)	2638(2)	14(1)
C(14)	8494(4)	1759(1)	3132(2)	14(1)
C(15)	8367(4)	1317(1)	2696(2)	16(1)
C(16)	10127(4)	1030(1)	3187(2)	21(1)
C(17)	10323(5)	599(1)	2733(2)	26(1)
C(18)	10625(4)	646(1)	1764(2)	26(1)
C(19)	8940(5)	942(1)	1274(2)	22(1)
C(20)	8910(4)	1368(1)	1746(2)	17(1)
C(21)	7443(4)	1696(1)	1240(2)	18(1)
C(22)	7685(4)	2129(1)	1679(2)	16(1)
C(23)	5688(4)	4312(1)	3695(2)	21(1)
C(24)	4785(4)	3308(1)	3862(2)	17(1)
C(25)	4691(4)	2098(1)	2680(2)	16(1)
C(26)	6118(4)	1114(1)	2736(2)	21(1)
C(27)	9755(5)	7003(1)	-376(2)	26(1)

Cl(1)	8006(1)	6887(1)	-1345(1)	38(1)
Cl(2)	11307(2)	6563(1)	28(1)	55(1)

Table 3c. Bond lengths [Å] and angles [°] for svp16.

_____

O(1)-C(12)	1.426(3)
O(1)-C(1)	1.440(3)
O(2)-C(11)	1.386(3)
O(3)-C(12)	1.410(3)
O(3)-C(11)	1.449(3)
O(4)-C(22)	1.443(3)
C(1)-C(2)	1.516(3)
C(1)-C(10)	1.540(3)
C(2)-C(3)	1.529(3)
C(3)-C(4)	1.530(3)
C(3)-C(8)	1.556(3)
C(4)-C(5)	1.527(4)
C(5)-C(6)	1.534(4)
C(6)-C(7)	1.535(4)
C(7)-C(8)	1.541(4)
C(8)-C(23)	1.536(4)
C(8)-C(9)	1.547(3)
C(9)-C(10)	1.541(3)
C(10)-C(11)	1.537(3)
C(10)-C(24)	1.542(3)
C(12)-C(13)	1.531(3)
C(13)-C(25)	1.539(3)
C(13)-C(22)	1.549(3)
C(13)-C(14)	1.557(3)
C(14)-C(15)	1.543(3)
C(15)-C(16)	1.540(3)
C(15)-C(26)	1.540(4)
C(15)-C(20)	1.546(4)
C(16)-C(17)	1.538(4)
C(17)-C(18)	1.531(4)
C(18)-C(19)	1.526(4)
C(19)-C(20)	1.530(3)
C(20)-C(21)	1.523(4)
C(21)-C(22)	1.522(3)

C(27)-Cl(2)	1.757(3)
C(27)-Cl(1)	1.767(3)
C(12)-O(1)-C(1)	109.45(17)
C(12)-O(3)-C(11)	112.82(18)
O(1)-C(1)-C(2)	111.59(19)
O(1)-C(1)-C(10)	109.28(19)
C(2)-C(1)-C(10)	113.4(2)
C(1)-C(2)-C(3)	107.5(2)
C(2)-C(3)-C(4)	114.2(2)
C(2)-C(3)-C(8)	112.5(2)
C(4)-C(3)-C(8)	111.9(2)
C(5)-C(4)-C(3)	110.2(2)
C(4)-C(5)-C(6)	112.1(2)
C(5)-C(6)-C(7)	111.9(2)
C(6)-C(7)-C(8)	113.0(2)
C(23)-C(8)-C(7)	108.8(2)
C(23)-C(8)-C(9)	111.0(2)
C(7)-C(8)-C(9)	108.4(2)
C(23)-C(8)-C(3)	112.4(2)
C(7)-C(8)-C(3)	107.3(2)
C(9)-C(8)-C(3)	108.77(19)
C(10)-C(9)-C(8)	116.5(2)
C(11)-C(10)-C(1)	104.59(19)
C(11)-C(10)-C(9)	109.83(19)
C(1)-C(10)-C(9)	107.21(19)
C(11)-C(10)-C(24)	108.1(2)
C(1)-C(10)-C(24)	111.9(2)
C(9)-C(10)-C(24)	114.7(2)
O(2)-C(11)-O(3)	107.24(19)
O(2)-C(11)-C(10)	111.0(2)
O(3)-C(11)-C(10)	109.54(18)
O(3)-C(12)-O(1)	110.68(19)
O(3)-C(12)-C(13)	109.28(19)
O(1)-C(12)-C(13)	109.41(18)
C(12)-C(13)-C(25)	108.95(19)

394

C(12)-C(13)-C(22)	107.51(19)
C(25)-C(13)-C(22)	111.5(2)
C(12)-C(13)-C(14)	106.36(19)
C(25)-C(13)-C(14)	114.1(2)
C(22)-C(13)-C(14)	108.12(19)
C(15)-C(14)-C(13)	117.4(2)
C(16)-C(15)-C(26)	108.7(2)
C(16)-C(15)-C(14)	108.8(2)
C(26)-C(15)-C(14)	110.8(2)
C(16)-C(15)-C(20)	107.5(2)
C(26)-C(15)-C(20)	112.7(2)
C(14)-C(15)-C(20)	108.1(2)
C(17)-C(16)-C(15)	112.8(2)
C(18)-C(17)-C(16)	112.5(2)
C(19)-C(18)-C(17)	112.4(2)
C(18)-C(19)-C(20)	110.5(2)
C(21)-C(20)-C(19)	113.2(2)
C(21)-C(20)-C(15)	111.6(2)
C(19)-C(20)-C(15)	111.9(2)
C(22)-C(21)-C(20)	111.2(2)
O(4)-C(22)-C(21)	106.50(19)
O(4)-C(22)-C(13)	112.3(2)
C(21)-C(22)-C(13)	113.1(2)
Cl(2)-C(27)-Cl(1)	112.64(17)

_____

Table 4c. Anisotropic displacement parameters ($Å^2$ x 10^3) for svp16. The anisotropic displacement factor exponent takes the form: $-2\pi^2[h^2 a^{*2}U^{11} + ... + 2 h k a^* b^* U^{12}]$

	U^{11}	U^{22}	U^{33}	U^{23}	U^{13}	U^{12}
O(1)	16(1)	12(1)	12(1)	-1(1)	-2(1)	-1(1)
O(2)	27(1)	22(1)	15(1)	0(1)	2(1)	0(1)
O(3)	18(1)	12(1)	10(1)	-1(1)	1(1)	0(1)
O(4)	28(1)	16(1)	13(1)	-2(1)	-2(1)	0(1)
C(1)	15(1)	11(1)	12(1)	-3(1)	0(1)	-1(1)
C(2)	20(1)	16(1)	12(1)	0(1)	1(1)	0(1)
C(3)	18(1)	13(1)	16(1)	-1(1)	2(1)	-1(1)
C(4)	28(2)	16(1)	20(1)	3(1)	4(1)	-1(1)
C(5)	24(2)	16(1)	30(2)	3(1)	5(1)	-2(1)
C(6)	25(2)	15(1)	30(2)	-3(1)	2(1)	-5(1)
C(7)	21(1)	16(1)	24(1)	-4(1)	2(1)	-2(1)
C(8)	16(1)	14(1)	18(1)	-1(1)	4(1)	1(1)
C(9)	17(1)	15(1)	15(1)	-2(1)	3(1)	0(1)
C(10)	14(1)	12(1)	12(1)	-1(1)	2(1)	0(1)
C(11)	16(1)	16(1)	11(1)	-2(1)	0(1)	-2(1)
C(12)	13(1)	13(1)	13(1)	0(1)	-1(1)	1(1)
C(13)	13(1)	13(1)	14(1)	-2(1)	-1(1)	1(1)
C(14)	15(1)	13(1)	14(1)	-2(1)	-1(1)	1(1)
C(15)	14(1)	13(1)	21(1)	-3(1)	0(1)	0(1)
C(16)	19(1)	16(1)	27(2)	-2(1)	-4(1)	3(1)
C(17)	22(2)	15(1)	40(2)	-4(1)	-3(1)	5(1)
C(18)	17(1)	18(1)	42(2)	-13(1)	2(1)	1(1)
C(19)	21(1)	18(1)	28(2)	-8(1)	4(1)	-1(1)
C(20)	13(1)	17(1)	20(1)	-6(1)	2(1)	-3(1)
C(21)	21(1)	19(1)	14(1)	-5(1)	2(1)	-2(1)
C(22)	19(1)	15(1)	13(1)	-2(1)	0(1)	-1(1)
C(23)	21(1)	17(1)	26(1)	-2(1)	6(1)	2(1)
C(24)	16(1)	17(1)	18(1)	0(1)	3(1)	0(1)
C(25)	14(1)	16(1)	19(1)	-3(1)	1(1)	-1(1)
C(26)	17(1)	16(1)	28(2)	1(1)	1(1)	-2(1)
C(27)	30(2)	28(2)	21(1)	4(1)	3(1)	4(1)

Cl(1)	35(1)	48(1)	31(1)	-9(1)	-5(1)	15(1)
Cl(2)	77(1)	66(1)	21(1)	3(1)	2(1)	48(1)

Table 5c. Hydrogen coordinates (x 10⁴) and isotropic displacement parameters (Å² x 10³) for svp16.

	x	y	z	U(eq)
H(2)	8670(40)	2799(10)	5530(20)	49(11)
H(4)	6320(60)	2647(5)	1417(18)	39(10)
H(1A)	9608	3252	3033	16
H(2A)	5790	3707	2315	20
H(2B)	7794	3602	1777	20
H(3A)	10189	3958	2867	19
H(4A)	8852	4359	1612	26
H(4B)	6958	4545	2126	26
H(5A)	9827	5038	2245	28
H(5B)	11545	4680	2604	28
H(6A)	8226	5030	3541	28
H(6B)	10799	5077	3812	28
H(7A)	9245	4562	4702	24
H(7B)	11118	4360	4202	24
H(9A)	9935	3685	4420	18
H(9B)	7772	3790	4845	18
H(11A)	9893	2952	4444	17
H(12A)	9654	2546	3084	16
H(14A)	10044	1846	3223	17
H(14B)	8005	1730	3718	17
H(16A)	11550	1177	3232	26
H(16B)	9773	981	3790	26
H(17A)	11580	442	3040	31
H(17B)	8992	430	2782	31
H(18A)	12103	757	1719	31
H(18B)	10510	362	1484	31
H(19A)	7479	809	1235	26
H(19B)	9295	987	671	26
H(20A)	10428	1483	1792	20
H(21A)	7824	1718	635	22

H(21B)	5907	1602	1205	22
H(22A)	9227	2225	1681	19
H(23A)	5316	4332	4294	32
H(23B)	4669	4119	3354	32
H(23C)	5591	4594	3422	32
H(24A)	4313	3011	3851	26
H(24B)	4092	3453	3336	26
H(24C)	4365	3447	4385	26
H(25A)	4053	2382	2603	24
H(25B)	4426	1985	3250	24
H(25C)	4020	1911	2213	24
H(26A)	5738	1135	3335	31
H(26B)	6166	814	2567	31
H(26C)	5020	1262	2333	31
H(27A)	10751	7236	-495	32
H(27B)	8871	7103	78	32

Table 6c. Torsion angles [°] for svp16.

_____

C(12)-O(1)-C(1)-C(2)	169.4(2)
C(12)-O(1)-C(1)-C(10)	-64.3(2)
O(1)-C(1)-C(2)-C(3)	-173.11(19)
C(10)-C(1)-C(2)-C(3)	62.9(3)
C(1)-C(2)-C(3)-C(4)	171.0(2)
C(1)-C(2)-C(3)-C(8)	-60.2(3)
C(2)-C(3)-C(4)-C(5)	-171.3(2)
C(8)-C(3)-C(4)-C(5)	59.5(3)
C(3)-C(4)-C(5)-C(6)	-54.4(3)
C(4)-C(5)-C(6)-C(7)	51.6(3)
C(5)-C(6)-C(7)-C(8)	-53.5(3)
C(6)-C(7)-C(8)-C(23)	-65.9(3)
C(6)-C(7)-C(8)-C(9)	173.3(2)
C(6)-C(7)-C(8)-C(3)	56.0(3)
C(2)-C(3)-C(8)-C(23)	-69.8(3)
C(4)-C(3)-C(8)-C(23)	60.3(3)
C(2)-C(3)-C(8)-C(7)	170.6(2)
C(4)-C(3)-C(8)-C(7)	-59.3(3)
C(2)-C(3)-C(8)-C(9)	53.6(3)
C(4)-C(3)-C(8)-C(9)	-176.4(2)
C(23)-C(8)-C(9)-C(10)	74.1(3)
C(7)-C(8)-C(9)-C(10)	-166.4(2)
C(3)-C(8)-C(9)-C(10)	-50.1(3)
O(1)-C(1)-C(10)-C(11)	60.9(2)
C(2)-C(1)-C(10)-C(11)	-173.9(2)
O(1)-C(1)-C(10)-C(9)	177.48(18)
C(2)-C(1)-C(10)-C(9)	-57.3(3)
O(1)-C(1)-C(10)-C(24)	-55.9(2)
C(2)-C(1)-C(10)-C(24)	69.3(3)
C(8)-C(9)-C(10)-C(11)	164.2(2)
C(8)-C(9)-C(10)-C(1)	51.1(3)
C(8)-C(9)-C(10)-C(24)	-73.8(3)
C(12)-O(3)-C(11)-O(2)	178.59(19)
C(12)-O(3)-C(11)-C(10)	58.1(2)

C(1)-C(10)-C(11)-O(2)	-174.87(19)
C(9)-C(10)-C(11)-O(2)	70.4(3)
C(24)-C(10)-C(11)-O(2)	-55.5(3)
C(1)-C(10)-C(11)-O(3)	-56.7(2)
C(9)-C(10)-C(11)-O(3)	-171.42(19)
C(24)-C(10)-C(11)-O(3)	62.7(2)
C(11)-O(3)-C(12)-O(1)	-59.2(2)
C(11)-O(3)-C(12)-C(13)	-179.73(19)
C(1)-O(1)-C(12)-O(3)	61.6(2)
C(1)-O(1)-C(12)-C(13)	-177.88(19)
O(3)-C(12)-C(13)-C(25)	56.6(2)
O(1)-C(12)-C(13)-C(25)	-64.7(2)
O(3)-C(12)-C(13)-C(22)	177.51(19)
O(1)-C(12)-C(13)-C(22)	56.2(2)
O(3)-C(12)-C(13)-C(14)	-66.9(2)
O(1)-C(12)-C(13)-C(14)	171.81(19)
C(12)-C(13)-C(14)-C(15)	-165.2(2)
C(25)-C(13)-C(14)-C(15)	74.6(3)
C(22)-C(13)-C(14)-C(15)	-50.0(3)
C(13)-C(14)-C(15)-C(16)	168.8(2)
C(13)-C(14)-C(15)-C(26)	-71.6(3)
C(13)-C(14)-C(15)-C(20)	52.3(3)
C(26)-C(15)-C(16)-C(17)	66.3(3)
C(14)-C(15)-C(16)-C(17)	-172.9(2)
C(20)-C(15)-C(16)-C(17)	-56.0(3)
C(15)-C(16)-C(17)-C(18)	52.6(3)
C(16)-C(17)-C(18)-C(19)	-50.0(3)
C(17)-C(18)-C(19)-C(20)	53.0(3)
C(18)-C(19)-C(20)-C(21)	173.7(2)
C(18)-C(19)-C(20)-C(15)	-59.1(3)
C(16)-C(15)-C(20)-C(21)	-172.2(2)
C(26)-C(15)-C(20)-C(21)	67.9(3)
C(14)-C(15)-C(20)-C(21)	-54.9(3)
C(16)-C(15)-C(20)-C(19)	59.7(3)
C(26)-C(15)-C(20)-C(19)	-60.1(3)
C(14)-C(15)-C(20)-C(19)	177.1(2)

C(19)-C(20)-C(21)-C(22)	-172.9(2)
C(15)-C(20)-C(21)-C(22)	59.7(3)
C(20)-C(21)-C(22)-O(4)	178.1(2)
C(20)-C(21)-C(22)-C(13)	-58.0(3)
C(12)-C(13)-C(22)-O(4)	-74.1(2)
C(25)-C(13)-C(22)-O(4)	45.3(3)
C(14)-C(13)-C(22)-O(4)	171.48(19)
C(12)-C(13)-C(22)-C(21)	165.3(2)
C(25)-C(13)-C(22)-C(21)	-75.4(3)
C(14)-C(13)-C(22)-C(21)	50.8(3)

Table 7c. Hydrogen bonds for svp16 [Å and °].

D-H...A	d(D-H)	d(H...A)	d(D...A)	<(DHA)
O(2)-H(2)...O(4)#1	0.850(2)	1.892(6)	2.737(3)	172(4)
O(4)-H(4)...O(1)	0.850(2)	1.94(2)	2.666(2)	143(3)

Symmetry transformations used to generate equivalent atoms:

#1 x+1/2,-y+1/2,z+1/2